



# SCOLIOSIS

a Universal Rotational (De)compensation of the Spine



UMC Utrecht

Steven de Reuver

# SCOLIOSIS

a Universal Rotational (De)compensation of the Spine

Steven de Reuver

## **Colofon**

|           |   |
|-----------|---|
| ISBN      | 978-90-393-7581-5                                     |
| Layout    | Steven de Reuver                                      |
| Printing  | Proefschriftmaken.nl                                  |
| Cover art | 'Scoliose van de Oude Gracht', Steven de Reuver, 2022 |

A large thank you to the following parties who supported this work (in alphabetical order):

|                        |   |                       |
|------------------------|---|-----------------------|
| Annafonds   NOREF      | Dutch Spine Society                         | Stichting Steun 22Q11 |
| ChipSoft               | Fondation Yves Cotrel                       | SYNTROPIQ             |
| Cresco Spine           | InSpine                                     | Telefield             |
| Dutch Scoliosis Center | Nederlandse Orthopaedische Vereniging (NOV) |                       |

© S. de Reuver, Utrecht, the Netherlands

All rights reserved. No part of this publication may be printed or utilized in any form without permission of the copyright holder.

**Scoliosis**  
**a Universal Rotational (De)compensation of the Spine**

Scoliose  
een Universele Rotatoire (De)compensatie van de Wervelkolom

**Proefschrift**

ter verkrijging van de graad van doctor aan de Universiteit Utrecht  
op gezag van de rector magnificus, prof.dr. H.R.B.M. Kummeling,  
ingevolge het besluit van het college voor promoties  
in het openbaar te verdedigen op

donderdag 28 september 2023 des middags te 2.15 uur

door

Steven de Reuver  
geboren op 3 juli 1993 te Vlissingen



**Promotoren**

prof. dr. René M. Castelein  
prof. dr. Moyo C. Kruyt

**Copromotoren**

dr. Tom P.C. Schlösser  
dr. Michiel L. Houben

**Beoordelingscommissie**

prof. dr. Cumhur (F.C.) Öner  
prof. dr. Aebele B. Mink van der Molen  
prof. dr. Keita Ito  
prof. dr. Rutger Jan (R.A.J.) Nijvelstein  
prof. dr. Barend J. van Royen

PhD Thesis



# Scoliosis

a Universal Rotational  
(De)compensation  
of the Spine

Steven de Reuver

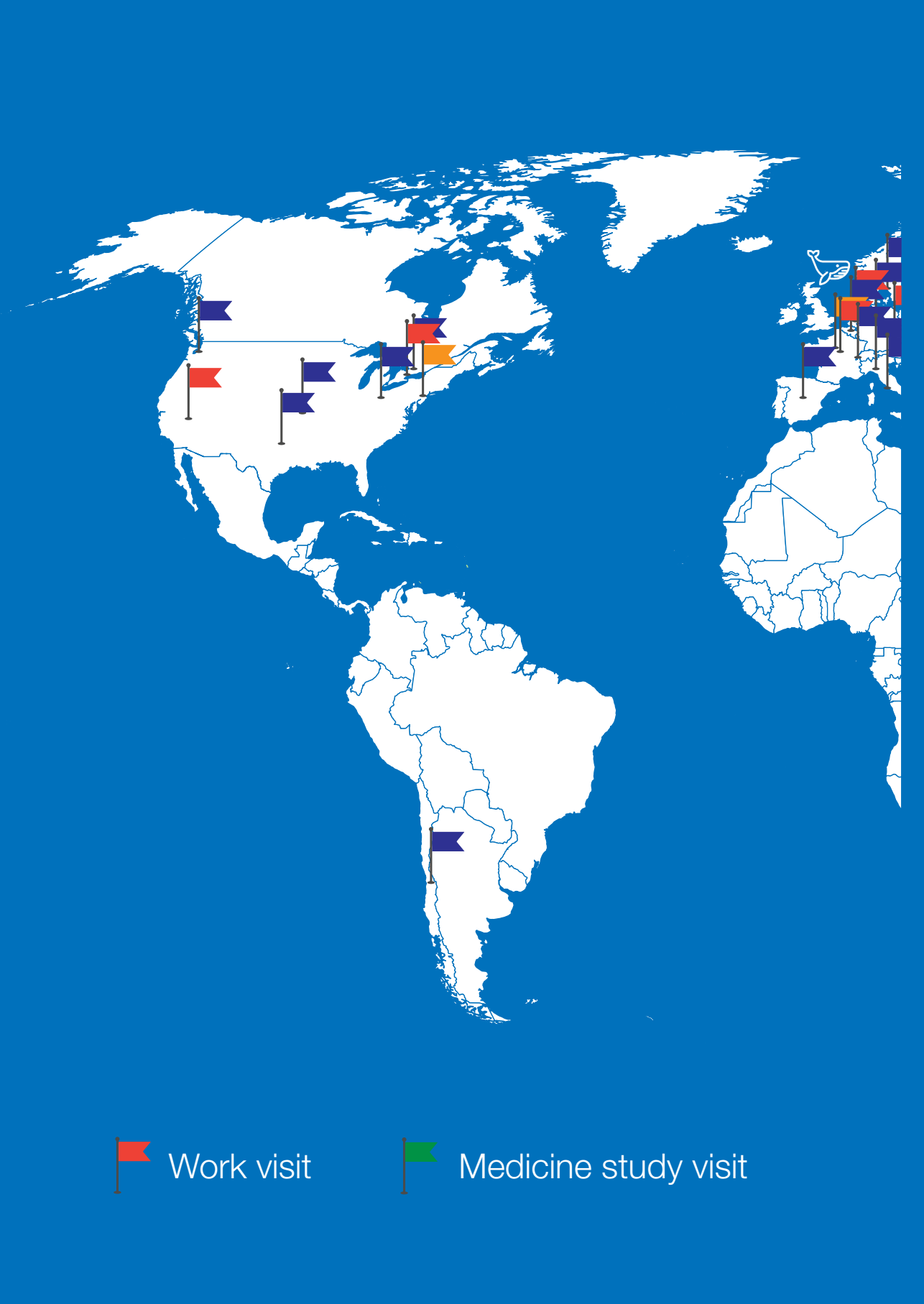


Voor al die ik liefheb

## Contents

| <b>Introduction</b>                              |   |     |
|--|---|-----|
| Chapter 1  | General introduction and Thesis Outline   | 17  |
| <b>Part I Growth of the Healthy Spine</b>        |   |     |
| Chapter 2  | Disc and Vertebral Body Morphology From Birth to Adulthood  | 35  |
| Chapter 3  | Morphological Changes of the Intervertebral Disc during Growth  | 49  |
| Chapter 4  | Ossification and Fusion of the Vertebral Ring Apophysis as an Important Part of Spinal Maturation   | 67  |
| Chapter 5  | The Changing Position of the Center of Mass of the Thorax during Growth in Relation to Pre-existent Vertebral Rotation  | 81  |
| Chapter 6  | Sagittal Spinal Profile development during Growth: a Cross-Sectional Pilot Study using Spinal Ultrasound and Statistical Shape Modeling                       | 93  |
| <b>Part II Scoliosis as a Universal Response</b> |   |     |
| Chapter 7  | Cross-validation of Ultrasound Imaging in Adolescent Idiopathic Scoliosis   | 107 |
| Chapter 8  | Anterior Lengthening in Scoliosis occurs only in the Disc and is Similar in Different types of Scoliosis  | 119 |
| Chapter 9  | The role of Sagittal Pelvic Morphology in the Development of Adult Degenerative Scoliosis   | 133 |
| Chapter 10                                       | What a Stranded Whale with Scoliosis can teach us about Human Idiopathic Scoliosis  | 145 |
| Chapter 11                                       | Convex-concave and Anterior-posterior Spinal Length Discrepancies in Adolescent Idiopathic Scoliosis with Major Right Thoracic curves versus Matched controls | 163 |

|   |  |     |
|---|--|-----|
| <b>Part III</b>   |  |     |
| <b>22q11.2 Deletion Syndrome as a Model for Scoliosis</b> |  |     |
| Chapter 12  | Updated Clinical Practice Recommendations for <i>Children</i> with 22q11.2 Deletion Syndrome – Musculoskeletal guidelines    | 177 |
| Chapter 13  | Updated Clinical Practice Recommendations for <i>Adults</i> with 22q11.2 Deletion Syndrome – Musculoskeletal guidelines      | 191 |
| Chapter 14  | The 22q11.2 Deletion Syndrome as a Model for Idiopathic Scoliosis - A Hypothesis   | 207 |
| Chapter 15  | 22q11.2 Deletion Syndrome as a Human Model for Idiopathic Scoliosis  | 221 |
| Chapter 16  | The role of 22q11.2 Deletion Syndrome in the Relationship between Congenital Heart Disease and Scoliosis                     | 237 |
| Chapter 17  | Genetic Overlap between Idiopathic Scoliosis and Schizophrenia in the General Population                                     | 251 |
| Chapter 18  | Ultrasound Shear Wave Elastography of the Intervertebral Disc and Idiopathic Scoliosis: A Systematic Review                  | 273 |
| Chapter 19  | Sagittal Curvature of the Spine as a Predictor for Pediatric Spinal Deformity Development                                    | 293 |
| Chapter 20  | Early Sagittal Shape of the Spine Predicts Scoliosis Development in a Syndromic Population: a Prospective Longitudinal Study | 309 |
| <b>Conclusion</b>   |  |     |
| Chapter 21  | Summary, General Discussion and Conclusions  | 325 |
|   | Nederlandse samenvatting   | 341 |
|   | List of Publications, Curriculum Vitae & Acknowledgements  | 353 |

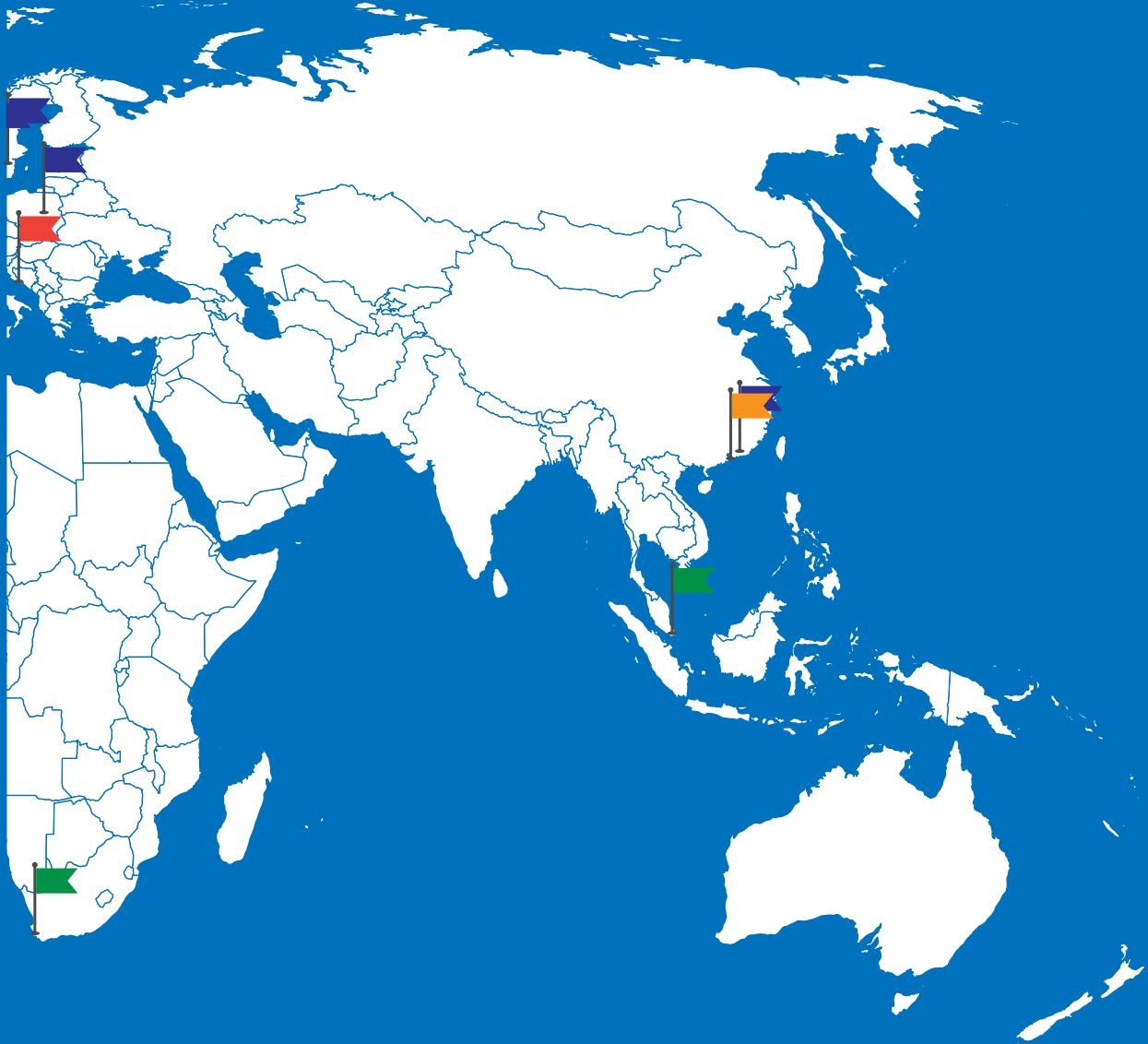


Work visit



Medicine study visit

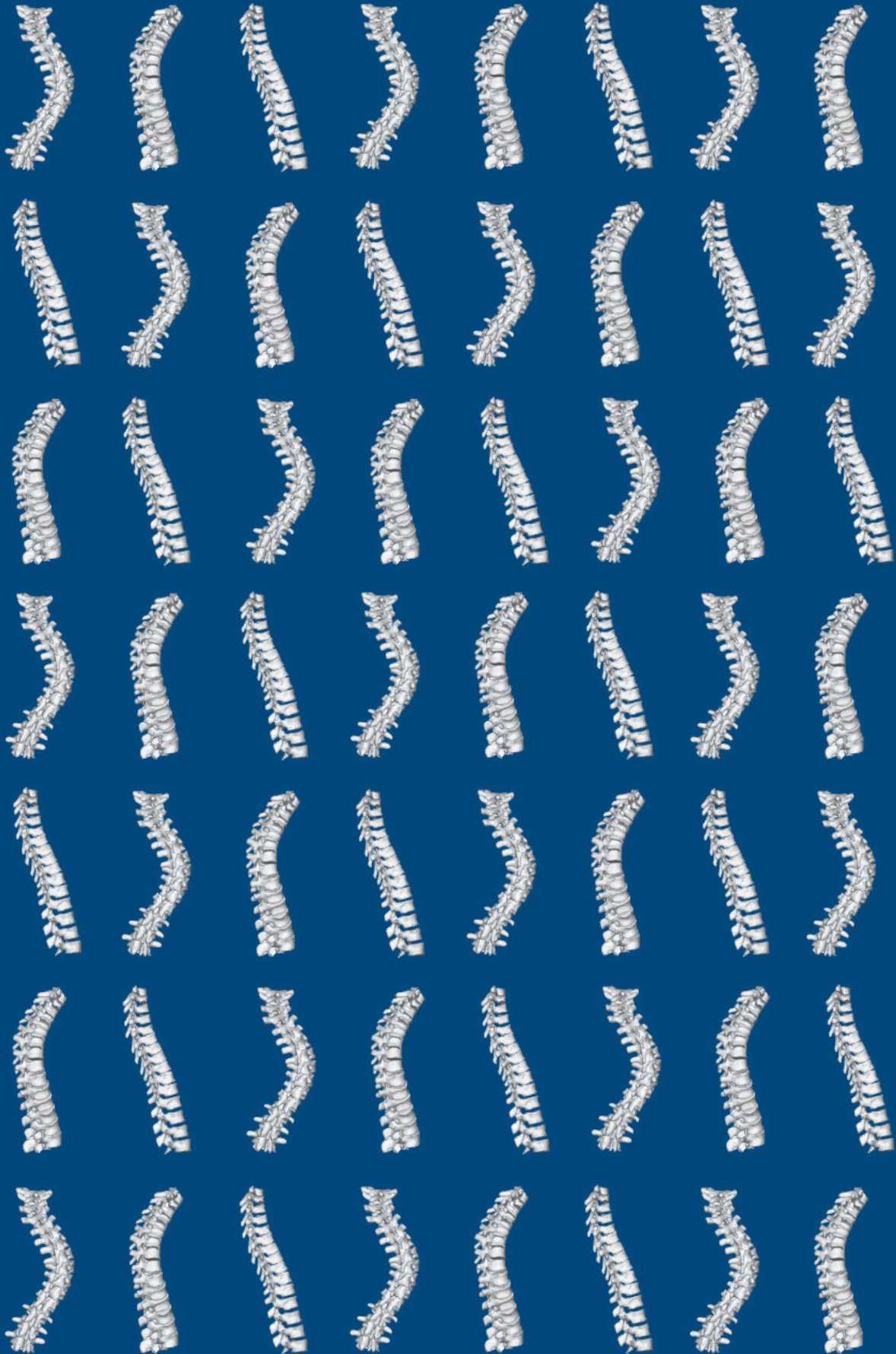


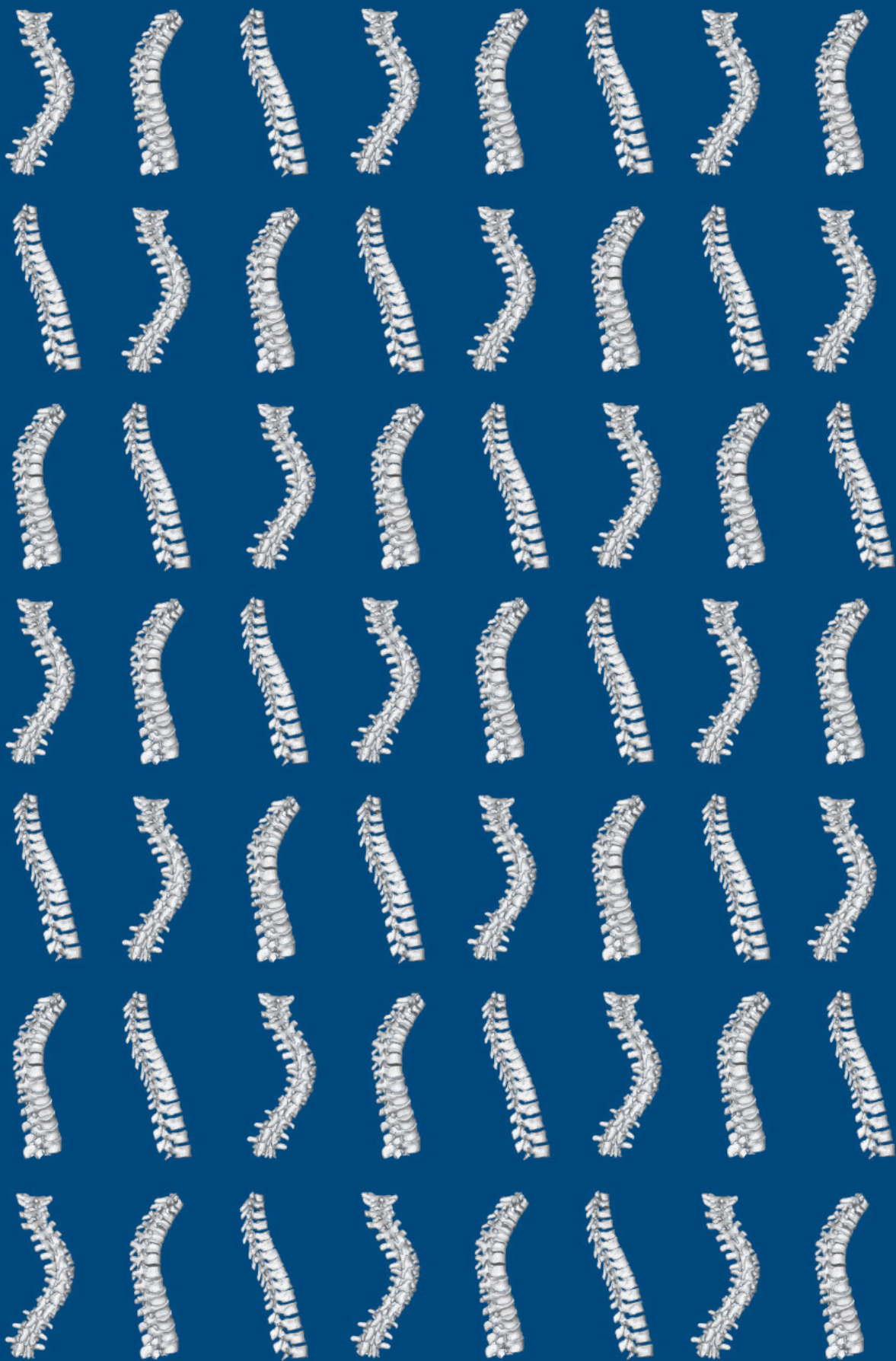


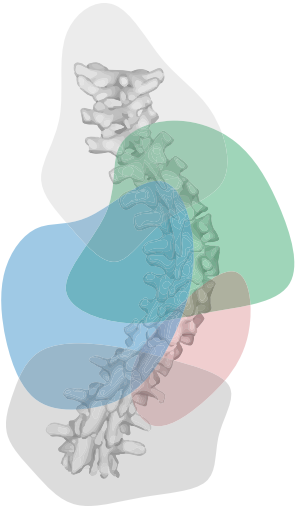
Grant collaborator



Co-author



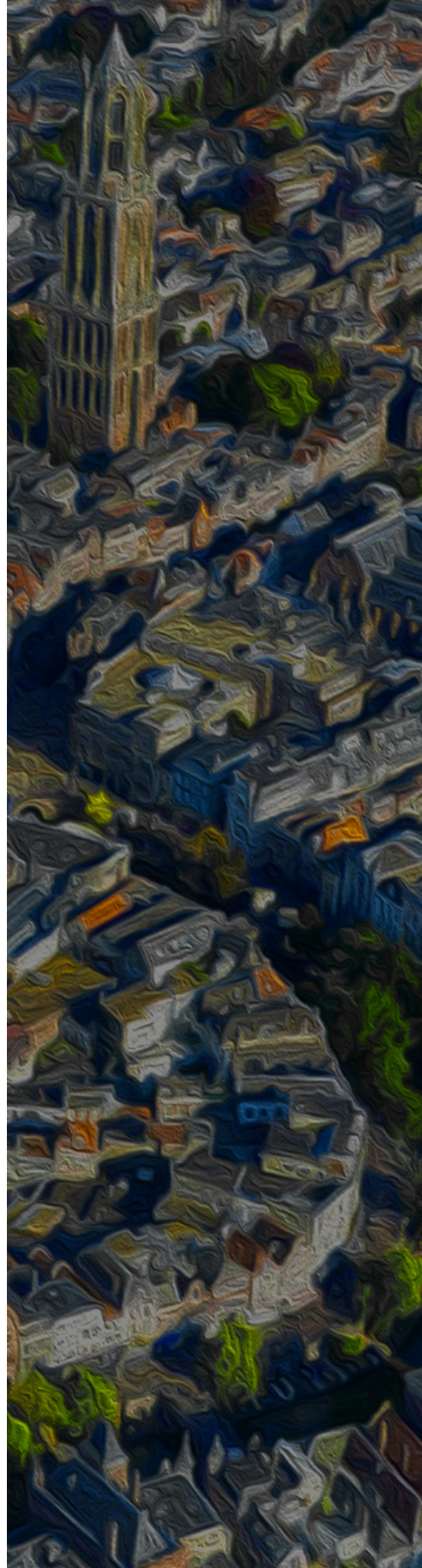






# 1

General Introduction  
and Thesis Outline



## Scoliosis

Scoliosis is a deformation of the spine characterized by a transverse plane rotation, coronal plane lateral deviation, and a lordosis in the sagittal plane (**Figure 1**). In severe cases, the spine can protrude anteriorly into the chest and distort the anatomy of the chest, which may have cardiopulmonary consequences for the young patients.<sup>1</sup> Scoliosis can develop due to a clear cause such as neuromuscular scoliosis in spinal muscular atrophy (SMA) patients, or congenital scoliosis due to a variety of inborn failures of formation or segmentation of vertebrae. However, the most common type of scoliosis spontaneously develops during growth, knows no clear underlying disorder and seems to occur only in humans.<sup>2,3</sup> This is called adolescent idiopathic scoliosis (AIS), and has a prevalence of 2-4% in the general population with an overrepresentation of females, especially in the more severe progressive curves.<sup>1</sup> As recently published by the European Commission, back pain and musculoskeletal disorders, of which AIS is a substantial part, are stated as under-researched medical conditions, while having a high burden for the patients and society as a whole.<sup>4</sup>

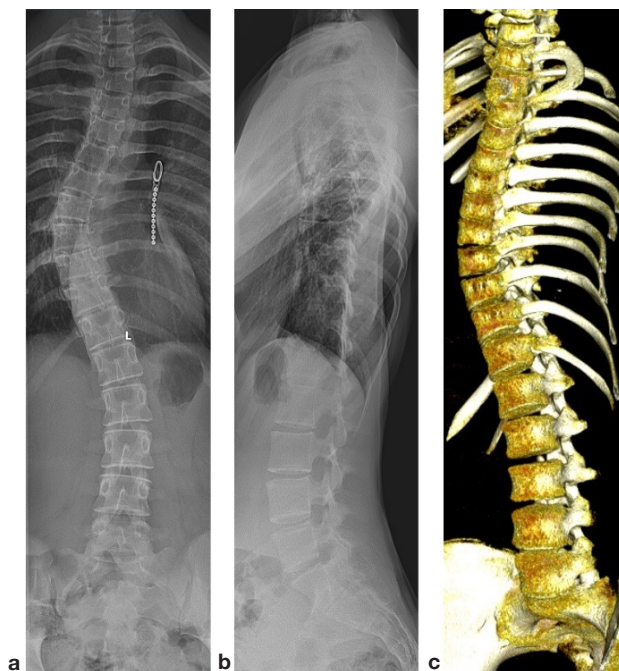


**Figure 1.** Posterior-anterior (a) and lateral (b) radiographs, and a 3D CT reconstruction of a 17 year old girl with a typical right-convex thoracic idiopathic scoliosis. Already on the lateral radiograph a thoracic hypokyphosis is visible, clinically often dubbed as ‘flat back’. On the antero-lateral view of the apex obtained with CT reconstruction (c), the apical lordosis becomes manifest.

Treatment is currently focused on limiting progression of the spinal curve until skeletal maturity, which can necessitate bracing therapy or spinal fusion surgery.<sup>1</sup> Unfortunately, although treatment with different brace concepts has proven to be effective,<sup>5,6</sup> prevention options for idiopathic scoliosis are lacking. This is because its etiology remains largely illusive, despite decades of quality research on the subject. Therefore, treatment is normally

only started for well-established cases, which already show many secondary adaptations of the spine and trunk. Many theories have been brought forward in search of the etiology of idiopathic scoliosis, that can roughly be divided into genetics, metabolomics, conditions of the central nervous system, and biomechanics.<sup>1,7-15</sup> In terms of biomechanics, the upright human spine involves segments with reduced stability in the horizontal plane, that may play an important role in idiopathic scoliosis initiation.<sup>16,17</sup>

### Human spinal structure and function

The human spine is unique, not in its basic anatomy nor because humans are bipedal, but in the way it is mechanically loaded, due to its unique sagittal alignment.<sup>18-21</sup> Since the times of the dinosaurs there have been many other bipedal animals, but all carry their center of mass in front of the pelvis when walking 'upright'. Humans are the only species that, in the sagittal plane, balance their center of mass straight above the pelvis by fully extending hips and knees, and thus more posterior than any other vertebrate, during upright stance and bipedal locomotion.<sup>18,22</sup> This orientation of the trunk begins with a unique lordosis between the ischial and iliac bones (the pelvic lordosis) and continues cranially with a lumbar lordosis.<sup>20</sup> As a consequence, a large portion of the thoracic and lumbar spine in humans is posteriorly inclined, even more so in the growing population (**Figure 2**).<sup>23</sup>

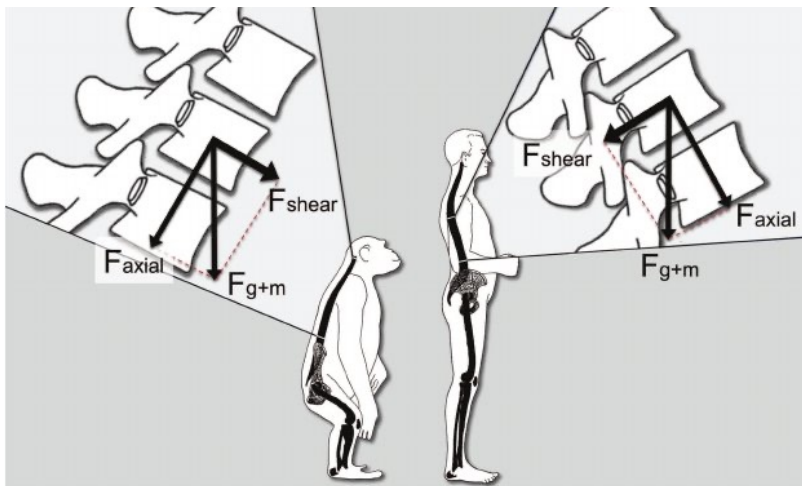
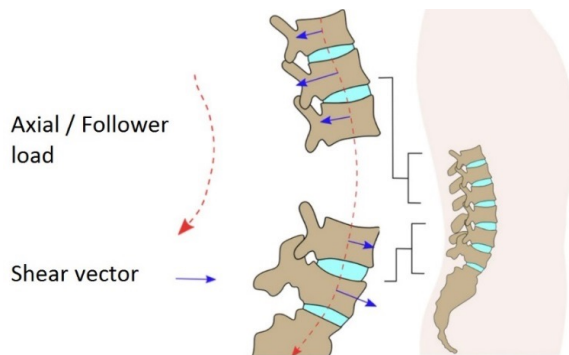


**Figure 2.** A simplification of the combined forces of gravity and trunk's muscles, that act on each vertebral body, and can be split into an axial vector along the spine and a shear vector perpendicular to it. This transverse shear force is directed anteriorly in all vertebrates besides humans, in which this shear load in a large portion of the spine, especially during growth, is posteriorly directed. Figure from Kouwenhoven et al.<sup>16</sup>

This leads to a different force play than in other bipedal as well as quadrupedal mammals, not only when upright, but, due to the continuously present muscle tension, basically always. This is explained in ex vivo biomechanical experiments with spinal segments, where the physiological situation of the trunk's mass and muscle tension is represented by a follower load.<sup>24</sup> This mainly involves an axial vector, with forces that act in a direction tangential to the spinal curvature, therefore perpendicular to the endplate. However, smaller force vectors do act on individual vertebrae, introducing shear forces in the sagittal plane, of which the direction depends on the orientation of each individual vertebra within the spinal curve (**Figure 3**). And as demonstrated in **figure 2**, while in all mammals except humans, this translates into a transverse plane vector that is directed anteriorly, in the posteriorly inclined segments in humans, a posteriorly directed transverse vector is introduced.<sup>16</sup>

**Figure 3.** The follower load tangential to the spinal curvature and the transverse shear force, of which the vector direction depends on the spinal segment's orientation.

Figure from Gudde et al.<sup>25</sup>



These force vectors have been demonstrated to play an important role in spinal stability, and their effect is visible in the healthy spine at micro level and can clearly manifest themselves in the symptomatic spine. At a micro level, studying the predominant orientation of the trabeculae in the cancellous bone demonstrates a difference between vertebrae that are oriented in anterior inclination, for instance L5, and those in posterior inclination, for instance L1 (**Figure 4**).<sup>25</sup>

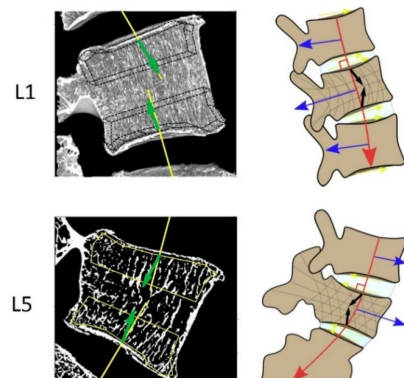


**Figure 4.** The primary trabecular orientation (green) in a posteriorly inclined (L1) and anteriorly inclined (L5) vertebrae, together with the axial/follower (red) and shear (blue) loads. Since anisotropic trabeculae orientation suggest a stereotypical load in that direction, these observations suggest there is, besides a relatively large axial compression, a smaller transverse component that differs per the vertebra's orientation. Figure partially adapted from Gudde et al.<sup>25</sup>



At a larger scale, these forces may become manifest throughout life, which can be most clearly observed in the degenerative spine, where disc degeneration has destabilized the spine. This may lead to different pathologies, dependent on which of the loads eventually succeed in disturbing the spinal equilibrium. For example, disc collapse as an expression of long-standing axial compression (**Figure 5a**), but also anterior (**Figure 5b**) or posterior (**Figure 5c**) vertebral slippage as an expression of anterior shear or posterior shear vectors acting on the segment.

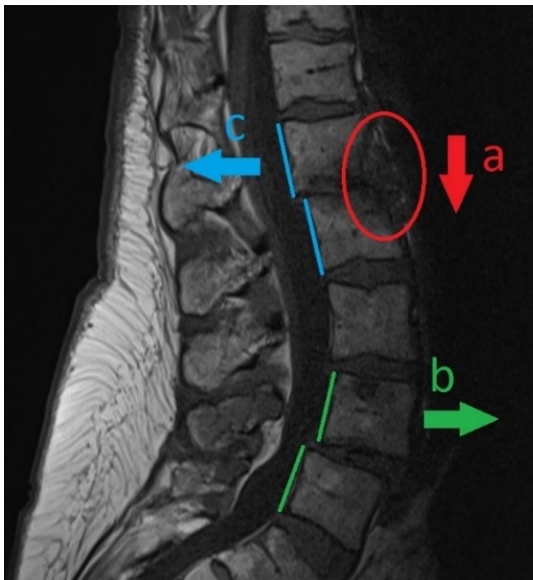
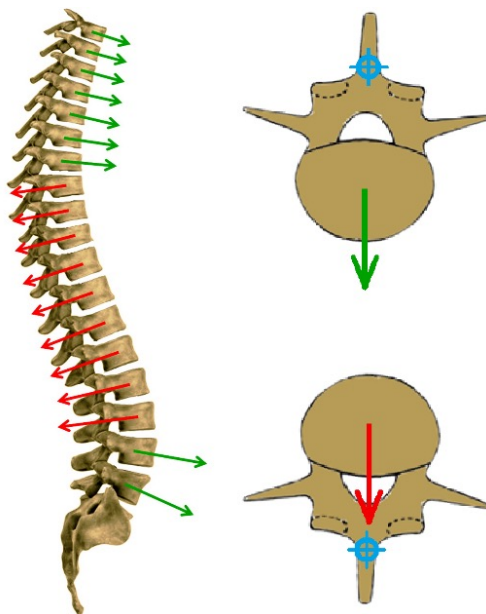


**Figure 5.** MRI of a degenerative lumbar spine with evidence of consequences of axial (**a**), and anteriorly (**b**) and posteriorly (**c**) directed forces that eventually disturbed the spinal equilibrium.

In essence there are thus three forces acting on the spine, axial, anteriorly directed and posteriorly directed, of which the axial force is the largest, but the shear forces have an impact on segmental rotational stability. Forces, when they exceed a certain threshold, will lead to a deformity, either acute or chronic. It has been postulated that an axial force that is chronically excessive to what the body can withstand will lead to a disturbance of longitudinal vertebral growth, or Scheuermann's disease. On the other hand, an excessive anteriorly directed force may lead to anterior slippage or spondylolisthesis. Interestingly the third, posteriorly directed force has not received much attention. All spines in nature except for the human, experience only anteriorly directed shear loads, which have been demonstrated to increase rotational stability, thus stabilizing the spine and protecting it from permanent rotational deformity. Only in humans, this anterior shear load is replaced, in certain ill-defined areas of the vertebral column, by a posteriorly directed shear load, that acts on all posteriorly inclined vertebrae and was shown to lead to a significant reduction of rotational stability of the involved segments.<sup>16,17</sup>

The presence of this phenomenon of posterior shear loading that introduces rotational instability of the human spine, is potentially explained by the posteriorly inclined spinal segment being fairly new on the evolutionary scale, while the basic anatomical ‘blueprint’ of the spine is much older and omnipresent among vertebrates. Apart from humans, this spinal orientation is usually one large kyphosis with gravity having an anterior transverse vector. In this configuration, the heavy but flexible anterior column and trunk is ‘hanging’ from the more rigid posterior facet joints and ligaments, i.e. a ‘stable equilibrium’.<sup>26</sup> In a reversed orientation, the spinal center of mass is balanced over the posterior elements acting as a fulcrum, i.e. a pendulum in an ‘unstable equilibrium’, which can only remain in equilibrium in a completely symmetrical orientation (**Figure 6**). Interestingly, it has been described that in the human spine there is a slight pre-existent vertebral rotation present due to organ anatomy, therefore the rotation’s direction (left- or right-sided) differs per vertebral level and also transfers sides during growth.<sup>27</sup>

**Figure 6.** The human sagittal spinal orientation on the left-hand side, which is anteriorly inclined in the upper thoracic and lower lumbar spine, and posteriorly inclined in the large segment in between. On the right-hand side, a ‘stable equilibrium’ is observed when the shear load is directed anteriorly (green), and the vertebral body is ‘hanging’ from the rigid posterior column acting as a fulcrum (blue). Vice versa, when the transverse vector of gravity is directed posteriorly (red) the vertebra is in an ‘unstable equilibrium’, since it is balancing straight over the fulcrum. Figure adapted from Schlösser et al.<sup>28</sup>



This human specific sagittal spinal alignment including the posteriorly inclined segments is not present at birth. In general, in utero and in newborns, the spine is C-shaped and practically one large kyphosis.<sup>29–31</sup> During growth, this transitions into the double S-shaped sagittal alignment we are all familiar with, but the exact process, its different phases, the exact morphology per phase, and timing are still not completely clear.<sup>23,32,33</sup> Therefore, the aim of **PART I** of this thesis is to describe the morphology and maturation of intervertebral discs and vertebral bodies, and the sagittal alignment of the normal spine during growth, making use of modern imaging acquisition and processing techniques.

## Imaging for idiopathic scoliosis

Follow-up of AIS patients with spinal imaging conventionally involves periodic free-standing full spine radiographs.<sup>34</sup> Additional imaging can be acquired with bi-planar radiography (EOS), computed tomography (CT), magnetic resonance imaging (MRI) or spinal ultrasound (**Figure 7**). Progress has been made to reduce ionizing radiation for AIS patients as much as possible, since the frequent radiographic imaging of this group has been associated with an increased incidence of malignancies later in life.<sup>35,36</sup>



**Figure 7.** Spinal imaging techniques for AIS, from left to right: conventional radiography, bi-planar radiography with EOS, a CT-scan, a 3D reconstruction from CT, a T2-weighted MRI and spinal ultrasound.

Besides alternatives for patient follow-up, advances in spinal imaging help in further unravelling AIS etiology. Modern imaging of the primary and compensatory curves in different kinds of scoliosis may help in various ways to identify the primary abnormality, preexistent abnormalities, growth disturbances, effect of biomechanical loading and in identification of secondary phenomena in AIS. For example, the once popular AIS etiology concept of relative anterior spinal overgrowth (RASO), that explains the anterior lengthening seen in AIS curves as a growth disorder of the bone, based on a vicious cycle of ever-increasing vertebral body wedging as a consequence of the Hueter-Volkman principle.<sup>10,11,37-39</sup> This concept sees AIS as an active bony overgrowth disorder. However, recent imaging studies showed that in AIS most anterior lengthening is in the discs with no active role for the bone.<sup>40,41</sup>

In this thesis, it is taken one step further, and the hypothesis is tested if scoliosis is a universal passive phenomenon, both in idiopathic and non-idiopathic patients, caused by rotational (de)compensation of the spine. In scoliosis with a clear cause such as neuromuscular disease, the stability is disturbed by a lack of neuromuscular control which causes the spine to decompensate. In congenital scoliosis on the other

hand, often large parts of the spine are anatomically normal, but these areas are forced to compensate for a rigid congenital bony anomaly. If all scoliosis types are essentially a similar passive mechanism, all scoliotic curves, also in crooked spines with known etiology, should have similar morphometric manifestations. And if scoliosis is a universal rotational (de)compensation of the spine across all etiological subtypes in humans, it remains unclear whether it is truly exclusive for humans. Therefore, the aim of **PART II** is to study scoliotic curves of different etiologies in relationship to AIS and determine if the statement and title of this thesis: ‘Scoliosis – a Universal Rotational (De)compensation of the Spine’ holds true.

### Scoliosis in 22q11.2 deletion syndrome

Before the development of the sophisticated genetic analysis techniques we know today, it was already known that siblings and especially monozygotic twins of AIS patients have an increased risk to develop scoliosis as compared to the general population.<sup>42</sup> The complex genetic architecture behind AIS deserves a thesis (or multiple theses) solely on that subject, however, genetic risk factors can also be utilized to our advantage in studying AIS etiology. The AIS prevalence of 2-4% is one of the major hurdles in prospective research, since large amounts of children need to be included before disease onset for sufficient statistical power. To overcome this, one approach is to utilize a subset of the population with a greatly increased risk to develop scoliosis: children with a microdeletion in the 22q11.2 region. 22q11.2 deletion syndrome (22q11.2DS), also known as DiGeorge syndrome or velocardiofacial (VCF) syndrome, is the most common microdeletion syndrome in humans with an estimated incidence of 1 in 992 unselected pregnancies and 1 in 2148 live births.<sup>43-45</sup> This microdeletion is sporadically inherited from one of the parents, however most patients (90%) acquire the deletion ‘de novo’ (**Figure 8**).<sup>43</sup>

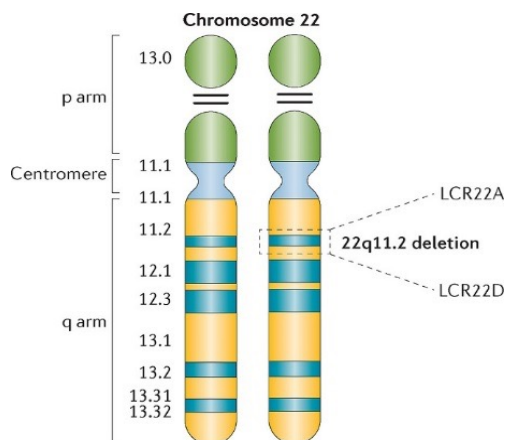


**Figure 8.** The microdeletion in patients with 22q11.2DS. The condition’s name describes that on one of their 22nd chromosomes, on the long arm (q-arm), a small section consisting of about 40 genes is missing leading to a variety of phenotypes. Figure from McDonald-McGinn et al.<sup>43</sup>

Compared to the general population, these children have a 20-fold increased risk of developing scoliosis during their growing years, with a lifetime prevalence of around 50%.<sup>46</sup> The University Medical Center Utrecht is the national center for pediatric 22q11.2DS care, and all patients within the Netherlands are invited for biennial follow-up at our multidisciplinary outpatient clinic. This is important, since, besides scoliosis, the syndrome is characterized by many different phenotypes both mild and severe, across all medical specialties. This includes: congenital heart disease (CHD), cleft palate, velopharyngeal insufficiency, immunodeficiency, autoimmunity, hypoparathyroidism, urologic anomalies, intellectual disability, autism spectrum disorder and schizophrenia (**Figure 9**).<sup>43</sup> Currently, it remains largely unknown whether different phenotypes associated to the 22q11.2 deletion are independent or clustered, and vice versa, whether the 22q11.2 deletion is a confounder for relationships between phenotypes in the general population, which has for instance been described for scoliosis and CHD.<sup>47</sup>

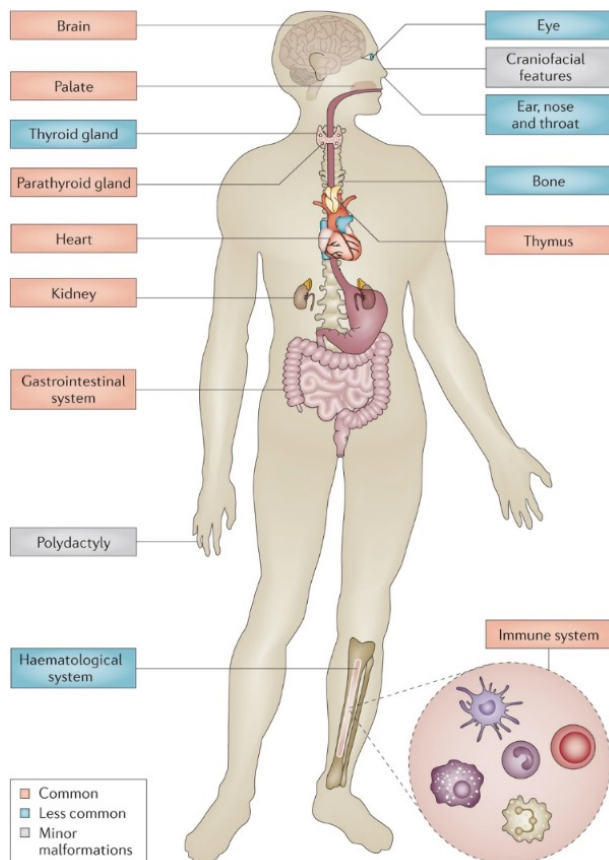


**Figure 9.** The organ (systems) involved in 22q11.2DS. There are currently about 180 phenotypes described associated with the syndrome, usually around seven are prominently present in each patient, however the composition of symptoms varies greatly per individual. Figure from McDonald-McGinn et al.<sup>43</sup>

The high prevalence of scoliosis in this population is scientifically interesting in itself and important for the young 22q11.2DS patients. Additionally, this patient population provides a unique opportunity to prospectively study the development of scoliosis. First, since the lifetime prevalence of scoliosis is 50% compared to 2-4% in the general population, this drastically decreases the needed sample size. Second, from the age of six, which is almost always before the (potential) onset of scoliosis, 22q11.2DS patients are followed-up as standard of care with full spine radiographs at a 2-year interval up until skeletal maturity. Therefore, the combination of identification of children before the onset of scoliosis and the standardized follow-up during childhood and adolescence, provide the opportunity to prospectively study the development of scoliosis in this model. However, the translatability from these prospective studies in 22q11.2DS to idiopathic scoliosis in the general population should be regarded with caution. For other diseases, this approach has already been successfully used. The study of psychotic, 'schizophrenia-like' disorders in the 22q11.2DS population has yielded important information on idiopathic schizophrenia in the general population.<sup>48</sup> For this 'model' to be of any scientific value for unraveling AIS etiology, the scoliosis in 22q11.2DS has to resemble idiopathic scoliosis in the general population. If so, it opens up an array of possibilities to test certain carefully selected phenomena associated with scoliosis development prospectively, which for the first time may identify causal relationships. Furthermore, if such causal risk factors for AIS can be identified, the 22q11.2DS patients will be the first to benefit from it.

This model should logically involve studying concepts already suggested to be associated to idiopathic scoliosis development in the general population, in this thesis two concepts are studied. The first concept is about the role of the intervertebral disc in AIS etiology, since morphometric differences between discs of AIS patients and controls have been demonstrated.<sup>49,50</sup> It is unknown whether there are already changes in the disc prior to the onset of scoliosis, however identifying children with discs 'at risk' for scoliosis would be a breakthrough. Studying the intervertebral disc properties in vivo is difficult due to obvious ethical concerns, especially in asymptomatic children. However, ultrasound based elastography performed with a standard abdominal probe, can measure the shear wave speed of the sound waves through the annulus fibrous tissue (**Figure 10**). Earlier studies of breast and liver tissue demonstrated that shear wave speed correlates to tissue stiffness and the elastic modulus, however for the intervertebral discs this has only been studied indirectly.<sup>51,52</sup> Interestingly, different elastography values were observed in lower lumbar discs between AIS patients and controls, and since these were thoracic curves, this could imply that these disc changes are not the result of the scoliosis, but potentially pre-existent.<sup>53</sup> To confirm this, a prospective analysis of disc elastography before the onset of scoliosis is necessary, for which the proposed 22q11.2DS model would fit well.



A second prospective study concept is regarding the posterior inclined segment of the sagittal human spine (**Figure 6**). If relatively increased posterior shear forces on the spine facilitate rotational instability, the magnitude of posterior inclination may be a risk factor for the development of idiopathic scoliosis. This comprises both the length and the inclination angle of this segment, and can be captured and quantified by measuring the posteriorly inclined triangle (PIT) area, for instance on standardized standing lateral spinal radiographs (**Figure 11**). A prospective study to determine if children with a higher PIT-area indeed have a higher risk for developing scoliosis, would be very well feasible in the 22q11.2DS model, since the 20-fold increased scoliosis risk sharply decreases the required sample size. Such a prospective study would be a great opportunity to identify a predictive relationship between the sagittal spinal profile and idiopathic scoliosis development, which has not been possible until today.

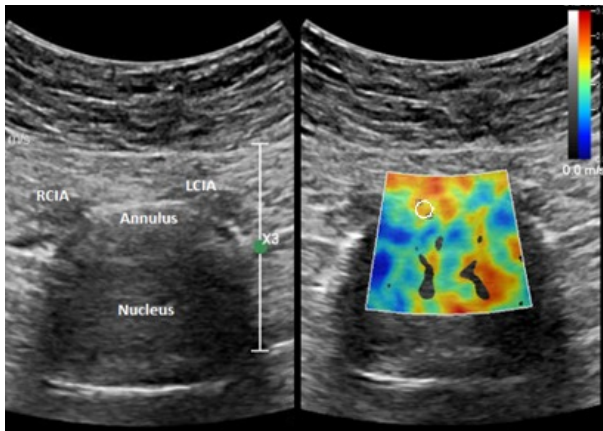


**Figure 10.** On the left-side a transverse plane view of an abdominal ultrasound of the L4-L5 intervertebral disc of a 9 year old, caudal from the aortic bifurcation between the left and right common iliac artery (RCIA/LCIA). The same image on the right-side but including the elastographic shear wave speed measurements taken in the anterior annulus fibrosus.

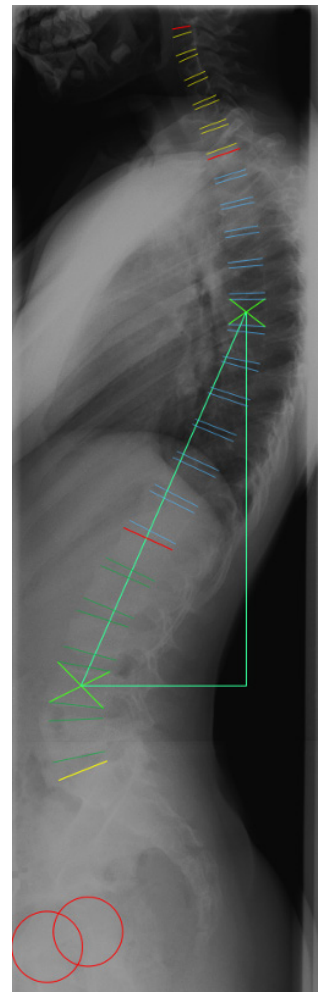


**Figure 11.** Lateral full-spine radiograph including the posteriorly inclined triangle (PIT) area.

The aim of **PART III** is to first study the orthopedic manifestations in 22q11.2DS including scoliosis and their clinical implication. Then the applicability of 22q11.2DS scoliosis as a 'model' for the prospective study of idiopathic scoliosis in the general population is explored. Also, other phenotypes of 22q11.2DS and their genetic background are compared to scoliosis as part of the syndrome. Lastly, a prospective and powered study is presented on the relationship between the magnitude of posterior inclination in pre-scoliotic 22q11.2DS patients, and the later development of scoliosis.

### **Aim and outline of this thesis**

This thesis sets out to describe the morphology, function and sagittal alignment of the 'healthy' spine during growth and in scoliotic curves of different etiologies in relationship to AIS. Furthermore, scoliosis in 22q11.2DS is explored as a 'model' for the prospective study to identify risk factors for idiopathic scoliosis. During the study of all research questions in this thesis, there is special attention for using the most advanced imaging techniques, decreasing the use of ionizing radiation and applying automated segmentation whenever possible.

In **PART I** the intervertebral disc, vertebral body morphology and sagittal alignment of the 'healthy' spine during growth are studied to answer the following questions:

- **Chapter 2:** How do vertebral bodies and intervertebral discs change in size in asymptomatic children during growth?
- **Chapter 3:** How do the annulus fibrosus and nucleus pulposus change in size and arrangement in asymptomatic children during growth?
- **Chapter 4:** What are the different stages of maturation of the ring apophysis throughout the spine during growth?
- **Chapter 5:** What is the position of the thoracic center of mass during growth, in relationship to pre-existent vertebral rotation?
- **Chapter 6:** Can ultrasound imaging of the spine and statistical shape modelling (SSM) describe the sagittal spinal profile of children before and after growth spurt?

In **PART II** this thesis transfers from the 'healthy' spine towards scoliosis, the following questions are studied:

- **Chapter 7:** Is spinal ultrasound accurate and valid for clinical curve severity measurements in AIS patients?



- **Chapter 8:** Is there relative anterior spinal overgrowth (RASO) of the bony vertebral bodies present in scoliosis, or does anterior spinal lengthening start in the disc, and in a similar manner in congenital scoliosis, neuromuscular scoliosis and AIS patients?
- **Chapter 9:** Is spino-pelvic alignment and thus spinal loading similar in adult degenerative scoliosis as compared to similar idiopathic adolescent scoliosis types?
- **Chapter 10:** By studying the rare occasion of post-traumatic scoliosis in a stranded whale, is there a similar scoliotic mechanism and compensatory curve morphology that is independent of cause and species?
- **Chapter 11:** What are the convex-concave and anterior-posterior length discrepancies in thoracic AIS, i.e. what is the exact disturbance of optimal spinal harmony?

In **PART III** scoliosis in 22q11.2 deletion syndrome as a model for AIS in the general population is studied by the following questions:

- **Chapter 12:** What are the clinical practice recommendations of scoliosis and other orthopedic manifestations in 22q11.2DS in children?
- **Chapter 13:** What are the clinical practice recommendations of scoliosis and other orthopedic manifestations in 22q11.2DS in adults?
- **Chapter 14:** Is scoliosis in 22q11.2DS a potential 'model' to study AIS in the general population, and how can this be studied?
- **Chapter 15:** Does scoliosis in 22q11.2DS morphologically and dynamically resemble AIS?
- **Chapter 16:** Is 22q11.2DS a confounder in the relationship between congenital heart disease (CHD) and scoliosis in the general population?
- **Chapter 17:** Is there genetic overlap between scoliosis in 22q11.2DS and another common phenotype: schizophrenia?
- **Chapter 18:** Is ultrasound shear wave elastography able to quantify intervertebral disc stiffness?
- **Chapter 19:** Are there certain sagittal curve patterns present before scoliosis development in 22q11.2DS?
- **Chapter 20:** Is the magnitude of posterior inclination of the spine a risk factor for scoliosis in syndromic patients?

## References

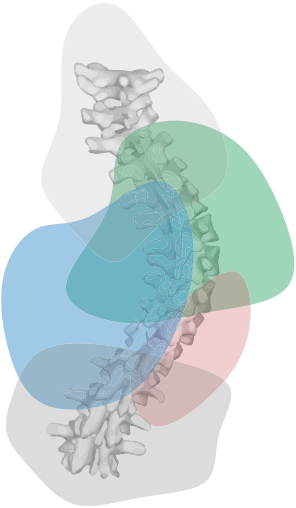
1. Cheng JC, Castelein RM, Chu WC, et al. Adolescent idiopathic scoliosis. *Nat Rev Dis Primers* 2015;1:15–30.
2. Kouwenhoven J-WM, Castelein RM. The pathogenesis of adolescent idiopathic scoliosis: review of the literature. *Spine (Phila Pa 1976)* 2008;33:2898–908.
3. Janssen MMA, de Wilde RF, Kouwenhoven J-WM, et al. Experimental animal models in scoliosis research: a review of the literature. *Spine J* 2011;11:347–58.
4. Directorate-General for Research and Innovation (European Commission). Scoping study on evidence to tackle high-burden under-researched medical conditions.
5. Costa L, Schlosser TPC, Jimale H, et al. The Effectiveness of Different Concepts of Bracing in Adolescent Idiopathic Scoliosis (AIS): A Systematic Review and Meta-Analysis. *J Clin Med*;10. May 15, 2021.
6. Weinstein SL, Dolan LA, Wright JG, et al. Effects of bracing in adolescents with idiopathic scoliosis. *N Engl J Med* 2013;369:1512–21.
7. Schlösser TPC, van der Heijden GJMG, Versteeg AL, et al. How “idiopathic” is adolescent idiopathic scoliosis? A systematic review on associated abnormalities. *PLoS One* 2014;9:e97461.
8. Somerville EW. Rotational lordosis; the development of single curve. *J Bone Joint Surg Br* 1952;34-B:421–7.
9. Dickson RA, Lawton JO, Archer IA, et al. The pathogenesis of idiopathic scoliosis. Biplanar spinal asymmetry. *J Bone Joint Surg Br* 1984;66:8–15.
10. Guo X, Chau WW, Chan YL, et al. Relative anterior spinal overgrowth in adolescent idiopathic scoliosis. Results of disproportionate endochondral-membranous bone growth. *J Bone Joint Surg Br* 2003;85:1026–31.
11. Newell N, Grant CA, Keenan BE, et al. Quantifying Progressive Anterior Overgrowth in the Thoracic Vertebrae of Adolescent Idiopathic Scoliosis Patients: A Sequential Magnetic Resonance Imaging Study. *Spine (Phila Pa 1976)* 2016;41:E382--7.
12. Stokes IAF, Burwell RG, Dangerfield PH. Biomechanical spinal growth modulation and progressive adolescent scoliosis – a test of the “vicious cycle” pathogenetic hypothesis: Summary of an electronic focus group debate of the IBSE. *Scoliosis* 2006;1:16.
13. Nicoladoni C. Anatomie und Mechanismus der Skoliose. In: Kocher, König, von Mikulicz, eds *Bibliotheca Medica Stuttgart*: Verlag von Erwin Nagele.
14. Roth M. [Idiopathic scoliosis and Scheuermann's disease: essentially identical manifestations of neuro-vertebral growth disproportion]. *Radiol Diagn (Berl)* 1981;22:380–91.
15. Porter RW. Can a short spinal cord produce scoliosis? *Eur Spine J* 2001;10:2–9.
16. Kouwenhoven J-WM, Smit TH, van der Veen AJ, et al. Effects of Dorsal Versus Ventral Shear Loads on the Rotational Stability of the Thoracic Spine. *Spine (Phila Pa 1976)* 2007;32:2545–50.
17. Homminga J, Lehr AM, Meijer GJM, et al. Posteriorly directed shear loads and disc degeneration affect the torsional stiffness of spinal motion segments: a biomechanical modeling study. *Spine (Phila Pa 1976)* 2013;38:E1313-9.
18. Alexander RM. Bipedal animals, and their differences from humans. *J Anat* 2004;204:321–30.
19. Washburn SL. The analysis of primate evolution with particular reference to the origin of man. *Cold Spring Harb Symp Quant Biol* 1950;15:67–78.
20. Abitbol MM. Evolution of the ischial spine and of the pelvic floor in the Hominoidea. *Am J Phys Anthropol* 1988;75:53–67.
21. Voutsinas SA, MacEwen GD. Sagittal profiles of the spine. *Clin Orthop Relat Res* 1986;235–42.
22. Bernhardt M, Bridwell KH. Segmental analysis of the sagittal plane alignment of the normal thoracic and lumbar spines and thoracolumbar junction. *Spine (Phila Pa 1976)* 1989;14:717–21.
23. Cil A, Yazici M, Uzumcugil A, et al. The evolution of sagittal segmental alignment of the spine during childhood. *Spine (Phila Pa 1976)* 2005;30:93–100.
24. Liebsch C, Graf N, Wilke H-J. The effect of follower load on the intersegmental coupled motion characteristics of the human thoracic spine: An in vitro study using entire rib cage specimens. *J Biomech* 2018;78:36–44.
25. Gudde A. A Multi-Scale Approach to Implications of the Preferred Vertebral Trabecular Orientation on Spine Biomechanics. *Semantic Scholar*.
26. Vercauteren M. *Dorso-lumbale Curvendistributie En Etiopathogenie Van De Scoliosis Adolescentium*. 1980.
27. Janssen MMA, Kouwenhoven J-WM, Schlösser TPC, et al. Analysis of preexistent vertebral rotation in the normal infantile, juvenile, and adolescent spine. *Spine (Phila Pa 1976)* 2011;36:E486-91.lumbar adolescent idiopathic scoliosis. *Spine J* 2014;14:282–90.
28. Schlösser TPC, Shah SA, Reichard SJ, et al. Differences in early sagittal plane alignment between thoracic and lumbar adolescent idiopathic scoliosis. *Spine J* 2014;14:282–90.
29. Bagnall KM, Harris PF, Jones PR. A radiographic study of the human fetal spine. 1. The development of the secondary cervical curvature. *J Anat* 1977;123:777–82.
30. O'Rahilly R, Muller F, Meyer DB. The human vertebral column at the end of the embryonic period proper. 1. The column as a whole. *J Anat* 1980;131:565–75.
31. Panattoni GL, Todros T. Postural aspects of the human fetal spine. Morphometric and functional study. *Panminerva Med*;30:250–3.
32. Schlösser TPC, Vincken KL, Rogers K, et al. Natural sagittal spino-pelvic alignment in boys and girls before, at and after the adolescent growth spurt. *Eur Spine J* 2015;24:1158–67.
33. Willner S, Johnson B. Thoracic kyphosis and lumbar lordosis during the growth period in children. *Acta Paediatr Scand* 1983;72:873–8.
34. Cobb JR. Outline for study of scoliosis. *The American Academy of Orthopaedic Surgeons Instr Course Lect* 1948;5:261–75.
35. Presciutti SM, Karukanda T, Lee M. Management decisions for adolescent idiopathic scoliosis significantly affect patient radiation exposure. *Spine J* 2014;14:1984–90.

36. Simony A, Hansen EJ, Christensen SB, et al. Incidence of cancer in adolescent idiopathic scoliosis patients treated 25 years previously. *Eur Spine J* 2016;25:3366–70.
37. Chu WCW, Lam WWM, Chan Y-L, et al. Relative shortening and functional tethering of spinal cord in adolescent idiopathic scoliosis?: study with multiplanar reformatted magnetic resonance imaging and somatosensory evoked potential. *Spine (Phila Pa 1976)* 2006;31:E19--25.
38. Stokes IA, Burwell RG, Dangerfield PH. Biomechanical spinal growth modulation and progressive adolescent scoliosis – a test of the “vicious cycle” pathogenetic hypothesis: Summary of an electronic focus group debate of the IBSE. *Scoliosis* 2006;1:16.
39. Volkman R. Verletzungen und Krankheiten der Bewegungsorgane. In: von Pitha und Billroth: Handbuch der allgemeinen und speciellen Chirurgie Bd II Teil II. Stuttgart: Ferdinand Enke. 1882.
40. Schlösser TPC, van Stralen M, Chu WCW, et al. Anterior Overgrowth in Primary Curves, Compensatory Curves and Junctional Segments in Adolescent Idiopathic Scoliosis. *PLoS One* 2016;11:e0160267.
41. Brink RC, Schlösser TPC, van Stralen M, et al. Anterior-posterior length discrepancy of the spinal column in adolescent idiopathic scoliosis-a 3D CT study. *Spine J* 2018;18:2259–65.
42. Kesling KL, Reinker KA. Scoliosis in twins: A meta-analysis of the literature and report of six cases. *Spine (Phila Pa 1976)* 1997;22:2009–15.
43. McDonald-McGinn DM, Sullivan KE, Marino B, et al. 22q11.2 deletion syndrome. *Nat Rev Dis Primers*;1 2015.
44. Grati FR, Molina Gomes D, Ferreira JCPB, et al. Prevalence of recurrent pathogenic microdeletions and microduplications in over 9500 pregnancies. *Prenat Diagn* 2015;35:801–9.
45. Blagojevic C, Heung T, Theriault M, et al. Estimate of the contemporary live-birth prevalence of recurrent 22q11.2 deletions: a cross-sectional analysis from population-based newborn screening. *CMAJ Open* 2021;9:E802–9.
46. Homans JF, Baldew VGM, Brink RC, et al. Scoliosis in association with the 22q11.2 deletion syndrome: An observational study. *Arch Dis Child* 2019;104:19–24.
47. Jordan CE, White RI, Fischer KC, et al. The scoliosis of congenital heart disease. *Am Heart J* 1972;84:463–9.
48. Gur RE, Bassett AS, McDonald-McGinn DM, et al. A neurogenetic model for the study of schizophrenia spectrum disorders: the International 22q11.2 Deletion Syndrome Brain Behavior Consortium. *Mol Psychiatry* 2017;22:1664–72.
49. Stokes IAF, Windisch L. Vertebral height growth predominates over intervertebral disc height growth in adolescents with scoliosis. *Spine (Phila Pa 1976)* 2006;31:1600–4.
50. Chen H, Schlösser TPC, Brink RC, et al. The Height-Width-Depth Ratios of the Intervertebral Discs and Vertebral Bodies in Adolescent Idiopathic Scoliosis vs Controls in a Chinese Population. *Sci Rep* 2017;7:46448.
51. Sarvazyan A, Hall TJ, Urban MW, et al. An overview of elasticity imaging - an emerging branch of medical imaging. *Curr Med Imaging Rev* 2011;7:255–82.
52. Vergari C, Rouch P, Dubois G, et al. Intervertebral disc characterization by shear wave elastography: An in vitro preliminary study. *Proc Inst Mech Eng H* 2014;228:607–15.
53. Vergari C, Chanteux L, Pietton R, et al. Shear wave elastography of lumbar annulus fibrosus in adolescent idiopathic scoliosis before and after surgical intervention. *Eur Radiol* 2020;30:1980–5.



# PART I

Growth of the  
Healthy Spine

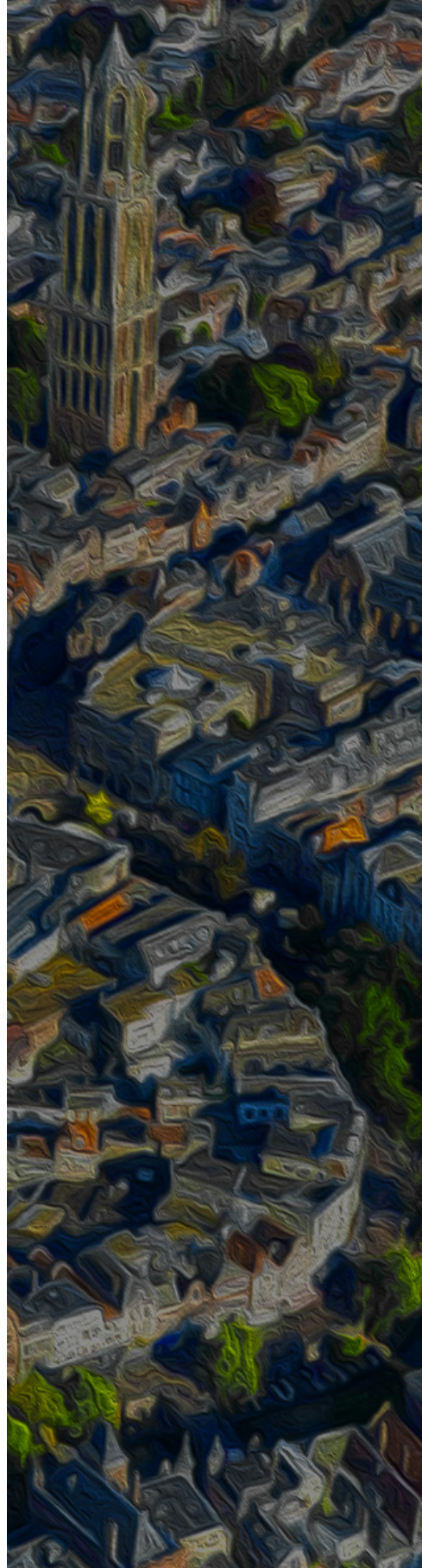


# 2

## Disc and Vertebral Body Morphology from Birth to Adulthood

Steven de Reuver  
Lorenzo Costa  
Hanna van Rheenen  
Casper S. Tabeling  
Justin V.C. Lemans  
Tom P.C. Schlösser  
Moyo C. Kruyt  
Marijn van Stralen  
René M. Castelein

*Spine. 2022 Apr 1;47(7):E312-E318.*



## ABSTRACT

**Study Design.** Cross-sectional.

**Objective.** The aim of this study was to describe the morphology of intervertebral discs and vertebral bodies during growth in asymptomatic children and adolescents.

**Summary of Background Data.** Earlier studies demonstrated that spinal growth occurs predominantly in vertebral bodies. This axiom introduced a vertebral-body-focus for unravelling etiological questions and achieve growth-modulation in young spinal deformity patients. Recent studies show the importance of the intervertebral discs in the early phases and possible etiology of pediatric spinal deformities. There is presently a paucity of 3D morphometric data of spinal elements during growth.

**Methods.** A database of 298 patients aged 0 to 21 that have received a computed tomography scan for indications not related to the spine was analyzed. Custom made software was used to semi-automatically measure intervertebral disc and vertebral body morphology, corrected for orientation in all 3 planes.

**Results.** Vertebral body height increased from birth up to adulthood, from 4-to-14 mm in the cervical, 6 to 20 mm in the thoracic, and 9 to 28 mm in the lumbar spine. This increase was 0.70 mm/year in males, more pronounced than females with 0.62 mm/year ( $P = 0.001$ ). Lumbar discs increased throughout growth from 4.4 to 9.0 mm, whereas thoracic discs only increased from 3.5 to 4.9 mm at age 4 and remained stable afterwards, similarly for cervical discs. The disc transverse surface area increased greatly and consistently throughout growth. Disc slenderness was stable in the lumbar spine during growth, but decreased in the thoracic and cervical spine. Overall, discs were more slender in females, especially around early adolescence.

**Conclusion.** The spine grows predominantly in the vertebral bodies. Thoracic discs increase in height only during the first years, whereas the transverse surface area continues to increase throughout growth, thus discs slenderness decreases. Relatively, female discs remained slenderer around growth-spurt. These measurements may assist future studies on the role of disc morphology in the etiology and treatment of spinal deformity.



## Introduction

Half a century ago, the ontogenetic changes in morphology of the intervertebral discs and vertebral bodies were evaluated in post-mortem and radiographic studies.<sup>1-6</sup> Since then, it is well known that height increase of the spine during growth in healthy children and adolescents is located predominantly in the vertebral bodies.<sup>2,3</sup> The height of intervertebral discs seemed to either increase slightly or remain relatively stable throughout growth.<sup>2,3</sup> Despite the monumental status of these articles, it must be acknowledged that available radiographic measurements of that period might not be precise compared to today's standards, especially for intervertebral discs, that are only a few millimeters tall in the first years of life. More recent studies showed that with use of three-dimensional (3D) imaging methods such as computed tomography (CT)-scanning, very precise morphological descriptions of spinal anatomy can be done, as was performed in 2015 by Peters et al. on the change in shape of thoracic vertebral bodies during growth.<sup>7</sup> However, no comprehensive analysis of the vertebral body and intervertebral disc morphology using modern 3D imaging methods has been done of the complete spine of healthy children and adolescents during growth.

Recent studies suggest the importance of intervertebral disc morphology, including height, width and slenderness (usually defined by a height-to-width ratio), as well as its attachment into the vertebral body, in the etiology of spinal deformity during pediatric growth.<sup>8</sup> Especially for adolescent idiopathic scoliosis, where most of the deformity was observed in the disc with the vertebral bodies largely retaining their original shape.<sup>9-12</sup> Stokes et al. observed a difference in height growth of discs and bodies between adolescent idiopathic scoliosis patients and controls.<sup>13</sup> Moreover, a recent biplanar radiography study by Vergari et al. and a CT-analysis by Chen et al. showed the spine in adolescent idiopathic scoliosis patients to be more slender than the asymptomatic population.<sup>14,15</sup> In these and earlier studies, it has been suggested that slenderness of the spine, and especially of the intervertebral discs, is a proposed risk factor for scoliosis. Potentially explained by lateral displacement and torsion of the spine, as present in scoliosis, occurs more easily in more slender structures.

Characterizing the shape of the vertebral bodies and intervertebral discs during growth is considered very important for determining the efficacy of - especially - early-onset scoliosis treatments. While many growth-friendly (i.e. fusion-less) treatments are able to facilitate spinal growth, the relative contribution of the vertebral bodies and the intervertebral discs to overall growth is unknown. Vertebral body growth can be related to the Hueter-Volkman principle, which states that epiphyseal growth is inhibited in areas of increased compressive stress and accelerated in areas of decreased compressive stress.<sup>16</sup> Present growth-friendly techniques aim at stabilizing and correcting the spinal deformity by utilizing the process of

local growth modulation using compression and/or distraction on the convexity and concavity respectively.<sup>17-19</sup> However, the effect of compression or distraction on the growth of intervertebral discs is yet unknown.

To put these and future observations into more perspective, it is essential to know the absolute measurements of both the vertebral bodies and the intervertebral disc, and their relative contribution to total spinal length at different ages, as they are of importance in patient-specific treatment. We hypothesize that spinal growth occurs mostly in vertebral bodies and that there is a decrease of disc slenderness with increasing age, we expect a difference between males and females with overall more slender discs in females. Therefore, the objective of this study is to describe with accurate 3D measurements the morphology of intervertebral discs and vertebral bodies during growth in asymptomatic children and adolescents.

## **Materials and Methods**

### Study population

For the present study an existing CT-scan research database from one tertiary children's hospital was used. The institutional ethics review board (IRB) approved a waiver of informed consent for this study. In line with institutional patient privacy guidelines, the age of patients could only be gathered exact to the year of age, so their date of birth is fully untraceable. Patients aged 0 to 21, with either a full body, thoracic-abdominal or thoracic CT-scan, made for indications not related to the spine were included. These indications were for example systemic infections or screening after larger traumatic injuries. Exclusion criteria were low-quality scans or incomplete visualization of individual spinal segments, evidence of spinal trauma, spinal pathology, anatomical abnormalities, and/or growth disorders.

### Measurements

Custom made for this study, in-house developed software for semiautomatic imaging analysis was used (ScoliosisAnalysis 7.3; Image Sciences Institute, Utrecht, The Netherlands, developed using MeVisLab, MeVis Medical Solutions AG, Bremen, Germany). With this software each vertebral body upper and lower endplate was segmented on CT-scans in the true transverse plane, corrected for the orientation in all three planes (**Figure 1A-C**). Note that for the youngest in our population, the most upper and lower portions segmented of the vertebral bodies were the primary ossification centers, since the future endplates are not yet ossified. The software automatically calculated the surface area and centroid of all endplates, and subsequently the height of vertebral bodies and intervertebral discs was calculated, defined as the distance between two adjacent centroids (**Figure 2**). This centroid distance

was chosen, since, during the software development, this showed to be most stable and less susceptible to individual sagittal spinal positioning (lordosis and kyphosis) causing a shift in endplate orientation, compared to other options such as the mean of the anterior-, posterior-, left- and right-height or the mean of the minimal and maximal distance between two endplates (**Figure 2**).

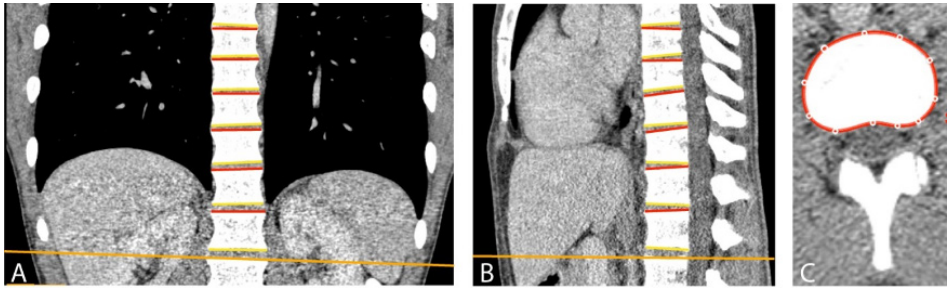


**Figure 1.** Custom made software for semi-automatic imaging analysis was used to correct for orientation in all three planes (**A,B**) to segment each vertebral body upper and lower endplate in the true transverse plane (**C**). The surface area and centroid of all segmented endplates were automatically determined.

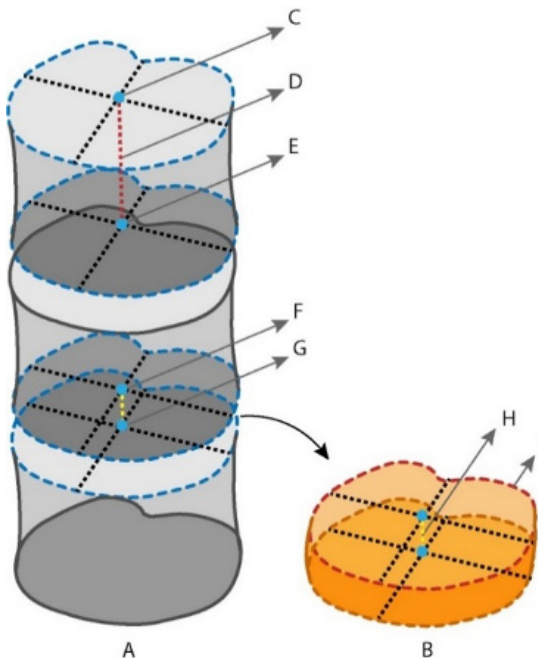


**Figure 2.** The intervertebral disc (**B**) was defined as the space between two adjacent endplates of the vertebrae above and below the disc (**A**). The height of a vertebral body (**D**) was defined as the distance between two adjacent endplate centroids (**C,E**) and similarly for the intervertebral disc height (**H**) between two adjacent endplate centroids (**F,G**).

### Outcome measures

The height and transverse surface area were calculated for each vertebral body and intervertebral disc in the section of the spine visible on the CT-scan. Specific analysis was done for the cervical, thoracic and lumbar spine. Also, the disc contribution to the segmental spinal height of a patient was calculated by dividing the intervertebral disc height by the sum of the height of that intervertebral disc and the vertebral body above for every complete pair visible on the CT-scan. For example:  $100\% \times ([Disc\ T8-9] / [Disc\ T8-9] + [Body\ T8])$ . Since this is a cross-sectional study, the growth-rate of vertebral bodies and intervertebral discs was defined as the mean height increase in millimeters compared to patients aged 1 year earlier.

### Statistical analysis

Vertebral body height, intervertebral disc height, were tested for normality of distribution with Q-Q plots, and thereafter stratified by sex and age. The difference and rate of change of height throughout growth was compared with a linear regression analysis, with age and male sex as (potential) independent variables. To visualize the change of height of vertebral bodies and intervertebral discs throughout growth, a locally estimated scatterplot smoothing (LOESS) curve was fitted to the scatter plot of each category. Following this analysis, the growth-rate was calculated as the height increase per year and visualized with bar graphs. The statistical significance level was set at 0.05. All analyses were performed with SPSS 25.0 for Windows (IBM, Armonk, NY).

## **Results**

### Study population

From 317 available CT-scan images in the database, a total of 19 were excluded for reasons: multiple CT-scans being of the same patient ( $n = 3$ ), low-quality or incomplete scans ( $n = 6$ ), and evidence of spinal pathology ( $n = 10$ ). Of the 298 included patients, 187 were male (61%) and the mean age was  $10.3 \pm 6.5$  and not significantly different between males and females ( $P = 0.963$ ). Of the included images, there were 69 full-body, 76 thoracic-abdominal, and 153 thoracic CT-scans.

### Spinal growth

The increase in height throughout the spine was predominantly present in the vertebral bodies, with the intervertebral discs increasing in height mostly in the first years of life (**Figure 3**). Specifically in the thoracic spine, the vertebral height increased throughout growth from  $6.3 \pm 0.7$  mm to  $20.3 \pm 1.4$  mm, whereas the intervertebral disc height increased only from

3.5 ± 0.4 mm to 4.9 ± 0.6 mm at age 4, whereafter it remained largely stable during the remaining growth (**Figure 3**). In the lumbar spine, vertebral body height increased from 9.0 ± 0.6 mm to 27.7 ± 1.9 mm during growth, and there was a constant increase in the lumbar intervertebral disc with the height doubling from 4.4 ± 0.4 mm to 9.0 ± 1.6 mm (**Figure 3**). Consequently, the overall contribution of the intervertebral disc to the total height of the spine decreased from 36.6% ± 2.5% to 20.2% ± 3.5%. Specifically in the lumbar spine from 32.5% ± 1.7% to 24.5% ± 3.9%, in the thoracic spine from 36.2% ± 2.8% to 18.0% ± 3.6% and in the cervical spine from 41.3% ± 3.5% to 23.2% ± 4.7%. Finally, throughout growth the overall height increase of thoracic vertebral bodies was 0.70 mm/year in males and 0.62 mm/year in females ( $P = 0.001$ ), with the steepest increase during early adolescence (**Figures 3 and 4**).

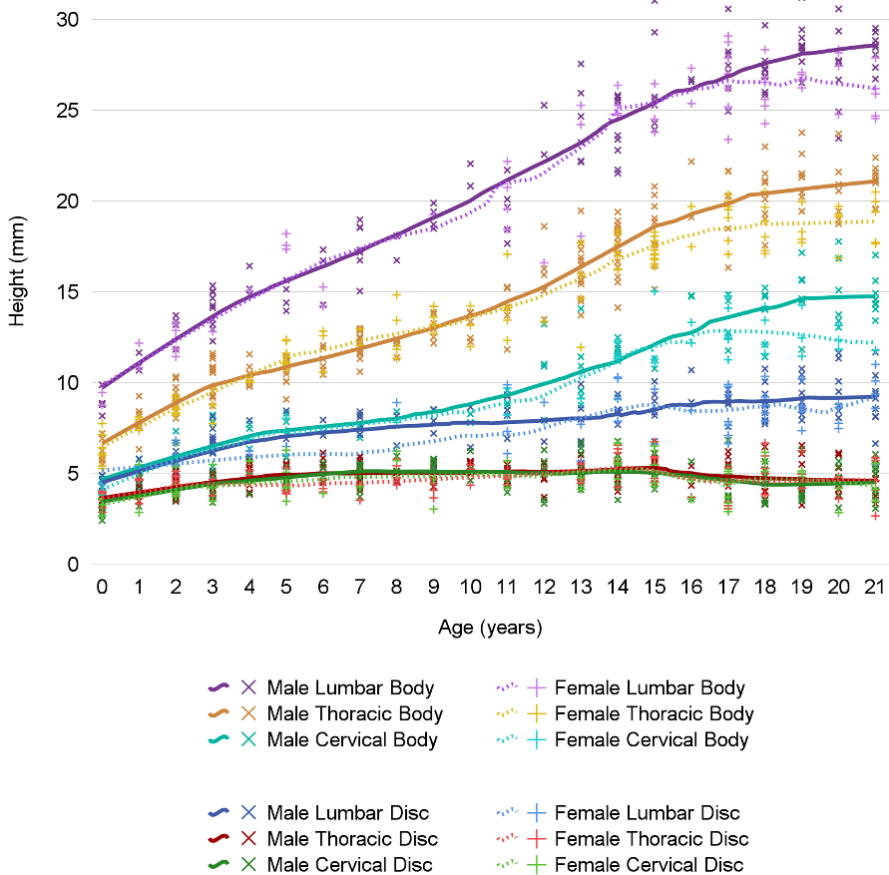


**Figure 3.** A scatter plot of the mean height in millimeters of intervertebral discs and vertebral bodies in the lumbar, thoracic and cervical spine per included patient is shown per year of age, stratified by sex. Furthermore a locally estimated scatterplot smoothing (LOESS) curve was fitted to each category.

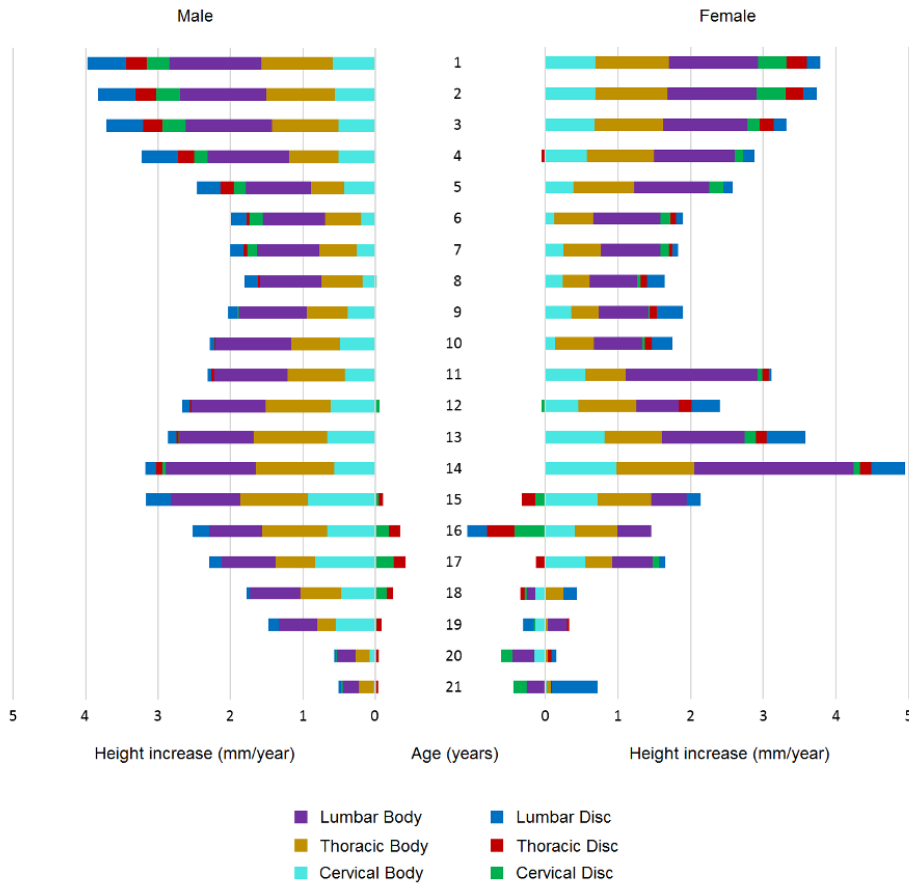


**Figure 4.** Bar graphs displaying the growth-rate of vertebral bodies and intervertebral discs per year in both males and females. In this study, the growth-rate was defined as the mean height increase in millimeters (mm) compared to patients aged 1 year earlier.

### Disc slenderness

The slenderness of intervertebral discs was stable in the lumbar spine throughout growth, but decreased in the thoracic and cervical spine with age. Overall, female discs were consistently more slender compared to males, but this phenomenon was especially visible around early adolescence at the time of the growth spurt. Peak height velocity is reached at age ~12 in girls and ~14 in boys, around peak height velocity female discs were more slender than male discs.<sup>20-24</sup>

## Discussion

The objective of this study was to describe the morphology of the intervertebral discs and vertebral bodies, their relative contribution to overall spinal length, and the slenderness of the discs, during growth in asymptomatic children and young adults. This cross-sectional analysis of nearly 300 children demonstrated a largely consistent increase of the vertebral body height throughout growth from 4 to 14 mm in the cervical, 6 to 20 mm in the thoracic, and 9 to 28 mm in the lumbar spine. In the thoracic spine this increase in height was significantly larger in males than females. For the intervertebral discs, we only observed a constant height increase throughout growth in the lumbar discs from 4.4 to 9.0 mm, whereas the thoracic discs increased from 3.5 to 4.9 mm at age 4 and remained stable throughout the remainder of growth, similarly for the cervical discs. Consequently, the overall discs contribution to spinal height decreased from 37% to 20%. The transverse surface area of intervertebral discs increased greatly and consistently throughout growth. Disc slenderness in the thoracic spine decreased throughout growth, but overall, discs remained more slender in females. At the age of presumed growth spurt, discs of females were overall more slender than in males.

These results confirm the observations of earlier studies that height increase of the spine during growth in healthy children and adolescents is located predominantly in the vertebral bodies.<sup>2,3</sup> Also, the observation in this study that lumbar intervertebral discs increase in height throughout growth, but thoracic and cervical discs only do so in the first years of life and thereafter remain relatively stable, confirms the earlier radiographic observations.<sup>2,3</sup> CT imaging and measurements allowed for analysis of the three-dimensional morphology of the intervertebral disc in this study during growth, presenting the novel findings that most of the increase in disc volume was present as an increase in transverse surface area, not of height. And that there was a larger, broader, and overall less slender disc in males compared to females throughout the complete growth, but especially at early adolescence.

The most obvious limitation of this study is that the optimal design for our research question would be a longitudinal study with multiple CT-scans of the same patient at different time points during growth. However, concerning the ionizing radiation burden, compounded by multiple CT-scans, this would be unethical to perform in an experimental setting. Therefore, the best option for the present study was a cross-sectional analysis of a database of already made CT-scans for indications not related to the spine. The intervertebral disc in this study was defined as the space between two adjacent endplates of the vertebrae above and below the disc (**Figure 2**). Therefore the exact shape of the disc could not be segmented, but only approximated as the space between two adjacent bony endplates, which can be visualized very well on CT-scan images (**Figure 1**). Potentially an MRI-based study could overcome

this limitation, however would introduce new limitations regarding the analysis of the bony vertebral body endplates, therefore a CT-based analysis for our research question was preferred. Also, the height of discs and bodies was defined as the centroid distance, as described in the methods section, this showed to be most stable and less susceptible to individual sagittal spinal positioning (kyphosis and lordosis) compared to other options. This is also important for the following limitation, that the CT-scan images were made supine, which it is known to influence the sagittal profile of the spine and therefore the overall shape of the intervertebral disc.<sup>25</sup> This could have influenced our observations compared to upright orientation and the effect of gravity on our study population. However, all CT-scans were made following the same supine protocol, and again the centroids distance is less susceptible to shift when orientation of the endplate changes (**Figure 2**). Last, the cross-sectional design of this study together with the limited number of females in certain age groups, could have induced minor inaccuracies to our goal to observe changes in intervertebral discs and vertebral body morphology during growth, by accounting for interpersonal differences between the included subjects. This can be observed in the female groups aged 15 to 21 years (**Figure 4**); however, this is mostly overcome by the large sample size of this study in the rest of the groups.

This study's absolute measurements of spinal elements during growth, including the observations that spinal growth is present mostly in vertebral bodies and is more pronounced in males, and that there is a decrease of disc slenderness throughout growth, with overall more slender discs in females, is essential knowledge in understanding the importance of intervertebral disc morphology in the etiology and treatment of pediatric spinal deformity. For example, to interpret the earlier observations that the scoliotic deformity in adolescent idiopathic scoliosis is present mostly in the disc and is associated with more slender spines.<sup>9-15</sup> The present observation of more slender discs in females, especially visible during early adolescence, could play a role in the overrepresentation of females in adolescent idiopathic scoliosis.<sup>26</sup> This is supported by earlier observations of a more slender spine in adolescent idiopathic scoliosis patients compared to asymptomatic controls.<sup>14,15</sup> A potential mechanical explanation could be that lateral displacement and torsion of the spine in scoliosis, occurs more easily in more slender structures.

Recently, there have also been several studies suggesting an important role of the intervertebral disc in the treatment of early onset scoliosis with traditional growing rod distractions.<sup>27,28</sup> These radiological studies have shown (in 2D and 3D) that epiphyseal growth with distraction-based growing rods, coincides with height- and volume loss of the intervertebral disc. The present study shows that in pre-adolescent normal growth, intervertebral disc volume increases while intervertebral disc height remains stable



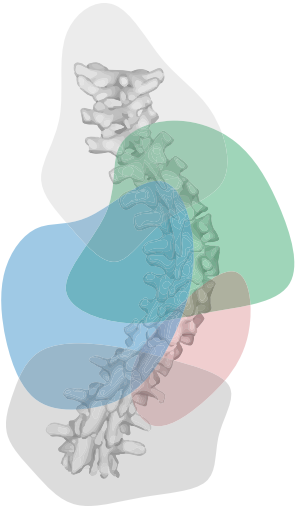
(thoracic) or increases somewhat (lumbar). The observation that both thoracic- and lumbar intervertebral discs under distraction decrease in height as well as volume is thus likely a direct result of distractive “growth-friendly” treatment. This phenomenon may be the cause for the “law of diminishing returns,” which is frequently observed when performing repeated lengthenings with traditional- or magnetically controlled growing rods.<sup>29,30</sup> Whether this disc height loss is a result of the distractive forces that are applied or of immobilization of the spanned segments is unknown and warrants further investigation. Prospective and/or causative research should build on the present observations and use it to their advantage to unravel the etiology and optimize treatments of pediatric spinal deformity.

In conclusion, height increase of the spine during growth is located predominantly in the vertebral bodies. Intervertebral discs appear to have a very different development, they increase slightly in height during the first years of life, whereafter only lumbar discs keep increasing, whereas cervical and thoracic discs remain at a stable height. The transverse surface area of discs increases greatly throughout growth, even more so in males. Therefore, the slenderness of intervertebral discs decreases overall, but thoracic discs of females are more slender, especially at early adolescence. This essential knowledge of relative height and slenderness during normal growth can assist in understanding the importance of intervertebral disc morphology in present as well as future studies, on the etiology and treatment of pediatric spinal deformity.

## References

1. Taylor JR. Growth of human intervertebral disc. *J Anat* 1970; 107:183–184.
2. Taylor JR. Growth of human intervertebral discs and vertebral bodies. *J Anat* 1975; 120:49–68.
3. Brander ME. Normal values of the vertebral body and intervertebral disk index during growth. *Am J Roentgenol Radium Ther Nucl Med* 1970; 110:618–627.
4. Bugyi B. [On the regularity of growth of the vertebrae of the thoraco-lumbar region in the x-ray picture]. *Anat Anz* 1959; 107:441–451.
5. Knutsson F. Growth and differentiation of the postnatal vertebra. *Acta Radiol* 1961; 55:401–408.
6. Schultz AB, Sørensen SE, Andersson GB, et al. Measurement of spine morphology in children, ages 10–16. *Spine (Phila Pa 1976)* 1984; 9:70–73.
7. Peters JR, Chandrasekaran C, Robinson LF, et al. Age- and gender-related changes in pediatric thoracic vertebral morphology. *Spine J* 2015; 15:1000–1020.
8. Costa L, de Reuver S, Kan L, et al. Ossification and fusion of the vertebral ring apophysis as an important part of spinal maturation. *J Clin Med* 2021; 10:3217
9. Brink RC, Schlösser TPC, van Stralen M, et al. Anterior-posterior length discrepancy of the spinal column in adolescent idiopathic scoliosis—a 3D CT study. *Spine J* 2018; 18:2259–2265.
10. Brink RC, Schlösser TPC, Colo D, et al. Anterior spinal overgrowth is the result of the scoliotic mechanism and is located in the disc. *Spine (Phila Pa 1976)* 2017; 42:818–822.
11. de Reuver S, Brink RC, Homans JF, et al. Anterior lengthening in scoliosis occurs only in the disc and is similar in different types of scoliosis. *Spine J* 2020; 20:1653–1658.
12. de Reuver S, Ijsseldijk LL, Homans JF, et al. What a stranded whale with scoliosis can teach us about human idiopathic scoliosis. *Sci Rep* 2021; 11:7218.
13. Stokes IAF, Windisch L. Vertebral height growth predominates over intervertebral disc height growth in adolescents with scoliosis. *Spine (Phila Pa 1976)* 2006; 31:1600–1604.
14. Vergari C, Karam M, Pietton R, et al. Spine slenderness and wedging in adolescent idiopathic scoliosis and in asymptomatic population: an observational retrospective study. *Eur Spine J* 2020; 29:726–736.
15. Chen H, Schlösser TPC, Brink RC, et al. The height-width-depth ratios of the intervertebral discs and vertebral bodies in adolescent idiopathic scoliosis vs controls in a Chinese population. *Sci Rep* 2017; 7:46448.
16. Mehlman CT, Araghi A, Roy DR. Hyphenated history: the Hueter-Volkman law. *Am J Orthop (Belle Mead NJ)* 1997; 26:798–800.
17. Wijdicks SPJ, Tromp IN, Yazici M, et al. A comparison of growth among growth-friendly systems for scoliosis: a systematic review. *Spine J* 2019; 19:789–799.
18. Wijdicks SPJ, Lemans JVC, Verkerke GJ, et al. The potential of spring distraction to dynamically correct complex spinal deformities in the growing child. *Eur Spine J* 2021;30:714–23
19. Lemans JVC, Wijdicks SPJ, Castelein RM, et al. Spring Distraction System for Dynamic Growth Guidance of Early Onset Scoliosis: 2 Year Prospective Follow-up of 24 Patients. *Spine J* 2021;21:671–81
20. Grave KC. Timing of facial growth: a study of relations with stature and ossification in the hand around puberty. *Aust Orthod J* 1973; 3:117–122.
21. Largo RH, Gasser T, Prader A, et al. Analysis of the adolescent growth spurt using smoothing spline functions. *Ann Hum Biol* 1978; 5:421–434.
22. Rauch F, Bailey DA, Baxter-Jones A, et al. The “muscle-bone unit” during the pubertal growth spurt. *Bone* 2004; 34:771–775.
23. Whiting SJ, Vatanparast H, Baxter-Jones A, et al. Factors that affect bone mineral accrual in the adolescent growth spurt. *J Nutr* 2004; 134:696S–700S.
24. Aksglaede L, Olsen LW, Sørensen TIA, et al. Forty years trends in timing of pubertal growth spurt in 157,000 Danish school children. *PLoS One* 2008; 3:e2728.
25. Bouaicha S, Lamanna C, Jentzsch T, et al. Comparison of the sagittal spine lordosis by supine computed tomography and upright conventional radiographs in patients with spinal trauma. *Biomed Res Int* 2014; 2014:967178.
26. Cheng JC, Castelein RM, Chu WC, et al. Adolescent idiopathic scoliosis. *Nat Rev Dis Prim* 2015; 1:15–30.
27. Lippross S, Girmond P, Lüders KA, et al. Smaller intervertebral disc volume and more disc degeneration after spinal distraction in scoliotic children. *J Clin Med* 2021; 10:2124.
28. Rong T, Shen J, Kwan K, et al. Vertebral growth around distal instrumented vertebra in patients with early-onset scoliosis who underwent traditional dual growing rod treatment. *Spine (Phila Pa 1976)* 2019; 44:855–865.
29. Sankar WN, Skaggs DL, Yazici M, et al. Lengthening of dual growing rods and the law of diminishing returns. *Spine (Phila Pa 1976)* 2011; 36:806–809.
30. Ahmad A, Subramanian T, Panteliadis P, et al. Quantifying the “law of diminishing returns” in magnetically controlled growing rods. *Bone Joint J* 2017; 99-B:1658–1664.



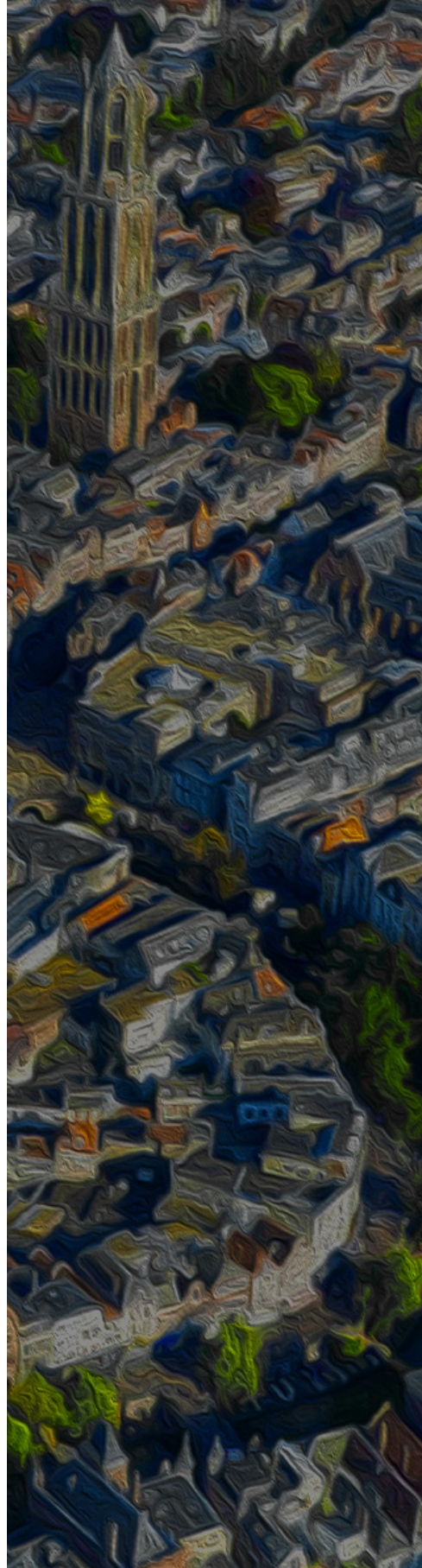


# 3

## Morphological Changes of the Intervertebral Disc during Growth

Aaron J.B.W.D. Moens  
Joëll Magré  
Moyo C. Kruyt  
René M. Castelein  
Steven de Reuver

*Spine (Phila Pa 1976). 2023 Jul. ePub ahead of print.*



## ABSTRACT

**Introduction.** Previous computed tomography (CT) studies approximated changes in the intervertebral disc (IVD) morphology during growth based on the bony vertebral endplates. More detailed insights, e.g. the relative proportions of the annulus fibrosus (AF) and nucleus pulposus (NP) during growth, remain unknown. The disc is the most important stabilizer of the spine and recent studies suggest the IVD plays a role in the etiology of pediatric spinal deformities, therefore understanding the general morphological development of the AF and NP during growth is important.

**Methods.** An existing database of children aged 0-18 years that had undergone magnetic resonance imaging (MRI) for indications unrelated to the spine were analyzed. The AF and NP were segmented semi-automatically from levels T1-L5. The parameters: mean IVD height, cross-sectional area, slenderness (height/width ratio), volume (ratio) and relative position of the centroid of the NP within the IVD in three directions (x,y,z) were extracted, and compared between age, sex and spinal level.

**Results.** IVD height increased barely during growth besides a moderate increase in the low-thoracic and lumbar spine during the first 5-10 years of life. The cross-sectional area of the IVD and thus the volume increased greatly and steadily during growth. IVD slenderness decreased slightly the first 3 years of life and remained relatively stable throughout the remainder of growth. Overall, IVDs were smaller and more slender in females, especially in the mid-thoracic spine and at early adolescence. In the upper- and mid-thoracic spine the NP comprises 10-12% of total IVD volume during growth and increases low-thoracic and lumbar to 20-25%. During growth the nucleus orientation is stable and centered in the right-left and cranial-caudal direction. In the anterior-posterior direction, the nucleus increasingly shifts with age, in line with the sagittal profile of the spine.

**Conclusion.** This MRI-based morphometric map describing the development of thoracic and lumbar IVDs during growth can be used as a reference for future studies on the role of the IVD in the etiology of different disc related disorders.

## Introduction

The intervertebral disc (IVD) is an important structure of the spine as it provides flexibility and stability.<sup>1</sup> The first published paper in English on the anatomy of the IVD was by John Cleland of Glasgow in 1890, where he stated the IVD represents a modified diarthrodial or synovial joint.<sup>2</sup> Until a published review of literature by Schmorl in 1928, the IVD was regarded as a structure of no great significance within the vertebral column.<sup>2</sup> Each IVD forms a fibrocartilaginous fusion or symphysis between adjacent vertebrae and can therefore be considered the most important spinal ligament. The IVD is made up of two functionally distinct regions: the outer fibrocartilaginous annulus fibrosus (AF) and the inner gel-like nucleus pulposus (NP).<sup>3</sup> The AF allows limited motion between adjacent vertebrae and can be regarded as an important (ligament) stabilizer of spine.<sup>1,4,5</sup> The NP allows for absorption of compression forces between vertebrae and provides flexibility to the spine.<sup>1,4-7</sup>

However, still not much is known on the morphological changes of the IVD during growth, especially for the changes that occur in the AF and the NP individually. More is known of the degenerating than of the maturing disc,<sup>8,9</sup> whereas many spine diseases such as scoliosis, Scheuermann's disease and spondylolisthesis may develop during the years that the spine, including the IVD, matures. During maturation, several changes occur within the composition of the IVD cellular matrix, as well as a decrease in vascularization towards the end of trunk growth in late puberty.<sup>10</sup> Part of the maturation process is a gradual ossification and ultimate fusion of the attachment of the disc, the ring apophysis, to the vertebral body, thus changing its mechanical properties. During adolescence, spinal loading significantly increases over a short period of time due to rapidly increasing body mass and moment arm. For harmonious development, bone and disc maturation must be in synchrony with that rapidly increasing spinal loading. In other words, mature loads can only be dealt with by mature supporting tissues.

Changes in morphology of the vertebral bodies and IVDs during growth were first assessed through post-mortem and radiographic studies.<sup>11,12</sup> Recent computed tomography (CT) studies described the three-dimensional (3D) morphometry of vertebral bodies during growth.<sup>13,14</sup> In these studies, IVD morphometries were approximated based on the vertebral endplates orientation, since the IVD itself is not visible on CT. This means that the individual contribution of the AF and NP could not be determined. As opposed to CT based approximations of the vertebral endplates, with magnetic resonance imaging (MRI) it is possible to distinguish the AF from the NP. Therefore, the main aim of this study is to accurately describe morphometric changes within the IVD and the relative volumetric contribution during growth in an asymptomatic population, based on MRI. This analysis involves



the assessment of several IVD morphological parameters: firstly height, cross-sectional area and slenderness. Secondly, MRI-specific parameters: AF and NP volume and the ratio between NP and IVD volume as a proxy for disc hydration status.

## Methods

### Study population

In this cross-sectional study, an existing database of T2-weighted MRI-scans of pediatric patients (aged 0-18 years) was analyzed. Scan indications were unknown due to data anonymization as required by the research ethics board. The MRI's dated from October 2011 to January 2019 and were made with a 1.5T Philips Achieva MRI-scanner in a single tertiary children's hospital. The scans were high resolution with a sagittal slice thickness of 3-4mm. Exclusion criteria were: scans of patients with (suspected) spinal pathology, incomplete scans (T1-L5 not fully imaged), sequences used with inability to distinguish the AF from the NP properly, malposition of the patient (i.e. hyperextended or rotated) and if a sagittal series was not available.

### Segmentation protocol

One of two trained observers segmented the AF and NP of the spinal levels T1-L5 (**Figure 1**) using Mimics software (v24.0, Materialise, Leuven, Belgium).<sup>15</sup> The NP was identified as a relatively hyperintense (water-rich) signal on T2-weighted images. First, the NP was segmented semi-automatically using thresholding to create a mask, highlighting the NP of each IVD. Since the grey values differed individually, the mask thresholds were determined by the observer specifically for each MRI-scan to maximize NP coverage. A second mask was created by setting a new threshold to invert the previous mask of the NP, highlighting both the AF and surrounding tissues. The AF was then segmented through visually identifying the AF and highlighting its area manually. This was performed for each AF of level T1-L5 in every sagittal slice containing part of the IVD. Finally, the segmentations were exported to 3-Matic (v15.0, Materialise, Leuven, Belgium) and refined using the 'wrap' tool, which results in smoothing out the model and filling in any minor gaps in the segmentation.

### Data extraction

In 3-Matic, the volumes ( $\text{mm}^3$ ) of the AF and NP were extracted from the segmentations.<sup>16</sup> The total volume of the IVD ( $V_{\text{IVD}}$ ) was calculated by adding up the volumes of the NP ( $V_{\text{NP}}$ ) and AF ( $V_{\text{AF}}$ ). The ratio between  $V_{\text{NP}}$  and  $V_{\text{IVD}}$  (volume ratio or hydration status) was calculated. To correct for patient orientation in the MRI scanner a new sagittal plane was

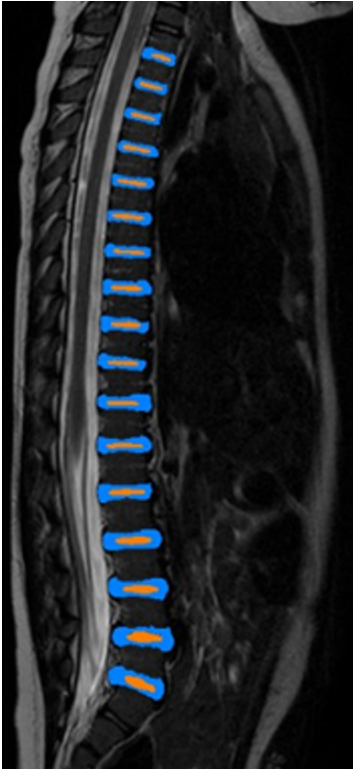


**Figure 1.** Segmentation of the nucleus pulposus (NP) in orange and annulus fibrosus (AF) in blue at levels T1-L5 on a sagittal MRI image.

defined by creating a plane through the centers of gravity of the AF of T1, L1 and the most posterior AF of the patient. A separate coordinate system was defined for each AF individually by their 3 inertia axes; x-axis (left-right), y-axis (anterior-posterior), z-axis (cranial-caudal). These individual coordinate systems were corrected for sagittal orientation by rotating around their z-axis until the y-axis is in line with the sagittal plane (**Figure 2**).

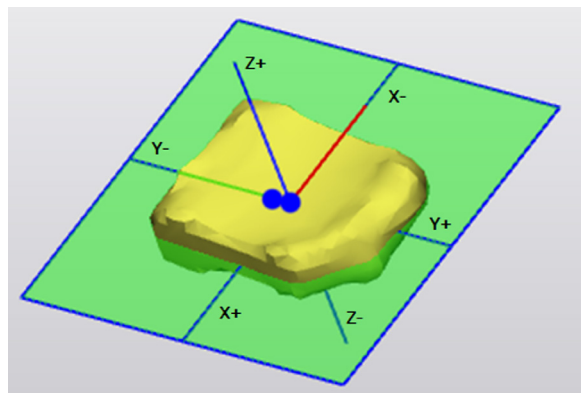


**Figure 2.** Nucleus orientation analysis. A new coordinate system ( $x,y,z$ ) was plotted in the center of both the IVD and NP. The relative center of the NP compared with the center of the total IVD was plotted and the distance between them calculated in three directions

IVD height in the center of gravity (mm) and cross-sectional area ( $\text{mm}^2$ ) in the xy-plane were extracted from 3-Matic for each AF. The distance between the center of gravity of the NP and IVD as a whole in the three principal planes was calculated for each IVD. Measurements were combined in three age groups (0-4/juvenile, 4-10/infantile, and 10-18/adolescent), as defined by the Scoliosis Research Society (SRS). Measurements were stratified into average values at four spinal levels: upper-thoracic (T1-T4), mid-thoracic (T5-T8), lower-thoracic (T9-T12) and lumbar (L1-L5), also according to SRS measurement manual.<sup>17</sup> Furthermore, a custom variable as a proxy for slenderness of an IVD, was calculated as the height divided by the square root of the cross-sectional area. In literature, many variants of a height-to-width ratio as a proxy for slenderness have been calculated in morphometric studies of the spine, however in this study the most simplest is used that corrects for the quadratic quantity surface area by taking the square root.<sup>18,19</sup>

### Statistical analysis

Simple scatterplots were made for  $V_{AF}$ ,  $V_{NP}$ , volume ratio ( $V_{NP}:V_{IVD}$ ), mean IVD height, cross-sectional area and slenderness versus age for males and females. To visualize the change in IVD morphological parameters during growth, a locally estimated scatterplot smoothing (LOESS) curve was fitted to each plot. Simple logistic regression was performed to test changes in IVD morphology with age. Changes in IVD morphology with increasing age were assessed with simple logistic regression, while differences between males and females were assessed with a multivariate regression analysis. An unpowered post-hoc t-test was performed between disc slenderness of the mid-thoracic spine in boys and girls aged 9-13, given the predominantly descriptive nature of this study. Intra-operator and inter-operator variability were assessed in 3 MRIs (102 individual segmentations) for the segmentation of the AF and NP separately and for the IVD as a whole. Values greater than 0.75 indicate good reliability and values over 0.90 excellent reliability.<sup>20</sup> Statistical significance was set at 0.05. All statistical analysis were performed with SPSS 27.0 for Windows (IBM, Armonk, NY, USA).

## **Results**

### Study population

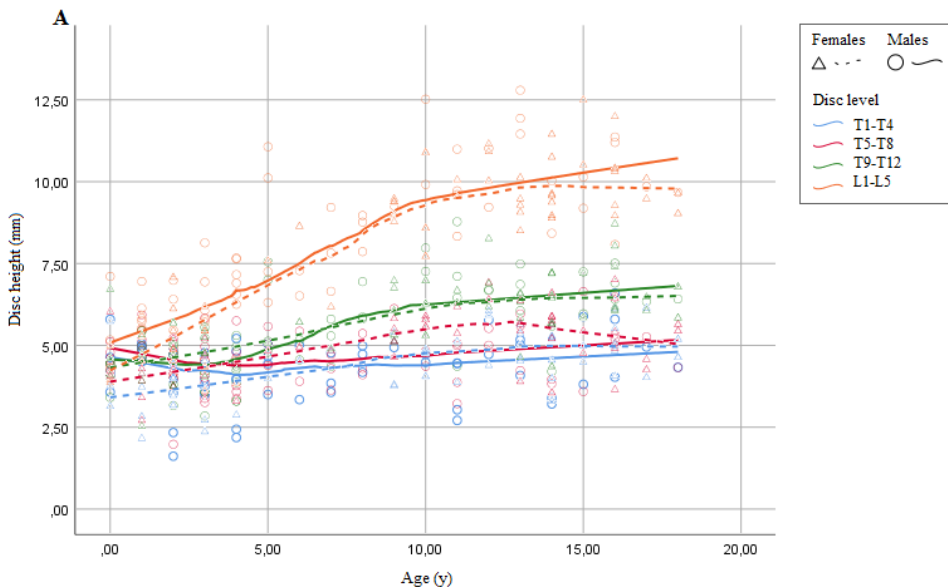
From 180 T2-weighted MRI scans in the database, a total of 126 patients aged 0 to 18 years were included (mean age  $7.7 \pm 5.7$ ) of which 67 (53%) were male (**Table 1**). A total of 4284 segmentations were included and analyzed (i.e. both the AF and NF of 2142 IVDs).

| Exclusion criterium       | Excluded scans (n=54) |
|---------------------------|-----------------------|
| Spine not fully imaged    | 13                    |
| No sagittal MRI available | 6                     |
| Poor scan quality         | 11                    |
| Spinal pathology          | 16                    |
| Malposition               | 1                     |
| Brain MRI                 | 3                     |
| Improper slice thickness  | 4                     |

**Table 1.** Excluded scans

### Intervertebral disc height and cross-sectional area

IVD height increased barely during growth besides a moderate increase in the low-thoracic and lumbar spine during the first 5-10 years of life, with males having a marginally higher mean IVD height than females. The IVD height in the upper- and mid-thoracic spine remained relatively stable at 5 mm. In the low-thoracic spine, height increased from 4 to 7 mm and in the lumbar spine from 5 to 10 mm. The IVD cross-sectional area showed a consistent increase throughout growth at all spinal levels and was overall significantly greater in males than females per age. The increase in cross-sectional area from birth to early adulthood was greater in males versus females (460% versus 325% for all spinal levels combined). Cross-sectional area growth increased least from birth to early adulthood in the upper-thoracic spine (males 420% versus females 250%) and most in the lumbar spine (males 520% versus females 390%). Absolute values per age and spinal level are presented in **Figure 3A** and **3B**.



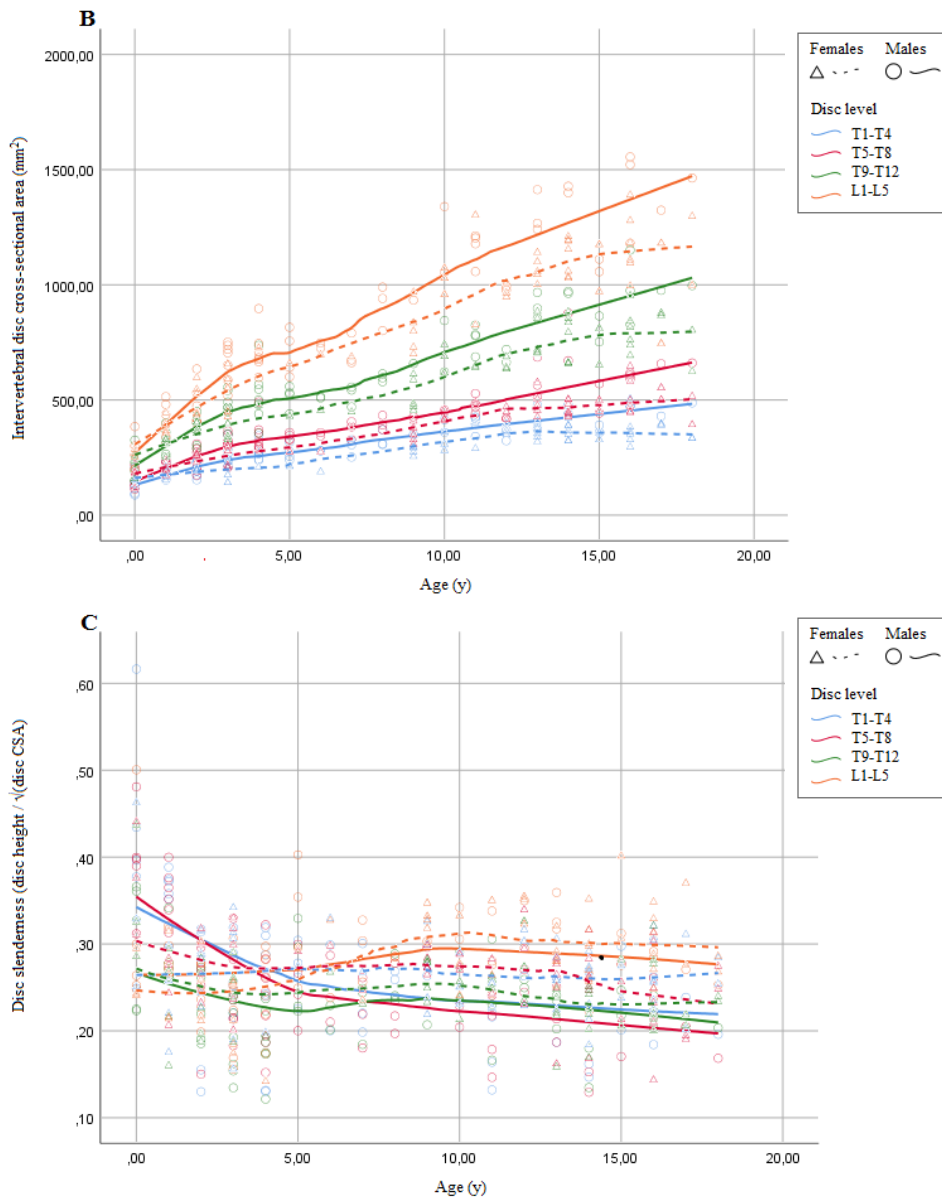


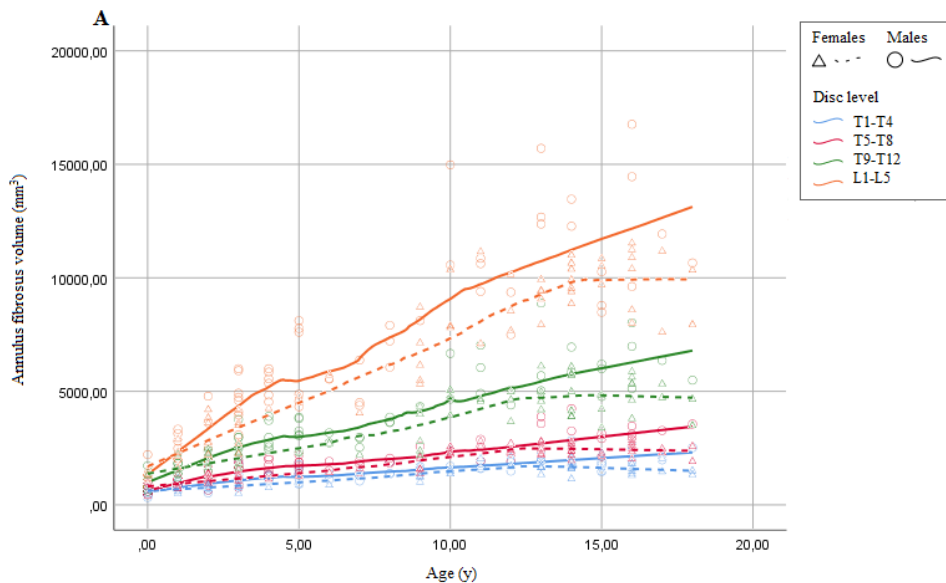
**Figure 3.** Scatterplot of (A) mean IVD height (mm), (B) mean IVD cross-sectional area (mm<sup>2</sup>) and (C) IVD slenderness of four intervertebral IVD level groups by age in males and females. Each dot represents the mean value at a IVD level in a single person. A LOESS regression line is fitted for each IVD level. CSA = cross-sectional area.

### Disc slenderness

Slenderness (height divided by the square root of the cross-sectional area) of the IVD tended to decrease during the first 3 years of life and remained relatively stable for the remainder of growth (**Figure 3C**). Overall, females had more slender IVDs compared to males ( $p = 0.025$ ). A large discrepancy was observed in mid-thoracic IVDs of females at early adolescence. Post-hoc analysis of children aged 9-13 showed that IVDs in the mid-thoracic spine were significantly more slender in females compared to males (0.23 vs 0.27,  $p < 0.001$ ).

### Intervertebral disc volume

The IVD volume increased consistently throughout growth.  $V_{AF}$  and  $V_{NP}$  both increase consistently from birth in both males and females. Males showed a significantly higher  $V_{AF}$  and  $V_{NP}$  than girls, at all IVD levels, regardless of age. Both  $V_{AF}$  and  $V_{NP}$  increased at a greater rate from cranial to caudal, more in males than in females. From birth to early adulthood,  $V_{AF}$  increased in the upper-thoracic area with 380% in males and with 260% in females, whereas in the lumbar spine this was 980% and 700% respectively. While the NP is smaller than the AF, relatively the  $V_{NP}$  increased more during growth than  $V_{AF}$ . From birth to early adulthood,  $V_{NP}$  increased in the upper-thoracic region with 360% in males and with 300% in females, whereas in the lumbar spine this was 1320% in males and 1180% in females respectively. Absolute values per age and spinal level are presented in **Figure 4A** and **4B**.



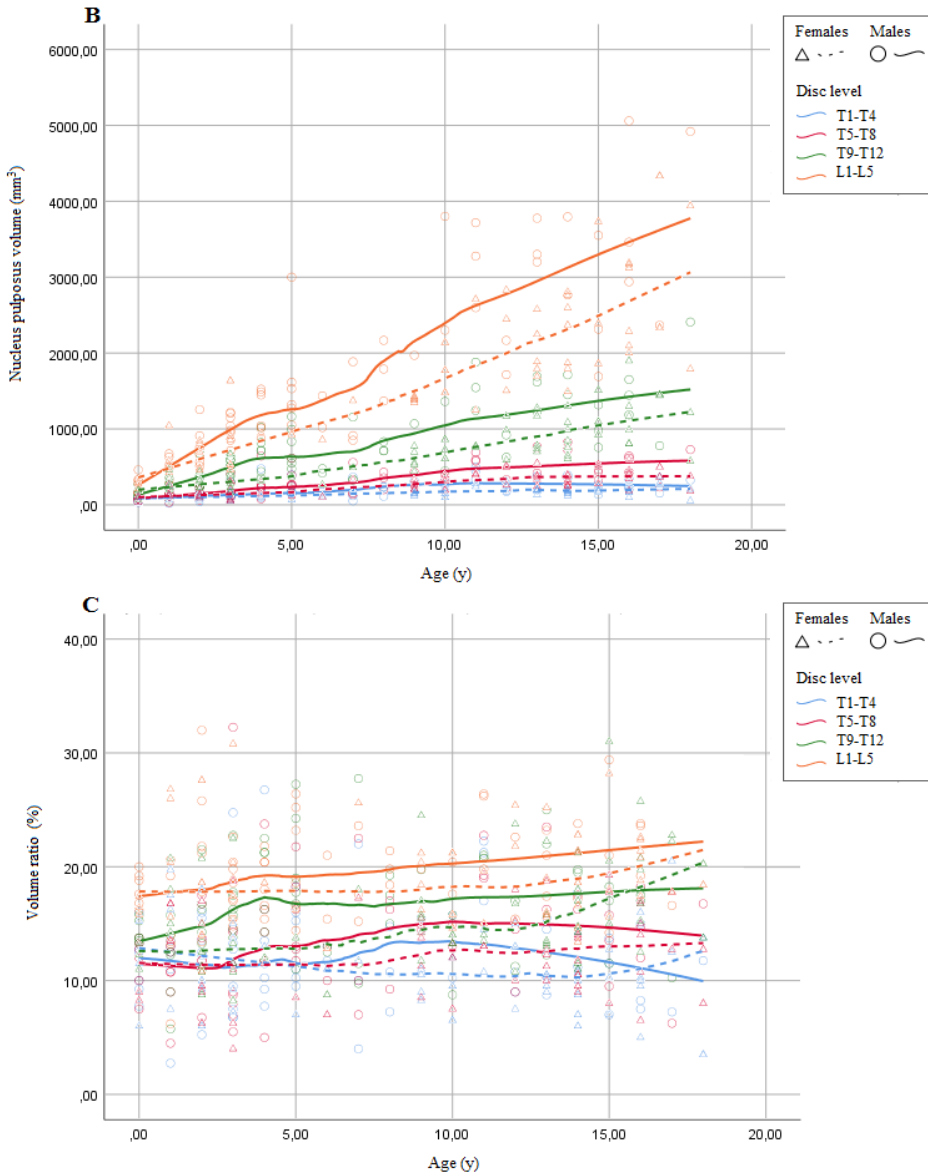


**Figure 4.** Scatterplot of (A) mean annulus fibrosus volume (mm<sup>3</sup>), (B) mean nucleus pulposus volume and (C) ratio of nucleus to IVD volume (%) of four intervertebral IVD level groups by age in males and females. Each dot represents the mean value at a IVD level in a single person. A Loess regression line is fitted for each IVD level.



The volume ratio in the upper- and mid-thoracic spine remained relatively stable throughout growth in both males and females, with the  $V_{NP}$  comprising around 10-12% of the  $V_{IVD}$ . The volume ratio increased slightly with age, indicating a relatively more hydrated IVD, mostly in the low-thoracic and lumbar spine in both males and females (**Figure 4C**). For males, this increase was low-thoracic from 14 to 19% and lumbar from 18 to 23%. For females, similar values were observed, as the volume ratio increased low-thoracic from 12 to 20% and lumbar from 17 to 25%.

### Nucleus orientation

Relative position of the nucleus within the IVD was assessed in three directions: x (left/right), y (anterior/posterior), and z (caudal/cranial). There was very little nucleus deviation in left/right orientation at all ages and spinal levels, and there was no nucleus deviation at all in the caudal/cranial direction. However, deviation of the nucleus was most apparent in the anterior/posterior direction, demonstrating differences among males and females and between age groups. In juveniles this male-female difference was less pronounced and the nucleus fairly centered, but in infants and more so in adolescents, the nucleus was positioned towards the convexity of the sagittal curve, anteriorly in the lumbar spine, posteriorly at the mid thoracic levels, and back to neutral in the upper thoracic spine. The absolute values for the changes in NP centroid can be seen in **Figure 5**.

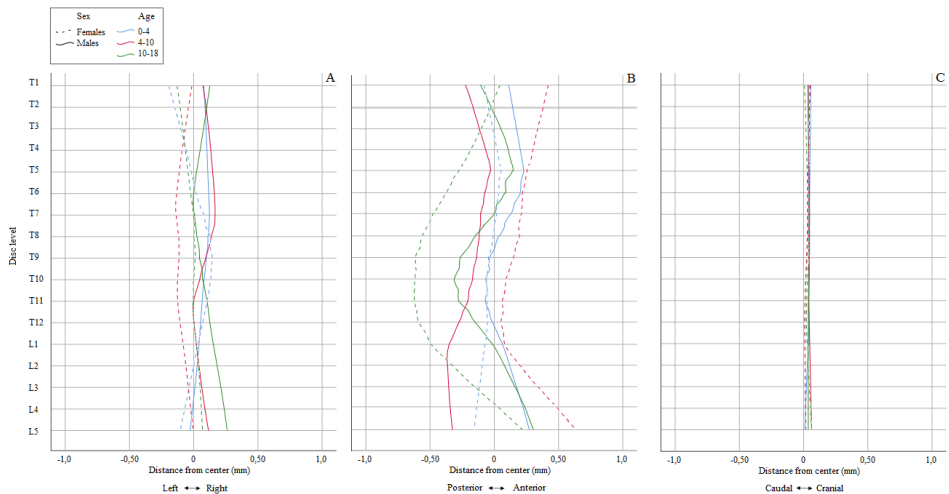


**Figure 5.** Relative change in center of mass of the nucleus pulposus within the intervertebral IVD throughout the spine, in three age groups, for males and females. Fitted with Loess regression lines, X: change in the left-right orientation (negative = towards the left, positive = towards the right). Y: change in the anteroposterior orientation (negative = more posterior, positive = more anterior). Z: change in the craniocaudal orientation (negative = more caudal, positive = more cranial)

### Inter- and intra-observer variability

In terms of intra-operator and inter-operator variability for segmentation of the AF, NF and IVD, ICC's were  $> 0.94$  (**Table 2**).

|                    | IVD              | AF               | NP               |
|--------------------|------------------|------------------|------------------|
| Inter-observer ICC | 0.98 (0.98-0.99) | 0.98 (0.93-0.99) | 0.96 (0.91-0.98) |
| Intra-observer ICC | 0.96 (0.94-0.97) | 0.94 (0.89-0.97) | 0.98 (0.95-0.99) |

**Table 2.** Inter-observer and intra-observer variability: Values are expressed as ICC (95% CI). ICC = intra-class correlation coefficient, IVD = intervertebral disc, AF = annulus fibrosus, NP = nucleus pulposus

### Discussion

Semi-automatic 3D-segmentation of MRI scans was used to cross-sectionally describe morphological changes of and within the IVD during growth in children from 0-18 without manifest spinal disorders. IVD height only increased slightly and just in the first 5-10 years of life. However, the cross-sectional area of the IVD and thus the volume increased greatly and consistently during growth. These results correspond with data from previously published CT-approximated analyses.<sup>13,14</sup> Overall, IVDs were larger in males compared to females. The nucleus comprises 10-12% of the IVD volume in the upper- and mid-thoracic spine and remains relatively stable throughout growth. In both males and females this ratio increased to around 20% in the low-thoracic and 25% in the lumbar spine in early adulthood. IVD slenderness, as a proxy for mechanical stability, decreases slightly in the first 3 years of life and remains stable afterwards. In a recent biplanar radiographic study by Vergari et al. and a CT-analysis by Chen et al., it was suggested that IVD slenderness may be a risk factor for scoliosis.<sup>19,21</sup> Of interest in the discussion on scoliosis etiology and pathogenesis, this study showed that female IVDs in the mid-thoracic spine at early adolescence were significantly higher and narrower, thus more slender than those of males. This may be interpreted as an area of decreased mechanical stability during this critical phase of development, assuming all other variables are evenly distributed. During growth the nucleus orientation is very stable and centered in the right-left and cranial-caudal direction, however in the anterior-posterior direction, the nucleus increasingly shifts with age, following or less likely, initiating the sagittal profile of the spine. This seems to indicate that the NP dynamically adapts to the shape of the disc and resultant pressure distribution.

These results confirmed and sharpened the CT based approximations: spinal height growth is mainly in the vertebral bodies, as in this study the IVD in the upper- and mid-thoracic spine increases from about 4 mm in height only to 5 mm from birth and plateaus at age 5-10, while lumbar IVDs show less of a plateau and increase from about 5 to 10 mm in height.<sup>14</sup> Novel data from this study demonstrate that growth patterns of the NP and AF appears to be similar in boys and girls, although  $V_{AF}$  seems to plateau at an earlier age in girls, probably due to the fact that girls enter their growth spurt at an earlier age compared to boys. There were no significant or distinct growth patterns of the absolute or relative  $V_{AF}$  or  $V_{NP}$  in boys and girls at their expected age of peak height velocity, which is around 13-14 for boys and 11-12 for girls.<sup>22</sup> This could possibly be due to the limited number of included participants at certain ages, or the fact that the skeletal maturity and age from maturity offset of included participants were unknown. Also, since spinal growth primarily occurs as a result of chondral ossification at the vertebral endplates, it may well be possible that the growth spurt is not reflected in AF and/or NP growth. Since dimensions of upper thoracic IVDs are generally much smaller compared to low-thoracic and lumbar IVDs, this made the transition between NP and AF in the scans less obvious. Differentiation in this area is more challenging and segmentation more susceptible to inaccuracies, which may also contribute to the non-significant findings at this spinal level.

In other studies, the ratio between  $V_{NP}$  and  $V_{IVD}$  or  $V_{NP}$  and  $V_{AF}$  is used as an indicator for IVD hydration.<sup>23</sup> Bolzinger et al. studied the hydration status of non-pathological lumbar IVDs in a pediatric population.<sup>10</sup> They reported a non-significant increase of IVD hydration by age and no statistically significant influence of sex, although hydration status was generally lower in girls. In this study, a significant increase in IVD hydration with age was seen, in the whole spine except for T1-T4. Bolzinger et al. hypothesized that lower IVD hydration in girls might be a contributing factor in the etiology of idiopathic scoliosis, which mostly affects girls in early puberty.<sup>8,24,25</sup> The influence of IVD volume and/or hydration status during growth on the development of idiopathic scoliosis is still unclear and requires further investigation. Violas et al. reported on pre- and postoperative lumbar IVD volume in 28 patients with scoliosis. They reported a trend towards the increase of IVD hydration in subjacent segments below arthrodesis.<sup>23</sup> Abelin-Genevois et al. demonstrated similar results, as NP volume increased on average by 30% in patients with adolescent idiopathic scoliosis after surgery, with total IVD volume remaining stable. Furthermore, disc hydration ratio improved further throughout a five-year follow-up.<sup>26</sup>

With the use of MRI, as opposed to previous CT-analyses, it was possible in this study to investigate not only IVD properties, e.g. height, cross-sectional area and slenderness, but also to distinguish the individual contribution of the AF and NP in the IVDs growth pattern. Furthermore, this study gave insight in the changes that occur in the IVD hydration status during growth, as well as the shift in NP centroid within the IVD. This semi-automatic 3D-segmentation of MRI scans provides a potent morphometric map of thoracic and lumbar IVDs during growth for future research, but has certain limitations. The indication for the MRI-scan was unknown due to randomization and blinding of patient data as required by the research ethics board. While major spinal pathology (such as trauma, inflammatory disease, scoliosis, or congenital anomalies) are easily detected, it cannot be guaranteed that certain spinal pathologies are included in this database (e.g. neurologic or metabolic), which might affect IVD in terms of volume, hydration status or otherwise. Next, thoracic IVD volumes were significantly smaller and thus grey values of the NP and AF are closer together, which sometimes creates difficulties in segmentation. The sagittal MRI images had a very high resolution, making the segmentation in the cranial-caudal and anterior-posterior direction very precise, however segmentation in the left-right direction was limited by the slice thickness of the MRI-scan, which was 3-4 mm in all cases. While the effects of this are random, it could mean that in this direction the segmentation was too small, resulting in an underestimation of IVD transverse cross-sectional surface area, and thus volume. Furthermore, it may also have a minor effect on the calculation of the change in nucleus position within the IVD in the left-right direction throughout growth. Finally, for some age groups, only a limited number of scans were available ( $n = 3$  for ages 6, 8, 17 and 18) This may distort the mean value reported if there is an older child with a relatively smaller IVD, or vice versa, and also impact significance of results.

We hypothesized that spinal alignment might influence the orientation of the NP within the IVD. The results showed no distinct left/right and caudal/cranial deviation of the NP at all ages and spinal levels. Interestingly, a trend was observed in the anterior/posterior direction, although in juveniles this was less pronounced and the nucleus fairly centered, but in infants and more so in adolescents, the nucleus was positioned anteriorly in the lumbar spine, posteriorly at the mid thoracic levels, and back to neutral in the and largely anteriorly in the upper thoracic and lumbar spine. While this effect was not statistically significant, most likely because the deviation is very slight and this descriptive study was not powered for this outcome, these results indicate the NP is subjected to the deformation of the IVD as part of the kyphosis and lordosis of the spine, and follows the development of the sagittal spinal profile during growth. Although it is known that the intra-uterine and infantile spine is in global kyphosis, lordosis develops with ambulation, and the adolescent spine gradually starts resembling the adult Roussouly types, this study contributes to the knowledge on sagittal spinal alignment at different ages.<sup>27</sup>

While this study's primary goal was objective morphometric description of the anatomy of the IVD during growth, interesting findings that may play a role in spinal deformity etiology were observed. IVDs were more slender in females, most outspoken in the mid-thoracic spine and at early adolescence. Interestingly, idiopathic scoliosis manifests itself mostly in females, and usually has its onset in early adolescence.<sup>24</sup> Furthermore, it has been demonstrated that the spine in patients with scoliosis is more slender compared to the healthy population.<sup>19,21</sup> Our observations may support the suggestions in these studies that spinal and specifically IVD slenderness is a potential risk factor for the development of scoliosis. The most frequent form of idiopathic scoliosis develops in girls in the mid-thoracic area during early adolescence, which is in line with these findings. The human spine is subject to rotation inducing forces throughout life,<sup>34,35</sup> these may only get a chance to lead to a deformity such as scoliosis when certain biomechanical circumstances are at its optimum. However, this suggestion based on cross-sectional descriptive data remains uncertain, and requires a prospective longitudinal confirmation or rejection.

In conclusion, IVD height increases minimally during growth in the low-thoracic and lumbar spine, whereas the transverse cross-sectional area and thus volume increases consistently at all spinal levels. IVD slenderness decreases slightly the first years. Female IVDs, especially mid-thoracic and at early adolescence, were significantly more slender than their male counterpart, or compared to other areas of the spine. This may have implications for scoliosis etiology or pathogenesis. In the upper- and mid-thoracic spine the NP comprises 10-12% of total IVD volume. This increases in the low-thoracic and lumbar area to 20-25% at the beginning of adulthood. Anterior-posteriorly, the NP center shifts slightly following the sagittal profile, becoming more pronounced with age. This MRI-based morphometric map can be used as a reference for future studies on the role of the IVD in the etiology of pediatric spinal deformities.

## References

1. Hudson, K. D., Alimi, M., Grunert, P., Härtl, R. & Bonassar, L. J. Recent advances in biological therapies for disc degeneration: Tissue engineering of the annulus fibrosus, nucleus pulposus and whole intervertebral discs. *Current Opinion in Biotechnology*.
2. Walmsley, R. & Bute, F. R. S. E. The Development and Growth of the Intervertebral Disc. *Edinb Med J* 60, 341 (1953).
3. Lawson, L. Y. & Harfe, B. D. Developmental mechanisms of intervertebral disc and vertebral column formation. *Wiley Interdiscip Rev Dev Biol* 6, e283 (2017).
4. Waxenbaum, J. A. & Fetterman, B. *Anatomy, Back, Intervertebral Discs*. StatPearls (2018).
5. Mok, G. S. P. et al. Comparison of three approaches for defining nucleus pulposus and annulus fibrosus on sagittal magnetic resonance images of the lumbar spine. *J Orthop Translat* (2016)
6. Drake, R., Vogl, A. & Mitchell, A. *Back*. in *Gray's Anatomy for students 64–79* (Churchill Livingstone Elsevier, 2014).
7. Haq, R., Aras, R., Besachio, D. A., Borgie, R. C. & Audette, M. A. 3D lumbar spine intervertebral disc segmentation and compression simulation from MRI using shape-aware models. *Int J Comput Assist Radiol Surg* (2015)
8. Oichi, T., Taniguchi, Y., Oshima, Y., Tanaka, S. & Saito, T. Pathomechanism of intervertebral disc degeneration. *JOR Spine* 3, (2020).
9. Rodrigues-Pinto, R., Richardson, S. M. & Hoyland, J. A. An understanding of intervertebral disc development, maturation and cell phenotype provides clues to direct cell-based tissue regeneration therapies for disc degeneration. *European Spine Journal* 23, 1803–1814 (2014).
10. Bolzinger, M. et al. MRI evaluation of the hydration status of non-pathological lumbar intervertebral discs in a pediatric population. *Orthopaedics and Traumatology: Surgery and Research* (2020)
11. Taylor, J. R. Growth of human intervertebral discs and vertebral bodies. *J Anat* 120, 49 (1975).
12. Brandner, M. E. Normal values of the vertebral body and intervertebral disk index during growth. *Am J Roentgenol Radium Ther Nucl Med* 110, 618–27 (1970).
13. Peters, J. R. et al. Age- and gender-related changes in pediatric thoracic vertebral morphology. *The Spine Journal* 15, 1000–1020 (2015).
14. de Reuver, S. et al. Disc and Vertebral Body Morphology From Birth to Adulthood. *Spine (Phila Pa 1976)* (2021).
15. Materialise. *Mimics Innovation Suite 23.0*. Preprint at (2020).
16. Materialise. *3-Matic 15.0*. Preprint at (2020).
17. O'Brien, M., Kulklo, T., Blanke, K. & Lenke, L. *Spinal Deformity Study Group Radiographic Measurement Manual*. Spinal Deformity Study Group Radiographic Measurement Manual (Medtronic Sofamor Danek USA, Inc., 2008).
18. Schultz, A. B., Sörensen, S. E. & Andersson, G. B. Measurement of spine morphology in children, ages 10–16. *Spine (Phila Pa 1976)* 9, 70–3.
19. Vergari, C. et al. Spine slenderness and wedging in adolescent idiopathic scoliosis and in asymptomatic population: an observational retrospective study. *Eur Spine J* 29, 726–736 (2020).
20. Koo, T. K. & Li, M. Y. A Guideline of Selecting and Reporting Intraclass Correlation Coefficients for Reliability Research. *J Chiropr Med* 15, 155–163 (2016).
21. Chen, H. et al. The Height-Width-Depth Ratios of the Intervertebral Discs and Vertebral Bodies in Adolescent Idiopathic Scoliosis vs Controls in a Chinese Population. *Sci Rep* 7, (2017).
22. Abbassi, V. Growth and normal puberty. *Pediatrics* 102, 507–512 (1998).
23. Violas, P., Estivalozes, E., Briot, J., Sales De Gauzy, J. & Swider, P. Quantification of intervertebral disc volume properties below spine fusion, using magnetic resonance imaging, in adolescent idiopathic scoliosis surgery. *Spine (Phila Pa 1976)* 32, (2007).
24. Cheng, J. C. et al. Adolescent idiopathic scoliosis. *Nat Rev Dis Primers* 1, 1–21 (2015).
25. Konieczny, M. R., Senyurt, H. & Krauspe, R. Epidemiology of adolescent idiopathic scoliosis. *J Child Orthop* 7, 3 (2013).
26. Abelin-Genevois, K. et al. Spino-pelvic alignment influences disc hydration properties after AIS surgery: a prospective MRI-based study. *Eur Spine J* 24, 1183–1190 (2015).
27. Roussouly, P., Gollogly, S., Berthonnaud, E. & Dimnet, J. Classification of the normal variation in the sagittal alignment of the human lumbar spine and pelvis in the standing position. *Spine (Phila Pa 1976)* 30, 346–353 (2005).
28. Castelein, R. M., van Dieën, J. H. & Smit, T. H. The role of dorsal shear forces in the pathogenesis of adolescent idiopathic scoliosis--a hypothesis. *Med. Hypotheses* 65, 501–8 (2005).
29. Homminga J, Lehr AM, Meijer GJM, et al. Posteriorly directed shear loads and disc degeneration affect the torsional stiffness of spinal motion segments: a biomechanical modeling study. *Spine (Phila Pa 1976)* 2013;38:E1313-9.





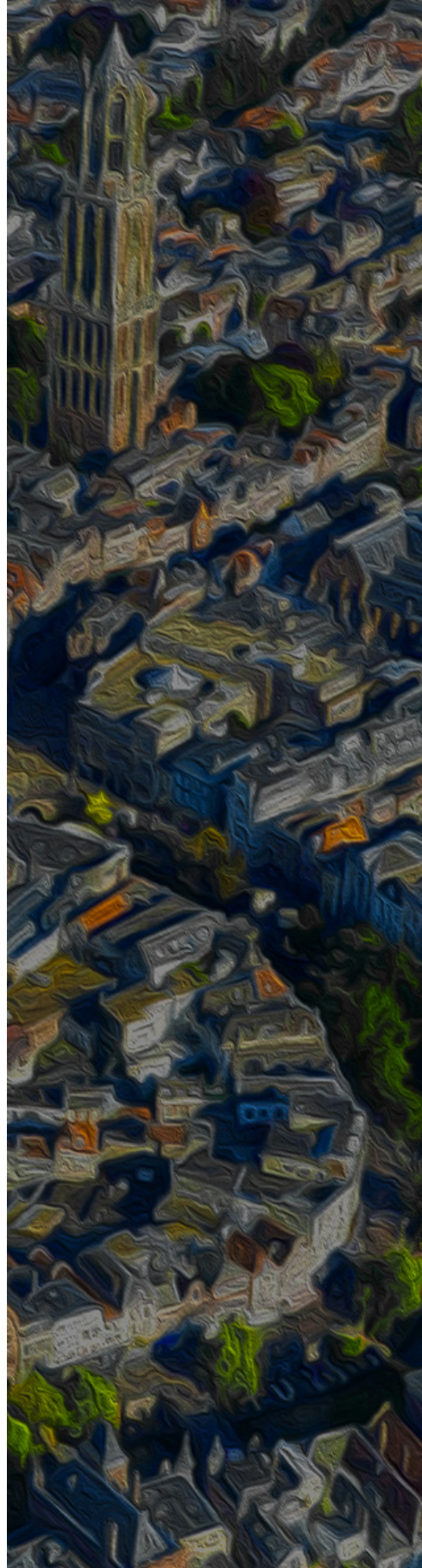


# 4

## Ossification and Fusion of the Vertebral Ring Apophysis as an Important Part of Spinal Maturation

Lorenzo Costa  
Steven de Reuver  
Luc Kan  
Peter Seevinck  
Moyo C. Kruyt  
Tom P.C. Schlösser  
René M. Castelein

*Journal of Clinical Medicine. 2021 Jul 21;10(15):3217.*



## ABSTRACT

In scoliosis, most of the deformity is in the disc and occurs during the period of rapid growth. The ring apophyses form the insertion of the disc into the vertebral body, they then ossify and fuse to the vertebrae during that same crucial period. Although this must have important implications for the mechanical properties of the spine, relatively little is known of how this process takes place. This study describes the maturation pattern of the ring apophyses in the thoracic and lumbar spine during normal growth. High-resolution CT scans of the spine for indications not related to this study were included. Ossification and fusion of each ring apophysis from T1 to the sacrum was classified on midsagittal and midcoronal images (4 points per ring) by two observers. The ring apophysis maturation (RAM) was compared between different ages, sexes, and spinal levels. The RAM strongly correlated with age ( $R = 0.892$ ,  $p < 0.001$ ). Maturation differed in different regions of the spine and between sexes. High thoracic and low lumbar levels fused earlier in both groups, but, around the peak of the growth spurt, in girls the mid-thoracic levels were less mature than in boys, which may have implications for the development of scoliosis.

## Introduction

The majority of pediatric spinal deformities develop during puberty when the body weight and dimensions increase rapidly, as the skeleton matures into its adult form. Recent studies have demonstrated the significant contribution of the intervertebral discs to the deformation of the spine in scoliosis.<sup>1-3</sup> For undisturbed and harmonious spinal development, rapidly increasing loads during the growth spurt require adequate maturation of the spine's stabilizers, of which the disc is an essential component.<sup>4</sup> Skeletal maturity is traditionally assessed on X-rays of the iliac crest, the hand, and wrists, or other growth cartilages remote from the spine. The most used classifications are the Risser grade based on ossification and fusion of the iliac apophysis and the Sanders simplified skeletal maturity scoring system, based on the maturation of the hand epiphyses.<sup>5,6</sup> Another classification is the Proximal Humerus Ossification System (PHOS).<sup>7</sup> This classification is a five-stage system that uses the proximal humeral physis in assessing skeletal maturity. These skeletal maturation scoring systems correlate with the Peak Height Velocity (PHV) during pubertal growth and the curve acceleration phase in scoliosis, however, they do not necessarily assess the maturation of different regions of the spine itself.<sup>6,8-10</sup>

After the formation of the three primary ossification centers for each vertebra (one for the body and two for the vertebral arch), the maturation of the spine continues with the closure of the neurocentral synchondroses from age 4–8.<sup>11</sup> The secondary ossification centers are the ring apophyses and the tips of the transverse and spinous processes.<sup>12</sup> The ring apophyses are not inside the epiphyseal plate and are not involved in the longitudinal growth of the spine.<sup>13</sup> During growth, they encircle the inferior and superior surfaces of the vertebral bodies. The outermost fibers of the annulus fibrosus, the Sharpey's fibers, insert into the ring apophysis and thus anchor the intervertebral disc to the two adjacent vertebrae (**Figure 1**).<sup>14-18</sup> During skeletal maturation, these initially cartilaginous insertions of the disc ossify and ultimately fuse to the vertebral bodies.<sup>19</sup> This process has important implications for the mechanical stability of the disc-vertebral body complex at a time when spinal loading increases rapidly, but very little is known about its different phases during growth.<sup>20,21</sup>

## Materials and Methods

### Study population

After a waiver from the ethical review board (ERB) for formal review of this retrospective study, pre-existing high-resolution Computed Tomography (CT) scans of the thorax and/or abdomen acquired from a tertiary pediatric hospital for indications not related to this study (e.g., trauma screening, pulmonary disease, and gastro-enteric disorders) were included

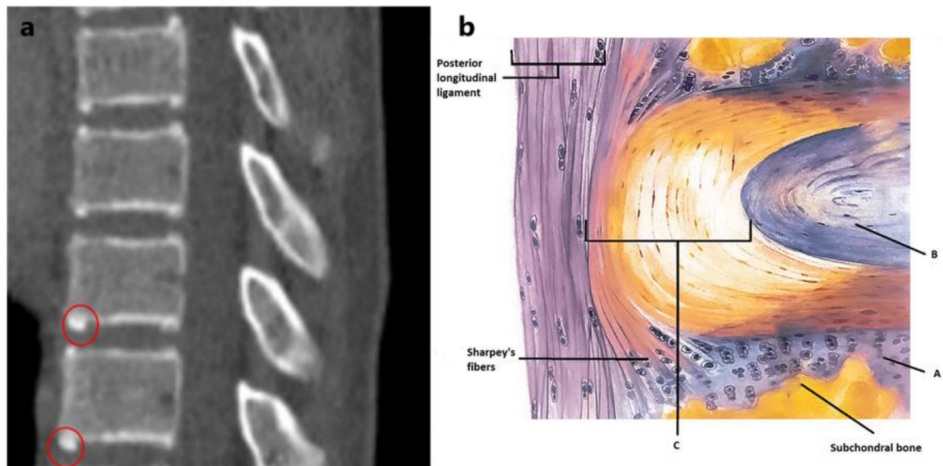


**Figure 1.** (a) A view of the ossified rings and the start of the fusion (red circles) to the vertebral body; (b) schematic anatomical view of the IVD and the attachment of the Sharpey's fibers to cartilage tissue. A: cartilaginous endplate. B: Nucleus pulposus. C: Anulus fibrosus.

from our local patient archiving and communications system (PACS). Inclusion criteria were patients between 6 and 21 years of age and available high-resolution images of the spine (slice thickness  $\leq 1$  mm and slice interval  $\leq 1.5$  mm). The ages of 6 and 21 were chosen based on previous studies by Woo et al. and Uys et al.<sup>13,19</sup> Exclusion criteria were the presence of spinal pathology, bone disorders (e.g., Scheuermann's disease), syndromes associated with growth disorders, growth hormone treatment, and insufficient CT-scan quality including movement artifacts. According to all available information, subjects represented healthy adolescents. A minimum of 10 subjects per age cohort was included. Age, sex, Risser grade, and proximal humeral ossification system (PHOS) were collected on the coronal survey scans.

### CT-scan analysis

The included CT scans were analyzed independently by two trained observers, who scored each vertebra separately blinded from each other. Multiplanar images of the exact mid-sagittal and mid-coronal plane of each individual vertebra were reconstructed, using the RadiAnt DICOM viewer© (RadiAnt, Poznan, Poland) (**Figure 2**). The window level was set to the bone. Ossification and/or fusion of the anterior, posterior, and lateral parts of each superior and inferior apophyseal ring was classified. If needed, the two observers viewed adjacent slices to confirm that suspected ossified structures were part of the ring apophysis, and discrepancies were resolved by consensus.

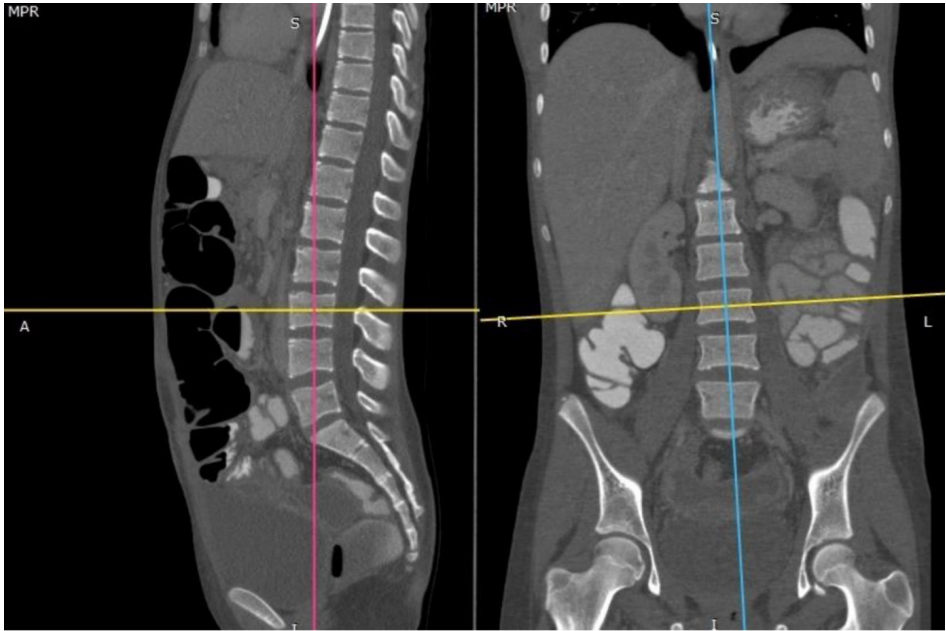


**Figure 2.** Mid-sagittal and mid-coronal reconstructions were used for each spinal level to describe the presence of ossification and fusion in four areas of each ring.

According to previous observations by Uys et al., and confirmed following a pilot study performed, the ossification and fusion of each region of interest (ROI) of the ring apophyses were scored as shown in **Figure 3.**<sup>19</sup>

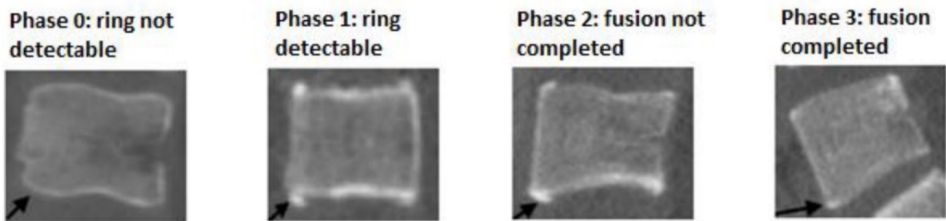


**Figure 3.** The four phases of maturation of the ring apophysis on mid-sagittal images. In phase 0 the rings are still in a cartilaginous stage and are not detectable on CT scans. In phase 1 the rings are ossified and can be seen on CT scans but have not yet started to fuse. In phase 2 the rings are starting to fuse with the bodies. In phase 3 the rings are completely fused with the vertebral bodies

Next, the overall ring apophysis maturation (RAM) of each ring was classified as:

- Stage 0: no ossification (phase 0) in all 4 ROI.
- Stage 1: Beginning of ossification (phase 1 in 1–3 ROI).
- Stage 2: Complete ossification (phase 1 in all 4 ROI).
- Stage 3: Incomplete fusion (phase 3 in 1–3 ROI).
- Stage 4: Complete fusion at all 4 points (phase 3 in all 4 ROI).

Intraclass correlation coefficients (kappa value) were calculated for the assessment of intra- and inter-observer reliability.

### Statistical analysis

Statistical analyses were performed using SPSS 25.0 for Windows (IBM, Armonk, NY, USA). The median, range, and IQR of the RAM were calculated for each age and spinal level for both sexes. The normality of distribution of the RAM within the study population was analyzed via Q-Q plots. The correlation between the RAM and age was tested with a non-parametric Spearman's rank test as well as for different areas of the rings. In the ring ossification stage (phase 1), the authors compared the sagittal plane (both anterior and posterior) with the coronal plane, with a standard t-test. The same procedure was done for fusion (phase 3). Different growth patterns between the lower thoracic and thoracolumbar spine and the other spinal sections were calculated through a generalized linear model. The correlation between the median RAM of the whole spine and the conventional skeletal maturity scores (Risser and PHOS) was analyzed with a Spearman's rank test. The p-value was set at 0.05.

## **Results**

### Study population

Out of 4775 available CT scans, 456 could be included in this study. Most exclusions were due to insufficient image quality. Of the included subjects, 50% were females. The CT scan images analyzed were 289 (63%) full-body, 82 (18%) thoracic, and 85 (19%) abdominal. Descriptive statistics of patients and CT scans are shown in **Table 1**.



| Population         |             |             |
|--------------------|-------------|-------------|
| Age                | Males       | Females     |
| 6                  | 15          | 17          |
| 7                  | 18          | 16          |
| 8                  | 13          | 13          |
| 9                  | 13          | 11          |
| 10                 | 11          | 12          |
| 11                 | 16          | 16          |
| 12                 | 17          | 20          |
| 13                 | 17          | 15          |
| 14                 | 14          | 19          |
| 15                 | 14          | 17          |
| 16                 | 16          | 12          |
| 17                 | 14          | 13          |
| 18                 | 12          | 14          |
| 19                 | 14          | 13          |
| 20                 | 12          | 11          |
| 21                 | 11          | 10          |
| Total (percentage) | 227 (49.7%) | 229 (50.3%) |
| Mean age           | 13.22       | 13.15       |
| SD                 | 4.52        | 4.44        |
| Range              | 6–21        | 6–21        |
| CT scans           |             |             |
| Selected CT scans  | 456         |             |
| Total-body n (%)   | 289 (63%)   |             |
| Thoracic n (%)     | 82 (18%)    |             |
| Abdominal n (%)    | 85 (19%)    |             |

**Table 1.** Patient demographics.

Ring apophysis maturation

Maturation of the ring apophysis is a process that varies for each age at different levels of the spine and differs between sexes. Furthermore, it does not strictly follow the same patterns and timing of the most common physes used for skeletal maturity assessment such as iliac apophysis (Risser), hand epiphysis (Sanders), and proximal humeral physis (PHOS). Ossification occurred from age 9–15 in males and 7–15 in females, fusion from 14–19 and 13–19, respectively. RAM correlated significantly with age ( $R = 0.892$ ) and both ossification and fusion occurred earlier in females ( $p = 0.002$ , **Figure 4**).

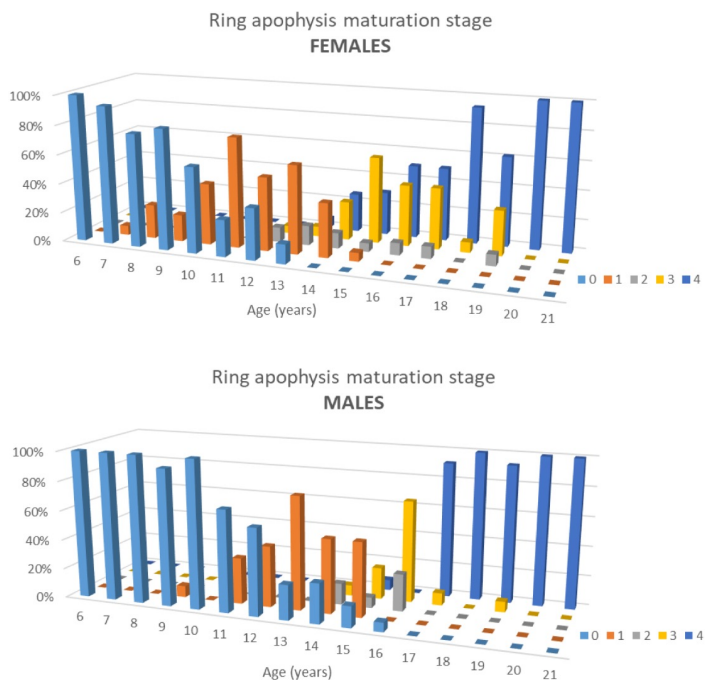


**Figure 4.** A 3-D histogram showing the percentiles of the different maturation stages of the apophyseal ring in females and males at different ages.

At age 21, 98% of the rings were completely fused (stage 4). Whereas ossification and fusion occurred on average between 9 and 19 in males and 7 and 19 in females, important differences were observed per spinal level, especially when related to the average age of the PHV (13 years of age in females and 15 in males) as can be seen in **Table 2** and **Figure 5**. Most differences between the sexes could be detected in the thoracic levels. In females at the age of 13, the median of RAM was stage 0 between T1 and T6 and stage 1 between T7 and T12. In 15-year old males, the median of maturation in spinal sections was stage 3 for T1 and T2 and stage 1 between T3 and T12.

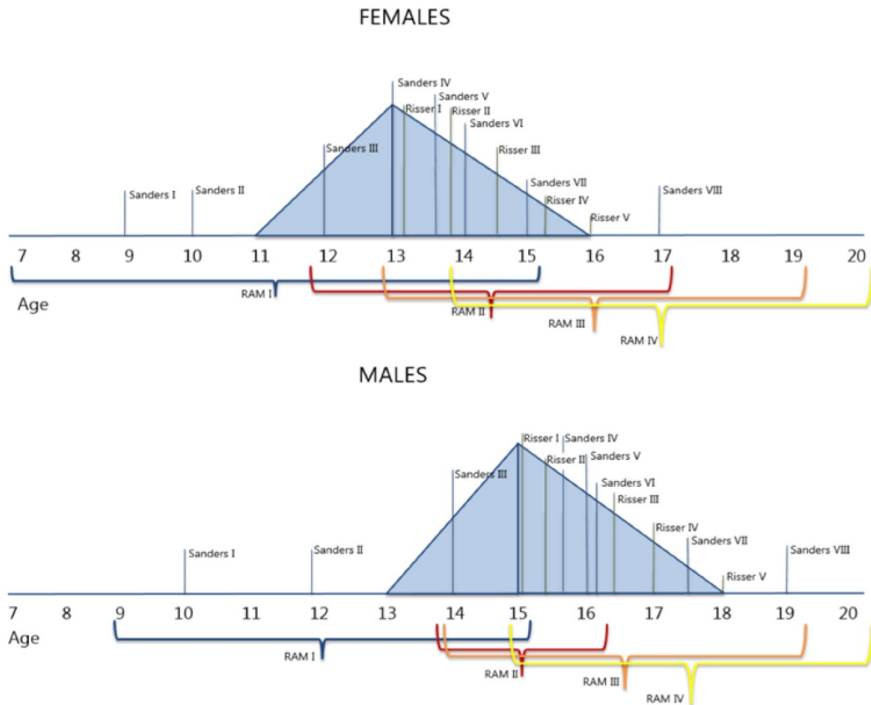


**Figure 5.** Figure based on Di Meglio et al. (2011) in which Sanders, Risser, and RAM classifications are correlated to growth velocity (and peak height velocity) in females and males.<sup>22</sup>

|     |  | M  |    |    |    | F  |    |    |    |    |     |    |    |    |    |    |    |    |    |    |  |
|-----|--|----|----|----|----|----|----|----|----|----|-----|----|----|----|----|----|----|----|----|----|--|
|     |  | 0  | 1  | 2  | 3  | 0  | 1  | 2  | 3  | 4  |     |    |    |    |    |    |    |    |    |    |  |
| AGE |  | 10 | 11 | 12 | 13 | 14 | 15 | 16 | 17 | 18 | AGE | 10 | 11 | 12 | 13 | 14 | 15 | 16 | 17 | 18 |  |
| T1  |  |    |    |    |    |    |    |    |    |    | T1  |    |    |    |    |    |    |    |    |    |  |
| T2  |  |    |    |    |    |    |    |    |    |    | T2  |    |    |    |    |    |    |    |    |    |  |
| T3  |  |    |    |    |    |    |    |    |    |    | T3  |    |    |    |    |    |    |    |    |    |  |
| T4  |  |    |    |    |    |    |    |    |    |    | T4  |    |    |    |    |    |    |    |    |    |  |
| T5  |  |    |    |    |    |    |    |    |    |    | T5  |    |    |    |    |    |    |    |    |    |  |
| T6  |  |    |    |    |    |    |    |    |    |    | T6  |    |    |    |    |    |    |    |    |    |  |
| T7  |  |    |    |    |    |    |    |    |    |    | T7  |    |    |    |    |    |    |    |    |    |  |
| T8  |  |    |    |    |    |    |    |    |    |    | T8  |    |    |    |    |    |    |    |    |    |  |
| T9  |  |    |    |    |    |    |    |    |    |    | T9  |    |    |    |    |    |    |    |    |    |  |
| T10 |  |    |    |    |    |    |    |    |    |    | T10 |    |    |    |    |    |    |    |    |    |  |
| T11 |  |    |    |    |    |    |    |    |    |    | T11 |    |    |    |    |    |    |    |    |    |  |
| T12 |  |    |    |    |    |    |    |    |    |    | T12 |    |    |    |    |    |    |    |    |    |  |
| L1  |  |    |    |    |    |    |    |    |    |    | L1  |    |    |    |    |    |    |    |    |    |  |
| L2  |  |    |    |    |    |    |    |    |    |    | L2  |    |    |    |    |    |    |    |    |    |  |
| L3  |  |    |    |    |    |    |    |    |    |    | L3  |    |    |    |    |    |    |    |    |    |  |
| L4  |  |    |    |    |    |    |    |    |    |    | L4  |    |    |    |    |    |    |    |    |    |  |
| L5  |  |    |    |    |    |    |    |    |    |    | L5  |    |    |    |    |    |    |    |    |    |  |
| S1  |  |    |    |    |    |    |    |    |    |    | S1  |    |    |    |    |    |    |    |    |    |  |

**Table 2.** The differences in mean maturation of the apophyseal ring females (in red, left-side) and in males (in blue, right-side) for each spinal level

For both males and females, the ossification of the inferior ring was earlier than the superior ring. In contrast, fusion was earlier in the superior ring. Furthermore, maturation does not appear to occur in all areas at the same time: ossification (phase 1) and fusion (phase 3) occurred half a year later (between 11 and 12 years, median 12) in the coronal than the sagittal plane ( $p = 0.031$ ). Finally, the high thoracic and low lumbar levels ossified later but fused earlier (while growth spurt was ceasing in females and mid-way in males) than the thoracolumbar levels (after the growth spurt has ceased in females and was ceasing in males).

#### Correlation with other skeletal maturity parameters

Although ring maturation varies per level studied, the overall RAM presented a clear correlation with the other two classifications. The Spearman's test between the RAM and Risser grade was 0.900 and between RAM and PHOS was 0.908.

### **Discussion**

This study provides a CT-based analysis of the maturation of the disc's fixation to the vertebral body, the ring apophysis, related to age, sex, and spinal levels. Knowledge of the maturation pattern of the ring apophysis is important in the management and etiologic understanding of developmental spine problems since the disc is considered the primary passive stabilizer of the spine.<sup>4,23,24</sup> Whether it is anchored to bone or cartilage during a period in life when body weight and dimensions increase rapidly is supposed to make a major difference for the mechanical properties of the system. Unlike what all traditional maturation parameters that Risser, PHOS, and Sanders suggest, spinal maturation differs per spinal level. Overall, ossification occurred from age 9–15 years in males and 7–15 in females, fusion from 14–19 and 13–19. Between 12–15 in females and 13–16 years old in males, the ring apophysis undergoes a massive change.<sup>25,26</sup> In girls, around their growth spurt, fewer vertebrae have started the maturation process than in boys, who, in general, have a growth spurt around two years later (**Table 2**).<sup>22</sup> The anterior and posterior parts, compared to the lateral parts, ossified and fused half a year earlier and the high thoracic and low lumbar levels fused earlier than the mid-thoracic and thoracolumbar. We observed an earlier fusion of the superior ring compared to the inferior ring as was also observed in earlier radiography studies.<sup>16,19</sup> Moreover, the observations that the inferior ring ossifies earlier than the superior one, that they have the same level of maturation at the age of 15–16, and finally that the superior ring overcomes the inferior one during the fusion stage is in line with the findings by Woo et al.<sup>13</sup> Not all of the spinal areas mature at the same time. This study showed a later fusion in the mid thoracic and thoracolumbar spine in both sexes, which is similar to the closure pattern of the Neuro Central Junction.<sup>11</sup> Interestingly, the most common curve type in Adolescent Idiopathic Scoliosis (AIS) patients is in the same region where ring apophysis maturation is slower.<sup>27</sup>

As mentioned previously, understanding the maturation of the spine is of key importance for the management of disturbances of its harmonious development. Nowadays, the most used technique to determine bone maturation is the Risser grade even though its accuracy is debated since the Risser stages do not reflect the exact growth activity in the vertebral endplates.<sup>6,9,10,28,29</sup> Even though other classifications such as Sanders are shown to be more reliable, a specific, spine-based classification of spine maturation is lacking. Furthermore, the spine continues to mature after Risser 4 and 5. Similar discrepancies have already been demonstrated by James et al. in 1958 in which in most cases of the studied x-rays, Risser 5 was not synchronous with the end of the ring maturation.<sup>18</sup> This delayed maturation, as compared to most of the long bones, may be relevant to better understand the response of the spine to the increased loads of the adolescent body during the growth spurt.

This topic is nicely displayed in the paper by Sanders et al. (2020).<sup>30</sup> The authors explained that the spine continues to grow longer than the lower extremities. Di Meglio et al. provided similar results in two of their studies, showing differences in yearly height gain velocity between the trunk and the lower limbs.<sup>22,31</sup> Furthermore, as the pelvis reflects the lower extremities more, it is clear that the Risser grade is not deeply connected to the growth of the spine which continues after the lower limb's growth has ceased.<sup>30</sup> Moreover, it is clear that Risser 1 occurs after the peak height velocity as shown previously by Di Meglio et al. and in Figure 5 while ring apophysis maturation varies, depending on spinal level, for each Risser stage.<sup>22</sup> Finally, inter- and intra-observer reliability of RAM was highly positive, resulting in a substantial agreement. Nevertheless, many differences between the RAM and other classifications could be detected. This might be due to the necessity to form age groups of the subjects.

This study gives an important insight into the maturation of the spine itself, showing interesting differences between the sexes and different anatomical areas. The area of the spine in which most common types of idiopathic scoliosis develop appears to mature later than the rest of the spine. Sharpey's fibers insert into the ring apophysis and thus anchor the intervertebral disc to the two adjacent vertebrae.<sup>19</sup> As it is a weak point, this ossification and fusion process might have important implications for the mechanical stability of the disc-vertebral body complex of the mid-thoracic and thoraco-lumbar sections at a time when spinal loading increases rapidly due to the growth spurt.<sup>20,21</sup> This may be important for understanding the patho-mechanism of idiopathic scoliosis. Furthermore, around the PHV females appear to have less matured rings if compared to males at the PHV. As most adolescent spine deformities occur mainly in this period and females have a less-matured spine, this could partly explain why the onset of these deformities is more common in females.

This study used an existing CT database to analyze ossification and fusion of the ring apophysis, obviously, this cannot be used in clinical practice because of radiation hygiene.<sup>32</sup> We are presently working on the further development of bone-MRIs, a new radiation-free technique, which uses MRI to create synthetic CT images based on deep-learning processes.<sup>33,34</sup> Possibly, in the near future, it can also be applied to the scoliotic spine, providing a true spine-based assessment of spinal maturation per level of the spine in a patient group that often undergoes MRI scanning as a regular procedure.

In conclusion, this study describes the maturation of the ring apophysis as the attachment of the disc to the vertebral body on CT images and shows that they ossify and fuse later in the mid-thoracic and thoraco-lumbar spine. Furthermore, related to the timing of their growth spurt, the female spine appears to be less mature than the male spine.

## References

1. Schlösser, T.P.; Shah, S.A.; Reichard, S.J.; Rogers, K.; Vincken, K.L.; Castelein, R.M. Differences in early sagittal plane alignment between thoracic and lumbar adolescent idiopathic scoliosis. *Spine J.* 2014, 14, 282–290.
2. Will, R.E.; Stokes, I.; Qiu, X.; Walker, M.R.; Sanders, J.O. Cobb Angle Progression in Adolescent Scoliosis Begins at the Intervertebral Disc. *Spine* 2009, 34, 2782–2786.
3. Grivas, T.B.; Vasiladias, E.; Malakasis, M.; Mouzakis, V.; Segos, D. Intervertebral disc biomechanics in the pathogenesis of idiopathic scoliosis. *Stud. Health Technol. Inform.* 2006, 123, 80–83.
4. Castelein, R.M.; Pasha, S.; Cheng, J.C.; Dubouset, J. Idiopathic Scoliosis as a Rotatory Decompensation of the Spine. *J. Bone Miner. Res.* 2020, 35, 1850–1857.
5. Risser, J.C. The Iliac Apophysis: An Invaluable Sign in the Management of Scoliosis. *Clin. Orthop. Relat. Res.* 1958, 11, 111–119.
6. Vira, S.; Husain, Q.; Jalai, C.; Paul, J.; Poorman, G.W.; Poorman, C.; Yoon, R.S.; Looze, C.; Lonner, B.; Passias, P.G. The Interobserver and Intraobserver Reliability of the Sanders Classification Versus the Risser Stage. *J. Pediatr. Orthop.* 2017, 37, e246–e249.
7. Li, D.; Cui, J.J.; DeVries, S.; Nicholson, A.D.; Li, E.; Petit, L.; Kahan, J.B.; Sanders, J.O.; Liu, R.W.; Cooperman, D.R.; et al. Humeral Head Ossification Predicts Peak Height Velocity Timing and Percentage of Growth Remaining in Children. *J. Pediatr. Orthop.* 2018, 38, e546–e550.
8. Sanders, J.O.; Khoury, J.G.; Kishan, S.; Browne, R.H.; Mooney, J.F.; Arnold, K.D.; McConnell, S.J.; Bauman, J.A.; Finegold, D. Predicting Scoliosis Progression from Skeletal Maturity: A Simplified Classification during Adolescence. *J. Bone Jt. Surg. Am. Vol.* 2008, 90, 540–553.
9. Modi, H.N.; Modi, C.H.; Suh, S.W.; Yang, J.-H.; Hong, J.-Y. Correlation and comparison of Risser sign versus bone age determination (TW3) between children with and without scoliosis in Korean population. *J. Orthop. Surg. Res.* 2009, 4, 36.
10. Noordeen, M.H.H.; Haddad, F.S.; Edgar, M.A.; Pringle, J. Spinal Growth and a Histologic Evaluation of the Risser Grade in Idiopathic Scoliosis. *Spine* 1999, 24, 535–538.
11. Schlösser, T.P.; Vincken, K.L.; Attrach, H.; Kuijff, H.J.; Viergever, M.A.; Janssen, M.M.; Castelein, R.M. Quantitative analysis of the closure pattern of the neurocentral junction as related to preexistent rotation in the normal immature spine. *Spine J.* 2013, 13, 756–763.
12. Skórzewska, A.; Grzymisławska, M.; Bruska, M.; Łupicka, J.; Woźniak, W. Ossification of the vertebral column in human foetuses: Histological and computed tomography studies. *Folia Morphol.* 2013, 72, 230–238.
13. Woo, T.D.; Tony, G.; Charan, A.; Lalam, R.; Singh, J.; Tyrrell, P.N.M.; Cassar-Pullicino, V.N. Radiographic morphology of normal ring apophyses in the immature cervical spine. *Skelet. Radiol.* 2018, 47, 1221–1228.
14. Taylor, J.R. Growth of human intervertebral discs and vertebral bodies. *J. Anat.* 1975, 120, 49–68.
15. Bernick, S.; Cailliet, R.; Levy, B. The Maturation and Aging of the Vertebrae of Marmosets. *Spine* 1980, 5, 519–524.
16. Edelson, J.G.; Nathan, H. Stages in the Natural History of the Vertebral End-Plates. *Spine* 1988, 13, 21–26.
17. Cheng, J.; Castelein, R.M.; Chu, W.; Danielsson, A.J.; Dobbs, M.B.; Grivas, T.; Gurnett, C.; Luk, K.D.; Moreau, A.; Newton, P.O. et al. Adolescent idiopathic scoliosis. *Nat. Rev. Dis. Prim.* 2015, 1, 15030.
18. Dimeglio, A.; Bonnel, F.; Canavese, F. Normal Growth of the Spine and Thorax. *Eur. Spine J.* 2011, 13–42.
19. Takeuchi, T.; Abumi, K.; Shono, Y.; Oda, I.; Kaneda, K. Biomechanical Role of the Intervertebral Disc and Costovertebral Joint in Stability of the Thoracic Spine. *Spine* 1999, 24, 1414–1420.
20. Waxenbaum, J.A.; Reddy, V.; Futterman, B.; Williams, C. Anatomy, Back, Intervertebral Discs. In *StatPearls* [Internet]; StatPearls Publishing: Treasure Island, FL, USA, 2021.
21. Gerver, W.; De Bruin, R. Growth velocity: A presentation of reference values in Dutch children. *Horm. Res.* 2003, 60, 181–184.
22. Tanner, J.; Davies, P.S. Clinical longitudinal standards for height and height velocity for North American children. *J. Pediatr.* 1985, 107, 317–329.
23. Choudhry, M.N.; Ahmad, Z.; Verma, R. Adolescent Idiopathic Scoliosis. *Open Orthop. J.* 2016, 10, 143–154.
24. Sanders, J.O.; McConnell, S.J.; Margraf, S.A.; Browne, R.H.; Cooney, T.E.; Finegold, D.N. Maturity Assessment and Curve Progression in Girls with Idiopathic Scoliosis. *J. Bone Jt. Surg. Am. Vol.* 2007, 89, 64–73.
25. Little, D.G.; Sussman, M.D. The Risser Sign. *J. Pediatr. Orthop.* 1994, 14, 569–575.
26. Sanders, J.O.; Karbach, L.E.; Cai, X.; Gao, S.; Liu, R.W.; Cooperman, D.R. Height and Extremity-Length Prediction for Healthy Children Using Age-Based Versus Peak Height Velocity Timing-Based Multipliers. *J. Bone Jt. Surg. Am. Vol.* 2021, 103, 335–342.
27. DiMeglio, A. Growth in Pediatric Orthopaedics. *J. Pediatr. Orthop.* 2001, 21, 549–555.
28. Ron, E. Cancer risks from medical radiation. *Health Phys.* 2003, 85, 47–59.
29. Florkow, M.C.; Zijlstra, F.; Willemsen, K.; Maspero, M.; Berg, C.A.T.V.D.; Kerkmeijer, L.G.W.; Castelein, R.M.; Weinans, H.; Viergever, M.A.; Van Stralen, M.; et al. Deep learning-based MR-to-CT synthesis: The influence of varying gradient echo-based MR images as input channels. *Magn. Reson. Med.* 2020, 83, 1429–1441.
30. Edmondston, S.; Song, S.; Bricknell, R.; Davies, P.; Fersum, K.; Humphries, P.; Wickenden, D.; Singer, K. MRI evaluation of lumbar spine flexion and extension in asymptomatic individuals. *Man. Ther.* 2000, 5, 158–164.



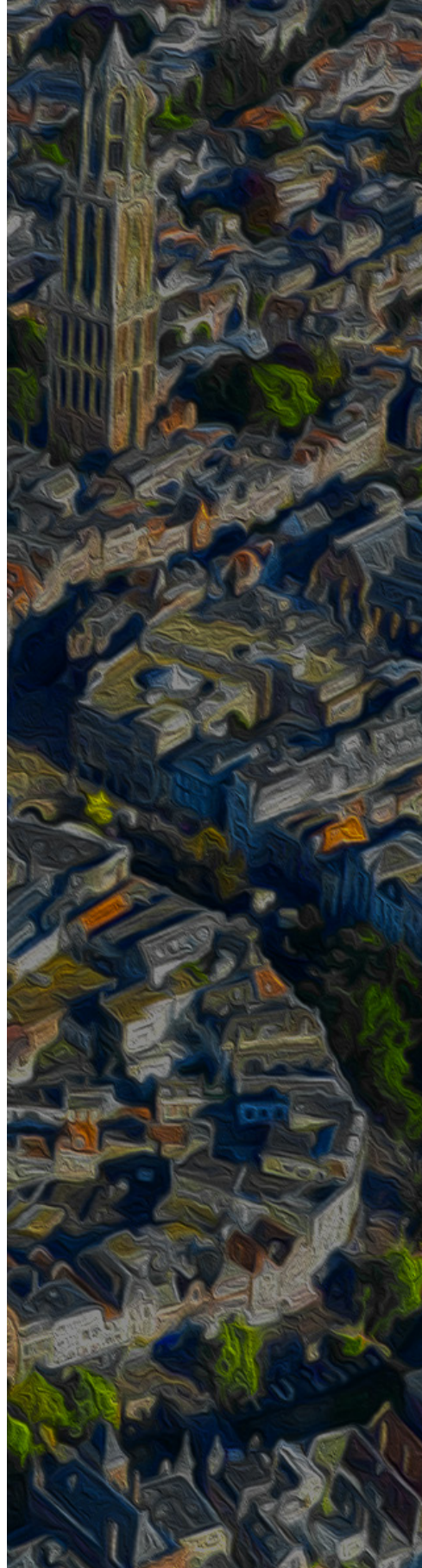


# 5

## The Changing Position of the Center of Mass of the Thorax During Growth in Relation to Pre-existent Vertebral Rotation

Steven de Reuver  
Rob C. Brink  
Jelle F. Homans  
Moyo C. Kruyt  
Marijn van Stralen  
Tom P.C. Schlösser  
René M. Castelein

*Spine. 2019 May 15;44(10):679-684.*



## ABSTRACT

**Study Design.** Cross-sectional.

**Objective.** The aim of this study was to analyze the thoracic center of mass (COM) position of children at different ages and evaluate its relation with the previously reported pre-existent rotational pattern of the normal spine.

**Summary of Background Data.** The normal, nonscoliotic thoracic spine is known to have a rotational pattern that changes direction during growth, a transition from left-sided toward right-sided rotation with increasing age. This matches the changing curve convexity seen when idiopathic scoliosis develops at different ages. Furthermore, the direction of pre-existent rotation was shown to be related to organ orientation; in situs inversus the rotation is opposite to situs solitus.

**Methods.** Computed tomography (CT) scans of the thorax of infantile (0–4 years,  $n = 40$ ), juvenile (4–10 years,  $n = 53$ ), and adolescent (10–18 years,  $n = 62$ ) children without spinal pathology were included from an existing database. The location of the COM inside the thorax was calculated based on Hounsfield-units, representing tissue mass. The COM offset was defined as the shortest distance to the midsagittal plane.

**Results.** At the infantile age, the COM was  $2.5 \pm 2.1$  mm on the right side, at juvenile age not significantly deviated, and at adolescent age  $3.1 \pm 2.3$  mm on the left side of the midsagittal plane. The mean COM offset correlated linearly with age ( $r = 0.77$ ,  $P < 0.001$ ).

**Conclusion.** The COM shifts from slightly on the right side of the thorax at the infantile age, to neutral at juvenile age, to the left at adolescent age. This corresponds to the earlier demonstrated change in direction of pre-existent rotation in the normal spine with age, as well as with the well-known changing direction, from left to right, of thoracic curve convexity in scoliosis at different ages.

## Introduction

Scoliosis is a three-dimensional (3D) deformity of the spine in which rotation plays a major role.<sup>1</sup> The direction of this rotation as part of the scoliotic deformity is related to age.<sup>1-3</sup> The Scoliosis Research Society (SRS) has divided age groups into infantile (0–4), juvenile (4–10), and adolescent (10–18). Most thoracic infantile idiopathic scoliotic curves are left-convex, whereas the curves are mostly right-convex at the adolescent age. In juvenile idiopathic scoliosis, the right- and left-convex curves are almost equally divided.<sup>4-8</sup> This pattern is well known for idiopathic scoliosis, and interestingly, identical patterns of much more subtle degrees of thoracic vertebral rotation were observed in the nonscoliotic pediatric spine.<sup>9,10</sup> Janssen et al. demonstrated that vertebral rotation of the nonscoliotic spine varies with age: left-sided rotation of thoracic vertebrae occurs mostly in infantile spines and right-sided rotation in adolescent spines.<sup>10</sup> Moreover, in scoliotic humans with situs inversus totalis, curve convexity of the main thoracic curve is opposite to what is seen in the general population.<sup>11</sup> Also, in nonscoliotic humans with situs inversus totalis, an opposite vertebral rotational pattern can be seen.<sup>12</sup> Apparently, asymmetrical mass distribution and pre-existent rotation are related. This led to the hypothesis that the mass distribution of the normal thorax shifts during growth and corresponds with the direction of the vertebral rotation.

## Materials and Methods

### Study population

For the purpose of this study, an already existing computed tomography (CT) scan database of a tertiary children's hospital was used.<sup>10</sup> This database contained 539 children from birth to the age of 18, who had undergone CT imaging between January 2005 and June 2009. Indications were not related to the spine, and were mostly infections, trauma, screening before bone marrow transplantation or immune-deficit disorders. A Philips Brilliance 16-P CT scanner (Philips Healthcare, Eindhoven, The Netherlands) was used for scanning with a slice thickness of 2 to 4 mm. Children with evidence of spinal trauma, spinal pathology (including scoliosis), anatomical anomalies, growth disorders, mental retardation, lung pathology, and incomplete scans were excluded. Children without a fully scanned thorax, children who were not positioned in a straight manner inside the gantry, and children with their arms on their thorax were excluded as well. The children were divided into three age groups based on the SRS age cohorts for scoliosis: infantile (0–4 years), juvenile (4–10 years), and adolescent (10–18 years).

### Computed tomographic (CT) measurements

To determine the location of the center of mass (COM) in the thorax, semi-automatic, in-house developed software was used (CenterOfMassAnalysis version 1.4; Image Sciences Institute,

Utrecht, The Netherlands, developed using MeVisLab, MeVis Medical Solutions AG, Bremen, Germany). The process consisted of three steps. First, the observer evaluated body positioning and scan quality, before segmenting the thorax by drawing a line around it in the coronal plane where the thorax was widest. This line passes through the upper endplate of T1, around the most lateral borders of all costae and through the diaphragm. This method was already described in CT-based studies on segmentation of the thorax (**Figure 1**).<sup>13</sup>

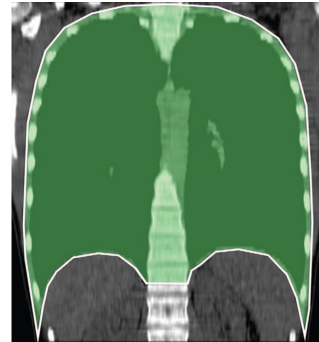


**Figure 1.** The first step of the computed tomographic (CT) measurement of the center of mass (COM) offset. The thorax was segmented by drawing a line through the upper endplate of vertebrae T1, outside of the lateral costae borders and following the diaphragm.

Second, the contour, as drawn in step 1, was copied to all coronal reconstructed slides of the CT scan, to make sure the whole thorax was segmented. During segmentation of the complete thorax, the mass of each separate voxel was calculated based on the Hounsfield unit, as a linear correlation has been shown between actual tissue-specific weight and Hounsfield units on corresponding CT scans.<sup>14,15</sup> Therefore, for COM calculation in this study, Hounsfield units were used as an index for mass per voxel. After the mass of each separate voxel in the thorax image was calculated, the software automatically calculated the exact COM position within the thorax (**Figure 2**).

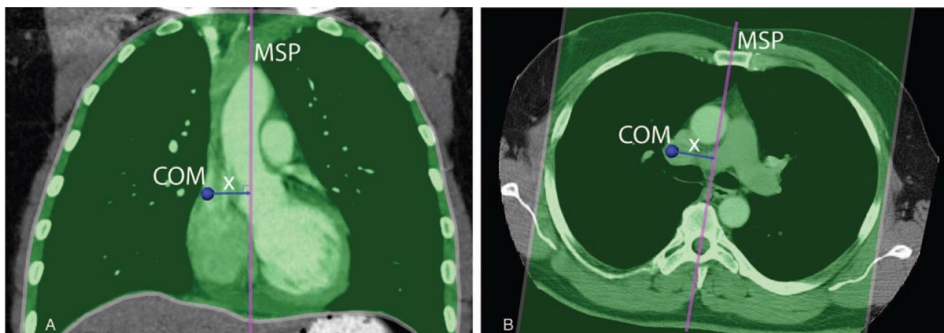


**Figure 2.** Coronal (A) and transversal (B) view of the computed tomographic (CT) measurement of the center of mass (COM) offset. The software used the contour drawn in step 1 in every coronal plane to create a three-dimensional (3D) image of the thorax. COM offset is the shortest distance ( $x$ ) to the midsagittal plane (MSP). Positive values indicate a right-sided COM offset.

Third, the COM offset was calculated, defined as the distance between the COM and the midsagittal plane of the thorax. The midsagittal plane was defined as using three points in the transverse plane: the midpoint of the sternum at level T4 and the centers of the spinal canal at level T1 and T12. The software then automatically drew the midsagittal plane through these three points and calculated the shortest distance from the established COM position to that plane in millimeters. Positive values indicate a right-sided COM offset (**Figure 3**). This new method of determining the midsagittal plane of the body by creating an actual plane determined by body parameters is less likely to be influenced by positioning than landmarks that are used in most other studies.<sup>9,10</sup> Two experienced observers performed the whole procedure. In addition, a random subset of 15 children were measured again in a separate setting to determine intra- and interobserver variability.

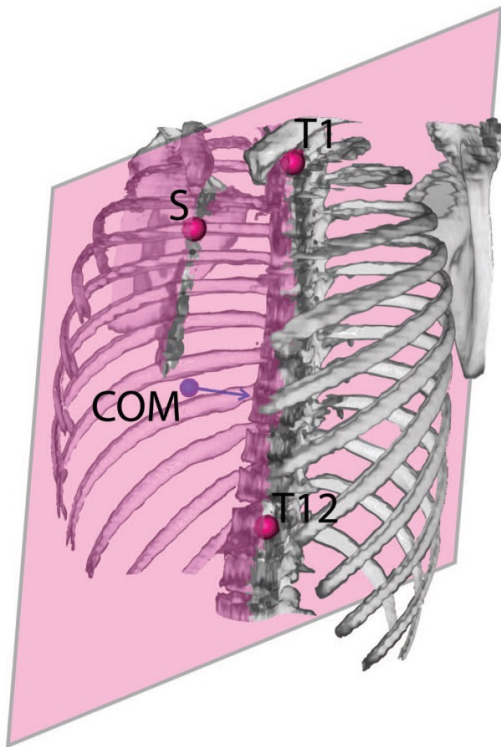


**Figure 3.** The last step in the process of computed tomographic (CT) measurement of the center of mass (COM) offset. After selection of midpoint sternum (S) at level T4 and the centers of the spinal canal at level T1 and T12, the midsagittal plane was automatically drawn and the software showed the COM location in relation to that plane, with the shortest distance to it in mm. Positive values indicate a right-sided COM offset.

### Statistical analysis

SPSS 23.0 for Windows (SPSS Inc., Chicago, IL) was used for statistical analysis. Shapiro-Wilk test was used to test normality of distribution of the COM offset in each age group. A one-sample t test was used to assess whether the offset in each age group was significant. One-way analysis of variances (ANOVA) and post-hoc Bonferroni corrected test analyzed the

mean difference in COM offset between the three age groups. Pearson correlation coefficient ( $r$ ) defined the relationship between the COM offset and age. The difference in COM offset between boys and girls, over all ages and within the three age groups, was analyzed with an unpaired  $t$  test. Intraclass correlation coefficients (ICC) were calculated for assessment of intra- and interobserver reliability. The statistical significance level was set at 0.05.

## Results

### Study population and reliability

A total of 384 children were excluded and 155 children included 40 infants, 53 juveniles, and 62 adolescents (**Table 1**). The ICCs of the intra- and interobserver reliability for measurement of the COM offset were 0.83 (95% confidence interval (95% CI): 0.51–0.94) and 0.88 (95% CI: 0.58–0.96).

|               | Infantiles (n = 40) | Juveniles (n = 53) | Adolescents (n = 62) |
|---------------|---------------------|--------------------|----------------------|
| Mean age (SD) | 2.1 (1.1)           | 6.7 (1.6)          | 13.6 (1.8)           |
| Girls (%)     | 20 (50)             | 18 (34)            | 21 (34)              |

*Patient characteristics of the infantile (0–4 years-old), juvenile (4–10 years-old), and adolescent (10–18 years-old) age cohorts. This table summarizes mean age with standard deviation (SD) and number of girls with percentage (%).*

**Table 1.** Patients characteristics

### Center of mass

Tests for normality showed a normal distribution in the infantile (0–4 years;  $P = 0.301$ ) and juvenile (4–10 years;  $P = 0.155$ ) group and a close to normal distribution in the adolescent group (10–18 years;  $P = 0.032$ ). From infantile to adolescent, the lateral offset of the thoracic COM changed from right-sided at infantile age ( $2.5 \pm 2.1$  mm from the midline;  $P < 0.001$ ), to neutral at juvenile age ( $0.3 \pm 2.1$  from the midline;  $P = 0.379$ ) to left-sided at adolescent age ( $3.1 \pm 2.3$  mm from the midline;  $P < 0.001$ ; **Table 2**). Moreover, the lateral offset of the COM of the trunk showed a significant correlation with age ( $r = 0.772$ ,  $P < 0.001$ ; **Figure 4**). Post-hoc analysis showed significant differences in mean COM offset between all three age cohorts ( $P < 0.001$ ). Mean COM offset was not significantly different between boys and girls of all ages ( $P = 0.534$ ), nor within the different age groups ( $P \geq 0.323$ ).

| Age Group, yrs     | Female | Male | Total          | $P$      |
|--------------------|--------|------|----------------|----------|
| Infantile (0–4)    | 2.2    | 2.7  | $2.5 \pm 2.1$  | $<0.001$ |
| Juvenile (4–10)    | 0.0    | 0.4  | $0.3 \pm 2.1$  | 0.379    |
| Adolescent (10–18) | –3.4   | –2.8 | $-3.1 \pm 2.3$ | $<0.001$ |

*Analysis of thoracic center of mass (COM) offset in mm compared with the midline in nonscoliotic children. Distance is shown in mm with standard deviation for total. Also,  $P$  value for mean COM offset per age group compared with midline is shown. Positive values indicate a COM location on the right side and negative values on the left side of the thorax. The level of significance was set at  $P < 0.05$ .*

**Table 2.** Center of mass offset



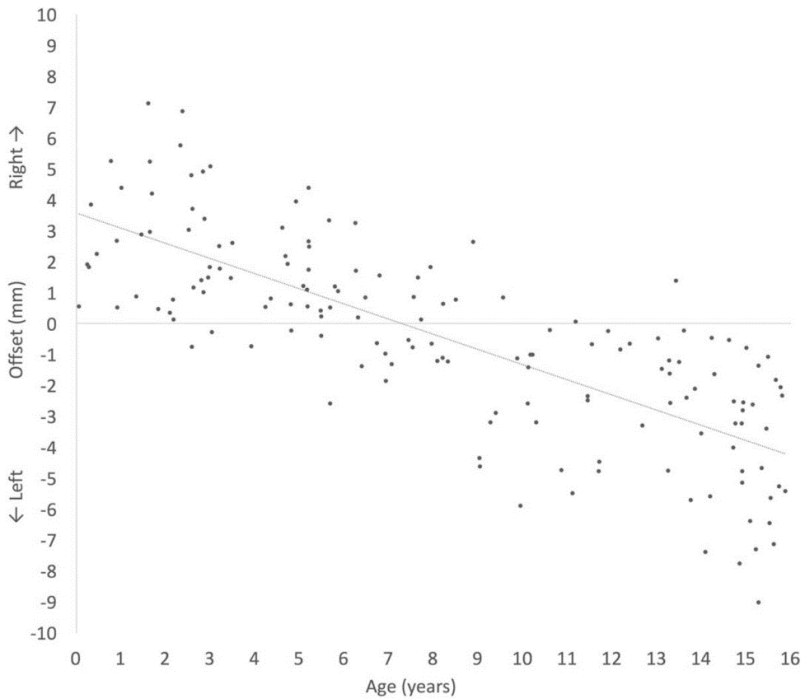


**Figure 4.** Scatter plot of all thoracic center of mass (COM) offset distances in mm per patient with age (continues) at time of computed tomographic (CT) investigation. Positive values indicate a COM on the right-side and negative values indicate a COM on the left-side of the midsagittal plane of the thorax. A trend line shows the correlation between COM and age ( $r = 0.772$ ,  $P < 0.001$ ).

## Discussion

A number of recent studies have summarized different theories on the etio-pathogenesis of idiopathic scoliosis.<sup>1,16</sup> This has led to a better understanding of the role of genetics and the unique biomechanics of the fully upright human spine and trunk. However, the reason why predominant curve direction changes from left- to right-sided during growth remained unclear.<sup>1,9-12,16</sup> Rotation of the spine is an essential part of idiopathic scoliosis, as nonscoliotic spine exhibits a rotational pattern that is identical in direction, although much smaller in magnitude, to what is seen in the most common types of idiopathic scoliosis at different ages.<sup>9,10,17</sup> It was also shown that the direction of this pre-existent rotation is related to the distribution of the organs inside the body, and not to handedness.<sup>12</sup> This led to the hypothesis that the distribution of mass inside the thorax is related to the direction of this pre-existent rotation, and that the center of mass therefore must change position during growth. Therefore, the aim of this study was to analyze the COM location of the normal infantile, juvenile, and adolescent thorax and evaluate its relation with this pre-existent thoracic vertebral rotation.

Analysis of the nonscoliotic spine and thorax in this study showed that the COM of the thorax is located on the right side of the midsagittal plane in the first years of life and gradually shifts toward the left side at adolescence ( $r = 0.722$ ,  $P < 0.001$ ; **Figure 4**). This shift corresponds inversely with the pre-existent rotational pattern of the nonscoliotic pediatric spine—as described in studies by Kouwenhoven et al,<sup>9</sup> Janssen et al,<sup>10</sup> and Schlösser et al<sup>11</sup>—and the known thoracic curve convexity and rotational pattern seen in idiopathic scoliosis, all shifting from left to right with increasing age.<sup>2-8,10</sup> These data suggest that in the pathogenesis of idiopathic scoliosis, the convexity of the thoracic curve is related to the COM offset of the thorax and the pre-existent vertebral rotation of the normal spine. This study thus addresses an important enigma in the pathogenetic mechanism of idiopathic scoliosis, but no conclusions on scoliosis etiology can be drawn based on these data.

For accurate and reproducible measurements, in this study a systematic, semi-automatic analysis method was used with high intra- and interobserver reliability. The method used in this study to segment the thorax—by drawing a line through upper endplate of vertebrae T1, around the lateral borders of the costae and following the diaphragm—is a method used in other CT-based studies on trunk segmentation as well.<sup>13</sup> In our study, the midsagittal plane was defined as the plane drawn through three points inside the body: midpoint sternum at level T4 and centers of the spinal canal at level T1 and T12. This is similar to the anterior-posterior line through center of the spinal canal and sternum at level T4 used in most previous CT studies on vertebral rotation or body mass.<sup>9,10</sup> Our method of using a plane out of three points provides the same or even better representation of the anatomical midline in the thorax, as it is less vulnerable to body positioning during the CT scan and the reference points are easily and accurately reproducible.

During growth, the relative size, as well as the location, of some of the organs in the human body vary with age.<sup>18-20</sup> For example, Antia et al<sup>18</sup> described a positive correlation between age and the distance of the heart apex from the midline. The changing position of the COM of the thorax during growth is probably the result of these relative organ transitions during growth. This is also true for intraabdominal organs; in infants, the liver volume is proportionately much greater than in adults (5% of the body weight vs. 2–2.7% in adults).<sup>19</sup> In children, intraabdominal organs are relatively larger than in adults when compared with the total body volume.<sup>20</sup> Unfortunately, our CT database consisted of very few fully scanned abdomen of children, with a large part including bowel contrast, which would interfere with COM calculations, which made it impossible to compare the position of the abdominal COM to the thoracic one in this study.



Multiple studies have already reported on the relation between organ anatomy and spinal rotation, both in the normal spine and in scoliosis: Kouwenhoven et al<sup>2</sup> studied the rotation of the spine in nonscoliotic subjects with situs solitus and situs inversus totalis; they found a mirror image rotational pattern in persons with normal organ anatomy as compared with situs inversus. Furthermore, handedness was shown not to be of influence on the direction of the spinal rotation.<sup>12</sup> Also, in a study of congenital heart disease patients of adolescent age, a strong association was shown between a right-sided aortic arch and a left-sided thoracic scoliotic curve.<sup>21</sup> And more recently, Schlösser et al<sup>11</sup> screened a population of patients with pulmonary ciliary dyskinesia, a disease characterized by a situs inversus totalis prevalence of 50% and a scoliosis prevalence slightly higher than idiopathic scoliosis in the normal population. In patients with both situs inversus totalis and scoliosis, they observed a 94% match between organ distribution and scoliosis curve convexity.<sup>11</sup>

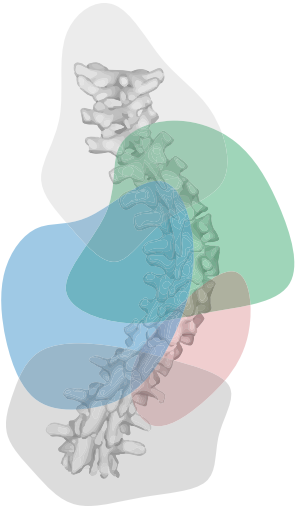
Our study demonstrates a relation between the changing eccentric position of the thoracic COM and the direction of pre-existent rotation of the thoracic spine during growth. It is, however, not able to answer questions of causality. Does the change in position of the COM initiate a change in rotational pattern, does rotation change direction first, leading to a change in position of the COM, or are both epiphenomena of a currently unknown cause of body asymmetry. In order to draw definitive conclusions on the causal relationship between COM offset and direction of rotation in the normal as well as the scoliotic thoracic spine, the COM position should be prospectively and longitudinally determined in a large cohort of normal children, and related to eventual scoliotic development. This obviously will never be possible using CT scanning due to radiation concerns.

In conclusion, the lateral offset of the COM inside the growing thorax shifts from the right side at the infantile age, to neutral at juvenile age, to left-sided at adolescent age. This corresponds to the well-known changing direction, from left to right, of thoracic curve convexity in scoliosis at different ages as well as the same changing direction of pre-existent rotation in the normal spine.

## References

1. Cheng JC, Castelein RM, Chu WC, et al. Adolescent idiopathic scoliosis. *Nat Rev Dis Primers* 2015; 1:15030.
2. Roaf R. The basic anatomy of scoliosis. *J Bone Joint Surg Br* 1966; 48:786–792.
3. Liljenqvist UR, Link TM, Halm HF. Morphometric analysis of thoracic and lumbar vertebrae in idiopathic scoliosis. *Spine (Phila Pa 1976)* 2000; 25:1247–1253.
4. Thompson SK, Bentley G. Prognosis in infantile idiopathic scoliosis. *J Bone Joint Surg Br* 1980; 62-B:151–154.
5. Wynne-Davies R. Familial (idiopathic) scoliosis. A family survey. *J Bone Joint Surg Br* 1968; 50:24–30.
6. James JL, Lloys-Roberts GC, Pilcher MF. Infantile structural scoliosis. *J Bone Joint Surg Br* 1959; 41-B:719–735.
7. Figueiredo UM, James JL. Juvenile idiopathic scoliosis. *J Bone Joint Surg Br* 1981; 63-B:61–66.
8. Chiu YL, Huang TJ, Hsu RW. Curve patterns and etiologies of scoliosis: analysis in a university hospital clinic in Taiwan. *Changgeng Yi Xue Za Zhi* 1998; 21:421–428.
9. Kouwenhoven JW, Vincken KL, Bartels LW, et al. Analysis of preexistent vertebral rotation in the normal spine. *Spine (Phila Pa 1976)* 2006; 31:1467–1472.
10. Janssen MM, Kouwenhoven JW, Schlösser TP, et al. Analysis of preexistent vertebral rotation in the normal infantile, juvenile, and adolescent spine. *Spine (Phila Pa 1976)* 2011; 36:E486–E491.
11. Schlösser TPC, Semple T, Carr SB, et al. Scoliosis convexity and organ anatomy are related. *Eur Spine J* 2017; 26:1595–1599.
12. Kouwenhoven JW, Bartels LW, Vincken KL, et al. The relation between organ anatomy and pre-existent vertebral rotation in the normal spine: magnetic resonance imaging study in humans with situs inversus totalis. *Spine (Phila Pa 1976)* 2007; 32:1123–1128.
13. Pearsall DJ, Reid JG, Livingston LA. Segmental inertial parameters of the human trunk as determined from computed tomography. *Ann Biomed Eng* 1996; 24:198–210.
14. Jiang H, Seco J, Paganetti H. Effects of Hounsfield number conversion on CT based proton Monte Carlo dose calculations. *Med Phys* 2007; 34:1439–1449.
15. Schneider W, Bortfeld T, Schlegel W. Correlation between CT numbers and tissue parameters needed for Monte Carlo simulations of clinical dose distributions. *Phys Med Biol* 2000; 45:459–478.
16. Kouwenhoven JW, Castelein RM. The pathogenesis of adolescent idiopathic scoliosis: review of the literature. *Spine (Phila Pa 1976)* 2008; 33:2898–2908.
17. Schlösser TP, Vincken KL, Attrach H, et al. Quantitative analysis of the closure pattern of the neurocentral junction as related to preexistent rotation in the normal immature spine. *Spine J* 2013; 13:756–763.
18. Antia AU, Maxwell SR, Gough A, et al. Position of the apex beat in childhood. *Arch Dis Child* 1978; 53:585–589.
19. Noda T, Todani T, Watanabe Y, et al. Liver volume in children measured by computed tomography. *Pediatr Radiol* 1997; 27:250–252.
20. Konus OL, Ozdemir A, Akkaya A, et al. Normal liver, spleen, and kidney dimensions in neonates, infants, and children: evaluation with sonography. *AJR Am J Roentgenol* 1998; 171:1693–1698.
21. Jordan CE, White RI Jr, Fischer KC, et al. The scoliosis of congenital heart disease. *Am Heart J* 1972; 84:463–469.



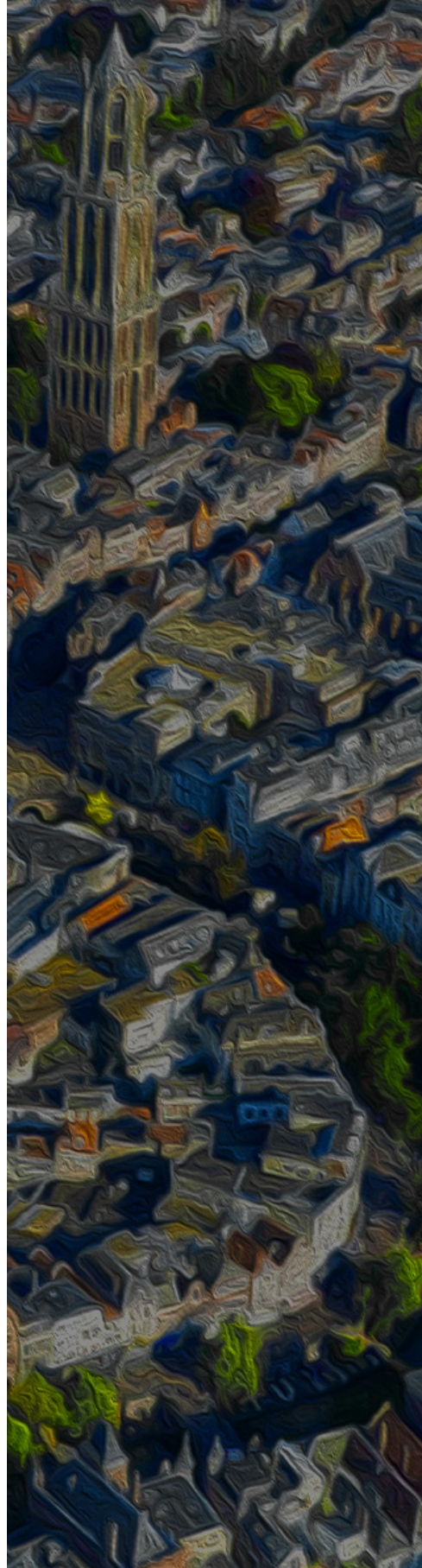


# 6

## Sagittal Spinal Profile development during Growth: a Cross-Sectional Pilot Study using Spinal Ultrasound and Statistical Shape Modeling

Steven de Reuver  
Rob C. Brink  
Willem Paul Gielis  
Timothy T.Y. Lee  
Tom P.C. Schlösser  
Moyo C. Kruyt  
René M. Castelein

*Under Peer-review.*



## ABSTRACT

**Purpose.** Little is known of sagittal spinal profile development during growth. The purpose of this pilot study is to evaluate the usefulness of dedicated upright spinal ultrasound and statistical shape modeling (SSM) to visualize and quantify the variability in sagittal profiles of the growing spine.

**Methods.** Forty-four asymptomatic boys and girls before and after the growth spurt underwent upright spinal ultrasound. The T4-L5 laminae were segmented in the sagittal plane to reconstruct the sagittal profile, SSM resulted in 7 principal components, 'modes', that explained 95% of shape variation in the included volunteers. Mode 1 and 2 explained random individual positioning, while mode 3 explained sagittal spinal shape variation.

**Results.** Before the growth spurt, boys were -0.65 standard deviation (SD) and girls -0.85 SD from the mean shape in mode 3, negative deviation indicated a less pronounced sagittal curvature with a longer posteriorly inclined segment including the high thoracic vertebrae. After the growth spurt +0.28 SD in boys and +0.74 SD in girls was observed, positive deviation indicated more pronounced sagittal curvature with a shorter posteriorly inclined segment. ICCs were 0.996 for intra- and 0.991 for interobserver reliability.

**Conclusions.** Upright spinal ultrasound and SSM is useful and reliable for radiation-free visualization and quantification of individual sagittal spinal shape in a normal pediatric population. The post-pubertal spine exhibited a different profile than the pre-pubertal. These pilot data can be utilized for longitudinal population studies on sagittal spinal development.

## Introduction

The different sagittal spinal shapes with their clinical consequences have been described for adults,<sup>1-4</sup> but much less is known of the growing population. Neonates exhibit a global kyphosis, sagittal curvatures develop as the child becomes ambulant and grows, but the normal sagittal spinal shape in children of different ages is poorly defined, despite the fact that differences in the sagittal plane have been shown to play a role in the development of spinal deformities.<sup>5-8</sup> Deeper knowledge of the age related changes in the pediatric sagittal spinal shape is therefore important, this knowledge should be obtained in the normal population and should avoid ionizing radiation as much as possible.

This pilot study uses dedicated spinal ultrasound, which is a validated technique to visualize the spine in 3D.<sup>9-13</sup> In addition, statistical shape modelling (SSM) is able to quantify subtle differences in shape to describe populations, compare subgroups, longitudinally follow inter-subject change and/or act as a biomarker/predictor.<sup>14-17</sup> The purpose of this study is to evaluate the usefulness of upright spinal ultrasound and SSM to visualize and quantify the sagittal profile of the growing spine before and after the growth spurt. Furthermore, we test the reliability of this method and provide a sample size calculation for future powered longitudinal studies.

## Methods

### Study population

In this pilot study two groups of healthy volunteers were included, either before their adolescent growth spurt (aged 7-11) or after the growth-spurt (aged 15-21). Since no radiographic skeletal age assessment was available, this was based on peak height velocity as reported in the literature.<sup>18-22</sup> Exclusion criteria were: any significant current health issue, a history of disease or surgery related to the spine, and not able to stand upright for more than two minutes. The Institutional Review Board (IRB) approved this study, after participants and/or their caregivers had given a written informed consent. (IRB number 19/137).

### Spinal ultrasound imaging

Of each included patient, an upright spinal ultrasound image was obtained with the Scolioscan system (model SCN801: Telefield Medical Imaging Ltd, Hong Kong), a system described, validated and tested for reliability in earlier studies (**Figure 1**).<sup>9-13</sup> The system is equipped with a linear ultrasound probe (center frequency of 7.5 MHz and width of 75 mm) for freehand scanning and a sensor to track the position and 3D orientation of the probe. Scanning takes one to two minutes. The spinal levels T1 to S1 are scanned while patients are upright with

their arms in natural position on the sides. During scanning, the system saves up to 1000 ultrasound images with their corresponding position and orientation in space. Subsequently, these images were combined with custom post-processing software (Telefield Medical Imaging Ltd, Hong Kong), to automatically create a 3D volume reconstruction of the spine.<sup>12</sup>



**Figure 1.** The Scolioscan system (model SCN801: Telefield Medical Imaging Ltd, Hong Kong), including a linear ultrasound probe and a sensor to track the position and three-dimensional orientation of the probe during scanning.

### Statistical Shape Modeling

In general, SSM starts with automatic or manual segmentation of individual shape. After shapes are normalized for absolute size, they are compiled into one mean shape of the study population. Then a principal component analysis is performed, a method to explain a large sum of variance by a select number of relevant quantities, i.e. the principal components. In SSM, different 'modes' are produced for each principal component and ranked based on how much of the total variation they explain. Sometimes mode 1 is therefore the most relevant, but not always, as the first mode(s) can explain positioning artefacts. Visually (by plotting the mode a certain standard deviation + and - from the mean to see what shape change the mode is explaining) or numerically (by statistical testing), the best mode to fit the study population and research question is selected. The final step of SSM is to extract the deviation of each patient from the population mean in the chosen mode, which may be compared between (sub)groups using statistics as one would do with any other parameter. identified of level T4-L5, for consistency always on the left side, to provide 14 landmarks, which were connected to retrieve the sagittal spinal profile (**Figure 2**).<sup>13</sup> In separate sessions, two investigators performed this procedure twice to analyze intra- and interobserver reliability. Subsequently, sagittal spinal profile variation within the study population was analyzed with



SSM using BoneFinder 1.3.4 (Manchester University, UK).<sup>14-17</sup> SSM was performed as described previously, the model was set to explain 95% in shape variation within all included volunteers. This resulted in 7 descriptive modes, mode 1 explained 61% of shape variation, which was 21% for mode 2 and 6% for mode 3, decreasing towards <1% in mode 7. These modes were visually and numerically analyzed by two observers, mode 1 and 2 explained individual positioning of the upper body with the upper spinal segment varying wildly, mode 1 resembled slouching and mode 2 flexion of the upper spine, with random distributions across the study population. In mode 3, the upper spinal segment remained stable and variation in sagittal shape within the spine was observed, additionally, this variation seemed not random as it numerically differed significantly per age group. With mode 3 as a reference, the deviation for each individual sagittal spinal shape was calculated as a standard deviation ( $\pm$  SD) from the mean population shape (= 0), to retrieve a numerical value of the direction and magnitude of the shape deviation from the mean population shape.

### Statistical analysis

For this pilot study descriptive statistics were performed. Per group, the mean shape deviation from the total population mean sagittal spinal shape was calculated. Intraclass correlation coefficients (ICCs) and their 95% confidence intervals (95%CI) were calculated for intra- and interobserver reliability of the sagittal shape segmentation, following upright ultrasound imaging, as part of the SSM method. Statistical analysis was performed in SPSS 25.0 for Windows (IBM, Armonk, NY, USA).

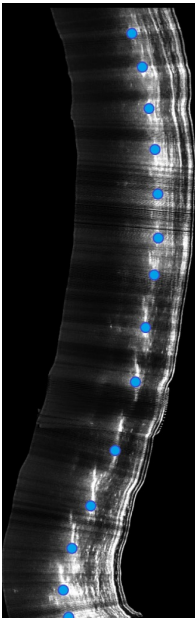


**Figure 2.** All participants received a three-dimensional ultrasound scan of the spine. A sagittal reconstruction of the spine left para-medial at the level of the laminae is displayed. For each spine, the posterior lamina cortex at level T4 to L5 was identified and segmented (blue dots), which were connected to retrieve the sagittal spinal profile.

## Results

### Study population

Forty-four volunteers without spinal pathology were recruited: Twelve boys (mean age  $9.5 \pm 1.3$ ) and seven girls (mean age  $9.4 \pm 1.5$ ) before growth spurt, and ten boys (mean age  $19.4 \pm 2.2$ ) and fifteen girls (mean age  $18.3 \pm 1.4$ ) after growth spurt.

### Statistical shape modeling

The SSM resulted in seven modes, of which mode three best described the variation of sagittal spinal shape, irrespective of absolute spinal length, in the complete study population. In this mode, deviation towards a less pronounced sagittal curvature with a less steep, but longer posteriorly inclined segment reaching into the higher thoracic regions was defined as negative up to  $-2.5$  SD. A more pronounced sagittal curvature with a steeper but shorter posteriorly inclined segment was considered positive up to  $+2.5$  SD (**Figure 3**).

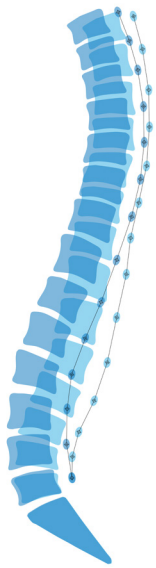
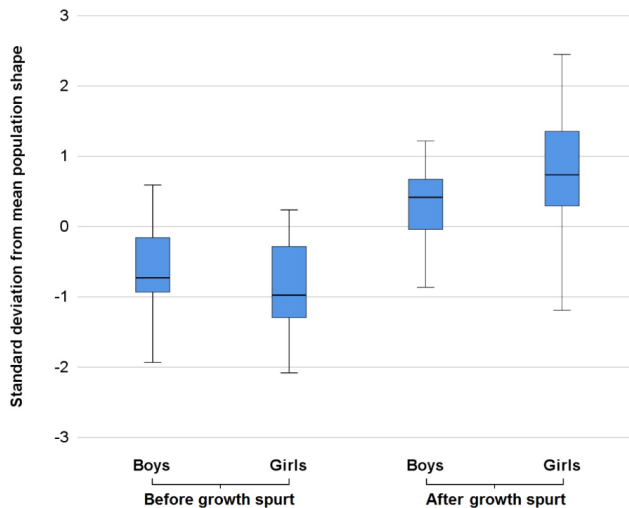


**Figure 3.** With statistical shape modelling (SSM) the variation in sagittal spinal shape was described from level T4 to L5. This is an illustration showing the differences in spinal shape between  $-2.5$  (light blue) and  $+2.5$  (dark blue) standard deviation from the mean of the population. Note that the SSM analysis is based on the laminae orientation, the vertebral bodies were added for visual reference.

**Figure 4.** Box plots of the sagittal spinal profile as analyzed with statistical shape modelling (SSM), the variation in shape per group from the population mean ( $\pm 0$  SD) is shown.



Compared to the mean population shape there was a negative deviation before growth spurt, indicating a less pronounced sagittal curvature, in both boys ( $-0.65 \pm 0.76$  SD) and girls ( $-0.85 \pm 0.84$  SD). After growth spurt there was a positive deviation, indicating a more pronounced sagittal curvature, in both boys ( $+0.28 \pm 0.62$  SD) and girls ( $+0.74 \pm 0.84$  SD; **Figure 4**). A visual reconstruction of the mean sagittal spinal shape per group following the SSM analysis is displayed in **Figure 5**. The upright ultrasound and SSM method had ICCs of 0.996 (95%CI: 0.993 - 0.998) for intra- and 0.991 (95%CI: 0.983 - 0.995) for interobserver reliability.

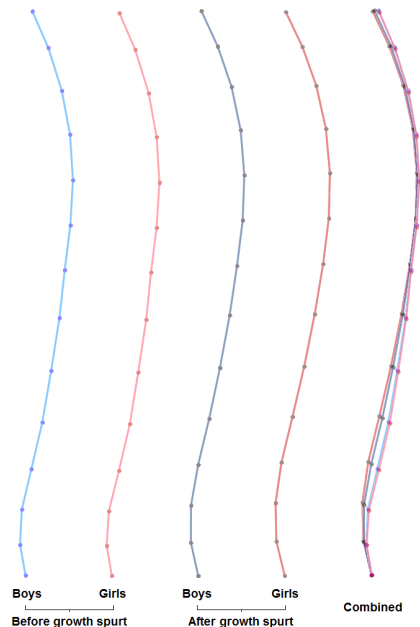


**Figure 5.** Following statistical shape modelling (SSM), the mean sagittal spinal shape from level T4 to L5, per group is displayed.

### Future studies

This upright ultrasound and SSM method has the potential to be used for longitudinal studies in the normal growing population and to study the relationship between sagittal spinal profile development and the onset of spinal deformities acquired during growth, such as AIS and hyperkyphosis. A well-known risk factor for the development of scoliosis is female sex.<sup>23</sup> The observed difference in sagittal profile between boys and girls of a certain age appeared to be limited and much less pronounced than the difference before and after growth spurt. To identify such a subtle difference in future longitudinal studies on the sagittal profile as a potential risk factor for developmental spinal deformities, the SSM data of boys and girls before the growth spurt ( $-0.65 \pm 0.76$  and  $-0.85 \pm 0.84$ ) was used for power calculation, resulting in a sample size to identify this difference of 251 per group (2-sided, 80% power,  $\alpha=5\%$ ).<sup>24</sup>

## Discussion

The individually determined sagittal spinal profile plays an important role in spinal deformity development.<sup>5-8</sup> Most research is hampered by a focus on already existing pathology, the use of ionizing radiation, an unnatural body/arm position and a poor understanding of sagittal profile development in the asymptomatic growing spine.<sup>25-32</sup> To overcome these hurdles, this pilot study aimed to test the feasibility of both ultrasound imaging and SSM to visualize and quantify the sagittal profile of the growing spine. In forty-four asymptomatic volunteers the variation of sagittal spinal shape was described, based on ultrasound imaging, with a SSM model (**Figure 3**). Compared to the mean, before growth spurt the spinal shape in boys (-0.65) and girls (-0.85) deviated negatively, whereas after growth spurt shape deviated positively in boys (+0.28) and girls (+0.74). The shape before the growth spurt was a less pronounced sagittal curvature with a less steep, but longer posteriorly inclined segment reaching into the higher thoracic regions. After the growth spurt, a more pronounced sagittal curvature with a steeper but shorter posteriorly inclined segment was observed (**Figure 5**).

The major advantage of this upright ultrasound and SSM method is the ease of obtaining free standing imaging of the spine with the arms in a relaxed anatomical position, without radiation and that it provides the ability to perform SSM with high reliability (ICCs of >0.99).<sup>9-13</sup> In addition, SSM has the potential to quantify more subtle differences in sagittal spinal shape, compared to predefined conventional sagittal parameters, such as T4-T12 thoracic kyphosis. This suggests that future studies are feasible on large cohorts to compare subgroups, longitudinally follow inter-subject variation and/or the use as a biomarker/predictor.<sup>5-8,14-17</sup> The ultimate goal of this approach is that this may allow for identification of certain sagittal spinal profiles that predispose for development of spinal deformity.

The current pilot assessed groups before (aged 7-11) and after (aged 15-21) pubertal growth spurt, since peak height velocity is at age ~12 in girls and ~14 in boys.<sup>18-22</sup> Within these age groups there are natural differences in sagittal spinal shape when considering the natural spread in sagittal profiles types as described by Roussouly for adults, and differences in maturity status related to calendar age.<sup>1</sup> Also, regarding the natural variation in sagittal profiles, this is influenced by pelvic morphology i.e. the pelvic incidence and sacral slope, with spinal ultrasound it is not possible to determine these, therefore in this study it is assumed they are distributed normally across the study population and most likely do not influence the results. Nevertheless, the effect of age on the sagittal profile was evident and appeared much more prominent than the differences between sexes. This phenomenon was also observed in a radiography study on natural sagittal profile development during growth, where many spinal

parameters significantly differed before and after growth spurt, but almost all did not differ between sexes.<sup>33</sup> This is similar to physical examination and radiographic observations of the sagittal profile with increasing age, evolving from the neonatal global kyphosis into the better defined but variable S-shape at maturity.<sup>1,28,34-39</sup>

This pilot utilized the population description and subgroup comparing capabilities of SSM. The logical next step for this method would be to perform longitudinal studies on the relationship between sagittal spinal profile and developmental of spinal deformities such as scoliosis or hyperkyphosis. Since the observed sagittal profile variation before growth spurt in this pilot was subtle, power calculation resulted in a fairly large required sample size of hundreds of scoliosis patients. Which would mean for a prospective cohort study in the general population, and a known scoliosis prevalence of 2-4%, thousands of children would have to be included before their growth spurt.<sup>23-24</sup> Obviously, this is a very conservative estimate, tested two-sided and based on the small sagittal profile differences between boys and girls before their growth spurt. If a bigger difference is expected for those at risk for scoliosis development, naturally a smaller study population may be sufficient.

In conclusion, this pilot study demonstrated that SSM combined with non-ionizing ultrasound imaging in a natural, free standing body position can visualize and quantify the subtle variations in individual sagittal shape. While the validity and reliability of upright spinal ultrasound was previously tested,<sup>9-13</sup> this study showed high intra- and interobserver reliability of the sagittal spinal profile segmentation technique and SSM applied on ultrasound images. The shape before the growth spurt was a less pronounced sagittal curvature with a less steep, but longer posteriorly inclined segment reaching into the higher thoracic regions. After growth spurt there was a more pronounced sagittal curvature with a steeper but shorter posteriorly inclined segment. Subtle differences in the sagittal profile, as observed between boys and girls before growth spurt, have an impact on biomechanical loading of the growing spine, rotational stability and thus the development of spinal deformities. Future powered longitudinal studies could utilize this ultrasound and SSM method to identify predictors for spinal deformity development in the sagittal profile, by including healthy children before disease onset.

## References

1. Roussouly P, Gollogly S, Berthonnaud E, Dimnet J (2005) Classification of the normal variation in the sagittal alignment of the human lumbar spine and pelvis in the standing position. *Spine (Phila Pa 1976)* 30:346–53
2. Le Huec JC, Thompson W, Mohsinaly Y, et al (2019) Sagittal balance of the spine. *Eur Spine J* 28:1889–1905
3. Iyer S, Sheha E, Fu MC, et al (2018) Sagittal Spinal Alignment in Adult Spinal Deformity: An Overview of Current Concepts and a Critical Analysis Review. *JBUS Rev* 6:e2
4. Glassman SD, Bridwell K, Dimar JR, et al (2005) The impact of positive sagittal balance in adult spinal deformity. *Spine (Phila Pa 1976)* 30:2024–9
5. Abelin-Genevois K, Sassi D, Verdun S, Roussouly P (2018) Sagittal classification in adolescent idiopathic scoliosis: original description and therapeutic implications. *Eur Spine J* 27:2192–2202
6. Schlösser TPC, Shah SA, Reichard SJ, et al (2014) Differences in early sagittal plane alignment between thoracic and lumbar adolescent idiopathic scoliosis. *Spine J* 14:282–90
7. Schlösser TPC, Castelein RM, Grobost P, et al (2021) Specific sagittal alignment patterns are already present in mild adolescent idiopathic scoliosis. *Eur Spine J* 30:1881–1887
8. Homans JF, Schlösser TPC, Pasha S, et al (2021) Variations in the sagittal spinal profile precede the development of scoliosis: a pilot study of a new approach. *Spine J* 21:638–641
9. Cheung C-WJ, Zheng Y (2010) Development of 3-D Ultrasound System for Assessment of Adolescent Idiopathic Scoliosis (AIS). pp 584–587
10. Zheng R, Chan ACY, Chen W, et al (2015) Intra- and Inter-rater Reliability of Coronal Curvature Measurement for Adolescent Idiopathic Scoliosis Using Ultrasonic Imaging Method-A Pilot Study. *Spine Deform* 3:151–158
11. Brink RC, Wijdicks SPJ, Tromp IN, et al (2018) A reliability and validity study for different coronal angles using ultrasound imaging in adolescent idiopathic scoliosis. *Spine J* 18:979–985
12. Zhou G-Q, Jiang W-W, Lai K-L, et al (2016) Semi-automatic Measurement of Scoliotic Angle Using a Freehand 3-D Ultrasound System Scolioscan. pp 341–346
13. Lee TT-Y, Jiang WW, Cheng CLK, et al (2019) A Novel Method to Measure the Sagittal Curvature in Spinal Deformities: The Reliability and Feasibility of 3-D Ultrasound Imaging. *Ultrasound Med Biol* 45:2725–2735
14. Lindner C, Thiagarajah S, Wilkinson JM, et al (2013) Accurate bone segmentation in 2D radiographs using fully automatic shape model matching based on regression-voting. *Med Image Comput Comput Assist Interv* 16:181–9
15. Lindner C, Thiagarajah S, Wilkinson JM, et al (2013) Development of a fully automatic shape model matching (FASMM) system to derive statistical shape models from radiographs: application to the accurate capture and global representation of proximal femur shape. *Osteoarthritis Cartil* 21:1537–44
16. Lindner C, Bromiley PA, Ionita MC, Cootes TF (2015) Robust and Accurate Shape Model Matching Using Random Forest Regression-Voting. *IEEE Trans Pattern Anal Mach Intell* 37:1862–74
17. Agricola R, Leyland KM, Bierma-Zeinstra SMA, et al (2015) Validation of statistical shape modelling to predict hip osteoarthritis in females: data from two prospective cohort studies (Cohort Hip and Cohort Knee and Chingford). *Rheumatology (Oxford)* 54:2033–41
18. Grave KC (1973) Timing of facial growth: a study of relations with stature and ossification in the hand around puberty. *Aust Orthod J* 3:117–22
19. Largo RH, Gasser T, Prader A, et al (1978) Analysis of the adolescent growth spurt using smoothing spline functions. *Ann Hum Biol* 5:421–34
20. Rauch F, Bailey DA, Baxter-Jones A, et al (2004) The "muscle-bone unit" during the pubertal growth spurt. *Bone* 34:771–5
21. Whiting SJ, Vatanparast H, Baxter-Jones A, et al (2004) Factors that affect bone mineral accrual in the adolescent growth spurt. *J Nutr* 134:696S–700S
22. Aksglaede L, Olsen LW, Sørensen TIA, Juul A (2008) Forty years trends in timing of pubertal growth spurt in 157,000 Danish school children. *PLoS One* 3:e2728
23. Cheng JC, Castelein RM, Chu WC, et al (2015) Adolescent idiopathic scoliosis. *Nat Rev Dis Prim* 1:15–30
24. Chow S-C, Shao J, Wang H (2008) *Sample Size Calculations in Clinical Research*. 2nd Ed. Chapman & Hall/CRC Biostatistics Series.
25. Marty C, Boisauvert B, Descamps H, et al (2002) The sagittal anatomy of the sacrum among young adults, infants, and spondyloolsthesis patients. *Eur Spine J* 11:119–25
26. Mendoza-Lattes S, Ries Z, Gao Y, Weinstein SL (2010) Natural history of spinopelvic alignment differs from symptomatic deformity of the spine. *Spine (Phila Pa 1976)* 35:E792–8
27. Pasha S (2019) 3D Deformation Patterns of S Shaped Elastic Rods as a Pathogenesis Model for Spinal Deformity in Adolescent Idiopathic Scoliosis. *Sci Rep* 9:16485
28. Cil A, Yazici M, Uzumcugil A, et al (2005) The evolution of sagittal segmental alignment of the spine during childhood. *Spine (Phila Pa 1976)* 30:93–100
29. Pruijs JEH, Keessen W, van der Meer R, van Wieringen JC (1995) School screening for scoliosis: the value of quantitative measurement. *Eur Spine J* 4:226–230
30. Dickson RA, Stamper P, Sharp AM, Harker P (1980) School screening for scoliosis: cohort study of clinical course. *BMJ* 281:265–267
31. Mac-Thiong J-M, Labelle H, Berthonnaud E, et al (2007) Sagittal spinopelvic balance in normal children and adolescents. *Eur Spine J* 16:227–234

32. Janssen MMA, Drevelle X, Humbert L, et al (2009) Differences in male and female spino-pelvic alignment in asymptomatic young adults: a three-dimensional analysis using upright low-dose digital biplanar X-rays. *Spine (Phila Pa 1976)* 34:E826-32
33. Schlösser TPC, Vincken KL, Rogers K, et al (2015) Natural sagittal spino-pelvic alignment in boys and girls before, at and after the adolescent growth spurt. *Eur Spine J* 24:1158–1167
34. Bagnall KM, Harris PF, Jones PR (1977) A radiographic study of the human fetal spine. 1. The development of the secondary cervical curvature. *J Anat* 123:777–82
35. O'Rahilly R, Muller F, Meyer DB (1980) The human vertebral column at the end of the embryonic period proper. 1. The column as a whole. *J Anat* 131:565–75
36. Willner S, Johnson B (1983) Thoracic kyphosis and lumbar lordosis during the growth period in children. *Acta Paediatr Scand* 72:873–8
37. Voutsinas SA, MacEwen GD (1986) Sagittal profiles of the spine. *Clin Orthop Relat Res* 235–42
38. Panattoni GL, Todros T Postural aspects of the human fetal spine. Morphometric and functional study. *Panminerva Med* 30:250–3
39. Bernhardt M, Bridwell KH (1989) Segmental analysis of the sagittal plane alignment of the normal thoracic and lumbar spines and thoracolumbar junction. *Spine (Phila Pa 1976)* 14:717–21





# PART II

Scoliosis as a  
Universal Respons

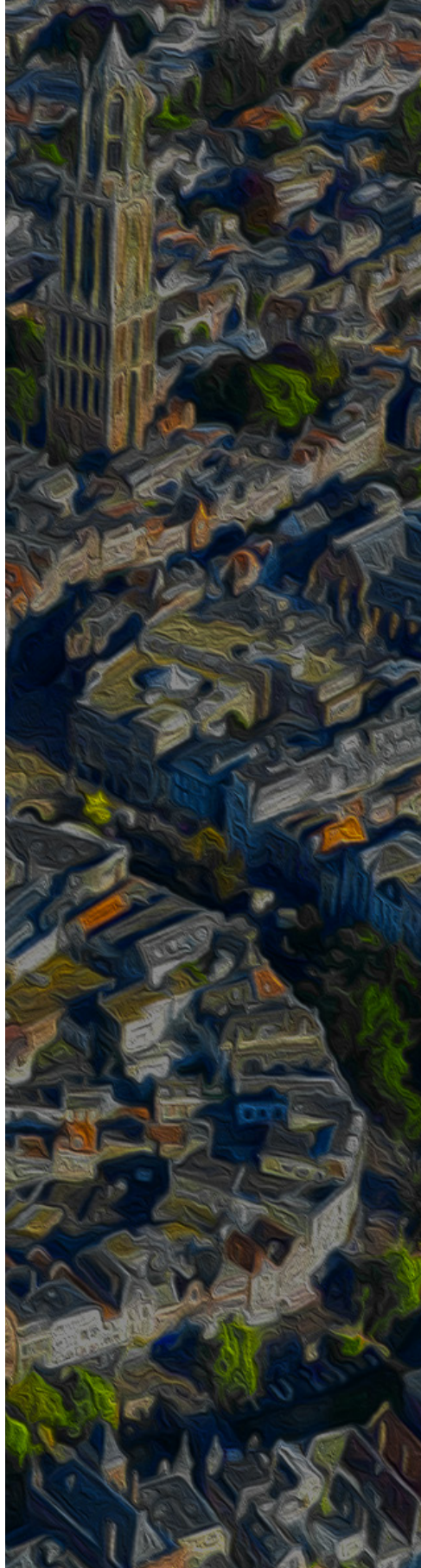


# 7

## Cross-validation of Ultrasound Imaging in Adolescent Idiopathic Scoliosis

Steven de Reuver  
Rob C. Brink  
Timothy T.Y. Lee  
Yong-Ping Zheng  
Frederik J.A. Beek  
René M. Castelein

*European Spine Journal. 2021 Mar;30(3):628-633.*



## ABSTRACT

**Purpose.** Adolescent idiopathic scoliosis (AIS) patients are exposed to 9–10 times more radiation and a fivefold increased lifetime cancer risk. Radiation-free imaging alternatives are needed. Ultrasound imaging of spinal curvature was shown to be accurate, however, systematically underestimating the Cobb angle. The purpose of this study is to create and cross-validate an equation that calculates the expected Cobb angle using ultrasound spinal measurements of AIS patients.

**Methods.** Seventy AIS patients with upright radiography and spinal ultrasound were split randomly in a 4:1 ratio to the equation creation (n=54) or validation (n=16) group. Ultrasound angles based on the spinous processes shadows were measured automatically by the ultrasound system (Scolioscan, Telefield, Hong Kong). For thoracic and lumbar curves separately, the equation: expected Cobb angle=regression coefficient×ultrasound angle, was created and subsequently cross-validated in the validation group.

**Results.** Linear regression analysis between ultrasound angles and radiographic Cobb angles (thoracic:  $R^2=0.968$ , lumbar:  $R^2=0.923$ ,  $p<0.001$ ) in the creation group resulted in the equations: *thoracic Cobb angle* =  $1.43 \times \text{ultrasound angle}$  and *lumbar Cobb angle* =  $1.23 \times \text{ultrasound angle}$ . With these equations, expected Cobb angles in the validation group were calculated and showed an excellent correlation with the radiographic Cobb angles (thoracic:  $R^2=0.959$ , lumbar:  $R^2=0.936$ ,  $p<0.001$ ). The mean absolute differences were  $6.5^\circ$ – $7.3^\circ$ . Bland–Altman plots showed good accuracy and no proportional bias.

**Conclusion.** The equations from ultrasound measurements to Cobb angles were valid and accurate. This supports the implementation of ultrasound imaging, possibly leading to less frequent radiography and reducing ionizing radiation in AIS patients.

## Introduction

Adolescent idiopathic scoliosis (AIS) is a complex three-dimensional (3D) deformity of the spine and trunk with severe consequences for young patients in terms of pain, possible cardiopulmonary compromise, psycho-social burden and disturbed self-image.<sup>1</sup> Patients with AIS are traditionally diagnosed and monitored with frequent upright anterior–posterior (AP) and lateral radiographs.<sup>2</sup> Additional imaging consists of magnetic resonance (MR) or computed tomography (CT) for surgical planning, to obtain in-depth 3D morphology or identification of spinal anomalies.<sup>1</sup> The major downside of radiography and CT is ionizing radiation: AIS patients are exposed to 9–10 times more radiation and have a lifetime relative risk of 4.8 for developing cancer as compared to the general population.<sup>3,4</sup> MRI is not ionizing, but is mostly made in supine position, and is expensive and time-consuming, and cortical bone is poorly visible on standard MR imaging.<sup>5</sup> Low-dose biplanar radiography (EOS imaging, Paris, France) is performed upright, but is not widely available and still utilizes ionizing radiation.<sup>6</sup> Because of these difficulties, other radiation-free methods to create a 3D image of the spine in upright position have been developed, like ultrasound imaging. Several authors described the use of ultrasound landmarks such as the spinous process (SP) and transverse process (TP) to measure the severity of the AIS curve, and good-to-excellent correlations were shown between ultrasound angles and radiographic Cobb angles.<sup>7–11</sup> However, ultrasound angles were systematically smaller as compared to radiographic Cobb angles. The relationship between angles measured with ultrasound and radiography is described in earlier studies, but an equation to calculate the expected Cobb angle based on the ultrasound angle has not yet been properly cross-validated.<sup>9–11</sup> Therefore, the purpose of the current study is to create and cross-validate an equation to calculate the expected Cobb angle of thoracic and lumbar curves based on the ultrasound angle of AIS patients.

## Methods

### Study population

Patients suspected of AIS who had a conventional upright radiography of the complete spine planned were consecutively recruited between 2016 and 2019. Patients not between 10 and 18 years of age, with spinal pathology other than AIS, previous spinal surgery, neurological symptoms and/or syndromes associated with growth disorders were excluded. The patients were included in a tertiary spine clinic in the Netherlands, and the study was approved by the local Medical Research Ethics Committee. After informed consent was obtained from all patients and/or their parents, an ultrasound scan was made on the same day as the radiography. Patients could not receive the ultrasound investigation at the same visit as the radiograph or with a failed radiography and/or ultrasound investigation was excluded. In this validation study, the included patients were split randomly in a 4:1 ratio and put in the equation creation group and the validation group, respectively.

### Ultrasound and radiographic measurements

The ultrasound scans were obtained using the Scolioscan system (Model SCN801: Telefield Medical Imaging Ltd., Hong Kong), as described and tested for reliability in earlier studies on scoliosis (**Figure 1**).<sup>9-14</sup> This system uses a linear ultrasound probe (center frequency of 7.5 MHz and a width of 75 mm) for freehand scanning and a sensor to track the position and 3D orientation of the probe while scanning. The patients stand upright with their arms on the side and can breathe normally during the scanning, which takes approximately 1–2 min.



**Figure 1.** *The Scolioscan system.*

After scanning from level S1 to level T1, the device creates a 2D coronal reconstruction of the spine and the system software automatically reconstructs a midline through the shadows of all SP, to calculate the thoracic and lumbar ultrasound angles (**Figure 2**). The radiographs, which were part of the standard care of the included AIS patients and made on the same day as the ultrasound images, were manually measured using software in the local picture archiving and communication system (PACS) to determine the thoracic and lumbar Cobb angles, as described by the Scoliosis Research Society.<sup>15</sup> Two observers measured each curve, and the mean of both observers was used in this study as the radiographic Cobb angle.

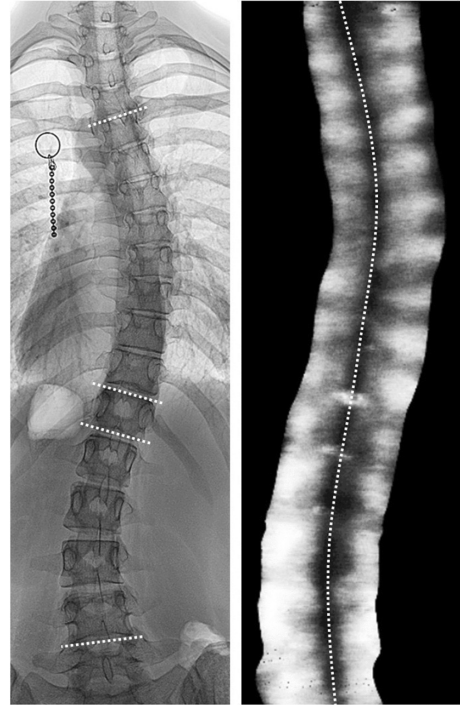


**Figure 2.** On the left side, the measurement of the Cobb angle on anterior–posterior radiography of the complete spine in an AIS patient is shown. On the right side, a coronal ultrasound image of the same patient is shown. The system software automatically drew a line through the bone shadows of all spinous process, to calculate the thoracic and lumbar ultrasound angles.

### Statistical analysis

Descriptive statistics were calculated for both groups (equation creation group and validation group): means, standard deviations and ranges for continuous variables such as age and Cobb angle (tested with independent samples t tests), and numbers and percentages for categorical variables such as the number of girls in each group (tested with Pearson's Chi-squared tests). A simple linear regression analysis between the ultrasound and radiographic Cobb angles described the determination coefficients ( $R^2$ ) and regression coefficients—without a constant in the equation—to create the equation: expected Cobb angle = regression coefficient  $\times$  ultrasound angle for both thoracic and lumbar curves. Additionally, the  $R^2$ -values for the linear regression analyses with a constant in the equation were described. In the validation group, the equations were used to calculate expected Cobb angles and were compared to the radiographic Cobb angles to test the validity (linear regression) and accuracy (mean absolute difference (MAD), maximum error and Bland–Altman plot) of the equations. Post hoc linear regression analyses between the difference and the mean of expected and radiographic Cobb angles were done for both thoracic and lumbar curves to check for proportional bias, i.e., if curve severity influences the amount of variation between expected and radiographic Cobb angles. SPSS Statistics 25.0.0 for Windows (IBM, Armonk, NY, USA) was used for statistical analysis. The level of significance was set at 0.05.

## Results

### Study population

From 86 initially recruited patients, five were excluded for being under the age of 10, one had a congenital spinal malformation, three could not be planned for ultrasound investigation on the same day as the radiograph, five had insufficient ultrasound investigations (two had their scapula excessively overlapping the thoracic spine, and three had loss of proper probe contact in the lumbar region) and two had insufficient radiography investigations. (One had only forward/lateral bending images, and one was taken seated.) Thereafter, a total of 70 patients were included, 54 in the equation creation group and 16 in the validation group. There were no significant differences in age, sex, ultrasound angles and radiographic Cobb angles (**Table 1**).

|                             | Creation group<br><i>n</i> = 54 | Validation group<br><i>n</i> = 16 | <i>p</i> |
|-----------------------------|---------------------------------|-----------------------------------|----------|
| Age (years)                 |                                 |                                   |          |
| Mean (SD)                   | 14.7 (2.0)                      | 13.9 (2.1)                        | 0.195    |
| Range                       | 10.1–17.5                       | 10.6–17.2                         |          |
| Girls                       |                                 |                                   |          |
| <i>n</i> (%)                | 43 (80%)                        | 13 (81%)                          | 0.887    |
| Ultrasound angle (°)        |                                 |                                   |          |
| Main thoracic curve         |                                 |                                   |          |
| Mean (SD)                   | 26.5 (14.1)                     | 23.1 (11.8)                       | 0.387    |
| Range                       | 5.5–73.6                        | 6.5–43.2                          |          |
| Main lumbar curve           |                                 |                                   |          |
| Mean (SD)                   | 20.4 (10.5)                     | 22.2 (10.4)                       | 0.566    |
| Range                       | 1.5–50.7                        | 3.4–44.9                          |          |
| Radiographic Cobb angle (°) |                                 |                                   |          |
| Main thoracic curve         |                                 |                                   |          |
| Mean (SD)                   | 38.4 (20.5)                     | 31.4 (19.1)                       | 0.226    |
| Range                       | 6.6–89.6                        | 2.8–56.1                          |          |
| Main lumbar curve           |                                 |                                   |          |
| Mean (SD)                   | 26.3 (13.0)                     | 29.4 (15.6)                       | 0.428    |
| Range                       | 1.5–61.9                        | 10.8–80.0                         |          |

*SD* standard deviation

**Table 1.** Patient characteristics

### Equation creation

Significant correlations were observed between ultrasound angles and radiographic Cobb angles of thoracic ( $R^2=0.968$  with no constant and  $R^2=0.859$  with constant in equation,  $p<0.001$ ) and lumbar ( $R^2=0.923$  with no constant and  $R^2=0.647$  with constant in equation,  $p<0.001$ ) curves. The linear regression coefficient for thoracic curves was 1.43 (95%CI:1.36–



1.50) and for lumbar curves was 1.23 (95%CI:1.13–1.32). So, the equations to calculate the expected Cobb angle based on the ultrasound angle were *thoracic Cobb angle* =  $1.43 \times \text{ultrasound angle}$  and *lumbar Cobb angle* =  $1.23 \times \text{ultrasound angle}$  (**Figure 3**).

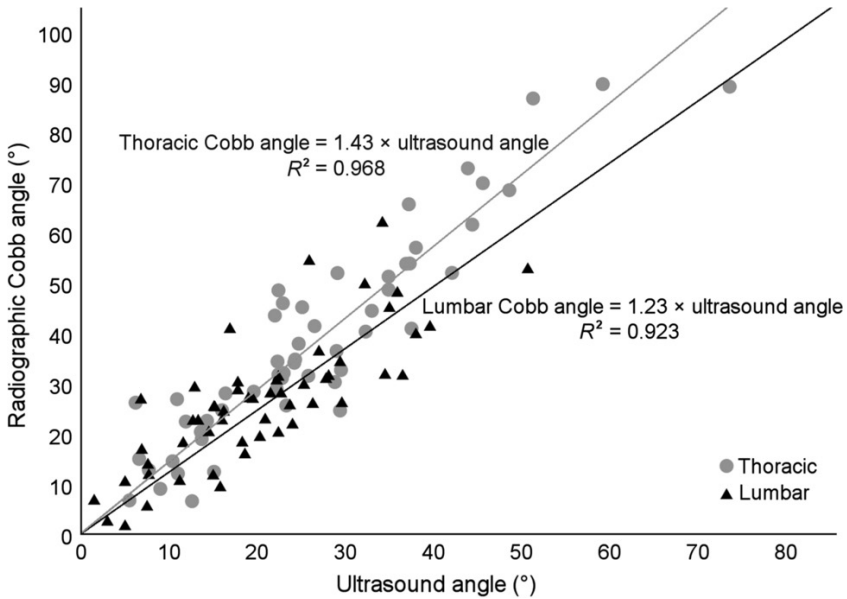


**Figure 3.** To create the equations, a linear regression analysis between ultrasound angles and radiographic Cobb angles in 54 AIS patients was done for thoracic and lumbar curves. The scatter plot, linear regression and equation:  $\text{Cobb angle} = \text{regression coefficient} \times \text{ultrasound angle}$ , are shown. The linear regression coefficient for thoracic curves was 1.43 (95% CI:1.36–1.50) and for lumbar curves was 1.23 (95% CI:1.13–1.32). Also, the coefficients of determination ( $R^2$ , with no constant in the equation) are shown for both linear regressions.

#### Equation validation

The expected Cobb angles (calculated with the created equation, based on ultrasound angles) correlated with the radiographic Cobb angles of thoracic ( $R^2 = 0.959$  with no constant and  $R^2 = 0.844$  with constant in equation,  $p < 0.001$ ) and lumbar ( $R^2 = 0.936$  with no constant and  $R^2 = 0.695$  with constant in equation,  $p < 0.001$ ) curves. The mean expected Cobb angle of the thoracic curves was  $33.0^\circ \pm 16.9^\circ$  and the radiographic Cobb angle was  $31.4^\circ \pm 19.1^\circ$  ( $p = 0.406$ ); the MAD was  $6.5^\circ \pm 3.9^\circ$  and the maximum error was  $14.3^\circ$ . For lumbar curves, the mean expected Cobb angle was  $27.2^\circ \pm 12.7^\circ$  and the mean radiographic Cobb angle was  $29.4^\circ \pm 15.6^\circ$  ( $p = 0.328$ ); the MAD was  $7.3^\circ \pm 4.7^\circ$  and the maximum error was  $18.9^\circ$ .

Bland–Altman plots between expected Cobb angles and radiographic Cobb angles are shown in **Figure 4**. There was no significant correlation between the difference and mean of expected and radiographic Cobb angles for thoracic ( $p=0.838$ ) and lumbar ( $p=0.140$ ) curves, indicating that there was no proportional bias, i.e., curve severity did not influence the amount of variation.

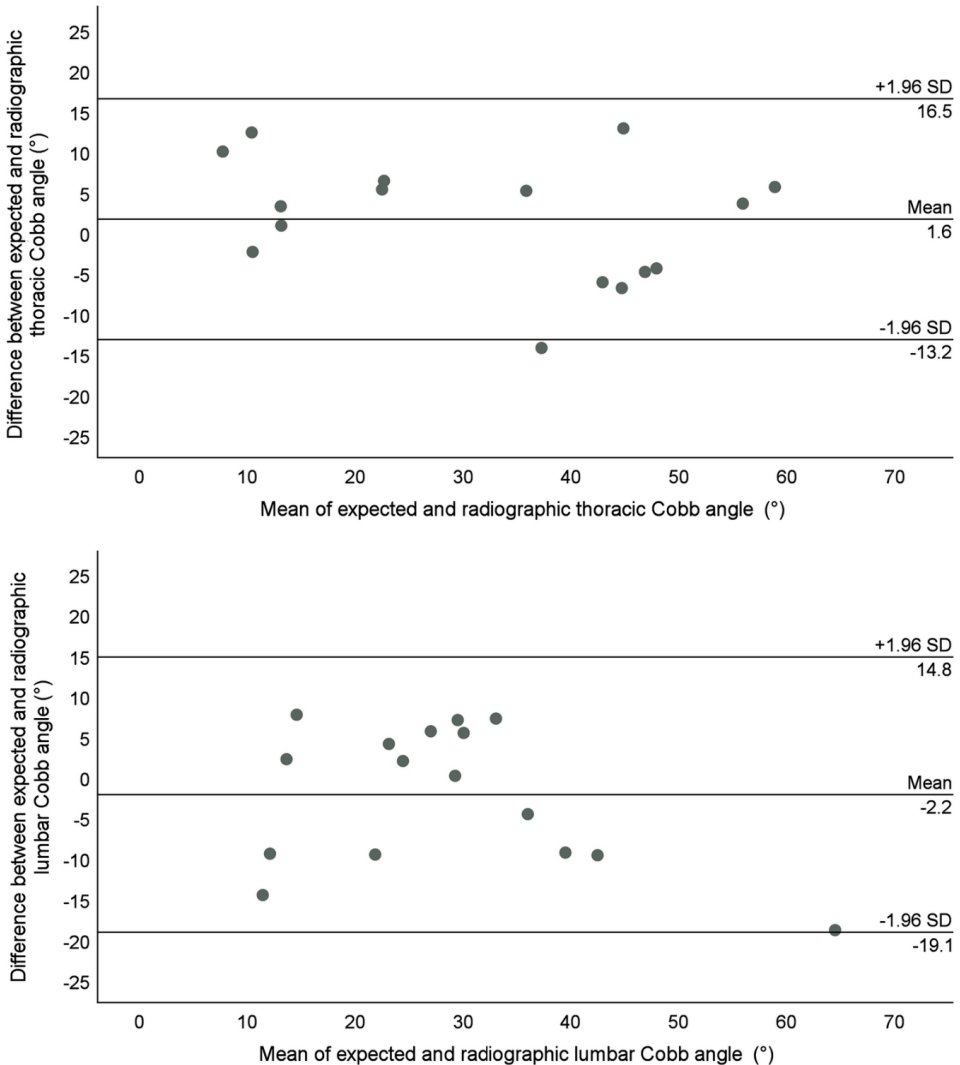


**Figure 4.** To show accuracy of the equations, the agreement between expected Cobb angle (calculated with thoracic Cobb angle =  $1.43 \times$  ultrasound angle and lumbar Cobb angle =  $1.23 \times$  ultrasound angle) and radiographic Cobb angle is shown in Bland–Altman plots, separately for thoracic (figure above) and lumbar curves (figure below).

## Discussion

Conventional upright radiography is the most used imaging method for the scoliotic spine, resulting in more radiation exposure and an increased incidence of cancer as compared to the general population.<sup>3,4</sup> To reduce the potential radiation, alternatives have been sought. Ultrasound imaging is a potential alternative, and good-to-excellent correlations were described previously between ultrasound angles and radiographic Cobb angles.<sup>7-11</sup> However, the ultrasound imaging systematically underestimates the radiographic Cobb angle, and therefore, to implement ultrasound in AIS clinics, a properly developed and validated equation is essential. The purpose of this study was to create and cross-validate an equation to calculate the expected Cobb angle using ultrasound measurements of the AIS spine. Excellent correlations between ultrasound angles and radiographic Cobb angles were observed for both thoracic ( $R^2=0.968$ ) and lumbar ( $R^2=0.923$ ) curves. The equations as derived from the data were *thoracic Cobb angle* =  $1.43 \times$  *ultrasound angle* and *lumbar Cobb angle* =  $1.23 \times$  *ultrasound angle*. The expected Cobb angles calculated by the equations were valid (excellent correlations with radiographic Cobb angles, thoracic:  $R^2=0.959$  and lumbar:  $R^2=0.936$ ) and accurate (**Figure 4**).

The correlations between the ultrasound and radiographic coronal spinal angles of AIS patients, as described in this study, are comparable to previous studies ( $R^2=0.722-0.991$ ).<sup>9-11</sup> Also, the regression coefficient between ultrasound angles and radiographic Cobb angle of 1.43 for thoracic curves and 1.23 for lumbar curves found in this study is in the range of previous studies (thoracic: 1.20–1.55 and lumbar: 1.15–1.34).<sup>9,10</sup>

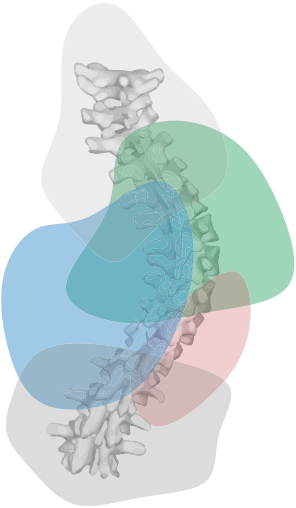
The concept of one spinal anatomical parameter strongly correlating with the Cobb angle and creating an equation to translate between these two is demonstrated before by Korovessis et al. in 1996 for the scoliometer used in physical examination of scoliosis patients.<sup>16</sup> The current study is the first to create and cross-validate an equation to calculate the expected Cobb angle using ultrasound measurements of the spine in AIS patients. The expected Cobb angles calculated by the equations were valid and accurate. Also, the MAD was  $6.5^\circ$  to  $7.3^\circ$  and the Bland–Altman plots show that the expected Cobb angle is in 23 out of 28 cases within  $10^\circ$  of the radiographic Cobb angle (**Figure 4**). This is comparable to the intra- and interobserver variability of around  $5^\circ$  reported for radiographic Cobb angle measurements of the same curve.<sup>17,18</sup> The automatic software method used in this study to determine ultrasound angles has ICCs for intra- and interobserver reliabilities of 1.00 and 1.00 for the same ultrasound image analyzed again and 0.97 and 0.94 for different ultrasound images of the same curve.<sup>10</sup> This is better than or at least similar to the ICCs of the conventional Cobb angle, ranging from 0.83 to 0.99 as determined on radiographs.<sup>19</sup>

The results of this study suggest that ultrasound measurements of curve severity in AIS are valid and accurate as conventional radiography. However, three important questions remain unanswered so far. First, despite demonstrating a similar variability in spinal curvature determination by ultrasound versus radiography, for ultrasound to replace radiography in AIS clinics, the level of accuracy and safety in determining clinically relevant cutoff points has to be studied, i.e., the sensitivity and specificity of the ultrasound system for indicating observation, exercise therapy, brace therapy and/or spinal surgery. Second, the cross-sectional design of this study makes it impossible to test validity and accuracy of monitoring curve progression, which can be tested when ultrasound and radiography data are gathered on multiple time points within the same AIS patient. Third, this study was conducted in AIS patients seen in a tertiary spine center in the Netherlands, and it remains unclear whether the equation can be used for other populations as well.

In conclusion, the spinal curvature in AIS measured by ultrasound can be accurately calculated to the expected Cobb angle with simple equations: *thoracic Cobb angle* =  $1.43 \times \text{ultrasound angle}$  and *lumbar Cobb angle* =  $1.23 \times \text{ultrasound angle}$ . This finding supports the possible implementation of ultrasound in AIS clinics, which can lead to less frequent radiography, lowering the cumulative ionizing radiation dose and subsequently the cancer risk in young AIS patients.

## References

1. Cheng JC, Castelein RM, Chu WC et al (2015) Adolescent idiopathic scoliosis. *Nat Rev Dis Prim* 1:15–30
2. Cobb JR (1948) Outline for study of scoliosis. *Am Acad Orthop Surg Instr Course Lect* 5:261–275
3. Presciutti SM, Karukanda T, Lee M (2014) Management decisions for adolescent idiopathic scoliosis significantly affect patient radiation exposure. *Spine J* 14:1984–1990
4. Simony A, Hansen EJ, Christensen SB et al (2016) Incidence of cancer in adolescent idiopathic scoliosis patients treated 25 years previously. *Eur Spine J* 25:3366–3370
5. Wehrli FW (2013) Magnetic resonance of calcified tissues. *J Magn Reson* 229:35–48
6. Newton PO, Khandwala Y, Bartley CE et al (2016) New EOS imaging protocol allows a substantial reduction in radiation exposure for scoliosis patients. *Spine Deform* 4:138–144
7. Suzuki S, Yamamuro T, Shikata J et al (1989) Ultrasound measurement of vertebral rotation in idiopathic scoliosis. *J Bone Joint Surg Br* 71:252–255
8. Zheng R, Chan ACY, Chen W et al (2015) Intra- and inter-rater reliability of coronal curvature measurement for adolescent idiopathic scoliosis using ultrasonic imaging method—a pilot study. *Spine Deform* 3:151–158
9. Zheng Y-P, Lee TT-Y, Lai KK-L et al (2016) A reliability and validity study for Scolioscan: a radiation-free scoliosis assessment system using 3D ultrasound imaging. *Scoliosis spinal Disord* 11:13
10. Brink RC, Wijdicks SPJ, Tromp IN et al (2018) A reliability and validity study for different coronal angles using ultrasound imaging in adolescent idiopathic scoliosis. *Spine J* 18:979–985
11. Wong Y, Lai KK, Zheng Y et al (2019) Is radiation-free ultrasound accurate for quantitative assessment of spinal deformity in idiopathic scoliosis (IS): a detailed analysis with EOS radiography on 952 patients. *Ultrasound Med Biol* 45:2866–2877
12. Cheung C-WJ, Zheng Y (2010) Development of 3-D ultrasound system for assessment of adolescent idiopathic scoliosis (AIS), pp 584–587
13. Cheung C-WJ, Siu-Yin Law, Yong-Ping Zheng (2013) Development of 3-D ultrasound system for assessment of adolescent idiopathic scoliosis (AIS): And system validation. In: 2013 35th Annual International Conference of the IEEE Engineering in Medicine and Biology Society (EMBC). IEEE, pp 6474–6477
14. Cheung C-WJ, Zhou G-Q, Law S-Y et al (2015) Ultrasound volume projection imaging for assessment of scoliosis. *IEEE Trans Med Imaging* 34:1760–1768
15. O'Brien MF, Kuklo TR, Blanke KM, Lenke LG (2008) Radiographic measurement manual. Medtronic Sofamor Danek USA, Memphis, USA, pp 11–30
16. Korovessis PG, Stamatakis MV (1996) Prediction of scoliotic cobb angle with the use of the scolioscan. *Spine (Phila Pa 1976)* 21:1661–1666
17. Morrissy RT, Goldsmith GS, Hall EC et al (1990) Measurement of the Cobb angle on radiographs of patients who have scoliosis. Evaluation of intrinsic error. *J Bone Joint Surg Am* 72:320–327
18. Carman DL, Browne RH, Birch JG (1990) Measurement of scoliosis and kyphosis radiographs. Intraobserver and interobserver variation. *J Bone Joint Surg Am* 72:328–333
19. Langensiepen S, Semler O, Sobottke R et al (2013) Measuring procedures to determine the Cobb angle in idiopathic scoliosis: a systematic review. *Eur Spine J* 22:2360–2371

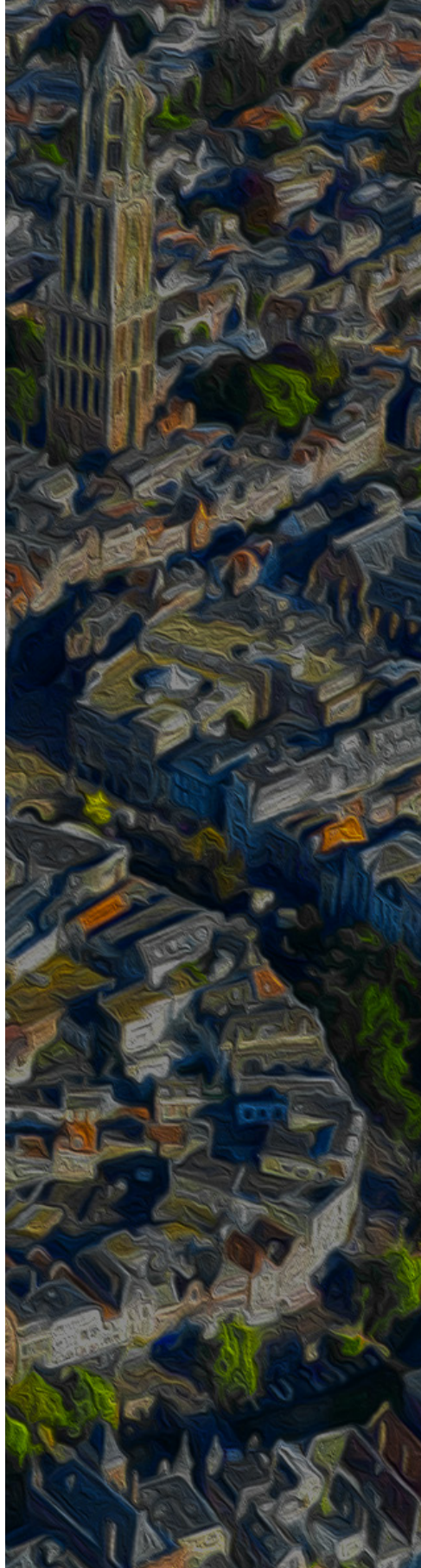


# 8

## Anterior Lengthening in Scoliosis occurs only in the Disc and is Similar in Different types of Scoliosis

Steven de Reuver  
Rob C. Brink  
Jelle F. Homans  
Ludvig Vavruch  
Hans Tropp  
Moyo C. Kruyt  
Marijn van Stralen  
René M. Castelein

*The Spine Journal. 2020 Oct;20(10):1653-1658.*



## ABSTRACT

**Background context.** Relative anterior spinal overgrowth was proposed as a generalized growth disturbance and a potential initiator of adolescent idiopathic scoliosis (AIS). However, anterior lengthening has also been observed in neuromuscular (NM) scoliosis and was shown to be restricted to the apical areas and located in the intervertebral discs, not in the bone. This suggests that relative anterior spinal overgrowth does not rightfully describe anterior lengthening in scoliosis, as it seems not a generalized active growth phenomenon, nor specific to AIS.

**Methods.** CT-scans were included of patients in whom a short segment congenital malformation had led to a long thoracic compensatory curve without bony abnormality. Out of 143 congenital scoliosis patients, 18 fit the criteria and compared with 30 nonscoliotic controls, 30 AIS and 30 NM scoliosis patients. Of each vertebral body and intervertebral disc in the compensatory curve, the anterior and posterior length was measured on CT-scans in the exact mid-sagittal plane, corrected for deformity in all three planes. The AP% was calculated for the total compensatory curve (Cobb-to-Cobb) and for the vertebral bodies and the intervertebral discs separately.

**Results.** The total AP% of the compensatory curve in congenital scoliosis showed lordosis (+1.8%) that differed from the kyphosis in nonscoliotic controls (-3.0%;  $p < .001$ ) and was comparable to the major curve in AIS (+1.2%) and NM scoliosis (+0.5%). This anterior lengthening was not located in the bone; the vertebral body AP% showed kyphosis (-3.2%), similar to nonscoliotic controls (-3.4%) as well as AIS (-2.5%) and NM scoliosis (-4.5%;  $p = 1.000$ ). However, the disc AP% showed lordosis (+24.3%), which sharply contrasts to the kyphotic discs of controls (-1.5%;  $p < .001$ ), but was similar to AIS (+17.5%) and NM scoliosis (+20.5%).

**Conclusions.** The current study on compensatory curves in congenital scoliosis confirms that anterior lengthening is part of the three-dimensional deformity in different types of scoliosis and is exclusively located in the intervertebral discs. The bony vertebral bodies maintain their kyphotic shape, which indicates that there is no active anterior bony overgrowth. Anterior lengthening appears to be a passive result of any scoliotic deformity, rather than being related to the specific cause of AIS.



## Introduction

Adolescent idiopathic scoliosis (AIS) is a three-dimensional (3D) deformity of the spine and trunk. Recent research has shed light on the role of the unique biomechanics that act on the fully upright human spine and its effect on rotational stability.<sup>1</sup> It has been known for a long time that, in idiopathic scoliosis, the anterior part of the spine is longer than posterior, transforming the global thoracic kyphosis into a rotated apical lordosis.<sup>2-4</sup> In earlier studies, this phenomenon was called relative anterior spinal overgrowth (RASO) and was suggested to be part of the etiology of AIS.<sup>5-7</sup> However, recent studies have shown that this additional anterior length is present in both the primary and compensatory curves in idiopathic scoliosis, predominantly around the apex, whereas the junctional zones do not exhibit this length discrepancy, thus excluding a generalized growth disturbance.<sup>8</sup> Furthermore, this phenomenon was found to be located exclusively in the intervertebral disc, while the bony structures (vertebral bodies) showed an anterior-posterior ratio similar to nonscoliotic controls.<sup>9</sup> That finding contradicts the often cited vicious cycle theory: uneven loading of a vertebra would result in decreased growth of the loaded side in accordance with the Heuter-Volkman law causing wedging of the vertebra and subsequently even more asymmetric loading and curve increase.<sup>10,11</sup> Finally, in neuromuscular (NM) scoliosis, the same phenomenon of additional anterior spinal length caused by anterior expansion of the disc was observed.<sup>12</sup>

These findings suggest that anterior lengthening is an integral part of a more generalized mechanism that occurs in more types of scoliosis. To confirm this hypothesis, a similar phenomenon would be expected in scoliosis of other origins. The objective of this study is to further elucidate the role of this anterior lengthening of the spine in the overall scoliotic mechanism. Therefore, we determined the anterior-posterior length discrepancy (AP%) in the compensatory thoracic curves of congenital scoliosis and compared the findings with the nonscoliotic spine and major curves of AIS and NM scoliosis.

## Materials and methods

### Study population

Computed tomography (CT) scans of every patient with a diagnosis of congenital scoliosis, made from February 2006 until February 2019 in a tertiary children's hospital, were screened by two observers. Patients who had a relatively short area of the spine with a congenital anomaly in the cervical/high-thoracic or lumbar/low-thoracic area, and had subsequently developed a compensatory thoracic scoliotic curve in the area of the spine without congenital anomalies, were included (**Figure 1**).

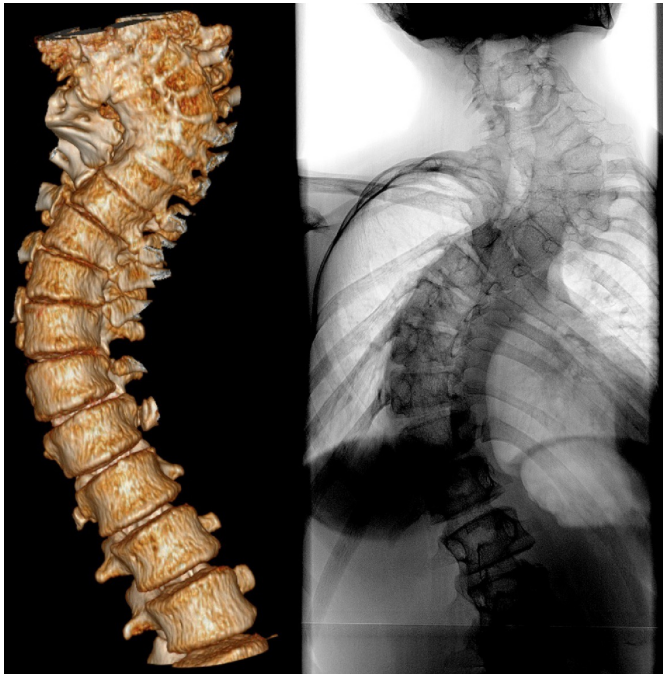


**Figure 1.** A reconstructed 3D image based on the CT-scan and an anterior-posterior radiograph of an included patient with congenital spinal anomalies (C2–T6). The thoracic compensatory curve (T7–L1, apex: disc T10/11, Cobb angle: 61°) with no congenital spinal anomalies, is the part of the spine that is analyzed in this study.

Compensatory curves were considered thoracic if the apex was anywhere at the level T2 through the T11–T12 disc, following the Scoliosis Research Society guidelines.<sup>13</sup> Patients not in supine position during CT scanning, with vertebral anomalies in all curves, with no thoracic compensatory curve, with incomplete CT scans (no visualization of all vertebrae in the compensatory curve), with compensatory curves smaller than 15° Cobb angle and/or with a history of spinal surgery before CT scanning were excluded (**Table 1**). Patient characteristics including sex and age at CT investigation were extracted from the electronic patients record. All included CT scans were assessed by a senior orthopedic surgeon to classify the congenital deformity that induced scoliosis, according to the classification of McMaster (**Table 1**).<sup>14</sup> Curve characteristics, including Cobb angles, level of apex and number of vertebrae in the compensatory thoracic curve were gathered using digitally reconstructed radiographs of the CT scans.<sup>13,15</sup> The congenital scoliosis patients were compared with nonscoliotic controls, AIS and NM scoliosis patients. These patients were part of an earlier published database of NM scoliosis patients (mostly diagnosed with cerebral palsy, psychomotor retardation, and muscular dystrophy) and age-matched AIS patients, of which we used the patient characteristics and CT scan data in the current study.<sup>12</sup>

**Excluded congenital scoliosis patients (n=125)**

|                                 |    |
|---------------------------------|----|
| Anomalies in all curves         | 29 |
| Compensatory curve not thoracic | 6  |
| Incomplete CT scan              | 33 |
| Cobb angle <15°                 | 17 |
| Post-operative CT scan only     | 40 |

**Included congenital scoliosis patients (n=18)**

|                         |    |
|-------------------------|----|
| Failure of formation    | 7  |
| Failure of segmentation | 11 |

**Table 1.** A total of 143 initial patients with congenital scoliosis were screened. The number of excluded patients per criterion is shown. Also, the primary congenital anomaly that induced scoliosis in the included patients is displayed.

CT measurements

CT scans were analyzed with in-house developed software (ScoliosisAnalysis 4.1; Image Sciences Institute, Utrecht, the Netherlands, developed with MeVisLab, MeVis Medical Solutions AG, Bremen, Germany) to determine the AP% in the true mid-sagittal plane of the thoracic compensatory curves in congenital scoliosis patients. This software used a validated and semiautomatic image processing method, with an intraclass correlation coefficient of 0.99 and an interclass correlation coefficient of 0.99 for determining the anterior-posterior length ratio, as is used in the current study.<sup>16</sup> The method consisted of three steps:

First, the observer selected the lower and upper endplate of each vertebra involved in the compensatory thoracic curve, between the two most tilted vertebrae in the coronal plane (Cobb-to-Cobb) as assessed on the digitally reconstructed radiograph.<sup>15</sup> In the true transverse plane of the endplate, achieved by correcting the sagittal and coronal tilt (**Figure 2a & 2b**), each endplate and adjacent spinal canal was manually segmented (**Figure 2c**).

Second, the semiautomatic software calculated the centroid of the vertebral endplate and spinal canal, and reconstructed a line through both points to get the anterior-posterior axis of each endplate. The anterior and posterior landmarks of the endplate were based on the intersection of this axis and the contours of the endplate, resulting in 3D Cartesian coordinates for each individual endplate of the compensatory thoracic curve (**Figure 2c**).

Third, the distance between the anterior midline point of the lower endplate and the upper endplate of the same vertebra was calculated, and similarly for the posterior points, to determine the anterior and posterior length of the vertebral body. The same points were used to determine the anterior and posterior length of the intervertebral disc. This analysis was done for all vertebral bodies and discs included in the curve (**Figure 2d**).

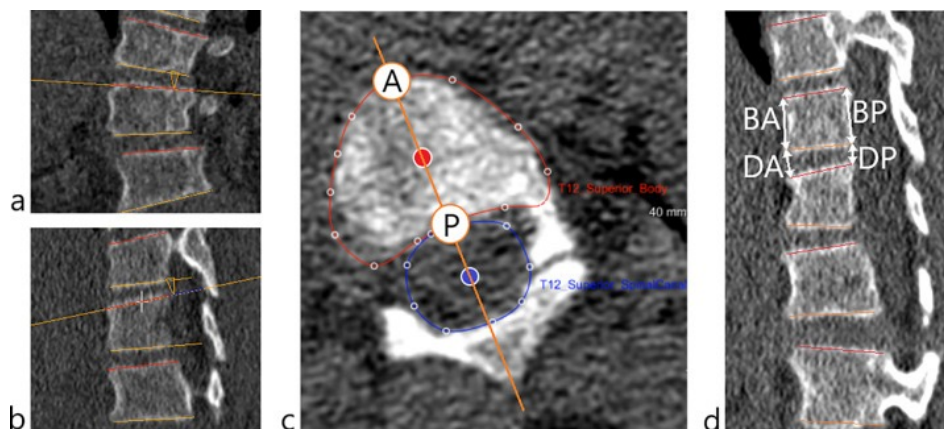


**Figure 2.** The method to determine the 3D orientation of the lower and upper endplates of included vertebrae in the compensatory thoracic curve is shown. CT-scans were assessed with use of semi-automatic software. First, the view was adjusted for coronal (**a**) and sagittal (**b**) tilt. Next, in the true transverse plane of the endplate, the vertebral body and spinal canal were manually segmented (**c**). The software automatically calculated the midpoint of the vertebral body and the spinal canal, and drew a line through both points to get the true anterior-posterior axis. The intersection of this axis with the vertebral body segmented cortex are the anterior (A) and posterior (P) landmarks of the endplate. This was done for all lower and upper endplates in the thoracic compensatory curve and 3D coordinates of all anterior and posterior landmarks were gathered. Finally, distances between them were calculated: the body-anterior (BA) length, body-posterior (BP) length, disc-anterior (DA) length and disc-posterior (DP) length (**d**).

#### Anterior-posterior length discrepancy

To describe the difference in length between the anterior and posterior side, the ratio was calculated as:  $[(\text{anterior length} - \text{posterior length}) / (\text{posterior length})] \times 100\%$ , shortened to AP%. The AP% was calculated for the total compensatory thoracic curve (Cobb-to-Cobb) in the congenital scoliosis patients, for the matched corresponding levels of nonscoliotic controls and for the primary thoracic curves in AIS and NM scoliosis. The AP% was calculated for the whole compensatory curve (total AP%), as well as the vertebral bodies (body AP%) and intervertebral discs (disc AP%). Positive values indicate that the anterior side is longer than the posterior side.

### Statistical analysis

For this study in congenital scoliosis patients, the required sample size was calculated based on earlier data of nonscoliotic controls, AIS and NM scoliosis.<sup>12</sup> To detect equivalence in body AP%, with 80% power, a two-sided alpha of 5%, an expected body AP% of -3.1% with a standard deviation (SD) of 3.4% and a two-sided testing margin of 3.0 percentage points (chosen because beyond this margin the AP% could be positive, ie, the bodies would be lordotic instead of kyphotic), a required sample size of 12 was calculated.<sup>17</sup> Descriptive statistics were calculated and means, ranges and SD were given for normally distributed parameters. For not normally distributed parameters, medians, ranges, and interquartile ranges were given. The differences in mean AP% between congenital scoliosis, controls, AIS and NM scoliosis were tested with one-way analyses of variances with post-hoc Bonferroni correction for six pair-wise comparisons between the four groups (the p-values were multiplied by six, analogous to testing to an adjusted alpha of 0.0083). The mean AP% results are presented with  $\pm$ SD to show variability of outcome within the groups. A simple linear regression analysis was performed between the mean disc AP% and the Cobb angle per group. Statistical analyses were performed with SPSS 25.0 for Windows (IBM, Armonk, NY, USA). The statistical significance level was set at 0.05.

## Results

### Study population

Of the 143 original patients with a congenital scoliosis and an available CT-scan, 125 were excluded and a total of 18 patients were included in the study. Exclusion reasons and the primary (congenital) diagnoses are described in **Table 1**, and the patient demographics are described in **Table 2**. From an earlier published database a total of 30 CT scans of nonscoliotic spines without other spinal anomalies were included as controls, and for comparison 30 patients with NM scoliosis and 30 patients with AIS were included as well.<sup>12</sup>

| <b>Excluded congenital scoliosis patients (n=125)</b> |    |
|---|----|
| Anomalies in all curves                               | 29 |
| Compensatory curve not thoracic                       | 6  |
| Incomplete CT scan                                    | 33 |
| Cobb angle <15°                                       | 17 |
| Post-operative CT scan only                           | 40 |
| <b>Included congenital scoliosis patients (n=18)</b>  |    |
| Failure of formation                                  | 7  |
| Failure of segmentation                               | 11 |

**Table 1.** Exclusion reasons and the primary (congenital) diagnoses

|  | <b>Congenital<br/>(n=18)</b> | <b>AIS<br/>(n=30)</b> | <b>NM<br/>(n=30)</b> | <b>Controls<br/>(n=30)</b> |
|--|------------------------------|-----------------------|----------------------|----------------------------|
| <b>Mean years of age±SD</b>                                  | 12.3±4.6                     | 15.3±2.4              | 15.4±4.2             | 15.2±1.2                   |
| <b>Range</b>   | 6–23                         | 11–19                 | 9–24                 | 11–17                      |
| <b>Number of girls (%)</b>                                   | 12 (67%)                     | 25 (83%)              | 17 (57%)             | 19 (63%)                   |
| <b>Mean Cobb angle±SD</b>                                    | 42.3°±14.9°                  | 55.8°<br>±12.9°       | 51.5°<br>±21.4°      |                            |
| <b>Range</b>   | 18°–79°                      | 21°–81°               | 19°–101°             |                            |
| <b>Median apex (IQR)</b>                                     | T9 (T7–T11)                  | T9 (T8–<br>T9)        | T8 (T7–<br>T10)      |                            |
| <b>Range</b>   | T2–T12                       | T6–T10                | T6–T12               |                            |
| <b>Median number of<br/>vertebrae in the<br/>curve (IQR)</b> | 6 (5–7)                      | 7 (7–8)               | 9 (8–9)              |                            |
| <b>Range</b>   | 4–8                          | 6–9                   | 5–12                 |                            |

**Table 2.** Demographics of included patients with congenital scoliosis, adolescent idiopathic scoliosis (AIS), neuromuscular (NM) scoliosis and controls.

### Total curve

The compensatory curves of the congenital scoliosis patients had a mean Cobb angle of  $42.3^\circ \pm 14.9^\circ$  with a range of  $18^\circ$  to  $79^\circ$  (**Table 2**). The mean AP% of the total thoracic compensatory curves (Cobb-to-Cobb) in congenital scoliosis patients was  $+1.8 \pm 4.7\%$ , indicating that the mean length of the spine at the anterior side was 1.8% greater than the posterior side, indicating a thoracic lordosis. This total AP% differed from the nonscoliotic control group, where the mean anterior length of the spine was shorter than the mean posterior length ( $-3.0 \pm 1.6\%$ ;  $p < .001$ ) indicating thoracic kyphosis. The total AP% in compensatory curves in congenital scoliosis ( $+1.8 \pm 4.7\%$ ) was not significantly different from the major curves in AIS ( $+1.2 \pm 2.2\%$ ) and NM scoliosis ( $+0.5 \pm 4.1\%$ ;  $p = 1.000$ ; **Figure 3**).

### Vertebral bodies

The mean body AP% of the vertebral bodies that were part of the thoracic compensatory curves in congenital scoliosis patients was  $-3.2 \pm 4.7\%$ , indicating kyphosis. This body AP% was not significantly different from controls ( $-3.4\% \pm 1.4\%$ ;  $p = 1.000$ ), as well as from the major curves in AIS and NM scoliosis ( $-2.5 \pm 2.6\%$  and  $-4.5 \pm 4.3\%$ ;  $p = 1.000$ ; **Figure 3**).

### Intervertebral discs

The mean disc AP% of the intervertebral discs that were part of the thoracic compensatory curves in congenital scoliosis patients was  $+24.3 \pm 12.9\%$ , indicating lordosis, which differed significantly from the kyphotic discs in controls ( $-1.5 \pm 5.6\%$ ;  $p < .001$ ). The disc AP% in compensatory curves in congenital scoliosis was not significantly different from the major curves in AIS ( $+17.5 \pm 12.7\%$ ) and NM scoliosis ( $+20.5 \pm 16.3\%$ ;  $p \geq .427$ ; **Figure 3**).

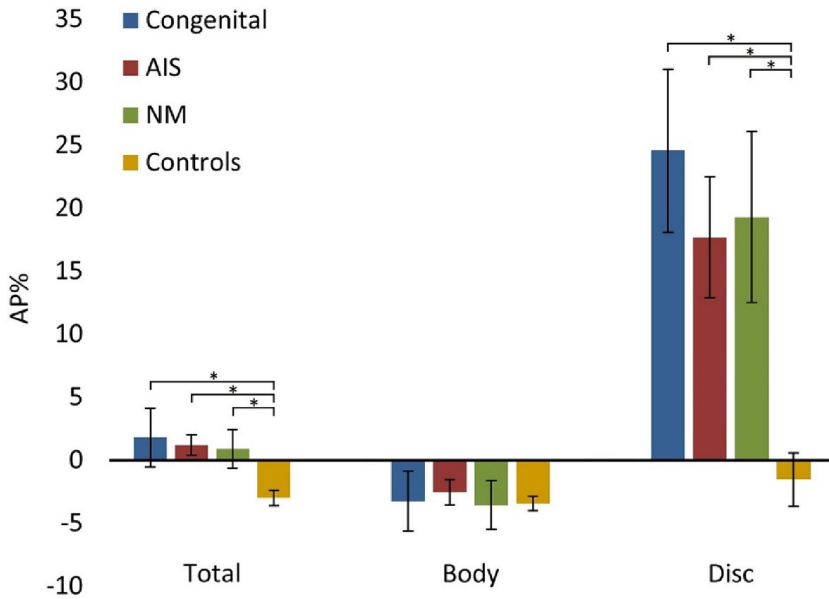


**Figure 3.** Results bar graph. The mean anterior-posterior length discrepancy (AP%) is shown for the total spine, the vertebral bodies and the intervertebral discs. This included the part of the spine involved in the compensatory thoracic curve in congenital scoliosis, the main thoracic curve in adolescent idiopathic scoliosis (AIS), the main thoracic curve in neuromuscular (NM) scoliosis and the corresponding levels in controls. Positive AP% indicates a larger anterior length than posterior length. The error bars indicate the 95% confidence interval of means. Significant differences are indicated with asterisks (\*).

### Curve severity and disc AP%

The mean disc AP% of congenital scoliosis, AIS and NM scoliosis patients showed a significant correlation with the Cobb angle of the included curves ( $p = .011$ ), that is, in severe curves the AP% of the disc was more pronounced (**Figure 4**).

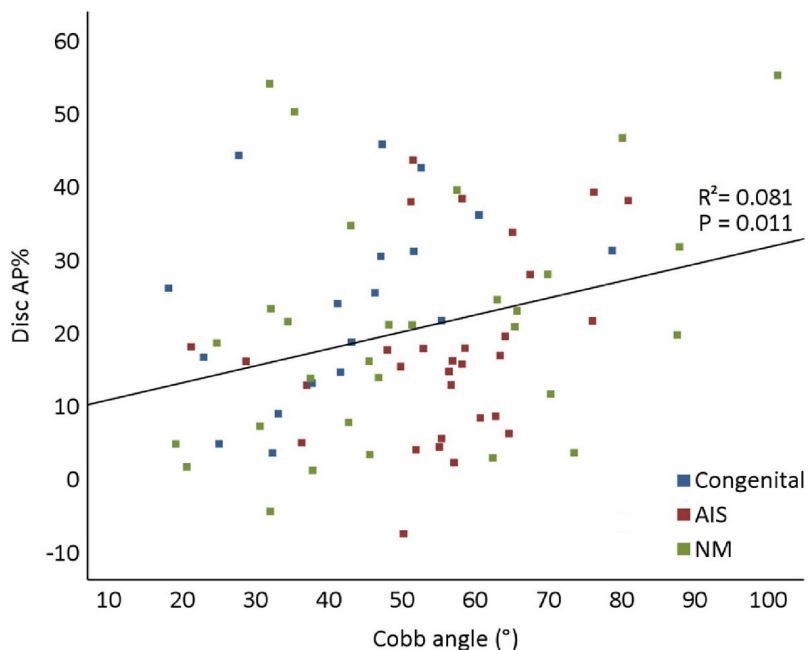


**Figure 4.** Disc vs. Cobb angle scatter plot. The mean anterior-posterior length discrepancy (AP%) of the intervertebral discs is plotted against the Cobb angle for all included patients with adolescent idiopathic scoliosis (AIS), congenital scoliosis and neuromuscular (NM) scoliosis. Linear regression analysis showed a significant correlation between curve severity (Cobb angle) and disc AP% ( $R^2=0.081$  and  $p=.011$ ).

## Discussion

The objective of this study was to find further evidence that anterior lengthening is a generalized mechanism that occurs in different types of scoliosis and that it consistently occurs in the disc, not in the bone. Isolated congenital malformations can induce long compensatory curves in otherwise normal areas of the spine, in an attempt to keep the spine aligned (**Figure 1**). We studied these compensatory curves in congenital scoliosis and found a thoracic lordosis (+1.8%), different from the kyphosis in nonscoliotic controls (−3.0%) and comparable to the major curves in AIS (+1.2%) and NM scoliosis (+0.5%). The results clearly show there was no anterior lengthening in the bony vertebrae, with a similar degree of vertebral kyphosis present in the congenital scoliosis patients (−3.2%), nonscoliotic controls (−3.4%), AIS (−2.5%), and NM scoliosis (−4.5%). This is consistent with the other recent studies on different types of scoliosis.<sup>9,12</sup> The intervertebral discs were lordotic in the compensatory curves in congenital scoliosis (+24.3%), which is in sharp contrast to the kyphotic discs of controls (−1.5%), but similar to the major curves in AIS (+17.5%) and NM scoliosis (+20.5%).



The finding of a thoracic lordosis in the scoliotic spine, instead of the normal thoracic kyphosis, was described in other studies on moderate to severe scoliosis.<sup>2-4,8</sup> However, multiple observations showed that the thoracic lordosis occurred primarily around the apex and the AP% was located exclusively in the disc, both in AIS and scoliosis of known origin (NM scoliosis).<sup>8,9,12</sup> These observations contradict the theory of a generalized anterior bony overgrowth or RASO, as part of the etiology of scoliosis.<sup>5-7</sup> Also, in the current study we observed a similar kyphotic shape of the vertebral bodies in all scoliosis types as well as nonscoliotic controls, this suggests that there is no change in bony growth in the mid-sagittal plane of the studied curve magnitudes that would fit with the vicious cycle theory as a propagator of scoliosis.<sup>10</sup> In a study of more severe and progressive scoliosis, changes in vertebral morphology in the mid-sagittal plane have been observed, although in this study the initial role of the disc was also acknowledged.<sup>18</sup> The observation in the current study of a statistically significant but weak positive correlation between disc AP% and the Cobb angle (**Figure 4**), could suggest that anterior lengthening of the disc is related to the severity of the scoliotic deformity.

In the current study, only complete CT scans of long compensatory thoracic curves in the otherwise normal spine, caused by a short congenital malformation above or below that compensatory curve, were included. This resulted in the exclusion of a large portion of congenital scoliosis patients which could have induced selection bias, despite the consecutive inclusion of all eligible patients from 2006 to 2019 of a single hospital. However, this was necessary since the strict exclusion criteria enabled comparison with recently published data on 3D morphology of AIS and NM scoliosis, as compared with nonscoliotic controls.<sup>12</sup> We were interested in the compensatory curves of congenital scoliosis, they were compared with the primary curves of AIS and NM scoliosis, thus making the underlying anatomy of the vertebrae comparable. We did not want to compare with secondary curves in AIS and NM scoliosis, since we also wanted to test the hypothesis that anterior lengthening is part of a generalized scoliotic mechanism, thus present in both primary and compensatory curves. All 3D measurements in the current study were performed on supine CT scans, excluding the effect of different gravitational loading between groups and making data fully comparable.

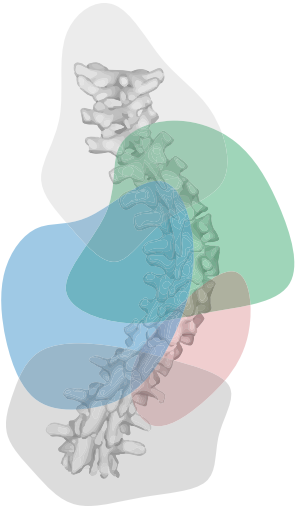
The results of the current study confirm that the lengthening of the anterior column of the spine is part of a more generalized mechanism that occurs in other types of scoliosis, irrespective of its etiology. This supports the notion that anterior lengthening or apical thoracic lordosis is not an active growth disturbance, but that it is part of every scoliotic mechanism and must be regarded as the result of the deformation, rather than its cause. Both the term RASO and the theory of vicious cycle imply active bony anterior overgrowth of the scoliotic spine, which was not observed by us in any of the studied types of scoliosis. Our explanation for the general

scoliotic mechanism is that scoliosis starts as a rotatory instability in the transverse plane, the rotation moves the involved vertebrae and discs away from the mid sagittal plane, resulting in axial unloading of the anterior spine. This results in passive expansion of the anterior side of the discs, which itself can be considered a vicious cycle, though not of the bone but rather of the soft tissues.

In conclusion, the current study on compensatory curves in congenital scoliosis expands earlier observations of anterior lengthening that appears to be part of the 3D deformity in different types of scoliosis and is exclusively located in the intervertebral discs. The bony vertebral bodies maintain their kyphotic shape, which indicates that there is no active anterior bony overgrowth. Anterior lengthening appears to be a passive result of any scoliotic deformity, rather than being related to the specific cause of AIS.

## References

1. JC Cheng, RM Castelein, WC Chu, AJ Danielsson, MB Dobbs, TB Grivas, et al. Adolescent idiopathic scoliosis *Nat Rev Dis Prim*, 1 (2015)
2. EW Somerville. Rotational lordosis; the development of single curve. *J Bone Joint Surg Br*, 34-B (1952), pp. 421-427
3. R Roaf. The basic anatomy of scoliosis. *J Bone Joint Surg Br*, 48 (1966), pp. 786-792
4. RA Dickson, JO Lawton, IA Archer, WP Butt. The pathogenesis of idiopathic scoliosis. Biplanar spinal asymmetry. *J Bone Joint Surg Br*, 66 (1984), pp. 8-15
5. X Guo, WW Chau, YL Chan, JCY Cheng. Relative anterior spinal overgrowth in adolescent idiopathic scoliosis. Results of disproportionate endochondral-membranous bone growth. *J Bone Joint Surg Br*, 85 (2003), pp. 1026-1031
6. WCW Chu, WWM Lam, Y-L Chan, BKW Ng, T-P Lam, K-M Lee, et al. Relative shortening and functional tethering of spinal cord in adolescent idiopathic scoliosis?: study with multiplanar reformat magnetic resonance imaging and somatosensory evoked potential. *Spine (Phila Pa 1976)*, 31 (2006), pp. E19-E25
7. N Newell, CA Grant, BE Keenan, MT Izatt, MJ Percy, CJ Adam. Quantifying progressive anterior overgrowth in the thoracic vertebrae of adolescent idiopathic scoliosis patients: a sequential magnetic resonance imaging study. *Spine (Phila Pa 1976)*, 41 (2016), pp. E382-E387
8. TPC Schlösser, M van Stralen, WCW Chu, T-P Lam, BKW Ng, KL Vincken, et al. Anterior overgrowth in primary curves, compensatory curves and junctional segments in adolescent idiopathic scoliosis. *PLoS One*, 11 (2016), Article e0160267
9. RC Brink, TPC Schlösser, M van Stralen, KL Vincken, MC Kruyt, SCN Hui, et al. Anterior-posterior length discrepancy of the spinal column in adolescent idiopathic scoliosis-a 3D CT study. *Spine J*, 18 (2018), pp. 2259-2265
10. IAF Stokes, RG Burwell, PH Dangerfield. Biomechanical spinal growth modulation and progressive adolescent scoliosis – a test of the “vicious cycle” pathogenetic hypothesis: Summary of an electronic focus group debate of the IBSE. *Scoliosis*, 1 (2006), p. 16
11. R Volkmann. Verletzungen und Krankheiten der Bewegungsorgane. von Pitha und Billroth Handb. der Allg. und speciellen Chir. Bd II Tl. II. Stuttgart Ferdinand Enke (1882)
12. RC Brink, TPC Schlösser, D Colo, L Vavruch, M van Stralen, KL Vincken, et al. Anterior spinal overgrowth is the result of the scoliotic mechanism and is located in the disc. *Spine (Phila Pa 1976)*, 42 (2017), pp. 818-822
13. O'Brien M, Kulkot, Blanke K, Lenke L. Radiographic measurement manual. 2008.
14. MJ McMaster. James IV lecture: congenital deformities of the spine. *J R Coll Surg Edinb*, 47 (2002), pp. 475-480
15. JR Cobb. Outline for study of scoliosis. *Am Acad Orthop Surg Instr Course Lect*, 5 (1948), pp. 261-275
16. TPC Schlösser, M van Stralen, RC Brink, WCW Chu, T-P Lam, KL Vincken, et al. Three-dimensional characterization of torsion and asymmetry of the intervertebral discs versus vertebral bodies in adolescent idiopathic scoliosis. *Spine (Phila Pa 1976)*, 39 (2014), pp. E1159-E1166
17. S-C Chow, J Shao, H Wang. Sample size calculations in clinical research (2nd Ed.), Chapman & Hall/CRC Biostatistics Series (2008)
18. RE Will, IA Stokes, X Qiu, MR Walker, JO Sanders, Cobb angle progression in adolescent scoliosis begins at the intervertebral disc. *Spine (Phila Pa 1976)*, 34 (2009), pp. 2782-2786

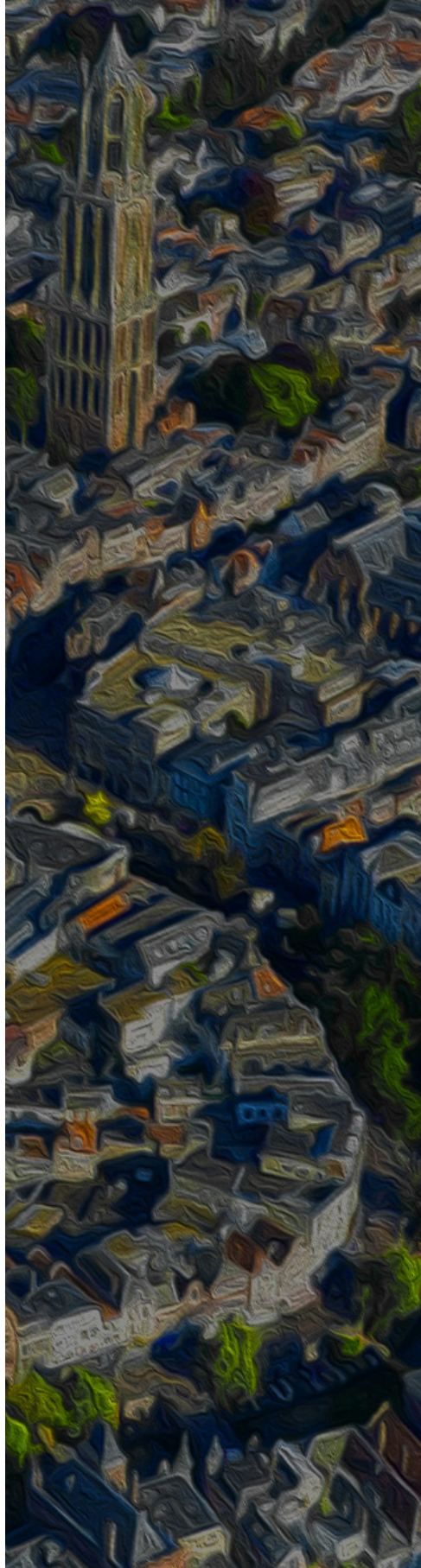


# 9

## The role of Sagittal Pelvic Morphology in the Development of Adult Degenerative Scoliosis

Steven de Reuver  
Philip P. van der Linden  
Moyo C. Kruyt  
Tom P.C. Schlösser  
René M. Castelein

*European Spine Journal. 2021 Sep;30(9):2467-2472.*



## ABSTRACT

**Purpose.** Pelvic morphology dictates the alignment and biomechanics of the spine. Recent observations in different types of adolescent idiopathic scoliosis indicate that individual pelvic morphology is related to the spinal levels in which scoliosis develops: primary lumbar adolescent scoliosis is associated with a higher pelvic incidence (PI) than thoracic scoliosis and non-scoliotic controls. We hypothesize that adult degenerative scoliosis (ADS) of the lumbar spine follows the same mechanical principles and is associated with a high PI.

**Methods.** This study used an existing CT-scan database, 101 ADS patients were sex and age matched to 101 controls. The PI was measured by two observers with multi-planar reconstruction, perpendicular to the hip-axis according to a previously validated technique.

**Results.** The PI was  $54.1^\circ \pm 10.8^\circ$  in ADS patients and  $47.7^\circ \pm 10.8^\circ$  in non-scoliotic controls ( $p < 0.001$ ). The median ADS curve apex was the disc L2-3 and median curve length was 4 vertebral levels. The mean supine Cobb angle was  $21^\circ \pm 8^\circ$  (ranged  $10^\circ$ - $47^\circ$ ). There was no significant correlation between PI and the apex level ( $p = 0.883$ ), the curve length ( $p = 0.418$ ) or the Cobb angle ( $p = 0.518$ ).

**Conclusions.** ADS normally develops de novo in the lumbar spine of patients with a higher PI than controls, similar to primary lumbar adolescent idiopathic scoliosis. This suggests a shared mechanical basis of both deformities. Pelvic morphology dictates spinal sagittal alignment, which determines the segments of the spine that are prone to develop scoliosis.

## Introduction

The unique upright sagittal profile of the human spine and its consequences for human spinal biomechanics provide an important mechanical basis for the development of spinal deformities.<sup>1-5</sup> Spinal alignment and consequent biomechanics are to a large extent determined by the pelvic incidence (PI), first described by Duval-Beaupère et al.<sup>6</sup> The PI describes position-independent sagittal pelvic morphology and is strongly related to the sagittal spinal configuration, making it ideal for studying and comparing spino-pelvic alignment.<sup>7</sup> Also, the PI is not influenced by potential spinal deformity and is therefore a pre-existent parameter, facilitating the study of cause-and-effect relationships. The PI can be measured on conventional lateral spinal radiographs that include both femoral heads. Recent studies show that the inaccuracy of the projection plane accounts for a variability of 3°–6° in PI when measured on conventional radiographs, compared to 0.8° when measured on 3D computed tomography (CT) images.<sup>8-11</sup> CT measurements, however, are acquired in a horizontal position and will never become popular for general assessment due to the high radiation burden, but existing databases of CT-scans obtained for indications such as polytrauma screening or malignancies, can be used for study purposes.

Earlier studies observed a higher PI in primary lumbar adolescent idiopathic scoliosis patients compared to primary thoracic curve types and to non-scoliotic controls.<sup>7,12-14</sup> In adolescents, pelvic morphology dictates the spinal alignment, where a higher PI corresponds with a more pronounced curvature of the spinal profile in the sagittal plane, including a steeper dorsally inclined segment of the thoracolumbar spine.<sup>15</sup> This dorsally inclined segment appears to be of causal importance. A recently published study demonstrated that the inclination and magnitude of this dorsally inclined area in the years before the onset of scoliosis, differs between those that will and will not develop scoliosis.<sup>16</sup>

Also in adults, it has been shown that the sagittal profile plays a role in the development of adult degenerative scoliosis (ADS) of the lumbar spine, suggesting the importance of spino-pelvic alignment also in this type of lumbar scoliosis.<sup>2,17,18</sup> We hypothesize a similar mechanical basis of both adolescent and adult de novo lumbar scoliosis. Plain radiography studies have already suggested the relationship of a slightly higher PI in ADS patients compared to either patients with milder ADS, poorly defined controls and/or a literature standard PI value.<sup>19-21</sup> The purpose of this study was to provide a thorough determination of the relationship between PI and ADS, by measuring the PI in an existing CT-scan database and compare ADS patients to a sex and age matched control population.

## Methods

### Study population

The Institutional Review Board (IRB) exempted patient informed consent for this retrospective cross-sectional comparative study (IRB number 19/642). All patients aged 40–80 that had received a full body CT-scan between 2011 and 2019 in our clinic and had a diagnosis of ADS with a Cobb angle  $> 10^\circ$  according to the Scoliosis Research Society guidelines were included.<sup>22</sup> Patients were included only if there was no history of spinal surgery, no previous hip arthroplasty, both femoral heads were visible on the CT-scan, no pelvic or vertebral fractures and no other spinal deformities, such as idiopathic scoliosis, were present. From the same hospital, patients aged 40–80 that had received a full-body CT-scan between 2011 and 2019 for indications not related to the spine were used as potential control patients and screened for the same criteria as the ADS patients except the presence of a scoliotic curve with a Cobb angle  $> 10^\circ$ . Before further analysis of the CT-scans and blinded for all baseline characteristics except sex and age, every included ADS patient was matched to a control patient of first the same sex, and thereafter of the closest age. Of the ADS patients and sex-age matched controls, basic characteristics of the spine were determined on digitally reconstructed radiographs of the CT-images: supine coronal Cobb angle, curve convexity, apex level and the curve length recorded as the number of vertebral bodies in the curve from Cobb-to-Cobb end vertebrae, following the Scoliosis Research Society guidelines.<sup>22</sup>

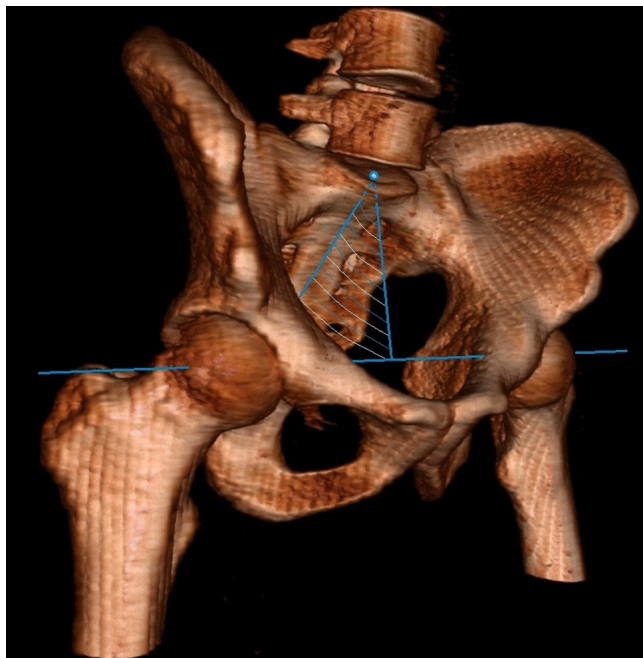


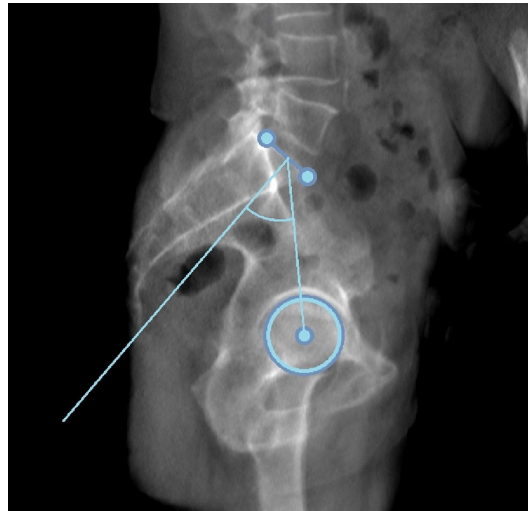
**Figure 1.** A three-dimensional (3D) CT reconstruction of the femoral heads, pelvis and lower lumbar spine. The pelvic incidence is shown in the light blue lined plane. PI is defined as the angle between the line from the femoral-heads-axis to the mid-point of the sacral endplate, and the line perpendicular to the sacral endplate.



### Three-dimensional pelvic incidence measurement

In the current study, we used a previously validated, accurate 3D method that uses sagittal plane reconstructions perpendicular to hip-axis.<sup>9,14</sup> The PI is measured as the angle between the line from the femoral-heads-axis to the mid-point of the sacral endplate, and the line perpendicular to the sacral endplate (**Figure 1**). The supine full body CT-scans of every included ADS patients and sex-age matched control were analysed by multi-planar reconstruction (MPR) to measure the PI (**Figure 2**).

**Figure 2.** Full body CT-scans of all included patients were analysed by multi-planar reconstruction (MPR) to get a three-dimensional (3D) image rotatable in all planes. The femoral heads were aligned and encircled by the observer to get the exact axis through the femoral heads. After selecting the sacral endplate, the pelvic incidence was measured as the angle between the line from the femoral-heads-axis to the mid-point of the sacral endplate, and the perpendicular line from the mid-point of the sacral endplate



### Statistical analysis

The required sample size was calculated based on an earlier study that measured the pelvic incidence with the same method on CT-scans of an asymptomatic control population ( $47.1^\circ \pm 10.0^\circ$ ).<sup>9</sup> To detect a difference of 5 degrees in PI or more with 80% power and a two-sided alpha of 5% in two equally sized groups (sampling ratio of 1), a required sample size of 63 per group was calculated.<sup>23</sup> All descriptive statistics were tested for normality with a Shapiro–Wilk test. For normally distributed parameters the mean, range and standard deviation (SD) were calculated and for not normally distributed parameters the median and interquartile range (IQR) were calculated. Percentages were shown for the categorical variables. The difference in PI between the two groups was analysed with an independent samples t test. A linear regression analysis between age and PI in both ADS patients and sex-age matched controls was performed. For curve characteristics, a Pearson's correlation test

between the apex level and curve convexity was performed, also the association between PI and the apex level, curve length and Cobb angle were analysed with an ordinal regression analysis. Statistical analyses were performed with SPSS 25.0 for Windows (IBM, Armonk, NY, USA). The statistical significance level was set at 0.05.

## Results

A total of 101 ADS patients were sex and age matched to 101 controls. The median age was 69 in ADS patients and 68 in the matched controls, 57% were female. In ADS patients, the median apex level was the disc L2-3, the mean coronal Cobb angle was  $21^\circ \pm 8^\circ$  and ranged from  $10^\circ$  to  $47^\circ$  (**Table 1**). Furthermore, all ADS curves had their apex in the lumbar area, in concurrence with earlier observations of de novo ADS, and 56% of these primary lumbar curves were left convex.<sup>24</sup> A higher lumbar apex level correlated significantly with a right convex curve ( $R=0.282$ ;  $p=0.004$ ).

|  | ADS                         | Control                     |
|--|-----------------------------|-----------------------------|
| N  | 101                         | 101                         |
| Median year of age                                 | 69                          | 68                          |
| Female   | 57%                         | 57%                         |
| Mean Cobb angle ( $\pm$ SD)                        | $21^\circ \pm 8^\circ$      |                             |
| Range  | $10^\circ$ to $47^\circ$    |                             |
| Convexity of lumbar curve                          | 56% left-sided              |                             |
| Median apex  | L2-3                        |                             |
| IQR  | L2 to L3                    |                             |
| Median curve length (included number of vertebrae) | 4                           |                             |
| IQR  | 3 to 5                      |                             |
| Pelvic incidence*                                  | $54.1^\circ \pm 10.8^\circ$ | $47.7^\circ \pm 10.8^\circ$ |

**Table 1.** Demographics and Results.

The PI was  $54.1^\circ \pm 10.8^\circ$  in ADS patients and  $47.7^\circ \pm 10.8^\circ$  in sex-age matched controls ( $p<0.001$ ; **Table 1**). Furthermore, there was a weak and slightly significant correlation between age and PI in both the ADS group ( $R=0.225$ ;  $p=0.024$ ) and the sex-age matched controls ( $R=0.197$ ;  $p=0.048$ ; **Figure 3**). There was no significant correlation between PI and the specific level of the apex ( $p=0.883$ ), the length of the scoliotic curve ( $p=0.418$ ) or the Cobb angle ( $p=0.518$ ).

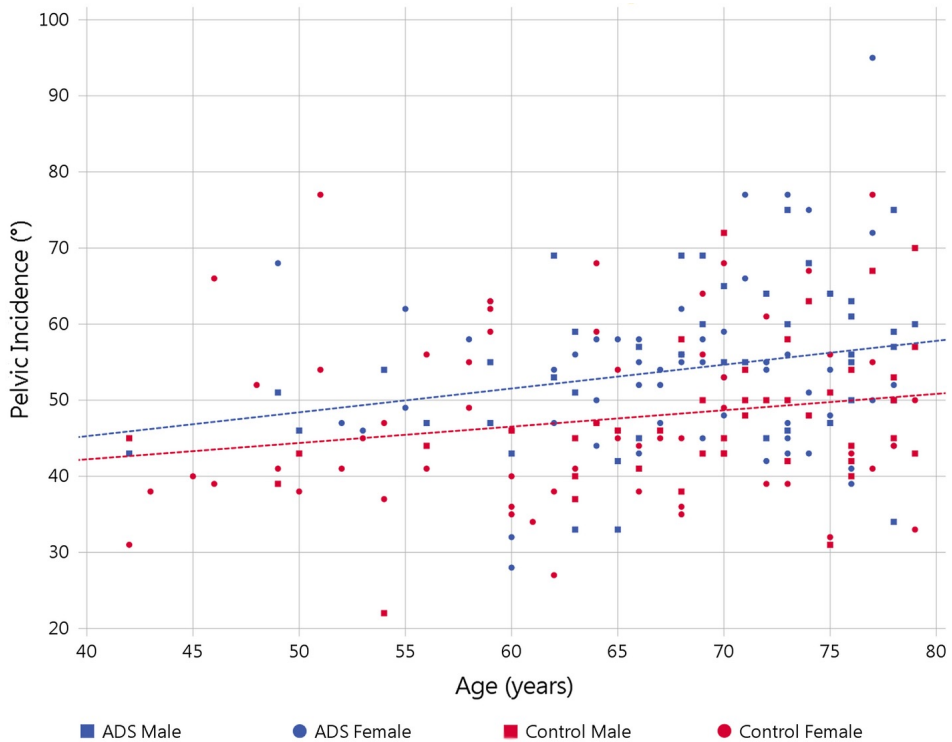


**Figure 3.** This scatter-plot shows the pelvic incidence and age for all males and females in the adult degenerative scoliosis (ADS) group and sex-age matched control group. Linear regression analysis showed a weak but significant correlation between age and pelvic incidence in both the ADS group ( $R=0.225$ ;  $p=0.024$ ) and the sex-age matched controls ( $R=0.197$ ;  $p=0.048$ ), indicated by the dashed lines in figure.

## Discussion

The mechanical basis of scoliosis is becoming more and more understood. The human spine has a unique sagittal profile, that renders certain spinal segments prone to decompensate into a scoliotic deformity.<sup>2,4,5</sup> How, why and when this decompensation starts is still matter of continuing investigations, however, not yet fully understood mechanical properties of the maturing as well as the degenerating disc as the primary passive stabilizer of the spine likely play a role in the pathogenesis of scoliosis.<sup>4,25,26</sup> Pelvic morphology influences the sagittal spinal profile, e.g. a higher PI typically results in a more pronounced sagittal spinal curvature and a steeper dorsal inclination of the lumbar spine.<sup>6,7,15</sup> Furthermore, a higher PI has been shown to be related to primary lumbar adolescent idiopathic scoliosis, whereas a lower PI was associated with primary thoracic curves and non-scoliotic controls.<sup>7,12-14</sup> In de novo

adult spinal deformities, the curvature normally develops in the lumbar spine during a phase in life when the torsional stiffness of the intervertebral disc decreases.<sup>18,24-29</sup> If mechanical characteristics, dictated by the sagittal pelvic morphology, play a role in the development of scoliosis, we expect a similar phenomenon of a higher PI in ADS as was observed in primary lumbar adolescent idiopathic scoliosis. So far, three radiographic studies indicated a slightly higher PI in ADS patients compared to either patients with milder ADS, controls and/or a literature standard PI value.<sup>19-21</sup>

This CT-based study with sex and age matched controls demonstrated that the PI was indeed higher in ADS than in non-scoliotic controls (54° vs 48°; **Table 1**). Since PI is not affected by the spinal deformity, this confirms the role of sagittal spino-pelvic alignment in the development of both idiopathic adolescent and adult degenerative de novo scoliosis. Using the same CT-based method for PI measurements, a similar but slightly larger PI difference of 51° in (thoraco)lumbar adolescent idiopathic scoliosis and 41° in matched controls was observed.<sup>14</sup> These overall lower PIs compared to the current observations of 54° in ADS and 48° in controls, are explained by the fact that children and adolescents are known to have a lower PI than adults.<sup>30-33</sup> This ageing effect was also observed in the current study (**Figure 3**). Furthermore, all ADS curves had their apex in the lumbar area, which is consistent with data from the literature (**Table 1**).<sup>24,25,28</sup> And a higher lumbar apex correlated significantly with a right-convex curve, which is in concurrence with observations that scoliotic curve convexity tends to follow the slight pre-existent rotational pattern present in the non-scoliotic spine.<sup>34</sup>

The three main strengths of the current study are: First, the comparison between ADS patients and a sex-age matched control population. Second, the study was powered to detect a difference of 5 degrees in PI or more.<sup>9,23</sup> And third, the use of 3D CT-scan images and a validated measurements method of the PI, which is more accurate than radiographic measurements.<sup>8-11</sup> Due to the inevitable nature of the CT-scans, made supine in contrast to the upright position during standard full spine radiography, a potential limitation is that some smaller ADS curves may have dropped below the 10-degree threshold in the supine position, and were therefore not included in the ADS group. Furthermore, it is possible that patients with an unknown history of adolescent idiopathic scoliosis with only a lumbar curve (Lenke 5), or similarly for adult idiopathic scoliosis, that developed a degenerative lumbar spine over time, were included in this study as ADS patients. However, the prevalence of this occurrence is likely to be very small compared to the reported ADS prevalence of 30–60%, and therefore the influence on the results is insignificant.<sup>25</sup>

The current and earlier studies again confirm the interaction between the sagittal spinal profile as dictated by the PI and the occurrence of scoliosis.<sup>1-7</sup> This strengthens the hypothesis of

a causal relationship between sagittal spinal morphology and development of both idiopathic adolescent and adult degenerative scoliosis.<sup>7,12-14</sup> In this causal mechanism, the individual's PI in itself is not a sufficient cause or 'trigger', but a component cause, predisposing patients with a specific spino-pelvic alignment to develop scoliosis in different areas of the spine, dependent of the sagittal profile, during two separate phases of life. In both adolescence and in later adulthood, important changes to spinal biomechanics occur.<sup>4,25,26</sup> We propose that the 'trigger' is a relative loss of equilibrium between the passive stabilizers, mainly the intervertebral discs, on the one hand and the spinal loading on the other. During adolescence, an imbalance can occur between rapidly increasing loads on the spine and the mechanical properties of the still maturing disc, where initially a cartilaginous insertion of the annulus fibrosus fibers changes into a bony insertion during puberty, with ossification and fusion of the ring apophysis to the vertebral endplate.<sup>35-37</sup> Similarly at later age, degeneration related loss of torsional stiffness can induce a segmental spinal instability under relatively constant spinal loading, a process potentially sped up by a high PI itself, by dictating a more pronounced lumbar lordosis, increasing local stress on intervertebral discs and therefore uneven degeneration may take place.<sup>18,29,38</sup>

However, for both phases in life, the spinal level where this (relative or absolute) loss of mechanical properties of the intervertebral discs will become manifest, appears to be dictated by the sagittal spinal profile. Explained by the Roussouly classification, a higher PI is associated with a more pronounced curvature of the spinal profile in the sagittal plane, including a steeper dorsally inclined segment of the lumbar spine.<sup>15</sup> The resultant dorsal shear forces in these sections are known to decrease rotational stability.<sup>2-17</sup> And already before scoliosis onset, this dorsally inclined segment was observed to be different between those that later developed a primary thoracic or a lumbar curve, or did not develop a scoliosis at all.<sup>16</sup> This suggests an important role for sagittal spino-pelvic alignment in a general mechanism of scoliosis development during two separate phases of life, characterized by a change in the balance between mechanical properties of the disc in relation to the spinal loading.

In conclusion, adult degenerative scoliosis develops de novo in the lumbar spine of patients with a higher PI than controls, similar to lumbar adolescent idiopathic scoliosis. This suggests a shared mechanical basis of both deformities. It is known that pelvic morphology dictates spinal sagittal alignment, which determines the segments of the spine that are prone to develop scoliosis. We hypothesize that whether and during which phase in life this will occur, depends on the mechanical properties of the passive stabilizers of the spine, predominantly the discs, either during maturation, or during degeneration.

## References

1. Marty C, Boisauvert B, Descamps H et al (2002) The sagittal anatomy of the sacrum among young adults, infants, and spondylolisthesis patients. *Eur Spine J* 11:119–125
2. Castelein RM, van Dieën JH, Smit TH (2005) The role of dorsal shear forces in the pathogenesis of adolescent idiopathic scoliosis—a hypothesis. *Med Hypotheses* 65:501–508
3. Cheng JC, Castelein RM, Chu WC et al (2015) Adolescent idiopathic scoliosis. *Nat Rev Dis Prim* 1:15–30
4. Castelein RM, Pasha S, Cheng JC, Dubouset J (2020) Idiopathic scoliosis as a rotatory decompensation of the spine. *J Bone Miner Res* 35:1850–1857
5. Pasha S (2019) 3D deformation patterns of s shaped elastic rods as a pathogenesis model for spinal deformity in adolescent idiopathic scoliosis. *Sci Rep* 9:16485
6. Duval-Beaupère G, Schmidt C, Cosson P (1992) A barycentric study of the sagittal shape of spine and pelvis: The conditions required for an economic standing position. *Ann Biomed Eng* 20:451–462
7. Legaye J, Duval-Beaupère G, Hecquet J, Marty C (1998) Pelvic incidence: A fundamental pelvic parameter for three-dimensional regulation of spinal sagittal curves. *Eur Spine J* 7:99–103
8. Vaz G, Roussouly P, Berthonnaud E, Dimnet J (2002) Sagittal morphology and equilibrium of pelvis and spine. *Eur Spine J* 11:80–87
9. Vrtovec T, Janssen MMA, Pernuš F et al (2012) Analysis of pelvic incidence from 3-dimensional images of a normal population. *Spine (Phila Pa 1976)* 37:E479–E485
10. Ghostine B, Sauret C, Assi A et al (2017) Influence of patient axial malpositioning on the trueness and precision of pelvic parameters obtained from 3D reconstructions based on biplanar radiographs. *Eur Radiol* 27:1295–1302
11. Moon JW, Shinn JK, Ryu D et al (2017) Pelvic incidence can be changed not only by age and sex, but also by posture used during imaging. *Korean J Spine* 14:77–83
12. Schlösser TPC, Shah SA, Reichard SJ et al (2014) Differences in early sagittal plane alignment between thoracic and lumbar adolescent idiopathic scoliosis. *Spine J* 14:282–290
13. Pasha S, Aubin C-E, Sangole AP et al (2014) Three-Dimensional Spinopelvic Relative Alignment in Adolescent Idiopathic Scoliosis. *Spine (Phila Pa 1976)* 39:564–570
14. Brink RC, Vavrouch L, Schlösser TPC et al (2019) Three-dimensional pelvic incidence is much higher in (thoraco)lumbar scoliosis than in controls. *Eur Spine J* 28:544–550
15. Roussouly P, Gollopy S, Berthonnaud E, Dimnet J (2005) Classification of the normal variation in the sagittal alignment of the human lumbar spine and pelvis in the standing position. *Spine (Phila Pa 1976)* 30:346–353
16. Homans JF, Schlösser TPC, Pasha S et al (2021) Variations in the sagittal spinal profile precede the development of scoliosis: a pilot study of a new approach. *Spine J* 21:638–641
17. Kouwenhoven J-WM, Smit TH, van der Veen AJ et al (2007) Effects of dorsal versus ventral shear loads on the rotational stability of the thoracic spine: a biomechanical porcine and human cadaveric study. *Spine (Phila Pa 1976)* 32:2545–2550
18. Homminga J, Lehr AM, Meijer GJM et al (2013) Posteriorly directed shear loads and disc degeneration affect the torsional stiffness of spinal motion segments: a biomechanical modeling study. *Spine (Phila Pa 1976)* 38:1313–1319
19. Hong J-Y, Suh S-W, Modi HN et al (2010) Correlation of Pelvic Orientation With Adult Scoliosis. *J Spinal Disord Tech* 23:461–466
20. Wang H, Ma L, Yang DL et al (2015) Radiological analysis of degenerative lumbar scoliosis in relation to pelvic incidence. *Int J Clin Exp Med* 8:22345–22351
21. Sun XY, Kong C, Zhang TT et al (2019) Correlation between multifidus muscle atrophy, spinopelvic parameters, and severity of deformity in patients with adult degenerative scoliosis: The parallelogram effect of LMA on the diagonal through the apical vertebra. *J Orthop Surg Res* 14:1–10
22. O'Brien MF, Kulklo TR, Blanke KM, Lenke LG (2008) Radiographic Measurement Manual. Spinal deformity study group (SDSG). Medtronic Sofamor Danek USA, Inc
23. Chow S-C, Shao J, Wang H (2008) Sample Size Calculations in Clinical Research, 2nd edn. Chapman & Hall/CRC Biostatistics Series, Boca Raton
24. McAviney J, Roberts C, Sullivan B et al (2020) The prevalence of adult de novo scoliosis: A systematic review and meta-analysis. *Eur Spine J* 29:2960–2969
25. Kelly A, Younus A, Lekgwara P (2020) Adult degenerative scoliosis – A literature review. *Interdiscip Neurosurg* 20:100661
26. Grivas TB, Vasilidis E, Malakasis M et al (2006) Intervertebral disc biomechanics in the pathogenesis of idiopathic scoliosis. *Stud Health Technol Inform* 123:80–83
27. de Vries AAB, Mullender MG, Pluymakers WJ et al (2010) Spinal decompensation in degenerative lumbar scoliosis. *Eur Spine J* 19:1540–1544
28. Aebi M (2005) The adult scoliosis. *Eur Spine J* 14:925–948
29. Kettler A, Rohlmann F, Ring C et al (2011) Do early stages of lumbar intervertebral disc degeneration really cause instability? Evaluation of an in vitro database. *Eur Spine J* 20:578–584
30. Schlösser TPC, Vincken KL, Rogers K et al (2015) Natural sagittal spino-pelvic alignment in boys and girls before, at and after the adolescent growth spurt. *Eur Spine J* 24:1158–1167
31. Schlösser TPC, Janssen MMA, Vrtovec T et al (2014) Evolution of the ischio-iliac lordosis during natural growth and its relation with the pelvic incidence. *Eur Spine J* 23:1433–1441
32. Mac-Thiong J-M, Berthonnaud É, Dimar JR et al (2004) Sagittal Alignment of the Spine and Pelvis During Growth. *Spine (Phila Pa 1976)* 29:1642–1647

33. Mac-Thiong J-M, Labelle H, Berthonnaud E et al (2007) Sagittal spinopelvic balance in normal children and adolescents. *Eur Spine J* 16:227–234
34. Kouwenhoven JW, Vincken KL, Bartels LW, Castelein RM (2006) Analysis of preexistent vertebral rotation in the normal spine. *Spine (Phila Pa 1976)* 31:1467–1472
35. Taylor JR (1975) Growth of human intervertebral discs and vertebral bodies. *J Anat* 120:49–68
36. Edelson JG, Nathan H (1988) Stages in the natural history of the vertebral end-plates. *Spine (Phila Pa 1976)* 13:21–26v
37. Uys A, Bernitz H, Pretorius S, Steyn M (2019) Age estimation from anterior cervical vertebral ring apophysis ossification in South Africans. *Int J Legal Med* 133:1935–1948
38. Bezci SE, Eleswarapu A, Klineberg EO, O'Connell GD (2018) Contribution of facet joints, axial compression, and composition to human lumbar disc torsion mechanics. *J Orthop Res* 36:2266–2273



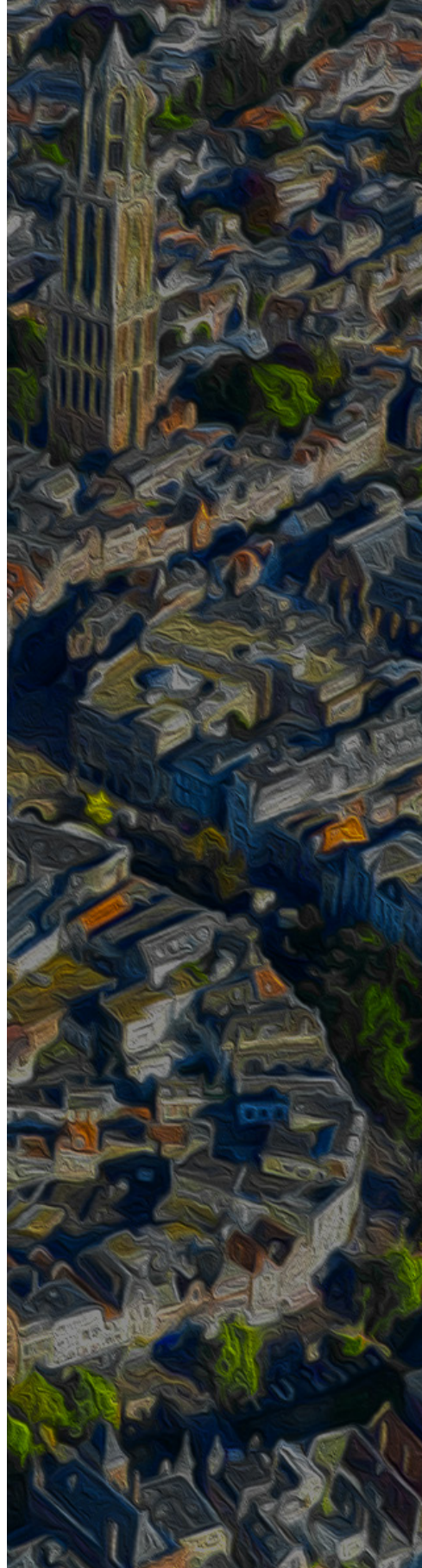


# 10

## What a Stranded Whale with Scoliosis can teach us about Human Idiopathic Scoliosis

Steven de Reuver  
Lonneke L. IJsseldijk  
Jelle F. Homans  
Dorien S. Willems  
Stefanie Veraa  
Marijn van Stralen  
Marja J.L. Kik  
Moyo C. Kruyt  
Andrea Gröne  
René M. Castelein

*Nature Scientific Reports. 2021 Mar 30;11(1):7218.*



## ABSTRACT

Scoliosis is a deformation of the spine that may have several known causes, but humans are the only mammal known to develop scoliosis without any obvious underlying cause. This is called 'idiopathic' scoliosis and is the most common type. Recent observations showed that human scoliosis, regardless of its cause, has a relatively uniform three-dimensional anatomy. We hypothesize that scoliosis is a universal compensatory mechanism of the spine, independent of cause and/or species. We had the opportunity to study the rare occurrence of scoliosis in a whale (*Balaenoptera acutorostrata*) that stranded in July 2019 in the Netherlands. A multidisciplinary team of biologists, pathologists, veterinarians, taxidermists, radiologists and orthopaedic surgeons conducted necropsy and imaging analysis. Blunt traumatic injury to two vertebrae caused an acute lateral deviation of the spine, which had initiated the development of compensatory curves in regions of the spine without anatomical abnormalities. Three-dimensional analysis of these compensatory curves showed strong resemblance with different types of human scoliosis, amongst which idiopathic. This suggests that any decompensation of spinal equilibrium can lead to a rather uniform response. The unique biomechanics of the upright human spine, with significantly decreased rotational stability, may explain why only in humans this mechanism can be induced relatively easily, without an obvious cause, and is therefore still called 'idiopathic'.

## Introduction

Scoliosis is a three-dimensional (3D) deformity of the spine and trunk, in which rotation of the vertebral column in the horizontal plane together with extension in the sagittal plane plays a consistent role, that may be caused by traumatic injury, syndromic conditions, congenital malformations or neuromuscular disease.<sup>1</sup> In mammals, the development of scoliosis without an obvious underlying cause is exclusively observed in humans, this is called ‘idiopathic’ scoliosis and is the most frequently observed type.<sup>1-3</sup> The condition occurs with a prevalence of 1–4% in otherwise healthy individuals, most commonly adolescent females.<sup>1</sup> Treatment is currently focused on limiting progression of the spinal curve until skeletal maturity, which can necessitate bracing therapy or spinal fusion surgery.<sup>1</sup> Many theories have been brought forward in search of the aetiology of idiopathic scoliosis.<sup>1,4-12</sup> Upright spinal biomechanics, that implies a reduction of stability in the horizontal plane, was shown to play an important role.<sup>13-19</sup> And while the shape of the scoliotic spine has been described for over a century,<sup>10,20,21</sup> recent observations have shown that the 3D anatomy is very uniform across human scoliosis with different aetiology, including vertebral rotation into the curve convexity and anterior lengthening of the intervertebral discs.<sup>22-26</sup>

We hypothesize that scoliosis is a universal compensatory mechanism of the spine, that consists of vertebral rotation into the convexity of the curve, accompanied by anterior lengthening of the intervertebral discs, that can be caused by different primary challenges to spinal equilibrium. One of these challenges, and a possible explanation of idiopathic scoliosis in humans is the unique upright posture with the centre of weight balanced straight above the pelvis, resulting in a unique biomechanical loading of the trunk.<sup>13-17,27</sup> This specific sagittal plane configuration of the human spine was shown to lead to decreased rotational stability, making it more prone than other spines in nature to decompensate into scoliosis.<sup>18,19,28,29</sup> Scoliosis is found rarely in other vertebrates than humans and is usually caused by anatomic abnormalities.<sup>30,31</sup>

Recently, we had the opportunity to study the compensatory curves in an anatomically normal area of the spine of a whale with a post-traumatic scoliosis. Whales are sea mammals that are not known to develop scoliosis spontaneously: several reports on cetaceans with scoliosis exist, however all cases have a clear cause which is mostly of traumatic origin, e.g. following ship collision.<sup>32-34</sup> In the current study we examined a young common minke whale (*Balaenoptera acutorostrata*), which was found stranded in July 2019 in the Netherlands with an obvious spine trauma and subsequent severe local post-traumatic scoliosis (**Figure 1**). This post-traumatic scoliosis initiated compensatory 3D curves in the area of the spine that was not affected by the trauma, apparently in an attempt of the animal to re-align its trunk.

We were interested in these compensatory curves, as they could provide insights into the more general, intrinsic mechanisms that govern alignment of the mammalian spine. A multidisciplinary team of biologists, pathologists, veterinarians, taxidermists, radiologists and orthopaedic surgeons studied the whale and conducted a necropsy and 3D imaging analysis of the spine and compared the findings to non-scoliotic whales. The aim of the study was to assess whether scoliosis is a universal compensatory mechanism that occurs independent of cause and/or species. The hypothesis tested in the current study was that the injured whale would re-align its trunk by creating compensatory curves in the essentially normal spine and that these curves show a similar 3D configuration as is observed in human scoliosis.



**Figure 1.** Photograph of the common minke whale (*Balaenoptera acutorostrata*) that washed ashore on the 8th of July 2019 at Texel, the Netherlands. Photograph by Pierre Bonnet (Ecomare, Texel).

## Results

### Post mortem findings

The common minke whale was a 403 cm long, 530 kg female juvenile, with an estimated age between 0.5 and 4 years.<sup>35</sup> Besides the clear lateral post-traumatic curvature of the spine, other important findings of external examination were multifocal areas of deep haemorrhage and oedema that were present in the subcutis and longissimus dorsi muscle, as well as the presence of blood tinge liquid in the spinal canal and congestion and haemorrhage of the brain. The animal had a poor nutritional condition (blubber layers of 20–25 mm) despite recent feeding.<sup>36</sup> Histology of the fractured vertebrae demonstrated fibrin deposits, some

eosinophilic granulocytes, and necrosis, indicative of chronic changes that were still ongoing. Therefore, the most likely cause of death was considered to be acute recent blunt trauma. Furthermore, there was clear evidence that earlier trauma had resulted in the fractures and other deformations of the lumbar vertebrae, which had led to a localized, post-traumatic deformity of the spine. Visual inspection showed that the deformity was mostly in the coronal plane with no significant lordosis or kyphosis at that region. This was further investigated after removing all of the soft tissues of the entire vertebral column. Visual inspection showed an epiphysiolysis at the left-side of the lower endplate of vertebra L3, a burst upper endplate at the right-side of vertebra L4 and fractured/missing spinous processes at multiple levels (Figure 2).

### Post-Traumatic Primary Curve



**Figure 2.** Photographs of the post-traumatic primary curve after removing the soft tissues. The dorsal overview on the right-hand side shows the post-traumatic primary, abrupt coronal curve at level L3/L4. Close-up inspection reveals an epiphysiolysis at the left-side of the lower endplate of vertebra L3, and a burst upper endplate at the right-side of vertebra L4. Furthermore, fractured spinous processes at multiple levels are present. There are multiple post mortem marks following tissue selection for histopathology, and also centre holes and screws that were drilled through the endplates in the process of framing the complete skeleton for museum display. These artefacts did not influence the presented post-traumatic features.



Furthermore, spinal curvatures were observed in the adjacent, anatomically normal parts of the spine, outside the traumatically affected area (**Figure 3**). Therefore, the thoracolumbar area was the suspected site of an acute (dorso-)lateral blunt traumatic injury, which subsequently initiated a double compensatory curve cranially and a single compensatory curve caudally in areas of the spine unaffected by the trauma (**Figure 4**). We analysed these compensatory curves in 3D and compared the morphology with the non-scoliotic spine of 10 control whales. The levels T11/12 (severe wedging) and L3/L4 (traumatic injury) were excluded before CT-scan analysis of the compensatory curvatures.

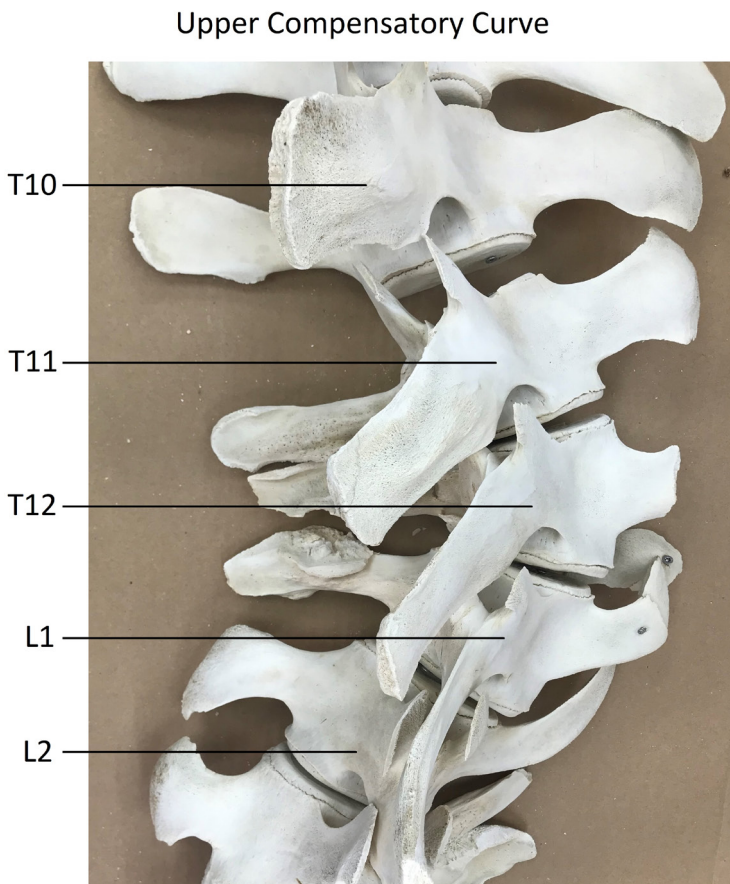


**Figure 3.** Close-up photograph of the apex of the upper compensatory curve, directly cranial of the post-traumatic primary curve, after removing the soft tissues. This compensatory curvature occurred in an (initially) anatomically normal part of the spine, unaffected by the trauma.

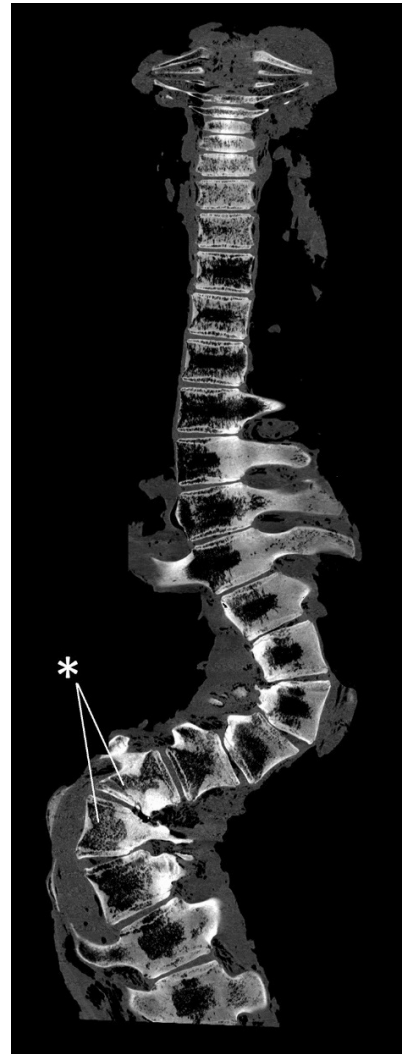


**Figure 4.** Dorsal view with the cranial side upwards from the CT-scan of level C1 to L7. The site of the blunt traumatic injury at level L3/L4 (indicated with an asterisk) initiated a double compensatory curve cranially and a single compensatory curve caudally.

#### CT-measurements

The 3D analysis of the compensatory curves showed a rotation of the vertebral bodies in the transverse plane into the convexity of the curve (**Figure 5**). The mean anterior–posterior length discrepancy (AP%) of the total compensatory curvature was +9.4% in the whale. This means that the anterior (ventral) length of the compensatory scoliotic curvature was 9.4% greater than the posterior (dorsal) length, indicating a regional lordosis. This is significantly different from the kyphosis in the same part of the spine in the non-scoliotic control group, with a total AP% of  $-2.1 \pm 0.4\%$ , meaning that the anterior length of the spine was 2.1% shorter

than the posterior length ( $p < 0.001$ ). On the contrary, the bony morphology of the vertebral bodies was similar to the controls; the vertebral body AP% of the whale was  $-2.5\%$ , which was comparable to the kyphotic shape of the vertebral bodies in controls with  $-1.8 \pm 0.8\%$  ( $p = 0.429$ ). Almost all anterior lengthening took place in the intervertebral discs, as the disc AP% in the compensatory curvature of the whale was  $+99.5\%$ , which meant a lordotic shape of the intervertebral discs with an anterior length almost twice the posterior length. This is in sharp contrast to the kyphosis in the discs of controls with  $-4.6 \pm 5.0\%$  ( $p < 0.001$ ). The AP% for the separate vertebral bodies and intervertebral discs at every level is shown in **Figure 6**.

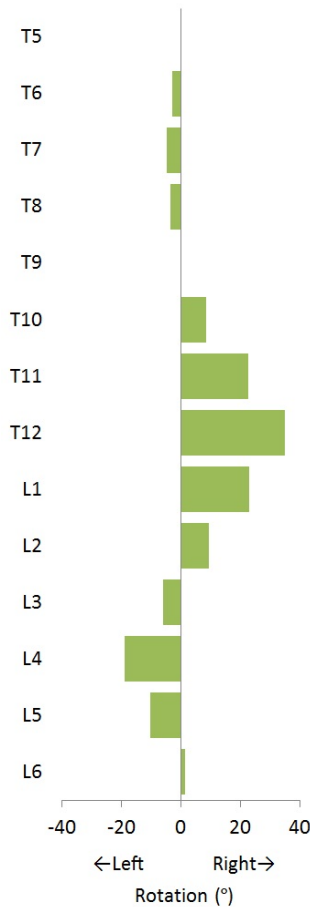


**Figure 5.** Of the whale with scoliosis, the rotation of the vertebral bodies in the transverse plane is shown in degrees. Positive values indicate that the anterior part of the vertebral body is pointing towards the right. All rotation of the vertebral bodies is into the convexity of the curve.



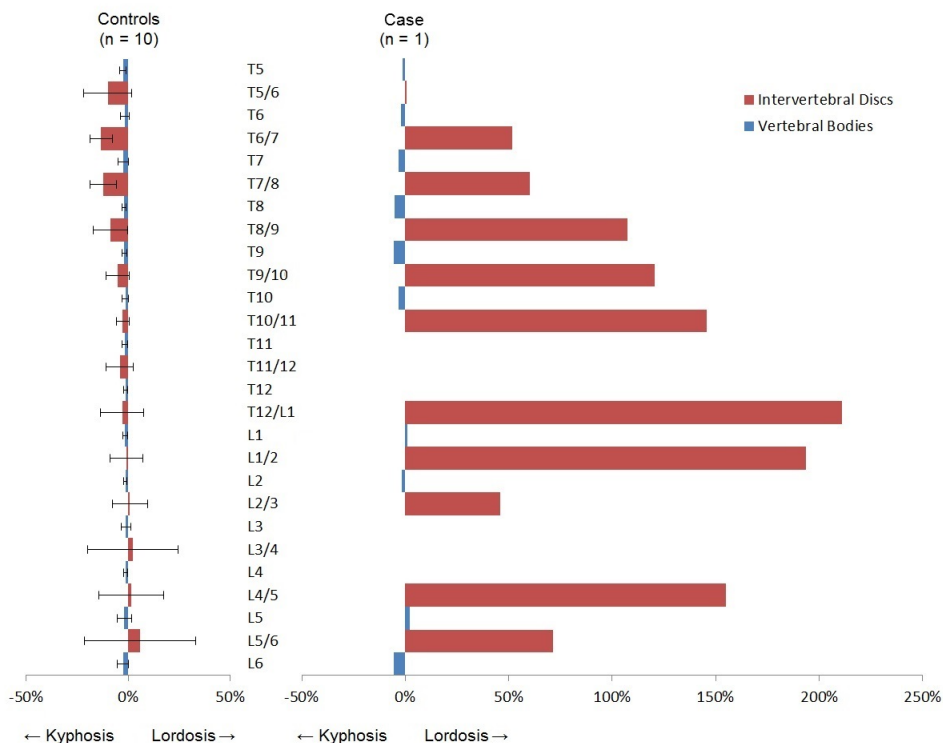


**Figure 6.** The mean anterior–posterior length discrepancy (AP%) with the standard deviation is shown for the intervertebral discs in red and the vertebral bodies in blue, for both the non-scoliotic controls and the whale with scoliosis. Endplates severely affected by trauma (L3/L4) and wedging (T11/T12) were excluded due to impossibility of proper CT-scan analysis. Positive AP% indicates a larger anterior length than posterior length.

**Discussion**

Idiopathic scoliosis is a 3D decompensation of a spine with no anatomical abnormalities, in an individual without underlying manifest disease.<sup>1</sup> In the search for its aetiology, many theories involving just as many of the body’s organ systems have been suggested to play a role.<sup>1,4–12</sup> The usually present lengthening of the anterior side of the thoracic spine in idiopathic scoliosis,<sup>5,6,37</sup> was suggested to be the result of a generalized bony overgrowth disorder (relative anterior spinal overgrowth; RASO), possibly as a compensation for a disturbance of synchronized growth between the neural and the osseous elements.<sup>7–9,38</sup> Recent observations have shown that this anterior lengthening occurs predominantly in the discs and is not restricted to idiopathic scoliosis.<sup>22–26</sup>

We propose that scoliosis is a rather universal compensatory mechanism that can occur as a response to a (perceived) disturbance of spinal equilibrium. The crucial difference between the human spine and that of other mammals is not in its anatomy, but in the way it is biomechanically loaded, not by the fact that man is bipedal (many species are) but by the fact that humans carry their center of mass more posteriorly than any other species.<sup>13-17,27</sup> This leads to a sagittal profile that makes the human spine, in comparison with any other spine in nature, quadrupedal and bipedal alike, a rotationally less stable structure.<sup>18,19,39</sup> This means that, whereas in other species often draconic measures are necessary to induce a scoliosis,<sup>3</sup> in humans much less is needed to initiate this mechanism. We propose that the possible value of scoliosis research in experimental animals is not in the primary, artificially induced curve, but in the response that follows in the untouched area of the spine, i.e. the compensatory curve. This is supported by the observation that compensatory curves in congenital scoliosis in humans show a very similar 3D morphology to idiopathic scoliosis,<sup>25</sup> and that in porcine tether induced scoliosis the compensatory curves outside the instrumented spinal segment showed a similar rotational deformity.<sup>40</sup>

The objective of the current study was to investigate the mechanism through which a scoliosis developed in the normal area of the spine, in an animal that is not known to develop a scoliosis spontaneously. We studied the 3D morphology of the compensatory curves that evolved around a traumatically induced coronal plane deformity in a whale. A (dorso-)lateral blunt traumatic injury caused a localized, acute, predominantly lateral deviation of the spine, that subsequently initiated 3D compensatory scoliotic curves in the anatomically normal areas of the spine. These compensatory curves showed rotation of the vertebral bodies into the convexity of the curve, and an apical lordosis (+9.4%), which differed significantly from the kyphosis in the spine of the control group (-2.1%). Although, since the animal was still growing, some wedging of vertebrae occurred, the vertebral bodies shape in the sagittal plane showed no difference with the normal, kyphotic shape of the vertebrae in the control group (-1.8%). The observed lordosis in the compensatory curves of the whale was exclusively located in the intervertebral discs, they showed severe anterior lengthening (+99.5%) which was in stark contrast with the kyphotic discs of controls (-4.6%). This 3D morphology is very similar to what is found in humans with idiopathic scoliosis, but also in human neuromuscular scoliosis as well as in the compensatory curve in human congenital scoliosis.<sup>22-25</sup>

The acute primary scoliosis caused by the traumatic accident, resulted in the head and tail of the whale being out of line and inhibiting proper locomotion and swimming manoeuvres. As many mammals have a vestibular reflex of self-righting,<sup>41,42</sup> the whale most likely compensated this trunk imbalance in an attempt to realign its head to its tail, inducing compensatory curves in the anatomically normal areas of the spine with a 3D morphology that strongly

resembles human scoliosis. Whereas most spines in nature require substantial effort to start a permanent rotational deformity due to the stabilizing action of gravity in combination with the trunk's muscles (i.e. the follower load),<sup>39,43</sup> the human spine is much less rotationally stable due to its unique sagittal profile with the body's centre of gravity straight above, rather than in front of the pelvis.<sup>13-17,27</sup> This reduces the stabilizing anterior shear loading and even induces posteriorly directed shear loads that render the involved spinal segments unstable in the horizontal plane.<sup>1,18,19,28,29,39,44</sup>

This rare occurrence of scoliosis in a species that is not known to develop a spinal curvature spontaneously, provided a unique chance to study scoliosis in a completely different model. A limitation of this study was that the common minke whale was not compared to non-scoliotic controls of the exact same species. This is due to the low frequency of stranded common minke whales in the Netherlands, in combination with their large size and weight exceeding the capacity of most CT-scanning facilities. However, the smaller harbour porpoise (*Phocoena phocoena*) share strong commonalities in spinal anatomy and were therefore used as controls in the current study.<sup>45,46</sup> Furthermore, the fractured and extensively deformed vertebrae were excluded since proper recognition of the anatomical planes was impossible during CT-scan analysis. However, visual inspection showed wedging mainly in the coronal plane and overview images in the sagittal plane of the CT-scan did not show a significant kyphosis at the site of traumatic injury. Therefore, we could exclude a post-traumatic kyphosis as the initiator of the apical lordosis observed in this study. Also, the observation of a lordosis or kyphosis could be influenced by the fact that the scoliotic whale, nor the controls were alive during CT-scanning and were positioned prone outside of their naturally aquatic habitat. We know from human scoliosis that kyphosis and lordosis are underestimated during prone or supine imaging compared to upright, but there is no difference between prone or supine.<sup>47</sup> Gravity obviously plays an important role in humans, but not in submerged mammals, therefore we feel that the influence of positioning on our results is limited.

The aim of this study was to analyse whether scoliosis can be considered a more generalized compensatory mechanism that occurs independent of cause and/or species. In line with our hypothesis, we observed that the compensatory curves that developed in the normal area of the spine of a whale, that suffered severe but localized trauma to the spine, show strong similarities in 3D configuration with different types of human scoliosis. This suggests a shared and rather uniform mechanical basis, implying that any perceived decompensation of spinal equilibrium can lead to a uniform response, with uniform 3D morphology. The unique biomechanics of the upright human spine,<sup>13-17,27</sup> with significantly decreased rotational stability,<sup>1,18,19,39,44</sup> may explain why only in humans this mechanism can be induced relatively easily, without an obvious cause, and is therefore still called 'idiopathic'.

## Methods

### Post mortem examination

Since 2008, cetaceans that stranded dead or died shortly after stranding on the Dutch coast are subjected to post mortem examination, which is conducted at the division of pathology of the Faculty of Veterinary Medicine (Utrecht University). The animals described in the current study were not used for scientific or commercial testing. All were free-living whales which died of natural causes or were euthanized on welfare grounds and not for the purpose of this, or other studies. Therefore, since there was no handling of live animals in the current study, according to institutional guidelines, no consent from the Animal Use Committee was required, and animal ethics committee approval was not applicable to this work. On the 8th of July 2019, a young common minke whale washed up on the North Sea beach of Texel, the Netherlands (**Figure 1**), and subsequently underwent post mortem investigation aiming to determine the cause of its death. A necropsy and tissue sampling procedure was conducted following internationally standardized guidelines.<sup>48</sup> This included the collection of the following measures: total length (measured from the tip of the rostrum to the fluke notch, in a straight line next to the body, in cm), weight (kg) and blubber thickness. The latter was measured immediately anterior to the dorsal fin at three locations (dorsal, lateral and ventral, in mm). Age class was determined based on total length and gross examination of reproductive organs. Tissue samples from various organs, as well as the vertebral bone, were fixed in 4% phosphate-buffered formalin, embedded in paraffin, cut into 4 µm sections, and stained with haematoxylin and eosin. Samples from vertebra were decalcified prior to paraffin imbedding and staining procedures.

### Diagnostic imaging

Upon gross examination of the whale, the spinal malformation was noted. The entire vertebral column was therefore wrapped in plastic sheets and submitted for computed tomography (CT)-scanning. The spine was positioned in ventral recumbency on the table of a 64-slice sliding gantry CT scanner (Somatom Definition AS, Siemens AG, München, Germany).

### Control group

As common minke whale strandings infrequently occur on the Dutch coast, a control group of the same species was not possible to acquire. Therefore, a control group was assembled of the harbour porpoise; a smaller member of the cetacean family and the most abundant whale species in the North Sea. Harbour porpoises are regularly subjected to post mortem examination and in a previous study focusing on their anatomy, animals were subjected for full-body CT-scan prior to the necropsies.<sup>49</sup> Ten cases which did not present spinal

abnormalities and were positioned straight during CT-scanning were selected from this database and used as a control group in this study.

### CT measurements

The orientation of the scanned whales in this study was defined the same way as in humans, with anterior indicating the ventral side and posterior indicating the dorsal side, and furthermore cranial, caudal, left and right as standard. The CT-scans of the whale and control group was measured with dedicated software (ScoliosisAnalysis 4.1; Image Sciences Institute, Utrecht, The Netherlands, developed with MeVisLab, MeVis Medical Solutions AG, Bremen, Germany) to measure the direction and amount of rotation, anterior and posterior height of vertebral bodies and vertebral discs in the exact mid-sagittal plane, corrected for deformity in all three planes. This software is in-house developed and validated with excellent intra- and interobserver reliability.<sup>50</sup> This semi-automated method is used and extensively described in multiple earlier studies.<sup>23,25,50,51</sup> For all upper and lower endplates in the included part of the spine, the observer adjusted the plane of view for coronal and sagittal tilt. In this true transverse plane, the vertebral body and spinal canal were manually segmented by the observer, whereafter the software automatically determined the 3D coordinates of the anterior and posterior point of the endplate, adjusted for rotation and deformity in all planes. The distances between these points were calculated to obtain the anterior and posterior heights of the vertebral bodies and intervertebral discs (**Figure 7**). This was done for all the compensatory curves (Cobb-to-Cobb). The corresponding levels of the spine analysed in the whale were also measured in controls. After measurements, the anterior–posterior length discrepancy (AP%) was calculated as  $[(\text{anterior length} - \text{posterior length})/(\text{posterior length})] \times 100\%$ , for the total compensatory curved spine, and for the vertebral bodies and the intervertebral discs separately. Endplates severely affected by trauma or wedging were excluded, as proper segmentation was not possible. Positive AP% values indicated that the anterior (ventral) side was longer than the posterior (dorsal) side.

### Statistical analysis

The mean AP% results for the total curve, the vertebral bodies and the intervertebral bodies were determined for the minke whale and for the non-scoliotic harbour porpoise control group given with  $\pm$  standard deviation. The differences in mean AP% between the scoliotic whale and non-scoliotic controls were tested with an independent samples T-test. Statistical analysis was performed in SPSS 25.0 for Windows (IBM, Armonk, NY, USA). The level of statistical significance was set at  $p \leq 0.05$ .

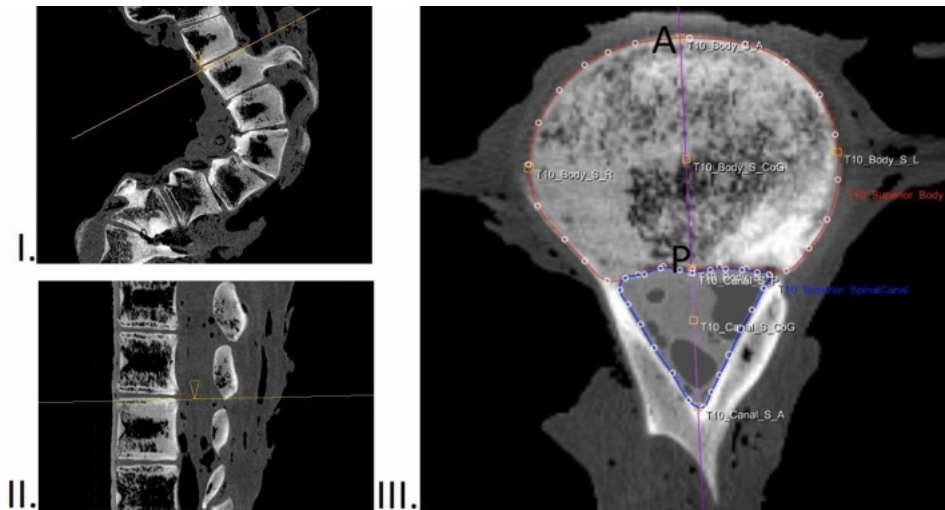


**Figure 7.** Method of 3D measurements on CT-scans in this study. For all upper and lower endplates, the observer adjusted the plane of view for coronal (I) and sagittal (II) tilt. In the true transverse plane, the vertebral body and spinal canal were manually segmented (III), whereafter the software automatically determined the 3D coordinates of the anterior (A) and posterior (P) point of the endplate, adjusted for rotation and deformity in all planes. The distances between these points were calculated to obtain the anterior and posterior heights of the vertebral bodies and intervertebral discs.

#### Animal ethics committee approval

The animals described in the current study were not used for scientific or commercial testing. All were free-living whales which died of natural causes or were euthanized on welfare grounds and not for the purpose of this, or other studies. Therefore, since there was no handling of live animals in the current study, according to institutional guidelines, no consent from the Animal Use Committee was required, and animal ethics committee approval was not applicable to this work.

**References**

1. Cheng JC, et al. Adolescent idiopathic scoliosis. *Nat. Rev. Dis. Prim.* 2015;1:15–30.
2. Kouwenhoven J-WM, Castelein RM. The pathogenesis of adolescent idiopathic scoliosis: Review of the literature. *Spine.* 2008;33:2898–2908.
3. Janssen MMA, de Wilde RF, Kouwenhoven J-WM, Castelein RM. Experimental animal models in scoliosis research: A review of the literature. *Spine J.* 2011;11:347–358.
4. Schlösser TPC, van der Heijden GJMG, Versteeg AL, Castelein RM. How 'idiopathic' is adolescent idiopathic scoliosis? A systematic review on associated abnormalities. *PLoS ONE.* 2014;9:e97461.
5. Somerville EW. Rotational lordosis; the development of single curve. *J. Bone Joint Surg. Br.* 1952;34-B:421–427.
6. Dickson RA, Lawton JO, Archer IA, Butt WP. The pathogenesis of idiopathic scoliosis. Biplanar spinal asymmetry. *J. Bone Joint Surg. Br.* 1984;66:8–15.
7. Guo X, Chau WW, Chan YL, Cheng JCY. Relative anterior spinal overgrowth in adolescent idiopathic scoliosis. Results of disproportionate endochondral-membranous bone growth. *J. Bone Joint Surg. Br.* 2003;85:1026–1031.
8. Newell N, et al. Quantifying progressive anterior overgrowth in the thoracic vertebrae of adolescent idiopathic scoliosis patients: A sequential magnetic resonance imaging study. *Spine.* 2016;41:E382–E387.
9. Stokes IAF, Burwell RG, Dangerfield PH. Biomechanical spinal growth modulation and progressive adolescent scoliosis—A test of the 'vicious cycle' pathogenetic hypothesis: Summary of an electronic focus group debate of the IBSE. *Scoliosis.* 2006;1:16.
10. Nicoladoni, C. Anatomie und Mechanismus der Skoliose. Kocher, König, von Mikulicz, eds. *Bibl. Medica.* Stuttgart Verlag von Erwin Nagele (1904).
11. Roth M. Idiopathic scoliosis and Scheuermann's disease: Essentially identical manifestations of neuro-vertebral growth disproportion. *Radiol. Diagn.* 1981;22:380–391.
12. Porter RW. Can a short spinal cord produce scoliosis? *Eur. Spine J.* 2001;10:2–9
13. Abitbol MM. Evolution of the ischial spine and of the pelvic floor in the Hominoidea. *Am. J. Phys. Anthropol.* 1988;75:53–67.
14. Voutsinas SA, MacEwen GD. Sagittal profiles of the spine. *Clin. Orthop. Relat. Res.* 1950;210:235–242.
15. Washburn SL. The analysis of primate evolution with particular reference to the origin of man. *Cold Spring Harb. Symp. Quant. Biol.* 1950;15:67–78.
16. Alexander RM. Bipedal animals, and their differences from humans. *J. Anat.* 2004;204:321–330.
17. Payne RC, et al. Morphological analysis of the hindlimb in apes and humans. II. Moment arms. *J. Anat.* 2006;208:725–742.
18. Kouwenhoven J-WM, et al. Effects of dorsal versus ventral shear loads on the rotational stability of the thoracic spine: A biomechanical porcine and human cadaveric study. *Spine.* 2007;32:2545–2550.
19. Homminga J, et al. Posteriorly directed shear loads and disc degeneration affect the torsional stiffness of spinal motion segments: A biomechanical modeling study. *Spine.* 2013;38:E1313–E1319.
20. Lovett RW. A contribution to the study of the mechanics of the spine. *Am. J. Anat.* 1903;2:457–462.
21. Lovett RW. The mechanism of the normal spine and its relation to scoliosis. *Bost. Med. Surg. J.* 1905;153:349–358.
22. Schlösser TPC, et al. Anterior overgrowth in primary curves, compensatory curves and junctional segments in adolescent idiopathic scoliosis. *PLoS ONE.* 2016;11:e0160267.
23. Brink RC, et al. Anterior-posterior length discrepancy of the spinal column in adolescent idiopathic scoliosis—a 3D CT study. *Spine J.* 2018;18:2259–2265.
24. Brink RC, et al. Anterior spinal overgrowth is the result of the scoliotic mechanism and is located in the disc. *Spine.* 2017;42:818–822.
25. de Reuver S, et al. Anterior lengthening in scoliosis occurs only in the disc and is similar in different types of scoliosis. *Spine J.* 2020;20:1653–1658.
26. Will RE, Stokes IA, Qiu X, Walker MR, Sanders JO. Cobb angle progression in adolescent scoliosis begins at the intervertebral disc. *Spine.* 2009;34:2782–2786.
27. Bernhardt M, Bridwell KH. Segmental analysis of the sagittal plane alignment of the normal thoracic and lumbar spines and thoracolumbar junction. *Spine.* 1989;14:717–721.
28. Pasha S. 3D deformation patterns of S shaped elastic rods as a pathogenesis model for spinal deformity in adolescent idiopathic scoliosis. *Sci. Rep.* 2019;9:16485.
29. Castelein RM, Pasha S, Cheng JC, Dubousset J. Idiopathic scoliosis as a rotatory decompensation of the spine. *J. Bone Miner. Res.* 2020;35:1850–1857.
30. Arkin AM. The mechanism of the structural changes in scoliosis. *J. Bone Joint Surg. Am.* 1949;31A:519–528.
31. Naique SB, et al. Scoliosis in an orangutan. *Spine.* 2003;28:E143–E145.
32. Sharp SM, et al. Gross and histopathologic diagnoses from North Atlantic right whale *Eubalaena glacialis* mortalities between 2003 and 2018. *Dis. Aquat. Organ.* 2019;135:1–31.
33. Weir CR, Wang JY. Vertebral column anomalies in Indo-Pacific and Atlantic humpback dolphins *Sousa* spp. *Dis. Aquat. Organ.* 2016;120:179–187.
34. Bertulli CG, et al. Vertebral column deformities in white-beaked dolphins from the eastern North Atlantic. *Dis. Aquat. Organ.* 2015;116:59–67.
35. Nielsen, N. H., Vikingsson, G. A., Hansen, S. H., Ditlevsen, S. & Heide-Jørgensen, M. P. Two techniques of age estimation in cetaceans: GLGs in teeth and earplugs, and measuring the AAR rate in eye lens nucleus. *NAMMCO Sci. Publ.* 10, (2017).
36. Christiansen F, Vikingsson GA, Rasmussen MH, Lusseau D. Minke whales maximise energy storage on their feeding grounds. *J. Exp. Biol.* 2013;216:427–436.

37. Roaf R. The basic anatomy of scoliosis. *J. Bone Joint Surg. Br.* 1966;48:786–792.
38. Chu WCW, et al. Relative shortening and functional tethering of spinal cord in adolescent idiopathic scoliosis? Study with multiplanar reformat magnetic resonance imaging and somatosensory evoked potential. *Spine.* 2006;31:E19–25.
39. Castelein RM, van Dieën JH, Smit TH. The role of dorsal shear forces in the pathogenesis of adolescent idiopathic scoliosis—A hypothesis. *Med. Hypotheses.* 2005;65:501–508.
40. Barrios C, et al. Novel porcine experimental model of severe progressive thoracic scoliosis with compensatory curves induced by interpedicular bent rigid temporary tethering. *J. Orthop. Res.* 2017;36:174–118266.
41. Spoor F, Bajpai S, Hussain ST, Kumar K, Thewissen JGM. Vestibular evidence for the evolution of aquatic behaviour in early cetaceans. *Nature.* 2002;417:163–166.
42. Spoor F, et al. The primate semicircular canal system and locomotion. *Proc. Natl. Acad. Sci. USA.* 2007;104:10808–10812.
43. Patwardhan AG, Meade KP, Lee B. A frontal plane model of the lumbar spine subjected to a follower load: Implications for the role of muscles. *J. Biomech. Eng.* 2001;123:212–217.
44. Janssen MM, Kouwenhoven JW, Castelein RM. The role of posteriorly directed shear loads acting on a pre-rotated growing spine: A hypothesis on the pathogenesis of idiopathic scoliosis. *Stud. Health Technol. Inform.* 2010;158:112–117.
45. Thewissen JGM, Cooper LN, George JC, Bajpai S. From land to water: The origin of whales, dolphins, and porpoises. *Evol. Educ. Outreach.* 2009;2:272.
46. Fordyce RE. Cetacean Evolution. *Encyclopedia of Marine Mammals.* Elsevier; 2018.
47. Brink RC, et al. Upright, prone, and supine spinal morphology and alignment in adolescent idiopathic scoliosis. *Scoliosis Spinal Disord.* 2017;12:6.
48. IJsseldijk, L. L., Brownlow, A. C. & Mazzariol, S. (eds). Best practice on cetacean post mortem investigation and tissue sampling. Joint ASCOBANS/ACCOBAMS document. (2019).
49. Willems, D., IJsseldijk, L. & Veraa, S. Vertebral pattern variation in the North Sea Phocoena phocoena by computed tomography. *Anat. Rec.* (2020).
50. Schlösser TPC, et al. Three-dimensional characterization of torsion and asymmetry of the intervertebral discs versus vertebral bodies in adolescent idiopathic scoliosis. *Spine.* 2014;39:E1159–E1166.
51. Brink RC, et al. A reliability and validity study for different coronal angles using ultrasound imaging in adolescent idiopathic scoliosis. *Spine J.* 2018;18:979–985.





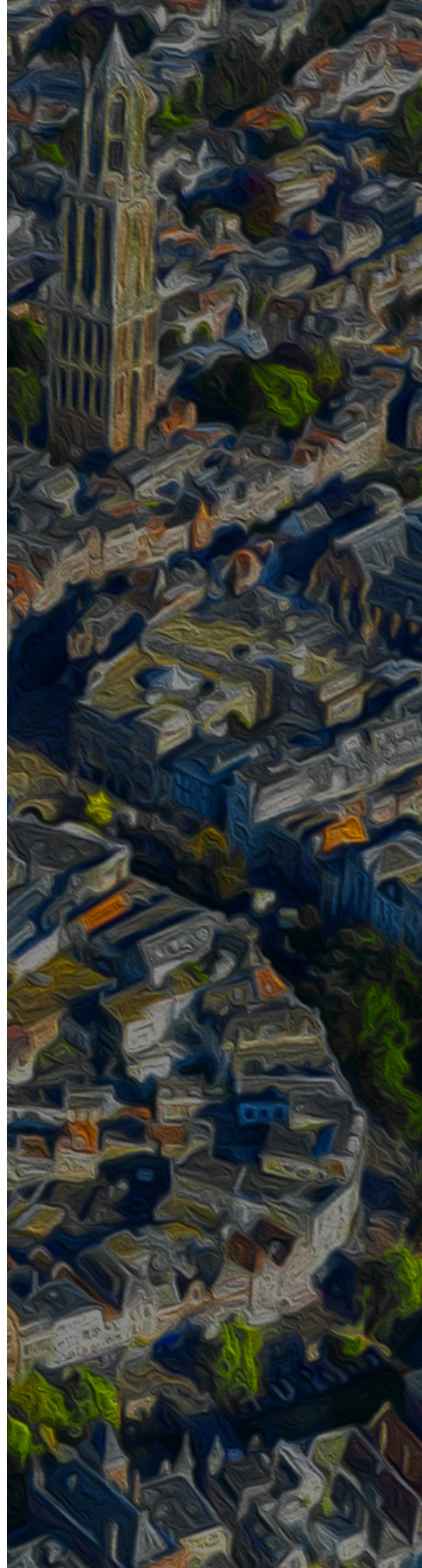


# 11

## Convex-concave and Anterior-posterior Spinal Length Discrepancies in Adolescent Idiopathic Scoliosis

Steven de Reuver  
Nick de Block  
Rob C. Brink  
Winnie C.W. Chu  
Jack C.Y. Cheng  
Moyo C. Kruyt  
René M. Castelein  
Tom P.C. Schlösser

*Spine Deformity*. 2023 Jan;11(1):87-93.



## ABSTRACT

**Purpose.** The apical deformation in adolescent idiopathic scoliosis (AIS) is a combination of rotation, coronal deviation and passive anterior lengthening of the spine. In AIS surgery, posterior-concave lengthening or anterior-convex shortening can be part of the corrective maneuver, as determined by the individual surgeon's technique. The magnitude of convex-concave and anterior-posterior length discrepancies, and how this needs to be modified to restore optimal spinal harmony, remains unknown.

**Methods.** CT-scans of 80 pre-operative AIS patients with right convex primary thoracic curves were sex- and age-matched to 80 healthy controls. The spinal length parameters of the main thoracic curves were compared to corresponding levels in controls. Vertebral body endplates and posterior elements were semi-automatically segmented to determine the length of the concave and convex side of the anterior column and along the posterior pedicle screw entry points while taking the 3D-orientation of each individual vertebra into account.

**Results.** The main thoracic curves showed anterior lengthening with a mean anterior-posterior length discrepancy of  $+ 3 \pm 6\%$ , compared to a kyphosis of  $- 6 \pm 3\%$  in controls ( $p < 0.01$ ). In AIS, the convex side was  $20 \pm 7\%$  longer than concave ( $0 \pm 1\%$  in controls;  $p < 0.01$ ). The anterior and posterior concavity were 7 and 22 mm shorter, respectively, while the anterior and posterior convexity were 21 and 8 mm longer compared to the controls.

**Conclusions.** In thoracic AIS, the concave shortening is more excessive than the convex lengthening. To restore spinal harmony, the posterior concavity should be elongated while allowing for some shortening of the posterior convexity.

## Introduction

From earlier three-dimensional (3D) morphometric studies on adolescent idiopathic scoliosis (AIS) it is known that besides rotation and coronal plane deviation, the apical deformation in AIS involves lordosis, mostly by anterior opening of the intervertebral discs.<sup>1,2</sup> In progressive AIS, surgical correction may be indicated. In general, scoliosis surgery aims to avoid further progression and restore 'healthy' spinal and trunk morphology as much as possible. Posterior scoliosis correction and spinal fusion is the most common technique used for AIS surgery, with in recent meta-analyses good long-term clinical outcomes.<sup>3-5</sup>

There are many different ways AIS can be corrected by posterior spinal fusion.<sup>3</sup> In general, 3D correction maneuvers of the thoracic curve normally consist of a complex combination of concave lengthening, convex shortening and medial translation of the apex back to the midline in the coronal plane, derotation in the axial plane and posterior apical translation and thoracic kyphosis restoration in the sagittal plane. Depending on the individual surgeon's preference, screws, hooks or laminar bands are used, and a certain strategy is chosen in which the corrections of the three main deformations (apical rotation, coronal curvature, thoracic lordosis) are prioritized, since usually not all three components can be fully reversed.<sup>3,6-9</sup>

That scoliosis is the complex result of deformation in all three anatomical planes is generally accepted. It is unknown, however, to what magnitude different sides of the spine lengthen or shorten in the pathogenesis of AIS. These patho-anatomical data can be helpful for further optimization of applied correction techniques in AIS surgery for 3-D restoration towards the morphology of a healthy spine. Therefore, the purpose of this study is to determine the convex-concave and anterior-posterior spinal length discrepancies of the main thoracic curve in primary thoracic AIS.

## Methods

### Study population

From existing pre-operative computed tomographic (CT) databases, patients with right-sided primary thoracic AIS (Lenke 1-4) and sex- and age matched healthy controls were included.<sup>10-14</sup> These patients received these CT-scans as part of their pre-operative work-up for planning of navigation guided pedicle screw placement, which in that university medical center is part of standard care for all idiopathic scoliosis patients with an indication for posterior instrumentation. Exclusion criteria were age < 10 or > 21 years, a left convex main thoracic curve, a primary lumbar curve, a main thoracic curve radiographic Cobb angle below 45° or insufficient CT-scan quality. Full-body CT-scans of the controls were acquired

for indications not related to the spine, for example screening for infection, trauma or malignancy. For the included AIS patients, conventional curve characteristics were measured on free standing full-spine radiographs, according to the Scoliosis Research Society guidelines.<sup>15</sup>

### Spinal length measurements

For each patient, the main thoracic curve was analyzed on the CT scan from Cobb-end to Cobb-end vertebra, as determined on the standing radiographs. For the matched control, the identical levels as in the AIS patient were analyzed. The CT-scan analyses were performed using in-house developed software (ScoliosisAnalysis 7.2, developed with MeVisLab, MeVis Medical Solutions AG, Bremen, Germany), that was previously validated for curve morphology assessment.<sup>2,11,16,17</sup>

One observer, semi-automatically segmented all the upper and lower vertebral body endplates and the spinal canal in the 'true' transverse plane by correcting for the coronal and sagittal angulation of each endplate (**Figure 1**). A line perpendicular to the mid-sagittal axis (based on the mid-points of the endplate and spinal canal) at the center of the endplate was used to localize the left and right side of each endplate. The midpoints between the upper and lower endplate points were automatically calculated and connected, to get the total concave and convex spinal length of the anterior column (**Figure 2**). On the posterior side, the intersections of the laminae and the transverse processes were identified bilaterally, corresponding to the pedicle screw entry points, which allowed measurement of the total concave and convex posterior spinal length (**Figures 1 & 2**).

To compare absolute and relative spinal length measurements and to correct for individual spinal size, the absolute data of the AIS patients was normalized based on the ratio of the mean total spinal segment length of the AIS group relative to the controls. The anterior-posterior length discrepancy was calculated as  $\frac{[(\text{anterior left} + \text{anterior right}) - (\text{posterior left} + \text{posterior right})]}{(\text{posterior left} + \text{posterior right})} \times 100\%$ . The convex-concave length discrepancy was calculated as  $\frac{[(\text{anterior right} + \text{posterior right}) - (\text{anterior left} + \text{posterior left})]}{(\text{anterior left} + \text{posterior left})} \times 100\%$ .

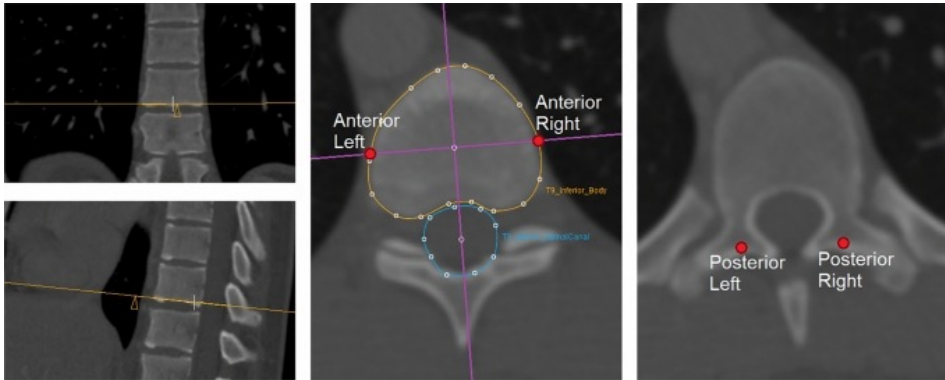
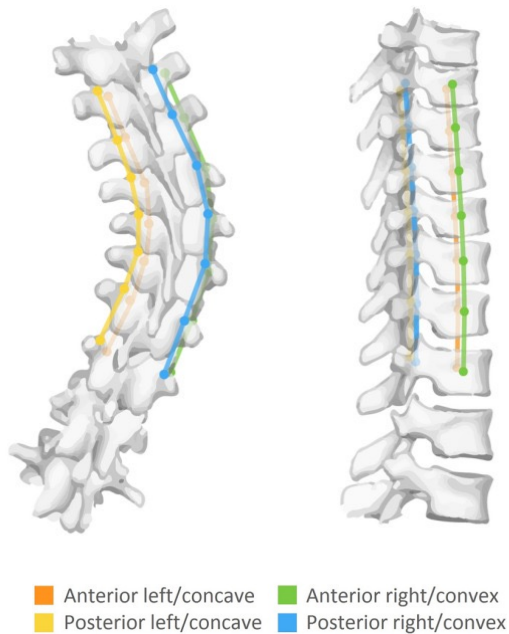


**Figure 1.** In the CT analysis software the upper and lower endplates of all vertebral bodies in the right-convex thoracic curves were segmented in the ‘true’ transverse plane. The spinal canal was also segmented to calculate the mid-sagittal axis, which intersects with the centroid of the endplate and the centroid of the canal. Perpendicular to the mid-sagittal axis at the centroid, the left and right point per was calculated. The mid-point between the upper and lower left point was calculated to retrieve the left anterior column point for each vertebrae, and similarly for the right side. Finally, on the transverse plane, where the intersections of the laminae and transverse process were visible, this was segmented to retrieve the left and right posterior column point per vertebrae.

**Figure 2.** Schematic figure from a posterior and right-side view of a right-convex thoracic scoliosis and four spinal length measurements of the Cobb-end to Cobb-end segment. Following segmentation (Figure 1) four points per vertebral body were calculated: anterior left, anterior right, posterior left and posterior right. This was done for all vertebrae in each right-convex thoracic AIS curve from Cobb-end to Cobb-end, and the same segment in a sex-age matched control. These points were connected on each side to retrieve the four spinal length measurements.



### Statistical analysis

Statistical analyses were performed in SPSS 26.0.0.1 for Windows (IBM, Armonk, NY, USA). Normality of distribution was tested via Q–Q plots. The difference in anterior–posterior length discrepancy and convex–concave length discrepancy between AIS and controls was analyzed with independent sample t tests. Differences in spinal length of each of the four sides was tested between the two groups with independent sample t tests. For the correlation with curve severity (Cobb angle) a non-parametric Spearman's rho test was performed. The statistical significance level was set at 0.05.

## Results

### Study population

Out of 118 AIS patients in the CT-database, eighty patients with right-convex primary thoracic AIS were included and sex and age matched to eighty controls. Thirty-eight were excluded: four for their age, two with a left convex thoracic curve, 21 with a lumbar primary curve, seven with a Cobb angle <45° and four with insufficient CT-scan quality. Patient and curve characteristics are shown in **Table 1**. Non-normalized spinal segment length was 146 mm in AIS and 160 mm in controls.

|                             | AIS patients (n = 80) | Matched controls (n = 80) |
|-----------------------------|-----------------------|---------------------------|
| Mean age (± SD)             | 16.0 ± 2.5            | 15.8 ± 2.2                |
| Range                       | 10–21                 | 10–21                     |
| Female sex                  | 68 (85%)              | 68 (85%)                  |
| Right convex thoracic curve | 80 (100%)             | –                         |
| Mean cobb angle (± SD)      | 69.5° ± 12.6°         | –                         |
| range                       | 46–109°               | –                         |
| Cobb angle group            |                       |                           |
| 45–60°                      | 15 (19%)              | –                         |
| 60–70°                      | 36 (45%)              | –                         |
| 70–80°                      | 12 (15%)              | –                         |
| > 80°                       | 17 (21%)              | –                         |
| Lenke curve type            |                       |                           |
| Type 1                      | 42 (53%)              | –                         |
| Type 2                      | 23 (29%)              | –                         |
| Type 3                      | 10 (13%)              | –                         |
| Type 4                      | 5 (6%)                | –                         |

**Table 1.** Patient demographic and radiographic curve characteristics



### Spinal length measurements

The mean anterior–posterior length discrepancy in AIS patients, along the endplates and along the pedicle entry points, was  $+3\pm 6\%$ , representing apical lordosis, compared to  $-6\pm 3\%$  in controls, representing physiological thoracic kyphosis ( $p < 0.01$ ). The mean convex–concave length discrepancy was  $+20\pm 7\%$  in AIS patients, compared to  $0\pm 1\%$  in controls ( $p < 0.01$ ). The normalized spinal length measurements (**Figure 2**) along the four ‘corners’ demonstrated a mean anterior–concave length of  $148\pm 29$  mm in AIS versus  $155\pm 30$  mm in controls (difference =  $-7$  mm,  $p=0.14$ ), an anterior–convex length of  $176\pm 29$  mm versus  $156\pm 30$  mm (difference =  $+21$  mm,  $p < 0.01$ ), a posterior–concave length of  $143\pm 25$  mm versus  $164\pm 31$  mm (difference =  $-22$  mm,  $p < 0.01$ ) and a posterior–convex length of  $172\pm 30$  mm versus  $164\pm 31$  mm (difference =  $+8$  mm,  $p=0.11$ ), respectively (**Figure 3**).

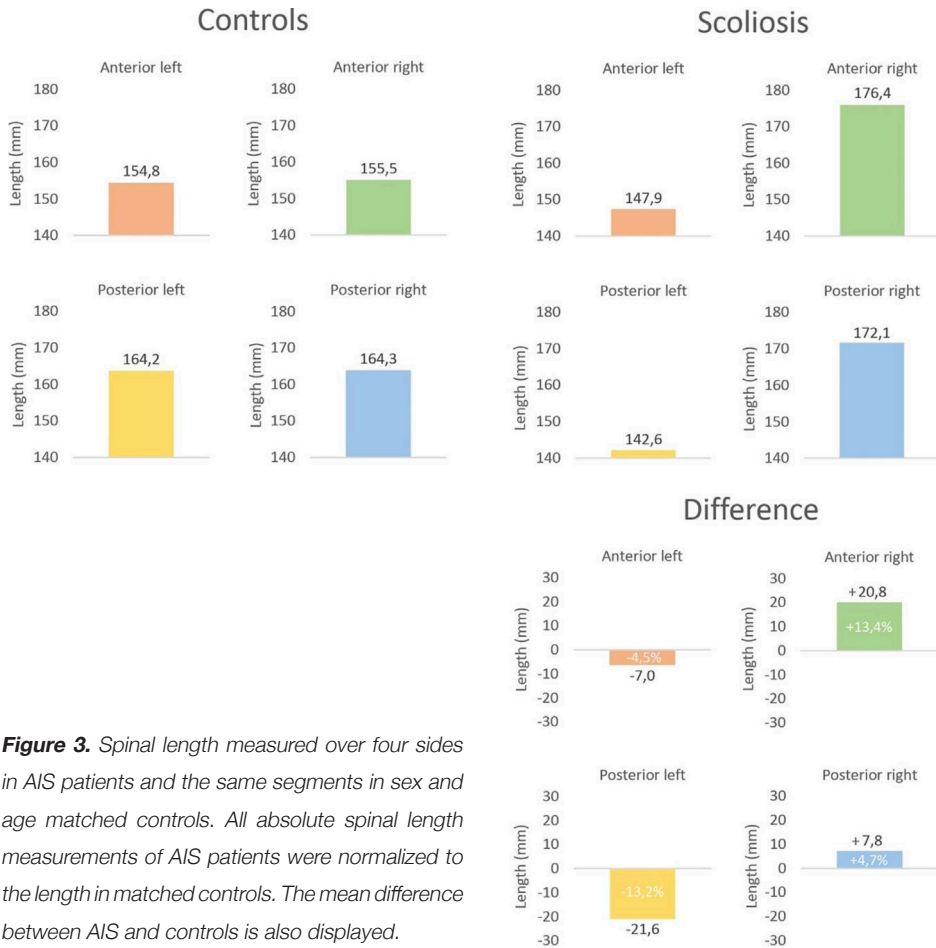


**Figure 3.** Spinal length measured over four sides in AIS patients and the same segments in sex and age matched controls. All absolute spinal length measurements of AIS patients were normalized to the length in matched controls. The mean difference between AIS and controls is also displayed.

After stratifying for curve severity into four groups, Cobb angle of 45–60°, 60–70°, 70–80° and over 80° (**Table 1**), the length discrepancies per group were compared to their matched control as displayed in **Figure 4**. The coronal curve severity Cobb angle correlated significantly with larger length discrepancies on the anterior-concavity ( $p=0.01$ ,  $r=-0.29$ ), anterior-convexity ( $p<0.01$ ,  $r=0.48$ ) and posterior-concavity ( $p=0.01$ ,  $r=-0.28$ ), but not with the posterior-convexity ( $p=0.46$ ).

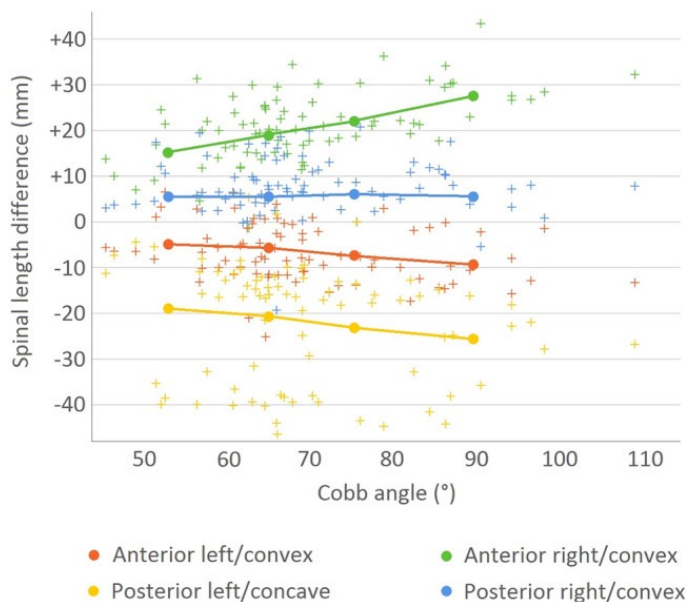


**Figure 4.** Scatter plot of the spinal length differences between AIS patients with different curve severities and the same segments in their respective sex and age matched controls. In addition, the mean values stratified per Cobb angle group: 45–60°, 60–70°, 70–80° and over 80° are overlaid.

## Discussion

In AIS surgery, much emphasis has been placed on restoring the 3D morphology of the spine to achieve a physiological alignment in all planes, to prevent adding on and junctional decompensation and to achieve an optimal configuration of the non-fused segments.<sup>3,6-9</sup> Although much has been published on the shape of the scoliotic spine in the sagittal plane, no studies have so far addressed the length discrepancies along the convex and concave side of the scoliotic curvature. The present sex- and age-matched cross-sectional CT-scan analysis confirms that there is an anterior–posterior length discrepancy: a lordosis (+3%) is present in the true sagittal plane in thoracic AIS compared to a normal kyphosis (–6%) in controls. This study adds to the previous literature a quantification of the convex–concave length discrepancy in AIS in the ‘true’ coronal plane: for the anterior and posterior column combined, the convexity is on average 20% longer than the concavity in AIS. When the length differences of the main thoracic curve in AIS were compared along the four ‘corners’

to the controls, the postero-concave shortening and anterior-convex lengthening were 2–3 fold greater than the contralateral lengthening/shortening, respectively (–7 mm and –22 mm at the anterior- and posterior-concavity, and +21 and +8 mm at the anterior- and posterior-convexity). With increasing curve severity, all segmental discrepancies, besides posterior-convex, increased as well.

Recent studies have already shown the anterior–posterior length discrepancy in AIS compared to controls, which is present as a relative anterior lengthening mostly of the intervertebral disc spaces, with less changes of the bone.<sup>1,2,11,18</sup> When ignoring the obvious rotational component in AIS, this could be conceptualized as ‘spinal bending’ over a transverse axis. However, it was unknown to what extent spinal sides contribute to the deformity in AIS. The current study demonstrates that in AIS there are not only length differences in anterior–posterior direction, but that the direction of deformation is more oblique and there is mostly ‘spinal bending’ over the anterior-convexity and posterior-concavity (**Figure 3**). In addition, and potentially relevant for AIS etiology, the posterior-convexity only lengthens a few millimeters and that this increase in length did not differ between curves that were more or less severe, unlike the 3 other spinal sides (**Figure 4**). This may be explained by ligaments and/or interlocking facets that limit posterior lengthening. By passive decompensation the spine rotates around this fairly rigid posterior-convex tether acting as the fulcrum, allowing for posterior-concavity shortening and anterior-convexity lengthening. These observations cannot be explained adequately by the simple hypothesis of AIS as a generalized anterior bony overgrowth disorder based on the principles of Hueter–Volkman.<sup>19–23</sup>

In an attempt to restore healthy spinal morphology by scoliosis correction surgery, the length discrepancies should ideally be reversed. If a posterior approach is preferred, the present data suggest that the posterior concavity needs to be lengthened significantly, while the posterior convexity needs to be shortened to a much smaller extent. On average in this pre-operative population, in absolute numbers this corresponds to a 22 mm posterior–concave lengthening and an 8 mm posterior–convex shortening. Similarly, but reversed, this could be applied to an anterior approach, for which the data suggest that the largest correction should be on the convexity, with a 21 mm anterior–convex shortening, 3 times the amount of an anterior–concave lengthening (**Figure 3 & 4**). The effectiveness of posterior spinal releases for unilateral lengthening has not been investigated to date.<sup>24</sup>

There are several limitations regarding this study. The first is the inevitable cross-sectional design, since it was impossible to prospectively study the change in morphology, foremost, because scoliosis patients are identified only with an already established scoliosis.

Furthermore, CT scans were obtained once for preoperatively for navigation or planning purposes. In the future, 3-D reconstructions of biplanar radiographs may allow for longitudinal assessment of the convex–concave length discrepancies during scoliosis progression. In addition, the individual changes in sagittal alignment during growth could potentially influence the analysis.<sup>25-27</sup> To mitigate this in a cross-sectional study, all AIS patients were matched to a control patient of the same sex and age, and the exact same spinal segment per AIS and control pair was analyzed. Another potential limitation of this study is that AIS patients were from another ethnic population than the controls. To correct for individual spinal length differences, the AIS patients were normalized to the mean spinal length of the controls. A third limitation is that, scoliosis curve severity and spinal alignment is usually assessed in a free-standing position, mainly on full spine radiographs, while the CTs were obtained in a non-weightbearing position. To mitigate potential influence of body positioning, the curve severity and Cobb end vertebrae were measured on free-standing full spine radiographs obtained at the same time as the CT. We know that both coronal curve severity, as well as different sagittal parameters, are different in the same patient between standing and prone/supine, but that these do not differ significantly between prone and supine 3-D scans.<sup>28</sup> Regarding the individual differences in curve flexibility, i.e., the difference between standing Cobb angle versus on CT, we hypothesize that because in this study larger curves generally showed bigger spinal length differentials, the curve that would retain higher Cobb angles on CT, in other words the less flexible curves, would have a larger differential in a supine position, and could require more intraoperative correction than the more flexible ones.

In conclusion, AIS is the complex result of rotation, coronal deviation and anterior lengthening of the spine, but to what extent each spinal side contributes and how much exactly should be reversed during scoliosis surgery has so far remained unknown. This sex- and age-matched CT-scan analysis confirms a lordosis in thoracic AIS compared to the kyphosis in controls. It demonstrates that the axis of spinal deformation is more oblique than in the coronal or sagittal plane: largely over the anterior–convex and posterior–concave side. This study provides rough targets of spinal length along the pedicle entry points to restore optimal spinal harmony during posterior scoliosis surgery: The posterior concavity should be distracted extensively (on average 22 mm) while allowing for a slight shortening (7 mm) on the convexity.

## References

1. Castelein RM, Pasha S, Cheng JCYC, et al. Idiopathic scoliosis as a rotatory decompensation of the spine. *J Bone Miner Res.* 2020;35:1850–1857.
2. de Reuver S, Brink RC, Homans JF, et al. Anterior lengthening in scoliosis occurs only in the disc and is similar in different types of scoliosis. *Spine J.* 2020;20:1653–1658.
3. Tambe AD, Panikkar SJ, Millner PA, et al. Current concepts in the surgical management of adolescent idiopathic scoliosis. *Bone Joint J.* 2018;100-B:415–424.
4. Chen L, Sun Z, He J, et al. Effectiveness and safety of surgical interventions for treating adolescent idiopathic scoliosis: a bayesian meta-analysis. *BMC Musculoskelet Disord.* 2020;21:427.
5. Lee ACH, Feger MA, Singla A, et al. Effect of surgical approach on pulmonary function in adolescent idiopathic scoliosis patients. *Spine (Phila Pa 1976)* 2016;41:E1343–E1355.
6. Pesenti S, Lafage R, Henry B, et al. Deformity correction in thoracic adolescent idiopathic scoliosis. *Bone Joint J.* 2020;102-B:376–382.
7. Mazda K, Ilharreborde B, Even J, et al. Efficacy and safety of posteromedial translation for correction of thoracic curves in adolescent idiopathic scoliosis using a new connection to the spine: the universal clamp. *Eur Spine J.* 2009;18:158–169.
8. Schlösser TP, Abelin-Genevois K, Homans J, et al. Comparison of different strategies on three-dimensional correction of AIS: which plane will suffer? *Eur Spine J.* 2021;30:645–652.
9. Acaroglu E, Doany M, Cetin E, et al. Correction of rotational deformity and restoration of thoracic kyphosis are inversely related in posterior surgery for adolescent idiopathic scoliosis. *Med Hypotheses.* 2019;133:109396.
10. Brink RC, Homans JF, de Reuver S, et al. A computed tomography-based spatial reference for pedicle screw placement in adolescent idiopathic scoliosis. *Spine Deform.* 2020;8:67–76.
11. Brink RC, Schlösser TPC, van Stralen M, et al. Anterior-posterior length discrepancy of the spinal column in adolescent idiopathic scoliosis—a 3D CT study. *Spine J.* 2018;18:2259–2265.
12. Brink RC, Homans JF, Schlösser TPC, et al. CT-based study of vertebral and intravertebral rotation in right thoracic adolescent idiopathic scoliosis. *Eur Spine J.* 2019;28:3044–3052.
13. de Reuver S, Brink RC, Homans JF et al (2018) The changing position of the center of mass of the thorax during growth in relation to pre-existent vertebral rotation. *Spine (Phila Pa 1976)* 44(10):679–684
14. de Reuver S, Costa L, van Rheenen H, et al. Disc and vertebral body morphology from birth to adulthood. *Spine (Phila Pa 1976)* 2021;47(7):E312–E318.
15. O'Brien MF, Kulklo TR, Blanke KM, Lenke LG (2008) Radiographic measurement manual. Spinal deformity study group (SDSG). Medtronic Sofamor Danek USA, Inc
16. Schlösser TPC, van Stralen M, Brink RC, et al. Three-dimensional characterization of torsion and asymmetry of the intervertebral discs versus vertebral bodies in adolescent idiopathic scoliosis. *Spine (Phila Pa 1976)* 2014;39.
17. de Reuver S, Costa L, van Rheenen H, et al. Disc and vertebral body morphology from birth to adulthood. *Spine (Phila Pa 1976)* 2021.
18. Schlösser TPC, van Stralen M, Chu WCW, et al. Anterior Overgrowth in primary curves, compensatory curves and junctional segments in adolescent idiopathic scoliosis. *PLoS ONE.* 2016;11:e0160267.
19. Guo X, Chau WW, Chan YL, et al. Relative anterior spinal overgrowth in adolescent idiopathic scoliosis results of disproportionate endochondral-membranous bone growth. *J Bone Joint Surg Br.* 2003;85:1026–1031.
20. Chu WCW, Lam WWM, Chan Y-L, et al. Relative shortening and functional tethering of spinal cord in adolescent idiopathic scoliosis?: Study with multiplanar reformat magnetic resonance imaging and somatosensory evoked potential. *Spine (Phila Pa 1976)* 2006;31:E19–25.
21. Newell N, Grant CA, Keenan BE, et al. Quantifying progressive anterior overgrowth in the thoracic vertebrae of adolescent idiopathic scoliosis patients: a sequential magnetic resonance imaging study. *Spine (Phila Pa 1976)* 2016;41:E382–E387.
22. Stokes IA, Burwell RG, Dangerfield PH. Biomechanical spinal growth modulation and progressive adolescent scoliosis—a test of the “vicious cycle” pathogenetic hypothesis: summary of an electronic focus group debate of the IBSE. *Scoliosis.* 2006;1:16.
23. Volkman R (1882) Verletzungen und Krankheiten der Bewegungsorgane. In: von Pitha und Billroth: Handbuch der allgemeinen und speciellen Chirurgie Bd II Teil II. Stuttgart: Ferdinand Enke
24. Holeywijn RM, Schlösser TPC, Bisschop A, et al. How does spinal release and ponte osteotomy improve spinal flexibility? The law of diminishing returns. *Spine Deform.* 2015;3:489–495.
25. Cil A, Yazici M, Uzunucugil A, et al. The evolution of sagittal segmental alignment of the spine during childhood. *Spine (Phila Pa 1976)* 2005;30:93–100.
26. Mac-Thiong J-M, Labelle H, Berthodnaud E, et al. Sagittal spinopelvic balance in normal children and adolescents. *Eur Spine J.* 2007;16:227–234.
27. Janssen MMA, Drevelle X, Humbert L, et al. Differences in male and female spino-pelvic alignment in asymptomatic young adults: a three-dimensional analysis using upright low-dose digital biplanar X-rays. *Spine (Phila Pa 1976)* 2009;34:E826–E832.
28. Brink RC, Colo D, Schlösser TPC, et al. Upright, prone, and supine spinal morphology and alignment in adolescent idiopathic scoliosis. *Scoliosis Spinal Disord.* 2017;12:6.



# PART III

22q11.2 Deletion Syndrome  
as a Model for Scoliosis





# 12

## Updated Clinical Practice Recommendations for *Children* with 22q11.2 Deletion Syndrome – Musculoskeletal guidelines

Sólveig Óskarsdóttir

Erik Boot

Terrence B. Crowley

Joanne C.Y. Loo

Jill M. Arganbright

Marco Armando

Adriane L. Baylis

Elemi J. Breetvelt

René M. Castelein

Madeline Chadehumbe

Christopher M. Cielo

Steven de Reuver

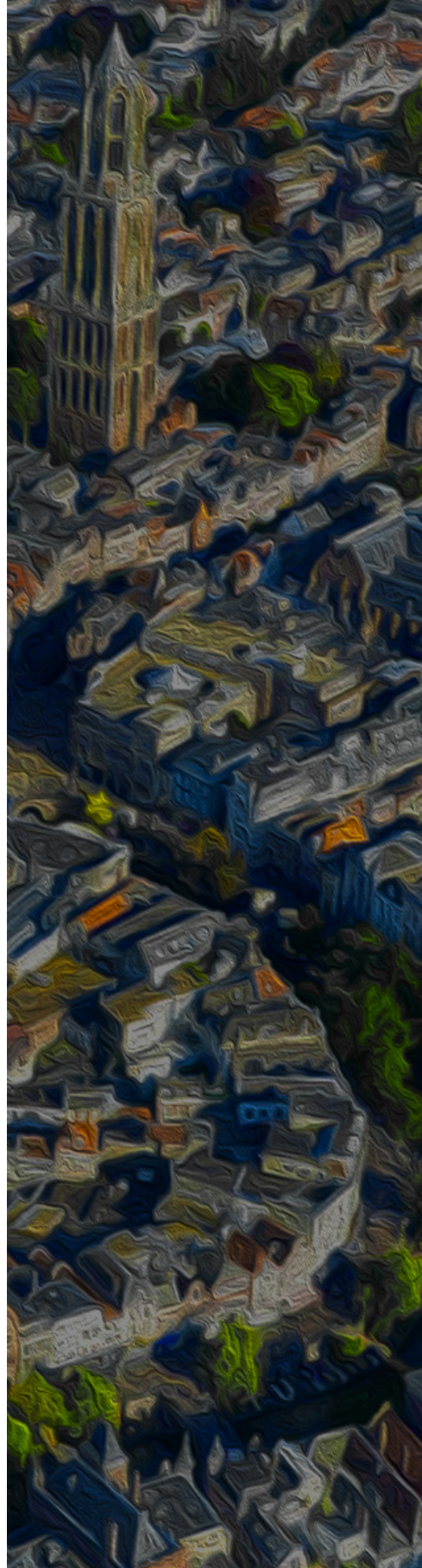
Jacob S. Vorstman

*[full author's list in the published article]*

Anne S. Bassett

Donna M. McDonald-McGinn

*Genetics in Medicine. 2023 Jan 31;100338.*



## **ABSTRACT**

This review aimed to update the clinical practice guidelines for managing children and adolescents with 22q11.2 deletion syndrome (22q11.2DS). The 22q11.2 Society, the international scientific organization studying chromosome 22q11.2 differences and related conditions, recruited expert clinicians worldwide to revise the original 2011 pediatric clinical practice guidelines in a stepwise process: (1) a systematic literature search (1992-2021), (2) study selection and data extraction by clinical experts from 9 different countries, covering 24 subspecialties, and (3) creation of a draft consensus document based on the literature and expert opinion, which was further shaped by survey results from family support organizations regarding perceived needs. Of 2441 22q11.2DS-relevant publications initially identified, 2344 received full-text reviews, including 1545 meeting criteria for potential relevance to clinical care of children and adolescents. Informed by the available literature, recommendations were formulated. Given evidence base limitations, multidisciplinary recommendations represent consensus statements of good practice for this evolving field. These recommendations provide contemporary guidance for evaluation, surveillance, and management of the many 22q11.2DS-associated physical, cognitive, behavioral, and psychiatric morbidities while addressing important genetic counseling and psychosocial issues.

## Introduction

22q11.2 deletion syndrome (22q11.2DS), a multisystem disorder including physical, cognitive, and behavioral issues of variable severity,<sup>1,2</sup> is the most common microdeletion syndrome in humans, with an estimated prevalence of 1 in 2148 live births and 1 in 992 pregnancies (Figure 1).<sup>3,4</sup> 22q11.2 deletion is the most frequent cause of DiGeorge syndrome and several other conditions previously described clinically (velocardiofacial syndrome, conotruncal anomaly face syndrome, Cayler cardiofacial) and a subset of patients with Opitz G/BBB syndrome.<sup>5-10</sup>

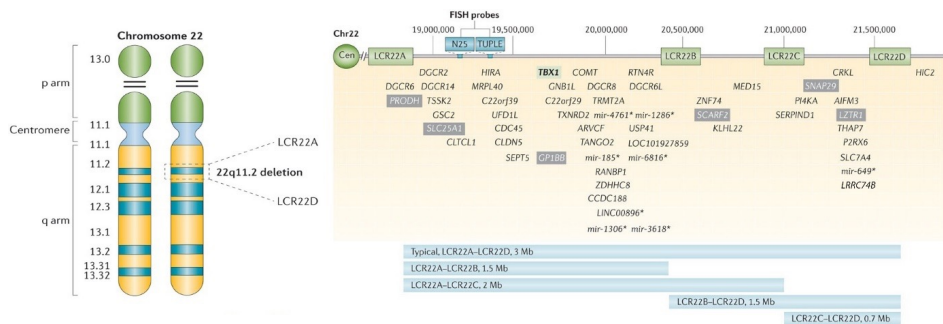


**Figure 1.** Chromosome 22 ideogram and genes within the 22q11.2 LCR22A-LCR22D region

22q11.2DS is often suspected because of congenital abnormalities, primarily cardiac and speech/language deficits, learning/behavioral problems, recurrent infections, and subtle dysmorphic features. Occasional cases are identified via newborn screening for severe combined immunodeficiency.<sup>1-11</sup> Feeding difficulties, hypocalcemia, and numerous structural anomalies may also be early alerting features.<sup>1</sup> Although awareness of 22q11.2DS has increased, the diagnosis is often delayed or missed, especially in those without serious congenital heart disease (CHD).<sup>12-14</sup> Clinical practice guidelines for managing patients with 22q11.2DS were first published in 2011.<sup>14</sup> Subsequent research has highlighted important novel associations. The aim in this study was to systematically review the literature and provide updated recommendations to facilitate optimal care for children and adolescents with 22q11.2DS.

## Materials and Methods

The 22q11.2 Society recruited expert clinicians worldwide to revise the original clinical practice guidelines for children through a stepwise process: (1) a systematic literature search, according to best practices (Preferred Reporting Items for Systematic Reviews and Meta-Analyses)<sup>15</sup> guided by a methodologist, (2) study selection and synthesis by the clinical

experts from 9 countries, covering 24 subspecialties, and (3) creation of a multidisciplinary consensus document using the Grading of Recommendations Assessment, Development and Evaluation framework (GRADE)<sup>16</sup> based on the literature and best practice and shaped by patient advocate survey results, with subsequent independent approval sought.

Inclusion criteria comprised any report with relevance to clinical care of individuals born with a 22q11.2 deletion involving the typical deletion region. Reports involving other conditions including distal 22q11.2 deletions or restricted to prenatal issues were excluded. Given the limited number of systematic studies in 22q11.2DS, a qualitative synthesis of the evidence was performed by a multidisciplinary panel of clinical experts, with review of all reports available from the systematic search.

Using the Grading of Recommendations Assessment, Development and Evaluation framework, high confidence evidence was deemed too limited to justify formal grading of individual recommendations with respect to the quality of available scientific literature or of fine gradations of strength.<sup>16</sup> Consensus recommendations were formulated based on the literature, consideration of being more beneficial than harmful, and best practice according to the experts involved (each having seen tens to hundreds of patients), and input from patient advocate survey results. The revised guidelines were subsequently approved for submission by 2 external reviewers (parent of a child with 22q11.2DS and a genetics expert), neither of whom were part of the guidelines updating process.

## **Results**

The systematic literature search initially identified 6018 publications regarding 22q11.2DS across the lifespan ([Online] Supplemental Figure 1); 3577 were excluded after initial screening (most were duplicates, or involved other conditions) and 97 could not be retrieved, resulting in 2344 reports included for full-text review. Thereafter, 26 reports were excluded as they had no relevance to clinical care. Of the final 2318 that met the inclusion criteria (list included in [Online] Supplemental Material, Study Selection and Data Extraction under Methods), 1545 were deemed to have potential relevance to children and adolescents.

The patient advocate survey results, completed by eight 22q11.2DS patient advocacy organizations, based in 7 countries on 3 continents and representing 7624 families, supported updated guidelines to improve: awareness for health care providers and the public; access to 22q11.2DS specific clinics, knowledgeable providers, and comprehensive care; and access to genetic testing and genetic counseling. The respondents ranked the top 5 most relevant

subspecialty areas of care, through a combination of free responses and checkboxes of predetermined options as (1) cardiology, (2) brain and behavior (psychiatry, neurology, early intervention, education), (3) genetics (testing, counseling, reproductive health), (4) ear, nose, and throat (ENT) (chronic infections, hearing, palate), and (5) immunology, rheumatology, hematology, and oncology. Regarding knowledge transfer, the respondents conveyed a need for guidelines to be shareable, portable, and available on the internet/social media.

The vast majority of scientific literature relevant to clinical management of children with 22q11.2DS involved study designs in low confidence categories,<sup>16</sup> with few randomized clinical trials, formal systematic reviews, or meta-analyses. Given the state of the scientific evidence available and the challenges inherent to 22q11.2DS that include multiple comorbidities and high inter-individual variability, recommendations in these updated guidelines were not formally graded on an individual basis.<sup>16</sup> The recommendations rather emphasize those with lowest harm and highest potential benefit for patients with this rare condition, informed by long term experience with patients and their families, that reflect current best practice.<sup>16</sup>

## Review and Practice Guidelines

### Brief overview

Pediatric care for patients with 22q11.2DS requires both generalists and specialists in multiple fields to appreciate the overall interrelated effects of associated medical and developmental features and their impact on well-being and quality of life. Basic knowledge about variable expressivity, severity of features, and changes over time, as well as an emphasis on family-centered care, are essential.<sup>17</sup>

Periodic assessments may identify new or anticipated features enabling early treatment. Preventive management of developmental issues can mitigate frustration and support achieving full potential. Coordination of care with multidisciplinary evaluations is required. Relatives, including parents, siblings, and often grandparents, benefit from information and support. Optimizing health, functioning, and quality of life is the overall goal of these recommendations

We summarize main features and management recommendations by system in the following sections and in corresponding tables. **Figure 2** presents the multisystem features, and **Table 1** highlights recommended assessments and health monitoring at diagnosis and by age. In this, international/local differences should be considered. Of note, these recommendations are most relevant to high-income countries and corresponding resources.

| Genetics   | Immunology  |
|--|---|
| Additional clinically relevant variant   | T cell lymphopenia  |
| <b>Prenatal</b>  | Recurrent infections  |
| Congenital heart disease (mostly conotruncal)  | Low immunoglobulins, humoral deficits   |
| Thymic hypoplasia/aplasia  | Asthma and allergies  |
| Dilated cavum septum pellucidum  | Autoimmune cytopenia (ITP, AHA)   |
| Palatal anomalies  | Juvenile idiopathic arthritis, vitiligo   |
| Renal anomalies, umbilical hernia  | <b>Hematology/Oncology</b>  |
| Skeletal (butterfly vertebrae, club foot, polydactyly)   | Low platelet numbers  |
| Polyhydramnios   | Bleeding, bruising, epistaxis   |
| Congenital diaphragmatic hernia, spina bifida  | Bernard-Soulier   |
| <b>Cardiology</b>  | Malignancy  |
| Congenital heart disease (mostly conotruncal)  | <b>Skeletal</b>   |
| Aortic arch anomalies (right aortic arch, vascular ring)   | Scoliosis   |
| Dilated aortic root  | Cervical spine anomalies  |
| <b>ENT /Palate/Speech</b>  | Butterfly vertebrae, 13 pairs of ribs   |
| Palatal anomalies (velopharyngeal dysfunction, SMCP, bifid uvula, overt cleft palate, CL/P)                | Recurrent patellar dislocations   |
| Speech disorders (especially hypernasality)  | Clubfoot, polydactyly, syndactyly   |
| Otitis media (acute or chronic with effusion)  | Craniosynostosis  |
| Hearing loss (conductive, sensorineural, mixed), cochlear abnormalities                                    | <b>Neurology</b>  |
| Airway anomalies (subglottic stenosis, laryngeal web)  | Hypotonia   |
| Obstructive sleep apnea  | Seizures/epilepsy   |
| Microtia, anotia, choanal atresia  | Microcephaly  |
| <b>Ophthalmology</b>   | Polymicrogyria, heterotopias, spina bifida, tethered cord, dystonia, Parkinsonism/Early onset Parkinson disease |
| Refractive errors (hyperopia/astigmatism)  | <b>General Surgery</b>  |
| Strabismus, exotropia/phoria, ptosis   | Hernia (all types)  |
| Sclerocornea   | Surgical complications (all types)  |
| Tortuous retinal vessels, posterior embryotoxon  | Congenital diaphragmatic hernia   |
| <b>Odontology</b>  | <b>Sleep</b>  |
| Caries   | Sleep pattern disturbances, obstructive sleep apnea   |
| Enamel defects   | <b>Cognitive Functioning and Development</b>  |
| Decreased saliva secretion   | Delayed gross motor milestones  |
| Delayed tooth eruption/agenesis  | Fine motor difficulties   |
| Malocclusion   | Delayed bladder control   |
| <b>Endocrinology</b>   | Developmental coordination disorder   |
| Hypocalcaemia/hypoparathyroidism   | Speech-language delay/disorders   |
| Hypothyroidism, hyperthyroidism  | Learning difficulties, cognitive deficits, NVLD   |
| Growth hormone deficiency  | Intellectual disabilities (mostly mild)   |
| <b>Growth</b>  | Visuo-spatial impairments   |
| Growth restriction in infancy and childhood  | <b>Psychiatry</b>   |
| Short stature  | Attention deficit disorder or ADHD  |
| Obesity in adolescence   | Autism spectrum disorder  |
| <b>Gastroenterology and Nutrition</b>  | Anxiety disorders   |
| Feeding difficulty   | Subclinical psychotic symptoms  |
| Constipation   | Schizophrenia spectrum disorders  |
| Gastrointestinal reflux disease, dysphagia   | Depression  |
| Aspiration, NG/G-tube feeds/Nissen fundoplication  | Anorexia  |
| Malformations (imperforate anus, Hirschsprung's, intestinal malrotation, esophageal/tracheal atresia, TEF) |   |
| Cyclical vomiting  |   |
| <b>Genitourinary</b>   |   |
| Renal anomalies (e.g. hydronephrosis, renal agenesis, multicystic/dysplastic kidney)                       |   |
| Dysfunctional voiding  |   |
| Males: cryptorchidism, hypospadias, phimosi  |   |
| Females: vaginal agenesis, absent uterus   |   |

| Key  |
|--|
| Common                                       |
| Less common                                  |
| Rare, but clinically relevant                |
| Common, but not requiring clinical attention |

Figure 2. Features and risks in children and adolescents with 22q11.2 deletion syndrome



| Assessments and Management   | At Diagnosis | Annual/<br>Biennial | 0-1 y | 1-5 y | 6-12 y | 13-18 y |
|--|--------------|---------------------|-------|-------|--------|---------|
| <b>Genetic</b>   |              |                     |       |       |        |         |
| Genetic testing (proband: MLPA or microarray; FISH if only available method) (parents: MLPA or FISH) <sup>a</sup>              | ✓            |                     |       |       |        |         |
| Genetic counseling (etiology, natural history, recurrence risk, prenatal/preconception screening/diagnostics)                  | ✓            | ✓                   |       |       |        | ✓       |
| Remaining allele/exome sequencing (when appropriate) <sup>b</sup>  | ✓            |                     |       |       |        |         |
| <b>General</b>   |              |                     |       |       |        |         |
| Consultation with clinician(s) experienced with 22q11.2DS <sup>c</sup>   | ✓            | ✓                   | ✓     | ✓     | ✓      | ✓       |
| Comprehensive history-taking (including family history)  | ✓            | ✓                   | ✓     | ✓     | ✓      | ✓       |
| Physical examination   | ✓            | ✓                   | ✓     | ✓     | ✓      | ✓       |
| Nutritional assessment, feeding, swallowing, GERD, constipation, and growth  | ✓            | ✓                   | ✓     | ✓     | ✓      | ✓       |
| Neurologic and developmental assessment (neurologic exam, milestones, sacral dimple, neuroimaging as needed)                   | ✓            |                     | ✓     | ✓     | ✓      | ✓       |
| Assessment of history of infections, allergy, asthma, autoimmunity, and malignancy   | ✓            | ✓                   | ✓     | ✓     | ✓      | ✓       |
| Assessment of access to specialized health care and community, developmental, and government resources                         | ✓            |                     | ✓     | ✓     | ✓      | ✓       |
| <b>Other clinical assessments</b>  |              |                     |       |       |        |         |
| Cardiac evaluation (using echocardiogram and EKG; determine arch sidedness)  | ✓            |                     |       |       |        |         |
| Long term follow-up for all with CHD; transition to GUCH if CHD  |              | ✓                   | ✓     | ✓     | ✓      | ✓       |
| Periodic screening for arrhythmias/EKG abnormalities and dilated aortic root <sup>d</sup>                                      |              |                     |       | ✓     | ✓      | ✓       |
| Periodic EKG screening in at-risk patients (antiepileptic/neuropsychiatric treatment, hypocalcemia, thyroid disease)           |              | ✓                   |       |       |        |         |
| Referral to cleft-palate team to assess for overt cleft, SMCP, and VPD (nasoendoscopy/videofluoroscopy as needed) <sup>e</sup> | ✓            |                     | ✓     | ✓     | ✓      | ✓       |
| Evaluation of speech and language by speech-language pathologist <sup>f</sup>  | ✓            |                     | ✓     | ✓     | ✓      | ✓       |
| Evaluation by otolaryngologist for recurrent otitis media and possible laryngo-tracheo-esophageal anomalies                    | ✓            |                     | ✓     | ✓     | ✓      | ✓       |
| Evaluation of hearing using audiogram +/- tympanometry   | ✓            | ✓                   | ✓     | ✓     | ✓      | ✓       |
| Ophthalmic evaluation/vision (refractive errors, strabismus, exotropia, sclerocornea, coloboma, ptosis)                        | ✓            |                     | ✓     | ✓     |        |         |
| Dental evaluation (measure saliva secretion rate from 6 y) <sup>g</sup>  |              |                     |       | ✓     | ✓      | ✓       |
| Endocrinological assessment (PTH, calcium, magnesium, creatinine, TSH, and free T4; GH studies as needed)                      | ✓            | ✓                   | ✓     | ✓     | ✓      | ✓       |
| Consider clinical (multidisciplinary) feeding and/or swallowing evaluation including assessment of airway <sup>h</sup>         |              |                     | ✓     | ✓     |        |         |
| Renal and bladder ultrasound   | ✓            |                     |       |       |        |         |
| Immunologic assessment: T- and B cell phenotyping <sup>i</sup>   | ✓            |                     | ✓     | ✓     |        | ✓       |
| Immunologic assessment: IgG, IgA, IgM, IgE levels (not before 6 mo)  |              |                     | ✓     | ✓     |        | ✓       |
| Immunologic assessment: vaccine responses <sup>j</sup>   |              |                     | ✓     | ✓     |        |         |
| Complete blood count and differential  | ✓            | ✓                   | ✓     | ✓     | ✓      | ✓       |
| Routine scoliosis screening with scoliometer and with x-ray when clinically indicated  |              |                     |       |       | ✓      | ✓       |
| Radiography of the cervical spine at age ~4 y to exclude instability <sup>k</sup>  |              |                     |       | ✓     |        |         |
| Sleep evaluation (consider polysomnography pre and post VPD repair), sleep hygiene recommendations <sup>l</sup>                |              |                     |       | ✓     | ✓      |         |
| <b>Cognitive development, academic functioning, and child psychiatry</b>   |              |                     |       |       |        |         |
| Assessment of cognitive/learning capacities including language domains with standardized measures                              | ✓            |                     |       | ✓     | ✓      | ✓       |

**Table 1.** Recommendations for periodic assessment and management of children and adolescents with 22q11.2 deletion syndrome at diagnosis, annually/biannually, and by age. For the full table legend please see the online version.

## Genetics & Genetic counseling

22q11.2DS is a contiguous gene deletion syndrome. Affected individuals have a heterozygous loss of 1 copy of the chromosome 22q11.2 region. Most deletions occur as de novo events but approximately 10% are inherited from a parent.<sup>12,18,19</sup> The typical 22q11.2 deletion originates from nonallelic homologous recombination between low copy repeats (LCRs),<sup>20-23</sup> most commonly LCR22A to LCR22D (85%-90%), resulting in an approximately 2.5 to 3 megabase (Mb) deletion involving approximately 50 protein-coding genes.<sup>1</sup> Smaller LCR22A to LCR22B (1.5 Mb) and LCR22A to LCR22C (2.0 Mb) deletions occur in 5% to 10% of the cases.<sup>1,18</sup> Rarer LCR22B to LCR22D and LCR22C to LCR22D deletions (~5%) occur with overlapping features as this region includes the important developmental gene CRKL associated with congenital heart disease and renal anomalies.<sup>12,24</sup> Distal deletions beyond LCR22D (involving other LCRs, LCR22E to LCR22H, OMIM 611867), comprising a distinct entity, should not be confused with 22q11.2DS and are not the subject of these recommendations.

Beginning in the 1990's, the 22q11.2 deletion was identified using fluorescence in situ hybridization (FISH) and probes located between LCR22A-LCR22B.<sup>18</sup> Later, multiplex-ligation dependent probe amplification became available, providing deletion sizing,<sup>25,26</sup> but both tests required an elevated index of suspicion. Chromosomal microarray analysis (CMA) identifies genome-wide copy number variants (CNVs), thus 22q11.2 deletions and their breakpoints and in a minority of patients any other relevant CNVs if present.<sup>27,28</sup> Even the common 2.5 Mb deletion is usually submicroscopic, ie, missed in karyotyping except for rare unbalanced translocations. Thus, CMA currently provides the most clinically useful information for diagnosis and genetic counseling, but we acknowledge that it may not be available or covered in many settings around the world.

Parental testing is always recommended to determine whether the 22q11.2 deletion is de novo or transmitted from a parent to provide care and genetic counseling for the affected parent.<sup>14,29</sup> This includes the opportunity to identify the rare parent with somatic mosaicism. Parents of a child with a de novo deletion have a small increased recurrence risk over the general population based on reports of germline mosaicism.<sup>19,20</sup> Reproductive counseling will include discussions regarding prenatal screening/definitive testing options. Affected individuals, both males and females, have a 50% chance of having a child with 22q11.2DS in each pregnancy. In addition to care recommendations, as for any newly diagnosed individual, risk of transmission and variable expressivity are key discussion points. Available reproductive options including prenatal screening and preconception options such as preimplantation genetic diagnostics using in vitro fertilization should also be reviewed.



## Clinical Practice Recommendations

For other systems than musculoskeletal, please refer to the full article:

<https://doi.org/10.1016/j.gim.2022.11.006>

### Musculoskeletal

Scoliosis, usually of adolescent idiopathic type, is common and may be clinically significant,<sup>30-33</sup> sometimes requiring bracing/spinal surgery.<sup>33-35</sup> Other skeletal issues sometimes requiring surgical intervention include patellar dislocation,<sup>33,36,37</sup> clubfoot,<sup>13,37-39</sup> polydactyly,<sup>13,40-41</sup> hammer toe and other foot anomalies.<sup>40-43</sup> Cervical/occipital anomalies found in almost all children are rarely consequential (although surgical intervention may be required),<sup>44-45</sup> likewise, for butterfly vertebrae and 13 pairs of ribs.<sup>41</sup> Several cases of juvenile idiopathic arthritis often polyarticular and associated with IgA deficiency have been reported.<sup>37,39,46,47</sup> Underrepresented in the literature are frequent nonspecific lower leg/foot pains,<sup>14</sup> which may be associated with pes planovalgus and may benefit from orthotics. Cramping pain from hypocalcemia and other causes, including juvenile idiopathic arthritis, should be considered.

Routine scoliosis screening is recommended, with scoliometer and with x-ray when clinically indicated, with some sites screening from age 6 years with radiography at 2-year intervals until skeletal maturity.<sup>31</sup> A one-time screening for cervical spinal anomalies and instability, with radiography including atlas-dens measurements in flexion and extension is recommended around age 4 years.<sup>30,44,48</sup> In older children and adolescents, if patellar dislocation is suspected, radiographs are indicated.

### Discussion

In these updated clinical practice guidelines, we provide recommendations for evaluation, management, and follow-up of children with 22q11.2DS from birth to 18 years of age. We outline associated features and the changing phenotype over the pediatric lifespan (**Figure 3**). The recommendations are based on the current state of knowledge and consensus by experts in the field from many countries. Although some recommendations are relevant for all, management must be targeted to suit the individual and the individual condition(s). In addition, local differences in health care, educational, social, and other systems need consideration. Coordination of care, involving generalists and specialists from a wide range of needed services, is important to help diminish the burden on patients and their families.

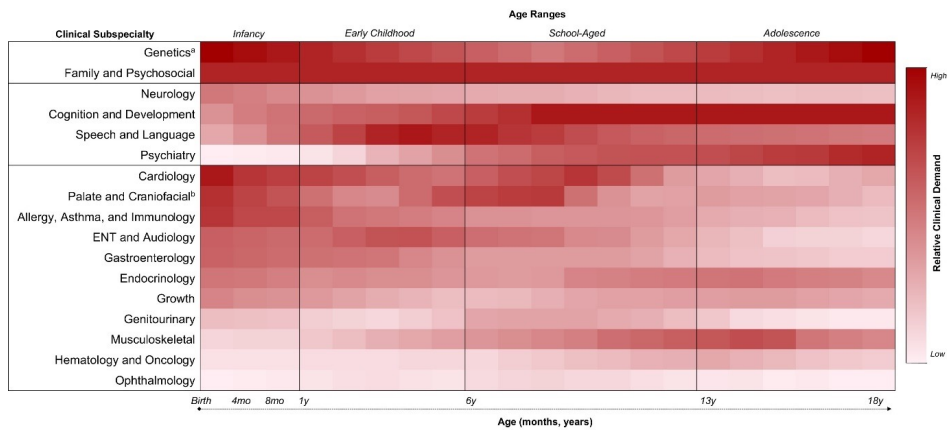


**Figure 3.** Multidisciplinary demand over time in children with 22q11.2DS

Since the publication of the first practical guidelines for managing patients with 22q11.2DS in 2011,<sup>14</sup> our knowledge and understanding of many associated features has increased, and recently, subspecialty guidelines have been developed for speech-language disorders and prenatal considerations.<sup>49</sup> Primarily observational research has included new data on physical features, such as the risk of developing scoliosis, and the developmental, cognitive, and psychiatric phenotypes that are of major concern to parents throughout the pediatric years and beyond. Research examining the evolving expression of 22q11.2DS across developmental ages and stages and interrelated effects of physical, neuropsychiatric, and developmental features reinforce the need for multidisciplinary care with a holistic view.

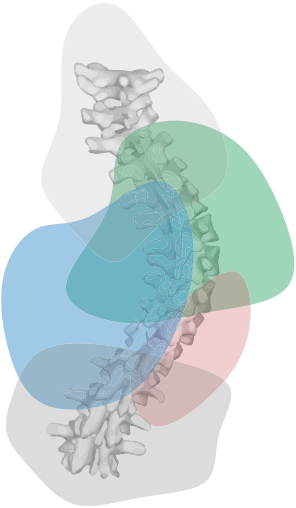
There remain many gaps however in our knowledge and understanding of this multisystem disorder. The lack of high-quality evidence limits the strength of the recommendations. Particularly, there is a need for well-designed studies to evaluate recommendations contained in these guidelines, determine possible differences for individuals with atypical nested 22q11.2 deletions, further contribute to the problematic area of predicting outcome, and assess current and novel treatment modalities. Such studies will strengthen our future recommendations so that we may move closer to our primary goal to optimize health, functioning, and quality of life for children with 22q11.2DS. The lack of systematic studies and high-quality evidence in 22q11.2DS made many steps and processes that would be typically undertaken in a rigorous systematic review not available.

Thus, these multidisciplinary pediatric recommendations, along with the companion adult recommendations,<sup>50</sup> represent consensus statements of good practice for this evolving field, including contemporary guidance for evaluation, surveillance, and management of the many 22q11.2DS-associated physical, cognitive behavioral, and psychiatric morbidities, while addressing important genetic counseling and psychosocial issues. As for our initial publication, these recommendations will continue to require updating, proposed for 5 years hence, as new information becomes available.

## References

1. McDonald-McGinn DM, Sullivan KE, Marino B, et al. 22q11.2 deletion syndrome. *Nat Rev Dis Primers*. 2015;1:15071.
2. McDonald-McGinn DM. 22q11.2 deletion – a tiny piece leading to a big picture. *Nat Rev Dis Primers*. 2020;6(1):33.
3. Blagojevic C, Heung T, Theriault M, et al. Estimate of the contemporary live-birth prevalence of recurrent 22q11.2 deletions: a cross-sectional analysis from population-based newborn screening. *CMAJ Open*. 2021;9(3):E802-E809.
4. Grati FR, Molina Gomes D, Ferreira JC, et al. Prevalence of recurrent pathogenic microdeletions and microduplications in over 9500 pregnancies. *Prenat Diagn*. 2015;35(8):801-809.
5. McDonald-McGinn DM, Hoffman E, Lairson A, McGinn DE, Zackai EH. Chapter 1 - 22q11.2 deletion syndrome: setting the stage. In: McDonald-McGinn DM, ed. *The Chromosome 22q11.2 Deletion Syndrome*. Academic Press; 2022:2-32.
6. Driscoll DA, Salvin J, Sellinger B, et al. Prevalence of 22q11 microdeletions in DiGeorge and velocardiofacial syndromes: implications for genetic counselling and prenatal diagnosis. *J Med Genet*. 1993;30(10):813-817
7. Burn J, Takao A, Wilson D, et al. Conotruncal anomaly face syndrome is associated with a deletion within chromosome 22q11. *J Med Genet*. 1993;30(10):822-824.
8. Giannotti A, Digilio MC, Marino B, Mingarelli R, Dallapiccola B. Cayler cardiofacial syndrome and del 22q11: part of the CATCH22 phenotype. *Am J Med Genet*. 1994;53(3):303-304.
9. McDonald-McGinn DM, Driscoll DA, Bason L, et al. Autosomal dominant "Opitz" GBBB syndrome due to a 22q11.2 deletion. *Am J Med Genet*. 1995;59(1):103-113.
10. McDonald-McGinn DM, LaRossa D, Goldmuntz E, et al. The 22q11.2 deletion: screening, diagnostic workup, and outcome of results; report on 181 patients. *Genet Test*. 1997;1(2):99-108.
11. Barry JC, Crowley TB, Jyonouchi S, et al. Identification of 22q11.2 deletion syndrome via newborn screening for severe combined immunodeficiency. *J Clin Immunol*. 2017;37(5):476-485.
12. Campbell IM, Sheppard SE, Crowley TB, et al. What is new with 22q? An update from the 22q and You Center at the Children's Hospital of Philadelphia. *Am J Med Genet A*. 2018;176(10):2058-2069.
13. Oskarsdottir S, Persson C, Eriksson BO, Fasth A. Presenting phenotype in 100 children with the 22q11 deletion syndrome. *Eur J Pediatr*. 2005;164(3):146-153.
14. Bassett AS, McDonald-McGinn DM, Devriendt K, et al. Practical guidelines for managing patients with 22q11.2 deletion syndrome. *J Pediatr*. 2011;159(2):332-339.e1.
15. Page MJ, McKenzie JE, Bossuyt PM, et al. The PRISMA 2020 statement: an updated guideline for reporting systematic reviews. *BMJ*. 2021;372:n71.
16. Guyatt GH, Oxman AD, Vist GE, et al. GRADE: an emerging consensus on rating quality of evidence and strength of recommendations. *BMJ*. 2008;336(7650):924-926.
17. Berens J, Wozow C, Peacock C. Transition to adult care. *Phys Med Rehabil Clin N Am*. 2020;31(1):159-170
18. Lu JH, Chung MY, Hwang B, Chien HP. Prevalence and parental origin in tetralogy of Fallot associated with chromosome 22q11 microdeletion. *Pediatrics*. 1999;104(1 Pt 1):87-90.
19. Green T, Gothelf D, Glaser B, et al. Psychiatric disorders and intellectual functioning throughout development in velocardiofacial (22q11.2 deletion) syndrome. *J Am Acad Child Adolesc Psychiatry*. 2009;48(11):1060-1068
20. Edelmann L, Pandita RK, Spiteri E, et al. A common molecular basis for rearrangement disorders on chromosome 22q11. *Hum Mol Genet*. 1999;8(7):1157-1167.
21. Guo T, Diacou A, Nomaru H, et al. Deletion size analysis of 1680 22q11.2DS subjects identifies a new recombination hotspot on chromosome 22q11.2. *Hum Mol Genet*. 2018;27(7):1150-1163.
22. Edelmann L, Pandita RK, Morrow BE. Low-copy repeats mediate the common 3-Mb deletion in patients with velo-cardio-facial syndrome. *Am J Hum Genet*. 1999;64(4):1076-1086.
23. Shaikh TH, Kurahashi H, Saitta SC, et al. Chromosome 22-specific low copy repeats and the 22q11.2 deletion syndrome: genomic organization and deletion endpoint analysis. *Hum Mol Genet*. 2000;9(4):489-501.
24. Rozas MF, Benavides F, León L, Repetto GM. Association between phenotype and deletion size in 22q11.2 microdeletion syndrome: systematic review and meta-analysis. *Orphanet J Rare Dis*. 2019;14(1):195
25. Fernández L, Lapunzina P, Arjona D, et al. Comparative study of three diagnostic approaches (FISH, STRs and MLPA) in 30 patients with 22q11.2 deletion syndrome. *Clin Genet*. 2005;68(4):373-378.
26. Vorstman JAS, Jalali GR, Rappaport EF, Hacker AM, Scott C, Emanuel BS. MLPA: a rapid, reliable, and sensitive method for detection and analysis of abnormalities of 22q. *Hum Mutat*. 2006;27(8):814-821.
27. Busse T, Graham JM Jr, Feldman G, et al. High-resolution genomic arrays identify CNVs that phenocopy the chromosome 22q11.2 deletion syndrome. *Hum Mutat*. 2011;32(1):91-97.
28. Cohen JL, Crowley TB, McGinn DE, et al. 22q and two: 22q11.2 deletion syndrome and coexisting conditions. *Am J Med Genet A*. 2018;176(10):2203-2214
29. Schindewolf E, Khalek N, Johnson MP, et al. Expanding the fetal phenotype: prenatal sonographic findings and perinatal outcomes in a cohort of patients with a confirmed 22q11.2 deletion syndrome. *Am J Med Genet A*. 2018;176(8):1735-1741
30. Homans JF, Tromp IN, Colo D, et al. Orthopaedic manifestations within the 22q11.2 Deletion syndrome: a systematic review. *Am J Med Genet A*. 2018;176(10):2104-2120.

31. Homans JF, Baldew VGM, Brink RC, et al. Scoliosis in association with the 22q11.2 deletion syndrome: an observational study. *Arch Dis Child*. 2019;104(1):19-24.
32. de Reuver S, Homans JF, Schlösser TPC, et al. 22q11.2 deletion syndrome as a human model for idiopathic scoliosis. *J Clin Med*. 2021;10(21):4823.
33. Bassett AS, Chow EW, Husted J, et al. Clinical features of 78 adults with 22q11 deletion syndrome. *Am J Med Genet A*. 2005;138(4):307-313.
34. Morava E, Lacassie Y, King A, Illes T, Marble M. Scoliosis in velo-cardio-facial syndrome. *J Pediatr Orthop*. 2002;22(6):780-783.
35. Cheng JC, Castelein RM, Chu WC, et al. Adolescent idiopathic scoliosis. *Nat Rev Dis Primers*. 2015;1:15030.
36. Boot E, Butcher NJ, van Amelsvoort TA, et al. Movement disorders and other motor abnormalities in adults with 22q11.2 deletion syndrome. *Am J Med Genet A*. 2015;167A(3):639-645.
37. Friedman N, Rienstein S, Yeshayahu Y, Gothelf D, Somech R. Post-childhood presentation and diagnosis of DiGeorge syndrome. *Clin Pediatr (Phila)*. 2016;55(4):368-373.
38. Poirsier C, Besseau-Ayasse J, Schluth-Bolard C, et al. A French multicenter study of over 700 patients with 22q11 deletions diagnosed using FISH or aCGH. *Eur J Hum Genet*. 2016;24(6):844-851.
39. Sullivan KE, McDonald-McGinn DM, Driscoll DA, et al. Juvenile rheumatoid arthritis-like polyarthritis in chromosome 22q11.2 deletion syndrome (DiGeorge anomalad/velocardiofacial syndrome/conotruncal anomaly face syndrome). *Arthritis Rheum*. 1997;40(3):430-436.
40. Ryan AK, Goodship JA, Wilson DI, et al. Spectrum of clinical features associated with interstitial chromosome 22q11 deletions: a European collaborative study. *J Med Genet*. 1997;34(10):798-804.
41. Ming JE, McDonald-McGinn DM, Megerian TE, et al. Skeletal anomalies and deformities in patients with deletions of 22q11. *Am J Med Genet*. 1997;72(2):210-215.
42. Derbent M, Yilmaz Z, Baltaci V, Saygili A, Varan B, Tokel K. Chromosome 22q11.2 deletion and phenotypic features in 30 patients with conotruncal heart defects. *Am J Med Genet A*. 2003;116A(2):129-135.
43. Vantrappen G, Devriendt K, Swillen A, et al. Presenting symptoms and clinical features in 130 patients with the velo-cardio-facial syndrome. The Leuven experience. *Genet Couns*. 1999;10(1):3-9.
44. Ricchetti ET, States L, Hosalkar HS, et al. Radiographic study of the upper cervical spine in the 22q11.2 deletion syndrome. *J Bone Joint Surg Am*. 2004;86(8):1751-1760.
45. Veerapandiyan A, Blalock D, Ghosh S, Ip E, Barnes C, Shashi V. The role of cephalometry in assessing velopharyngeal dysfunction in velocardiofacial syndrome. *Laryngoscope*. 2011;121(4):732-737.
46. Sato S, Kawashima H, Suzuki K, Nagao R, Tsuyuki K, Hoshika A. A case of juvenile idiopathic polyarticular arthritis complicated by IgA deficiency in 22q11 deletion syndrome. *Rheumatol Int*. 2011;31(8):1089-1092.
47. Pelkonen P, Lahdenne P, Lantto R, Honkanen V. Chronic arthritis associated with chromosome deletion 22q11.2 syndrome. *J Rheumatol*. 2002;29(12):2648-2650.
48. Torg JS, Ramsey-Emrhein JA. Management guidelines for participation in collision activities with congenital, developmental, or postinjury lesions involving the cervical spine. *Clin Sports Med*. 1997;16(3):501-530.
49. Blagowidow N, Nowakowska B, Schindewolf E, et al. Prenatal Screening and Diagnostic Considerations for 22q11.2 Microdeletions. *Genes*. 2023;14(1):160.
50. Boot E, Oskarsdottir S, Loo JCY, et al. Updated clinical practice recommendations for managing adults with 22q11.2 deletion syndrome. *Genet Med*. 2023;25:100344.



# 13

## Updated Clinical Practice Recommendations for *Adults* with 22q11.2 Deletion Syndrome – Musculoskeletal guidelines

Erik Boot

Sólveig Óskarsdóttir

Joanne C.Y. Loo

Terrence B. Crowley

Ani Orchanian-Cheff

Danielle M. Andrade

Jill M. Arganbright

René M. Castelein

Christine Cserti-Gazdewich

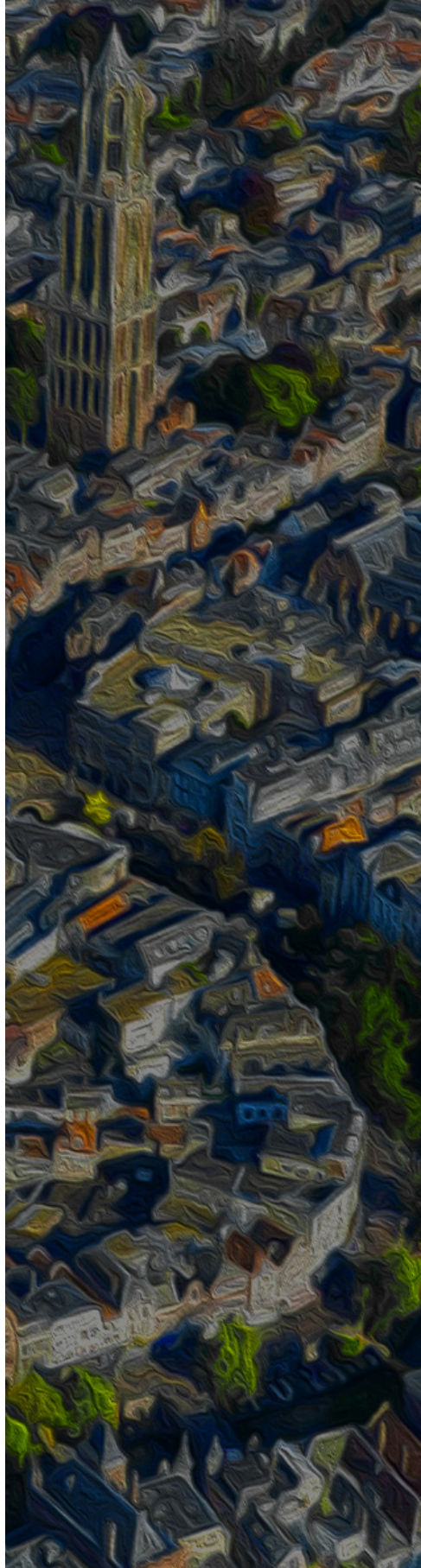
Steven de Reuver

*[full author's list in the published article]*

Donna M. McDonald-McGinn

Anne S. Bassett

*Genetics in Medicine. 2023 Jan 31;100344*



## **ABSTRACT**

This review aimed to update the clinical practice guidelines for managing adults with 22q11.2 deletion syndrome (22q11.2DS). The 22q11.2 Society recruited expert clinicians worldwide to revise the original clinical practice guidelines for adults in a stepwise process according to best practices: (1) a systematic literature search (1992-2021), (2) study selection and synthesis by clinical experts from 8 countries, covering 24 subspecialties, and (3) formulation of consensus recommendations based on the literature and further shaped by patient advocate survey results. Of 2441 22q11.2DS-relevant publications initially identified, 2344 received full-text review, with 2318 meeting inclusion criteria (clinical care relevance to 22q11.2DS) including 894 with potential relevance to adults. The evidence base remains limited. Thus multidisciplinary recommendations represent statements of current best practice for this evolving field, informed by the available literature. These recommendations provide guidance for the recognition, evaluation, surveillance, and management of the many emerging and chronic 22q11.2DS-associated multisystem morbidities relevant to adults. The recommendations also address key genetic counseling and psychosocial considerations for the increasing numbers of adults with this complex condition.



## Introduction

22q11.2 deletion syndrome (22q11.2DS), the most common microdeletion syndrome in humans,<sup>1</sup> is a multisystem disorder associated with congenital and later-onset health issues, with an estimated prevalence of 1 in 2148 live births (4.7 per 10,000) based on a recent population-based newborn screening study (**Figure 1**).<sup>2</sup> Despite the prevalence, substantial morbidity, and availability of clinical testing, 22q11.2DS, previously known as DiGeorge syndrome or velo-cardio-facial syndrome, remains largely unrecognized in adults by both health care providers and society at large.

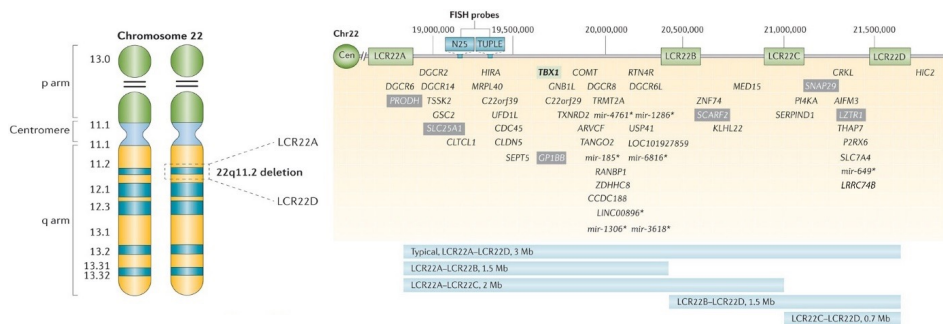


**Figure 1.** Chromosome 22 ideogram and genes within the 22q11.2 LCR22A-LCR22D region

The first clinical practice guidelines for managing adults with 22q11.2DS were published in 2015.<sup>3</sup> Subsequently, there has been considerable new research on associated conditions and functioning. With a growing adult population with 22q11.2DS, owing primarily to improved detection and clinical care of children, updated guidance is needed. Using a systematic review of the literature published between 1992-2021, we have updated the 2015 clinical practice guidelines for adults with 22q11.2DS. Adults are defined in this study as age 18 years and older, thus spanning transition from pediatric care to the elderly age range.

## Materials and Methods

The 22q11.2 Society recruited expert clinicians worldwide to revise the original clinical practice guidelines for adults in a stepwise process: (1) a systematic literature search according to best practices (Preferred Reporting Items for Systematic Reviews and Meta-Analyses, 2020; [Online] Supplemental Figure 1),<sup>4</sup> guided by a methodologist, (2) study selection and synthesis by these clinical experts from 8 countries, covering 24 subspecialties, and (3) creation of a multidisciplinary consensus document using the Grading of Recommendations Assessment, Development and Evaluation framework,<sup>5</sup> based on the literature, best practice, and shaped by patient advocate survey results, with subsequent independent approval sought.

Inclusion criteria comprised any report with relevance to clinical care of individuals born with a 22q11.2 deletion involving the typical 22q11.2 deletion region (ie, overlapping the low-copy repeats (LCRs) LCR22A to LCR22B region and most commonly overlapping the LCR22A to LCR22D region; see Genetics section and Figure 1). Reports involving other conditions, such as distal 22q11.2 deletions or restricted to prenatal issues, were excluded. Given the limited number of systematic studies, eg, randomized controlled trials, in the 22q11.2DS literature, a qualitative synthesis of the evidence was performed by a multidisciplinary panel of clinical experts, with review of all reports available from the systematic search.

Using the Grading of Recommendations Assessment, Development, and Evaluation framework, high confidence evidence was deemed too limited to justify formal grading of individual recommendations with respect to the quality of available scientific literature or of fine gradations of strength.<sup>5</sup> Draft recommendations per subspecialty/topic were formulated based on critical appraisal of the literature, consideration of being more beneficial than harmful, and best practice per the experts involved (each having seen tens to hundreds of adult patients with 22q11.2DS), while incorporating input from patient advocate survey results. The revised document was subsequently approved for submission by 2 external reviewers (a family member of an adult with 22q11.2DS and a genetics expert), neither of whom were part of the guidelines updating process.

## Results

The systematic literature search (January 1, 1992 to April 14, 2021) initially identified 6018 citations putatively related to 22q11.2DS across the lifespan ([Online] Supplemental Figure 1); 3577 were excluded after screening (most were duplicates or involved other conditions) and 97 were not able to be retrieved. This resulted in 2344 reports included for full-text review, of which a final 2318 met inclusion criteria. Of these, 894 were deemed to have potential relevance to adults. See Supplemental Table 2 for the list of the 2441 articles that were sought for retrieval.

The patient advocate survey results, completed by eight 22q11.2DS patient advocacy organizations, based in 7 countries on 3 continents and representing 7624 families, prioritized updated guidelines to improve awareness among health care providers and the public; access to 22q11.2DS specific clinics, knowledgeable providers, and comprehensive care; and access to genetic testing and genetic counseling. They ranked the top 5 most relevant subspecialty areas of care, regardless of age, as cardiology; brain and behavior (psychiatry,

neurology, early intervention, education); genetics (testing, counseling, reproductive health); ear, nose, and throat (chronic infections, hearing, palate); and immunology, rheumatology, and hematology-oncology. Regarding knowledge transfer, the respondents conveyed a need for guidelines to be shareable, portable, and available on the internet/social media.

The vast majority of scientific literature relevant to clinical management of adults with 22q11.2DS involved study designs in low confidence categories,<sup>5</sup> with vanishingly few randomized clinical trials, formal systematic reviews, or meta-analyses. Given the state of the scientific evidence available and the challenges inherent to 22q11.2DS, which include multiple comorbidities and high interindividual variability, recommendations in these updated guidelines were not formally graded on an individual basis.<sup>5</sup> Globally, the recommendations should therefore be considered to be weak (ie, conditional or individualized), in all cases emphasizing those with lowest harm and highest potential benefit for patients with this rare condition, informed by long-term experience with patients with 22q11.2DS and their families, that reflect current best practice.<sup>5</sup>

## **Clinical Practice Recommendations—General Aspects of Management**

### Brief overview

Adults with 22q11.2DS require follow-up, regardless of age at diagnosis. There may be congenital/early-onset manifestations of 22q11.2DS with persisting ramifications, but in virtually all cases, later-onset conditions emerge that require clinical attention. Knowledge about the high variability in number and severity of manifestations and 22q11.2DS-related risks is essential. Periodic assessments may reveal (previously) undetected medical conditions, enabling early treatment, and should be tailored to different life stages.

The multisystem nature and developmental complexity of 22q11.2DS demand broad consideration of signs and symptoms (**Figures 2 & 3**), with visits therefore often necessitating considerable time and effort. Having an interested/informed generalist involved for patient care/follow-up/coordination is advantageous.

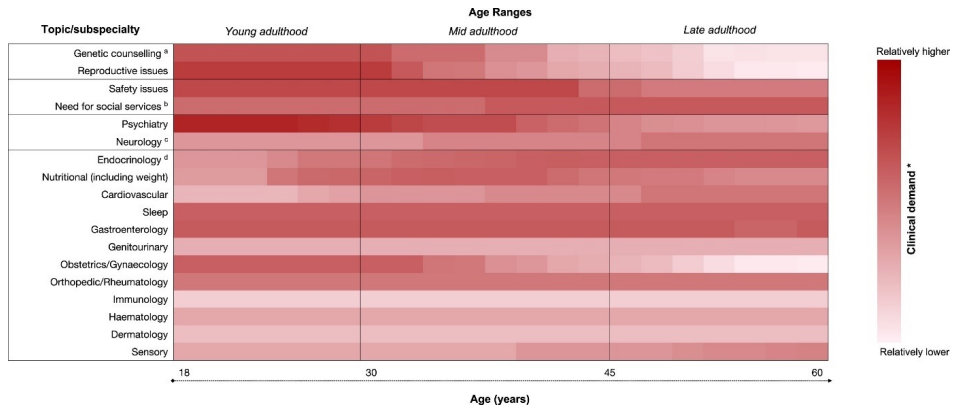


**Figure 2.** Estimated multidisciplinary demand over time for adults with 22q11.2 deletion syndrome

Typically, for the associated conditions, standard management and treatment strategies apply, as for idiopathic forms of each condition, with similar efficacy expected. The main caveat is that 22q11.2DS-related comorbidity demands attention by all clinicians, regardless of their subspecialty, with balancing of risks/benefits for proposed treatments. Repetition and reinforcement of information, written summaries, and use of simple diagrams and visual aids to illustrate major points can be helpful. Involvement of families and/or caregivers, who often provide monitoring/oversight of treatment compliance and results, is usually essential.<sup>3</sup>

Patients and relatives/caregivers require their own individual time with professionals. Personalized medical information cards may be useful.<sup>6</sup> Optimizing lifetime health and functioning is the overall goal and includes clear coordination between all involved. **Figure 3** presents the multisystem features and **Table 1** an overview of recommendations for periodic assessments and health monitoring, in order of their clinical relevance to 22q11.2DS and the clinical attention typically required.<sup>3,7</sup> International/local differences should be considered. Of note, however, these recommendations are most relevant to high-income countries and with corresponding resources.

|  |  |
|--|--|
| Genetics   |  |
| Additional clinically relevant variant                           |  |
| Cognitive and adaptive functioning                               |  |
| Intellectual disabilities  |  |
| Intellectual decline   |  |
| Deficits in adaptive functioning                                 |  |
| Impairments in executive functions                               |  |
| Psychiatry   |  |
| Anxiety disorders  |  |
| Psychotic disorders, schizophrenia                               |  |
| Autism spectrum disorders  |  |
| Persisting attention deficit disorders                           |  |
| Substance-use disorders  |  |
| Catatonia  |  |
| Neurology  |  |
| Seizures, often secondary, recurrent                             |  |
| Epilepsy   |  |
| Parkinsonism, early-onset Parkinson's disease                    |  |
| Other motor disorders (e.g., dystonia, myoclonus)                |  |
| Asymmetric facies / hemifacial paresis                           |  |
| White matter hyperintensity signals on MRI                       |  |
| Endocrinology and metabolism                                     |  |
| Hypocalcaemia / hypoparathyroidism                               |  |
| Hypomagnesemia   |  |
| Thyroid disease, usually hypothyroidism                          |  |
| Obesity  |  |
| Type 2 diabetes  |  |
| Cardiology / cardiovascular and respiratory                      |  |
| Congenital heart disease requiring follow-up                     |  |
| Hypertension, arrhythmia / heart failure, aortic root dilatation |  |
| Lymphedema   |  |
| Asthma   |  |
| Sleep  |  |
| Sleep pattern disruptions  |  |
| Obstructive sleep apnea  |  |
| Gastroenterology   |  |
| General GI symptoms (e.g., constipation, dysphagia)              |  |
| Gastro-esophageal reflux disease                                 |  |
| Cholelithiasis   |  |
| Fatty liver  |  |
| Genitourinary, gynecology  |  |
| Congenital anomalies, renal cysts, renal failure                 |  |
| Menstrual disorders (e.g., dysmenorrhea)                         |  |
| Sexual and reproductive health / obstetrics                      |  |
| Sexual / reproductive knowledge deficits                         |  |
| High-risk sexual behaviours / STIs                               |  |
| Pregnancy and delivery complications                             |  |
| General surgery  |  |
| Surgical complications (all types)                               |  |
| Hernias, all types   |  |
| Pilonidal sinus, varicose veins                                  |  |
| Skeletal   |  |
| Scoliosis of varying degrees                                     |  |
| Patellar dislocation   |  |
| Clubfoot   |  |
| Arthritis, rheumatoid and others                                 |  |
| Minor vertebral / rib anomalies                                  |  |
| Immunology and related   |  |
| Autoimmune disease and atopy                                     |  |
| Poor vaccine responses   |  |
| Recurrent infections   |  |
| Haematology and oncology   |  |
| Mild-moderate thrombocytopenia / mild cytopenias                 |  |
| Immune thrombocytopenia (ITP) / hemolytic anemia                 |  |
| Impaired hemostasis (e.g. epistaxis, menorrhagia)                |  |
| Anemia of chronic disease  |  |
| Possible increased risk of cancer                                |  |
| Sensory deficits   |  |
| Refractive errors requiring glasses                              |  |
| Hearing loss (especially high-frequency loss)                    |  |
| Severe olfactory deficits  |  |
| Tortuosity of retinal vessels                                    |  |
| Dental   |  |
| Dental caries  |  |
| Enamel hypoplasia, low saliva secretion                          |  |
| Malocclusion   |  |
| Aging and outcome  |  |
| Multimorbidity and polypharmacy                                  |  |
| Elevated premature mortality risk                                |  |
| Key  |  |
| Common   |  |
| Less common  |  |
| Rare, but clinically relevant                                    |  |
| Common, but not requiring clinical attention                     |  |

Figure 3. Features and risks in adults with 22q11.2 deletion syndrome.

| Assessments and Management   | At Diagnosis/Initial Assessment | At Follow-up (Every 1-2 y) |
|--|---------------------------------|----------------------------|
| <b>Genetic</b>   |                                 |                            |
| Parental genetic testing (FISH, MLPA, or microarray) <sup>a</sup>  | ✓                               |                            |
| Genetic counseling (including recurrence risk, update on natural history, management)  | ✓                               | ✓                          |
| Family planning, reproductive and prenatal counseling  | ✓                               | ✓                          |
| Additional genetic testing <sup>b</sup>  | If applicable                   |                            |
| <b>General</b>   |                                 |                            |
| Consultation with clinician(s) experienced with 22q11.2DS <sup>c</sup>   | ✓                               | ✓                          |
| Comprehensive history-taking (including family history), systems review, and medication review   | ✓                               | ✓                          |
| Assessment of need for/coordination with specialist(s) providing care  | ✓                               | ✓                          |
| Nutritional assessment; diet and exercise counseling   | ✓                               | ✓                          |
| Sleep evaluation (consider polysomnography), sleep hygiene recommendations   | ✓                               | ✓                          |
| Vaccination counseling, other standard preventive health care measures   | ✓                               | ✓                          |
| Assessment of functioning (including hygiene), care/supports (family/community/government), safety issues (eg, financial, internet)  | ✓                               | ✓                          |
| <b>Physical examination and additional diagnostic tests</b>  |                                 |                            |
| BMI, resting heart rate, blood pressure  | ✓                               | ✓                          |
| 22q11.2DS-relevant laboratory tests <sup>d</sup>   | ✓                               | ✓                          |
| Echocardiogram   | ✓ <sup>^</sup>                  |                            |
| Abdominal ultrasound   | ✓ <sup>^</sup>                  |                            |
| Routine care/hearing, vision, dental assessment <sup>e</sup>   | ✓                               | ✓                          |
| <b>Targeted clinical assessments<sup>f</sup></b>   |                                 |                            |
| CNS—psychiatric, neurologic, neurocognitive assessments (including for anxiety, psychosis, seizures, movement disorders, formal testing of cognitive and adaptive functioning/ADL) | ✓                               | ✓                          |
| Congenital cardiac (ACHD) and cardiovascular risk assessment   | ✓                               | ✓                          |
| Endocrinology  | ✓                               | ✓                          |
| Genitourinary, obstetrics/gynecology assessment (including contraception, pregnancy risks, and safe sex counseling)  | ✓                               | ✓                          |
| Hematology, gastroenterology, orthopedic/rheumatology, respirology, immunology, otolaryngology, ophthalmology, dermatology   | ✓                               | ✓                          |

**Table 1.** Recommendations for periodic assessments and management of adults with 22q11.2 deletion syndrome. For the full table legend please see the online version.

## Genetic testing and related issues

22q11.2DS is a contiguous gene deletion syndrome, ie, affected individuals have loss of 1 copy at the 22q11.2 locus. Most deletions occur as de novo (spontaneous) events, unrelated to maternal or paternal age.<sup>8</sup> Approximately 5% to 10% are inherited from a parent who may be unaware of their genetic diagnosis, with clinical features ranging from characteristic to relatively mild.<sup>9-12</sup> Males and females with the 22q11.2 deletion have a 50% chance of transmitting the deletion at each pregnancy. Genetic testing should be offered to all parents of affected patients, regardless of age.<sup>3,9-12</sup> When neither parent has the deletion, reproductive counselling includes a small elevated recurrence risk due to the rare report of germline mosaicism.<sup>13,14</sup> Notably, features in an affected parent do not predict possible findings in affected offspring and vice versa. A genetic diagnosis and genetic counseling can be helpful at any age and regardless of reproduction-related issues.<sup>3,15</sup>

Recurrent 22q11.2 deletions originate from nonhomologous allelic recombination between LCRs.<sup>16,17,18</sup> The most common 22q11.2 deletion occurs between LCR22s A to D (85%-90%). This approximately 2.5 to 3-megabase (Mb) deletion involves more than 40 protein-coding genes.<sup>1</sup> Smaller nested proximal 1.5 Mb (LCR22A to LCR22B) and 2.0 Mb (LCR22A to LCR22C) deletions account for 5% to 10% of deletions.<sup>1,19</sup> Rarer LCR22B to LCR22D and LCR22C to LCR22D nested distal deletions appear to have an overlapping phenotype.<sup>20</sup> Distal deletions beyond LCR22D (involving other LCRs, LCR22E to LCR22H) should not be confused with 22q11.2DS<sup>21</sup> and are not the subject of these clinical practice recommendations.

Several laboratory techniques are available to confirm or exclude the presence of a 22q11.2 deletion, including chromosomal microarray analysis (CMA), which identifies genome-wide copy number variants (CNVs). CMA results provide information on 22q11.2 deletion size and the presence of additional clinically relevant genome-wide CNVs.<sup>1</sup> Two other commonly available methods require an index of suspicion: fluorescence in situ hybridization and multiplex-ligation dependent probe amplification. Standard fluorescence in situ hybridization probes target the proximal LCR22A to LCR22B region and cannot determine deletion size nor identify deletions outside of the proximal LCR22A to LCR22B region, eg, LCR22B to LCR22D.<sup>1,19</sup> Multiplex-ligation dependent probe amplification interrogates the LCR22A to LCR22D region using several probes, providing information on deletion size but not about changes beyond this region.<sup>22,23</sup> Except for very rare translocations, karyotyping will not detect 22q11.2 deletions.

Patients with atypical features should prompt consideration of additional relevant variants. These may not be rare in 22q11.2DS<sup>24</sup> and include genome-wide CNVs and other pathogenic variants,<sup>25</sup> and variants on the remaining chromosome 22 allele that unmask an autosomal recessive condition.<sup>19</sup> CMA reveals CNVs; exome or genome sequencing may reveal other types of variants.<sup>26</sup> Limitations of most genetic tests include high cost, limited availability, and lack of reimbursement or coverage by health systems.

### **Aging and outcome**

The lifetime burden of illness is substantial, with concurrence of medical conditions (multimorbidity)<sup>27</sup> comparable with that of the general population several decades older.<sup>28,29</sup> At relatively young ages, adults with 22q11.2DS have increased vulnerability to age-related diseases including obesity, type 2 diabetes, Parkinson disease (PD), and hearing loss.<sup>30-35</sup> Life expectancy for adults on average is less than that expected for unaffected relatives.<sup>36</sup> Probability of survival to age 45 years has been reported to be approximately 95% for those

and 72% for those with major CHD (eg, tetralogy of Fallot, truncus arteriosus); no significant effects of intellectual disability or treated major psychiatric illness were detected.<sup>56</sup> Deaths are most commonly due to cardiovascular causes, even when compared with other individuals with CHD, and with proportionately more sudden cardiac deaths in individuals with 22q11.2DS.<sup>36-40</sup>

Further studies at older ages are required to better define natural history. To date, most reports involve adults in their mid-30s on average.<sup>3</sup> Multimorbidity and related polypharmacy<sup>29</sup> urge the need for a holistic, proactive, multisystem approach versus one solely focused on demand-driven care or on one organ system. Medication reviews may optimize appropriate prescribing.<sup>41</sup> Monitoring and prompts for medication intake are often needed. At any age, selected patients and families could potentially benefit from palliative care support. Long-term planning, eg, as parents/primary caregivers age, may involve siblings, partners, and/or agencies and others in the circle of care.

There is substantial variability in intellect in adults with 22q11.2DS. The most prevalent full scale IQ is in the borderline range (70 to 85).<sup>42</sup> 22q11.2DS imparts on average a 30 IQ point deficit relative to parental IQ,<sup>43</sup> with expectations lower for those with an inherited deletion<sup>44</sup> and somewhat higher for those with a nested LCR22A to LCR22B deletion.<sup>45</sup> Regardless of intellect, specific learning disabilities/impairments in cognitive functioning may be present. Although there are often no significant differences between verbal and performance IQ in adults with 22q11.2DS,<sup>42,46</sup> many have relative strength in verbal abilities, thus may have a “hidden disability.” Executive functions, such as problem solving, flexibility, working memory, concentration, and impulse inhibition, may be differentially affected.<sup>47</sup> Thinking is often literal or concrete, arithmetic particularly challenging, and social cognition is frequently affected, with difficulty recognizing emotions or sarcasm and interpreting others’ intentions and behavior (theory of mind).<sup>46-49</sup> Collectively, cognitive deficits may contribute to poor social judgment and decision-making. Some individuals may be impulsive, emotionally immature, and/or lack critical judgment yet be desirous of friendship. These factors increase the risk of experiencing traumatic events such as financial and/or sexual exploitation, bullying/abuse, and safety issues, including those related to the internet.<sup>50,51</sup> Challenges may be compounded by reluctance and/or inability to admit to or recognize deficits and/or to ask for assistance.

Levels of adaptive functioning also vary widely. Higher IQ, better executive functioning, and absence of psychotic illness predict better overall adaptive functioning, on average. More than 60% of adults are employed in the open market or assisted employment.<sup>46,47</sup> Most require assistance with completing forms, managing money, and making complex life and



and work decisions. Some require more basic help, eg, assistance with or reminders for personal hygiene. Although many meet criteria for intellectual disability, severe disabilities are relatively rare.

## Clinical Practice Recommendations

For other systems than musculoskeletal, please refer to the full article:

<https://doi.org/10.1016/j.gim.2022.11.012>

## Musculoskeletal

Clinically relevant manifestations include scoliosis,<sup>52-54</sup> recurrent patellar dislocation,<sup>52</sup> musculoskeletal pain, persisting juvenile idiopathic and later-onset forms of arthritis (eg, psoriatic, osteoarthritis),<sup>55-56</sup> clubfoot,<sup>57-58</sup> hammertoes and other foot abnormalities. Recurrent limb pains may relate to flat feet, vitamin D deficiency, or possibly mitochondrial dysfunction.<sup>59</sup> There are also reports of exercise intolerance and reduction in bone mass.<sup>60</sup>

Routine history and physical examination, eg, for scoliosis (early adulthood) and joint abnormalities, are recommended with radiographic screening weighed against radiation exposure. Standard management for individual conditions is recommended. Severe scoliosis or recurrent patellar dislocation may require bracing or surgical management.<sup>52,61,62</sup> Employment restrictions and accommodations may be warranted.

13

## Discussion

Since the publication of the initial clinical practice guidelines for managing adults with 22q11.2DS,<sup>3</sup> research has served to emphasize the evolving expression and complex care required at all life stages in 22q11.2DS (**Tables 1** and **Figures 2 and 3**). In addition to previously associated conditions, recent studies have revealed and/or confirmed associations with endocrinopathies and neurologic disorders that require proactive attention and need to be taken into account when following up those with 22q11.2DS.

Limitations imposed by the very nature of this complex condition and the lack of studies meeting formal criteria for high-quality evidence, ie, randomized controlled trials vs observational studies, constrained the ability of the panel to meet all of the requirements of a systematic review of the 2318 articles, including the 894 related to adults. The inherent variability and multisystem complexity of 22q11.2DS increase risk of bias (eg, sample selection)

for all study types.<sup>5</sup> The recommendations are most relevant to higher-income countries. Collectively, these issues limit the overall strength of the recommendations. Mitigating this were the expert panel's conservative approach to the recommendations, focus on optimizing potential benefit and minimizing harm, and avoidance of an overprescriptive approach at this relatively early stage of the field. The emphasis is on clinical judgment tailored to the individual patient and situation in the context of appreciating the multisystem and evolving features of 22q11.2DS.

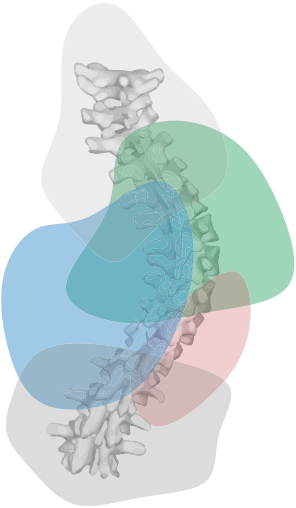
Most importantly, the adult 22q11.2DS population remains understudied. There is an urgent need for data on the natural history of 22q11.2DS, especially studies of older patients and prospective outcome research. Such research and accounting for multisystem complexity and ascertainment would facilitate systematic treatment trials, both pharmacologic and nonpharmacologic, including early interventions as well as studies of illness burden and long-term planning. This information is also key for future global 22q11.2DS clinical practice guidelines review/updating, proposed for 5 years hence in addition to subspecialty-specific guidelines planned for the near future.<sup>15,63</sup> All will benefit from involving both patients and their families and caregivers. Increasing our knowledge may empower the expertise of health care providers, whether or not they are associated with 22q11.2DS-specific clinics, and increase awareness about 22q11.2DS, thereby improving comprehensive care for all patients.

## References

1. McDonald-McGinn DM, Sullivan KE, Marino B, et al. 22q11.2 deletion syndrome. *Nat Rev Dis Primers*. 2015;1:15071.
2. Blagojevic C, Heung T, Theriault M, et al. Estimate of the contemporary live-birth prevalence of recurrent 22q11.2 deletions: a cross-sectional analysis from population-based newborn screening. *CMAJ Open*. 2021;9(3):E802-E809.
3. Fung WLA, Butcher NJ, Costain G, et al. Practical guidelines for managing adults with 22q11.2 deletion syndrome. *Genet Med*. 2015;17(8):599-609.
4. Page MJ, McKenzie JE, Bossuyt PM, et al. The PRISMA 2020 statement: an updated guideline for reporting systematic reviews. *BMJ*. 2021;372:n71.
5. Guyatt GH, Oxman AD, Vist GE, et al. GRADE: an emerging consensus on rating quality of evidence and strength of recommendations. *BMJ*. 2008;336(7650):924-926.
6. Loo JCY, Boot E, Corral M, Bassett AS. Personalized medical information card for adults with 22q11.2 deletion syndrome: an initiative to improve communication between patients and healthcare providers. *J Appl Res Intellect Disabil*. 2020;33(6):1534-1540.
7. Bassett AS, McDonald-McGinn DM, Devriendt K, et al. Practical guidelines for managing patients with 22q11.2 deletion syndrome. *J Pediatr*. 2011;159(2):332-339.e1.
8. Delio M, Guo T, McDonald-McGinn DM, et al. Enhanced maternal origin of the 22q11.2 deletion in velocardiofacial and DiGeorge syndromes. *Am J Hum Genet*. 2013;92(3):439-447.
9. McDonald-McGinn DM, Tonnesen MK, Laufer-Cahana A, et al. Phenotype of the 22q11.2 deletion in individuals identified through an affected relative: cast a wide FISHing net. *Genet Med*. 2001;3(1):23-29.
10. Vogels A, Schevenels S, Cayenberghs R, et al. Presenting symptoms in adults with the 22q11 deletion syndrome. *Eur J Med Genet*. 2014;57(4):157-162.
11. Vantrappen G, Devriendt K, Swillen A, et al. Presenting symptoms and clinical features in 130 patients with the velo-cardio-facial syndrome. The Leuven experience. *Genet Couns*. 1999;10(1):3-9.
12. Digilio MC, Angioni A, De Santis M, et al. Spectrum of clinical variability in familial deletion 22q11.2: from full manifestation to extremely mild clinical anomalies. *Clin Genet*. 2003;63(4):308-313.
13. Kasprzak L, Der Kaloustian VM, Elliott AM, Shevell M, Lejtenyi C, Eydoux P. Deletion of 22q11 in two brothers with different phenotype. *Am J Med Genet*. 1998;75(3):288-291.
14. Chen W, Li X, Sun L, Sheng W, Huang G. A rare mosaic 22q11.2 microdeletion identified in a Chinese family with recurrent fetal conotruncal defects. *Mol Genet Genomic Med*. 2019;7(8):e847.
15. Blagowidow N, Nowakowska B, Schindewolf E, et al. Prenatal screening and diagnostic considerations for 22q11.2 microdeletions. *Genes*. 2023;14:160.
16. Edlmann L, Pandita RK, Morrow BE. Low-copy repeats mediate the common 3-Mb deletion in patients with velo-cardio-facial syndrome. *Am J Hum Genet*. 1999;64(4):1076-1086.
17. Edlmann L, Pandita RK, Spiteri E, et al. A common molecular basis for rearrangement disorders on chromosome 22q11. *Hum Mol Genet*. 1999;8(7):1157-1167.
18. Shaikh TH, Kurahashi H, Saitta SC, et al. Chromosome 22-specific low copy repeats and the 22q11.2 deletion syndrome: genomic organization and deletion endpoint analysis. *Hum Mol Genet*. 2000;9(4):489-501.
19. Morrow BE, McDonald-McGinn DM, Emanuel BS, Vermeesch JR, Scambler PJ. Molecular genetics of 22q11.2 deletion syndrome. *Am J Med Genet A*. 2018;176(10):2070-2081.
20. Burnside RD. 22q11.2 deletion syndromes: a review of proximal, central, and distal deletions and their associated features. *Cytogenet Genome Res*. 2015;146(2):89-99.
21. Busse T, Graham JM Jr, Feldman G, et al. High-resolution genomic arrays identify CNVs that phenocopy the chromosome 22q11.2 deletion syndrome. *Hum Mutat*. 2011;32(1):91-97.
22. Fernandez L, Lapunzina P, Arjona D, et al. Comparative study of three diagnostic approaches (FISH, STRs and MLPA) in 30 patients with 22q11.2 deletion syndrome. *Clin Genet*. 2005;68(4):373-378.
23. Vorstman JAS, Jalali GR, Rappaport EF, Hacker AM, Scott C, Emanuel BS. MLPA: a rapid, reliable, and sensitive method for detection and analysis of abnormalities of 22q. *Hum Mutat*. 2006;27(8):814-821.
24. Cohen JL, Crowley TB, McGinn DE, et al. 22q and two: 22q11.2 deletion syndrome and coexisting conditions. *Am J Med Genet A*. 2018;176(10):2203-2214.
25. Bassett AS, Lowther C, Merico D, et al. Rare genome-wide copy number variation and expression of schizophrenia in 22q11.2 deletion syndrome. *Am J Psychiatry*. 2017;174(11):1054-1063.
26. Durmaz AA, Karaca E, Demkow U, Toruner G, Schoumans J, Cogulu O. Evolution of genetic techniques: past, present, and beyond. *Biomed Res Int*. 2015;2015:461524.
27. Barnett K, Mercer SW, Norbury M, Watt G, Wyke S, Guthrie B. Epidemiology of multimorbidity and implications for health care, research, and medical education: a cross-sectional study. *Lancet*. 2012;380(9836):37-43.
28. Bassett AS, Chow EWC, Husted J, et al. Clinical features of 78 adults with 22q11 deletion syndrome. *Am J Med Genet A*. 2005;138(4):307-313.
29. Malecki SL, Van Mil S, Graffi J, et al. A genetic model for multimorbidity in young adults. *Genet Med*. 2020;22(1):132-141.
30. Butcher NJ, Kiehl TR, Hazrati LN, et al. Association between early-onset Parkinson disease and 22q11.2 deletion syndrome: identification of a novel genetic form of Parkinson disease and its clinical implications. *JAMA Neurol*. 2013;70(11):1359-1366.
31. Mok KY, Sheerin U, Sim  n-S  nchez J, et al. Deletions at 22q11.2 in idiopathic Parkinson's disease: a combined analysis of genome-wide association data. *Lancet Neurol*. 2016;15(6):585-596.

32. Verheij E, Derks LSM, Stegeman I, Thomeer HGXM. Prevalence of hearing loss and clinical otologic manifestations in patients with 22q11.2 deletion syndrome: a literature review. *Clin Otolaryngol*. 2017;42(6):1319-1328.
33. Boot E, Butcher NJ, Udow S, et al. Typical features of Parkinson disease and diagnostic challenges with microdeletion 22q11.2. *Neurology*. 2018;90(23):e2059-e2067
34. Voll SL, Boot E, Butcher NJ, et al. Obesity in adults with 22q11.2 deletion syndrome. *Genet Med*. 2017;19(2):204-208.
35. Van L, Heung T, Malecki SL, et al. 22q11.2 microdeletion and increased risk for type 2 diabetes. *EClinicalmedicine*. 2020;26: 100528.
36. Van L, Heung T, Graffi J, et al. All-cause mortality and survival in adults with 22q11.2 deletion syndrome. *Genet Med*. 2019;21(10):2328-2335.
37. Campbell IM, Sheppard SE, Crowley TB, et al. What is new with 22q? An update from the 22q and You Center at the Children's Hospital of Philadelphia. *Am J Med Genet A*. 2018;176(10):2058-2069.
38. Repetto GM, Guzm'an ML, Delgado I, et al. Case fatality rate and associated factors in patients with 22q11 microdeletion syndrome: a retrospective cohort study. *BMJ Open*. 2014;4(11):e005041.
39. Kawu D, Woudstra OI, van Engelen K, et al. 22q11.2 deletion syndrome is associated with increased mortality in adults with tetralogy of Fallot and pulmonary atresia with ventricular septal defect. *Int J Cardiol*. 2020;306:56-60.
40. van Mil S, Heung T, Malecki S, et al. Impact of a 22q11.2 micro-deletion on adult all-cause mortality in tetralogy of Fallot patients. *Can J Cardiol*. 2020;36(7):1091-1097.
41. Cooper JA, Cadogan CA, Patterson SM, et al. Interventions to improve the appropriate use of polypharmacy in older people: a Cochrane systematic review. *BMJ Open*. 2015;5(12):e009235.
42. van Amelsvoort T, Henry J, Morris R, et al. Cognitive deficits associated with schizophrenia in velo-cardio-facial syndrome. *Schizophr Res*. 2004;70(2-3):223-232.
43. Fiksinski AM, Heung T, Corral M, et al. Within-family influences on dimensional neurobehavioral traits in a high-risk genetic model. *Psychol Med*. 2022;52:3184-3192.
44. Gothelf D, Aviram-Goldring A, Burg M, et al. Cognition, psychosocial adjustment and coping in familial cases of velocardiofacial syndrome. *J Neural Transm (Vienna)*. 2007;114(11):1495-1501.
45. Zhao Y, Guo T, Fiksinski A, et al. Variance of IQ is partially dependent on deletion type among 1,427 22q11.2 deletion syndrome subjects. *Am J Med Genet A*. 2018;176(10):2172-2181.
46. Butcher NJ, Chow EWC, Costain G, Karas D, Ho A, Bassett AS. Functional outcomes of adults with 22q11.2 deletion syndrome. *Genet Med*. 2012;14(10):836-843.
47. Fiksinski AM, Breetvelt EJ, Lee YJ, et al. Neurocognition and adaptive functioning in a genetic high risk model of schizophrenia. *Psychol Med*. 2019;49(6):1047-1054
48. Frascarelli M, Padovani G, Buzzanca A, et al. Social cognition deficit and genetic vulnerability to schizophrenia in 22q11 deletion syndrome. *Annali Dell'Istituto Superiore di Sanita*. 2020;56(1):107-113.
49. Accinni T, Buzzanca A, Frascarelli M, et al. Social cognition impairments in 22q11.2DS individuals with and without psychosis: A comparison study with a large population of patients with schizophrenia. *Schizophrenia Bulletin Open*. 2021;3(1):1-10.
50. Buijs PCM, Boot E, Shugar A, Fung WLA, Bassett AS. Internet safety issues for adolescents and adults with intellectual disabilities. *J Appl Res Intellect Disabil*. 2017;30(2):416-418.
51. Palmer LD, Heung T, Corral M, Boot E, Brooks SG, Bassett AS. Sexual knowledge and behaviour in 22q11.2 deletion syndrome, a complex care condition. *J Appl Res Intellect Disabil*. 2022;35(4):966-975.
52. Bassett AS, Chow EWC, Husted J, et al. Clinical features of 78 adults with 22q11 deletion syndrome. *Am J Med Genet A*. 2005;138(4):307-313
53. Homans JF, Baldew VGM, Brink RC, et al. Scoliosis in association with the 22q11.2 deletion syndrome: an observational study. *Arch Dis Child*. 2019;104(1):19-24.
54. de Reuver S, Homans JF, Schl'osser TPC, et al. 22q11.2 deletion syndrome as a human model for idiopathic scoliosis. *J Clin Med*. 2021;10(21):4823.
55. Davies K, Stiehm ER, Woo P, Murray KJ. Juvenile idiopathic poly-articular arthritis and IgA deficiency in the 22q11 deletion syndrome. *J Rheumatol*. 2001;28(10):2326-2334.
56. Sullivan KE, McDonald-McGinn DM, Driscoll DA, et al. Juvenile rheumatoid arthritis-like polyarthritis in chromosome 22q11.2 deletion syndrome (DiGeorge anomalous/velocardiofacial syndrome/conotruncal anomaly face syndrome). *Arthritis Rheum*. 1997;40(3):430-436.
57. Oskarsdottir S, Persson C, Eriksson BO, Fasth A. Presenting phenotype in 100 children with the 22q11 deletion syndrome. *Eur J Pediatr*. 2005;164(3):146-153.
58. Poirsier C, Besseau-Ayasse J, Schluth-Bolard C, et al. A French multicenter study of over 700 patients with 22q11 deletions diagnosed using FISH or aCGH. *Eur J Hum Genet*. 2016;24(6):844-851
59. Napoli E, Tassone F, Wong S, et al. Mitochondrial citrate transporter-dependent metabolic signature in the 22q11.2 deletion syndrome. *J Biol Chem*. 2015;290(38):23240-23253.
60. Stagi S, Lapi E, Gambineri E, et al. Bone density and metabolism in subjects with microdeletion of chromosome 22q11 (del22q11). *Eur J Endocrinol*. 2010;163(2):329-337.
61. Cheng JC, Castelein RM, Chu WC, et al. Adolescent idiopathic scoliosis. *Nat Rev Dis Primers*. 2015;1:15030.
62. Morava E, Lacassie Y, King A, Illes T, Marble M. Scoliosis in velo-cardio-facial syndrome. *J Pediatr Orthop*. 2002;22(6):780-783.
63. Oskarsdottir S, Boot E, Crowley TB, et al. Updated clinical practice recommendations for managing children with 22q11.2 deletion syndrome. *Genetic Med*. 2023;25:100338



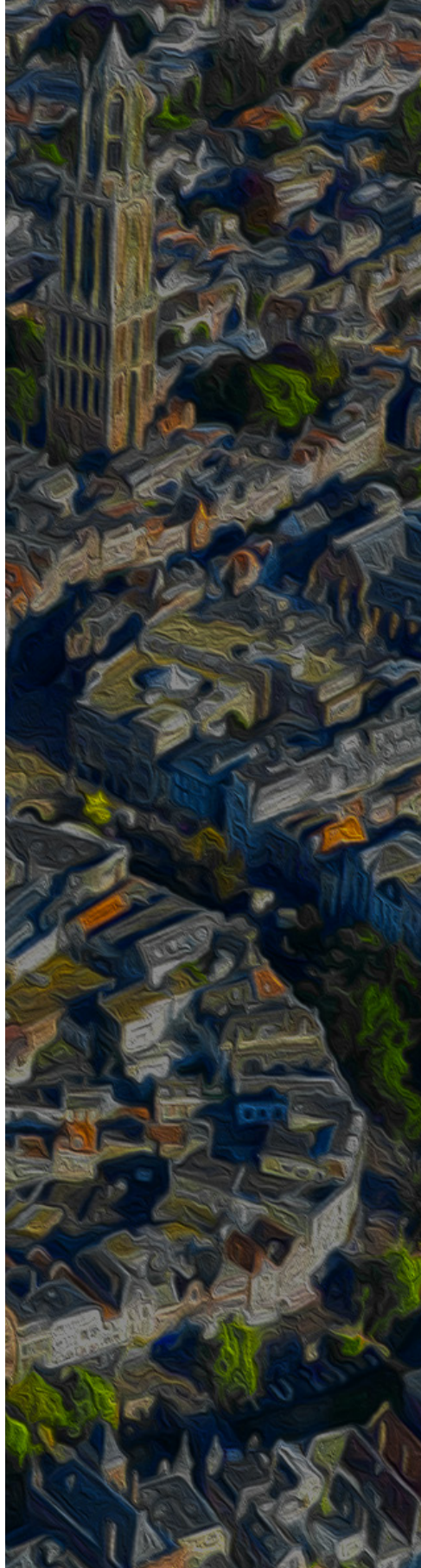


# 14

## The 22q11.2 Deletion Syndrome as a Model for Idiopathic Scoliosis - A Hypothesis

Jelle F. Homans  
Steven de Reuver  
Elemi J. Breetvelt  
Jacob A.S. Vorstman  
Vincent F.X. Deeney  
John M. Flynn  
Donna M. McDonald-McGinn  
Moyo C. Kruyt  
René M. Castelein

*Medical Hypotheses. 2019 Jun;127:57-62.*



## **ABSTRACT**

Adolescent idiopathic scoliosis (AIS), defined as a lateral deviation of the spine of at least ten degrees, is a classic enigma in orthopaedics and affects 1-4% of the general population. Despite (over) a century of intensive research, the etiology is still largely unknown. One of the major problems in all existing AIS research is the fact that most patients come to medical attention after onset of the curve. Therefore, it is impossible to know whether current investigated parameters are causative, or an effect of the scoliosis. Moreover, up until now there is no known animal model that captures the core features of AIS. In order to identify causal pathways leading to AIS we propose another approach, which has been of great value in other medical disciplines: To use a subset of the population, with a higher risk for a certain disease as a “model” for the general population. Such a “model” may allow the identification of causative mechanisms that might be applicable to the general population. The 22q11.2 deletion syndrome (22q11.2DS) is the most common microdeletion syndrome and occurs in ~1:3000-6000 children and 1:1000 pregnancies. Nearly half of the population of patients with 22q11.2DS develop a scoliosis that in most cases resembles AIS as far as age at onset and curve pattern. We postulate that within 22q11.2DS certain causal pathways leading to scoliosis can be identified and that these are applicable to the general population.



## Introduction

Scoliosis is a three-dimensional (3D) rotational deformity of the spine and trunk which has major consequences for the patient in terms of self-image, pain and the serious impact of possible invasive treatments (brace therapy and/or scoliosis surgery).<sup>1,2</sup> A scoliosis is defined as a lateral deviation of the spine of at least ten degrees Cobb angle (**Figure 1**).<sup>3</sup>

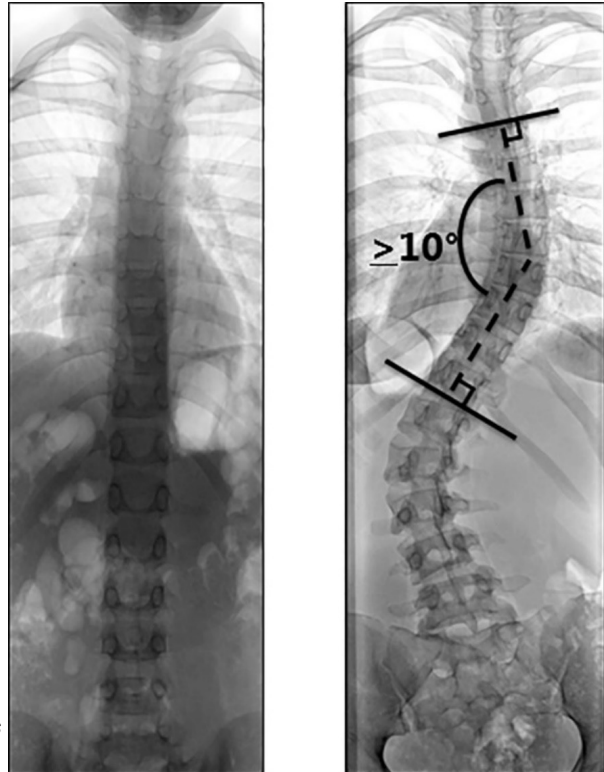


**Figure 1.** A scoliosis (right image) is diagnosed as a curve  $\geq 10$  degrees.

Several known causes for scoliosis exist (congenital and neuromuscular scoliosis). However, the majority of patients have an adolescent idiopathic scoliosis (AIS), for which the cause is, to a large extent, unknown. The majority of AIS patients are healthy and well-functioning up to the age of the pubertal growth spurt. AIS affects 1–4% of the general population and is a classic enigma within orthopedics.<sup>2</sup> Although recent research has elucidated the role of genetics and the biomechanics of the upright human spine, the true cause of this disorder, and thus the potential for prevention, has remained largely undiscovered.<sup>2,4-8</sup> As a result, surgery is the main treatment option in AIS patients with curves exceeding 45–50 degrees.<sup>2,9</sup>

There are two important reasons why there is such a variety of theories and why the etiopathogenesis, is still to a large extent unraveled:

1. Patients with AIS are identified as such after the onset of the scoliosis. Therefore, it is impossible to identify causative factors of the curve onset. As a consequence, in current research, it is unknown whether correlated parameters are the cause, the consequence or an epiphenomenon of the scoliosis.<sup>2,5</sup>

2. There is no animal that, without experimental intervention, develops a scoliosis. Specific genes are known to play a role in the development of scoliosis, as shown by the curvature developed within e.g. the mutant guppy syndrome curveback or POC-5 zebrafish.<sup>10,11</sup> However, as shown by multiple large genetic studies it is clear that the development of idiopathic scoliosis is not limited to one gene and/or pure mendelian inheritance.<sup>2</sup> On the contrary, the development of idiopathic scoliosis is known to be multifactorial (a combination of genetic, metabolic, the central nervous system, biomechanics and environmental factors).<sup>2</sup> Thus, in order to investigate the (combination of) multiple pathways leading to scoliosis and to understand the development of idiopathic scoliosis we have to investigate man: Only humans carry the body's center of gravity straight above the pelvis due to a pelvic and lumbar lordosis. All other animals, quadrupedal and bipedal alike, carry the body's center of gravity in front of the pelvis. Man has a unique biomechanical loading of the spine that introduces dorsal shear forces, that have been shown to cause a loss of rotational stability (**Figure 2**).<sup>8,12,13</sup>

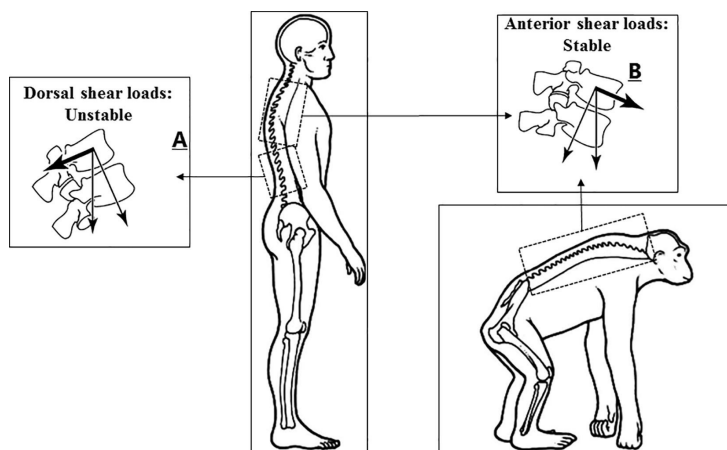


**Figure 2.** There are unique differences between human and all other animals. Humans have the center of gravity straight above the pelvis, while all other animals (including the bipedal ones) carry the body's center of gravity in front of the pelvis, leading to different biomechanical circumstances. Certain parts of the human spine experience dorsally directed shear loads (**A**), while other parts and all other animals only have anteriorly directed shear loads (**B**). The dorsal shear loads have been shown to decrease rotational stability in the affected segments. Compiled from Castelein et al.<sup>12</sup>

There is a large gap of knowledge in the etio-pathogenesis of scoliosis, which needs to be bridged in order to reach the next step in scoliosis care: Primary prevention (prevent the development of scoliosis) and/or secondary prevention (identify the patients in an early stage in order to prevent surgery). Therefore, we propose another possibility, which has been of great value in other medical disciplines: To prospectively investigate a subset of the population, with a higher risk for a certain disease, as a model for the general population. For AIS, patients with the 22q11.2 deletion syndrome (22q11.2DS) could be such a population to study, since 50% develops a scoliosis and the majority of patients has a scoliosis resembling AIS as far as age at onset and curve pattern.<sup>14</sup>

In humans, 22q11.2DS, is the most common microdeletion syndrome with a prevalence of ~1 in 3–6 thousand live births and 1 in 1000 unselected pregnancies.<sup>15–18</sup> Patients with 22q11.2DS, prior to the identification of the chromosomal etiology, may have been diagnosed with a variety of clinical described entities such as the DiGeorge syndrome, velocardiofacial syndrome or conotruncal anomaly face syndrome.<sup>19</sup> The clinical features associated with this condition vary greatly within and between individuals.<sup>20</sup> Numerous clinical features are now known to be associated with 22q11.2DS including common conditions such as congenital heart disease (CHD, 25–60%), endocrinopathies such as hypocalcemia (55%), immunodeficiency (77%), cognitive deficits (>95%) and psychiatric illness including schizophrenia (25%), and less frequently associated problems such as congenital diaphragmatic hernia and imperforate anus.<sup>20,21</sup>

On the other hand, the clinical features of 22q11.2DS can be relatively mild and the diagnosis tends to be missed. In fact, we treated multiple patients for presumed AIS that later turned out to suffer from 22q11.2DS. Scoliosis is present in about 50% of patients with 22q11.2DS, compared to about 1–4% in the general population.<sup>14,22</sup> We postulate that the population of individuals with 22q11.2DS can be used as a model to study scoliosis in a unique, prospective manner, starting from genetic risk to the emergence of first signs of (spine) abnormalities. We hypothesize that these insights will be informative for our understanding of the causal pathways leading to scoliosis in the general population.

#### Lessons learned from other high-risk populations

In the field of gynecology, the Sjögren-Larsson syndrome is proposed as a model for preterm labor and in the field of psychiatry 22q11.2DS is regarded as a model for idiopathic schizophrenia.<sup>23,24</sup> The 22q11.2 deletion is found to be the most prevalent and strongest single genetic risk factor for developing schizophrenia. The correlation between 22q11.2DS and schizophrenia has long been established; multiple studies confirm that approximately

one out in four patients with 22q11.2DS develop schizophrenia.<sup>20,23,25</sup> On the other hand, within the general population, out of all patients with schizophrenia only one in 100–200 have the 22q11.2 deletion.<sup>20,26</sup> This led to establishment of the International 22q11.2DS Brain and Behavior Consortium (a large group of international experts representing 22 clinical and five genomic sites) that aims to identify causal mechanisms leading to schizophrenia in 22q11.2DS and elaborating on that, investigate if these causal mechanisms are applicable to the general population. The large a-priori chance of conversion to schizophrenia in 22q11.2DS, leads to a dramatic decrease in required sample size to identify causative mechanisms of schizophrenia within 22q11.2DS.<sup>27</sup> Using this approach, multiple studies showed that several parameters, such as prematurity, lower global neurocognitive performance, poorer premorbid functioning and a decrease in intelligence quotient years before the onset of schizophrenia, pose an increased risk of developing schizophrenia at a later stage.<sup>25,27,28</sup> Obviously, preterm labor and schizophrenia are two disorders very distinct from scoliosis, however the onset of all three are thought to be multifactorial. By the use of a model as proposed, we can prospectively study one or more causative factors within a subgroup, and possibly extrapolate these findings to the general population.<sup>2,20,24</sup>

#### Neuromuscular versus idiopathic scoliosis

Neuromuscular scoliosis is a distinct spinal curvature which is caused by a disorder of the muscles and/or central nervous system. Common causes are cerebral palsy, myelodysplasia, spinal muscular atrophy (SMA) or Duchenne's muscular dystrophy.<sup>29</sup> These patients do not have the ability to maintain postural balance, are often wheelchair bound, and develop a C-curved scoliosis already at a very early stage of development (**Figure 3**). Both the underlying condition, the age at onset and the curve type are very different from AIS. Moreover, in neuromuscular scoliosis (e.g. Duchenne and spinal muscular atrophy) the risk of curve progression and subsequent surgical treatment is much higher as compared to AIS.<sup>2,30</sup>

#### Scoliosis within 22q11.2DS

Scoliosis is an important part of the multi-morbidity seen in association with 22q11.2DS, with a prevalence of about 50%.<sup>14</sup> In 22q11.2DS, as well as in the general population, scoliosis usually develops during the growth spurt.<sup>2,14</sup> Moreover, the majority of patients with 22q11.2DS have an idiopathic-like curve pattern. Lastly, although during development gross motor milestones like crawling, cruising, walking are slightly behind peers and siblings, patients with 22q11.2DS, in general are fully ambulant.<sup>31</sup> This leads to our hypothesis that within 22q11.2DS causal pathways resulting in scoliosis can be identified and that these may also play a role in the general population.

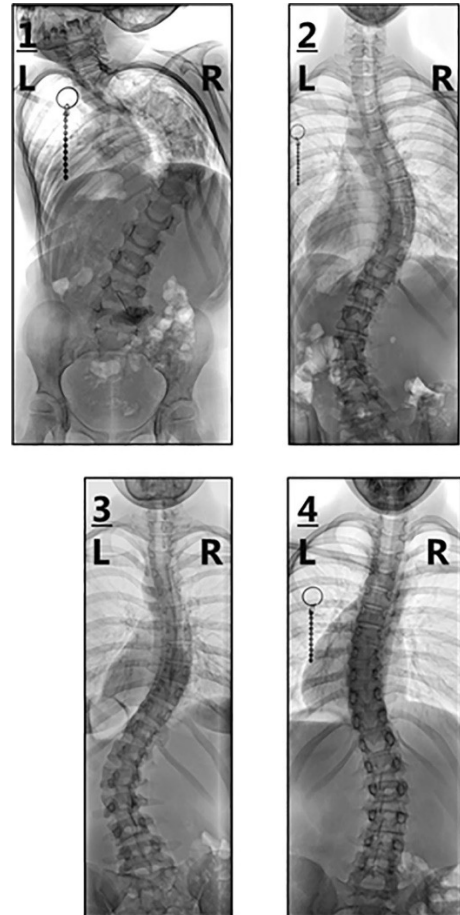


**Figure 3.** **1:** A five year old spinal muscular atrophy patient with a scoliosis neuromuscular scoliosis (C-shape, right thoracic) **2:** A 14 year old patient with an adolescent idiopathic scoliosis (S-shape, right thoracic, left lumbar) **3:** A 16 year old 22q11.2 Deletion Syndrome patient with a scoliosis (S-shape, right thoracic, left lumbar) **4:** A seven year old 22q11.2 Deletion Syndrome patient with a scoliosis (S-shape left thoracic, right lumbar).

### Testing the hypothesis

In order to test the hypothesis that the scoliosis in patients with 22q11.2DS can serve as a model for idiopathic scoliosis, four important factors, of the development of idiopathic scoliosis, should be determined within the 22q11.2DS population:

1. Does the scoliosis in 22q11.2DS behave like AIS?
2. What is the prevalence of intraspinal anomalies in 22q?
3. What is the neuromuscular status of 22q11.2DS patients as compared to AIS?
4. What is the condition of essential soft tissue structures, such as the intervertebral discs (IVD)?

### Does the scoliosis in 22q11.2DS behave like AIS?

In order to investigate whether the 22q11.2DS is comparable with AIS, both the curve pattern and the progression rate of patients with 22q11.2DS should be compared with AIS. This is illustrated by the fact that within neuromuscular scoliosis both of these factors are very different as compared to AIS. The majority of patients with 22q11.2DS has an idiopathic-like curve scoliosis pattern and a relatively mild scoliosis as shown by the fact that 16% of all 22q11.2DS scoliosis patients eventually require scoliosis surgery.<sup>14,32</sup> In AIS, 13.2% of the patients require brace and/or surgical treatment (2.4% of all the AIS patients require surgical treatment).<sup>33</sup> It is not possible to compare the progression rate of AIS and 22q11.2DS scoliosis based on need for surgical treatment. With the introduction of brace therapy, the need for scoliosis surgery in AIS decreased dramatically.<sup>34</sup> In 22q11.2DS, associated symptoms such as CHD and psychological status, can influence the compliance for brace therapy. Therefore, we should focus on the rate of progression. According to a recent systematic review by Negrini et al. the pooled estimated progression prevalence (defined as > 5 degrees curve progression) within juvenile and adolescent idiopathic scoliosis was 49% and the rate of scoliosis progression ranged from 2.2 to 9.6 degrees per year. We hypothesize that the patients with 22q11.2DS with an idiopathic-like curve have a comparable progression rate as in idiopathic scoliosis.

### What is the prevalence of intraspinal anomalies in 22q?

In a recent systematic review it was shown that, approximately ten percent of all AIS patients have intraspinal anomalies as shown on MRI.<sup>35</sup> In some cases this is linked to the development of scoliosis (e.g. a tethered cord) and subsequently in that case it is not deemed as AIS. However, how the majority of the intraspinal anomalies found in AIS relate to the development of idiopathic scoliosis remains unclear.<sup>35</sup> Therefore, there is no consensus on whether all AIS patients, prior to surgery, should receive an MRI or only the patients with atypical curves or abnormal neurologic findings.<sup>35</sup> From the point of view of our hypothesis it would be preferable if the scoliosis patients with 22q11.2DS have a similar percentage and/or a similar sort of intraspinal anomalies as AIS patients and not anomalies that are directly related to scoliosis development. However, it is currently unknown whether patients with 22q11.2DS, with an idiopathic-like curve, have a similar rate of intraspinal anomalies as compared to the AIS population.

### What is the neuromuscular status of 22q11.2DS patients as compared to AIS?

Although AIS patients are -by definition- considered to be normal apart from their spinal deformity, various subtle differences that may be cause or effect, with the normal population have been described. As discussed, there is a large difference between AIS patients and

neuromuscular scoliosis patients with regards to their postural balance and body control. However, in AIS, there are small differences with respect to the neuromuscular status as compared to the general, non-scoliotic population. For example, in a gait analysis study, there was a significantly higher postural instability in AIS that included limb load symmetry, sway length and velocity in anteroposterior and latero-lateral directions.<sup>36</sup> Once again, it cannot be determined if these differences are the cause or the effect of the disorder. It is currently unknown whether the subtle neuromuscular differences (as present in AIS) also occur between patients with 22q11.2DS with and without a scoliosis. More research should be performed on the possible neuromuscular differences in patients with 22q11.2DS with and without scoliosis, in order to, analyse whether these differences are causative or an effect of the scoliosis.

What is the condition of essential soft tissue structures, such as the intervertebral discs (IVD)?

In AIS patients, it was demonstrated that the curves were characterized by a much greater deformation in the intervertebral discs (IVD) as compared to the vertebral bodies.<sup>37,38</sup> The increase in curve magnitude, during adolescent skeletal growth and maturation, occurs mostly through disc wedging during the rapid growth spurt and vertebral wedging occurs later and to a lesser extent.<sup>39</sup> In other words, within the general population it is known that the intervertebral disk plays an important role in the development of scoliosis. Yet, whether there are primary IVD differences between the population that does and does not develop a scoliosis is unknown. In 22q11.2DS, we should analyze the possible disc property differences of patients with and without scoliosis. Hereafter, with intensive monitoring of the 22q11.2DS patients starting at a young age, we have the opportunity to analyze possible differences in the disc properties before the onset of the scoliosis.

Patients with 22q11.2DS are prone to develop scoliosis; in 22q11.2DS nearly half of the patients develop scoliosis, while within the general population scoliosis occurs in 1–4%. The major question is why do 50% of the patients with 22q11.2DS develop scoliosis and moreover what are the differences between the 22q11.2DS patients with and without a (progressive) scoliosis. There may be small differences between the patients with 22q11.2DS and the general population (e.g. a slight delay in milestone development). Yet, as opposed to AIS, in 22q11.2DS we have the opportunity to compare the parameters before the onset of the scoliosis and thus truly determine whether these parameters are the cause or the consequence of the scoliosis. Our hypothesis is that the 22q11.2DS scoliosis behaves the same as compared to AIS and by prospectively identifying differences between the 22q11.2DS patients with and without a scoliosis, we can identify causal mechanisms between these groups and subsequently expand these findings to the general population.

## Discussion

Scoliosis has severe consequences for the patient in terms of self-image and pain and in severe cases possible cardiopulmonary compromise.<sup>1,40</sup> Moreover, surgical treatment as well as brace therapy, that consists of rigid and constraining braces that have to be worn extensively in an emotionally vulnerable period of life, is a severe burden on the patient. Last, apart from the impact of the spinal deformity on the quality of life of the patient, scoliosis patients are also a considerable economic burden to society: it is the spinal deformity most frequently seen by general practitioners, pediatricians and orthopedic surgeons, and current therapies are very costly.<sup>2,41,42</sup> Therefore, the ultimate goal of scoliosis care is to prevent the development and/or deter progression, thereby eliminating the need for brace/surgical treatment. The first step to prevent the development of scoliosis within a patient is to identify the etio-pathogenesis of this deformity. It is well recognized that the development of scoliosis is multifactorial, and in order to truly elucidate its cause, new approaches are needed.<sup>2</sup>

The identification of causal pathways leading to scoliosis within 22q11.2DS, will lead to a large improvement in care for the population of patients with 22q11DS, both in primary and secondary prevention. At the same time, we hypothesize that the causative mechanisms leading to scoliosis within 22q11.2DS are applicable to the general population and thereby, this can lead to the improvement of care for a disease troubling 1–4% of the general population. The majority of patients with 22q11.2DS have an idiopathic-like curve scoliosis pattern and a relatively mild scoliosis as shown by the fact that 16% of all patients with 22q11.2DS eventually require scoliosis surgery.<sup>12,30</sup> To investigate the differences between 22q11.2DS patients with and without a scoliosis and with a non progressive and (rapid) progressive scoliosis will be the next step. Within the 22q11.2DS population we have the opportunity to analyze metabolic, the central nervous system, biomechanics and environmental factors, but also genetic factors: Possible differences within the deletion and/or genetic variances outside of the 22q11.2 deletion.

From a scientific perspective, a limitation of the 22q11.2DS population as a model for the general population could be that CHD are common (25–60%) in 22q.<sup>14,20,21</sup> The limitation would be that already four decades ago, a correlation between the appearance of congenital heart defects (CHD) and the development of scoliosis in the general population was shown.<sup>43-45</sup> Multiple theories were formed for why CHD leads to a scoliosis. First, different biomechanical forces, due to altered aortic configuration, could possibly cause an increased risk in developing scoliosis.<sup>43,44</sup> Second, surgery on an immature thoracic cage may result in altered growth and an increased scoliosis risk.<sup>45-47</sup> Yet, in a recent study, no relation between a thoracotomy/sternotomy for CHD and scoliosis was found.<sup>48</sup>



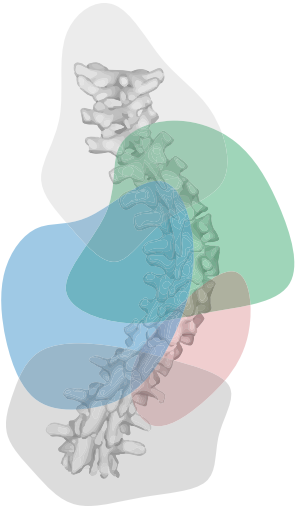
There are conflicting results on the correlation between CHD and scoliosis. Moreover, in none of these studies genetic testing of (all) the patients was performed. Subsequently, it is unknown whether (a subset of) the included patients in these studies may have had 22q11.2DS.<sup>43-47</sup> This is important because 22q11.2DS is the second greatest risk factor for CHD and the symptoms of 22q11.2DS can be subtle leading to underdiagnoses of 22q11.2DS.<sup>19,20</sup> Interestingly, in a recent study, in which all the patients had the 22q11.2DS diagnosis there was no association between CHD and scoliosis.<sup>14</sup> In other words, it is possible that actually 22q11.2DS was the reason that these patients developed both a CHD and a scoliosis.

Patients with 22q11.2DS are at an increased (~25 times fold) risk for the development of scoliosis. The major question is what are the factors that determine whether a scoliosis develops, or not. Moreover, what are the factors that lead to a progressive scoliosis that necessitates surgery in 16% of the 22q11.2DS patients. Within 22q11.2DS we have the opportunity to truly investigate this multifactorial pathway and in the end, possibly, extrapolate them to the general population.

## References

1. Nicoladoni C. Anatomie und mechanismus der skoliose. Kocher, König, von Mikulicz. Eds *Bibl Medica Stuttgart*, Ger Verlag von Erwin Nagele 1904.
2. Cheng JC, Castelein RM, Chu WC, et al. Adolescent idiopathic scoliosis. *Nat Rev Dis Prim* 2015;1:1–20.
3. Terms SRSTC and WG on SCRG of. Revised Glossary of Terms 2000. <http://www.srs.org/professionals/online-education-and-resources/glossary/revised-glossary-of-terms>.
4. Kouwenhoven JMW, Castelein M, Castelein RM. The pathogenesis of adolescent idiopathic scoliosis: review of the literature. *Spine (Phila Pa 1976)* 2008;33:2898–908.
5. Schlösser TPC, Van Der Heijden GJMG, Versteeg AL, Castelein RM. How “idiopathic” is adolescent idiopathic scoliosis? A systematic review on associated abnormalities. *PLoS ONE* 2014;9:1–10.
6. Gorman KF, Julien C, Moreau A. The genetic epidemiology of idiopathic scoliosis. *Eur Spine J* 2012;21:1905–19.
7. Kesling K, Reinker K. Scoliosis in twins. A meta-analysis of the literature and report of six cases. *Spine (Phila Pa 1976;1997(22):2009–14*.
8. Kouwenhoven JW, Smit TH, van der Veen AJ, Kingma I, van Dieën JH, Castelein RM. Effects of dorsal versus ventral shear loads on the rotational stability of the thoracic spine: a biomechanical porcine and human cadaveric study. *Spine (Phila Pa 1976)* 2007;32:2545–50.
9. Weinstein SL, Dolan LA, Cheng JCY, Danielsson A, Morcuende JA. Adolescent idiopathic scoliosis. *Lancet* 2008;371:1527–37.
10. Patten SA, Margarite-Jeannin P, Bernard JC, et al. Functional variants of POC5 identified in patients with idiopathic scoliosis. *J Clin Invest* 2015;125:1124–8.
11. Gorman KF, Tredwell SJ, Breden F. The mutant guppy syndrome curveback as a model for human heritable spinal curvature. *Spine (Phila Pa 1976)* 2007;32:735–41.
12. Castelein RM, van Dieën JH, Smit TH. The role of dorsal shear forces in the pathogenesis of adolescent idiopathic scoliosis – A hypothesis. *Med Hypotheses* 2005;65:501–8.
13. Janssen MM, Kouwenhoven JW, Castelein RM. The role of posteriorly directed shear loads acting on a pre-rotated growing spine: a hypothesis on the pathogenesis of idiopathic scoliosis. *Stud Health Technol Inform* 2010;158:112–7.
14. Homans JF, Baldew VGM, Brink RC, et al. Scoliosis in association with the 22q11.2 deletion syndrome: an observational study. *Arch Dis Child* 2019;104:19–24.
15. Oskarsdóttir S, Vujic M, Fasth A. Incidence and prevalence of the 22q11 deletion syndrome: a population-based study in Western Sweden. *Arch Dis Child* 2004;89:148–51.
16. Montcel Tezenas Du, S, Mendizabai H, Ayme S, Levy A, Philip N. Prevalence of 22q11 microdeletion. *J Med Genet* 1996;33:719.
17. Botto LD, May K, Fernhoff PM, et al. A population-based study of the 22q11.2 deletion: phenotype, incidence, and contribution to major birth defects in the population. *Pediatrics* 2003;112:101–7.
18. Grati FR, Molina Gomes D, Ferreira JCPB, et al. Prevalence of recurrent pathogenic microdeletions and microduplications in over 9500 pregnancies. *Prenat Diagn* 2015;35:801–9.
19. Bassett AS, McDonald-McGinn DM, Devriendt K, et al. Practical guidelines for managing patients with 22q11.2 deletion syndrome. *J Pediatr* 2011;159:332–9.
20. McDonald-McGinn DM, Sullivan KE, Marino B, et al. 22q11.2 deletion syndrome. *Nat Rev Dis Prim* 2015;1(15071):1–19.
21. Unolt M, Versacci P, Anaclerio S, et al. Congenital heart diseases and cardiovascular abnormalities in 22q11.2 deletion syndrome: from well-established knowledge to new frontiers. *Am J Med Genet Part A* 2018;176A:2087–96.
22. Asher MA, Burton DC. Adolescent idiopathic scoliosis: Natural history and long term treatment effects. *Scoliosis* 2006;1:1–10.
23. Insel TR, Grent-‘t-Jong T, Uhlhaas PJ, et al. Rethinking schizophrenia. *Nature* 2010.
24. Staps P, Fuijkschoot J, Hogeveen M, Willemsen MAA. Understanding preterm birth: Sjögren-Larsson Syndrome as a model. *Eur J Paediatr Neurol* 2017;21:e43
25. Van L, Boot E, Bassett AS. Update on the 22q11.2 deletion syndrome and its relevance to schizophrenia. *Curr Opin Psychiatry* 2017;30:191–6.
26. Costain G, Lionel AC, Merico D, et al. Pathogenic rare copy number variants in community-based schizophrenia suggest a potential role for clinical microarrays. *Hum Mol Genet* 2013;22:4485–501.
27. Gur RE, Bassett AS, McDonald-McGinn DM, et al. A neurogenetic model for the study of schizophrenia spectrum disorders: The International 22q11.2 Deletion Syndrome Brain Behavior Consortium. *Mol Psychiatry* 2017;22:1664–72.
28. Vorstman JAS, Breetvelt EJ, Duijff SN, Cognitive, et al. Decline preceding the onset of psychosis in patients With 22q11.2 deletion syndrome. *JAMA Psychiatry* 2015;72:377–85.
29. Cagnetti D, Keeny HM, Samdani AF, et al. Neuromuscular scoliosis complication rates from 2004 to 2015: a report from the Scoliosis Research Society Morbidity and Mortality database. *Neurosurg Focus* 2017;43:E10.
30. Garg S. Management of scoliosis in patients with Duchenne muscular dystrophy and spinal muscular atrophy: a literature review. *J Pediatr Rehabil Med* 2016;9:23–9.
31. Roizen NJ, Antshel KM, Fremont W, et al. 22q11.2DS deletion syndrome: developmental milestones in infants and toddlers. *J Dev Behav Pediatr* 2007;28:119–24.
32. Homans JF, Tromp IN, Colo D, et al. Orthopaedic manifestations within the 22q11.2 Deletion syndrome: a systematic review. *Am J Med Genet A* 2017:1–17.
33. Luk KDK, Lee CF, Cheung KMC, et al. Clinical effectiveness of school screening for adolescent idiopathic scoliosis. *Spine (Phila Pa 1976)* 2010;35(35):1607–14.

34. Weinstein SL, Dolan LA, Wright JG, Dobbs MB. Effects of bracing in adolescents with idiopathic scoliosis. *N Engl J Med* 2013;369:1512–21.
35. Heemskerk JL, Kruyt MC, Colo D, Castelein RM, Kempen DHR. Prevalence and risk factors for neural axis anomalies in idiopathic scoliosis: a systematic review. *Spine J* 2018;18:1261–71.
36. Kramers-De Quervain IA, Müller R, Stacoff A, Grob D, Stüssi E. Gait analysis in patients with idiopathic scoliosis. *Eur Spine J* 2004;13:449–56.
37. Schlösser TPC, van Stralen M, Brink RC, et al. Three-dimensional characterization of torsion and asymmetry of the intervertebral discs versus vertebral bodies in adolescent idiopathic scoliosis. *Spine (Phila Pa 1976)* 2014;39:E1159–66.
38. Grivas TB, Vasiliadis E, Malakasis M, Mouzakis V, Segos D. Intervertebral disc biomechanics in the pathogenesis of idiopathic scoliosis. *Stud Health Technol Inform* 2006;123:80–3.
39. Will RE, Stokes IA, Qiu X, Walker MR, Sanders JO. Cobb angle progression in adolescent scoliosis begins at the intervertebral disc. *Spine (Phila Pa 1976)* 2009;34:2782–6.
40. Roaf R. The basic anatomy of scoliosis. *J Bone Jt Surg Br* 1966;48:786–92.
41. Parent S, Newton PO, Wenger DR. Adolescent idiopathic scoliosis: etiology, anatomy, natural history, and bracing. *Instr Course Lect* 2005;54:529–36.
42. Roach JW, Mehlmán CT, Sanders JO. Does the outcome of adolescent idiopathic scoliosis surgery justify the rising cost of the procedures? *J Pediatr Orthop* 2011;31:77–80.
43. Beals R, Kenney K, Lees M. Congenital heart disease and idiopathic scoliosis. *Clin Orthop Relat Res* 1972;89:112–6.
44. Jordan CE, White RI, Fischer KC, Neill C, Dorst JP. The scoliosis of congenital heart disease. *Am Heart J* 1972;84:463–9.
45. Van Biezen FC, Bakx PA, De Villeneuve VH, Hop WC. Scoliosis in children after thoracotomy for aortic coarctation. *J Bone Joint Surg Am* 1993;75:514–8.
46. Ruiz-Iban MA, Burgos J, Aguado HJ, et al. Scoliosis after median sternotomy in children with congenital heart disease. *Spine (Phila Pa 1976)*;2005(30):E214–8.
47. Gilsanz V, Boechat IM, Birnberg FA, King JD. Scoliosis after Thoracotomy for Esophageal Atresia. *AJRAmerican J Roentgenol* 1983;141:457–60.
48. Feiz HH, Afrasiabi A, Parvizi R, Safarpour A, Fouladi RF. Scoliosis after thoracotomy/sternotomy in children with congenital heart disease. *Indian J Orthop* 2012;46:77–80.

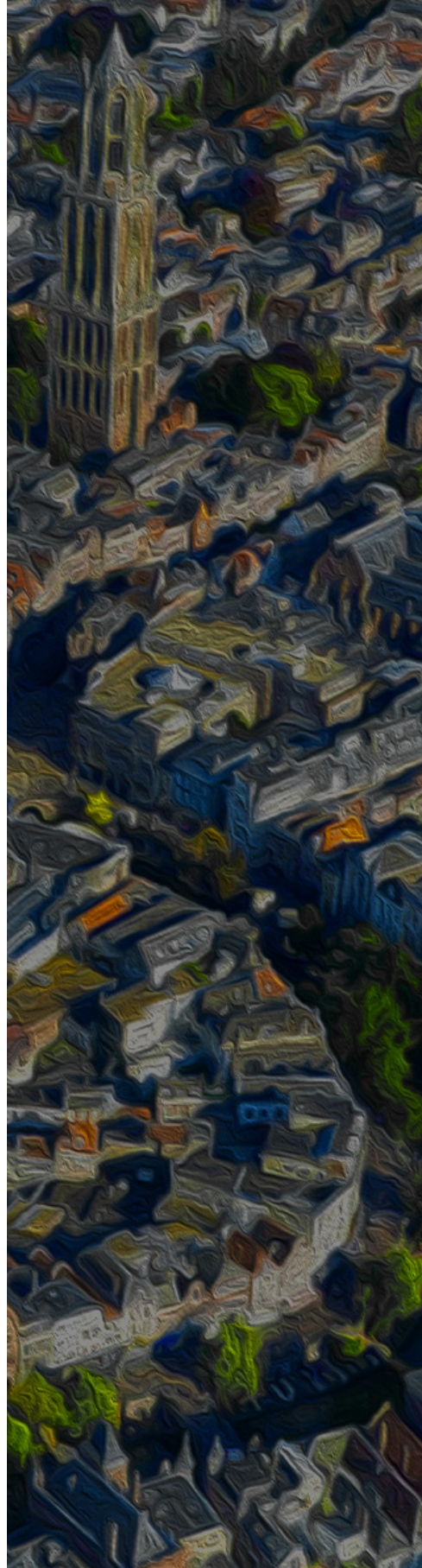


# 15

## 22q11.2 Deletion Syndrome as a Human Model for Idiopathic Scoliosis

Steven de Reuver  
Jelle F. Homans  
Tom P.C. Schlösser  
Michiel L. Houben  
Vincent F.X. Deeney  
Terrence B. Crowley  
Ralf Stücker  
Saba Pasha  
Moyo C. Kruyt  
Donna M. McDonald-McGinn  
René M. Castelein

*Journal of Clinical Medicine.* 2021 Oct 20;10(21):4823.



## ABSTRACT

To better understand the etiology of idiopathic scoliosis, prospective research into the pre-scoliotic state is required, but this research is practically impossible to carry out in the general population. The use of 'models', such as idiopathic-like scoliosis established in genetically modified animals, may elucidate certain elements, but their translatability to the human situation is questionable. The 22q11.2 deletion syndrome (22q11.2DS), with a 20-fold increased risk of developing scoliosis, may be a valuable and more relevant alternative and serve as a human 'model' for idiopathic scoliosis. This multicenter study investigates the morphology, dynamic behavior, and presence of intraspinal anomalies in patients with 22q11.2DS and scoliosis compared to idiopathic scoliosis. Scoliosis patients with 22q11.2DS and spinal radiography ( $n = 185$ ) or MRI ( $n = 38$ ) were included (mean age  $11.6 \pm 4.2$ ; median Cobb angle  $16^\circ$ ) and compared to idiopathic scoliosis patients from recent literature. Radiographic analysis revealed that 98.4% of 22q11.2DS patients with scoliosis had a curve morphology following predefined criteria for idiopathic curves: eight or fewer vertebrae, an S-shape and no inclusion of the lowest lumbar vertebrae. Furthermore, curve progression was present in 54.2%, with a mean progression rate of  $2.5^\circ/\text{year}$ , similar to reports on idiopathic scoliosis with 49% and  $2.2\text{-}9.6^\circ/\text{year}$ . The prevalence of intraspinal anomalies on MRI was 10.5% in 22q11.2DS, which is also comparable to 11.4% reported for idiopathic scoliosis. This indicates that 22q11.2DS may be a good model for prospective studies to better understand the etiology of idiopathic scoliosis.

## Introduction

Scoliosis is a deformity of the spine and trunk that can have a clear cause, such as neuromuscular disease or congenital spinal malformation; however, the majority of cases are referred to as ‘idiopathic’ and occur in otherwise healthy adolescents.<sup>1</sup> Idiopathic scoliosis is quite common, with a prevalence of 2–4% in the general population, but its exact etiology remains clouded, despite important recent discoveries about genetics and the role of human upright spinal biomechanics.<sup>1–6</sup> Knowing the exact cause(s) is of utmost importance for potential scoliosis prevention and optimal treatment. The problem with current human etiology research is that, by necessity, only patients with an already established idiopathic scoliosis are studied; therefore, it is impossible to distinguish cause from effect.<sup>1,3</sup>

Prospective cohort research, which follows the development of scoliosis starting in the pre-scoliotic spine, is practically impossible in the general population due to practical and ethical obstacles: the prevalence of idiopathic scoliosis would require thousands of children to be included for sufficient statistical power, and there would have to be periodic follow-ups with full spine radiographs, raising ionizing radiation concerns. The next best option is to use a ‘model’ with better availability or a higher idiopathic scoliosis prevalence—for instance, an animal model. Unfortunately, idiopathic scoliosis is a disease unique to humans, mainly due to our unique upright spinal biomechanics.<sup>7</sup> Earlier studies demonstrated that the computation of spinal biomechanics, for instance, with finite element models, can help understand idiopathic scoliosis.<sup>8</sup> Additionally, idiopathic-like scoliosis can be established in genetically modified animals such as zebrafish, pinealectomized chickens, or bipedal-forced mice; however, the translatability of this model to the human situation is questionable.<sup>9–12</sup>

To prospectively study the etiology of idiopathic scoliosis, a human model is therefore preferred but has not yet been described. In other fields of medicine, such as psychiatry, the innovative use of a subset of the population with a high risk of a certain disease has been used and validated to serve as a ‘model’ for the disease in the general population.<sup>13</sup> This approach obviously also has scientific limitations, but if the model sufficiently resembles the condition in the general population, it can yield important information on specific aspects of the earliest phases of the disorder that cannot otherwise be studied prospectively.

The 22q11.2 deletion syndrome (22q11.2DS), the most common cause of DiGeorge syndrome, is the most common microdeletion syndrome in humans, with an incidence of 1 in 992 unselected pregnancies and 1 in 2148 live births.<sup>14–16</sup> Compared to the general population, these children have a 20-fold increased risk of developing scoliosis during their growing years, with a prevalence of around 50%.<sup>17</sup> Children with 22q11.2DS are often

identified before or shortly after birth, well before potential scoliosis onset, are usually known in the pediatric circuit, and could therefore be studied prospectively.<sup>18,19</sup> It is currently unknown if scoliosis in 22q11.2DS sufficiently resembles idiopathic scoliosis in the general population, which is a prerequisite to be used as a 'model'. This study focused on the morphology, dynamic behavior, and presence of intraspinal anomalies, all of which are quantifiable features relevant to idiopathic scoliosis development. These were studied in 22q11.2DS and scoliosis patient cohorts from multiple centers and compared to what is reported in the literature for idiopathic scoliosis in the general population.

## **Materials and Methods**

### Study population

The local Ethical Review Boards of the three hospitals involved approved this study and waived the necessity of explicit (parental) informed consent since data were collected as part of standard care and were handled anonymously. In all participating centers, spinal radiographs are made of each patient at two-year intervals as part of a global standard 22q11.2DS follow-up protocol.<sup>20</sup>

From databases of two specialized 22q11.2DS centers, patients with an available full spine radiograph were extracted. All patients that were ambulant, had a genetically confirmed 22q11.2 deletion (via FISH, 22q11.2 specific MLPA, CGH, or SNP micro-array), were aged >4, and had scoliosis defined as a Cobb angle >10° were included.<sup>21</sup> Patients with congenital spinal anomalies (based on spinal radiography review) that induced congenital scoliosis were excluded since the pathoetiology varies greatly from the development of idiopathic scoliosis.<sup>22</sup> Additionally, non-ambulant patients (based on the patient's chart review) were excluded. Sex, age at the time of radiography, and data on comorbidities were collected. For the further analysis of curve progression, all included patients with at least one year of radiographic follow-up were analyzed.

Additionally, patients were included from a database of a third specialized 22q11.2DS center, where patients with scoliosis frequently receive an MRI of the spine for indications such as pain, fast progression, or pre-operative screening. Patients with congenital spinal anomalies or with only post-operative MRIs were excluded. These MRIs were analyzed for intraspinal anomalies.



### Radiographic analysis

One trained and experienced observer (JH), blinded for all other clinical parameters, analyzed all radiographs in chronological order. First, the Cobb angle was measured of all scoliotic curve(s), and the location of the major curve (i.e., the largest) was noted as either thoracic (apex at T2 – disc T11/T12), thoracolumbar (apex at T12 – L1), or lumbar (apex at disc L1/L2 – L4), according to the Scoliosis Research Society guideline.<sup>21</sup> Next, curve morphology was determined based on the first available radiograph of each patient, according to the criteria determined by Abul-Kasim et al. in 2010.<sup>23</sup> Curves were classified as non-idiopathic if three conditions were met: (1) the Cobb-to-Cobb segment exceeded eight vertebrae, (2) the curve was C-shaped, and (3) the curve included the lowest or second-lowest lumbar vertebra (**Figure 1**). The findings in the 22q11.2DS patients in this study were compared to reference observations in idiopathic and non-idiopathic scoliosis patients in the general population.<sup>23</sup>

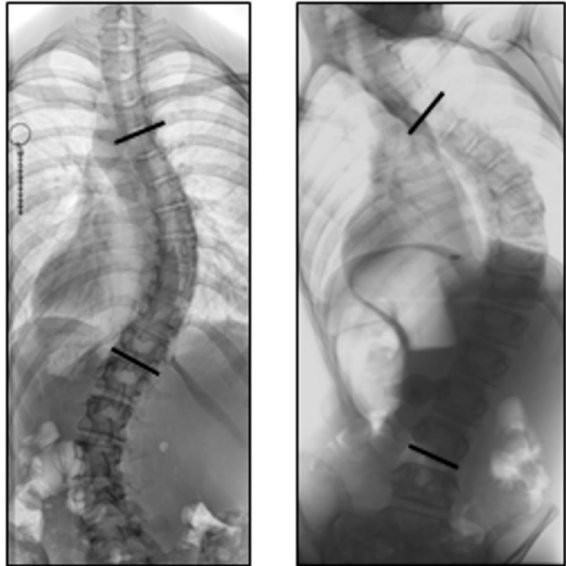


**Figure 1.** Two examples of different scoliosis curve types. On the left is an idiopathic-like curve, which is S-shaped with the apex of the major curve located at vertebral level T9 and a curve length of 8 vertebrae. On the right is a non-idiopathic neuromuscular-like curve, which is C-shaped with a curve length of 12 vertebrae, and a lower-end vertebra located at level L4.

Furthermore, the progression of scoliosis curve severity was analyzed by measuring the Cobb angle on the first and last radiograph available for each patient with at least one year of follow-up. A progressive curve was defined as at least a 5° increase over the follow-up period.<sup>24</sup> Additionally, if a patient had received brace treatment or surgery, the curve was considered progressive. Of all 22q11.2DS patients with progressive scoliosis, the curve progression rate in degrees of Cobb angle per year was calculated and compared to reference values of idiopathic scoliosis in the general population, as described in a meta-analysis by Di Felice et al. in 2018.<sup>24</sup>

### MRI analysis

Of the spinal MRIs made of 22q11.2DS patients with scoliosis, all reports were screened for the presence of intraspinal anomalies and annotated as described by the clinically involved radiologist at the time of investigation. The rate of intraspinal anomalies in 22q11.2DS patients with scoliosis was compared to that reported in idiopathic scoliosis in the general population, as described in a meta-analysis by Heemskerk et al. in 2018.<sup>25</sup>

### Statistical analysis

The age at diagnosis, sex, curve progression (< or >5°), and presence of spinal anomalies in the 22q11.2DS patients in this study were compared to data on idiopathic scoliosis in the general population from literature. Normality of distribution was tested with Q–Q plots, the means ± standard deviations were calculated for normally distributed variables, and medians and interquartile ranges (IQR) were calculated for not normally distributed variables. Since data were compiled from multiple cohorts with different criteria, no comparative statistics were performed to produce irrelevant p-values. The descriptive statistical analyses were performed with SPSS 25.0 for Windows (IBM, Armonk, NY, USA).

## **Results**

### Study population

From two databases, 206 patients with 22q11.2DS, scoliosis, and a full spine radiograph were retrieved; after 21 exclusions, 185 patients were included for radiographic analysis (**Figure 2**). From these 185 patients, a further 48 had at least one year of radiographic follow-up and were included for analysis of their scoliosis curve progression. Finally, for the MRI analysis, after nine exclusions, 38 patients were included for analysis of the rate of intraspinal anomalies.

The mean age at diagnosis of scoliosis in 22q11.2DS patients was  $11.6 \pm 4.2$ , and 92 (49.7%) were female (**Figure 3**). In literature, the mean age at idiopathic scoliosis diagnosis in the general population varies due to different screening and diagnosis protocols but is reported at 9.5–13.6.<sup>26-28</sup> Furthermore, the ratio of females to males in idiopathic scoliosis is reported as 1.44 to 1, corresponding to 59% females.<sup>26</sup>

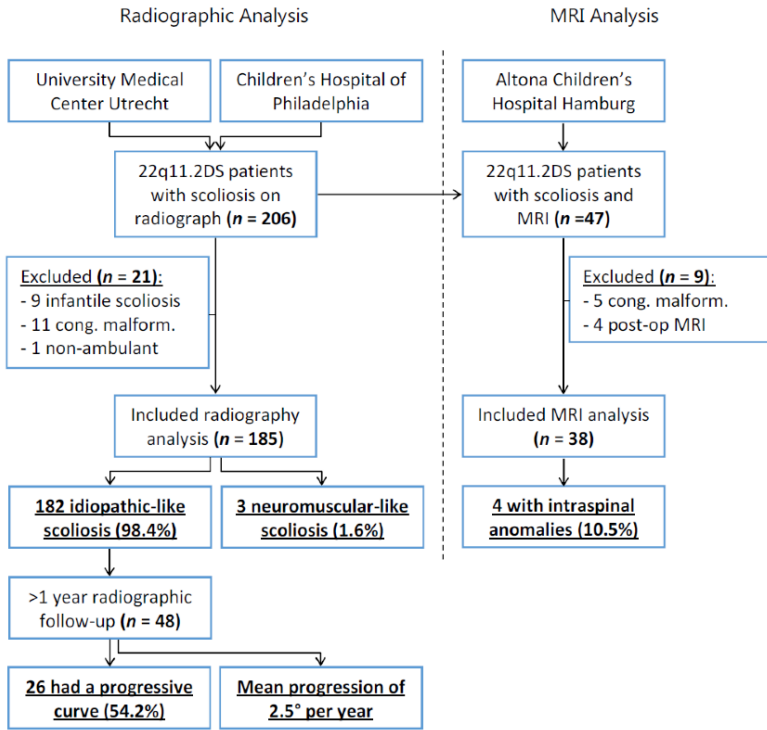
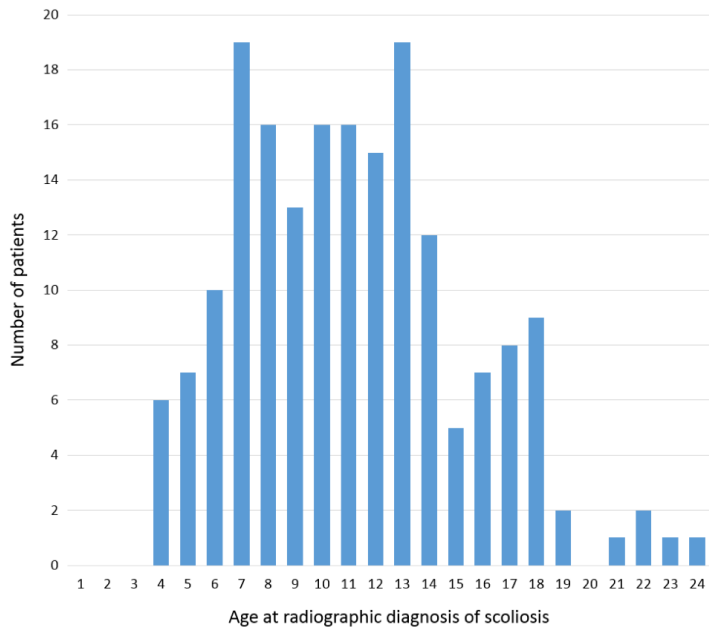


**Figure 2.** Flowchart shows the inclusion and exclusion of patients in the current study.

**Figure 3.** The age distribution at the moment of initial radiographic diagnosis of scoliosis. In the 185 included 22q11.2 deletion syndrome patients in this study, the mean age at diagnosis was  $11.6 \pm 4.2$ .



### Radiographic analysis

Of the 185 patients with 22q11.2DS and scoliosis, the median Cobb angle was 16° (IQR: 13–25°). A total of 182 patients (98.4%) had an idiopathic-like curve based on Abul-Kasim's criteria (**Table 1**).<sup>23</sup> The other three patients (1.6%) fitted the criteria for neuromuscular-like scoliosis. Remarkably, the proportion of S-shaped curves was 69%, much higher than the 18% reported earlier for idiopathic scoliosis (**Table 1**).<sup>23</sup> Of the 48 patients with at least one year of radiographic follow-up, the mean age at scoliosis diagnosis was 9.8 ± 2.7, and the median follow-up was 3.4 years (IQR: 2.3–5.1). There was a curve progression of at least 5° in 26 patients (54.2%), at an average progression rate of 2.5° per year, ranging from 1.4° to 5.0°. This is very comparable to idiopathic scoliosis, which has a reported proportion of 49% and a similar rate of 2.2–9.6° per year in the general population.<sup>24</sup>

|   | Current Study | Abul-Kasim et al. (2010) <sup>1</sup> |                  |
|---|---------------|---------------------------------------|------------------|
|   | 22q11.2DS     | Idiopathic Scoliosis                  | Neuro. Scoliosis |
| <i>n</i>                                  | 185           | 77                                    | 21               |
| Major curve location                      |               |                                       |                  |
| - Thoracic                                | 79 (43%)      | 52 (68%)                              | 5 (24%)          |
| - Thoracolumbar                           | 54 (29%)      | 13 (17%)                              | 12 (57%)         |
| - Lumbar                                  | 52 (28%)      | 12 (16%)                              | 4 (19%)          |
| Median curve length in N° vertebrae (IQR) | 6 (5–7)       | 7 (7–8)                               | 10 (9–11)        |
| >8 vertebrae in curve                     | 18 (10%)      | 3 (4%)                                | 19 (90%)         |
| Curve morphology                          |               |                                       |                  |
| - S-shape                                 | 127 (69%)     | 14 (18%)                              | 0 (0%)           |
| - C-shape                                 | 58 (31%)      | 63 (82%)                              | 21 (100%)        |
| Lower-end vertebra                        |               |                                       |                  |
| - L3+                                     | 114 (62%)     | 62 (81%)                              | 5 (24%)          |
| - L4                                      | 67 (36%)      | 15 (19%)                              | 8 (38%)          |
| - L5                                      | 4 (2%)        | 0 (0%)                                | 8 (38%)          |
| Fulfilled criteria for <sup>2</sup>       |               |                                       |                  |
| - Neuro. scoliosis                        | 3 (2%)        | 0 (0%)                                | 16 (76%)         |
| - Idiopathic scoliosis                    | 183 (98%)     | 77 (100%)                             | 5 (24%)          |

**Table 1.** Curve characteristics of the 185 ambulant 22q11.2 deletion syndrome patients with scoliosis next to references values of the idiopathic and neuromuscular scoliosis. From Abul-Kasim et al. (2010). 1Reprinted by Permission of SAGE Publications, Ltd.<sup>23</sup>. 2The combination of a Cobb-to-Cobb curve length > 8 vertebrae, a C-shaped curve, and the location of the lower-end vertebrae at the lowest or second-lowest lumbar vertebrae is determined as a non-idiopathic (neuromuscular) curve pattern.<sup>23</sup>

### MRI analysis

Out of 38 scoliosis patients with 22q11.2DS and an available MRI of the complete spine, four patients (10.5%) had a total of five intraspinal anomalies. The different anomalies were one tonsillar herniation, one extradural cyst, one intraspinal lipoma, and two vertebral body abnormalities. This is comparable to a prevalence of 11.4% in idiopathic scoliosis in the general population (**Table 2**).<sup>25</sup>

|                                       | Current Study       | Heemskerk et al. (2018) <sup>1</sup> |
|---------------------------------------|---------------------|--------------------------------------|
|                                       | 22q11.2DS           | Idiopathic Scoliosis                 |
| <i>n</i>                              | 38                  | 8622                                 |
| Spinal anomaly:                       |                     |                                      |
| -Isolated syrinx                      |                     | 318 (3.7%)                           |
| -Isolated Arnold-Chiari malf.         |                     | 259 (3.0%)                           |
| -Arnold-Chiari malf. with syrinx      |                     | 218 (2.5%)                           |
| -Tethered cord                        |                     | 49 (0.57%)                           |
| -Dural ectasia                        |                     | 33 (0.38%)                           |
| -Cerebral or intra/paraspinal tumors  |                     | 22 (0.26%)                           |
| -Tonsillar herniation                 | 1 (3%)              | 20 (0.23%)                           |
| -Diastematomyelia                     |                     | 19 (0.22%)                           |
| -Abnormal position of conus           |                     | 10 (0.12%)                           |
| -Extra- or intradural cysts           | 1 (3%)              | 6 (0.07%)                            |
| -Intraspinal lipoma                   | 1 (3%)              | 5 (0.06%)                            |
| -Discopathy                           |                     | 4 (0.05%)                            |
| -Hydrocephalus                        |                     | 3 (0.03%)                            |
| -Vertebral body abnormality           | 2 (5%) <sup>2</sup> | 3 (0.03%) <sup>3</sup>               |
| -Hydromyelia                          |                     | 2 (0.02%)                            |
| -Cranio-cervical junctional narrowing |                     | 1 (0.01%)                            |
| -Cerebellar angioma                   |                     | 1 (0.01%)                            |
| -Dandy-Walker syndrome                |                     | 1 (0.01%)                            |
| -Arteriovenous fistula                |                     | 1 (0.01%)                            |
| -Not specified                        |                     | 88 (1%)                              |

**Table 2.** Intraspinal anomalies in 38 patients with 22q11.22 deletion syndrome and scoliosis compared to idiopathic scoliosis in the general population, as described by Heemskerk et al. (2018).

<sup>1</sup>Compiled from the systematic review and meta-analysis as performed by Heemskerk et al.<sup>25</sup>

<sup>2</sup>Patient 1: Mild osteophytic ridging at T10-T11 and T11-T12 with Schmorl's nodes and decreased disc height at these levels. Patient 2: Vertical cleft in the midline of the T7 vertebral body.

<sup>3</sup>Hemangioma or lipoma in vertebral body.

## Discussion

The problem with the current etiology research on idiopathic scoliosis is that only established cases can be studied, and prospective research before the onset of the deformity is unfeasible in the general population.<sup>1,3</sup> The solution is the use of a 'model'; however, currently, for idiopathic scoliosis, only 'models' of genetically or anatomically modified small animals exist.<sup>7,9-12</sup> This study investigated the relevance of a human 'model' for idiopathic scoliosis by using a subset of the population with a high risk for the disease. Children with 22q11.2DS have a 20-fold increased prevalence of scoliosis at around 50% and are usually prospectively followed from birth.<sup>14,17,18</sup> The purpose of this multicenter study was to analyze the morphology, dynamic behavior, and presence of intraspinal anomalies in scoliosis patients from 22q11.2DS cohorts in comparison to idiopathic scoliosis.

Over two hundred patients with 22q11.2DS and scoliosis were compared to thousands of patients with idiopathic scoliosis from the recent literature. The mean age at diagnosis of scoliosis in patients with 22q11.2DS was 11.6, and 49.7% were females. In idiopathic scoliosis, this is reported as 9.5–13.6 years old and 59% females.<sup>26-28</sup> This broad range of reported age at diagnosis is caused by the many different scoliosis screening protocols in different countries. However, if scoliosis in 22q11.2DS onsets at the same age as idiopathic scoliosis, the mean age at diagnosis in patients with 22q11.2DS is likely to be lower since spinal radiography is part of the standard follow-up, promoting early diagnosis. The vast majority of included patients with 22q11.2DS and scoliosis (98.4%) had a curve morphology that was consistent with predefined criteria for an idiopathic curve.<sup>23</sup> Additionally, the proportion of progressive curves (54.2%) and the rate of curve progression (2.5° per year) was similar to reports on idiopathic scoliosis, with 49% being progressive at a rate of 2.2–9.6° per year.<sup>24</sup> Finally, the prevalence of intraspinal anomalies in 22q11.2DS patients with scoliosis was 10.5%, which was similar to the 11.4% prevalence in idiopathic scoliosis in the general population.<sup>25</sup>

There are multiple classification systems that describe the curve morphology pattern in scoliosis. The well-known King and Lenke classifications were created mainly for surgical planning by distinguishing stiffer/structural curves from non-structural curves rather than distinguishing between idiopathic and non-idiopathic scoliosis.<sup>29,30</sup> Abul-Kasim et al. showed that non-idiopathic curves display distinct morphologic characteristics on upright standing spinal radiographs, including the scoliosis shape, the curve length, and the contribution of the lowest lumbar vertebrae to the curve (**Figure 1**). These characteristics were translated into three criteria to distinguish idiopathic from non-idiopathic curves, which were used in this study of 22q11.2DS scoliosis.<sup>23</sup> While these three criteria are all assessed from

anterior–posterior standing spinal radiographs, idiopathic scoliosis is a 3D deformation of the spine and trunk, including vertebral rotation and sagittal plane deformation. However, since lateral radiographs were not routinely made in all participating centers, these were not analyzed in this study. Furthermore, accurate assessment of the sagittal spinal profile is notoriously unreliable on lateral radiographs, especially in more severe curves with a larger Cobb angle, due to coupling of the spinal curvature in all three planes.<sup>31,32</sup>

Besides the global curve morphology criteria for idiopathic scoliosis, the curve behavior over time was also reckoned as relevant. Although similar values for the proportion and rate of curve progression were observed in 22q11.2DS scoliosis in comparison to idiopathic scoliosis, this should be interpreted with caution since scoliosis progression is heavily influenced by age, sex, curve location, and curve magnitude, all parameters that were not normalized or matched in this study.<sup>24,33</sup> Additionally, in the 22q11.2DS cohort, there was a median follow-up difference between the progressive curves (4.4 years) and non-progressive curves (2.5 years); therefore, the number of progressive curves in 22q11.2DS might be underestimated by this study. Future studies, with, for instance, an age- and sex-matched design, could aim to confirm the similarities in curve behavior between 22q11.2DS and idiopathic scoliosis. The addition of an MRI-based analysis to this study was mainly to exclude intraspinal anomalies as an important cause of scoliosis in 22q11.2DS. Indeed, the intraspinal anomaly prevalence was comparable to idiopathic scoliosis.<sup>25</sup>

Although this study demonstrated similarities in curve morphology and behavior between scoliosis in 22q11.2DS and idiopathic scoliosis, the validity of 22q11.2DS as a ‘model’ has obvious limitations. First, the absence of typical non-idiopathic features that were identified for neuromuscular scoliosis does not imply that the curve is similar to idiopathic scoliosis. On the contrary, more subtle differences could be observed, such as the distribution between thoracic, thoracolumbar, and lumbar curves, as well as the contribution of L4 to the curve. Second, in this study, patients with congenital spinal anomalies that induced congenital scoliosis were excluded. This was because in the general population, and most likely also in 22q11.2DS, the pathoetiology of congenital scoliosis varies greatly from the development of idiopathic scoliosis.<sup>22</sup> It is known that in 22q11.2DS, the rate of congenital spinal malformations, especially in the cervical spine, is higher than the general population; therefore, if 22q11.2DS scoliosis were to be used as a ‘model’ to study idiopathic scoliosis, the congenital curves should be excluded.<sup>34</sup> Third, 22q11.2DS is a multisystem syndrome with many phenotypes resulting, for example, in hypocalcemia and a lower bone mineral density in half of the patients.<sup>14,35</sup> Interestingly, a proportion of patients with idiopathic scoliosis in the general population have lower bone mineral density.<sup>36-39</sup> Irrespective of a 22q11.2 deletion,

a lower bone mineral density might be an independent risk factor for idiopathic-like scoliosis. Additionally, congenital heart disease is prevalent in 22q11.2DS, and for many decades, congenital heart disease has been linked to scoliosis in the general population.<sup>40,41</sup> Recent observations in different cohorts demonstrate that the 22q11.2 deletion itself is a confounder in this relationship and that in both the general population and in 22q11.2DS, congenital heart disease itself is not a large scoliosis risk factor.<sup>42</sup> Finally, children with 22q11.2DS differ from the general population in frequent phenotypes such as slow maturation, short stature, and articular laxity, which could all influence scoliosis development, but their exact effects are currently unknown. Future studies using 22q11.2DS scoliosis as a model should aim to normalize these as much as possible, for instance, by determining the individual offset from maturity, i.e., the difference between chronological age and biological maturity.<sup>43</sup>

For a scientific 'model' to be valid, the disease of the 'model' must sufficiently resemble the condition in the general population before it can be used to study etiological aspects of the disorder. Of course, any 'model' is at best an approximation of the true disease; this holds true for the often-used animal model as well. Scoliosis in 22q11.2DS does have differences from true idiopathic scoliosis in the general population, but this study demonstrated many important similarities in curve morphology and behavior. A future goal could be to utilize this 'human model' in prospective studies on idiopathic scoliosis etiology—for example, to study the spinal sagittal profile before scoliosis onset and its influence on scoliosis development.<sup>8,44</sup> Another option is to examine whole-genome sequencing in patients with scoliosis and 22q11.2DS, and those in the general population, as a clue to identifying the genomic etiology. Studying psychotic, 'schizophrenia-like' disorders in the 22q11.2DS population has yielded important information on idiopathic schizophrenia, a disorder that also seems exclusive to humans in the general population.<sup>13</sup> We propose to use the same approach in idiopathic scoliosis research.

In conclusion, to better understand idiopathic scoliosis etiology, prospective research on the pre-scoliotic spine is needed but is practically impossible in the general population. Animal models can help, but a validated human model would be superior. This study explored scoliosis in patients with 22q11.2DS as a possible human 'model' for idiopathic scoliosis. These patients have a 20-fold increased scoliosis risk and a curve morphology that resembles idiopathic scoliosis. Additionally, the curve dynamic behavior, in terms of prevalence and rate of curve progression and the prevalence of intraspinal anomalies, closely mimicked idiopathic scoliosis. This suggests that 22q11.2DS scoliosis may be a very relevant 'model' to prospectively study and help better understand certain aspects of idiopathic scoliosis etiology in the general population.

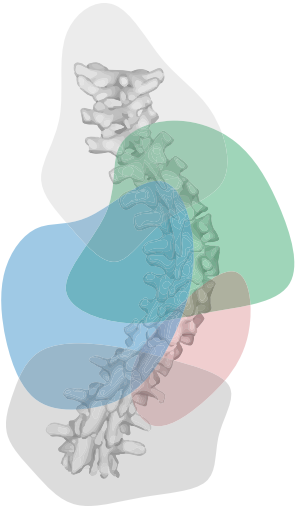


## References

1. Cheng, J.C.; Castelein, R.M.; Chu, W.C.; Danielsson, A.J.; Dobbs, M.B.; Grivas, T.B.; Gurnett, C.A.; Luk, K.D.; Moreau, A.; Newton, P.O.; et al. Adolescent idiopathic scoliosis. *Nat. Rev. Dis. Prim.* 2015, 1, 15–30.
2. Kouwenhoven, J.-W.M.; Castelein, R.M. The pathogenesis of adolescent idiopathic scoliosis: Review of the literature. *Spine* 2008, 33, 2898–2908.
3. Schlösser, T.P.C.; van der Heijden, G.J.M.G.; Versteeg, A.L.; Castelein, R.M. How “idiopathic” is adolescent idiopathic scoliosis? A systematic review on associated abnormalities. *PLoS ONE* 2014, 9, e97461.
4. Gorman, K.F.; Julien, C.; Moreau, A. The genetic epidemiology of idiopathic scoliosis. *Eur. Spine J.* 2012, 21, 1905–1919.
5. Kesling, K.L.; Reinker, K.A. Scoliosis in twins: A meta-analysis of the literature and report of six cases. *Spine* 1997, 22, 2009–2015.
6. Kouwenhoven, J.W.; Smit, T.H.; van der Veen, A.J.; Kingma, I.; van Dieën, J.H.; Castelein, R.M. Effects of dorsal versus ventral shear loads on the rotational stability of the thoracic spine: A biomechanical porcine and human cadaveric study. *Spine* 2007, 32, 2545–2550.
7. Castelein, R.M.; Pasha, S.; Cheng, J.C.Y.C.; Dubousset, J. Idiopathic Scoliosis as a Rotatory Decomensation of the Spine. *J. Bone Miner. Res.* 2020, 35, 1850–1857.
8. Pasha, S.; de Reuver, S.; Homans, J.F.; Castelein, R.M. Sagittal curvature of the spine as a predictor of the pediatric spinal deformity development. *Spine Deform.* 2021, 9, 923–932.
9. Janssen, M.M.A.; de Wilde, R.F.; Kouwenhoven, J.-W.M.; Castelein, R.M. Experimental animal models in scoliosis research: A review of the literature. *Spine J.* 2011, 11, 347–358.
10. Boswell, C.W.; Ciruna, B. Understanding Idiopathic Scoliosis: A New Zebrafish School of Thought. *Trends Genet.* 2017, 33, 183–196.
11. Machida, M.; Dubousset, J.; Imamura, Y.; Iwaya, T.; Yamada, T.; Kimura, J. An experimental study in chickens for the pathogenesis of idiopathic scoliosis. *Spine* 1993, 18, 1609–1615.
12. Bobyn, J.D.; Little, D.G.; Gray, R.; Schindeler, A. Animal models of scoliosis. *J. Orthop. Res.* 2015, 33, 458–467.
13. Gur, R.E.; Bassett, A.S.; McDonald-McGinn, D.M.; Bearden, C.E.; Chow, E.; Emanuel, B.S.; Owen, M.; Swillen, A.; Van den Bree, M.; Vermeesch, J.; et al. A neurogenetic model for the study of schizophrenia spectrum disorders: The International 22q11.2 Deletion Syndrome Brain Behavior Consortium. *Mol. Psychiatry* 2017, 22, 1664–1672.
14. McDonald-McGinn, D.M.; Sullivan, K.E.; Marino, B.; Philip, N.; Swillen, A.; Vorstman, J.A.S.; Zackai, E.H.; Emanuel, B.S.; Vermeesch, J.R.; Morrow, B.E.; et al. 22Q11.2 Deletion Syndrome. *Nat. Rev. Dis. Prim.* 2015, 1, 1–19.
15. Grati, F.R.; Molina Gomes, D.; Ferreira, J.C.P.B.; Dupont, C.; Alesi, V.; Gouas, L.; Horelli-Kuitunen, N.; Choy, K.W.; Garcia-Herrero, S.; de la Vega, A.G.; et al. Prevalence of recurrent pathogenic microdeletions and microduplications in over 9500 pregnancies. *Prenat. Diagn.* 2015, 35, 801–809.
16. Blagojevic, C.; Heung, T.; Theriault, M.; Tomita-Mitchell, A.; Chakraborty, P.; Kernohan, K.; Bulman, D.E.; Bassett, A.S. Estimate of the contemporary live-birth prevalence of recurrent 22q11.2 deletions: A cross-sectional analysis from population-based newborn screening. *Can. Med Assoc. Open Access J.* 2021, 9, E802–E809.
17. Homans, J.F.; Baldew, V.G.M.; Brink, R.C.; Kruyt, M.C.; Schlösser, T.P.C.; Houben, M.L.; Deeney, V.F.X.; Crowley, T.B.; Castelein, R.M.; McDonald-McGinn, D.M. Scoliosis in association with the 22q11.2 deletion syndrome: An observational study. *Arch. Dis. Child.* 2019, 104, 19–24.
18. Homans, J.F.; de Reuver, S.; Breetvelt, E.J.; Vorstman, J.A.S.; Deeney, V.F.X.; Flynn, J.M.; McDonald-McGinn, D.M.; Kruyt, M.C.; Castelein, R.M. The 22q11.2 deletion syndrome as a model for idiopathic scoliosis—A hypothesis. *Med. Hypotheses* 2019, 127, 57–62.
19. Campbell, I.M.; Sheppard, S.E.; Crowley, T.B.; McGinn, D.E.; Bailey, A.; McGinn, M.J.; Unolt, M.; Homans, J.F.; Chen, E.Y.; Salmons, H.I.; et al. What is new with 22q? An update from the 22q and You Center at the Children’s Hospital of Philadelphia. *Am. J. Med. Genet. Part. A* 2018, 176, 2058–2069.
20. Bassett, A.S.; McDonald-McGinn, D.M.; Devriendt, K.; Digilio, M.C.; Goldenberg, P.; Habel, A.; Marino, B.; Oskarsdottir, S.; Philip, N.; Sullivan, K.; et al. Practical Guidelines for Managing Patients with 22q11.2 Deletion Syndrome. *J. Pediatr.* 2011, 159, 332–339.
21. O’Brien, M.; Kulklo, T.; Blanke, K.; Lenke, L. Spinal Deformity Study Group Radiographic Measurement Manual; Medtronic Sofamor Danek USA, Inc.: Memphis, TN, USA, 2008.
22. McMaster, M.J.; Ohtsuka, K. The natural history of congenital scoliosis. A study of two hundred and fifty-one patients. *J. Bone Jt. Surg. Am.* 1982, 64, 1128–1147.
23. Abul-Kasim, K.; Ohlin, A. Curve Length, Curve Form, and Location of Lower-End Vertebra as a Means of Identifying the Type of Scoliosis. *J. Orthop. Surg.* 2010, 18, 1–5.
24. Di Felice, F.; Zaina, F.; Donzelli, S.; Negrini, S. The Natural History of Idiopathic Scoliosis during Growth: A Meta-Analysis. *Am. J. Phys. Med. Rehabil.* 2018, 97, 346–356.
25. Heemskerck, J.L.; Kruyt, M.C.; Colo, D.; Castelein, R.M.; Kempen, D.H.R. Prevalence and risk factors for neural axis anomalies in idiopathic scoliosis: A systematic review. *Spine J.* 2018, 18, 1261–1271.
26. Sung, S.; Chae, H.-W.; Lee, H.S.; Kim, S.; Kwon, J.-W.; Lee, S.-B.; Moon, S.-H.; Lee, H.-M.; Lee, B.H. Incidence and Surgery Rate of Idiopathic Scoliosis: A Nationwide Database Study. *Int. J. Environ. Res. Public Health* 2021, 18, 8152.

27. Strahle, J.; Smith, B.W.; Martinez, M.; Bapuraj, J.R.; Muraszko, K.M.; Garton, H.J.L.; Maher, C.O. The association between Chiari malformation Type I, spinal syrinx, and scoliosis. *J. Neurosurg. Pediatr.* 2015, 15, 607–611.
28. Yilmaz, H.; Zateri, C.; Kusvuran Ozkan, A.; Kayalar, G.; Berk, H. Prevalence of adolescent idiopathic scoliosis in Turkey: An epidemiological study. *Spine J.* 2020, 20, 947–955.
29. King, H.A.; Moe, J.H.; Bradford, D.S.; Winter, R.B. The selection of fusion levels in thoracic idiopathic scoliosis. *J. Bone Jt. Surg. Am. Vol.* 1983, 65, 1302–1313.
30. Lenke, L.G.; Betz, R.R.; Harms, J.; Bridwell, K.H.; Clements, D.H.; Lowe, T.G.; Blanke, K. Adolescent idiopathic scoliosis. A new classification to determine extent of spinal arthrodesis. *J. Bone Jt. Surg.-Ser. A* 2001, 83, 1169–1181.
31. Schlösser, T.P.C.; Shah, S.A.; Reichard, S.J.; Rogers, K.; Vincken, K.L.; Castelein, R.M. Differences in early sagittal plane alignment between thoracic and lumbar adolescent idiopathic scoliosis. *Spine J.* 2014, 14, 282–290.
32. Sullivan, T.B.; Reighard, F.G.; Osborn, E.J.; Parvaresh, K.C.; Newton, P.O. Thoracic Idiopathic Scoliosis Severity Is Highly Correlated with 3D Measures of Thoracic Kyphosis. *J. Bone Jt. Surg.* 2017, 99, e54.
33. Lonstein, J.; Carlson, J. The prediction of curve progression in untreated idiopathic scoliosis during growth Untreated of Curve Scoliosis in Growth. *J. Bone Jt. Surg.* 1984, 66, 1061–1071.
34. Homans, J.F.; Tromp, I.N.; Colo, D.; Schlösser, T.P.C.; Kruyt, M.C.; Deeney, V.F.X.; Crowley, T.B.; McDonald-McGinn, D.M.; Castelein, R.M. Orthopaedic manifestations within the 22q11.2 Deletion syndrome: A systematic review. *Am. J. Med. Genet. Part. A* 2018, 176, 2104–2120.
35. Stagi, S.; Lapi, E.; Gambineri, E.; Salti, R.; Genuardi, M.; Colarusso, G.; Conti, C.; Jenuso, R.; Chiarelli, F.; Azzari, C.; et al. Thyroid function and morphology in subjects with microdeletion of chromosome 22q11 (del(22)(q11)). *Clin. Endocrinol.* 2010, 72, 839–844.
36. Cheng, J.C.; Qin, L.; Cheung, C.S.; Sher, A.H.; Lee, K.M.; Ng, S.W.; Guo, X. Generalized low areal and volumetric bone mineral density in adolescent idiopathic scoliosis. *J. Bone Miner. Res.* 2000, 15, 1587–1595.
37. Cook, S.D.; Harding, A.F.; Morgan, E.L.; Nicholson, R.J.; Thomas, K.A.; Whitecloud, T.S.; Ratner, E.S. Trabecular bone mineral density in idiopathic scoliosis. *J. Pediatr. Orthop.* 1987, 7, 168–174.
38. Sadat-Ali, M.; Al-Othman, A.; Bubshait, D.; Al-Dakheel, D. Does scoliosis causes low bone mass? A comparative study between siblings. *Eur. Spine J.* 2008, 17, 944–947.
39. Burner, W.L.; Badger, V.M.; Sherman, F.C. Osteoporosis and acquired back deformities. *J. Pediatr. Orthop.* 1982, 2, 383–385.
40. Beals, R.K.; Haglund Kenny, K.; Lees, M.H. Congenital heart disease and idiopathic scoliosis. *Clin. Orthop. Relat. Res.* 1972, 89, 112–116.
41. Jordan, C.E.; White, R.I.; Fischer, K.C.; Neill, C.; Dorst, J.P. The scoliosis of congenital heart disease. *Am. Heart J.* 1972, 84, 463–469.
42. Homans, J.F.; de Reuver, S.; Heung, T.; Silversides, C.K.; Oechslin, E.N.; Houben, M.L.; McDonald-McGinn, D.M.; Kruyt, M.C.; Castelein, R.M.; Bassett, A.S. The role of 22q11.2 deletion syndrome in the relationship between congenital heart disease and scoliosis. *Spine J.* 2020, 20, 956–963.
43. Mirwald, R.L.; Baxter-Jones, A.D.G.; Bailey, D.A.; Beunen, G.P. An assessment of maturity from anthropometric measurements. *Med. Sci. Sports Exerc.* 2002, 34, 689–694.
44. Homans, J.F.; Schlosser, T.P.C.; Pasha, S.; Kruyt, M.; Castelein, R. Variations in the sagittal spinal profile precede the development of scoliosis: A pilot study of a new approach. *Spine J.* 2021, 21, 638–641.



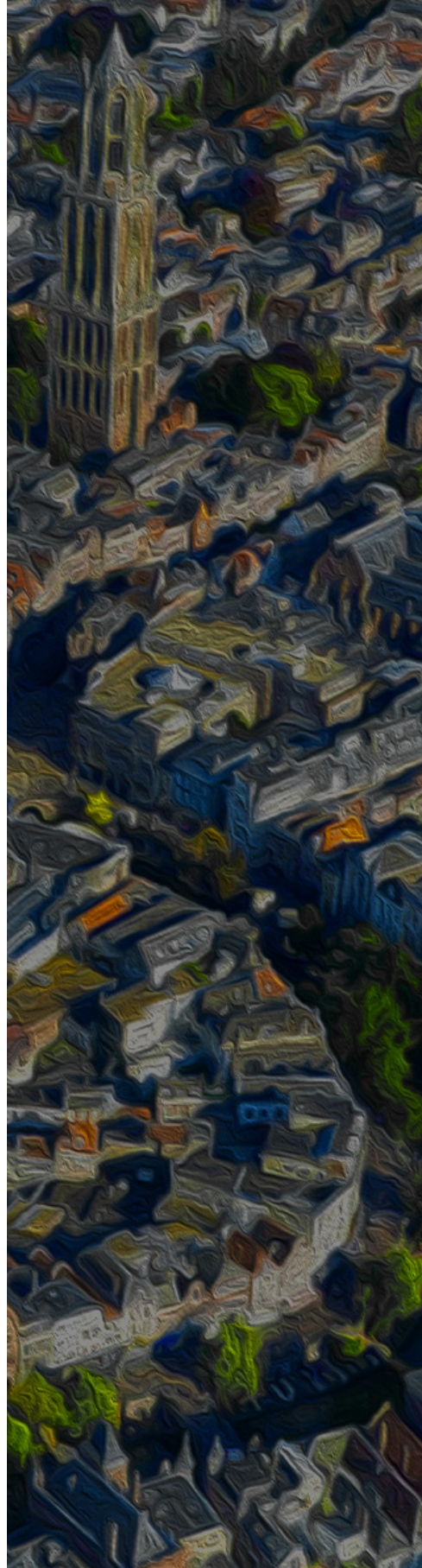


# 16

## The role of 22q11.2 Deletion Syndrome in the Relationship between Congenital Heart Disease and Scoliosis

Jelle F. Homans  
Steven de Reuver  
Tracy Heung  
Candice K. Silversides  
Erwin N. Oechslin  
Michiel L. Houben  
Donna M. McDonald-McGinn  
Moyo C. Kruyt  
René M. Castelein  
Anne S. Bassett

*The Spine Journal. 2020 Jun;20(6):956-963*



## ABSTRACT

**Introduction.** For over four decades, clinicians and researchers have suggested a relationship between congenital heart disease (CHD) and scoliosis, attributed to either the disease itself or to the long-term effects of cardiac surgery on the immature thoracic cage. However, no study has yet accounted for 22q11.2 deletion syndrome (22q11.2DS), the second most common cause of CHD after Down syndrome. 22q11.2DS has a scoliosis risk of 50%, but within 22q11.2DS a previous report found no significant association between scoliosis and CHD. We, hypothesize that scoliosis in a CHD cohort would be related to an underlying 22q11.2 deletion.

**Methods.** A well-characterized existing database of 315 adults with CHD (primarily tetralogy of Fallot), with (n=86) and without (n=229) 22q11.2DS, matched by sex and CHD severity, and excluding other known syndromic diagnoses. We compared the scoliosis prevalence of patients with 22q11.2DS and CHD patients to the prevalence of scoliosis in a cohort of adults with 22q11.2DS without CHD based on medical records. We systematically determined the presence of scoliosis (Cobb angle  $\geq 10^\circ$ ) in all included patients using chest radiographs, blind to genetic diagnosis. Besides 22q11.2DS, we analyzed other suspected risk factors for scoliosis using a regression model: thoracotomy before the age of 12 years, severe CHD type and sex.

**Results.** The prevalence of scoliosis in adults with CHD and 22q11.2DS (n=46, 53.5%) was significantly greater than in those without 22q11.2DS (n=18, 7.9%,  $p < .0001$ ). The presence of a 22q11.2 deletion (OR 25.4, 95%CI 11.2-57.4,  $p < .0001$ ), a history of thoracotomy before the age of 12 years (OR 3.5, 95%CI 1.6-8.1,  $p = .0027$ ) and most complex CHD class (OR 2.3, 95%CI 1.1-4.7,  $p = .0196$ ), but not sex, were significant independent predictors of scoliosis. In the 22q11.2DS group, a right-sided aortic arch was associated with a left convex curve ( $p = .036$ ).

**Conclusions.** The prevalence of scoliosis in those with CHD but without a 22q11.2 deletion approximates that of the general population. However, in the CHD population with a 22q11.2 deletion, the prevalence of scoliosis approximates that of others with 22q11.2DS. The pediatric surgical approach and severity of CHD were weaker independent contributors as compared to the 22q11.2 deletion. The results support the importance of a genetic diagnosis of 22q11.2DS to the risk of developing scoliosis in individuals with CHD. The 22q11.2 deletion may represent a common etiopathogenetic pathway for both CHD and scoliosis, possibly involving early laterality mechanisms.

## Introduction

For over four decades, researchers and clinicians have suggested a relationship between congenital heart disease (CHD) and scoliosis (a three-dimensional rotational deformity of the spine and trunk),<sup>1,2</sup> for which several possible mechanisms have been proposed.<sup>3-5</sup> These include biomechanical forces, for example due to altered aortic configuration during development,<sup>3,4</sup> or effects of cardiac surgery on an immature thoracic cage disturbing symmetrical growth.<sup>6-8</sup> Scoliosis can have important consequences, including respiratory dysfunction and in severe cases brace therapy or spinal surgery.<sup>2</sup> The majority of patients have adolescent idiopathic scoliosis (AIS), which has an estimated general population prevalence of 1%–9%, and for which the cause is still largely unknown.<sup>2,9</sup> It is widely accepted, however that genetic as well as biomechanical factors play an important role in the etiopathogenesis of AIS. There is a higher concordance of scoliosis in monozygotic twins (73%) and dizygotic twins (36%) than in unrelated individuals.<sup>10</sup> Notably, recent reports indicate that rare pathogenic copy number variants (CNVs) play a role in the development of AIS,<sup>11,12</sup> as they do in CHD.<sup>13</sup> Also, in nature AIS only occurs in fully upright bipedal man.<sup>14-16</sup>

The 22q11.2 deletion associated with 22q11.2 deletion syndrome (22q11.2DS), formerly known as DiGeorge or velocardiofacial syndrome, is a prime example of a rare pathogenic CNV.<sup>17</sup> The 22q11.2 deletion has an estimated prevalence of 1 in 3000 live births and is characterized by early and later onset conditions, including CHD and scoliosis.<sup>17</sup> In the present study, we used data obtained from an adult CHD cohort to test the hypothesis that the higher prevalence of scoliosis in CHD is related to an underlying 22q11.2 deletion, while accounting for pediatric cardiac surgery and CHD severity.

## Methods

### Study population

To determine the scoliosis prevalence in the adult ( $\geq 17$  years) CHD population, patients were included from an existing sample followed at a specialized adult CHD hospital.<sup>18-21</sup> All data in this study are part of ongoing studies approved by the local Research Ethics Board.

**Figure 1** shows the sample derivation and individuals included and excluded from the present study. We used data available from an existing database for a well-characterized sample of adults with CHD, including CHD type (mostly tetralogy of Fallot),<sup>20</sup> cardiac surgical history, laterality of aortic arch, and presence of musculoskeletal anomalies.<sup>18-21</sup> CHD complexity was classified as simple, moderate, and severe, following the 2018 guidelines from the American Heart Association and American College of Cardiology.<sup>22</sup> We confined the sample to adults with CHD and sufficient molecular genetic data (mostly standard clinical genetic testing and/or research-based genome-wide microarray),<sup>18-21</sup> to determine presence or absence of

a 22q11.2 deletion.<sup>17,18</sup> We used these molecular data to determine individuals confirmed to have the typical chromosome 22q11.2 deletion, that is, at least including the low copy repeat region (LCR)22A-LCR22B and most commonly involving the 2.5 megabase LCR22A-LCR22D region (the 22q11.2DS group),<sup>17,18</sup> and a comparison group comprising those confirmed to have no typical 22q11.2 deletion (the no 22q11.2DS group). The comparison group was selected in a 2–3 to 1 ratio, matching for sex and CHD severity class, by a research-analyst blind to scoliosis status.

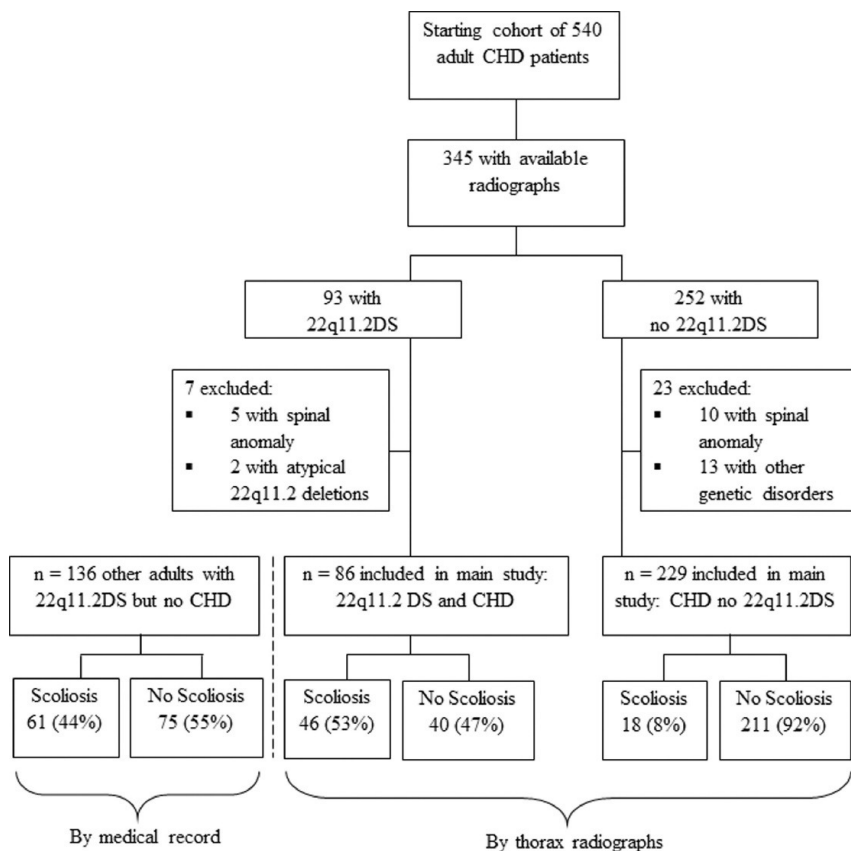


**Figure 1.** Flowchart of the sample studied.

Exclusion criteria were absence of a chest radiograph obtained between 17 and 40 years of age, presence of an atypical nested (eg, LCR22B-LCR22D, LCR22C-LCR22D) chromosome 22q11.2 deletion,<sup>17,18</sup> congenital spinal anomalies or variants (eg, hemivertebra, butterfly vertebrae, and Klippel-Feil), or a documented genetic or other syndromic disorder other than 22q11.2DS (eg, VACTERL, CHARGE, Klinefelter, Goldenhar, Pallister Killian, hemihypertrophy, or fetal ethanol syndromes) (**Figure 1**). After these exclusions the sample comprised 315 adults with CHD, either with or without a 22q11.2 deletion.



### Chest radiograph assessment

One trained observer, who was blinded to 22q11.2 deletion status and medical history, assessed the earliest upright chest radiograph available at the adult CHD hospital. The observer first screened each radiograph for the presence of congenital spinal anomalies (if present, patients were excluded, n=15, **Figure 1**) and signs of surgery in the past, including sternotomy wires for cardiac surgery (**Figure 2**) or spondylodesis material indicating surgically corrected scoliosis. The radiographs were then analyzed according to the Scoliosis Research Society – the observer recorded the number of thoracic vertebrae and (visible) lumbar vertebrae, the presence of scoliosis (a lateral deviation of the spine, defined as a Cobb angle [the angle between the two most tilted vertebrae]  $\geq 10^\circ$ ), the number of curves and the most severe (ie, major) curve, the convexity of the curve, the apex, and the number of involved vertebrae.<sup>23,24</sup> The laterality of the aortic arch was also assessed (**Figure 2**) and these data checked against those previously recorded in medical records.

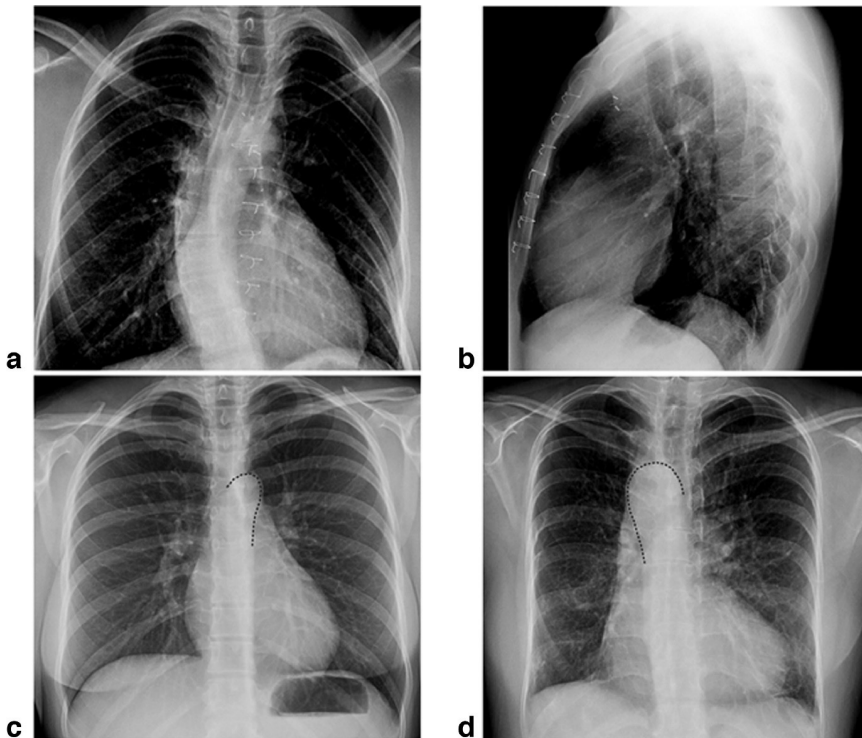


**Figure 2.** Findings during chest radiography assessment. In the case of a history of sternotomy, sternal wires can be visible from a coronal view (**a**) and sagittal view (**b**) of the chest radiograph. While the aortic arch is normally left sided (**c**), in this group of CHD patients the aortic arch is sometimes right-sided (**d**). Dashed guidelines are drawn over Figures 2c and 2d to indicate the aortic arch position.

### Scoliosis in 22q11.2DS patients without CHD

We also determined the prevalence of scoliosis in a cohort of adults with 22q11.2DS who had no CHD followed at a specialty clinic for adults with 22q11.2DS at the same hospital as those with CHD.<sup>18-21</sup> Inclusion criteria were adults ( $\geq 17$  years) with a 22q11.2 deletion as confirmed by standard molecular methods<sup>25,26</sup> and no CHD present, as determined by echocardiogram (n=136).<sup>27</sup> We used the same exclusion criteria for the CHD cohort except that, in the absence of comparable chest radiograph data, we determined the presence of scoliosis from medical records that provided documentation of scoliosis, that is, from physical examination and/or spine radiograph. This method was validated by comparing the presence of scoliosis based on such medical records documentation versus that based on direct examination of chest radiographs within the group of 22q11.2DS patients with CHD (data available for n=69 of the total n=86).

### Statistical analysis

Descriptive statistics were performed using Fisher exact test and if normally distributed (determined with Shapiro-Wilk's test) the means of continuous variables were compared using independent samples t test. Mann-Whitney U tests were used if distribution was non-normal. The main analysis used a logistic regression model to assess possible contributory factors to the development of scoliosis in CHD – presence of a 22q11.2 deletion, sex, CHD severity class, and thoracotomy under age of 12 years. The variance inflation factor and tolerance methods were used to determine that there was no multicollinearity between variables. Post-hoc chi-square ( $\chi^2$ ) tests and degrees of freedom (df) for the regression model and odds ratios (OR) and 95% confidence intervals (95% CI) for every predictor were reported. Statistical analysis was done in SPSS 25.0 for Windows (IBM, Armonk, NY, USA) and/or SAS. The statistical significance level was set at 0.05, two-tailed.

## **Results**

A total of 315 patients with a CHD formed the main sample studied 86 with and 229 without 22q11.2DS (**Table 1**). By design, there was no significant between-group sex or CHD severity class differences. Mean age at chest radiography was significantly older in the no 22q11.2DS group (**Table 1**). Although the majority of patients had a sternotomy before the age of 12 years, a significantly greater proportion of those in the no 22q11.2DS group had thoracotomy whereas the 22q11.2DS group was enriched for those who had no cardiac surgery before age 12 years or where there was uncertainty about the surgical approach (**Table 1**).

| Variables   | 22q11.2DS<br>(n=86) | No 22q11.2DS*<br>(n=229) | p Value          |
|---|---------------------|--------------------------|------------------|
| Female sex (%)  | 39 (45.4%)          | 108 (47.2%)              | .8009*           |
| Mean age in years at time of thoracic radiograph (SD)     | 22.7 (5.0)          | 26.9 (6.4)               | <b>&lt;.0001</b> |
| CHD severity class†                                       |                     |                          |                  |
| Mild-moderate   | 56 (65.1%)          | 139 (60.7%)              | 0.5163*          |
| Severe  | 30 (34.9%)          | 90 (39.3%)               |                  |
| Cardiac surgery before age 12 years‡                      |                     |                          |                  |
| Sternotomy only   | 55 (64.0%)          | 124 (54.2%)              | 0.1270           |
| Thoracotomy (with/without sternotomy)                     | 15 (17.4%)          | 83 (36.2%)               | <b>.0016</b>     |
| No cardiac surgery or uncertain cardiac surgical approach | 16 (18.6%)          | 22 (9.6%)                | <b>.0339</b>     |

**Table 1.** Characteristics of the 315 adults with congenital heart disease (CHD) studied, comparing those with and without 22q11.2 deletion syndrome (22q11.2DS). Significant findings are indicated in **bold font**. By design, the no 22q11.2DS group was matched a priori to the 22q11.2DS group by sex and CHD severity class. †CHD severity class was determined following the 2018 guidelines from the American Heart Association and American College of Cardiology<sup>22</sup> mild and moderate severity classes were combined given small numbers for the mild subgroup. ‡The surgical approach was determined based on the medical records. The patients could either fall in the sternotomy only group (first category), the lateral thoracotomy group with or without a sternotomy (second category) or in the group in which it was uncertain whether the patients had surgery paediatric cardiac and/or it was uncertain what kind of surgical approach was used (third category).

### Scoliosis in adults with CHD

Of the 64 individuals with scoliosis within the CHD cohort studied, the scoliosis prevalence was significantly greater in the 22q11.2DS group (n=46, 53.5%, 95% CI: 42.7–64.2) than in the no 22q11.2DS CHD group (n=18, 7.9%, 95% CI: 4.3–11.4; p<.0001). The logistic regression model was highly significant ( $X^2=94.6$ , df=4, p<.0001). Consistent with our hypothesis, the presence of a 22q11.2 deletion was the most significant predictor of scoliosis (OR 25.4, 95% CI: 11.2–57.4; p<.0001), followed by thoracotomy before the age of 12 years and CHD severity (**Table 2**). A secondary analysis using the same predictors (except 22q11.2 deletion) but restricting to the 229 adults with CHD and no 22q11.2DS, showed that the regression model remained significant ( $X^2=13.4$ , df=3, p=.0039) but only thoracotomy before the age of 12 years was a significant predictor of scoliosis (OR 4.4, 95% CI: 1.5–13.2; p=.0078); CHD severity was nonsignificant (OR 2.0, 95% CI: 0.7–5.6, p=.183). A further secondary analysis examined the model to predict scoliosis in only 22q11.2DS patients ( $X^2=8.6$ , df=3, p=.035); this showed no significant predictors for scoliosis, with a trend only for CHD severity (p=.057).

| Predictor variables                | Total<br>(n=315) | Scoliosis (n=64,<br>20.3%) | No scoliosis<br>(n=251, 79.7%) | Logistic regression<br>analysis |               |                  |
|------------------------------------|------------------|----------------------------|--------------------------------|---------------------------------|---------------|------------------|
|                                    |                  |                            |                                | OR                              | 95% CI        | p                |
| 22q11.2 deletion<br>syndrome       | 86               | 46 (53.5%)                 | 40 (46.5%)                     | 25.4                            | 11.2–<br>57.4 | <b>&lt;.0001</b> |
| Thoracotomy before<br>age 12 years | 98               | 24 (24.5%)                 | 74 (75.5%)                     | 3.5                             | 1.6–8.1       | <b>.0027</b>     |
| Severe CHD                         | 120              | 32 (26.7%)                 | 88 (73.3%)                     | 2.3                             | 1.1–4.7       | <b>.0196</b>     |
| Female sex                         | 147              | 35 (23.8%)                 | 112 (76.2%)                    | 1.7                             | 0.9–3.3       | .1309            |

**Table 2.** Factors contributing to scoliosis risk in 315 adults with CHD. Significant findings are indicated in **bold font**. Likelihood ratio for regression model:  $\chi^2=94.6$ ,  $df=4$ ,  $p<.0001$ .

**Table 3** presents further details of the scoliosis in this cohort; there were no significant differences found between the two groups on the parameters assessed. Only a minority had scoliosis surgery, nonsignificantly fewer in the 22q11.2DS than the no 22q11.2DS group. Six of those who did not have scoliosis surgery had thoracic scoliosis with a Cobb angle greater than 45°, all in the 22q11.2DS group; no individual in the no 22q11.2DS group had a Cobb angle over 40°. The median number of visible lumbar vertebrae was 2, with an interquartile range of 2–3. Based on the chest radiographs, we were able to determine eight individuals with lumbar scoliosis (**Table 3**).

#### Scoliosis convexity and aortic arch laterality

With respect to the 51 adults with CHD and thoracic scoliosis, the majority had the typical scoliotic curve convexity to the right, with no significant difference between the 22q11.2DS and no 22q11.2DS groups (**Table 3**). Amongst the 35 individuals with 22q11.2DS and a major thoracic scoliotic curve, there were 21 with a normal left-sided aortic arch, 15 (71%) of whom had a right convex scoliosis curve. There were 14 with a right-sided aortic arch, 5 (36%) with a right convex scoliosis curve, demonstrating a significant association between right-sided aortic arch and left convex thoracic curve ( $p=.036$ ).

#### Scoliosis in adults with 22q11.2DS without CHD

There was a clinical history of scoliosis in 61 of 136 adults with 22q11.2DS and no CHD (44.9%, 95% CI: 36.8%–53.2%) based on medical records data. Of the 69 patients with 22q11.2DS and a CHD, where data from both medical records and direct examination of radiography were available to assess for the presence of scoliosis, there was agreement in presence/absence of scoliosis for 61 individuals (88.4%), supporting the validity of the medical records method.

**Table 3.** Radiographic parameters of the scoliosis in the 64 adults with scoliosis in the CHD cohort studied, comparing those with and without 22q11.2DS. IQR, interquartile range; T, level of thoracic vertebra.

| Variables   | 22q11.2DS with scoliosis (n=46) | No 22q11.2DS with scoliosis (n=18) | p Value |
|---|---------------------------------|------------------------------------|---------|
| Major scoliosis curve type (total n=64)                     |                                 |                                    |         |
| Cervicothoracic   | 0 (0%)                          | 1 (5.6%)                           | .2812   |
| Thoracic  | 35 (76.1%)                      | 16 (88.9%)                         | .3200   |
| Thoracolumbar   | 3 (6.5%)                        | 1 (5.6%)                           | 1.0000  |
| Lumbar  | 8 (17.4%)                       | 0 (0%)                             | .0930   |
| Scoliosis surgery   | 6 (13.0%)                       | 5 (27.8%)                          | .2667   |
| Subset with major thoracic scoliosis without surgery (n=41) |                                 |                                    |         |
| Median degree of Cobb angle (IQR)                           | 21.3 (17–41)                    | 23.7 (20–28)                       | .9758   |
| Range   | 11–111                          | 13–40                              |         |
| Median number of vertebrae involved (IQR)                   | 6 (5–7)                         | 6 (6–8)                            | .3309   |
| Range   | 4–9                             | 4–8                                |         |
| Apex of curve (vertebra)                                    | T6 (T4–T8)                      | T8 (T6–T9)                         | .0675   |
| Range   | T3–T9                           | T3–T10                             |         |

## Discussion

For the past four decades, the role of CHD in development of scoliosis has been noted as a partial explanation of the enigma of scoliosis pathogenesis. However, in no previous study was a major risk factor for both entities taken into account: the 22q11.2 deletion. The present study provides the first evidence of the significant impact of the 22q11.2 deletion in the development of scoliosis in a cohort of adult CHD patients. Importantly, the prevalence of scoliosis in the no 22q11.2DS CHD cohort was found to be nearly similar to the prevalence of scoliosis in the general population.<sup>2,9</sup>

The results are consistent with previous studies reporting high prevalence of scoliosis in 22q11.2DS of about 50%,<sup>28</sup> compared with general population expectations of about 1%–9%.<sup>2,9</sup> The scoliosis prevalence in the general population varies greatly, with estimates from 0.5% to 5.2% based on physical examination.<sup>29</sup> However, in two independent studies using chest radiographs and a definition of scoliosis as a Cobb angle of  $\geq 10^\circ$ , the scoliosis prevalence in the general population was reported as 9.3% and 13.4%, respectively.<sup>9,30</sup> The scoliosis prevalence of 8% we found in the no 22q11.2DS CHD population in this study thus appears comparable to that of the general population when assessed radiographically. Taken together, the results may indicate that in previous studies unrecognized 22q11.2DS could be a confounder for reported associations between CHD and the development of scoliosis.

AIS is more common in females,<sup>31</sup> whereas we found that in 22q11.2DS, the prevalence of scoliosis is about equal between females and males, consistent with previous reports.<sup>28</sup> In the general population, early onset scoliosis (age <10 years) comes closer to a 1:1 female:male ratio.<sup>23,33</sup> Prospective studies in 22q11.2DS, investigating the differences between males and females in the development of scoliosis and between patients with and without a scoliosis, might therefore help shed light on the scoliosis development in the general population.<sup>34</sup> The type of scoliosis, both in the 22q11.2DS and no 22q11.2DS group is comparable to that of the general population, with the majority having a major thoracic curve.<sup>35</sup> This finding supports the hypothesis that the 22q11.2 deletion population, which has a high risk to develop an idiopathic-like scoliosis, can be used as a model to study the development of scoliosis.<sup>28,34</sup>

Recent studies have suggested a general role for CNVs in the development of AIS.<sup>11,12</sup> Sadler et al. reported that 16p11.2 duplications explain nearly 1% of AIS cases, in a study restricted to patients without major development impairment or major congenital anomalies.<sup>12</sup> Given that the 22q11.2DS population is characterized by broad phenotypic heterogeneity, with developmental impairment and congenital anomalies (eg, CHD) as common features, many patients with 22q11.2DS and scoliosis may have been excluded from the Sadler et al. study. Nonetheless they reported two patients with 22q11.2DS in their cohort of 1,197 AIS patients, reinforcing the importance of considering clinical genetic testing by microarray in AIS, as in CHD.<sup>13</sup> In the present study, for the main regression model, and in the secondary analysis of the no 22q11.2DS group, pediatric thoracotomy was a significant predictor of scoliosis. This could be explained by the fact that a thoracotomy is an asymmetrical procedure on an immature thoracic cage, which may lead to a disturbance of symmetrical growth and an increased scoliosis risk, as proposed by others.<sup>6-8</sup> However, in the literature, results are mixed as to whether and which type of cardiac surgery, including sternotomy, is associated with scoliosis risk.<sup>4,6-8,36</sup> Further studies, taking genetic syndrome status into account, are needed.

A right-sided aortic arch is rare with an estimated incidence of 0.1% in the general population, yet in 22q11.2DS a right-sided aortic arch is relatively common.<sup>37</sup> In the present study of CHD, in patients with 22q11.2DS we found that a right-sided aortic arch was associated with a left convex curve in patients with a major thoracic scoliosis. There was a similar finding in a previous study of 119 CHD patients where all eight scoliosis patients with a right-sided aortic arch had a left convex thoracic curve.<sup>4</sup> This phenomenon may be explained by the principle of inverted organ anatomy and spinal lateralization. In patients with scoliosis, one study found that scoliotic curve convexity was predominantly to the right in patients with normal organ anatomy (situs solitus), and to the left in patients with situs inversus totalis.<sup>38</sup> Also, laterality of the center of mass in the thorax is related to slight spinal rotation in the opposite direction in patients without scoliosis.<sup>39</sup> Although no causality can be concluded based on these former

studies, our findings make the biomechanical theory of an aortic arch to the right side increasing the chance of a left convex scoliotic curve appear plausible.

As the first study to report the scoliosis prevalence in CHD patients, while taking 22q11.2DS into account this study had several advantages but also some limitations. The study was based on a relatively large existing database of CHD patients, in which all patients had genetic testing to confirm or rule out the 22q11.2 deletion.<sup>18-21</sup> Moreover, in order to find the prevalence of scoliosis not caused by congenital spinal malformations, patients with a congenital spinal malformation were excluded. However, since the radiographs were made in order to visualize the thorax, the radiographs capture only the first several (lumbar) spine in most cases (median two visible lumbar vertebrae). Therefore, it might be possible that patients with an undetectable lumbar congenital malformation remain in the sample. Also, the eight adults with 22q11.2DS and lumbar scoliosis in the study sample may be an underestimation of the true number of patients with a lumbar scoliosis in the sample. However, since the lumbar spine is partly visible and the most common type of scoliosis is thoracic scoliosis, it is likely that these numbers are low. We excluded radiographs of patients under age 17 years and older than 40 years, in order to find the definitive prevalence of scoliosis. The younger age group may not yet have developed a scoliosis, whereas scoliosis in the older age group may be related to degenerative scoliosis.<sup>40</sup> We also excluded patients with other syndromic forms of CHD; scoliosis is known to occur more often in other syndromes.<sup>41</sup> In the present study, available data for 136 adults with 22q11.2DS but no CHD indicated a scoliosis prevalence of 45% based on medical records data. This may be an underestimate given that the determination of scoliosis, either at an age still at risk for the development of scoliosis or based on physical examination, could lead to lower scoliosis prevalence than radiographic determination in an adult population. Importantly however, within the 22q11.2DS subgroup with CHD, we demonstrated a high level of agreement (88.4%) between medical records data and chest radiograph methods of determining scoliosis. There may be other risk factors for the development of scoliosis we did not assess. For example, the methods used would not rule out the presence of neurologic anomalies, although we expect that number to be small in 22q11.2DS.<sup>17</sup>

In conclusion, the results of this study support the importance of clinical genetic testing for 22q11.2 deletions in patients with CHD, and the relevance of 22q11.2DS, in understanding the risk for scoliosis in the CHD population. With respect to the CHD population without 22q11.2DS, the scoliosis prevalence is comparable to that of the general population, with a slightly increased risk for those who underwent a thoracotomy as a child. These findings suggest that the 22q11.2 deletion may represent a common genetic pathway for the development of CHD and of scoliosis. Future studies using this genetic model may help determine the pathogenesis of both these complex developmental conditions.



## References

1. Nicoladoni C. Anatomie und mechanismus der skoliose. In: Kocher, Konig, von Mikulicz, editors. *Bibliotheca medica*. Stuttgart, Germany: Verlag von erwin nagele; 1904.
2. Cheng JC, Castelein RM, Chu WC, Danielsson AJ, Dobbs MB, Grivas TB, et al. Adolescent idiopathic scoliosis. *Nat Rev Dis Prim* 2015;1:1–20.
3. Beals R, Kenney K, Lees M. Congenital heart disease and idiopathic scoliosis. *Clin Orthop Relat Res* 1972;89:112–6.
4. Jordan CE, White RI, Fischer KC, Neill C, Dorst JP. The scoliosis of congenital heart disease. *Am Heart J* 1972;84:463–9.
5. Lui GK, Saidi A, Bhatt AB, Burchill LJ, Deen JF, Earing michael G et al. Diagnosis and management of noncardiac complications in adults with congenital heart disease: a scientific statement from the American Heart Association. *Circulation* 2017;136:e348–92.
6. Gilsanz V, Boechat IM, Birnberg FA, King JD. Scoliosis after thoracotomy for esophageal atresia. *AJRAmerican J Roentgenol* 1983;141:457–60.
7. Durning RP, Scoles PV, Fox OD. Scoliosis after thoracotomy in tracheoesophageal fistula patients. A follow-up study. *J Bone Jt Surg - Ser A* 1980;62:1156–9.
8. Roclawski M, Sabiniewicz R, Potaz P, Smoczyński A, Pankowski R, Mazurek T, et al. Scoliosis in patients with aortic coarctation and patent ductus arteriosus: does standard posterolateral thoracotomy play a role in the development of the lateral curve of the spine? *Pediatr Cardiol* 2009;30:941–5.
9. Urrutia J, Besa P, Bengoa F. A prevalence study of thoracic scoliosis in Chilean patients aged 10-20 years using chest radiographs as a screening tool. *J Pediatr Orthop Part B* 2018;27:159–62.
10. Kesling K, Reinker K. Scoliosis in twins. A meta-analysis of the literature and report of six cases. *Spine (Phila Pa 1976)* 1997;22: 2009–14.
11. Buchan JG, Alvarado DM, Haller G, Aferol H, Miller NH, Dobbs MB, et al. Are copy number variants associated with adolescent idiopathic scoliosis? *Clin Orthop Relat Res* 2014;472:3216–25.
12. Sadler B, Haller G, Antunes L, Bledsoe X, Morcuende J, Giampietro P, et al. Distal chromosome 16p11.2 duplications containing SH2B1 in patients with scoliosis. *J Med Genet* 2019;1–7;
13. Costain G, Silversides CK, Bassett AS. The importance of copy number variation in congenital heart disease. *NPJ Genom Med* 2016;14:1–11.
14. Castelein RM, van Dieen JH, Smit TH. The role of dorsal shear forces in the pathogenesis of adolescent idiopathic scoliosis - a hypothesis. *Med Hypotheses* 2005;65:501–8.
15. Janssen MMA, de Wilde RF, Kouwenhoven J-WM, Castelein RM. Experimental animal models in scoliosis research: a review of the literature. *Spine J* 2011;11:347–58.
16. Kouwenhoven JW, Smit TH, van der Veen AJ, Kingma I, van Dieen JH, Castelein RM. Effects of dorsal versus ventral shear loads on the rotational stability of the thoracic spine: a biomechanical porcine and human cadaveric study. *Spine (Phila Pa 1976)* 2007;32:2545–50.
17. McDonald-McGinn DM, Sullivan KE, Marino B, Philip N, Swillen A, Vorstman JAS, et al. 22q11.2 deletion syndrome. *Nat Rev Dis Prim* 2015;1:1–19.
18. Van L, Heung T, Graffi J, Ng E, Malecki S, Mil S Van, et al. All-cause mortality and survival in adults with 22q11.2 deletion syndrome. *Genet Med* 2019:1–8.
19. Chin-yeo NJ, Costain G, Swaby J, Silversides CK, Bassett AS. Reproductive fitness and genetic transmission of tetralogy of Fallot in the molecular age. *Circ Cardiovasc Genet* 2014;7:102–9.
20. Silversides CK, Lionel AC, Costain G, Merico D, Migita O, Liu B et al. Rare copy number variations in adults with tetralogy of Fallot implicate novel risk gene pathways. *PLoS Genet* 2012;8:1–14.
21. Piran S, Bassett AS, Grewal J, Swaby J-A, Morel C, Oechslin EN et al. Patterns of cardiac and extracardiac anomalies in adults with tetralogy of fallot. *Am Heart J* 2011;161:131–7.
22. Stout KK, Daniels CJ, Aboulhosn JA, Bozkurt B, Broberg CS, Colman JM, et al. 2018 AHA/ACC guideline for the management of adults with congenital heart disease: a report of the American College of Cardiology/American Heart Association Task Force on clinical practice guidelines. *Circulation* 2018;139:e698–800
23. O'Brien M, Kulklo T, Blanke K, Lenke L. *Radiographic measurement manual*. 2008.
24. Kane WJ. Scoliosis prevalence: a call for a statement of terms. *Clin Orthop Relat Res* 1977;126:43–6.
25. Bassett AS, Chow EWC, Husted J, Weksberg R, Caluseriu O, Webb GD, et al. Clinical features of 78 adults with 22q11 deletion syndrome. *Am J Med Genet Part A* 2005;138 A:307–13.
26. Bassett A, Van L, Butcher N, Chow E, Ogura L, Costain G. Fetal growth and gestational factors as predictors of schizophrenia in a high risk genetic subtype. *Biol Psychiatry* 2015;77:326S–7S.
27. Bassett AS, McDonald-McGinn DM, Devriendt K, Digilio MC, Goldenberg P, Habel A, et al. Practical guidelines for managing patients with 22q11.2 deletion syndrome. *J Pediatr* 2011;159:332–9.
28. Homans JF, Baldew VGM, Brink RC, Kruyt MC, Schlosser TPC, Houben ML et al. Scoliosis in association with the 22q11.2 deletion syndrome: an observational study. *Arch Dis Child* 2019;104:19–24.
29. Konieczny MR, Senyurt H, Krauspe R. Epidemiology of adolescent idiopathic scoliosis. *J Child Orthop* 2013;7:3–9.
30. Chen JB, Kim AD, Allan-Blitz L, Shamie AN. Prevalence of thoracic scoliosis in adults 25 to 64 years of age detected during routine chest radiographs. *Eur Spine J* 2016;25:3082–7.



31. Luk KDK, Lee CF, Cheung KMC, Cheng JCY, Ng BKW, Lam TP et al. Clinical effectiveness of school screening for adolescent idiopathic scoliosis. *Spine (Phila Pa 1976)* 2010;35:1607–14.
32. Chiu YL, Huang TJ, Hsu RW. Curve patterns and etiologies of scoliosis: analysis in a university hospital clinic in Taiwan. *Chang Yi Xue Za Zhi* 1998;21:421–8.
33. Figueiredo UMM, James JIPI. Juvenile idiopathic scoliosis. *J Bone Jt SurgeryBritish* 1981;63-B:61–6.
34. Homans JF, Reuver S De, Breetvelt EJ, Vorstman JAS, Deeney VFX, Flynn JM, et al. The 22q11.2 deletion syndrome as a model for idiopathic scoliosis – a Hypothesis. *Med Hypotheses* 2019;127:57–62.
35. Lenke LG, Betz RR, Harms J, Bridwell KH, Clements DH, Lowe TG et al. Adolescent idiopathic scoliosis: a new classification to determine extent of spinal arthrodesis. *J Bone Jt SurgeryAmerican Vol* 2001;83-A:1169–81.
36. Feiz HH, Afrasiabi A, Parvizi R, Safarpour A, Fouladi RF. Scoliosis after thoracotomy/sternotomy in children with congenital heart disease. *Indian J Orthop* 2012;46:77–80.
37. D'Antonio F, Khalil A, Zidere V, Carvalho JS. Fetuses with right aortic arch: a multicenter cohort study and meta-analysis. *Ultrasound Obstet Gynecol* 2016;47:423–32.
38. Schlosser TPC, Semple T, Carr SB, Padley S, Loebinger MR, Hogg C, et al. Scoliosis convexity and organ anatomy are related. *Eur Spine J* 2017;26:1595–9.
39. de Reuver S, Brink RC, Homans JF, Kruyt MC, van Stralen M, Schlosser TPC, et al. The changing position of the center of mass of the thorax during growth in relation to pre-existent vertebral rotation. *Spine (Phila Pa 1976)* 2019;44:679–84.
40. Silva FE, Lenke LG. Adult degenerative scoliosis: evaluation and management. *Neurosurg Focus* 2010;28:1–10.
41. Levy BJ, Schulz JF, Fornari ED, Wollowick AL. Complications associated with surgical repair of syndromic scoliosis. *Scoliosis* 2015;10:1–16.

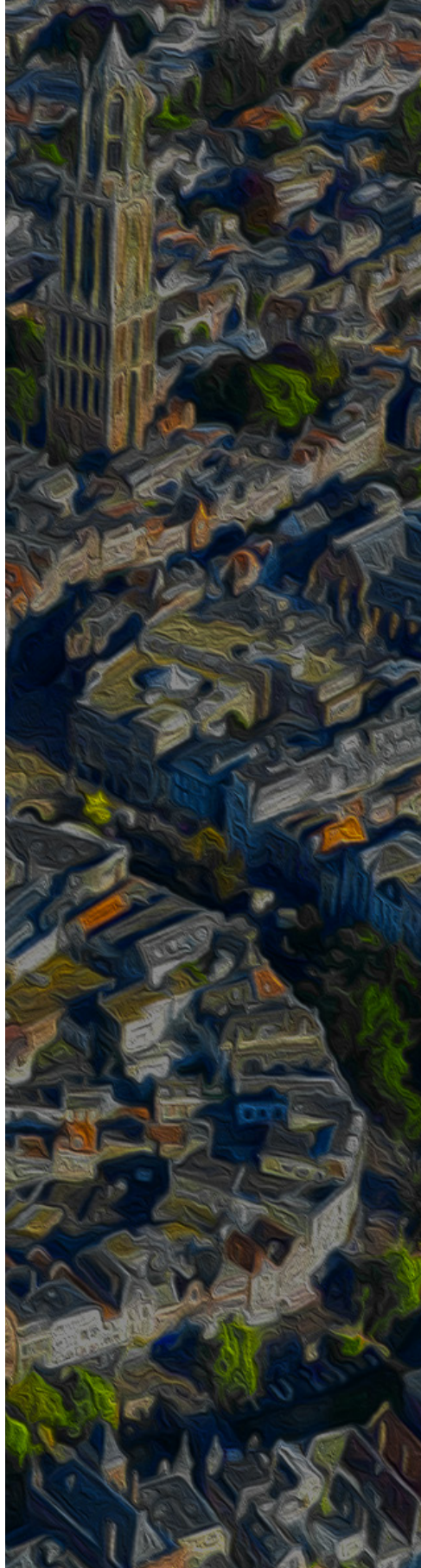


# 17

## Genetic Overlap between Idiopathic Scoliosis and Schizophrenia in the General Population

Steven de Reuver  
Worrawat Engchuan  
Mehdi Zarrei  
Jacob A.S. Vorstman  
René M. Castelein  
Elemi J. Breetvelt

*Major revisions*



## ABSTRACT

**Introduction.** Adolescent idiopathic scoliosis (AIS) and schizophrenia are two very distinct conditions with a poorly understood etiology that both emerge in otherwise healthy young adolescents. Children with 22q11.2 deletion syndrome (22q11.2DS), a microdeletion consisting of 47 genes and prevalent in 1:2,148 live births, have a 20-fold increased risk for both AIS and schizophrenia. In the general population, excluding 22q11.2DS, both conditions are also associated and genetic studies suggest the involvement of genes and genetic variants implicated in central nervous functioning. We aim to study other genetic overlap between both conditions in the general population, and determine the role of genes in the 22q11.2 region, in terms of common variants but also their gene-networks and biopathways.

**Methods.** For all analyses we used summary statistics from genome-wide association studies (GWAS); two on AIS (n=11,210) and one on schizophrenia (n=36,989) At first, we compared the ranking of all single-nucleotide polymorphisms (SNPs) associated to both AIS and schizophrenia based on their significance and analyzed overlap. Second, we used *in silico* analyses, to test gene-networks enrichment for the most significant SNPs, and determined the involvement of genes in the 22q11.2 region. Post-hoc, biological pathways were explored.

**Results.** The top 3% of the most significant SNPs for both conditions showed a cluster, which could not be attributed to chance ( $p < 3e^{-4}$ ). In addition, the *in silico* analyses revealed significant (corrected  $p < 0.05$ ) overlap between schizophrenia and both AIS cohorts. There was a 26-41% overlap with gene-networks involving genes in the 22q11.2 region, but SNPs in this region did not overlap with the most significant SNPs from the GWAS. Biopathways enriched in both AIS cohorts were related to cell (membrane) processes and signalling, together with synaptic and other neuron functioning and development.

**Conclusion.** In addition to sharing 22q11.2DS as a rare genetic variant, AIS and schizophrenia also share common genetic risk variants, and genes important in AIS and schizophrenia show overlap. Gene-networks enriched by the most significant SNPs for both conditions overlap with gene-networks involving genes in the 22q11.2 region. However, SNPs in 22q11.2 region are not overrepresented in the most significant SNPs in AIS nor schizophrenia. Finally, gene-networks implicated in the risk for both conditions indicate the involvement of biopathways related to cellular signaling and neuron and brain development.

## Introduction

Idiopathic scoliosis, a common condition of the spine, and schizophrenia, a severe mental health condition, both emerge in otherwise healthy young adolescents and can have a tremendous impact on the quality of life.<sup>1,2</sup> The conditions are rarely studied together and thus-far there is little converging evidence that adolescent idiopathic scoliosis (AIS) and schizophrenia share many risk-factors or biological pathways. The etio-pathogenesis of both conditions is thought to be multifactorial, involving a complex genomic architecture, with genetic variation encompassing a spectrum of extremely rare to common variants, with variable effect-sizes.<sup>1,3</sup>

Interestingly, the two conditions share one important genetic risk variant; the 22q11.2 deletion syndrome (22q11.2DS).<sup>4</sup> While classifying as a rare genetic disorder, 22q11.2DS is one of the most prevalent among rare recurrent pathogenic copy-number variants (CNVs) with an incidence of 1 in 992 unselected pregnancies and 1 in 2,148 live births.<sup>5-7</sup> Phenotypic manifestations of 22q11.2DS are highly variable and can affect multiple organ systems.<sup>5</sup> Amongst others, the syndrome is strongly and consistently associated with an increased risk for AIS with ~50% compared to ~3% in the general population, and a similarly increased risk for schizophrenia of ~25%, compared to ~1% in the general population, making 22q11.2DS one of the largest single genetic risk factors for both conditions.<sup>1,2,8,9</sup> Other conditions associated with 22q11.2DS show no clustering within cohorts of 22q11.2DS carriers, in other words having one condition is not increasing the risk for developing another condition associated with the 22q11.2DS.<sup>10-12</sup> Apparently, the 22q11.2 deletion can strongly but independently increase the risk for these conditions. Also since for AIS and schizophrenia there are no reports that the conditions cluster together within clinical 22q11.2DS cohorts. However, interestingly, in a large Swedish general population study a modest association between the two conditions was found.<sup>13</sup> This association could be in part explained by undetected 22q11.2DS carriers (scoliosis in 22q11.2DS carriers has a different classification in the ICD-10) and carriers of other (ultra) rare CNVs associated with both conditions within that general population sample,<sup>14</sup> but given the rarity of these CNVs, it is unlikely to explain all of the observed association between AIS and schizophrenia.

Possibly the two conditions share other (genetic) risk factors. And although the Swedish population study is to our knowledge the only study investigating the association between AIS and schizophrenia, other studies suggest the involvement of the central nervous system (CNS) in the etiology of AIS. These studies investigated abnormal regional cerebral cortical thickness, different relative brain structure volumes and shapes,<sup>15-17</sup> and CNS functioning, from neurophysiology to proprioception and vestibular functioning.<sup>18-20</sup> In addition,

genetic AIS studies suggest the involvement of axonal guidance, CNS development and neuro-osseous growth modulators in the pathophysiology of AIS.<sup>21-23</sup> Finally, some of the genes implicated by the genome wide association studies (GWAS) into AIS are also associated with neurodevelopmental disorders.<sup>24-26</sup> Possibly the association between AIS and schizophrenia in the general population and the co-occurrence in the 22q11.2DS is mitigated by CNS functioning and CNS genes. Identifying other genetic overlap between the AIS and Schizophrenia might provide better understanding of their genomic architecture and contribute to further elucidation of the phenotypic impact of the 22q11.2 region, exploring overlap on the level of common genetic variants would be an important first step.

In this study, we explored the genetic overlap between AIS and schizophrenia in the general population, i.e., in subjects without 22q11.2DS, while focusing on common genetic variants using summary statistics from GWAS. Furthermore, we looked at the potential overlap between gene-networks most strongly associated with the two conditions and gene-networks containing genes in the 22q11.2 region. Finally, we explored which biopathways might be involved in mitigating the shared risk for both conditions based on our findings. The study was an explorative study, primarily aiming at generating hypotheses.

## Methods

We applied two different approaches using summary statistics from GWAS studies. The relatively modest sample sizes of the available genetic studies of AIS, together with their mixed ancestry, hampers some of the classical genetic approaches, like linkage disequilibrium score regression (LDSC) and genomic restricted maximum likelihood (GREML), to determine the overlap between two conditions. In the first step of this study, we compared the ranking of all SNPs, i.e., intergenic, intronic and exonic SNPs, based on their significance, using the  $-\log_{10}$  of the p-value, of condition association. In the second step, we performed *in silico* analyses to determine the overlap of gene-networks of the genes harvesting the most significant SNPs in GWAS, and that of genes in the 22q11.2 region. Finally, we explored what biological pathways overlap the SNPs that significantly overlap between the two conditions. See **figure 1** for a study overview.

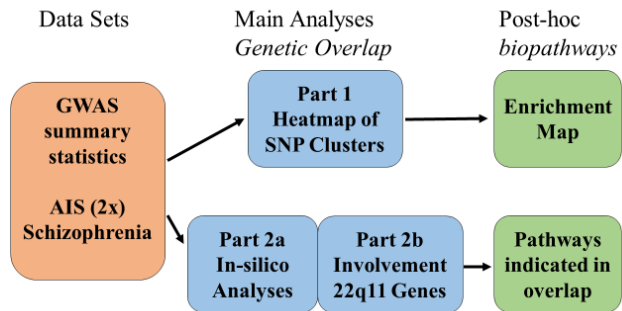


**Figure 1.** Flow-chart of the method used in this study.

### Study populations

In this study, we analyzed the overlap between common single-nucleotide polymorphism (SNP), of AIS and schizophrenia using summary statistics from two GWASs for AIS and one GWAS for schizophrenia. The data for AIS was retrieved from a 2018 meta-analysis of six GWASs with 7,956 cases from Japan, Hong Kong and USA, referred to as AIS cohort 1.<sup>25</sup> For replication purposes, a recent additional Japanese GWAS from 2019 with 3,254 cases was included, referred to as AIS cohort 2.<sup>24</sup> For schizophrenia, we used the data of 36,989 cases from the 2009 Psychiatric Genomics Consortium (PGC) meta-analyses.<sup>27</sup>

#### 1. SNP overlap between AIS and schizophrenia

In this step, we used a hypothesis-free approach comparing all SNPs. We focused on SNP overlap that was more than could be explained by a random variation, regardless of which statistical tests are used. To do so, we selected SNPs that were present in both AIS cohort 1 and in the schizophrenia cohort, leaving 3.35M SNPs, then we ordered the SNPs based on the rank order of their significance independently in both AIS and schizophrenia, with the least significant SNPs having the lowest rank-number and the most significant SNPs the highest rank-number. We created 30 evenly spaced categories for each condition, thus with an equal number of SNPs in each subset We made a cross table for these categories, with the null hypothesis of no genetic overlap between the two conditions indicated by random distribution of the cells. We used the heatmap function from r-package stats to create a heatmap of this 30x30 cross-table, suppressing reordering and creating dendrograms. We determined z-scores for the deviance of the cell-count from of the mean cell-count, to test for significance. We conservatively considered z-scores below -4 and above 4 as thresholds for significance regardless of the underlying distribution. Based on our estimation (see **supplement data part 1** for details) we argue that if there is meaningful clustering this will be in the right upper quadrant of the 30x30 matrix. Post hoc we used a Bonferroni

correction to correct for multiple testing, assuming a normal distribution of the deviance from the mean cell-count. We repeated this procedure for AIS cohort 2, with 5.90M SNPs present in both cohorts. Finally, we performed a sensitivity analysis to estimate the probability of observing the same pattern based on 20k random permutations.

## 2. In silico validation and 22q11.2 region analysis

To validate the findings from step 1, we performed an in silico gene-network analysis to determine the overlap between AIS and schizophrenia. This analysis was based on the genes tagged by the most significant SNPs in the GWAS of both conditions. To avoid any sex biases in different disorders, we included only autosomal variants. To avoid inclusion of false positive variants with a pseudo protective effect ( $OR < 1$ ), we only retained those with an odds ratio (OR) of more than one in the analysis. We used Web-based ANNOVAR (wANNOVAR)<sup>28</sup> to annotate the variants. Variants within upstream and downstream regions of the genes were tagged. We selected top 100 genes from each GWAS where one list was used as a reference set, while another was used as a query set of genes. GeneMania was used to give the interaction scores to genes not in the reference set, for the genes within the reference set, the maximum interaction score was assigned.<sup>29</sup> We then used GeneMania again to expand the query set (by 100, 200, ..., 900, 1000 genes). The enrichment analysis was done using GSEAPreranked with genes ranked by interaction score as pre-ranked list and expanded query set as a gene-set.<sup>30</sup> Multiple-test correction was automatically done by GSEAPreranked among different expanded query sets. We explored whether a potential overlap in gene-network between AIS and schizophrenia is mitigated by the overlap with genes in the 22q11.2 region. We conducted gene-network analyses between the genes based on the top results from GWAS and the 47 genes in the genomic region affected by the 22q11.2DS. See **figure 1** for an overview of the methods used.

## 3. Post-hoc analyses: Biological and functional pathway analysis

We explored which biological pathways enriched with the SNPs in cells showing the most significant overlap between schizophrenia and AIS. These biological pathways might provide information about how the shared genetic variants mitigating the vulnerability for both AIS and schizophrenia at a functional level. We used SNPs in the most significant cells from step 1 to explore the shared biological pathways. We used the online portal g:Profiler (<https://biit.cs.ut.ee/gprofiler/gost>), accessed 17th January 2023, the SNPs IDs were used as input, we did not prioritize SNPs within the strata, we used a conservative adjusted p-value of 0.00005 as significance threshold. See **supplement data part 2** for details about the selected databases for comparison.



To visualize the results, we applied Cytoscape (v3.9.1) and its plugin, EnrichmentMap (v3.3.4) to illustrate them in a network of enriched biological pathways called “enrichment map”.<sup>31</sup> In an enrichment map, nodes are biological pathways and edges are relationship between them. Here we used a Jaccard’s index of the genes overlapped to depict the relationship. Only edges with a Jaccard’s index of at least 0.35 were displayed. To reduce the density of highly correlated networks we applied a step-down approach to reduce the similarity and make the network sparser. To do so, we first ranked the result by the p-values from the most to the least significance. Then, we went down the list and if we found similar biological pathways (Jaccard’s index > 0.5), we discarded the one with higher p-value from the network. The results of both AIS cohort 1 and AIS cohort 2 were then projected on the same network. In addition, we compared the biological pathways implicated in both gene-network implicated in the GWAS and gene-networks overlapping with genes in the 22q11.2 critical region. To do so, for each of the gene lists (i.e., top GWAS gene lists, and 47 genes in 22q11.2 region), we extracted a gene subset with GeneMania score above the mean of GeneMania score of all the genes, this subset was the genes driving enrichment in GSEAPreranked analysis. Then, the overlap between two conditions and between each individual condition and 22q11.2 gene-network were defined. We then applied g:Profiler and obtained a list of significant biological pathways (i.e., p-value < 0.00005) for each pair of overlaps (e.g. schizophrenia and AIS cohort 1 overlap vs schizophrenia and 22q11.2DS overlap). To determine the level of overlap, Jaccard’s index was calculated for all combinations of gene lists from GWASs and gene network from 22q11.2 region. Finally, we determined the distribution of SNP types in the most significant cells and strata.

## Results

### 1. SNP overlap between AIS and schizophrenia

The heatmap (**figure 2**) showed that the vast majority of the cell-counts do not deviate from the mean cell-count, except for cells containing the most significant SNPs for both conditions, in the extreme upper-right quadrant. The same pattern was observed for both AIS1 and AIS2. In the analysis comparing the AIS1 and schizophrenia 2 cells had z-scores above 4 and in the analysis comparing AIS2 and schizophrenia 4 cells had z-scores above 4. In **supplement data part 3**, the histograms of the corresponding z-scores for the deviance from the mean cell-counts are presented, suggesting a normal distribution of the deviation from the mean count. In fact, z-scores were above 5 for all 6 cells with counts above the threshold. Post-hoc, we used Bonferroni correction of the p-values for each cell, the corrected p-values for the cells showing most overlap were all below 3e-04. The sensitivity analysis showed that is very unlikely, with a probability of 1 in 2 million, that our observations can be explained by random chance (**supplement data part 5**).

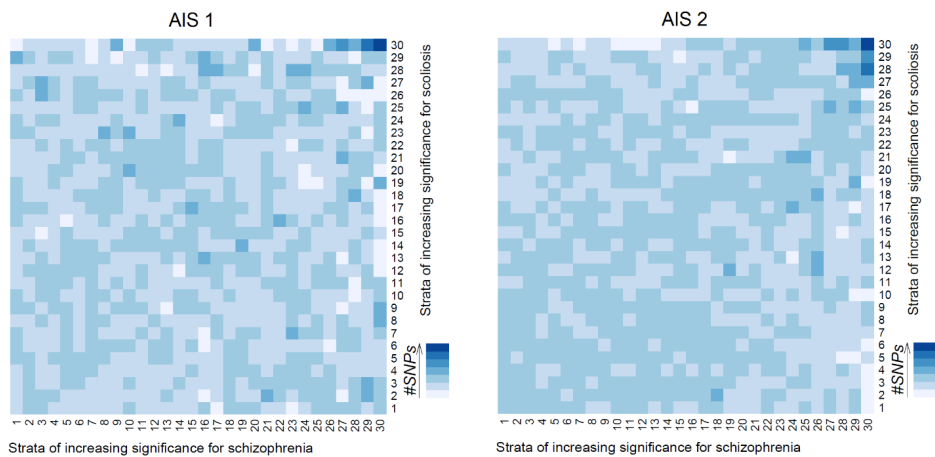


**Figure 2.** Results from analysis 1, displayed as heat maps of SNPs ranked based on significance from GWAS and split in 30 same sized categories with number 30 being the most significant ones, for AIS on the Y-axis and schizophrenia on the X-axis, on the left for AIS cohort 1 and on the right AIS cohort 2. Darker blue colors indicate the Z-scores, i.e. a higher overlap of SNPs of AIS and schizophrenia than expected from a random distribution.

## 2. In silico validation and 22q11.2 region analysis

We found a significant overlap between gene networks of the two disorders when an inclusive extension of the network was done. See **table 1** for results from the in silico gene-network analysis. For overlap between AIS cohort 1 and schizophrenia cohort we see that expanding the number of genes in the schizophrenia cohort reveals a significant result (corrected  $p < 0.05$  with at least 500 extended genes), but not for increasing the number of genes in AIS cohort 1. When comparing AIS cohort 2 and the schizophrenia cohort increasing the number of genes in both conditions reveals a significant overlap (corrected  $p < 0.05$  with at least 600 extended genes in schizophrenia and at least 800 extended genes in AIS cohort 2). These results suggest that the top GWAS signals of both disorders share similar functions or pathways, and are also in line with the observations in part 1.

| Extension | Comparison (Reference – Query) |              |            |      |            |             |            |              |
|-----------|--------------------------------|--------------|------------|------|------------|-------------|------------|--------------|
|           | AIS1 – SCZ                     |              | SCZ – AIS1 |      | AIS2 – SCZ |             | SCZ – AIS2 |              |
|           | NES                            | P            | NES        | P    | NES        | P           | NES        | P            |
| 100       | 0.86                           | 0.9          | 0.91       | 0.7  | 1.0        | 0.5         | 1.1        | 0.2          |
| 200       | 0.93                           | 0.8          | 1.02       | 0.4  | 1.03       | 0.3         | 1.14       | 0.1          |
| 300       | 1.03                           | 0.3          | 1.03       | 0.3  | 1.09       | 0.1         | 1.19       | <b>0.03</b>  |
| 400       | 1.07                           | 0.1          | 1.05       | 0.3  | 1.08       | 0.1         | 1.18       | <b>0.01</b>  |
| 500       | 1.14                           | <b>0.005</b> | 1.08       | 0.2  | 1.12       | <b>0.01</b> | 1.16       | <b>0.03</b>  |
| 600       | 1.15                           | <b>0.001</b> | 1.08       | 0.1  | 1.17       | <b>0</b>    | 1.15       | <b>0.02</b>  |
| 700       | 1.16                           | <b>0</b>     | 1.09       | 0.09 | 1.18       | <b>0</b>    | 1.15       | <b>0.01</b>  |
| 800       | 1.19                           | <b>0</b>     | 1.07       | 0.1  | 1.19       | <b>0</b>    | 1.16       | <b>0.005</b> |
| 900       | 1.19                           | <b>0</b>     | 1.07       | 0.1  | 1.22       | <b>0</b>    | 1.14       | <b>0.008</b> |
| 1000      | 1.19                           | <b>0</b>     | 1.06       | 0.1  | 1.22       | <b>0</b>    | 1.15       | <b>0.005</b> |

**Table 1.** Gene-network based enrichment analysis between disorders. \*Abbreviation: NES = Normalized Enrichment Score, P = Corrected p-value \*\* bold text indicates significant result.

The sub analysis focusing on the potential overlap between the genes in the 22q11.2 region and AIS and schizophrenia revealed significant overlap for AIS cohort 2 and schizophrenia cohort, while for AIS cohort 1, the overlap only became significant by extension of the network to 600 genes (**Table 2**).

| Extension | Query |              |      |             |      |             |
|-----------|-------|--------------|------|-------------|------|-------------|
|           | SCZ   |              | AIS1 |             | AIS2 |             |
|           | NES   | P            | NES  | P           | NES  | P           |
| 100       | 1.01  | 0.4          | 1.04 | 0.2         | 1.10 | <b>0.05</b> |
| 200       | 1.09  | <b>0.04</b>  | 1.02 | 0.3         | 1.18 | <b>0</b>    |
| 300       | 1.12  | <b>0.005</b> | 1.06 | 0.09        | 1.22 | <b>0</b>    |
| 400       | 1.10  | <b>0.01</b>  | 1.04 | 0.2         | 1.23 | <b>0</b>    |
| 500       | 1.11  | <b>0.001</b> | 1.05 | 0.1         | 1.23 | <b>0</b>    |
| 600       | 1.13  | <b>0</b>     | 1.06 | <b>0.04</b> | 1.23 | <b>0</b>    |
| 700       | 1.16  | <b>0</b>     | 1.04 | 0.08        | 1.24 | <b>0</b>    |
| 800       | 1.17  | <b>0</b>     | 1.04 | 0.09        | 1.25 | <b>0</b>    |
| 900       | 1.18  | <b>0</b>     | 1.04 | 0.07        | 1.27 | <b>0</b>    |
| 1000      | 1.19  | <b>0</b>     | 1.04 | 0.08        | 1.28 | <b>0</b>    |

**Table 2.** Gene-network based enrichment analysis in 22q11.2DS region. \*Abbreviation: NES = Normalized Enrichment Score, P = Corrected p-value. \*\* bold text indicates significant result.



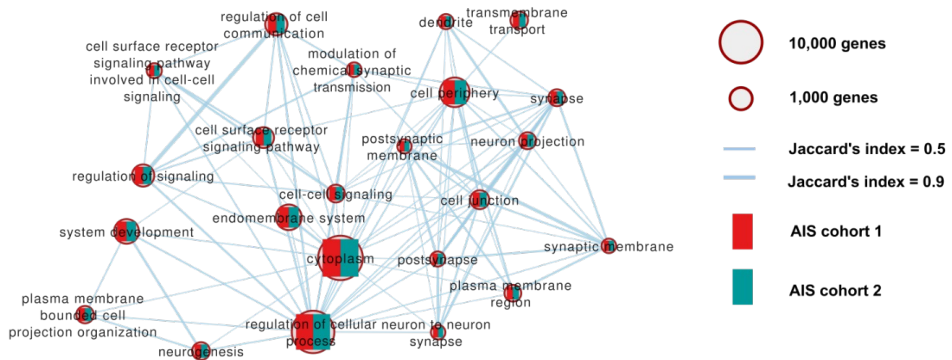


**Figure 3.** Biopathway analysis of AIS cohort 1 (red) and AIS cohort 2 (green). The figure on the previous page displays the pathways significant in either one of the cohorts. Above is a zoom-in of the previous image, displaying the pathways significant in both of the 2 AIS cohorts.

## Discussion

In this study we explored the potential genetic overlap between AIS and schizophrenia in the general population using common genetic variants. Analysis of GWAS summary statistic data demonstrated that there is significant overlap in SNPs strongest associated with both conditions. This indicates that a proportion of common genetics variants involved in AIS are also associated with schizophrenia. Additionally, using *in silico* analyses, we observed that genes important in AIS and schizophrenia also showed more overlap than expected randomly across the genome. Furthermore, only two handfuls of SNPs in the 22q11.2 region are present in cells containing the most significant SNPs for AIS and schizophrenia (0.017%), so it is unlikely that the observed overlap in gene-networks is driven by common variants in the 22q11.2 region. But interestingly, the enriched gene-networks for both AIS and schizophrenia do show overlap with gene-networks enriched for genes in the 22q11.2 region. Finally, exploration of biological pathways demonstrated that common variants associated with both AIS and schizophrenia, are enriched in biological regulation pathways and synaptic/neuron function pathways.

Besides theories about CNS involvement in the multifactorial etiology of AIS, as discussed in the introduction, several other concepts and theories have been postulated in literature. For example, a low BMI, low leptin levels and osteopenia have all been associated with AIS, however it remains unclear whether their occurrence is cause or effect.<sup>22,32,33</sup> Furthermore, in terms of biomechanics, axial rotational instability,<sup>34</sup> which occur when posteriorly directed shear loads are applied to the spine,<sup>35</sup> may play a role. These loads are present in posteriorly directed vertebrae, which are only present in the unique upright spines

of humans,<sup>36</sup> and interestingly AIS is also only observed in humans.<sup>37</sup> Since almost all studies are performed on patients or models of already established scoliosis, it is challenging to infer causality. Until recently a prospective study showed that the relative size and angulation of the posteriorly directed spinal segments increase scoliosis risk.<sup>38</sup> Further biomechanical concepts are a mismatch between vertebral column height growth and either the spinal cord or the surrounding muscles and tendons, acting as a tether causing the spine to buckle,<sup>39–41</sup> or asymmetrical loading for still unclear reasons causing a runaway Hueter–Volkmann effect of asymmetric bone growth.<sup>42,43</sup> Metabolic theories include the concept of platelet calmodulin<sup>44</sup> or melatonin (pathway) dysfunctioning.<sup>32,45</sup> Finally, central cord tethering and the resulting lower cerebral tonsils has also been implicated in the etiology of AIS.<sup>46,47</sup> Given the variety in theories, with hardly any prospective evidence supporting causality, we did not have any hypothesis on if the biopathway analysis would show anything significant, and which biopathways it would involve. Interestingly in our study, the pathways that were significantly enriched in two distinct AIS cohorts were mostly on cell (membrane) processes and signaling, but also contained multiple synaptic and other neuron functioning and development, suggesting the involvement of basic cell and neuro regulating mechanisms in the etiology of AIS.

The major limitation of this study is the modest sample size of available GWAS data for AIS, in particular AIS1, and because we used summary statistics we were not able to combine the two AIS GWAS. This very likely limited our ability to detect all relevant signals of genetic association. This might explain why the *in silico* analyses required expansion of the number of genes to 600 to reveal significant overlap between 22q11.2 genes for AIS cohort 1, and also help explain why the comparison between SCZ and AIS 1 showed a smaller effect size and trend-level p-values. Notwithstanding these limitations, we believe that the main finding in this study is valid, as is also suggested by the extremely low likelihood of finding based on random sampling (**supplement data part 1**). Another point to consider is that even with the mixed ancestral background in the AIS cohorts we observe strong consistency in the results for AIS cohorts 1 and 2.

In conclusion, this study is the first to report genetic overlap between AIS and schizophrenia in the general population, focusing on common genetic variants. Our findings are consistent with previous observations of shared rare genetic risk between both conditions, while adding evidence for shared common risk alleles. This explorative study generates new hypotheses about the etiopathogenesis of AIS and the shared genetic risk and genomic architecture of both AIS and schizophrenia. Possibly subtle alterations in neuron and brain development play a role in the risk for AIS as one of the many multifactorial causes. And, in addition to 22q11.2DS, a group of common genetic variants also increase the risk for both AIS and

schizophrenia. This suggests a shared genetic risk encompassing the full range of genetic variation from rare to common. An interesting question is whether the observed shared genetic risk acts through (a) biological mechanism(s) involved in both conditions, or more indirectly through the alteration of regulatory elements in the genome. Another interesting observation is that although SNPs in the 22q11.2 region do not explain the observed genetic overlap on the level of common genetic variants, some gene-networks enriched by genes with this shared genetic risk for AIS and schizophrenia show also enrichment of genes in the 22q11.2 region. Possibly, in some genes in gene-networks variation in common genetic variants are likely to have phenotypic consequences, while for other genes in the same network, dosage change can have functional effect, such as is the case for some of the genes in the 22q11.2 region. Whether the non-coding SNPs associated with an increased risk for both conditions play a role in a larger functional (regulatory) genetic network is an exciting new hypothesis which requires further exploration. Finally, the biological pathways enriched by SNPs associated with both AIS and schizophrenia are pathways well conserved throughout evolution, the question is why and how they play a role in the shared risk for two uniquely human conditions.

## References

1. Cheng JC, Castelein RM, Chu WC, et al. Adolescent idiopathic scoliosis. *Nature reviews Disease primers* 2015;1:15–30.
2. Fung WLA, Butcher NJ, Costain G, et al. Practical guidelines for managing adults with 22q11.2 deletion syndrome. *Genetics in Medicine* 2015;17:599–609.
3. Gorman KF, Julien C, Moreau A. The genetic epidemiology of idiopathic scoliosis. *European Spine Journal* 2012;21:1905–19.
4. Malecki SL, Van Mil S, Graffi J, et al. A genetic model for multimorbidity in young adults. *Genetics in Medicine* 2020;22:132–41.
5. McDonald-McGinn DM, Sullivan KE, Marino B, et al. 22q11.2 deletion syndrome. *Nature reviews Disease primers*;1 2015.
6. Grati FR, Molina Gomes D, Ferreira JCPB, et al. Prevalence of recurrent pathogenic microdeletions and microduplications in over 9500 pregnancies. *Prenatal Diagnosis* 2015;35:801–9.
7. Blagojevic C, Heung T, Theriault M, et al. Estimate of the contemporary live-birth prevalence of recurrent 22q11.2 deletions: a cross-sectional analysis from population-based newborn screening. *CMAJ open* 2021;9:E802–9.
8. Van L, Boot E, Bassett AS. Update on the 22q11.2 deletion syndrome and its relevance to schizophrenia. *Current Opinion in Psychiatry* 2017;30:191–6.
9. Homans JF, de Reuver S, Breetvelt EJ, et al. The 22q11.2 deletion syndrome as a model for idiopathic scoliosis - A hypothesis. *Medical hypotheses* 2019;127:57–62.
10. Vorstman JAS, Breetvelt EJ, Thode KI, et al. Expression of autism spectrum and schizophrenia in patients with a 22q11.2 deletion. *Schizophr Res* 2013;143:55–9.
11. Fiksinski AM, Breetvelt EJ, Duijff SN, et al. Autism Spectrum and psychosis risk in the 22q11.2 deletion syndrome. Findings from a prospective longitudinal study. *Schizophr Res* 2017;188:59–62.
12. Homans JF, de Reuver S, Heung T, et al. The role of 22q11.2 deletion syndrome in the relationship between congenital heart disease and scoliosis. *Spine J* 2020;20:956–63.
13. Malmqvist M, Tropp H, Lyth J, et al. Patients With Idiopathic Scoliosis Run an Increased Risk of Schizophrenia. *Spine Deformity* 2019;7:262–6.
14. Mulle JG, Gambello MJ, Sanchez Russo R, et al. 3q29 Recurrent Deletion. 1993.
15. Wang D, Shi L, Liu S, et al. Altered topological organization of cortical network in adolescent girls with idiopathic scoliosis. *PLoS one* 2013;8:e83767.
16. Domenech J, García-Martí G, Martí-Bonmatí L, et al. Abnormal activation of the motor cortical network in idiopathic scoliosis demonstrated by functional MRI. *European spine journal* : official publication of the European Spine Society, the European Spinal Deformity Society, and the European Section of the Cervical Spine Research Society 2011;20:1069–78.
17. Liu T, Chu WCW, Young G, et al. MR analysis of regional brain volume in adolescent idiopathic scoliosis: neurological manifestation of a systemic disease. *Journal of magnetic resonance imaging* : JMIR 2008;27:732–6.
18. Chen Z, Qiu Y, Ma W, et al. Comparison of somatosensory evoked potentials between adolescent idiopathic scoliosis and congenital scoliosis without neural axis abnormalities. *The spine journal* : official journal of the North American Spine Society 2014;14:1095–8.
19. Simoneau M, Lamothe V, Hutin E, et al. Evidence for cognitive vestibular integration impairment in idiopathic scoliosis patients. *BMC neuroscience* 2009;10:102.
20. Shi L, Wang D, Chu WCW, et al. Automatic MRI segmentation and morphoanatomy analysis of the vestibular system in adolescent idiopathic scoliosis. *NeuroImage* 2011;54 Suppl 1:S180–8.
21. Chu WCW, Lam WWM, Chan Y-L, et al. Relative shortening and functional tethering of spinal cord in adolescent idiopathic scoliosis?: study with multiplanar reformat magnetic resonance imaging and somatosensory evoked potential. *Spine* 2006;31:E19–25.
22. Clark EM, Taylor HJ, Harding I, et al. Association between components of body composition and scoliosis: a prospective cohort study reporting differences identifiable before the onset of scoliosis. *Journal of bone and mineral research* : the official journal of the American Society for Bone and Mineral Research 2014;29:1729–36.
23. Steppan CM, Swick AG. A role for leptin in brain development. *Biochemical and biophysical research communications* 1999;256:600–2.
24. Kou I, Otomo N, Takeda K, et al. Genome-wide association study identifies 14 previously unreported susceptibility loci for adolescent idiopathic scoliosis in Japanese. *Nat Commun* 2019;10:3685.
25. Khanshour AM, Kou I, Fan Y, et al. Genome-wide meta-analysis and replication studies in multiple ethnicities identify novel adolescent idiopathic scoliosis susceptibility loci. *Hum Mol Genet.* September 2018.
26. O’Roak BJ, Vives L, Girirajan S, et al. Sporadic autism exomes reveal a highly interconnected protein network of de novo mutations. *Nature* 2012;485:246–50.
27. Schizophrenia Working Group of the Psychiatric Genomics Consortium. Biological insights from 108 schizophrenia-associated genetic loci. *Nature* 2014;511:421–7.
28. Chang X, Wang K. wANNOVAR: annotating genetic variants for personal genomes via the web. *Journal of medical genetics* 2012;49:433–6.
29. Franz M, Rodriguez H, Lopes C, et al. GeneMANIA update 2018. *Nucleic acids research* 2018;46:W60–4.
30. Subramanian A, Kuehn H, Gould J, et al. GSEA-P: a desktop application for Gene Set Enrichment Analysis. *Bioinformatics (Oxford, England)* 2007;23:3251–3.
31. Merico D, Isserlin R, Stueker O, et al. Enrichment map: a network-based method for gene-set enrichment visualization and interpretation. *PLoS one* 2010;5:e13984.

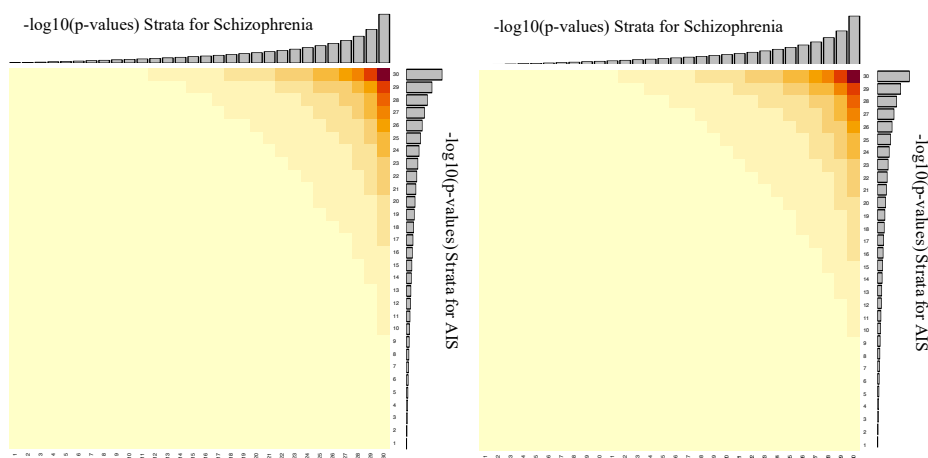


32. Azeddine B, Letellier K, Wang DS, et al. Molecular determinants of melatonin signaling dysfunction in adolescent idiopathic scoliosis. *Clinical orthopaedics and related research* 2007;462:45–52.
33. Burwell RG, Aujla RK, Grevitt MP, et al. Pathogenesis of adolescent idiopathic scoliosis in girls - a double neuro-osseous theory involving disharmony between two nervous systems, somatic and autonomic expressed in the spine and trunk: possible dependency on sympathetic nervous system and hormon. *Scoliosis* 2009;4:24.
34. Wong C. Mechanism of right thoracic adolescent idiopathic scoliosis at risk for progression; a unifying pathway of development by normal growth and imbalance. *Scoliosis* 2015;10:2.
35. Homminga J, Lehr AM, Meijer GJM, et al. Posteriorly directed shear loads and disc degeneration affect the torsional stiffness of spinal motion segments: a biomechanical modeling study. *Spine* 2013;38:E1313-9.
36. Schlösser TPC, Janssen MMA, Vrtovec T, et al. Evolution of the ischio-iliac lordosis during natural growth and its relation with the pelvic incidence. *European Spine Journal* 2014;23:1433–41.
37. Janssen MMA, de Wilde RF, Kouwenhoven J-WM, et al. Experimental animal models in scoliosis research: a review of the literature. *The spine journal : official journal of the North American Spine Society*. 2011.
38. de Reuver S, Homans JF, Houben ML, et al. Early sagittal shape of the spine as a risk factor for scoliosis. submitted.
39. Roth M. Idiopathic scoliosis from the point of view of the neuroradiologist. *Neuroradiology* 1981;21:133–8.
40. Porter RW. The pathogenesis of idiopathic scoliosis: uncoupled neuro-osseous growth? *European spine journal : official publication of the European Spine Society, the European Spinal Deformity Society, and the European Section of the Cervical Spine Research Society* 2001;10:473–81.
41. Chu WC, Lam WM, Ng BK, et al. Relative shortening and functional tethering of spinal cord in adolescent scoliosis - Result of asynchronous neuro-osseous growth, summary of an electronic focus group debate of the IBSE. *Scoliosis* 2008;3:8.
42. Stokes IAF, Burwell RG, Dangerfield PH. Biomechanical spinal growth modulation and progressive adolescent scoliosis – a test of the “vicious cycle” pathogenetic hypothesis: Summary of an electronic focus group debate of the IBSE. *Scoliosis* 2006;1:16.
43. Veldhuizen AG, Wever DJ, Webb PJ. The aetiology of idiopathic scoliosis: biomechanical and neuromuscular factors. *European spine journal : official publication of the European Spine Society, the European Spinal Deformity Society, and the European Section of the Cervical Spine Research Society* 2000;9:178–84.
44. Lowe TG, Burwell RG, Dangerfield PH. Platelet calmodulin levels in adolescent idiopathic scoliosis (AIS): can they predict curve progression and severity? Summary of an electronic focus group debate of the IBSE. *European spine journal : official publication of the European Spine Society, the European Spinal Deformity Society, and the European Section of the Cervical Spine Research Society* 2004;13:257–65.
45. Moreau A, Wang DS, Forget S, et al. Melatonin signaling dysfunction in adolescent idiopathic scoliosis. *Spine* 2004;29:1772–81.
46. Deng M, Hui SCN, Yu FWP, et al. MRI-based morphological evidence of spinal cord tethering predicts curve progression in adolescent idiopathic scoliosis. *Spine J* 2015;15:1391–401.
47. Chu WCW, Lam WWM, Chan Y-L, et al. Relative shortening and functional tethering of spinal cord in adolescent idiopathic scoliosis?: study with multiplanar reformat magnetic resonance imaging and somatosensory evoked potential. *Spine (Phila Pa 1976)* 2006;31:E19-25.

## Supplementary data

### 1. Position of potential relevant deviation in cell count

In the analyses in part 1 we try to reject the hypothesis that if there is no genetic overlap between AIS and schizophrenia the distribution of the p-values for both conditions will be independent resulting in a normal distribution of the number of SNPs in cells in the matrix. To test deviations from this expected distribution it is important to also take the position in the matrix into consideration. Many SNPs in GWAS have p-values close to 1, indicating very little evidence for an association with the condition under study. Clustering in cells in the matrix with SNPs with p-values close to 1 will therefore be biologically less meaningful. To get an impression in which cells we can expect a potentially meaningful clustering we multiplied two vectors containing the  $-\log_{10}$  of the mean p-value of for each stratum for AIS and schizophrenia creating a  $30 \times 30$  matrix. Any product of  $-10 \log$  of p-values close to 1 will approximate 0. We consider deviations from the normal distribution in cells with a product close to zero as a change finding. In **supplement figures 1a&b** the distribution across the matrix is shown in a heatmap, with the  $-\log_{10}$  of the mean p-value for each stratum. Based on this we expect only relevant findings in the right upper quadrant.



**Supplement figures 1a&b.** The  $30 \times 30$  matrices for the product of the  $-\log_{10}$  of the mean p-values for each stratum for AIS and schizophrenia. The  $-\log_{10}$  for the mean of the p-values for each stratum are provided in the upper and right axes.

## 2. List of databases used for enrichment map

### **Gene Ontology**

GO molecular function  
GO cellular component  
GO biological process

### **Biological pathways**

KEGG  
Reactome  
WikiPathways

### **Regulatory motifs in DNA**

miRTarBase

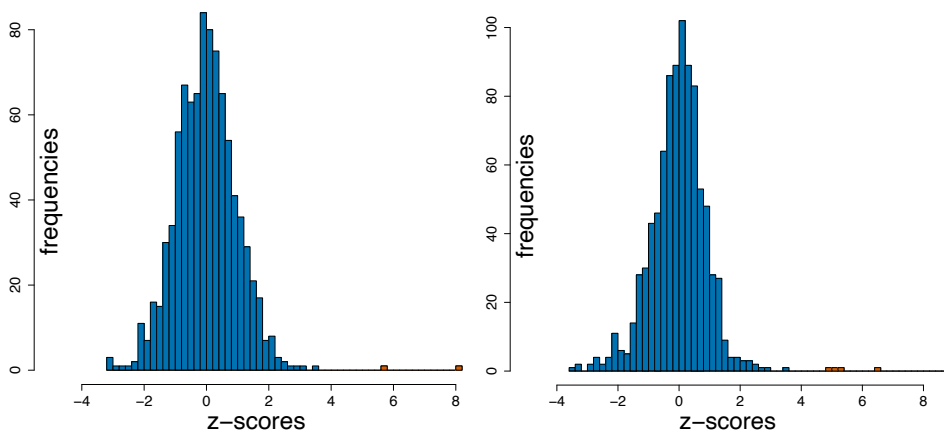
### **Protein databases**

Human Protein Atlas  
CORUM

### **Human phenotype ontology**

HP

## 3. Histogram for z-scores



**Supplement figure 2.** Distribution of z-scores from the heat map of analysis A in figure 2, AIS cohort 1 on the left and AIS cohort 2 on the right.

## 4. Most significant pathways overlapping with SNPs from part 2

| Term Name                               | Term ID    | p-value (-log10) AIS 1 |
|---|------------|------------------------|
| protein binding                         | GO:0005515 | 4.5                    |
| cytoplasm                               | GO:0005737 | 12.1                   |
| cell surface receptor signaling pathway | GO:0007166 | 4.6                    |
| multicellular organism development      | GO:0007275 | 7.7                    |
| nervous system development              | GO:0007399 | 7.0                    |
| regulation of cell communication        | GO:0010646 | 5.5                    |
| postsynaptic density                    | GO:0014069 | 5.4                    |
| neurogenesis                            | GO:0022008 | 6.6                    |
| regulation of signaling                 | GO:0023051 | 4.8                    |
| cell junction                           | GO:0030054 | 7.5                    |
| neuron differentiation                  | GO:0030182 | 5.4                    |
| asymmetric synapse                      | GO:0032279 | 5.8                    |
| multicellular organismal process        | GO:0032501 | 6.3                    |
| developmental process                   | GO:0032502 | 6.8                    |
| synapse                                 | GO:0045202 | 10.1                   |
| generation of neurons                   | GO:0048699 | 5.3                    |
| system development                      | GO:0048731 | 8.8                    |
| anatomical structure development        | GO:0048856 | 6.9                    |
| cellular response to stimulus           | GO:0051716 | 4.3                    |
| cell periphery                          | GO:0071944 | 4.6                    |
| postsynapse                             | GO:0098794 | 11.2                   |
| neuron to neuron synapse                | GO:0098984 | 5.7                    |
| postsynaptic specialization             | GO:0099572 | 4.7                    |

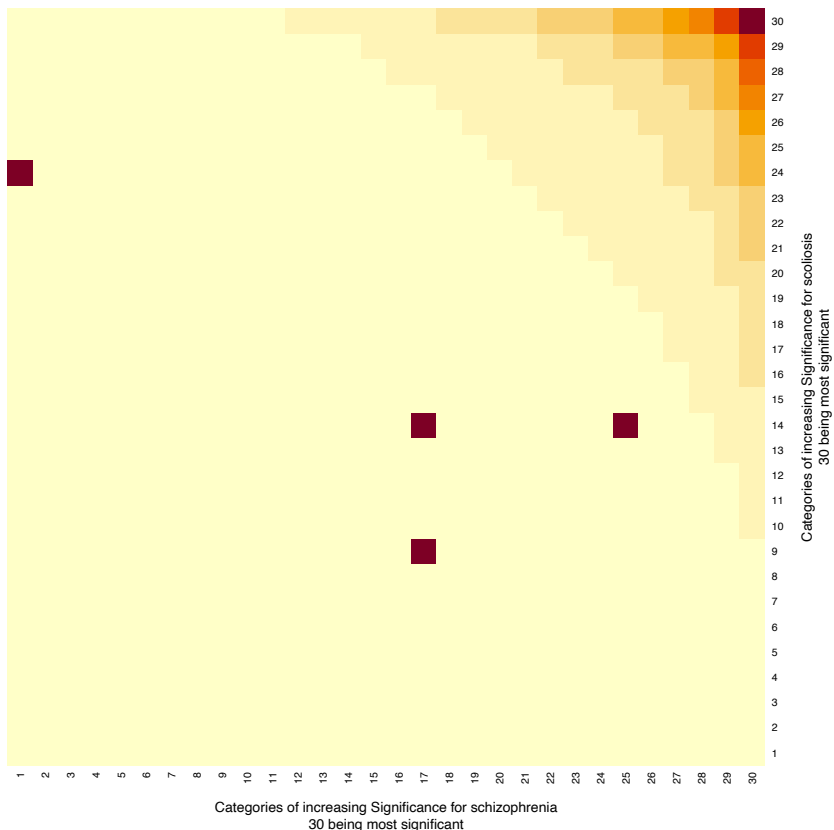
  

| Term Name                               | Term ID    | p-value (-log10) AIS 2 |
|---|------------|------------------------|
| protein binding                         | GO:0005515 | 5.6                    |
| cytoplasm                               | GO:0005737 | 6.7                    |
| cell surface receptor signaling pathway | GO:0007166 | 4.9                    |
| multicellular organism development      | GO:0007275 | 11.7                   |
| nervous system development              | GO:0007399 | 12.9                   |
| regulation of cell communication        | GO:0010646 | 5.8                    |
| postsynaptic density                    | GO:0014069 | 5.9                    |
| neurogenesis                            | GO:0022008 | 7.0                    |
| regulation of signaling                 | GO:0023051 | 5.8                    |
| cell junction                           | GO:0030054 | 5.0                    |
| neuron differentiation                  | GO:0030182 | 7.4                    |
| asymmetric synapse                      | GO:0032279 | 5.7                    |
| multicellular organismal process        | GO:0032501 | 9.1                    |
| developmental process                   | GO:0032502 | 12.3                   |
| synapse                                 | GO:0045202 | 6.3                    |
| generation of neurons                   | GO:0048699 | 6.7                    |
| system development                      | GO:0048731 | 13.8                   |
| anatomical structure development        | GO:0048856 | 11.0                   |
| cellular response to stimulus           | GO:0051716 | 4.3                    |
| cell periphery                          | GO:0071944 | 5.9                    |
| postsynapse                             | GO:0098794 | 4.6                    |
| neuron to neuron synapse                | GO:0098984 | 5.8                    |
| postsynaptic specialization             | GO:0099572 | 5.1                    |

**Supplement Table 1.** Most significant pathways from analyses in part 2, for cohort AIS 1 (top) and AIS 2 (bottom).

## 5. Sensitivity analysis

In the analysis we used conservative z-score threshold to identify cells with a deviation of the expected distribution, and all cells with z-score above 4 were positioned in the extreme upper right quadrant, and their z-scores were all above 5. To further explore the validity of these findings we performed a sensitivity analysis where we randomly reassigned the rank number of the p-value and reiterated the procedure in part 1, we did this 10k times for both AIS1 and AIS2. For each round we determined the number cells with z-scores above 5 and their position in the matrix. In total, so in 20k permutations, we found 4 cells (1 per 5000 experiments) with z-scores above 5 and all were positioned outside the expected area in the matrix, see **supplement figure 3**. This procedure shows that our observation cannot be contributed to random change, we estimate the probability of finding in total 6 cells with z-scores above five in two independent analyses to be smaller than 1 in 2.5 million.



**Supplement Figures 3.** The 30x30 matrices for the product of the  $-\log_{10}$  of the mean p-values for each stratum for AIS1 and schizophrenia. The 4 cells with corresponding z-scores above 5 in the 20,000 permutation are plotted in the heatmap and are positioned outside the expected area based on supplement data part 1.

## 6. Proportions of SNP-types

**Supplementary tables 2a&b** showing proportions of different types of SNPs in both analyses from part 1. Details are given for the cells showing overlap (column 1), and for the strata with the most significant SNPs for AIS and schizophrenia.

| SNP types                       | overlap (%) | AIS (%) | schizophrenia (%) |
|---------------------------------|-------------|---------|-------------------|
| Exonic                          | 0.77        | 0.63    | 0.72              |
| Intergenic                      | 45.23       | 51.53   | 46.41             |
| Intronic                        | 46.73       | 39.44   | 44.28             |
| ncRNA_exonic                    | 0.15        | 0.36    | 0.37              |
| ncRNA_intronic                  | 4.79        | 5.75    | 0                 |
| ncRNA_splicing                  | 0.01        | 0       | 5.31              |
| (up- and downstream, UTR3&UTR5) | 2.32        | 2.29    | 2.91              |

Table 2a. AIS 1

| SNP types                       | overlap (%) | AIS (%) | schizophrenia (%) |
|---------------------------------|-------------|---------|-------------------|
| Exonic                          | 0.97        | 0.67    | 0.79              |
| Intergenic                      | 42.84       | 50.96   | 46.42             |
| Intronic                        | 45.42       | 39.01   | 43.8              |
| ncRNA_exonic                    | 0.46        | 0.41    | 0.44              |
| ncRNA_intronic                  | 6.53        | 0       | 0                 |
| ncRNA_splicing                  | 0.01        | 6.41    | 5.46              |
| (up- and downstream, UTR3&UTR5) | 3.77        | 2.54    | 3.09              |

Table 2b. AIS 2





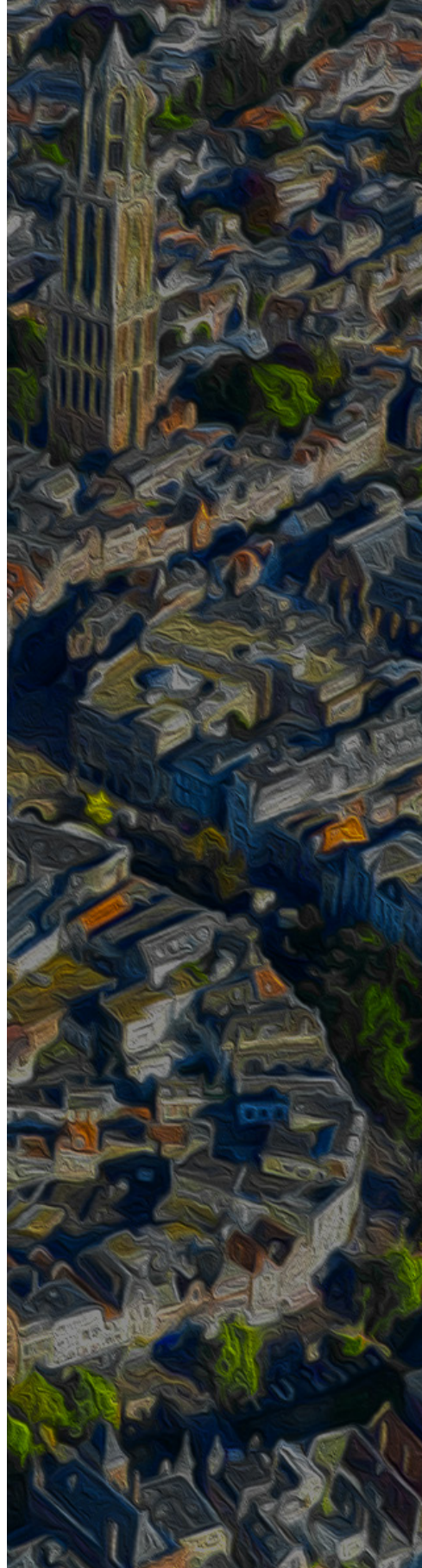


# 18

## Ultrasound Shear Wave Elastography of the Intervertebral Disc and Idiopathic Scoliosis: a Systematic Review

Steven de Reuver  
Aaron J.B.W.D. Moens  
Moyo C. Kruyt  
Rutger A.J. Nievelstein  
Keita Ito  
René M. Castelein

*Ultrasound in Medicine & Biology*, 2022 May;48(5):721-729.



## ABSTRACT

Ultrasound shear wave elastography is a radiation-free and low-cost technique for evaluating the mechanical properties of different tissues. This study systematically reviewed all relevant literature on shear wave elastography of the intervertebral disc. The purpose was twofold: first, to determine the validity of the elastography method, that is, the correlation between elastographically measured shear wave speed and disc mechanical properties, and inter-/intra-operator reliability; and second, to explore if disc elastography is potentially useful in identifying children at risk for idiopathic scoliosis. This systematic review was performed according to the PRISMA (Preferred Reporting Items for Systematic Reviews and Meta-analyses) guidelines. A comprehensive search was performed in PubMed and Embase, and study quality was assessed using the AXIS (Appraisal Tool for Cross-sectional Studies) critical appraisal instrument. Seven articles were included. Three animal *ex vivo* studies reported moderate-to-good correlations between shear wave speed and disc mechanical properties ( $r = 0.45-0.81$ ). Three studies reported high intra-operator repeatability (intra-class correlation coefficient [ICC] 0.94-0.99) and inter-operator reproducibility (ICC 0.97-0.98). Four clinical studies measured shear wave speed in asymptomatic children. Two studies reported significantly higher shear wave speeds in scoliosis patients compared with healthy controls, measured in discs both inside and outside the scoliotic curve. In conclusion, shear wave elastography appears reliable in assessing intervertebral disc mechanical characteristics. Despite its promising capabilities to distinguish patients with asymptomatic from those with pathological discs, the exact correlation between disc mechanical properties and shear wave speed remains unclear.

## Introduction

Adolescent idiopathic scoliosis (AIS) is the most prevalent form of scoliosis: a three-dimensional structural deformity of the spine, which includes lateral curvature, anteroposterior deviation and axial rotation, without any obvious underlying condition.<sup>1,2</sup> The prevalence is 2-4% in the general population and it mostly affects females in early puberty.<sup>3</sup> AIS can lead to severe trunk deformities causing poor self-image, pain and in severe cases cardiopulmonary compromise, which often requires spinal fusion surgery.<sup>4-8</sup> Despite decades of quality research, the exact etiology of AIS remains largely unknown, in contrast to congenital, neuromuscular and other types of scoliosis.<sup>3</sup>

Recently, it has been proposed that AIS is a multifactorial condition most likely involving a mismatch between the mechanical properties of the maturing intervertebral disc (IVD) and the rapidly increased loading due to the pubertal growth spurt.<sup>9</sup> In patients with AIS, the deformity occurs primarily in the IVD while the bony vertebral bodies retain their shape, and differences in mechanical properties between scoliotic IVDs and normal controls have been described.<sup>10-12</sup> The main problem with elucidating the role of the IVD in the etiology of AIS, is the invasive nature of harvesting IVD tissue to study its mechanical properties, especially since it concerns a population of young age. Additionally, most studies on AIS etiology include patients with already established scoliotic curves, therefore distinguishing between cause and effect is practically impossible. We hypothesize that in AIS patients, pathological mechanical IVD properties may already be present before the onset and/or progression of the scoliotic curve. If this were to be true, and these IVD properties could easily and safely be measured in children, this could potentially be used as a proxy for the risk of AIS development and progression of the scoliotic curve. Unfortunately, there currently is no established diagnostic method for non-invasive characterization of the IVD to determine the tissue's mechanical properties.

Several non-invasive elasticity imaging techniques exist, that aim to quantify mechanical properties of the examined tissue. In general, elasticity imaging techniques are used to gather information on tissue elasticity and can be applied to organs located deeper in the body, which provides new opportunities for screening and diagnosis.<sup>13</sup> Over the past few decades, numerous emerging elasticity imaging techniques have been developed and researched.<sup>14</sup> Early elasticity imaging techniques in the 1970s and 1980s used static loading and an external vibrator to generate stress in tissues, after which modified color Doppler was used to track tissue displacement and measure tissue stiffness.<sup>15,16</sup> In the late 1990s an alternative quasi-static approach was developed to remotely measure tissue elasticity via manual compression or cardiovascular/respiratory pulsation, now known as strain elastography.<sup>17</sup> This was soon

followed by the development of dynamic shear wave elastography to measure the shear wave speed (SWS), which directly relates to the elastic moduli of the tissue, as opposed to strain elastography.<sup>18,19</sup> In contrast to strain elastography, shear wave elastography uses a focused acoustic radiation force to generate shear waves within the organ of interest, which allows for measurement of the propagation speed to locally quantify the tissue stiffness.<sup>20</sup> Since 2005, increasingly more manufacturers have added the shear wave elastography option to their standard ultrasound systems.<sup>14</sup> Shear wave elastography is now regularly used in clinical practice to evaluate the breast, liver, prostate, and musculoskeletal tissues.<sup>21-24</sup> Therefore, in this systematic review, we explore the feasibility of shear wave elastography to assess IVD mechanical properties, through the measurement of SWS.

Non-invasive mechanical characterization of the IVD through shear wave elastography may provide new opportunities for early diagnosis and etiological research on AIS. However, to date, there is no systematic literature review on the current status of shear wave elastography of the IVD and its uses in AIS patients. Therefore, the purpose of this systematic review is two-fold: The first goal is to determine the validity of shear wave elastography in quantifying IVD mechanical properties (i.e. the correlation between SWS and apparent disc stiffness and/or elastic modulus, usually indirectly determined in ex vivo animal experiments) and the inter- and intra-operator reliability. The second goal is to analyze shear wave elastography measurements of the IVD in healthy populations and in children with AIS, and explore the usefulness of the method in identifying children at-risk for idiopathic scoliosis.

## **Materials and Methods**

### Search strategy and study selection

This systematic review was performed according to the PRISMA (Preferred Reporting Items for Systematic Reviews and Meta-Analysis) guideline.<sup>25</sup> A comprehensive search was performed in PubMed and Embase. The search string included all relevant terms and synonyms for “elastography”, “ultrasonography” and “intervertebral disc”, combined by “and”. All terms were required to be mentioned in either title or abstract of the study (**Appendix A**). Duplicates were removed. The reference lists of all included studies were reviewed for additional articles missed in the initial search. Two reviewers independently identified studies and reviewed title and abstract for relevance using predetermined in- and exclusion criteria. Any discrepancies were resolved through discussion. All irrelevant articles to the purpose of this study based on title or abstract were dismissed. Full text was reviewed if eligibility was uncertain after screening title and abstract. The search was conducted up until the October 15th of 2021. The search language was in English. There were no restrictions on publication date or status.

### Inclusion and exclusion criteria

Both ex vivo animal studies and human in vivo studies on shear wave elastography of the IVD were included in this review if full English text was available. Only studies were included that had their protocol approved by a local ethics committee, institutional review board (IRB) and/or institutional animal care and use committee (IACUC). In vivo studies had to be conducted in asymptomatic people or in patients with AIS. Studies in patients with pathology other than AIS were excluded. Further exclusion criteria were the use of elastography techniques other than ultrasound-based ones, such as MRI or optical coherence elastography, or when they studied tissues different than the IVD. When multiple articles were published on results within the same study population, only the most comprehensive or most recent article was included to prevent duplication bias.

### Quality assessment

The AXIS critical appraisal tool for cross-sectional studies was used to assess the quality of the included studies.<sup>26</sup> The criteria include 20 items scored 'yes', 'no', 'don't know' or 'not applicable (n/a)'. The AXIS tool contains 7 criteria related to study design, 7 related to quality of reporting and 6 items on potential bias (**Appendix B**). The AXIS tool does not provide a fixed cut-off value for high or low study quality. Therefore, in line with earlier studies using AXIS, it was decided that in this systematic review studies scoring 5 or more criteria negatively were considered low quality. Criteria scored 'n/a' were not taken into account in this consideration.

### Data extraction and analysis

A data form was created containing the following data from the included articles: title, first author, year of publication, country, study design, study population, study sample and the main results. The main outcomes of interest were: the correlation between ex vivo SWS measurements of the annulus fibrosus and apparent IVD stiffness or elastic modulus, the repeatability (intra-operator) and reproducibility (inter-operator) of the elastography measurements, and SWS measurements in healthy controls and AIS patients. Due to the heterogeneity of study designs and study populations, a quantitative meta-analysis was not performed. The intra-class correlation coefficient (ICC) was considered to be excellent (ICC: > 0.90), good (ICC: 0.75-0.90), moderate (ICC: 0.50-0.75) or poor (ICC: < 0.50).<sup>27</sup> The correlation coefficient (r) was regarded very good to excellent (r: 0.75-1.00), moderate to good (r: 0.50-0.75) or poor (r: 0.25-0.50).<sup>28</sup>

## Results

### Study selection and quality assessment

The inclusion procedure of the articles for this systematic review is shown in the PRISMA flow diagram (**Figure 1**).<sup>25</sup> A total of seven studies were included. Three animal ex vivo studies reported on the correlation between SWS measurements of the annulus fibrosus and apparent IVD stiffness and/or elastic modulus. Repeatability and/or reproducibility was reported by one ex vivo and two clinical studies. Two studies reported the SWS in healthy controls and two other studies compared SWS in healthy controls to patients with AIS. All seven included studies were of high quality according to the AXIS critical appraisal tool (**Appendix B**). Recurrent negative criteria were either a lack of sample size justification, a lack of discussion of study limitations, unclear funding sources, and/or conflicts of interest possibly affecting study outcomes.

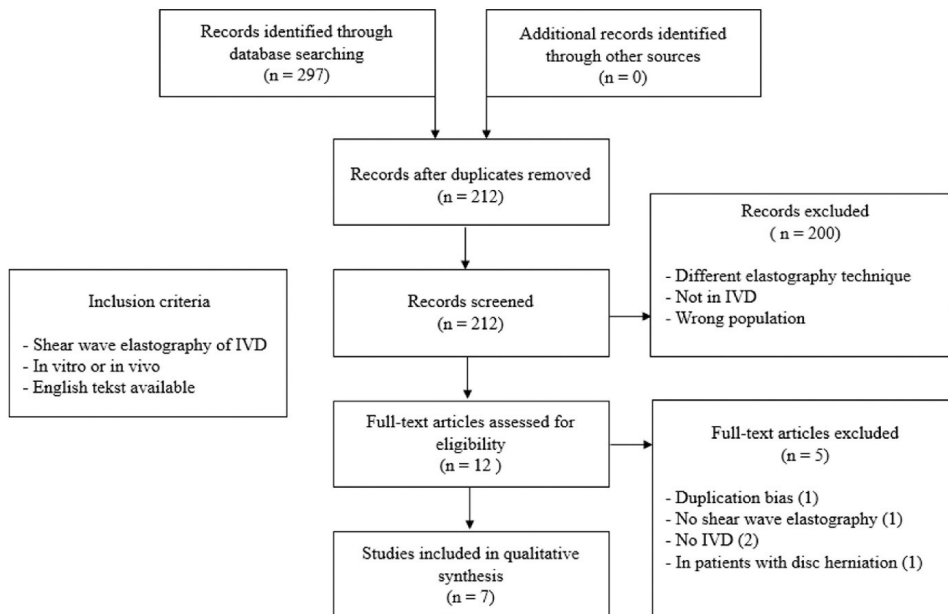


**Figure 1.** Preferred Reporting Items for Systematic Reviews and Meta-analyses flow diagram.

### Study characteristics

All included studies were published between 2013 and 2020. The majority of included studies were conducted at the same institute (**Table 1**). Three ex vivo studies reported on correlations between SWS and mechanical properties of either bovine or porcine IVDs.<sup>29-31</sup> A total of four clinical studies included a population of asymptomatic adults, asymptomatic children and a combination of asymptomatic children and children with AIS.<sup>32-35</sup>

| Article               | Year | Study population      | n  | IVD level                     | Main outcome   |
|-----------------------|------|-----------------------|----|-------------------------------|--|
| <i>Ex vivo</i>        |      |                       |    |                               |  |
| Vergari et al.        | 2013 | Oxtails               | 8  | n/a                           | SWS and IVD stiffness correlation                                    |
| Vergari et al.        | 2014 | Oxtails               | 11 | n/a                           | SWS and IVD stiffness correlation, intra-operator ICC, repeatability |
| Chotar-Vasseur et al. | 2015 | Porcine IVDs          | 8  | Pig 1: T15–L5<br>Pig 2: L1–L4 | SWS and IVD stiffness correlation                                    |
| <i>In vivo</i>        |      |                       |    |                               |  |
| Vergari et al.        | 2014 | Asymptomatic adults   | 47 | C6–C7 or C7–T1                | SWS, intra-/inter-operator ICC, repeatability, reproducibility       |
| Vergari et al.        | 2016 | Asymptomatic children | 31 | L5–S1 or L4–L5                | SWS, intra-/inter-operator ICC, repeatability, reproducibility       |
| Langlais et al.       | 2018 | Asymptomatic children | 30 | L3–L4, L4–L5 and L5–S1        | SWS  |
| Vergari et al.        | 2020 | AIS patients          | 30 | L3–L4, L4–L5 and L5–S1        | SWS  |
|                       |      | Asymptomatic children | 59 |                               |  |
|                       |      | AIS patients          | 25 |                               |  |

**Table 1.** Overview of included studies. AIS = adolescent idiopathic scoliosis; ICC = intra-class correlation coefficient; IVD = intervertebral disc; n/a = not available; SWS = shear wave speed.

### Correlation between SWS and mechanical properties

Three *ex vivo* studies reported on the correlation between SWS measurements in the annulus fibrosus and apparent stiffness and/or elastic modulus. In these studies, multiple cycles of axial compression, at loads ranging between 0 and 400N, were applied to the bovine or porcine intervertebral segments to produce a repeatable mechanical response. The slope in the produced force-displacement curve represents the material stiffness. Since IVD height and surface area is known, stress-strain curves can be calculated from force-displacement curves, from which the elastic modulus can be calculated. After the final cycle, the segment is unloaded and then loaded again after which the position is held to induce stress-relaxation, during which the elastography measurements were taken.

The reported correlation coefficient ( $r$ ) in these three studies varied from 0.45 to 0.81 (**Table 2**). The first study by Vergari et al. reported a significant correlation ( $r = 0.45$ ) between SWS and IVD stiffness for pooled data ( $n = 40$ ).<sup>29</sup> A later study reported significant correlations ( $r = 0.63 - 0.70$ ) between three measured variables under axial loading: SWS, IVD stiffness, and the apparent elastic modulus.<sup>30</sup> Chotar-Vasseur et al. performed a linear regression analysis between the IVDs apparent elastic modulus and elastographically measured SWS of the annulus fibrosus at different preloads of 10, 200 and 400 N. A coefficient of determination  $R^2$  of 0.66 was reported, corresponding to a correlation coefficient of  $r = 0.81$ .<sup>31</sup>



| Article                    | Year | Repeatability (intra-operator) |           | Reproducibility (inter-operator) |      | SWS and IVD stiffness correlation<br>Correlation coefficient, <i>r</i> | Average SWS (m/s) |           |
|----------------------------|------|--------------------------------|-----------|----------------------------------|------|--|-------------------|-----------|
|                            |      | SWS variation<br>(m/s)         | ICC       | SWS variation<br>(m/s)           | ICC  |  | Asymptomatic      | AIS       |
| <i>Ex vivo</i>             |      |                                |           |                                  |      |  |                   |           |
| Vergari et al.             | 2013 |                                |           |                                  |      | 0.45   |                   |           |
| Vergari et al.             | 2014 | ±0.39 (7%)                     | 0.96–0.99 |                                  |      | 0.63–0.70  |                   |           |
| Chotar-Vas-<br>seur et al. | 2015 |                                |           |                                  |      | 0.81   |                   |           |
| <i>In vivo</i>             |      |                                |           |                                  |      |  |                   |           |
| Vergari et al.             | 2014 | ±0.20 (7%)                     | 0.94–0.98 | 0.30 (10%)                       | 0.97 |  | 3.0 ± 0.4         |           |
| Vergari et al.             | 2016 | ±0.22 (7.5%)                   | 0.96–0.98 | 0.25 (8.7%)                      | 0.98 |  | 2.9 ± 0.5         |           |
| Langlais et al.            | 2018 |                                |           |                                  |      |  | 3.0 ± 0.3         | 3.5 ± 0.3 |
| Vergari et al.             | 2020 |                                |           |                                  |      |  | 3.1 ± 0.5         | 4.0 ± 0.5 |

**Table 2.** Main results. AIS = adolescent idiopathic scoliosis; ICC = intra-class correlation coefficient; IVD = intervertebral disc; SWS = shear wave speed.

### Repeatability and reproducibility

One ex vivo study and two clinical studies reported on the repeatability (intra-operator) of the shear wave elastography to measure the SWS in the annulus fibrosus (**Table 2**). The variation within repeated measurements was 0.20–0.39 m/s (7.0–7.5% coefficient of variation), while the ICCs for intra-operator reliability ranged between 0.94 and 0.99.<sup>30,32,33</sup> Two clinical studies reported reproducibility (inter-operator), in which the SWS variation was 0.25–0.30 m/s (8.7–10.0% coefficient of variation). The ICCs for inter-operator reliability ranged between 0.97 and 0.98.<sup>32,33</sup>

### Shear wave speed in asymptomatic patients

Two studies reported solely on SWS measurements in healthy controls (**Table 2**). In 47 asymptomatic adults (mean age  $36.5 \pm 12.6$ ), a mean SWS of  $3.0 \pm 0.4$  m/s was reported, measured at level C6–C7 and C7–T1.<sup>32</sup> Similar values for SWS were reported in 31 asymptomatic children aged 6 to 17, with a mean SWS in the annulus fibrosus of the IVD at level L4–L5 and L5–S1 of  $2.9 \pm 0.5$  m/s.<sup>33</sup>

### Shear wave speed in AIS and healthy controls

Two other studies measured SWS values in asymptomatic children, but also compared to measurements in children with AIS. In the study by Langlais et al (2018), SWS measurements in IVDs of 30 asymptomatic children (mean age  $13 \pm 1.9$ ) were compared to 30 patients with thoracic or lumbar AIS (mean age  $13 \pm 2.0$ , mean Cobb angle:  $28.8^\circ \pm 10.4^\circ$ ).<sup>34</sup> In this study, the SWS was measured with ultrasound elastography at the lower lumbar level (L3–S1), which in AIS patients mostly is outside of the spinal area affected by scoliosis. In asymptomatic children the SWS measured  $3.0 \pm 0.3$  m/s



and in AIS patients  $3.5 \pm 0.3$  m/s (2.7-4.8 m/s), while it is known from earlier ex vivo studies that a higher SWS is correlated with increased disc stiffness.<sup>29-31</sup> No significant difference between IVD levels (L3-L4, L4-L5, L5-S1) was observed within both groups, and SWS was significantly higher at all disc levels in AIS patients compared to healthy controls ( $p < 0.02$ ). Furthermore in this study a high SWS measured in multiple consecutive discs was associated with increased risk of curve progression. Subgroup analysis demonstrated a mean SWS in stable scoliosis of  $3.3 \pm 0.3$  m/s, in progressive scoliosis of  $3.7 \pm 0.3$  m/s, in pre-treatment progressive scoliosis of  $4.0 \pm 0.3$  m/s, and in scoliosis during treatment of  $3.3 \pm 0.3$  m/s (**Figure 2**) These data might suggests a possible form of regenerative capacity of the disc during treatment, however the SWS is mostly measured in IVDs outside of the affected part of the spine.

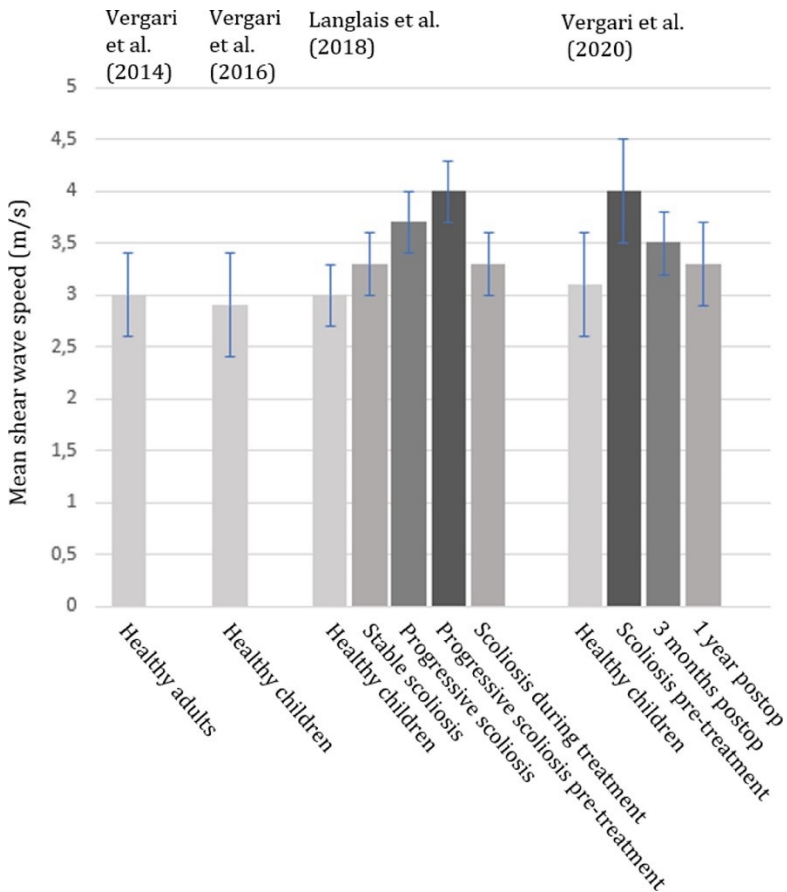


**Figure 2.** Subgroup analysis of shear wave speed. Error bars indicate standard deviations.

The latest study by Vergari et al. (2020) reported SWS data in lower lumbar discs of 59 asymptomatic children (mean age  $13 \pm 2$ ) and 25 severe AIS patients with mostly thoracic curves (mean age  $15 \pm 1.5$ , mean Cobb angle  $57^\circ \pm 14^\circ$ ), before and after surgical intervention.<sup>35</sup> SWS was significantly higher in pre-operative AIS patients at  $4.0 \pm 0.5$  m/s compared to asymptomatic children at  $3.1 \pm 0.5$  m/s. Three months post-operative, the mean SWS in AIS patients showed a non-statistically significant decrease to  $3.5 \pm 0.3$  m/s, and after a further 1 year a significant decrease to  $3.3 \pm 0.4$  m/s, a similar value to asymptomatic controls. Furthermore, a weak correlation between Cobb angle and a lower SWS was observed ( $r = 0.40$ ,  $p = 0.05$ ). Similar SWS values were found for AIS patients with thoracic ( $3.8 \pm 0.4$  m/s) and thoracolumbar curves ( $3.9 \pm 0.4$  m/s). Only one of the included patients had a lumbar curve, with a mean SWS of 5.1 m/s.

## Discussion

The purpose of this systematic review was two-fold. The first aim was to determine the validity of shear wave elastography (i.e. the correlation with mechanical disc properties) and inter/intra-operator reliability. The second aim was to examine if disc-elastography is potentially useful in identifying children at-risk for idiopathic scoliosis. Studies were reviewed that reported on the correlation between elastographically measured SWS in the annulus fibrosus and apparent IVD stiffness and/or elastic modulus. Furthermore, studies that reported on the repeatability and reproducibility of SWS measurements were reviewed, as well as studies that measured the SWS in IVDs of patients with AIS and asymptomatic controls. The initial search resulted in 262 records, of which seven articles were included.

Three ex vivo studies of animal tissue reported a moderate-to-good correlation between SWS measured in the annulus fibrosus and apparent IVD stiffness or elastic modulus ( $r = 0.45-0.81$ ). An excellent intra-operator repeatability (ICC: 0.94-0.99) and inter-operator reproducibility (ICC: 0.97-0.98) was reported. Four in vivo studies were included in this review, of which two solely in asymptomatic controls and two in both asymptomatic children and patients with (mostly) thoracic AIS. In these two studies, a significantly higher SWS was observed in AIS patients compared to asymptomatic controls. This may suggest that the IVDs in AIS patients both in- and outside the scoliotic curve are stiffer than in asymptomatic children, since a higher SWS correlates with an increased IVD stiffness. This could indicate that AIS involves pathological IVDs in the entirety of the spinal column, although it is most likely that IVDs adjacent to or within the curve will be affected more. But since only two studies included patients with AIS, no definitive conclusions can be drawn and more studies are necessary to investigate the uses of shear wave elastography in identifying children at risk for scoliosis.

Three animal ex vivo studies reported a varying correlation coefficient of 0.45 to 0.81 between SWS of the annulus fibrosus and apparent IVD stiffness or elastic modulus under different loads, suggesting that the variability in SWS might also be confounded by something other than just the IVD stiffness. For example, in the study by Chotar-Vasseur et al., almost a doubling of the SWS was demonstrated under 400N axial compression compared to 10N.<sup>31</sup> In addition, there was no significant correlation between the stiffness of unloaded IVDs and SWS.<sup>30</sup> Therefore, elastographically measured SWS is most likely also influenced by other tissue properties of the IVD such as hydration status, age and size, or even technical variability in the elastography method itself. It has been demonstrated by denucleation that the nucleus pulposus plays a more pronounced role on IVD stiffness in the low force range, whereas at a higher reference force of 400N, the mechanical behavior of the IVD is dominated by the annulus fibrosus and stiffness is minimally affected by denucleation.<sup>36,37</sup> The three ex vivo studies included in this review reported the correlation between SWS and apparent IVD mechanical properties under different circumstances, making it challenging to draw robust conclusions on the true relationship between shear wave elastography and IVD mechanical properties. Ideally, SWS measured with ultrasound elastography should solely reflect changes in disc stiffness. However, it remains unclear exactly what and to what extent, external factors are involved and how these should be accounted for. A further investigation into the role of the IVD anisotropy caused by its lamellar build-up should be performed to better understand how loading affects the elastic modulus in different planes.

Three studies reported excellent values (ICC: > 0.90) with moderate to strong evidence for both repeatability and reproducibility. Elastography of the IVD seems to be less operator dependent compared to superficial organs, breast or muscles. Because the IVD is located deeper inside the body, it might be less susceptible to operator dependent force of application of the ultrasound probe, which could explain the high repeatability and reproducibility compared to other tissues.<sup>38</sup>

Four clinical studies provided values for healthy controls and two studies observed in AIS an increase in SWS with progression of the scoliotic curve, while a decrease was observed after surgical correction and stabilization (**Figure 2**). Overall, the SWS in lower lumbar discs measured by elastography was significantly higher in patients with (mostly) thoracic AIS compared to healthy controls.<sup>34,35</sup> This may suggest that throughout the spine, in both the scoliotic and unaffected areas, the IVDs are stiffer in patients with AIS compared to asymptomatic controls. In an earlier study, it was suggested that the spinal curvature severity in scoliosis patients was associated with a stiffer spine.<sup>39</sup> Therefore, it was expected that a positive correlation between SWS and Cobb angle would exist. However, no significant

positive correlation was found in either Langlais et al. (2018) and even a trend towards a negative correlation in Vergari et al. (2020). This can be due to a lack of statistical power, or as mentioned in Vergari et al. (2020), the aggressive bracing of more severely affected patients, which may influence disc hydration and its mechanical properties.

In the clinical elastography studies in this review, the IVDs at the lower lumbar levels were measured, whereas the scoliosis was present (mostly) in the thoracic spine. One MRI study in AIS patients demonstrated that the deterioration of the IVD is greater within the spinal curvature than in asymptomatic regions of the spine.<sup>40</sup> Therefore, the measured SWS differences between AIS patients and asymptomatic controls could be an underrepresentation of the IVD stiffness differences within the curve. Support for this hypothesis could be found in the study by Vergari et al. (2020), in which there was one patient included with a lumbar scoliosis. In this patient the SWS was measured in or close to the scoliotic curve with a mean SWS of 5.1 m/s, which was the highest value reported amongst all patients. The studies by Langlais et al (2018) and Vergari et al. (2020) measured SWS in lower lumbar IVDs in patients with AIS. A similar increase in SWS was observed in both patients with thoracic and (thoraco)lumbar scoliosis, compared to asymptomatic controls. This suggests that in patients with AIS, the characteristics of the IVD may be different throughout the entire spine and not just in the affected area. Therefore, the different IVD mechanical properties may not solely be a result of the scoliotic deformity, but might be already present before the onset of scoliosis.

The main limitations of this systematic review were not methodological but related to the outcome, since six out of seven included studies were carried out at the same institute. Furthermore, only two included studies tested shear wave elastography in a clinical setting on patients with AIS. There was a limited number of studies on the subject, with large variability in both study design and study population characteristics. Of the seven included studies, data was only analyzed descriptively, since no meta-analysis could be performed. Finally, relatively small sample sizes and heterogeneity in reported data made thorough comparison and interpretation of the results difficult, and therefore this systematic review only provides an overview of current literature on ultrasound-based shear wave elastography of the IVD in relation to scoliosis, with a few tentative conclusions.

Current diagnostic techniques for early stage AIS have a high accuracy when used together, for instance a sensitivity of 93.8% and a specificity of 99.2% can be reached with the Adam's forward bend test, scoliometer measurement and Moiré topography combined.<sup>41</sup> Despite this, these techniques are only applicable in patients with an already established curve. This systematic review demonstrates that ultrasound shear wave elastography is able to make a

distinction between scoliotic and non-scoliotic patients by measuring shear wave speed through the annulus fibrosus of IVDs outside the scoliotic curve, as a proxy for mechanical properties of the IVD, specifically stiffness. This could imply that disc properties of patients that develop scoliosis are different even before the onset of scoliosis. If that is true, this technique can be used as a predictor, especially in high-risk populations, before the onset of a scoliosis. Such a high risk population could be patients with 22q11.2 deletion syndrome, a group that was described as a human model for idiopathic scoliosis in the general population, as they develop an idiopathic-like scoliosis with an incidence of ~50%.<sup>42,43</sup> Another possible use of ultrasound elastography could be the use in the follow-up of AIS patients to detect those at risk for progression at an early state, allowing for more aggressive non-surgical treatment and possibly preventing surgery in the long run.

In conclusion, this study systematically reviewed all relevant literature on shear wave elastography of the intervertebral disc, with the purpose to determine the validity, reliability and potentially useful in identifying children at-risk for idiopathic scoliosis. Excellent repeatability and reproducibility were reported with moderate to strong levels of evidence. Multiple studies demonstrated a correlation between elastographically measured SWS and the apparent stiffness/elasticity of IVDs under axial loading, however with a large variation and under different circumstances. While it is promising that in clinical studies ultrasound elastography could make a distinction between IVDs in patients with and without AIS, the correlation between SWS measurements and disc stiffness and possible confounding factors is not yet fully understood.

## References

1. Illés T, Tunyogi-Csapó M, Somoskeöy S. Breakthrough in three-dimensional scoliosis diagnosis: Significance of horizontal plane view and vertebra vectors. *European Spine Journal* 2011;20:135–43.
2. Kuklo TR, Potter BK, O'Brien MF, et al. Reliability Analysis for Digital Adolescent Idiopathic Scoliosis Measurements. *Journal of Spinal Disorders & Techniques* 2005;18:152–9.
3. Cheng JC, Castelein RM, Chu WC, et al. Adolescent idiopathic scoliosis. *Nat Rev Dis Primers* 2015;1:15–30.
4. Lonner B, Yoo A, Terran JS, et al. Effect of spinal deformity on adolescent quality of life: Comparison of operative scheuermann kyphosis, adolescent idiopathic scoliosis, and normal controls. *Spine* 2013;38:1049–55.
5. Choudhry MN, Ahmad Z, Verma R. The Open Orthopaedics Journal Adolescent Idiopathic Scoliosis. *The Open Orthopaedics Journal* 2016;10:143–54.
6. Johnston CE, Stephens Richards B, Sucato DJ, et al. Correlation of preoperative deformity magnitude and pulmonary function tests in adolescent idiopathic scoliosis. *Spine* 2011;36:1096–102.
7. Tsigliannis T, Grivas T. Pulmonary function in children with idiopathic scoliosis. *Scoliosis* 2012;7:7.
8. Koumbourlis AC. Scoliosis and the respiratory system. *Paediatric Respiratory Reviews* 2006;7:152–60.
9. Castelein RM, Pasha S, Cheng JCYC, et al. Idiopathic Scoliosis as a Rotatory Decomposition of the Spine. *Journal of Bone and Mineral Research* 2020;35:1850–7.
10. Yu J, Fairbank JCT, Roberts S, et al. The elastic fiber network of the annulus fibrosus of the normal and scoliotic human intervertebral disc. *Spine* 2005;30:1815–20.
11. Grivas TB, Vasiladis E, Malakasis M, et al. Intervertebral disc biomechanics in the pathogenesis of idiopathic scoliosis. In: *Studies in Health Technology and Informatics*. 2006:80–3.
12. de Reuver S, Brink RC, Homans JF, et al. Anterior lengthening in scoliosis occurs only in the disc and is similar in different types of scoliosis. *The spine journal : official journal of the North American Spine Society* 2020;20:1653–8.
13. Gennisson J-LL, Deffieux T, Fink M, et al. *Ultrasound elastography: Principles and techniques*. 2013.
14. Sarvazyan A, Hall TJ, Urban MW, et al. An overview of elasticity imaging - an emerging branch of medical imaging. *Current medical imaging reviews* 2011;7:255–82.
15. Dickinson R, Hill CR. An ultrasonic method of analyzing tissue motion. *The British Journal of Radiology* 1980;53:626–7.
16. Dickinson RJ, Hill CR. Measurement of soft tissue motion using correlation between A-scans. *Ultrasound in Medicine and Biology* 1982;8:263–71.
17. Shiina T, Nightingale KR, Palmeri ML, et al. WFUMB Guidelines and Recommendations for Clinical Use of Ultrasound Elastography: Part 1: Basic Principles and Terminology. *Ultrasound in Medicine & Biology* 2015;41:1126–47.
18. Garra BS. Elastography: history, principles, and technique comparison. *Abdominal Imaging* 2015;40:680–97.
19. Taljanovic MS, Gimber LH, Becker GW, et al. Shear-wave elastography: Basic physics and musculoskeletal applications. *Radiographics* 2017;37:855–70.
20. Shiina T, Nightingale KR, Palmeri ML, et al. WFUMB Guidelines and Recommendations for Clinical Use of Ultrasound Elastography: Part 1: Basic Principles and Terminology. *Ultrasound in Medicine & Biology* 2015;41:1126–47.
21. Cong R, Li J, Guo S. A new qualitative pattern classification of shear wave elastography for solid breast mass evaluation. *European Journal of Radiology* 2017;87:111–9.
22. Yoon HM, Kim SY, Kim KM, et al. Liver Stiffness Measured by Shear-wave Elastography for Evaluating Intrahepatic Portal Hypertension in Children. *Journal of Pediatric Gastroenterology and Nutrition* 2017;64:892–7.
23. Rouvière O, Melodelima C, Hoang Dinh A, et al. Stiffness of benign and malignant prostate tissue measured by shear-wave elastography: a preliminary study. *European Radiology* 2017;27:1858–66.
24. Moreau B, Vergari C, Gad H, et al. Non-invasive assessment of human multifidus muscle stiffness using ultrasound shear wave elastography: A feasibility study. *Proceedings of the Institution of Mechanical Engineers Part H, Journal of engineering in medicine* 2016;230:809–14.
25. Moher D, Liberati A, Tetzlaff J, et al. Preferred reporting items for systematic reviews and meta-analyses: The PRISMA statement. *PLoS Medicine*;6.
26. Downes MJ, Brennan ML, Williams HC, et al. Development of a critical appraisal tool to assess the quality of cross-sectional studies (AXIS). *BMJ Open* 2016;6:e011458.
27. Koo TK, Li MY. A Guideline of Selecting and Reporting Intra-class Correlation Coefficients for Reliability Research. *Journal of Chiropractic Medicine* 2016;15:155–63.
28. Dawson B, Trapp RG. *Basic & Clinical Biostatistics*. 4th ed. AccessMedicine, McGraw-Hill Medical; 2004.
29. Vergari C, Rouch P, Dubois G, et al. Intervertebral disc characterisation by elastography: A preliminary study. *Computer Methods in Biomechanics and Biomedical Engineering* 2013;16:275–7.
30. Vergari C, Rouch P, Dubois G, et al. Intervertebral disc characterization by shear wave elastography: An in vitro preliminary study. *Proceedings of the Institution of Mechanical Engineers, Part H: Journal of Engineering in Medicine* 2014;228:607–15.
31. Chotar-Vasseur Y, Cachon T, Ponsard B, et al. In vitro comparison between mechanical properties and elastographic characterization of porcine intervertebral disc. *Computer Methods in Biomechanics and Biomedical Engineering* 2015;18:1906–7.
32. Vergari C, Rouch P, Dubois G, et al. Non-invasive biomechanical characterization of intervertebral discs by shear wave ultrasound elastography: a feasibility study. *European Radiology* 2014;24:3210–6.

33. Vergari C, Dubois G, Vialle R, et al. Lumbar annulus fibrosus biomechanical characterization in healthy children by ultrasound shear wave elastography. *European Radiology* 2016;26:1213–7.
34. Langlais T, Vergari C, Pietton R, et al. Shear-wave elastography can evaluate annulus fibrosus alteration in adolescent scoliosis. *European Radiology* 2018;28:2830–7.
35. Vergari C, Chanteux L, Pietton R, et al. Shear wave elastography of lumbar annulus fibrosus in adolescent idiopathic scoliosis before and after surgical intervention. *European Radiology* 2020;30:1980–5.
36. Cannella M, Arthur A, Allen S, et al. The role of the nucleus pulposus in neutral zone human lumbar intervertebral disc mechanics. *Journal of Biomechanics* 2008;41:2104–11.
37. Shea M, Takeuchi TY, Wittenberg RH, et al. A comparison of the effects of automated percutaneous discectomy and conventional discectomy on intradiscal pressure, disk geometry, and stiffness. *Journal of Strength and Conditioning Research* 1994;8:317–25.
38. Kot BCW, Zhang ZJ, Lee AWC, et al. Elastic Modulus of Muscle and Tendon with Shear Wave Ultrasound Elastography: Variations with Different Technical Settings. *PLoS ONE*;7.
39. Deviren V, Berven S, Kleinstueck F, et al. Predictors of Flexibility and Pain Patterns in Thoracolumbar and Lumbar Idiopathic Scoliosis. *Spine* 2002;27:2346–9.
40. Huber M, Gilbert G, Roy J, et al. Sensitivity of MRI parameters within intervertebral discs to the severity of adolescent idiopathic scoliosis. *Journal of Magnetic Resonance Imaging* 2016;44:1123–31.
41. Dunn J, Henrikson NB, Morrison CC, et al. Screening for Adolescent Idiopathic Scoliosis. *JAMA* 2018;319:173.
42. Homans JF, Baldew VGM, Brink RC, et al. Scoliosis in association with the 22q11.2 deletion syndrome: An observational study. *Archives of Disease in Childhood* 2019;104:19–24.
43. Homans JF, de Reuver S, Breetvelt EJ, et al. The 22q11.2 deletion syndrome as a model for idiopathic scoliosis - A hypothesis. *Med Hypotheses* 2019;127:57–62.

## Appendix A

Search Syntax: The search was performed on October 15th 2021.

### Pubmed

("elastography"[Title/Abstract] OR "Elasticity Imaging Techniques"[MeSH Terms])

AND

("ultrasound"[Title/Abstract] OR "Ultrasonography"[Title/Abstract] OR  
"Ultrasonography"[MeSH Terms])

AND

("intervertebral disc"[Title/Abstract] OR "IVD"[Title/Abstract] OR "nucleus pulposus"[Title/  
Abstract] OR "annulus fibrosus"[Title/Abstract] OR "Intervertebral Disc"[MeSH Terms]  
OR "cartilage"[Title/Abstract] OR "Cartilage"[MeSH Terms] OR "spine"[Title/Abstract] OR  
"spine"[MeSH Terms] OR "scoliosis"[Title/Abstract] OR "scoliosis"[MeSH Terms])

Filters:

### Embase

('elastography':ti,ab,kw OR 'elastography'/exp)

AND

('ultrasound':ti,ab,kw OR 'ultrasound'/exp OR 'ultrasonography':ti,ab,kw OR  
'echography':ti,ab,kw OR 'echography'/exp)

AND

('intervertebral disc':ti,ab,kw OR 'IVD':ti,ab,kw OR 'nucleus pulposus':ti,ab,kw OR 'annulus  
fibrosus':ti,ab,kw OR 'intervertebral disk'/exp OR 'cartilage':ti,ab,kw OR 'cartilage'/exp OR  
'spine':ti,ab,kw OR 'spine'/exp OR 'scoliosis':ti,ab,kw OR 'scoliosis/exp')

Filters:

Publication type: article



## Appendix B

Quality assessment: The included studies were appraised using the AXIS appraisal tool for Cross-Sectional Studies (Downes et al. 2016).<sup>26</sup> The 20 scored criteria can be seen below:

| Articles                    | 1 | 2 | 3 | 4   | 5   | 6   | 7   | 8   | 9   | 10 | 11 | 12 | 13  | 14  | 15 | 16 | 17 | 18 | 19 | 20  |
|-----------------------------|---|---|---|-----|-----|-----|-----|-----|-----|----|----|----|-----|-----|----|----|----|----|----|-----|
| Vergari et al. (2013)       | √ | √ | × | n/a | n/a | n/a | n/a | n/a | n/a | √  | √  | √  | n/a | n/a | √  | √  | √  | ×  | √  | n/a |
| Vergari et al. (2014)       | √ | √ | √ | √   | √   | √   | n/a | √   | √   | √  | √  | √  | n/a | n/a | √  | √  | √  | √  | √  | √   |
| Vergari et al. (2014)       | √ | √ | × | n/a | n/a | n/a | n/a | n/a | n/a | √  | √  | √  | n/a | n/a | √  | √  | √  | ×  | ×  | n/a |
| Chotarvasseur et al. (2015) | √ | √ | × | n/a | n/a | n/a | n/a | n/a | n/a | √  | √  | √  | n/a | n/a | √  | √  | √  | ×  | ×  | n/a |
| Vergari et al. (2016)       | √ | √ | × | √   | √   | √   | n/a | √   | √   | √  | √  | √  | n/a | n/a | √  | √  | √  | √  | ×  | √   |
| Langlais et al. (2018)      | √ | √ | × | √   | √   | √   | n/a | √   | √   | √  | √  | √  | n/a | n/a | √  | √  | √  | √  | √  | √   |
| Vergari et al. (2020)       | √ | √ | × | √   | √   | √   | n/a | √   | √   | √  | √  | √  | n/a | n/a | √  | √  | √  | √  | √  | √   |

√ = yes; × = no; n/a = not applicable

### Introduction

1. Were the aims/objectives of the study clear?

### Methods

2. Was the study design appropriate for the states aim(s)?

3. Was the sample size justified?

4. Was the target/reference population clearly defined?
5. Was the sample frame taken from an appropriate population base so that it closely represented the target/reference population under investigation?
6. Was the selection process likely to select subjects/participants that were representative of the target/reference population under investigation?
7. Were measures undertaken to address and categorise non-responders?
8. Were the risk factor and outcome variables measured appropriate to the aims of the study?
9. Were the risk factor and outcome variables measured correctly using instruments/measurements that had been trialed, piloted or published previously?
10. Is it clear what was used to determine statistical significance and/or precision estimates?
11. Were the methods (including statistical methods) sufficiently described to enable them to be repeated?

#### Results

12. Were the basic data adequately described?
13. Does the response rate raise concerns about non-response bias?
14. If appropriate, was information about non-responders described?
15. Were the results internally consistent?
16. Were the results presented for all the analyses described in the methods?

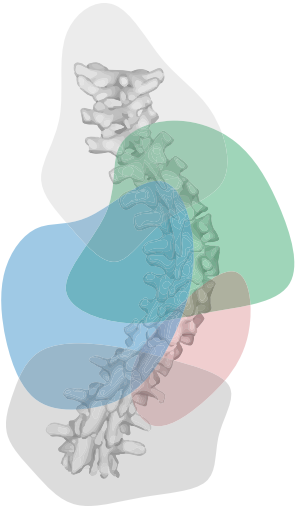
#### Discussion

17. Were the authors' discussions and conclusions justified by the results?
18. Were the limitations of the study discussed?

#### Other

19. Were there not any funding sources or conflicts of interest that may affect the authors' interpretation of results?
20. Was ethical approval or consent of participants attained?



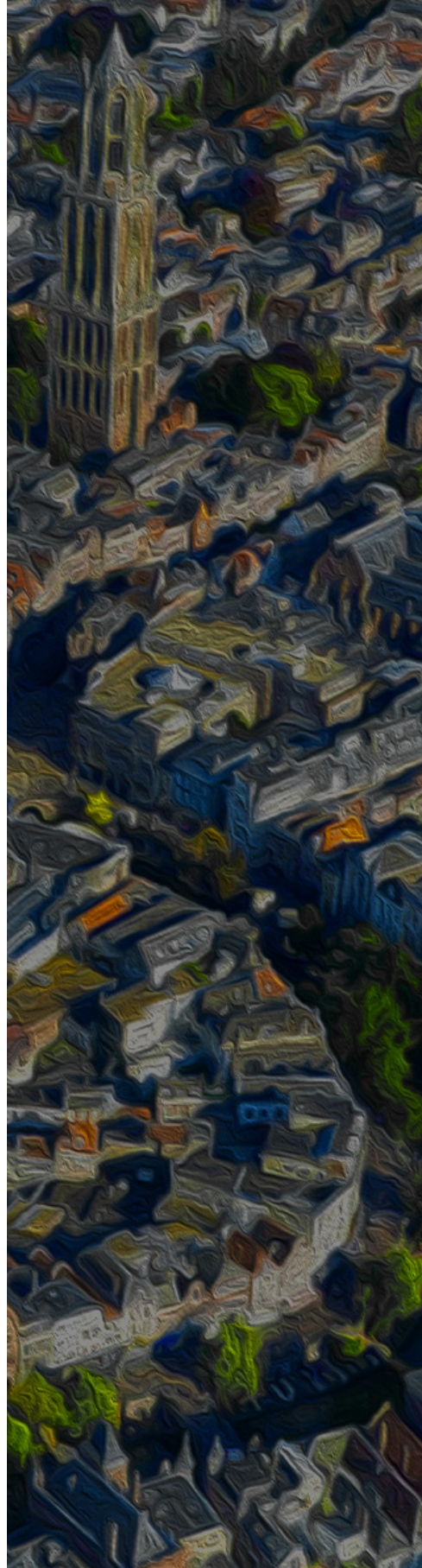


# 19

## Sagittal Curvature of the Spine as a Predictor for Pediatric Spinal Deformity Development

Saba Pasha  
Steven de Reuver  
Jelle F. Homans  
René M. Castelein

*Spine Deformity. 2021 Jul;9(4):923-932.*



## ABSTRACT

**Introduction.** The sagittal curvature of the spine is hypothesized to play an important role in induction of spinal deformities in adolescent idiopathic scoliosis. We previously showed an S shaped flexible rod, with the same curvature as the pediatric sagittal spinal curve, produces scoliotic-like deformities under physiologic loading. Yet, detailed characteristics of the pediatric sagittal spinal curves associated with higher risk of scoliosis are not well defined.

**Methods.** A total of 32 patients in a population with a high prevalence of idiopathic-like scoliosis, 22q11.2 deletion syndrome (22q), were included and followed up for at least two-years. We developed a reduced order finite element model (FEM) of the sagittal profile of these 32 patients where the spine was modeled as an S shaped elastic rod. We related the geometrical parameters of the sagittal curves and the deformed FEM of the corresponding S shaped rods to the risk of scoliosis development at two-year follow-up in this cohort.

**Results.** Variations in the sagittal curvature in the cohort of 22q patients resulted in five different deformity patterns shown by finite element analyses. Two sagittal plane deformity pattern groups had high rate of scoliosis development (86% and 100%) whereas the other 3 groups had less than 50% rate of scoliosis development (40%, 33%, and 0%). The pre-scoliotic position of the inflection point (where lordosis turns into kyphosis), the ratio of the spinal curvatures above and below the inflection point, and the length of the spinal curve above and below the inflection point were significantly different between the five deformity patterns groups,  $p < 0.05$ .

**Conclusion.** Combination of geometrical parameters of the sagittal profile prior to onset of scoliosis can relate to the development of spinal deformity in pediatric population.

## Introduction

Adolescent idiopathic scoliosis (AIS) presents as a 3D deformity of the spinal column with an onset around puberty in otherwise healthy adolescents.<sup>1</sup> Understanding the pathogenesis of the disease is the first step in developing methods for early diagnosis, prevention, and effective management of the condition. Several hypotheses have been proposed on the pathogenesis of the spinal deformity development in AIS.<sup>2-5</sup> Among these theories, the sagittal curvature of the spine is believed to play a role in induction of scoliosis.<sup>6-9</sup> Posteriorly inclined vertebrae were thought to cause rotational instability due to posteriorly directed shear load in a slightly pre-rotated spine.<sup>2,6</sup> Another theory, the rod theory, borrowed concepts from mechanics of the slender rod deformation to explain the patterns of the spinal deformity development in AIS from a mechanical standpoint alone.<sup>8</sup> Based on this theory, where spine is modeled as an S shaped elastic slender rod, the overall shape of the sagittal profile of the spine during the period of fast growth can dictate the mechanical loading of the spine and the 3D deformation patterns.<sup>9</sup> It was shown analytically that such S shaped curve deforms in 3D under physiological loading where the deformation patterns are a function of the geometrical parameters of rod including the magnitude of the two opposing curvatures and the position of the inflection point.<sup>7-10</sup> It remains to determine whether the geometrical parameters of the spinal sagittal curve can be biomarkers of the spinal deformity development in juvenile patients.

As AIS occurs in non-symptomatic children access to pediatric spinal radiographs prior to the onset of scoliosis are scarce. To overcome this problem, we use a pediatric cohort with a high prevalence of scoliosis that strongly resembles AIS i.e., 22q11.2 deletion syndrome (22q),<sup>11</sup> in order to determine whether specific patterns of the sagittal curvature of the pre-scoliotic patients can be linked to the risk of spinal deformity development. By studying this population, we evaluate the role of the geometrical parameters as manifested in the sagittal curvature of the spine prior to onset of the spinal deformity development using the rod theory to determine the mechanical biomarkers of the disease. The goal of the study was to evaluate the relationship between the geometrical parameters of the sagittal curvature of the spine prior to onset of scoliosis and the risk of spinal deformity development in a cohort of 22q patients. However, as the geometrical parameters of the sagittal curves dictate the mechanical loading of the rod in a non-linear fashion,<sup>7,9,10</sup> instead of relating the sagittal curve parameters and the risk of scoliosis directly, we related the deformation patterns of the S shaped rods (sagittal curvature) to the risk of scoliosis. We hypothesized that deformation patterns relate to the sagittal curvature parameters of the spine and are significantly different between the scoliotic and non-scoliotic children.

## Methods

### Study population

All eligible patients before the onset of scoliosis were included from an ongoing prospective cohort study on orthopedic manifestations in 22q, which is part of the outpatient 22q clinic of a tertiary university medical center and approved by the local Research Ethics Board. The inclusion criteria were a confirmed 22q deletion following genomic testing, available coronal and sagittal spinal radiographs prior to skeletal maturity (age of 8–10 years and Risser sign of 0) and without scoliosis (Cobb angle  $< 10^\circ$ ), and at least two-year follow-up. Spinal radiographs with pelvic rotation or any hand positioning other than finger tips on the zygomatic bone or clavicles were excluded.<sup>12</sup> Patients with any other known musculoskeletal or neuromuscular conditions were excluded. The two year follow up images were used to determine whether the patient developed a spinal curve exceeding  $10^\circ$  using the Cobb method.<sup>13</sup> These follow up images were used to group the patients into scoliotic and non-scoliotic groups.

### Sagittal profile characteristics

A medical student determined the vertebral centroids manually. The 2D coordinates of the sagittal spinal radiographs were stored using a program developed in MATLAB (The MathWorks Inc, Natick, Massachusetts). These centroids were connected to determine the sagittal spinal centerline. The centerlines were multiplied by the same factor in all directions in a way that normalized height was achieved (T1–L5 distance).<sup>14</sup> The sagittal profile was characterized by the following four geometric parameters, as shown in **Figure 1**. The first three parameters were selected as they uniquely define the S shape curvature of the spine and were shown previously to impact the mechanical loading of the curved rod.<sup>7–10</sup> The fourth parameter was also added as it had been suggested to play a role in induction of scoliosis in clinical studies.<sup>2,15</sup>

1. The position of the inflection point This point was determined as the vertebral level at which the direction of the spinal curvature changed. The position of the inflection point was presented as the number of the vertebrae between the T1 and the inflection point.

2. The ratio of the spinal positive and negative curvatures The curvature of the 2D sagittal spinal centerline was calculated discretely at each vertebral level using three consecutive points on the spinal centerline by calculating the radius of the oscillating circle that best fits the sagittal curvature at each point (**Figure 1**).<sup>16</sup> As such, the curvatures at T1 and L5 were not calculated. The ratio was calculated as the mean curvatures of the curve above the inflection point ( $k_1$ ) divided by the mean of curvature magnitudes below the inflection points ( $k_2$ ). The mean curvature in each segment is calculated by averaging the curvature values of all the vertebral levels in that section of the spine.



3. The ratio of the spinal lengths above and below the inflection point. This ratio determines the arc length of the 2D sagittal curves above the inflection point ( $L_1$ ) divided by the arc length below the inflection point ( $L_2$ ).

4. The posteriorly inclined spine. The posteriorly inclined spine was determined by the direction of the curvature vectors, which is perpendicular to the centerline at each vertebral level. A curvature vector in the first (both X and Y in positive directions) or third (both X and Y in negative directions) quadrant of the coordinate system determined the posteriorly inclined section of the spine (**Figure 1**).

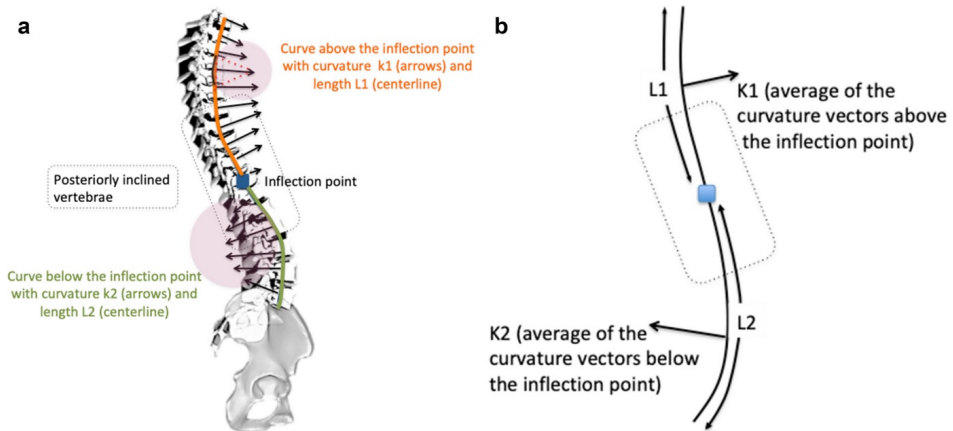


**Figure 1.** The sagittal characteristic of the spine. The position of the inflection point and spinal curvature at each vertebral level are shown. The curvature is maximal at the sagittal apices and the smallest at the area close to the inflection point. The posteriorly inclined vertebrae were determined based on the alignment of the curvature vectors.

#### Reduced-order finite element model of the S shaped (sagittal curve) rods

The sagittal curve of the spinal centerlines of the cohort at the first visit was used to develop a reduce-order finite element model of the spine.<sup>8</sup> The model was described before in details and the main components of it are as follows: This model consists of an S shaped elastic isotropic rod model with a circular cross section of 1 mm, Young's modulus of 1000P, and Poisson ratio of 0.3.<sup>8</sup> Gravitational load, to simulate the weight,<sup>17</sup> and a small axial torsion along the Z-axis ( $1e-4$  N-mm), to allow 3D deformation,<sup>18</sup> were applied to the rod model. The L5 was fixed in space and the T1 was allowed to only move vertically.<sup>8</sup> These variables generated rod deformations that were representative of the scoliotic spinal deformity<sup>7-10</sup> and the deformation patterns resembled the spinal deformity in scoliosis.<sup>8,9</sup>

A finite element model, as described, was developed for each of the patients at the first visit, using the isotropically normalized sagittal curves. The axial projection of the deformed S shaped rod, representing each patient, as a result of this simulation. The patterns of deformation of each of the curved rods (sagittal curves) were clustered based on the deformation shape (loop versus lemniscate) and proximity of the loop shaped deformations to each of the axes' of the coordinate system ( $\pm X$  and  $\pm Y$  axes). The geometrical characteristics of the sagittal profile corresponding to different axial deformation patterns were determined using the four aforementioned sagittal parameters (inflection point, curvature ratios, length ratios, and length of the posteriorly inclined section of the spine).

### Statistical analyses

The sagittal profile characteristics at the first visit were compared between the non-scoliotic and scoliotic subgroups using a Mann–Whitney U test. The sagittal profile characteristics of the axial subtypes, determined from the finite element analysis of the elastic rod model, were also compared statistically using a Kruskal–Wallis test followed by a Dunn test. Finally, the prevalence of scoliosis in each of the axial subtypes was determined and compared between the male and female patients in each group.

Our methodology as such follows these steps: (1) Medical image acquisition of the non-scoliotic 22q patients, (2) Centerline identification, (3) Developing the finite element model of the centerlines and determining the deformity pattern subtypes. (4) Calculating 5 discrete parameters of the sagittal curvature in each of the deformity pattern subtypes, and finally (5) Relating the sagittal curvature parameters to the risk of spinal deformity development at two year follow-up in each of the deformity pattern types.

## **Results**

### Study population

32 patients out of 150 patients in the database met the inclusion criteria and were included in the study. 16 patients developed a scoliotic curve and 16 did not show a spinal deformity exceeding  $10^\circ$  at two-year follow up. Patients with scoliosis at the final visit are marked (**Figure 2**).

The summary statistics of the patients' age, skeletal age (Risser sign), and the main curve severity at the first and most recent visits are summarized in **Table 1**. The age, Risser sign, and Cobb angle were significantly different between the two visits,  $p < 0.05$ .

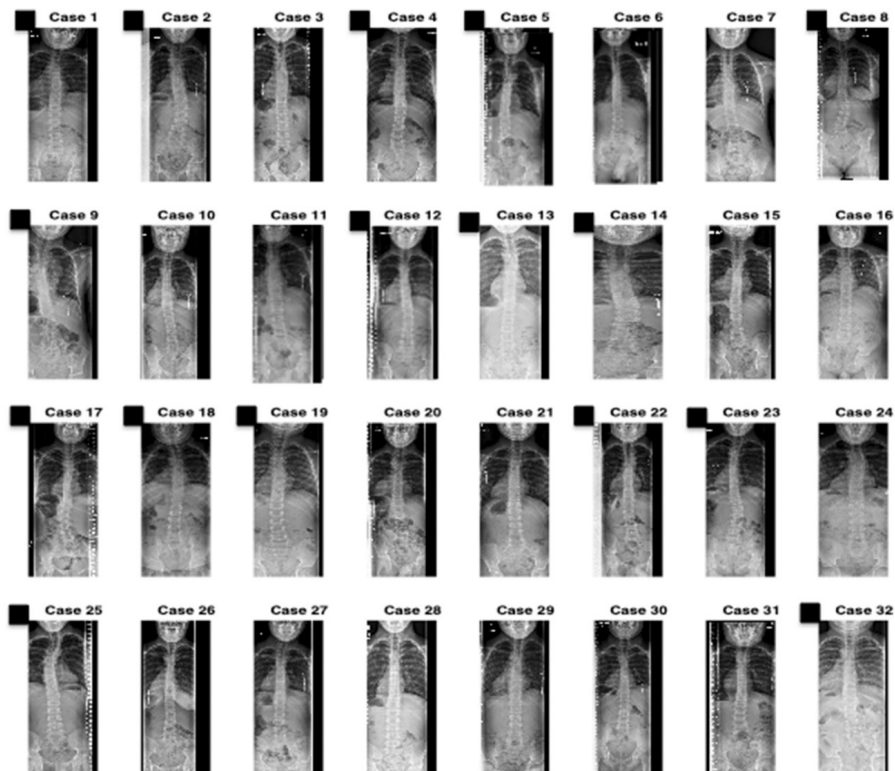


**Figure 2.** The frontal curves at the most recent follow up

| Visit                 | Parameters                     | Total $N=32$    | Non-scoliotic  |                | Scoliotic       |                |
|-----------------------|--------------------------------|-----------------|----------------|----------------|-----------------|----------------|
|                       |                                |                 | Female, $n=7$  | Male, $n=12$   | Female, $n=5$   | Male, $n=8$    |
| First visit           | Age (Year)                     | $10.4 \pm 2.3$  | $9.9 \pm 2.7$  | $10.7 \pm 2.3$ | $10.4 \pm 1.6$  | $10.5 \pm 2.6$ |
|                       | Risser sign                    | 0               | 0              | 0              | 0               | 0              |
|                       | Main Cobb angle ( $^{\circ}$ ) | $< 10$          | $< 10$         | $< 10$         | $< 10$          | $< 10$         |
| Most recent follow-up | Age (Year)                     | $14.2 \pm 2.4$  | $13.0 \pm 2.2$ | $14.2 \pm 2.7$ | $15.3 \pm 1.5$  | $14.6 \pm 2.2$ |
|                       | Risser sign                    | $1.6 \pm 1.8$   | $1.0 \pm 1.2$  | $1.7 \pm 1.8$  | $2.7 \pm 1.1$   | $1.6 \pm 2.2$  |
|                       | Main Cobb angle ( $^{\circ}$ ) | $19.2 \pm 12.1$ | $< 10$         | $< 10$         | $24.6 \pm 18.3$ | $15.8 \pm 4.5$ |

**Table 1.** Summary of the demographic data in the scoliotic and non-scoliotic cohorts

### Sagittal curvature of scoliotic versus non-scoliotic patients

The inflection point and the magnitude of curvature at each vertebral level (length of the black vectors) are shown in, the four sagittal geometrical parameters were not significantly different between the scoliotic and non-scoliotic groups,  $p > 0.05$  (**Figure 3**).

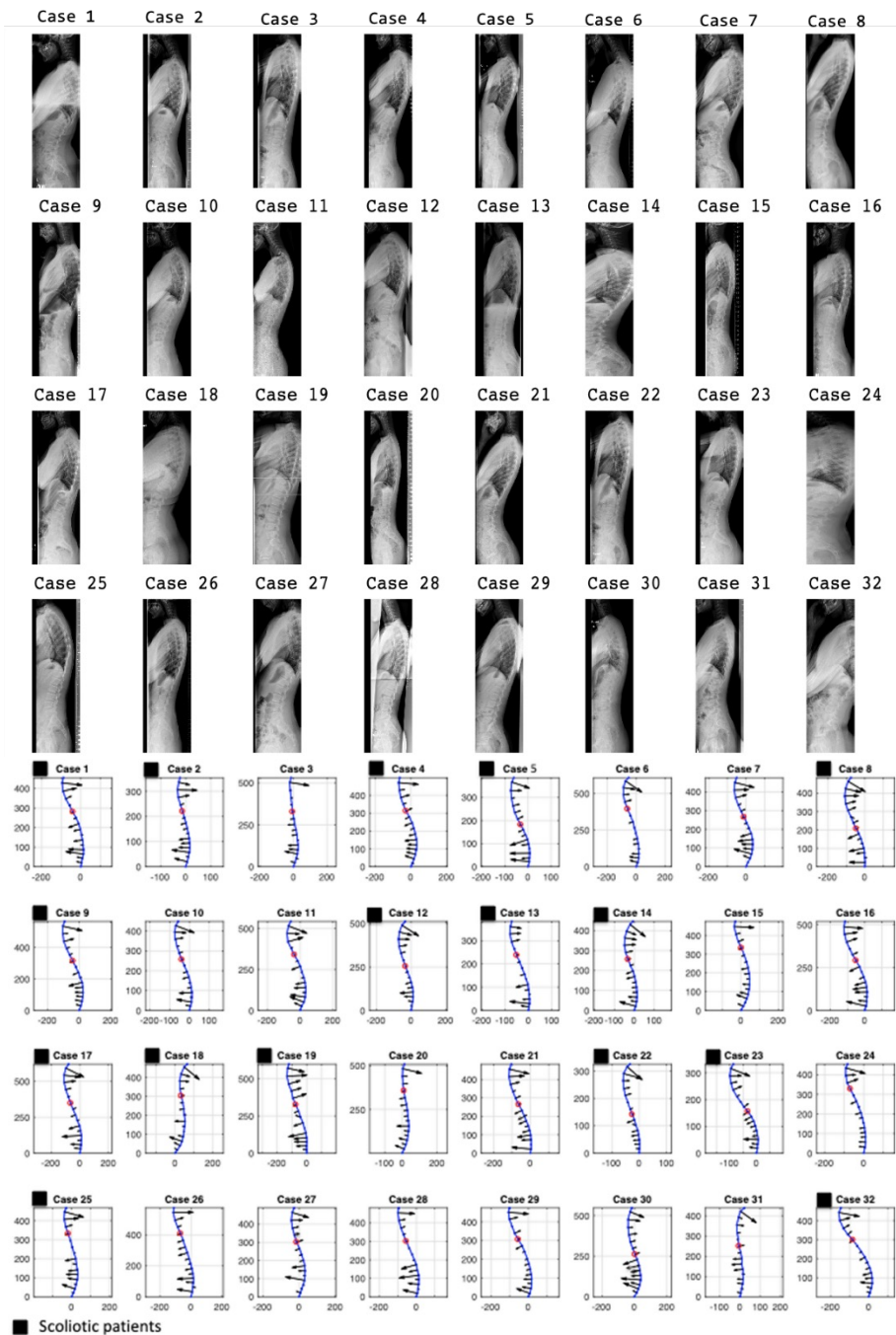


**Figure 3.** Above: the sagittal curvature of the cohort. Below: the position of the inflection point (red circle) and the curvature of the sagittal profile at each vertebral level are shown (black vectors). The lengths of the vector represent the magnitude of the curvature.

Elastic rod model and axial deformation patterns classification

The average of different axial projection patterns after deformation of the elastic rod models and average sagittal profile associated with each axial group is shown in **Figure 4**. A total of 5 different axial projection patterns were determined. **Table 2** summarizes the sagittal curvatures parameters associated with each of these axial projections. The position of the inflection point and the L1/L2 ratio were significantly different between Types 2 and 5,  $p < 0.05$ . The k1/k2 curvature ratios were significantly different between types 3 and 4,  $p < 0.05$ . Type 1 had the highest and type 4 had the lowest number of posteriorly inclined vertebrae but the differences were not statistically significant,  $p > 0.05$ . **Figure 5** shows these axial deformation patterns for each rod model based on the sagittal curvature of the 32 patients.

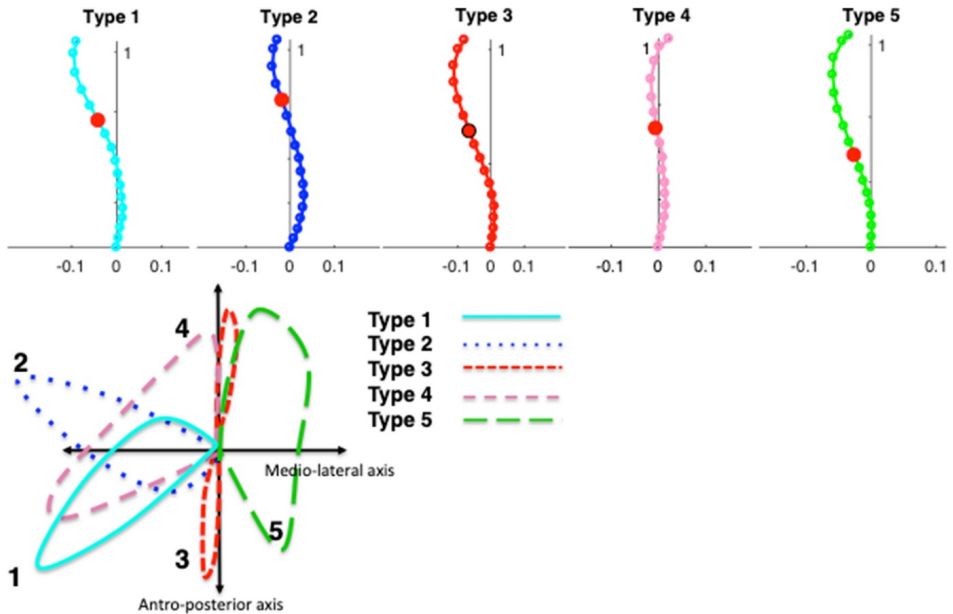


**Figure 4.** The average of the axial deformation patterns of the 2D S shaped elastic rods. Types 1, 2, 4, and 5 had a loop shaped projection. Type 3 had a lemniscate projection. Types 1, 2, and 4 were deformed to the left side as opposed to the type 5, which was deformed to the right side. Type 1 and 2 had an elongated shape along the medio-lateral axis and were almost mirror-image of each other with respect to the medio-lateral axis. Type 3 had similar deformed lengths along the medio-lateral and antro-posterior axes. The sagittal curvatures associated with each axial type are presented in Table 2.

| Axial subgroup | Inflection point (vertebral level) | Curvature ratio $k1/k2$ | Length ratio $L1/L2$ | Number of Posteriorly inclined vertebrae |
|----------------|------------------------------------|-------------------------|----------------------|--|
| $n=10$         | $6.1 \pm 0.5$                      | $1.5 \pm 0.3$           | $0.8 \pm 0.2$        | $8.3 \pm 1.3$                            |
| $n=9$          | $5.8 \pm 1.1^*$                    | $1.4 \pm 0.7$           | $0.6 \pm 0.3^*$      | $8.0 \pm 2.0$                            |
| $n=7$          | $7.5 \pm 1.0$                      | $1.4 \pm 0.5^*$         | $1.0 \pm 0.2$        | $6.8 \pm 2.4$                            |
| $n=3$          | $6.7 \pm 0.5$                      | $1.9 \pm 0.4^*$         | $0.9 \pm 0.1$        | $6.5 \pm 3.7$                            |
| $n=3$          | $8.5 \pm 0.2^*$                    | $1.5 \pm 0.3$           | $1.5 \pm 0.3^*$      | $7.0 \pm 0.9$                            |

**Table 2.** The sagittal curve characteristics in the 5 axial subtypes of the rod models. \*Statistically significant differences ( $p < 0.05$ ).

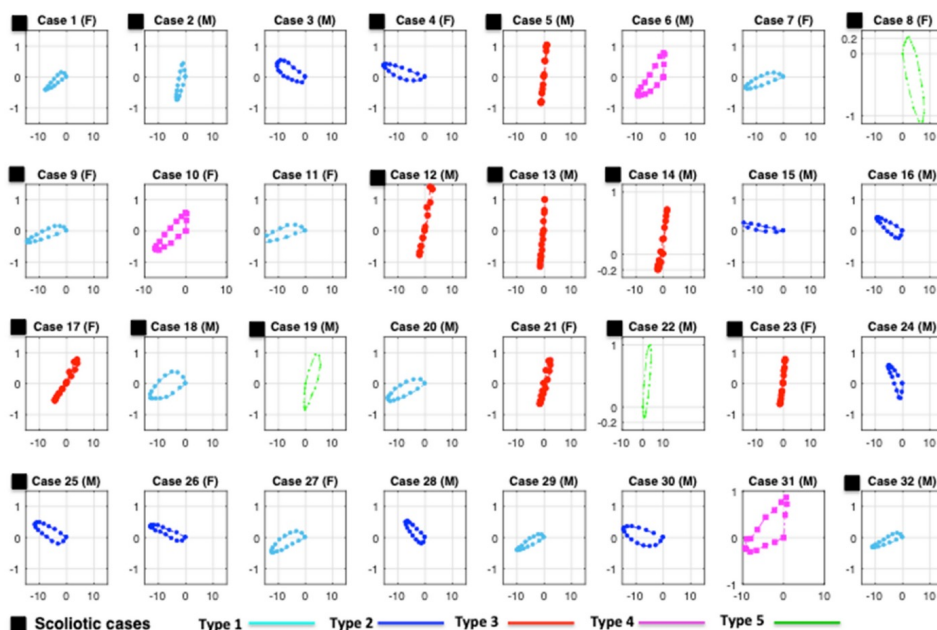


**Figure 5.** The axial deformation patterns of the rod models based on the sagittal curves of the cohort at their first visit. None of the patients had scoliosis at this stage. Scoliotic patients are marked.

Prevalence of scoliosis in the axial subtypes

**Table 3** summarizes the number of scoliotic and non-scoliotic patients in each of the axial subtypes along with their sagittal curve characteristics. None of the patients in Type 4 developed scoliosis while all patients in Type 5 developed scoliosis (**Figure 5**). Only one out of 7 patients in Type 3 was non-scoliotic.

| Axial subgroup       | Inflection point (vertebral level) | Curvature ratio k1/k2 | Length ratio L1/L2   | Number of posteriorly inclined vertebrae |
|----------------------|------------------------------------|-----------------------|----------------------|--|
| <i>Scoliotic</i>     |                                    |                       |                      |  |
| n=4, 40%             | 6.3±0.5                            | 1.6±0.2**             | 0.7±0.2 <sup>§</sup> | 8.5±1.0                                  |
| n=3, 33%             | 5.3±0.5 <sup>¶</sup>               | 2.1±0.8*              | 0.5±0.1 <sup>§</sup> | 7.3±1.5                                  |
| n=6, 86%             | 7.4±1.1                            | 1.3±0.5               | 1.0±0.2              | 6.6±2.6                                  |
| n=0, 0%              | –                                  | –                     | –                    | –  |
| n=3, 100%            | 8.5±0.2                            | 1.5±0.3               | 1.5±0.3 <sup>§</sup> | 7.0±0.9                                  |
| <i>Non-scoliotic</i> |                                    |                       |                      |  |
| n=6, 60%             | 6.3±0.6                            | 1.3±0.2**             | 0.8±0.3              | 8.2±1.5                                  |
| n=6, 67%             | 5.3±1.2                            | 1.0±0.2*              | 0.7±0.3              | 8.3±2.2                                  |
| n=1, 14%             | 8.0±0.0                            | 1.6±0.0               | 1.1±0.0              | 8.0±0.0                                  |
| n=3, 100%            | 6.7±0.5                            | 1.9±0.4               | 0.9±0.1              | 6.5±3.7                                  |
| n=0, 0%              | –                                  | –                     | –                    | –  |

**Table 3.** Sagittal curve characteristics in the scoliotic and non-scoliotic patients in each of the axial subgroups. Significantly different pair of variables are marked with the same symbol ( $p < 0.05$ ).

The position of the inflection point and L1/L2 ratio were significantly different between the Types 1 and 2 and Type 5 only in the scoliotic group,  $p < 0.05$  and k1/k2 ratios was higher in the scoliotic patients in Type1 and Type 2 compared to the non-scoliotic patients in these two types (**Table 3**). The one non-scoliotic patient in type 3 was not statistically compared with the scoliotic patients in this subtype.

#### Sex-specific sagittal profiles

Table 4 summarizes the rate of scoliosis in each of these 5 groups for male and female patients separately. Types 3 and 5 had the highest rate of scoliosis, 86% and 100%, respectively of which 100% of the female patients in these two types developed a scoliotic curve at the most recent follow-up (**Figure 2**). The prevalence of scoliosis in Types 1 and 2 remained lower than 50% for both male and female patients except for male patients in Type 1, which was at 60%.

| Cluster | Scoliotic cases (Number and percent) | Prevalence of scoliosis in male patients within each cluster (%) | Prevalence of scoliosis in female patients within each cluster |
|---------|--------------------------------------|--|--|
| n=10    | n=4, 40%                             | 60   | 20   |
| n=9     | n=3, 33%                             | 29   | 50   |
| n=7     | n=6, 85%                             | 60   | 100  |
| n=3     | n=0, 0%                              | 0  | 0  |
| n=3     | n=3, 100%                            | 100  | 100  |

**Table 4.** The prevalence of scoliosis in each axial subtypes of the rod model for male and female patients.



## Discussion

We used a mechanical model of the spine to show how different sagittal curvatures of the spine in a pediatric population deform in different patterns. We also showed some of these deformation patterns are linked to higher risk of scoliosis development (Types 3 and 5) while other deformation patterns had below 50% risk of deformity development at two-year follow-up (Types 1, 2, and 4). Several hypotheses have been proposed to explain the pathogenesis of scoliosis.<sup>5,6,14,19-22</sup> Genetic factors were suggested on the ground of familial occurrence of the disease and were tested in several animal models.<sup>5,19,20</sup> Biomechanical factors of the upright spine were particularly emphasized, as scoliosis and bipedalism are unique to human.<sup>2</sup> The sagittal curvature of the spine was shown to vary between the scoliotic and non-scoliotic patients at early stage of deformity development.<sup>6,14,21</sup> However, specific parameters of the sagittal curve that differentiate between the scoliotic and non-scoliotic patients were not quantified. In an analytical model of the S shaped rods under bending and torsion, it was shown that the deformation patterns of the rod could be due to variations in the position of the inflection point of the S shaped curve and the magnitude of the rod curvature above and below the inflection point,<sup>7,9,10,14</sup> because these parameters impact the magnitude and direction of the moments that deform the rod in 3D.<sup>7,9,10</sup> However, in the current study, instead of using the sagittal parameters directly, we used the axial deformation subtypes to determine the groups with higher risk of scoliosis. This is because the geometrical parameters of a curved rod are non-linearly related to the mechanical loading of the rod. Since the mechanical loading of the rod changes as the rod deforms, the final shape of the deformed rod can be a better presentation of the mechanical loading of the rod. This was confirmed in our results when the four geometrical parameters of the sagittal curvature of the spine were compared between the scoliotic and non-scoliotic types and no significant difference was found but the axial deformity pattern types were associated with increased risk of scoliosis (**Table 3**).

Our analysis determined deformation groups associated with high (Types 3 and 5) and low (Types 1, 2, 4) risk of scoliosis development. By comparing the scoliotic and non-scoliotic patients in Types 1 and 2, we learned that in these two groups a higher  $k_1/k_2$  ratio, while the  $L_1/L_2$  remains the same, is linked to scoliosis development (**Table 3**). A higher  $k_1$  with respect to  $k_2$  may allow a larger posterior translation of segment of the spine while still keep the head above the pelvis. This also relates to previous observation where a posteriorly inclined spine was observed in the sagittal profile of the early stage AIS patients.<sup>6</sup> Only one patient in Type 3 was non-scoliotic which makes the comparison between the scoliotic and non-scoliotic sagittal curve patterns challenging (**Table 3**). In Type 4 as the arc length of kyphotic and lordotic sections becomes close to equal (increase in  $L_1/L_2$  with respect the Type 1–3), transition between the  $k_1$  and  $k_2$ , may occur over a longer arclength which makes the changes in the curvature between the lordotic and kyphotic spine smoother (**Figure 4**). In comparison to Type 4, as the inflection point moves lower in the spine in Type 5 ( $L_1/L_2 = 1.5$ ),



the reverse of the sagittal profile in Types 1 and 2 is observed; a larger kyphotic curve connects to a smaller lordosis with an arc length without curvature connecting the two curves. This sagittal type was shown previously to result in a loop shaped axial projection associate with lumbar scoliotic patients.<sup>7</sup> As also shown in **Figure 2**, cases 8, 19 and 22 with this sagittal curve type (Type 5) all have a thoracolumbar/lumbar deformity. Finally, we should add that in an analytical rod various S shaped curvatures may endure the same mechanical loading resulting in similar deformation patterns. However, the sagittal curve patterns that can be adopted by human spine are limited compared to the theoretically produced curve patterns. This can justify why some sagittal curve patterns associated with higher risk of scoliosis could be detected.

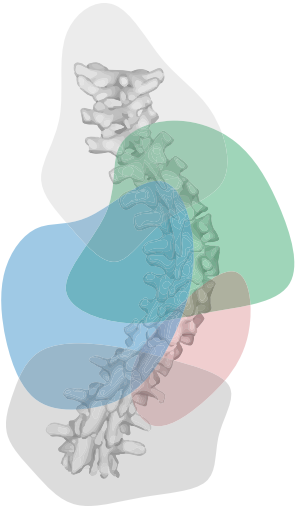
Limitations of the study are small cohort and short follow-up. 22q patients, as a patient group with a high prevalence of scoliosis,<sup>11</sup> were used as a model to study risk of pediatric idiopathic scoliosis in this study as access to the pre-scoliotic images are challenging in the normal population. We acknowledge that, although 22q patients have AIS-like deformity,<sup>11</sup> their curve patterns and the thus the sagittal curves leading to such curve patterns may vary from the AIS patients. Application of radiation free imaging modalities can be an attractive alternative, which allows a more comprehensive analysis of the sagittal curvature in the normal population. Longer follow-ups are required to determine if the slight deformities at the most recent follow-up (**Figure 2**) can lead to curve severity ranges that require bracing or surgery. The role of growth as a factor that can be linked to risk of scoliosis development in different sagittal curve types was not considered and will be the subject of our future work. We only analyzed the role of the sagittal curvature on the 3D deformation of the pediatric spine. It should be noted that scoliosis occurs if the increase in the moments due to a specific shape of the spine is not tolerated by the stabilizing mechanisms of the spine, i.e. discs and muscles. While the shape of the sagittal curve can be a factor that dictates the mechanical loading of the spine, the mismatch between the loading and stabilizing forces should be also considered when evaluating the mechanical factors associated with spinal deformity. We underline that this analysis was performed using standardized standing radiographs where special attention was paid to patients arm positioning,<sup>12</sup> as such other arm positing (hands on the wall or a bar) may adversely impact the result of this analysis.

In conclusion, geometrical parameters of the sagittal curve, namely the position of inflection point,  $k_1/k_2$  ratio and L1/L2 ratio, were different between the five axial deformity pattern groups. Two of the deformity pattern groups had a high prevalence of scoliosis while other three had less than 50% rate of spinal deformity development. The early screening, particularly using non-ionized imaging modalities in the normal population can be a reasonable future step to better identify the sagittal profile parameters associated with pediatric scoliosis with a potential use in early diagnosis of pediatric scoliosis.

## References

1. Roaf R (1966) The basic anatomy of scoliosis. *J Bone Joint Surg Br* 48:786–792
2. Kouwenhoven JW, Smit TH, van der Veen AJ, Kingma I, van Dieën JH, Castelein RM (2007) Effects of dorsal versus ventral shear loads on the rotational stability of the thoracic spine: a biomechanical porcine and human cadaveric study. *Spine (Phila Pa 1976)* 32:2545–2550.
3. Stokes IA, Burwell RG, Dangerfeld PH, IBSE, (2006) Biomechanical spinal growth modulation and progressive adolescent scoliosis—a test of the “vicious cycle” pathogenetic hypothesis: summary of an electronic focus group debate of the IBSE. *Scoliosis* 1:16.
4. Guo X, Chau WW, Chan YL, Cheng JC (2003) Relative anterior spinal overgrowth in adolescent idiopathic scoliosis. Results of disproportionate endochondral-membranous bone growth. *J Bone Joint Surg Br* 85:1026–1031.
5. Burwell RG (2003) Aetiology of idiopathic scoliosis: current concepts. *Pediatr Rehabil* 6:137–170.
6. Schlösser TP, Shah SA, Reichard SJ, Rogers K, Vincken KL, Castelein RM (2014) Differences in early sagittal plane alignment between thoracic and lumbar adolescent idiopathic scoliosis. *Spine J* 14:282–290.
7. Neelakantan S, Purohit PK, Pasha S (2020) A Semi-Analytic Elastic Rod Model of Pediatric Spinal Deformity. *J Biomech Eng*.
8. Pasha S (2019) 3D Deformation Patterns of S Shaped Elastic Rods as a Pathogenesis Model for Spinal Deformity in Adolescent Idiopathic Scoliosis In. *Scientific Reports* 9(1):16485
9. Pasha S (2020) What causes different coronal curve patterns in idiopathic scoliosis? *bioRxiv*.
10. Neelakantan S, Purohit PK, Pasha S (2020) A reduced-order model of the spine to study pediatric scoliosis. *Biomech Model Mechanobiol*.
11. Homans JF, Baldew VGM, Brink RC, Kruyt MC, Schlösser TPC, Houben ML, Deeney VFX, Crowley TB, Castelein RM, McDonald-McGinn DM (2019) Scoliosis in association with the 22q11.2 deletion syndrome: an observational study. *Arch Dis Child* 104:19–24.
12. Pasha S, Capraro A, Cahill PJ, Dormans JP, Flynn JM (2016) Biplanar spinal stereoradiography of adolescent idiopathic scoliosis: considerations in 3D alignment and functional balance. *Eur Spine J* 25:3234–3241.
13. Cobb J (1948) Outline for the study of scoliosis. *Am Acad Orthop Surg Inst Lect* 5:261–275
14. Pasha S, Hassanzadeh P, Ecker M, Ho V (2019) A hierarchical classification of adolescent idiopathic scoliosis: Identifying the distinguishing features in 3D spinal deformities. *PLoS ONE* 14:e0213406.
15. Castelein RM, van Dieën JH, Smit TH (2005) The role of dorsal shear forces in the pathogenesis of adolescent idiopathic scoliosis—a hypothesis. *Med Hypotheses* 65:501–508.
16. Legar JC (1999) Menger curvature and rectifiability. *Ann Math* 149:831–869
17. Pasha S, Aubin CE, Labelle H, Parent S, Mac-Thiong JM (2015) The biomechanical effects of spinal fusion on the sacral loading in adolescent idiopathic scoliosis. *Clin Biomech (Bristol, Avon)* 30:981–987.
18. de Reuver S, Brink RC, Homans JF, Kruyt MC, van Stralen M, Schlösser TPC, Castelein RM (2019) The Changing Position of the Center of Mass of the Thorax During Growth in Relation to Pre-existent Vertebral Rotation. *Spine (Phila Pa 1976)* 44:679–684
19. Londono D, Kou I, Johnson TA, Sharma S, Ogura Y, Tsunoda T, Takahashi A, Matsumoto M, Herring JA, Lam TP, Wang X, Tam EM, Song YQ, Fan YH, Chan D, Cheah KS, Qiu X, Jiang H, Huang D, TSRHC IS Clinical Group, International Consortium for Scoliosis Genetics, Su P, Sham P, Cheung KM, Luk KD, Gordon D, Qiu Y, Cheng J, Tang N, Ikegawa S, Wise CA, Group JSCR (2014) A meta-analysis identifies adolescent idiopathic scoliosis association with LBX1 locus in multiple ethnic groups. *J Med Genet* 51:401–406.
20. Xu L, Wu Z, Xia C, Tang N, Cheng JCY, Qiu Y, Zhu Z (2019) A Genetic Predictive Model Estimating the Risk of Developing Adolescent Idiopathic Scoliosis. *Curr Genomics* 20:246–251.
21. Pasha S, Baldwin K (2019) Preoperative Sagittal Spinal Profile of Adolescent Idiopathic Scoliosis Lenke Types and Non-Scoliotic Adolescents: A Systematic Review and Meta-Analysis. *Spine (Phila Pa 1976)* 44:134–142.
22. Castelein RM, Pasha S, Cheng JCY, Dubousset J (2020) Idiopathic Scoliosis as a Rotatory Decomensation of the Spine. *J Bone Miner Res* 35 (10):1850–1857



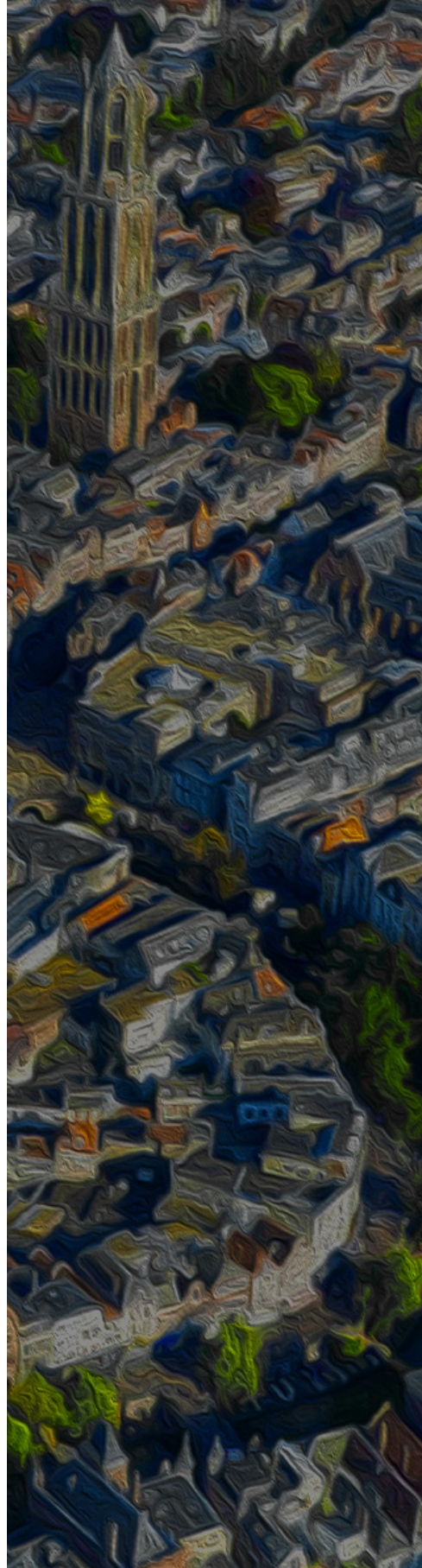


# 20

Early Sagittal Shape of the Spine  
Predicts Scoliosis Development in  
a Syndromic Population:  
a Prospective Longitudinal Study

Steven de Reuver  
Jelle F. Homans  
Michiel L. Houben  
Tom P.C. Schlösser  
Keita Ito  
Moyo C. Kruyt  
René M. Castelein

*Under Peer-review.*



## ABSTRACT

**Background.** Scoliosis is a deformation of the spine and trunk that, in its more severe forms, creates a life-long burden of disease and requires intensive treatment. Only for congenital scoliosis the cause is unequivocal; aberrant development of vertebrae leads to an unphysiological curvature of the spine. In neuromuscular and syndromic scoliosis, there is an associated recognizable condition, but the patho-mechanism of spinal decompensation remains elusive. For adolescent idiopathic scoliosis, no underlying condition can be defined, and the patho-mechanism is even more of a mystery. In this study, the early sagittal shape of the spine before scoliosis onset is defined and related to later scoliosis development, in a population with 22q11 deletion syndrome. These children have, amongst other features, a 50% chance of developing scoliosis that shares characteristics with idiopathic scoliosis: age of onset, curve morphology, and progression rate.

**Methods.** This is a prospective cohort study of patients with 22q11.2 deletion syndrome that were followed with spinal radiographs during adolescent growth. All children that initially had no scoliosis at skeletally immaturity (risser 0-1), and were followed with spinal radiographs at 2 year intervals until skeletal maturity (risser 3-5), were included. We were interested in the segment of the spine that has previously been shown to be rotationally unstable, the posteriorly inclined segment, to determine if that was predictive for later scoliosis development. To quantify this area, the previously described parameter 'posteriorly inclined triangle' (PIT), integrating both steepness and length of the segment at risk, was measured at inclusion.

**Results.** Of 50 children initially without scoliosis (mean age at inclusion  $10.7 \pm 1.7$ , mean follow-up  $4.8 \pm 1.6$  years), 24 (48%) developed scoliosis. An above average PIT-area ( $>60\text{cm}^2$ ) at inclusion, showed a relative risk of 2.55 (95%CI:1.22-5.34). PIT-shape was correlated with curve type, a longer, less steep hypotenuse predicting thoracic scoliosis, a steeper inclination with shorter hypotenuse predicting lumbar scoliosis.

**Conclusion.** This prospective study identified one mechanical parameter, posterior spinal inclination as a risk factor for development of scoliosis in this syndromic population.

## Introduction

The cause of most types of scoliosis is unknown, even if an underlying disorder can be defined.<sup>1</sup> In congenital scoliosis, malformation and abnormal growth of vertebrae understandably can lead to a progressive malformation of the spine.<sup>2</sup> In other scoliosis types with a 'known' origin such as a syndromic or neuromuscular disease, the underlying condition does not explain the patho-mechanism of the disorder. At the other end of the spectrum, in idiopathic scoliosis, not even an underlying pathology can be defined, and the cause has remained elusive.<sup>1</sup> Previous studies have suggested that the sagittal shape of the spine plays a role in the initiation of scoliosis, those vertebrae that are backwardly inclined in the sagittal plane being subject to dorsal shear forces, which have been shown to render those vertebrae rotationally unstable in the transverse plane.<sup>3-12</sup> To prove this concept in idiopathic scoliosis would require prospective studies using ionizing imaging in a very large healthy population, making them ethically and practically very difficult or impossible to carry out.

In this study, we prospectively studied differences in the sagittal shape of the pre-adolescent and non-scoliotic spine in patients with the 22q11.2 deletion syndrome (22q11.2DS). These patients have many different manifestations in many organ systems, but also develop a scoliosis in 50% of the cases.<sup>13</sup> More specifically, the length and tilt angle of the dorsally inclined segment, before the appearance of scoliosis, was quantified. To capture both length and tilt angle, we developed the concept of the 'Posteriorly Inclined Triangle' or PIT (**Figure 1**). This triangle can have different shapes depending on the length and steepness of the hypotenuse, but its surface area is an expression of the overall magnitude of the dorsally directed, de-stabilizing vectors. This concept was first explored in a pilot study including sample size calculations for the current study.<sup>14</sup> The aim of the present study is to evaluate the predictive value of the PIT, and we hypothesize that already before scoliosis onset, children that ultimately develop scoliosis have more posteriorly directed vectors acting on their spine as expressed by a larger PIT. In addition, we expected that the shape of the initial triangle (the length and steepness of the hypotenuse) determines which vertebrae are at risk and is thus related to the ultimate scoliotic curve type.

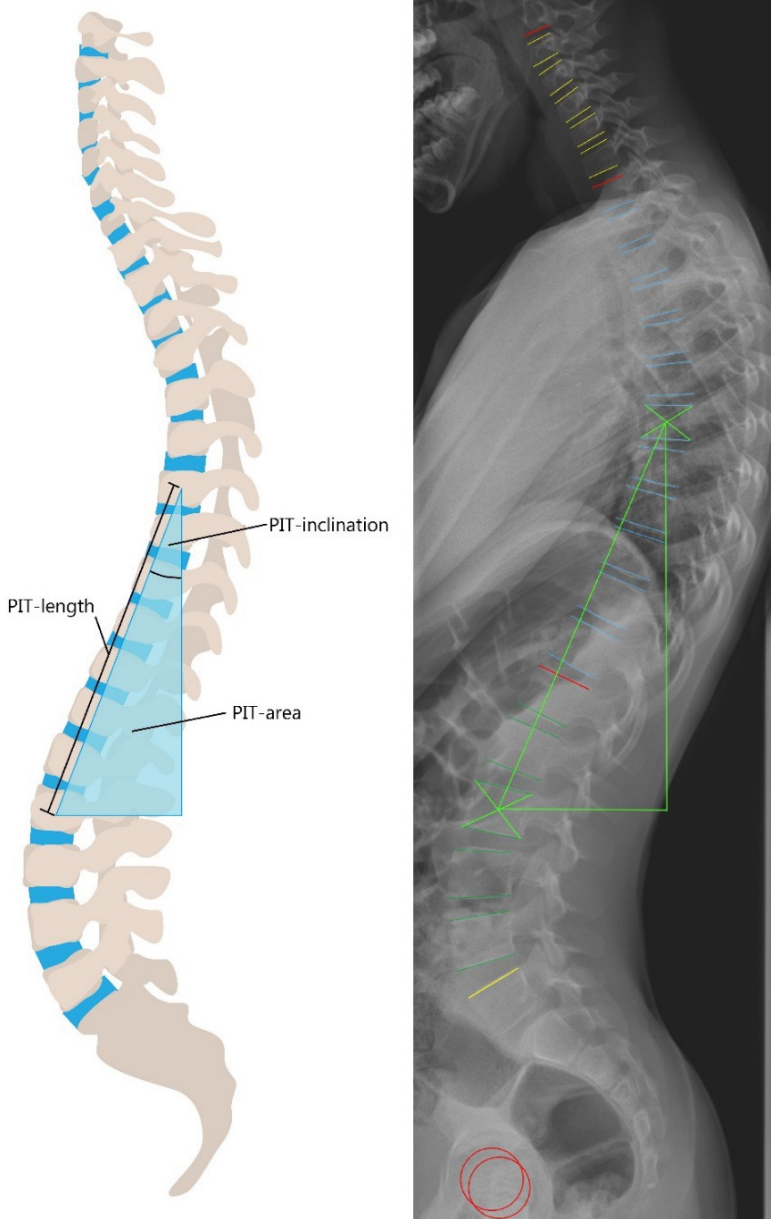


**Figure 1.** On the left a schematic view of the sagittal spine with the posterior inclined triangle (PIT), defined as the right-angled triangle between the centroid of the most upper and lower posteriorly inclined vertebral bodies. On the right side the analysis of the lateral radiograph using Surgimap software: The vertebral body endplates and femoral heads were semi-automatically segmented. Between the automatically generated centroids of the most cranial and caudal posteriorly inclined vertebra, the 'PIT' (posteriorly inclined triangle; bright green) was automatically generated and its area measured.



## Methods

### Participant population

This prospective cohort study is reported according to the STrengthening the Reporting of OBservational studies in Epidemiology (STROBE) statement guidelines for observational studies.<sup>15</sup> The University Medical Center Utrecht (The Netherlands) functions as the national referral center for patients with a confirmed diagnosis of 22q11.2DS, where they are followed up at regular multidisciplinary outpatient clinic visits from first diagnosis until adulthood. In agreement with an institutional review board IRB approved procedure, all caregivers of patients are asked for broad consent to anonymously use the patient chart data for research. From age 6, all 22q11.2DS patients are screened for orthopedic manifestations once every two years, including anterior-posterior and lateral full spine radiographs as part of their routine follow-up. The institutional review board (IRB) approved an exempt of individual informed consent for the current study. We aimed to include 50 consecutive eligible patients, aged 8 to 13, that had no scoliosis at first presentation (Cobb angle  $<10^\circ$ ) on their standing coronal full spine radiograph and were skeletally immature (Risser stage 0-1).<sup>16,17</sup> In this study, patients were followed at least every two years and until skeletal maturity (Risser stage 3-5). Patients with additional genetic syndromes, growth hormone therapy, congenital vertebral anomalies, spine surgery or other orthopedic manifestations influencing the spine or posture, and those with insufficient radiographic examination, for example not being able to stand upright without support, were excluded

### Posteriorly Inclined Triangle

All radiographic measurements were performed in Surgimap imaging software version 2.3.2.1 (Nemaris Inc., NY, USA), a validated software for measuring spinopelvic parameters.<sup>18</sup> Blinded for the outcome, one trained observer analyzed the free-standing lateral full-spine radiographs, acquired in a standardized manner, of every participant at inclusion, at that time all subjects were skeletally immature and the ones with scoliosis on the coronal radiograph had been excluded. First, the observer utilized the 'spinal wizard' of the Surgimap software to segment both femoral heads and all vertebral body endplates and made adjustments where necessary (**Figure 1**). Second, the software automatically calculated the inclination of each vertebral body based on the upper endplate in the sagittal plane, and the centroid was annotated of the most cranial and most caudal posteriorly inclined vertebra. Third, the right-angled triangle between these two points and the vertical was drawn and three parameters were gathered: the PIT-area was automatically calculated following the basic formula:  $0.5 * \text{width} * \text{height}$ , the PIT-length as the length of the hypotenuse and the PIT-inclination as the angle between the hypotenuse and the vertical (**Figure 1**). Finally, the pelvic incidence (a widely used pelvic parameter and important in sagittal spinal alignment, measured as the angle between the line from the femoral-heads-axis to the mid-point

of the sacral endplate)<sup>19</sup>, and the line perpendicular to the sacral endplate and spinal length from T1 to S1 were measured, both also in the sagittal plane, using the same Surgimap software's 'spinal wizard' and annotated by the observer. The spinal length T1-S1 was used to normalize the PIT and account for absolute body size. This was done by calculating the ratio between each patient's individual T1-S1 length and the study's population mean, with no distinction between sex since T1-S1 was not significantly different between males and females. With this ratio, the PIT-area and PIT-length could be normalized without loss of the physical units cm and cm<sup>2</sup>.

### End of follow-up

To qualify presence or absence of scoliosis, the patient had to be skeletally mature (Risser  $\geq 3$ ) and follow up had to be at least two years. The most recent free-standing posterior-anterior full-spine radiograph was analyzed. The presence and curve size of scoliosis (Cobb  $\geq 10^\circ$ ), level of the apex and the corresponding curve type, primary thoracic or primary (thoraco) lumbar, were determined according to the Scoliosis Research Society guidelines.<sup>20</sup>

### Statistical analysis

Based on an earlier pilot study we identified a factor 1.5 difference in magnitude of the PIT-area between those that would and would-not develop scoliosis.<sup>14</sup> Using the means and standard deviations of the PIT-area from that study, to have enough statistical power to compare 2 means (2-sided, alpha of 5% and 80% power), with a sampling ratio of 1 (i.e. equal groups), we would need 25 per group and given the known prevalence of 50% in 22q11.2DS, the required sample size was 50 participants.<sup>14,21</sup> Baseline characteristics as sex and age, together with the follow-up interval, were gathered. The normalized PIT-area, the normalized PIT-length, the PIT-inclination and the pelvic incidence showed a normal distribution, as tested with Q-Q plots. Three groups were compared based on the outcome of the last radiograph: 1. no scoliosis, 2. primary thoracic scoliosis and 3. primary (thoraco)lumbar scoliosis. The difference in sex was analyzed with a Fisher's exact test. The difference in age, follow-up, normalized PIT-area, normalized PIT-length, PIT-inclination and pelvic incidence between the three groups was analyzed with a one-way analysis of variances (ANOVA) with post-hoc independent t-test and Bonferroni correction. After the study population was split by either an above or below average PIT-area (60 cm<sup>2</sup>), the relative risk for scoliosis and 95% confidence intervals (95%CI) were calculated. Second, the population was stratified into six ordinal groups (0-30, 30-45, 45-60, 60-75, 75-90 and 90+ cm<sup>2</sup>) and the fraction of scoliosis per group was calculated. The final analysis was a multivariable linear regression with PIT-length and PIT-inclination as predictors for the apex level of the eventual main scoliotic curve. Statistical analyses were performed with SPSS 27.0 for Windows (IBM, Armonk, NY, USA). The statistical significance level was 0.05.

## Results

### Participant population

A total of 50 participants were consecutively included after 6 exclusions: 1 additional 7p21 duplication, 1 butterfly vertebra, 1 vertebral bar, 1 non-ambulant, 2 malpositioned lateral radiographs. The mean age at inclusion was  $10.7 \pm 1.7$  and the mean follow-up was  $4.8 \pm 1.6$  years. As patients that already had scoliosis (Cobb angle  $>10$ ) were not included, the mean Cobb angle at inclusion was 5.0 (range 0.0-9.7) with no significant differences between those that did and did not develop scoliosis during follow-up ( $p=0.770$ ). At the last follow up, 8 had a Risser stage 3, 21 a Risser stage 4 and 21 a Risser stage 5. As expected, 24 of the 50 subjects (48%) had developed a scoliosis, 12 with a primary thoracic and 12 with a (thoraco) lumbar curve (**Table 1**).

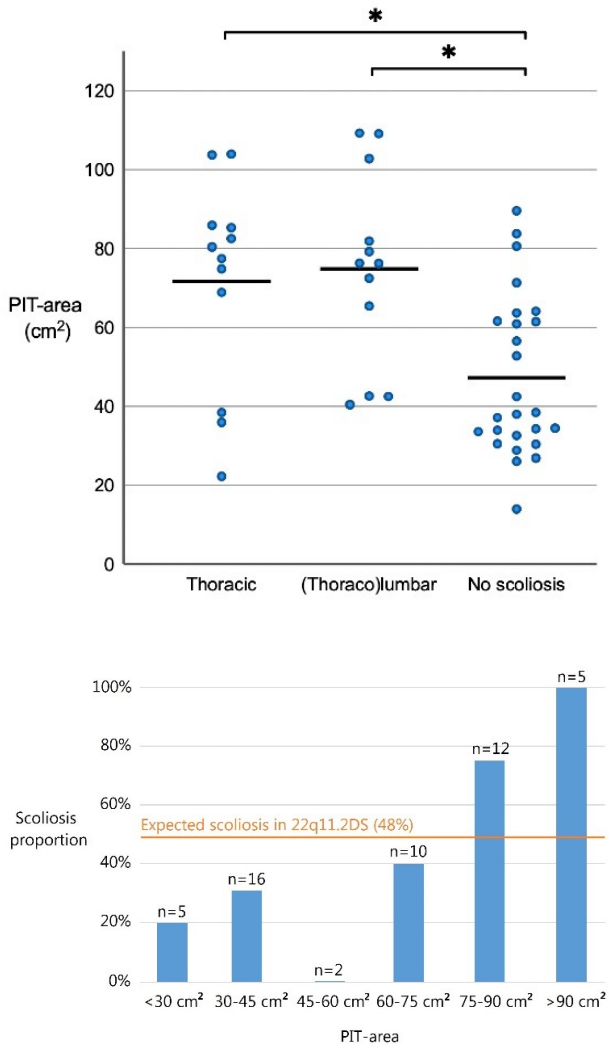
|  | Thoracic scoliosis | (Thoraco)lumbar scoliosis | No scoliosis   | P after correction |
|--|--------------------|---------------------------|----------------|--------------------|
| N  | 12                 | 12                        | 26             |                    |
| Males (%)  | 6 (50%)            | 6 (50%)                   | 15 (56%)       | 0.87               |
| Age at inclusion   | $10.6 \pm 1.9$     | $10.5 \pm 2.0$            | $10.9 \pm 1.5$ | 0.79               |
| Follow-up (years)  | $4.6 \pm 1.5$      | $5.4 \pm 1.9$             | $4.5 \pm 1.5$  | 0.26               |
| <u>Pre-adolescent radiographic parameters at inclusion</u> |                    |                           |                |                    |
| PIT-area (cm <sup>2</sup> )                                | $72 \pm 26$        | $75 \pm 25$               | $47 \pm 20$    | $<0.001^a$         |
| PIT-length (cm)  | $24 \pm 3$         | $22 \pm 2$                | $18 \pm 2$     | $<0.001^b$         |
| PIT-inclination (°)  | $15 \pm 4$         | $20 \pm 5$                | $16 \pm 5$     | $0.045^c$          |
| Pelvic incidence (°)                                       | $35 \pm 5$         | $44 \pm 8$                | $37 \pm 7$     | $0.006^d$          |

**Table 1.** This table shows the pre-adolescent clinical and radiographic parameters, stratified by end of follow-up outcome: thoracic scoliosis, (thoraco)lumbar scoliosis or no scoliosis. Figures represent number (percentage) or mean ( $\pm$ SD). The post-hoc tests with Bonferroni corrections showed: a) no difference in normalized PIT-area between thoracic and (thoraco)lumbar scoliosis, but both were larger than in no scoliosis ( $p \leq 0.01$ ). b) PIT-length differed between all three groups ( $p \leq 0.047$ ). c) Segment inclination angle was larger in (thoraco)lumbar than thoracic scoliosis ( $p=0.048$ ), both not different from no scoliosis. And d) pelvic incidence was not different between thoracic scoliosis and no scoliosis, but significantly higher in (thoraco)lumbar scoliosis ( $p \leq 0.015$ ). PIT = posteriorly inclined triangle.

Posteriorly Inclined Triangle area

The area of the PIT in participants that would later develop a scoliosis was  $73 \pm 25 \text{ cm}^2$ , over 1.5 times greater than the  $47 \pm 20 \text{ cm}^2$  in the ones that did not develop scoliosis. This effect was similar for both scoliosis types, with a mean normalized PIT-area of  $72 \pm 26 \text{ cm}^2$  in primary thoracic, and  $75 \pm 25 \text{ cm}^2$  in primary (thoraco)lumbar scoliosis (**Table 1; Figure 2**). We observed an above average PIT-area of  $60 \text{ cm}^2$  or higher at inclusion in 18 of 24 patients that eventually developed scoliosis, compared to 9 of 26 without scoliosis, i.e. a relative risk of 2.55 (95%CI:1.22-5.34; **Figure 2**). Comparing PIT-area subgroups, scoliosis developed in 20% in the lowest group (PIT-area  $0\text{-}30 \text{ cm}^2$ ) and in 100% in the highest group (PIT-area  $>90 \text{ cm}^2$ ).

**Figure 2.** The results with above a plot of the normalized PIT-area measured at inclusion of the study for each included patient and stratified by scoliosis type or no scoliosis at end of follow-up. Horizontal bars indicate the mean PIT-area, statistically significant differences are annotated with an asterisk (\*). On the bottom is shown the proportion of scoliosis cases stratified by normalized PIT-area at study inclusion, together with the overall 48% as observed in the 22q11.2DS population of this study.



### Shape of the posterior inclined segment

The normalized hypotenuse length of the PIT was longest in thoracic scoliosis with  $24\pm 3$  cm, versus  $22\pm 2$  cm in lumbar scoliosis and shortest in no scoliosis with  $18\pm 2$  cm. The triangle was narrower but higher in thoracic scoliosis with  $15\pm 4^\circ$ , compared to (thoraco)lumbar scoliosis with  $20\pm 5^\circ$  ( $p=0.048$ ), but both were not significantly different from no scoliosis with  $16\pm 5^\circ$  (**Table 1, Figure 4**). In a multivariable linear regression of the 24 scoliosis cases, both PIT-height ( $r = 0.436$ ,  $p = 0.022$ ) and PIT-inclination ( $r = -0.443$ ,  $p = 0.020$ ) were significant predictors for the apex level of the eventual main scoliotic curve (**Figure 3**). Examples of one participant per group to demonstrate the PIT before curve onset is displayed in **figure 4**.

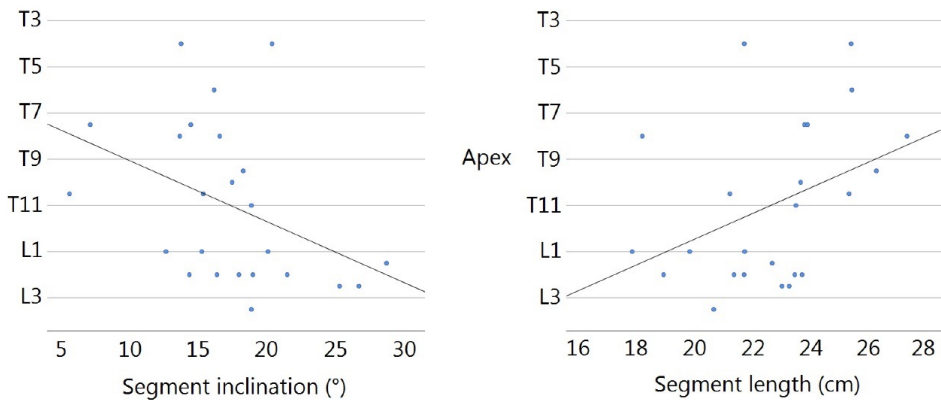


**Figure 3.** For all patients that had developed a scoliosis ( $n = 24$ ), a scatter plot is shown of the PIT-length and PIT-inclination, compared to the apex level of the main scoliotic curve. Multivariable linear regression analysis showed that both normalized PIT-length ( $r = 0.436$ ,  $p = 0.022$ ) and PIT-inclination ( $r = -0.443$ ,  $p = 0.020$ ), at inclusion, were significant predictors for the apex level of the eventual main scoliotic curve.

### Pelvic incidence

The pelvic incidence at inclusion in the overall group that later developed scoliosis was not significantly different from those without scoliosis at follow up. When distinguishing between type of scoliosis, the pelvic incidence was  $35\pm 5^\circ$  in thoracic scoliosis, similar to no scoliosis with  $37\pm 7^\circ$ , but it was significantly higher with  $44\pm 8^\circ$  (**Table 1**) in those that developed a (thoraco)lumbar scoliosis.

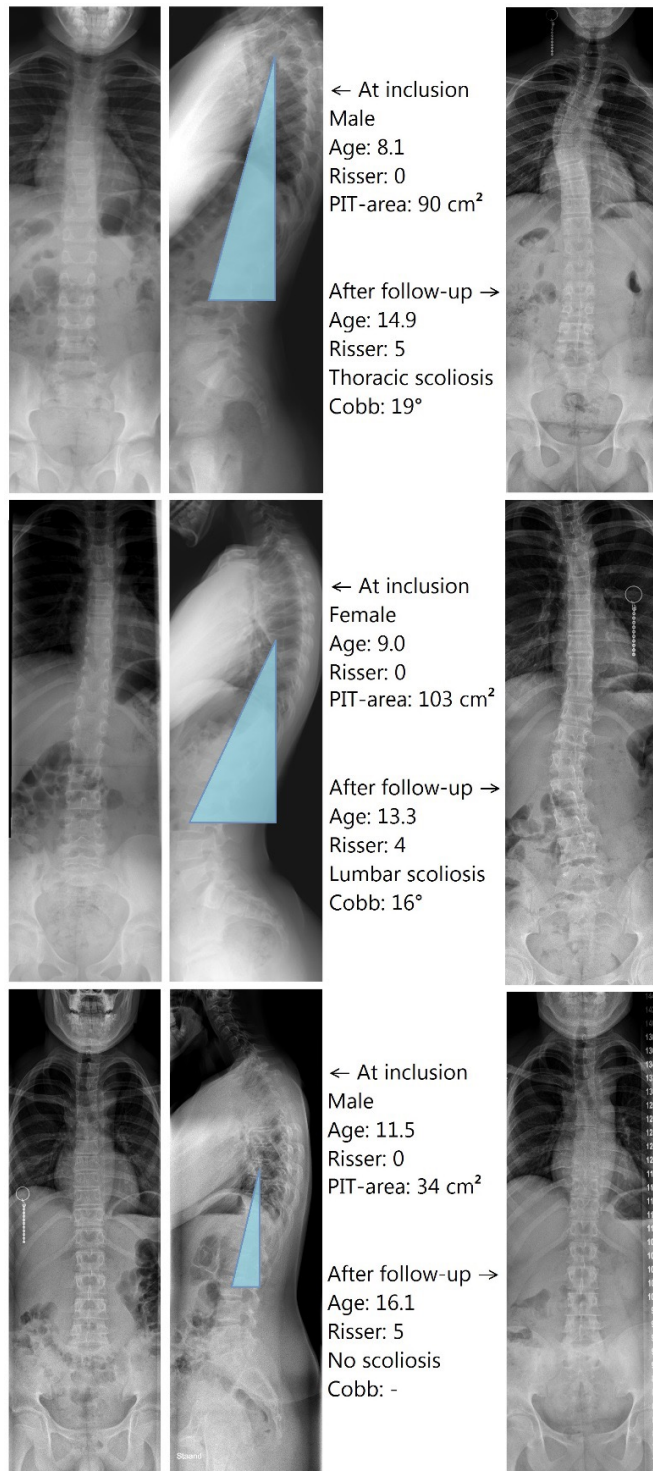


**Figure 4.** Examples of three participants, demonstrating a larger PIT-area before the development of scoliosis compared to no scoliosis. Note the slender PIT in thoracic scoliosis versus wider PIT in (thoraco)lumbar scoliosis.

## Discussion

Sagittal plane spinal alignment has long been considered to play an important role in the development of scoliosis.<sup>3-13</sup> However, since all studies in scoliosis research are done on already established cases, it is impossible to distinguish if these differences in sagittal profile were the cause of the deformity, or its effect. This study demonstrated, in a syndromic population that develops scoliosis in a high percentage of cases, for the first time prospectively, the role of the sagittal profile and dorsal shear loads in the later development of scoliosis. We believe this is the best achievable evidence as prospective studies using ionizing radiation in a healthy pediatric population with an incidence of the disorder of 2-4%, to study the relationship between the sagittal profile and the development of scoliosis are ethically and technically not feasible.<sup>22</sup> Furthermore, biomechanical animal research is not an option to resolve this specific question, as no animal model exists that reflects the unique spino-pelvic sagittal alignment of the human spine, and its biomechanical loading.<sup>23</sup>

The current study demonstrates clearly that the sagittal shape of the spine is a risk factor for development of scoliosis in an initially straight spine. The posteriorly inclined spinal segment, quantified by the PIT-area, strongly determined the risk to ultimately develop scoliosis in our study population. The PIT-area is larger for scoliotics than non-scoliotics, but not different for primary thoracic or (thoraco)lumbar curves. However the shape of the PIT dictates in which area of the spine scoliosis will develop. A more slender, higher and more vertical PIT precedes thoracic curves and a broader, lower and more horizontal PIT precedes (thoraco) lumbar scoliosis. These distinct PIT shapes are essentially part of the known natural variation in sagittal spinal profile and pelvic shapes as described in adults by the Roussouly types.<sup>24</sup> Our results show indeed that a high pelvic incidence, which is associated with a higher sacral slope and thus a larger lumbar lordosis, is consequently also associated with a shorter and steeper posteriorly inclined segment, and with the development of (thoraco)lumbar scoliosis. This confirms earlier observations in populations with already established idiopathic scoliosis or adult degenerative scoliosis.<sup>12,25-28</sup>

This study emphasizes the role of spinal biomechanics and corresponding dorsal shear forces, as determined by the sagittal profile, in a selected subpopulation with a likelihood of 50% to develop scoliosis. We have shown before, in different experimental models, that dorsal shear on spinal segments leads to a reduction of rotational stability in the horizontal plane, and this rotation is a characteristic and possibly initiating feature of scoliosis.<sup>6,29</sup> When observing the variation of the PIT between the cases and the controls at inclusion, the difference is very distinct, however in this cohort there is no strict threshold for scoliosis development (**Figure 3**). Although the analysis of PIT-area for above or below average (60 cm<sup>2</sup>) was not powered for, it already showed a significant relative risk of 2.55, stressing the

strength of the PIT-area as a risk factor in our study population. A small PIT-area seems to protect for scoliosis development in this population, however, the scoliosis risk (20%) in this group is still well above the prevalence of scoliosis in the general adolescent population so this increased risk is a general characteristic throughout the 22q11.2DS population. The risk of scoliosis development in subjects with a relatively large PIT area ( $>75 \text{ cm}^2$ ) is more than 4-fold compared to subjects with a smaller PIT area.

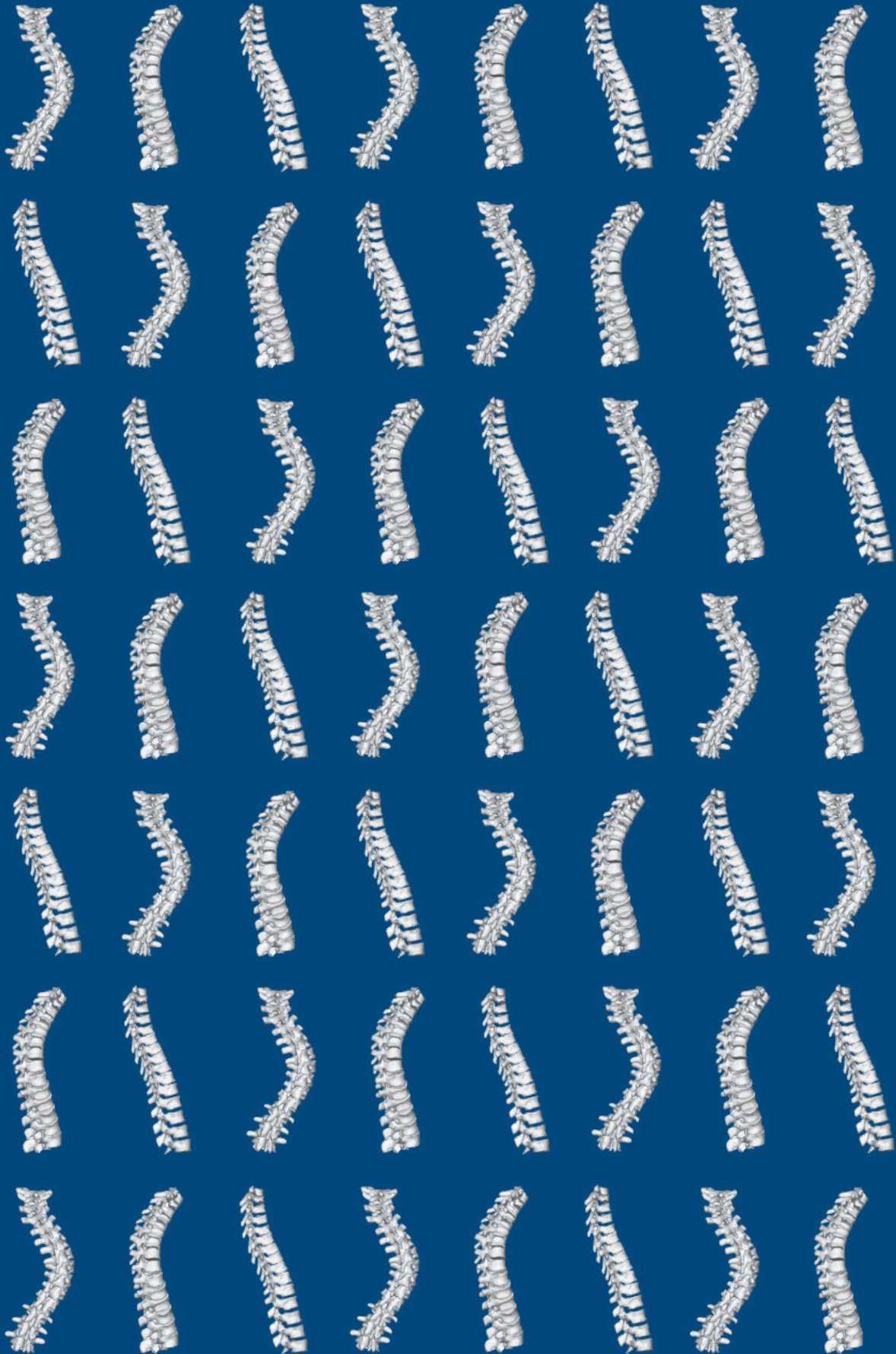
This indicates that posterior inclination and dorsal shear forces play an important role within the etiology of scoliosis, as a distinct risk factor, in the sense that the sagittal profile dictates which areas of the spine are rendered less stable in the horizontal (transverse) plane. Of course, every human, also in the general population, has a posteriorly inclined segment, but not all get scoliosis. It appears that a larger PIT-area predisposes to the development of scoliosis, but additional 'triggers', or enabling circumstances, are needed. Whether scoliosis actually occurs depends on the balance between the rotation inducing forces and the spine's stabilizers, of which the intervertebral discs are very important. A vulnerable period occurs when the body is rapidly increasing in size and weight, and the intervertebral disc may still be in its own process of maturation, i.e. during the adolescent growth spurt.<sup>30</sup> Interestingly, the increased risk in 22q11.2DS patients to develop scoliosis cannot be explained by an increased dorsal inclination itself, as children from the general population aged 8 to 13 have a mean PIT-area that is even slightly greater (derived from a previously investigated cohort, unpublished data). This indicates that important additional factors still remain to be identified as the cause of the high scoliosis risk in 22q11.2DS. This 22q11.2DS population, that is under close medical scrutiny at our institution, with a scoliosis prevalence of ~50% compared to 2-4% in the general population, allowed for a prospective analysis of the role of the sagittal profile in the later development of scoliosis.<sup>1,13</sup> Obviously, scoliosis in this population is different from idiopathic scoliosis, although they both develop during growth in an anatomically normal and initially straight spine and share certain characteristics.<sup>31,32</sup> Extrapolation to the general population, however, should obviously be done with caution.

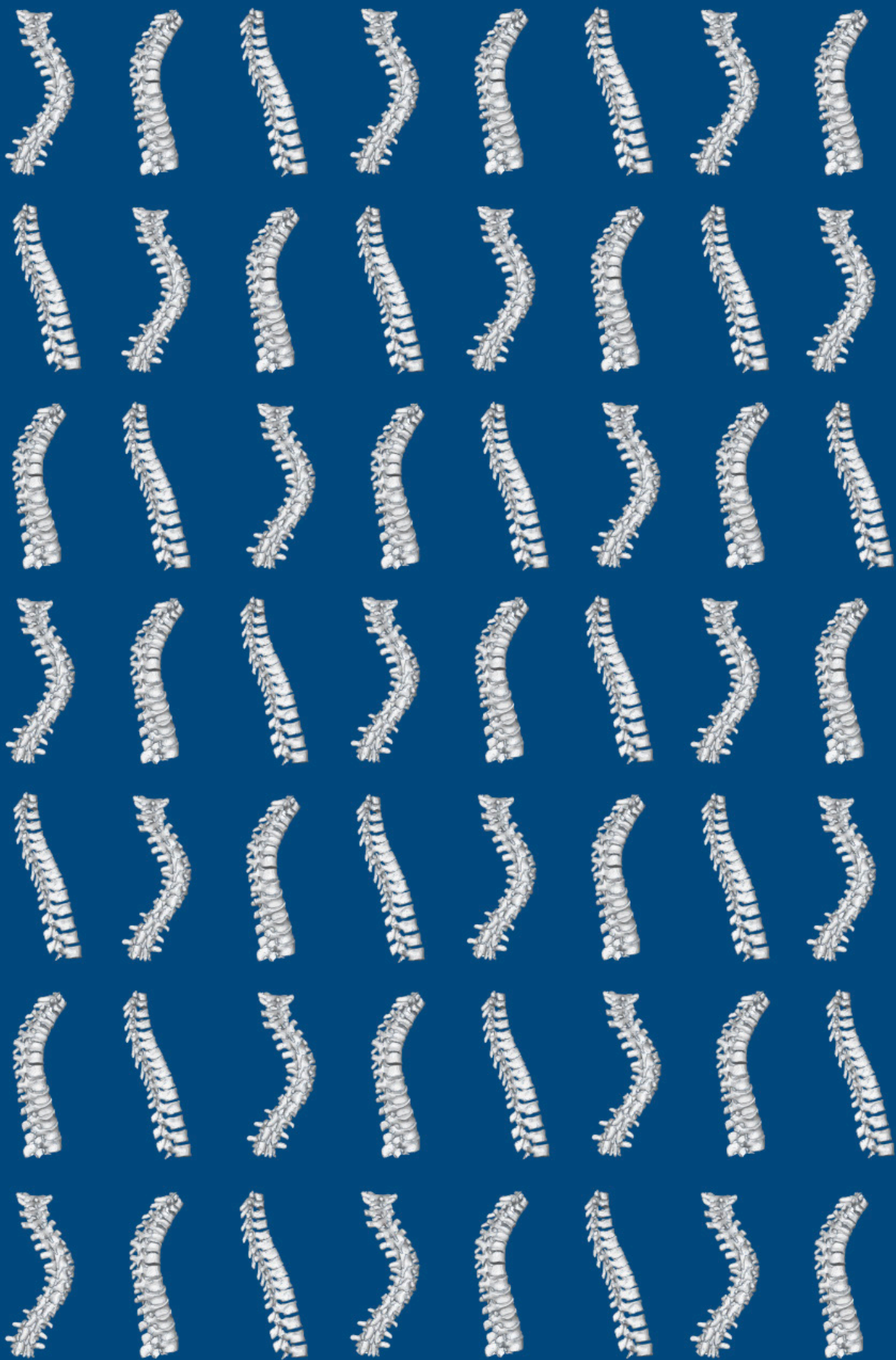
In conclusion, this prospective cohort study identified the magnitude of overall (length combined with inclination angle) dorsal inclination as a risk factor for development of scoliosis, in a syndromic population. The initial pre-adolescent sagittal spinal profile was shown to differ between the ones that do, or do not eventually develop a scoliosis during adolescence. Furthermore, the PIT-shape was shown to determine the type of scoliosis, a higher and narrower triangle precedes the development of thoracic scoliosis and a broader and lower triangle precedes (thoraco-)lumbar scoliosis. This substantiates an important biomechanical component, related to differences in individual spinal shape during growth as a risk factor for scoliosis development in this population.

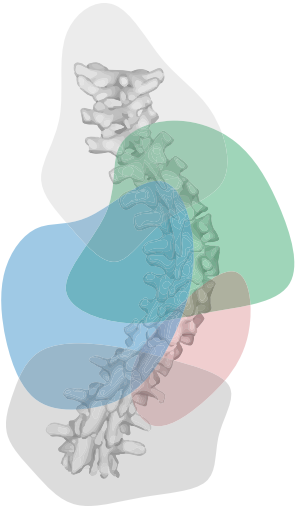


## References

1. Cheng JC, Castelein RM, Chu WC, et al. Adolescent idiopathic scoliosis. *Nat Rev Dis Primers* 2015;1:15–30.
2. McMaster MJ, Ohtsuka K. The natural history of congenital scoliosis. A study of two hundred and fifty-one patients. *J Bone Joint Surg Am* 1982;64:1128–47.
3. Abelin-Genevois K, Sassi D, Verdun S, et al. Sagittal classification in adolescent idiopathic scoliosis: original description and therapeutic implications. *Eur Spine J* 2018;27:2192–202.
4. Pasha S. 3D Deformation Patterns of S Shaped Elastic Rods as a Pathogenesis Model for Spinal Deformity in Adolescent Idiopathic Scoliosis. *Sci Rep* 2019;9:16485.
5. Castelein RM, van Dieën JH, Smit TH. The role of dorsal shear forces in the pathogenesis of adolescent idiopathic scoliosis--a hypothesis. *Medical hypotheses* 2005;65:501–8.
6. Castelein RM, Pasha S, Cheng JCYC, et al. Idiopathic Scoliosis as a Rotatory Decompensation of the Spine. *Journal of Bone and Mineral Research* 2020;35:1850–7.
7. de Reuver S, IJsseldijk LL, Homans JF, et al. What a stranded whale with scoliosis can teach us about human idiopathic scoliosis. *Scientific reports* 2021;11:7218.
8. Von Meyer H. Die mechanik der skoliose. *Archiv für pathologische Anatomie und Physiologie und für klinische Medicin* 1866;35:225–53.
9. Roaf R. The basic anatomy of scoliosis. *The Journal of bone and joint surgery British volume* 1966;48:786–92.
10. Dickson RA. The aetiology of spinal deformities. *Lancet (London, England)* 1988;1:1151–5.
11. Somerville EW. Rotational lordosis; the development of single curve. *The Journal of bone and joint surgery British volume* 1952;34-B:421–7.
12. Schlösser TPC, Shah SA, Reichard SJ, et al. Differences in early sagittal plane alignment between thoracic and lumbar adolescent idiopathic scoliosis. *Spine J* 2014;14:282–90.
13. Homans JF, Baldew VGM, Brink RC, et al. Scoliosis in association with the 22q11.2 deletion syndrome: An observational study. *Arch Dis Child* 2019;104:19–24.
14. Homans JF, Schlösser TPC, Pasha S, et al. Variations in the sagittal spinal profile precede the development of scoliosis: a pilot study of a new approach. *The Spine Journal* 2021;21:638–41.
15. von Elm E, Altman DG, Egger M, et al. The Strengthening of Reporting of Observational Studies in Epidemiology (STROBE) statement: guidelines for reporting observational studies. *Lancet (London, England)* 2007;370:1453–7.
16. Hacquebord JH, Leopold SS. In brief: The Risser classification: a classic tool for the clinician treating adolescent idiopathic scoliosis. *Clinical orthopaedics and related research* 2012;470:2335–8.
17. Sanders JO, Khoury JG, Kishan S, et al. Predicting Scoliosis Progression from Skeletal Maturity: A Simplified Classification During Adolescence. *The Journal of Bone and Joint Surgery-American Volume* 2008;90:540–53.
18. Lafage R, Ferrero E, Henry JK, et al. Validation of a new computer-assisted tool to measure spino-pelvic parameters. *The Spine Journal* 2015;15:2493–502.
19. Legaye J, Duval-Beaupère G, Hecquet J, et al. Pelvic incidence: A fundamental pelvic parameter for three-dimensional regulation of spinal sagittal curves. *European Spine Journal* 1998;7:99–103.
20. O'Brien MF, Kulklo TR, Blanck KM, et al. *Radiographic Measurement Manual*. 2008.
21. Chow S-C, Shao J, Wang H. *Sample Size Calculations in Clinical Research*. 2nd Ed. Chapman & Hall/CRC Biostatistics Series.; 2008.
22. Presciutti SM, Karukanda T, Lee M. Management decisions for adolescent idiopathic scoliosis significantly affect patient radiation exposure. *Spine J* 2014;14:1984–90.
23. Janssen MMA, de Wilde RF, Kouwenhoven J-WM, et al. Experimental animal models in scoliosis research: a review of the literature. *The spine journal : official journal of the North American Spine Society* 2011;11:347–58.
24. Roussouly P, Gollogly S, Berthonnaud E, et al. Classification of the normal variation in the sagittal alignment of the human lumbar spine and pelvis in the standing position. *Spine (Phila Pa 1976)* 2005;30:346–53.
25. Legaye J, Duval-Beaupère G, Marty C, et al. Pelvic incidence: a fundamental pelvic parameter for three-dimensional regulation of spinal sagittal curves. *European Spine Journal* 1998;7:99–103.
26. Brink RC, Vavrouch L, Schlösser TPC, et al. Three-dimensional pelvic incidence is much higher in (thoraco) lumbar scoliosis than in controls. *European Spine Journal* 2019;28:544–50.
27. Pasha S, Aubin C-E, Sangole AP, et al. Three-Dimensional Spinopelvic Relative Alignment in Adolescent Idiopathic Scoliosis. *Spine* 2014;39:564–70.
28. de Reuver S, van der Linden P, Kruyt MC, et al. The Role of Sagittal Pelvic Morphology in the Development of Adult Degenerative Scoliosis. *European Spine Journal*.
29. Kouwenhoven JW, Smit TH, van der Veen AJ, et al. Effects of dorsal versus ventral shear loads on the rotational stability of the thoracic spine: a biomechanical porcine and human cadaveric study. *Spine* 2007;32:2545–50.
30. Costa L, de Reuver S, Kan L, et al. Ossification and Fusion of the Vertebral Ring Apophysis as an important part of spinal maturation. *J Clin Med*.
31. de Reuver S, Homans JF, Schlösser TPC, et al. 22q11.2 Deletion Syndrome as a Human Model for Idiopathic Scoliosis. *J Clin Med*;10.
32. Abul-Kasim K, Ohlin A. Curve Length, Curve Form, and Location of Lower-End Vertebra as a Means of Identifying the Type of Scoliosis. *Journal of Orthopaedic Surgery* 2010;18:1–5.



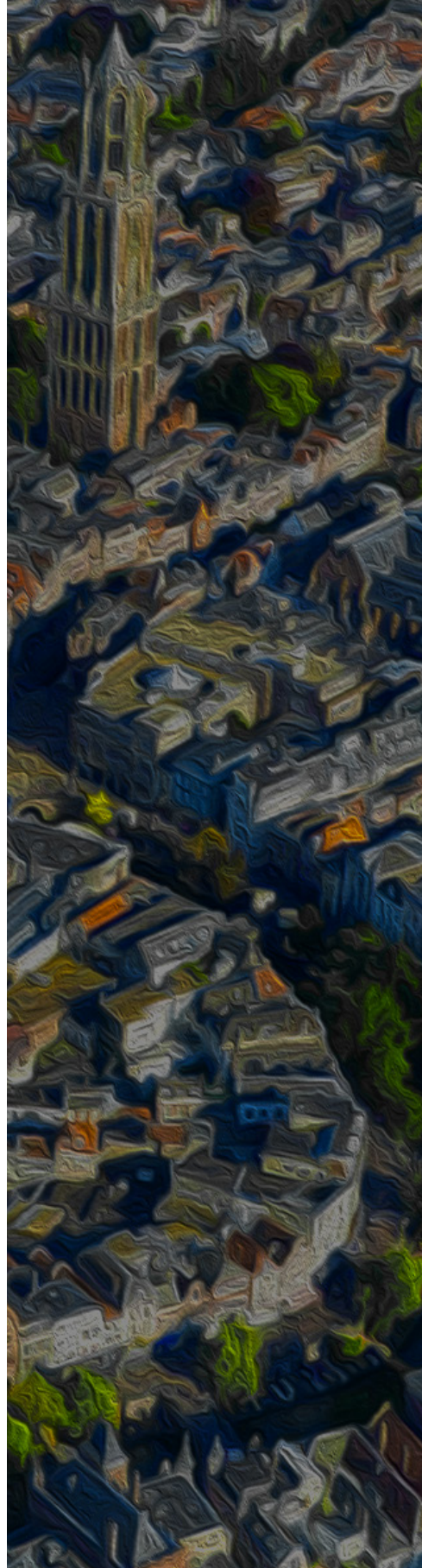






# 21

Summary, General Discussion  
and Conclusions



### Thesis summary

The introduction of this thesis in **Chapter 1**, elaborated on the unique human sagittal spinal alignment including a posteriorly inclined segment.<sup>1-5</sup> This segment's orientation introduces, in contrast to 'physiological' anterior loads, posteriorly directed shear loads to the spine which have been demonstrated to significantly reduce rotational stability.<sup>6,7</sup>

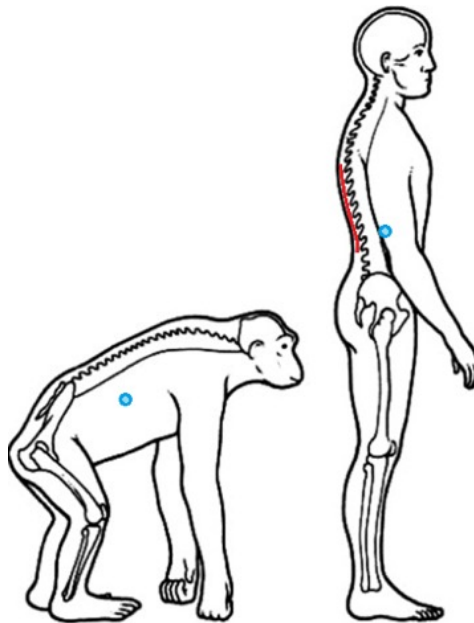


**Figure 1.** Humans are the only species that in the sagittal plane, balance their center of mass straight above the pelvis and thus more posterior, as a consequence a large portion of the spine is posteriorly inclined.

Three loads act on the spine: axial, anterior and posterior of which the axial load is the greatest. It has been generally accepted that excessive axial and anterior loads during growth can lead to well know deformities as Scheuermann's disease or spondylolisthesis. Our group has developed the concept that the third well known childhood deformity, scoliosis, is initiated by an overload of that third force, the posterior shear load. In this chapter a summary is provided of the results of the studies that were carried out to answer the study questions as mentioned in **Chapter 1**. For each of the three parts these findings are discussed, before this thesis ends with the final conclusions and future perspectives.

## Growth of the Healthy Spine

In **PART I** of this thesis, the intervertebral disc and vertebral body morphology, and the sagittal alignment in the ‘healthy’ spine during growth, were described with modern imaging techniques. It has been well known that the spine grows predominantly in the vertebral bodies, but precise measurements had never been published.<sup>8</sup> In **Chapter 2** these measurements were performed on CT, the vertebral body height increase was confirmed, while it was demonstrated that thoracic discs increase in height only during the first years and remain stable thereafter (**Figure 2**). Since the transverse surface area continues to increase throughout growth, discs slenderness decreases and female discs remained relatively more slender around growth-spurt.

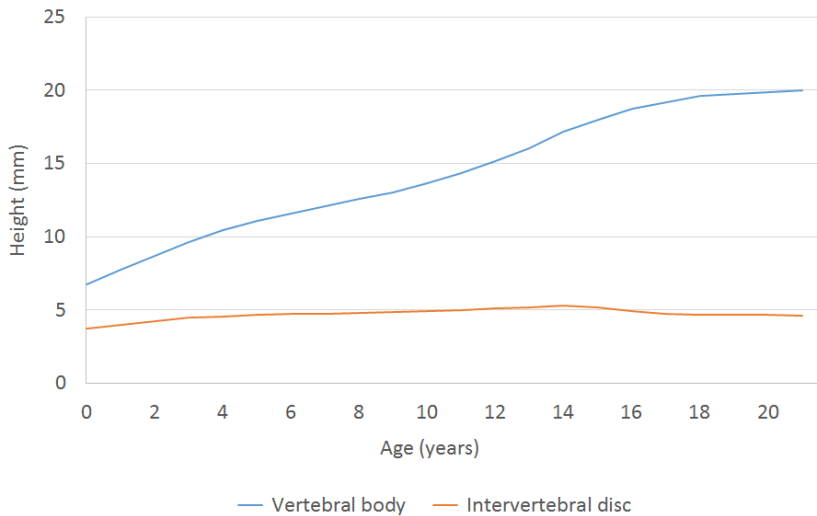


**Figure 2.** Mean height of vertebral bodies and intervertebral discs in the thoracic spine during growth.

This was confirmed in the MRI analysis of **Chapter 3**, furthermore, it was observed that the disc transverse cross-sectional area and volume increased consistently, with a stable volume ratio of the annulus fibrosus and nucleus pulposus, and overall larger discs in males. During growth the nucleus orientation within the disc is stable and centered in the right-left and cranial-caudal direction, however in the anterior-posterior direction, the nucleus increasingly shifts with age, following the sagittal profile of the spine. Disc slenderness decreased slightly in the first 3 years of life and remains stable afterwards, interestingly, female discs, especially the mid-thoracic ones in early adolescence, were more slender than those of males. Since

idiopathic scoliosis manifests itself mostly in females, in the mid-thoracic area in early adolescence, it could be speculated that this has to do with the taller and more narrow, thus less robust discs in this area.<sup>9</sup> Furthermore, it has been demonstrated that the spine in patients with scoliosis is more slender compared to the healthy population.<sup>10,11</sup> This suggests that disc slenderness is a potential risk factor for the development of scoliosis.

Stability of the spine and resistance to rotational forces also has to do with the way the disc is anchored to the spine. The Sharpey's fibers insert into the ring apophysis and thus anchor the intervertebral disc to the two adjacent vertebrae.<sup>12</sup> As it is a weak point, this is a process that might have important implications for the mechanical stability of the disc-vertebral body complex of the thoraco-lumbar sections at a time that spinal loading increases rapidly due to growth spurt.<sup>13</sup> In **Chapter 4** this was studied based on CT, different RAM (Ring Apophysis Maturation) stages that describe the process of ossification and fusion of the ring apophysis to the vertebral body, were mapped throughout growth. It was observed that RAM was later in the mid-thoracic and thoraco-lumbar spine, and relative to growth spurt timing, female spines were less mature than males. These findings may be important for understanding the patho-mechanism of idiopathic scoliosis, in terms of the timing of scoliosis onset at early growth spurt, the preferred location of the apex being mid thoracic and the overrepresentation of females.

In **Chapter 5**, it was observed that the thoracic center of mass shift from slightly right-sided at infantile age, to neutral at juvenile age, to left-sided at adolescent age. This corresponds to the earlier demonstrated change in direction of pre-existent rotation in the normal spine with age, as well as with the well-known changing direction, from left to right, of thoracic curve convexity in scoliosis at different ages.<sup>14-16</sup> This finding explains curve direction in scoliosis and underlines the biomechanical component of AIS.

**Chapter 6** demonstrated that statistical shape modeling (SSM) combined with non-ionizing ultrasound imaging, could visualize and quantify the subtle variations in individual sagittal shape. The shape before the growth spurt was a less pronounced sagittal curvature with a less steep, but longer posteriorly inclined segment reaching into the higher thoracic regions. After growth spurt there was a more pronounced sagittal curvature with a steeper but shorter posteriorly inclined segment (**Figure 3**).



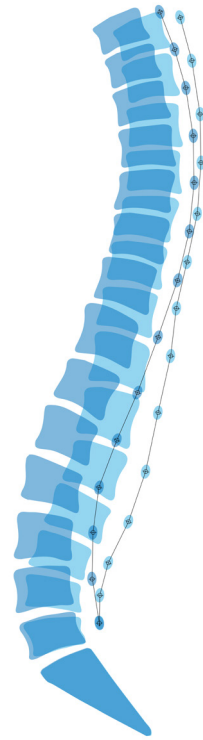


**Figure 3.** Before the growth-spurt a less pronounced sagittal profile (light blue) and after the growth-spurt more pronounced (dark blue).

Before these chapters, there was a general idea of spinal height increase mostly being in the vertebral bodies during growth, and the sagittal alignment shifting from a C-shape in infants to the typical S-shape of upright humans. The studies of **PART I** provide a much broader and accurate description of the morphology of the elements that make up the spine during growth. Furthermore, a more delicate and radiation free method for sagittal shape studies is presented. However, there are limitations, mainly that ‘growth’ was described based on cross-sectional data of different individuals, while a longitudinal design would probably be more accurate. This was not possible due to availability of data and ethical concerns, and by having large sample sizes in these studies, it was attempted to compensate for the cross-sectional designs. The results of these chapters are a large quantity of data, that will assist future studies with specific research questions on idiopathic scoliosis etiology, but already give some insights themselves. For instance, disc slenderness and severity of the posteriorly inclined segment are already present in the normal spine, varying inter-individually or between boys and girls, but potentially also play a role the initiation of idiopathic scoliosis.

## Scoliosis as a Universal Response

In **PART II** the morphology of the scoliotic spine, and the potential similarities between scoliosis of different etiologies and species, was studied. In **Chapter 7**, an attempt was made to address the radiation concerns of conventional spinal imaging, and it was demonstrated that spinal ultrasound Cobb angle measurements showed an excellent correlation with radiographs as the gold standard. Since ultrasounds are performed from the back, and measurements are based on the location of the spinous processes and the laminae/ the posterior structures which are less laterally deviated than the more anterior vertebral bodies used on radiographs, the Cobb angle was systematically underestimated. In this study, this was solved by generating equations: *thoracic Cobb angle* =  $1.43 \times$  *ultrasound angle* and *lumbar Cobb angle* =  $1.23 \times$  *ultrasound angle*, which showed good accuracy and no proportional bias, supporting the implementation of ultrasound imaging.

In **Chapter 8**, compensatory curves in congenital scoliosis were observed to have anterior lengthening exclusively of the intervertebral discs, similar to AIS and neuromuscular scoliosis, therefore confirming this is part of the three-dimensional deformity in different types of scoliosis (**Figure 4**). Furthermore, the bony vertebral bodies maintained their kyphotic shape in AIS, similar to the other scoliosis types as well as normal controls, which indicates that there is no active anterior bony overgrowth, in contrast to the earlier postulated theory of RASO (relative anterior spinal overgrowth). Anterior lengthening appears to be a passive result of any scoliotic deformity, rather than being related to the specific cause of AIS.

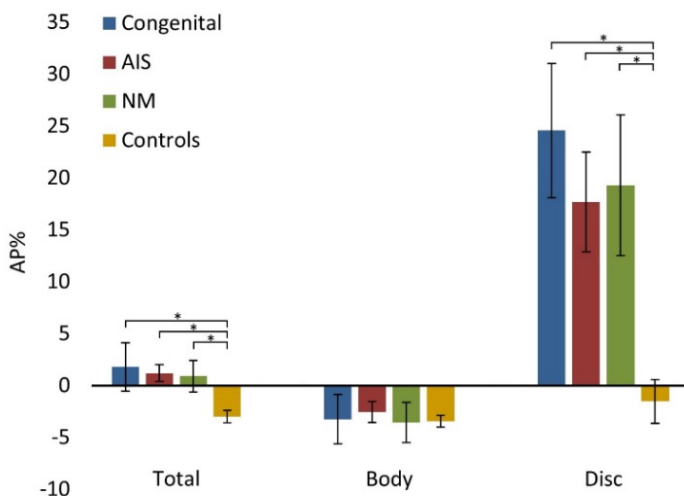


**Figure 4.** Similar anterior lengthening (positive AP%) of intervertebral discs with no changes to the slight kyphosis in vertebral bodies is seen in compensatory congenital, AIS and neuromuscular (NM) scoliosis.

Another scoliosis type, adult degenerative scoliosis (ADS), was studied in **Chapter 9**. ADS is generally considered a different entity than AIS with different patho-mechanical background. It was observed that ADS normally develops *de novo* in the lumbar spine of patients with a higher pelvic incidence than controls, similar to primary lumbar AIS. Since the pelvic incidence dictates the sagittal spinal profile, this suggests the importance of both in scoliosis etiology, and stresses another shared mechanical basis of scoliotic deformities with different etiologies. Phrased differently, pelvic morphology dictates spinal sagittal alignment, which determines the segments of the spine that are prone to develop scoliosis, both in the growing adolescent spine and the aging degenerative spine. Degenerative adult scoliosis can be considered the last stage of idiopathic scoliosis.

In **Chapter 10**, the compensatory scoliosis in the anatomically normal part of a stranded whale caused by traumatic injury, showed similar apex rotation into the curve convexity and anterior opening of the intervertebral discs space as the scoliosis types in humans, including AIS. This suggests that any decompensation of spinal equilibrium, or spinal compensation initiated by an external factor in the case of the whale, can lead to a rather uniform response, independent of the cause or species (**Figure 5**). It takes a severe trauma for a whale to develop scoliosis, the trauma eventually- after sufficient time to gradually develop the compensatory scoliosis- killed the animal. In humans, due to their much less rotationally stable spinal configuration, much more subtle disturbances of equilibrium are sufficient to initiate the same chain of events.

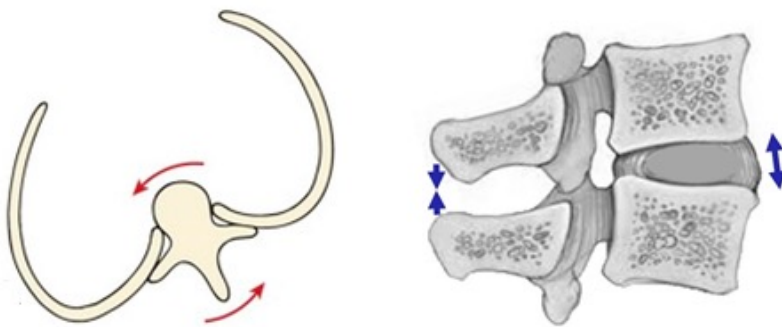


**Figure 5.** *The universal mechanism of scoliosis, including transverse plane rotation into the curve convexity and anterior opening of the disc, as observed in scoliosis indifferent of etiology and species.*

Finally, in **Chapter 11** the spinal length of the scoliotic curve in AIS was measured over four corners: anterior-convex, anterior-concave, posterior-convex and posterior-concave. Besides the expected global convexity lengthening and thoracic lordosis, a strong posterior concavity shortening was observed, while the posterior convexity was slightly longer in AIS compared to controls. To restore spinal harmony during posterior surgery, the posterior concavity should be elongated while allowing for some shortening of the posterior convexity.

Before this thesis, it was generally accepted that idiopathic scoliosis involves a hypokyphosis/lordosis, with the clinically present 'flat-back' and visible on radiographs. The later observed relative anterior lengthening in AIS, called RASO with the suggestion that the normal synchronicity of anterior and posterior vertebral growth is disturbed. This thesis rejects the concept of active anterior bony overgrowth as well as the idea that this is exclusive for AIS. Based on the observations of **PART II**, regarding the segmental lordosis as part of the scoliotic mechanism, it could be rejected that there is any form of bony (over)growth at the anterior part of the spine. It was observed that the relative anterior lengthening specifically is anterior opening of the intervertebral discs. Furthermore, it was confirmed that this mechanism is not only observed in AIS, but in scoliosis of different etiologies (neuromuscular, congenital and traumatic) and also in another species., however unlikely the occurrence of scoliosis is in this species. Therefore, the results confirm the title of this thesis, that scoliosis is a universal rotational (de)compensation of the spine, which can be initiated by any cause for disturbed equilibrium, in the spine of any species.

### **22q11.2 Deletion Syndrome as a Model for Scoliosis**

In **PART III** scoliosis in 22q11.2 deletion syndrome and the resemblance to AIS in the general population, and the potential to serve as a 'model' was studied. As mentioned in **Chapter 12 & 13**, 22q11.2DS has an estimated incidence of 1 in 2148 live births and is characterized by a scoliosis prevalence of around 50%.<sup>17-20</sup> The hypothesis to use 22q11.2DS scoliosis as a 'model' for AIS was postulated in **Chapter 14**, describing that the 20-fold increased risk over the general population of developing scoliosis strongly reduces the necessary sample size for prospective studies. **Chapter 15** supported the legitimacy of using 22q11.2DS scoliosis as a model for AIS by demonstrating great morphological and dynamic similarity: 98.4% of 22q11.2DS patients with scoliosis had a curve morphology following predefined criteria for idiopathic curves: eight or fewer vertebrae, involved in the curve, an S-shape and no inclusion of the lowest lumbar vertebrae. Furthermore, curve progression was present in 54.2%, with a mean progression rate of 2.5°/year, similar to reports on idiopathic scoliosis.

In **Chapter 16** the historical association between the occurrences of scoliosis and congenital heart disease (CHD) in the general population was addressed. The results showed that the 22q11.2 deletion was a big confounder in this relationship, since the prevalence of scoliosis in those with CHD but without a 22q11.2 deletion approximates that of the general population, contradicting earlier studies on the subject. Another common phenotype in 22q11.2DS is schizophrenia, and since in the general population schizophrenia had been associated to scoliosis, the genetic overlap between both was studied in **Chapter 17**.<sup>21</sup> This study showed that in addition to 22q11DS, there is also genetic overlap for common variants in the general population between AIS and schizophrenia. Also, gene-networks implicated in the risk for both conditions indicate the involvement of biopathways related to cellular signaling and neuron and brain development.

The final three chapters explored the use of this model. In **Chapter 18**, a systematic literature review on shear wave elastography of the intervertebral disc showed excellent repeatability and reproducibility of the ultrasound method, but a large variation in the correlation between shear wave speed measured in the disc and the tissue's apparent stiffness/elasticity. Although the data is not part of this thesis, following the findings of the systematic review this chapter, a prospective study is currently underway, and elastographies have been performed in both 22q11.2DS and asymptomatic children at pre-growth spurt age. At baseline, elastography measurements of the intervertebral discs L4/5 of their still straight spines, showed no significant differences between 22q11.2DS patients and those from the general population. However, after the next 5 years of follow-up, half of 22q11.2DS patients will have developed a scoliosis, and it can be analyzed whether the elastography measurements were different at inclusion from those that remain without scoliosis. In **Chapter 19**, a first unpowered prospective exploration with this model demonstrated that pre-scoliotic 22q11.2DS patients grouped by geometrical sagittal spine parameters to form five axial deformity pattern groups, all had very different rates of scoliosis development after two year of follow-up.

Finally, the climax of this thesis was in **Chapter 20**, where the 22q11.2DS model was used to its full potential for a powered prospective study. In this study, a larger 'PIT' (Posteriorly Inclined Triangle) area in the sagittal spinal profile of asymptomatic children with 22q11.2DS was identified as a prospective risk factor for later scoliosis development. Additionally, in those that developed scoliosis, it was observed that the sagittal spinal profile before curve onset not only dictated the scoliosis onset, but also the type of curve, i.e. thoracic versus (thoraco)lumbar (**Figure 6**).

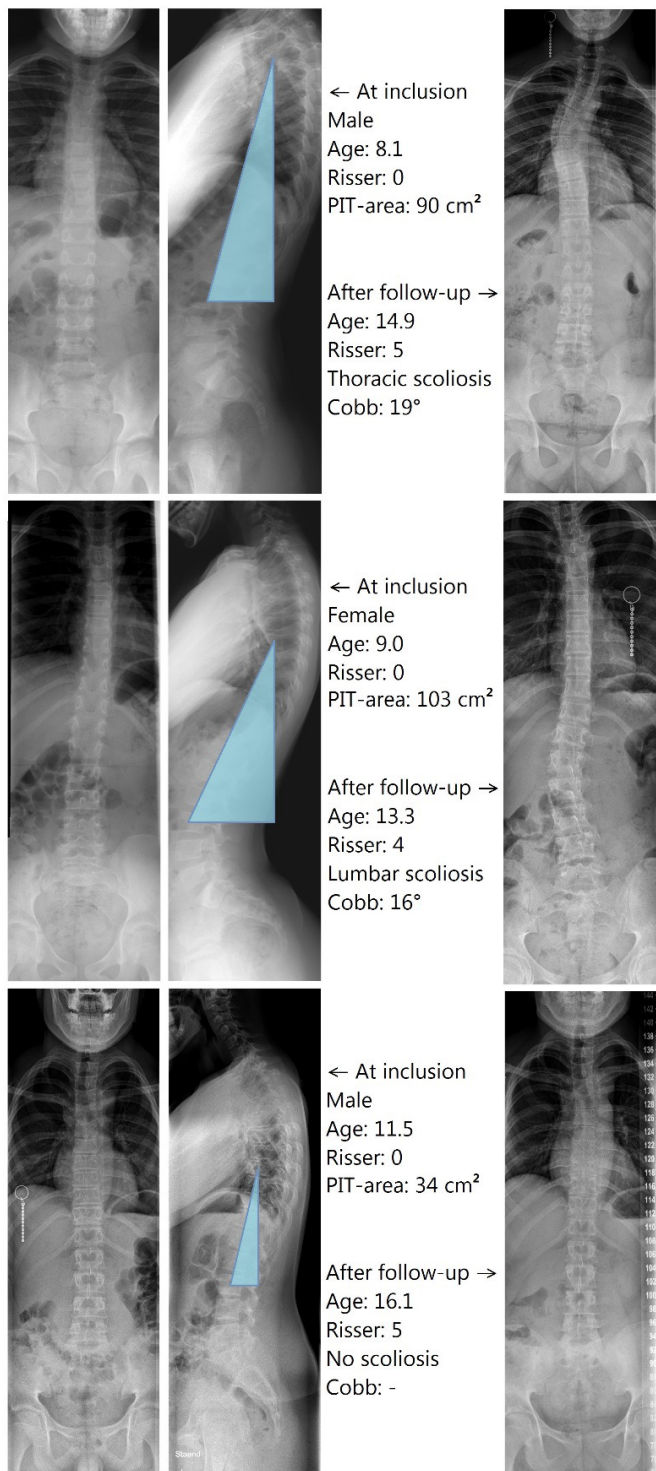


**Figure 6.** Examples of three participating children with 22q11.2DS, demonstrating a larger Posteriorly Inclined Triangle (PIT) area before the development of scoliosis compared to no scoliosis. Note the slender PIT in thoracic scoliosis versus wider PIT in (thoraco)lumbar scoliosis.

The exploration and validation of 22q11.2DS scoliosis as a 'biomechanical model' for AIS in **PART III**, and its final utilization, demonstrated the important implications for the role of the intervertebral disc and the sagittal spinal profile in scoliosis etiology. However, the use of this model has certain limitations. Earlier studies described scoliosis in 22q11.2DS as 'syndromic' or 'neuromuscular', which disqualified it to be a model for AIS. Although the results of this thesis show morphological and dynamic similarity of 22q11.2DS scoliosis to AIS, the translatability remains uncertain and the results should be interpreted with caution. This holds true for any model, it is always, at best, an approximation of the subject under study. However, if important findings in the 22q11.2DS model can be replicated for AIS in a general population cohort, this may aid in identifying those at risk for AIS in the general population.

### **Final conclusions and future perspectives**

The uniqueness of human sagittal spinal alignment and its link to the distinct phenomenon of AIS are the basis for this thesis. With contemporary imaging techniques, the current knowledge on the spinal structure during pediatric growth was broadened and deepened. Also this thesis introduced and verified radiation-free ultrasound to analyze the healthy and scoliotic spine, bypassing the ethical concerns of radiographic studies and reducing ionizing radiation in standard AIS care. Some of the presented study populations in this thesis were relatively small, therefore the next step would be ultrasound and MRI based studies of the general population, to prospectively describe the spinal structure, if possible in relationship to the development of scoliosis and other spinal deformities.

Arguably most importantly, this thesis aimed to shed light on the role of both the posteriorly inclined segment and posteriorly directed shear loads in the etiology of AIS. It was observed that already discrete differences are present in the straight spine, that may play a role in the development of AIS later in life. For instance disc slenderness, which was especially found to be present in girls in their mid-thoracic area during early adolescence, may be important. However, stronger prospective evidence was presented on the severity of the posteriorly inclined segment as risk factor for scoliosis. In scoliotic spines of different etiologies it was demonstrated, that axial rotation into the curve convexity combined with lordosis, i.e. anterior opening of the rotated intervertebral discs, are a universal phenomenon among idiopathic, non-idiopathic and compensatory scoliotic curves in any species. Therefore, it seems to be a response to any cause of disturbance of spinal equilibrium. Finally, the scoliosis in 22q11.2DS was shown to morphologically and dynamically resemble AIS, supporting the use as a 'model', and prospectively determine the importance of the intervertebral disc and the sagittal spinal profile in AIS etiology.

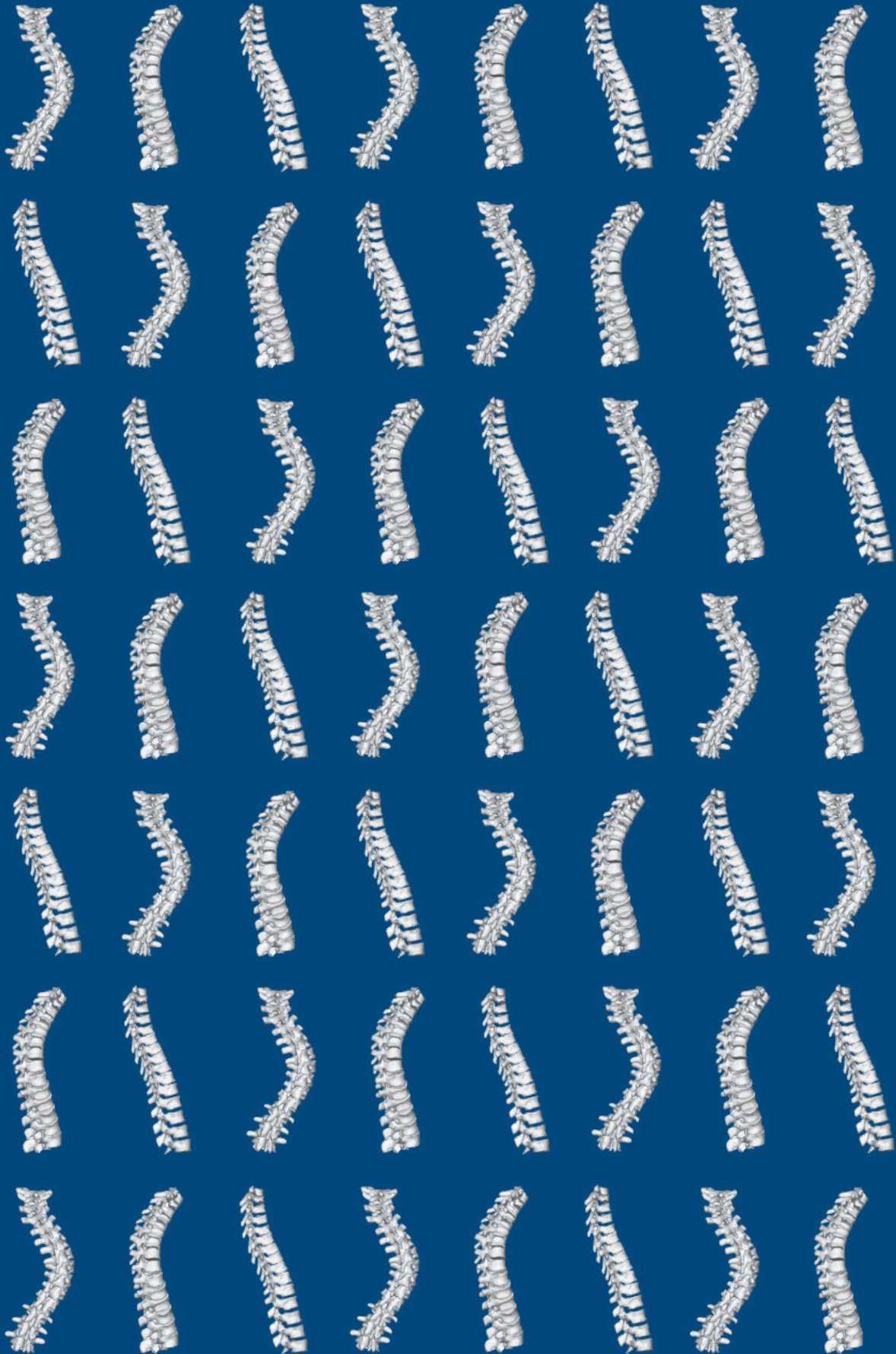
The logical next step is further unraveling idiopathic scoliosis etiology with powered prospective studies, opportunistically involving the 22q11.2DS model, to discern cause from effect in phenomena associated to AIS development. The identification of risk factors for idiopathic scoliosis, that are already present in the spine before curve onset, including but not limited to intervertebral disc mechanical properties or sagittal alignment as presented in this thesis, should be the most important goal of future studies. While important clues in AIS etiology have historically been drawn from retrospective studies, prospective research is the only way to truly confirm or discard these clues, distinguishing between cause and effect of the disorder and contribute certainties to the ongoing effort of taking the 'I' out of AIS. Identifying causal factors that are already present before AIS development, may be used as biomarkers in identifying those at risk for AIS in the general population. Screening and prevention currently have next to no place in AIS clinical care, while this has been proven to be the most effective way in battling a disease, especially on population level.

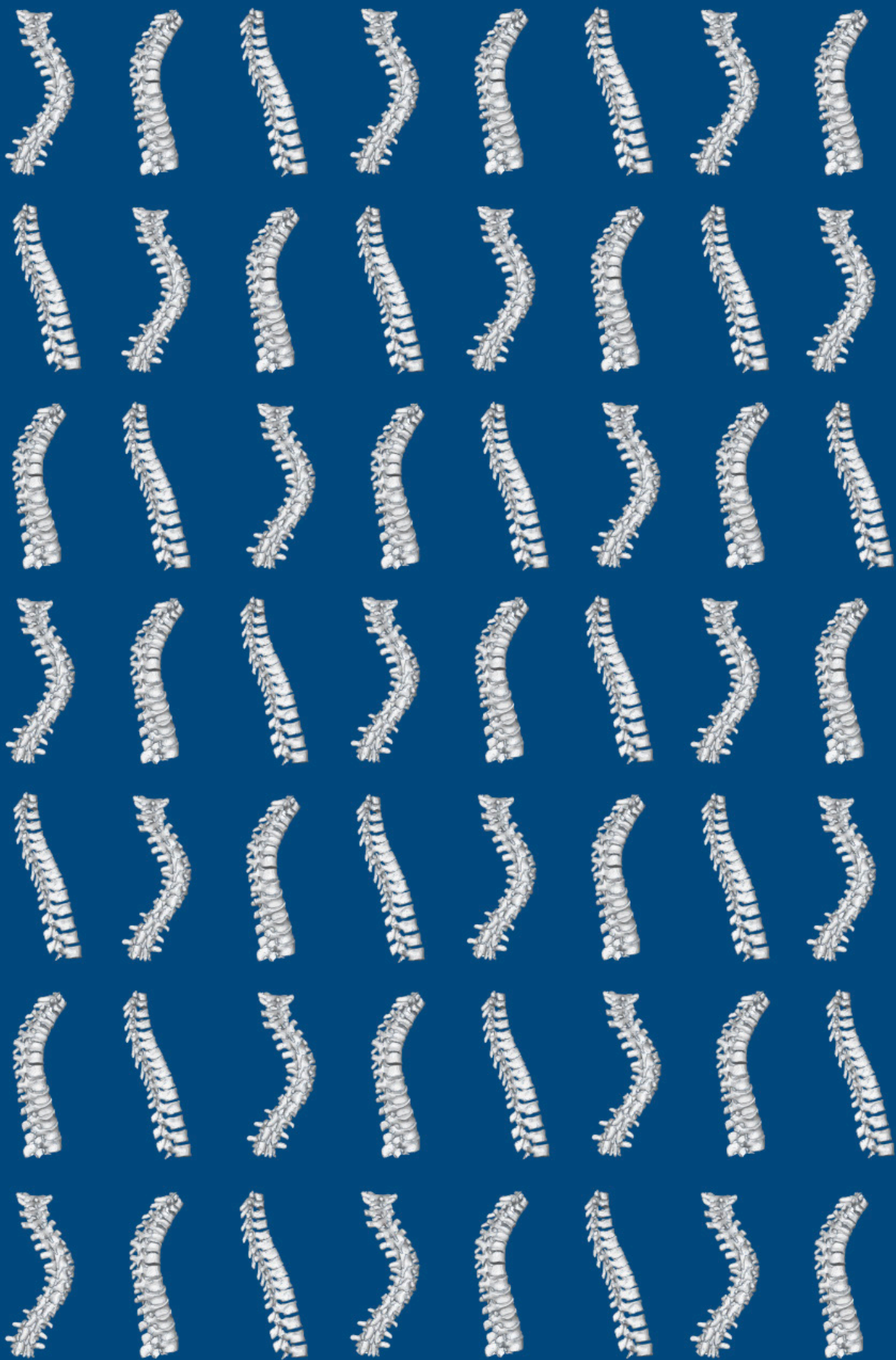
It is time to take the big leap, and transfer the focus from watchful waiting and treatment of secondary symptoms, towards developing prevention that targets the primary disease process.

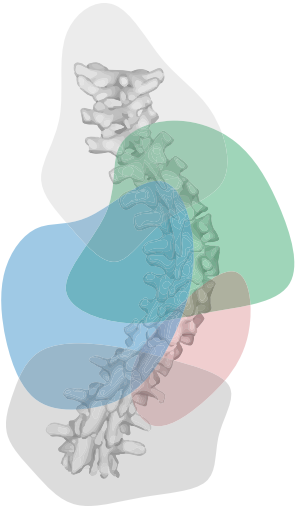


## References

1. Bernhardt M, Bridwell KH. Segmental analysis of the sagittal plane alignment of the normal thoracic and lumbar spines and thoracolumbar junction. *Spine (Phila Pa 1976)* 1989;14:717–21.
2. Alexander RM. Bipedal animals, and their differences from humans. *J Anat* 2004;204:321–30.
3. Washburn SL. The analysis of primate evolution with particular reference to the origin of man. *Cold Spring Harb Symp Quant Biol* 1950;15:67–78.
4. Abitbol MM. Evolution of the ischial spine and of the pelvic floor in the Hominoidea. *Am J Phys Anthropol* 1988;75:53–67.
5. Voutsinas SA, MacEwen GD. Sagittal profiles of the spine. *Clin Orthop Relat Res* 1986;235–42.
6. Kouwenhoven J-WM, Smit TH, van der Veen AJ, et al. Effects of Dorsal Versus Ventral Shear Loads on the Rotational Stability of the Thoracic Spine. *Spine (Phila Pa 1976)* 2007;32:2545–50.
7. Homminga J, Lehr AM, Meijer GJM, et al. Posteriorly directed shear loads and disc degeneration affect the torsional stiffness of spinal motion segments: a biomechanical modeling study. *Spine (Phila Pa 1976)* 2013;38:E1313–9.
8. Taylor JR. Growth of human intervertebral discs and vertebral bodies. *J Anat* 1975;120:49–68.
9. Cheng JC, Castelein RM, Chu WC, et al. Adolescent idiopathic scoliosis. *Nat Rev Dis Primers* 2015;1:1–21.
10. Vergari C, Karam M, Pietton R, et al. Spine slenderness and wedging in adolescent idiopathic scoliosis and in asymptomatic population: an observational retrospective study. *Eur Spine J* 2020;29:726–36.
11. Chen H, Schlösser TPC, Brink RC, et al. The Height-Width-Depth Ratios of the Intervertebral Discs and Vertebral Bodies in Adolescent Idiopathic Scoliosis vs Controls in a Chinese Population. *Sci Rep*;7. April 18, 2017.
12. Uys A, Bernitz H, Pretorius S, et al. Age estimation from anterior cervical vertebral ring apophysis ossification in South Africans. *Int J Legal Med* 2019;133:1935–48.
13. Makino T, Kaito T, Sakai Y, et al. Asymmetrical ossification in the epiphyseal ring of patients with adolescent idiopathic scoliosis. *Bone Joint J* 2016;98-B:666–71.
14. Janssen MMA, Kouwenhoven J-WM, Schlösser TPC, et al. Analysis of preexistent vertebral rotation in the normal infantile, juvenile, and adolescent spine. *Spine (Phila Pa 1976)* 2011;36:E486–91.
15. Figueiredo UM, James JI. Juvenile idiopathic scoliosis. *J Bone Joint Surg Br* 1981;63-B:61–6.
16. Roaf R. The basic anatomy of scoliosis. *J Bone Joint Surg Br* 1966;48:786–92.
17. Homans JF, Baldew VGM, Brink RC, et al. Scoliosis in association with the 22q11.2 deletion syndrome: An observational study. *Arch Dis Child* 2019;104:19–24.
18. McDonald-McGinn DM, Sullivan KE, Marino B, et al. 22q11.2 deletion syndrome. *Nat Rev Dis Primers*;1. 2015.
19. Grati FR, Molina Gomes D, Ferreira JCPB, et al. Prevalence of recurrent pathogenic microdeletions and microduplications in over 9500 pregnancies. *Prenat Diagn* 2015;35:801–9.
20. Blagojevic C, Heung T, Theriault M, et al. Estimate of the contemporary live-birth prevalence of recurrent 22q11.2 deletions: a cross-sectional analysis from population-based newborn screening. *CMAJ Open* 2021;9:E802–9.
21. Malmqvist M, Tropp H, Lyth J, et al. Patients With Idiopathic Scoliosis Run an Increased Risk of Schizophrenia. *Spine Deform* 2019;7:262–6.

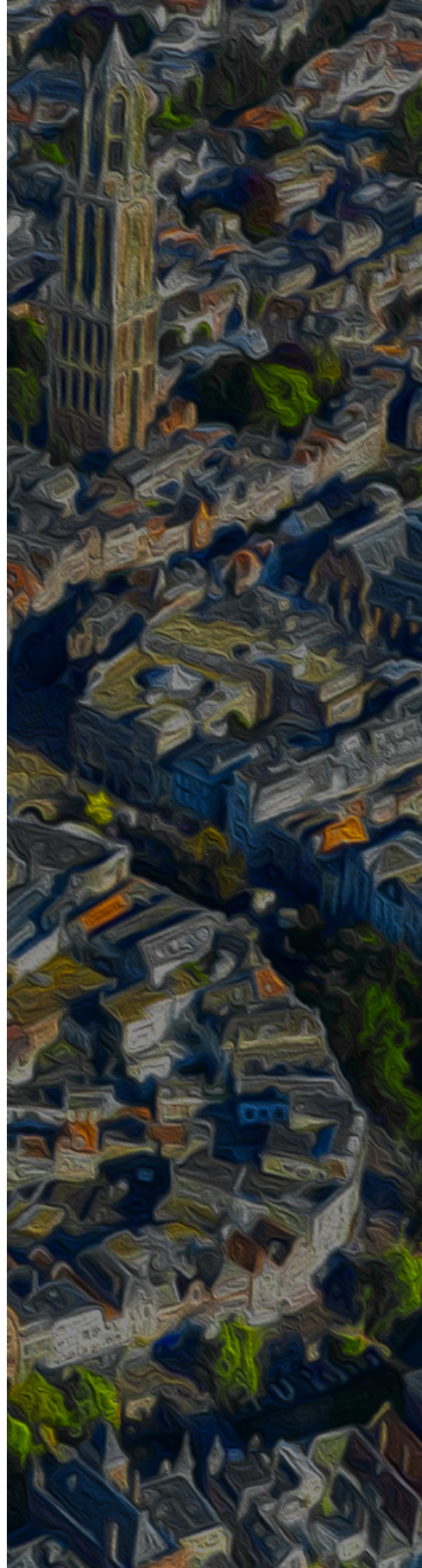








## Nederlandse Samenvatting



## Probleembeschrijving

Dit proefschrift bestudeert de meest voorkomende aandoening van de rug bij kinderen: adolescente idiopathische scoliose (AIS). Deze verkromming van de rug ontstaat meestal spontaan tijdens de groei, en de exacte oorzaak ervan is vooralsnog niet bekend. Wel zijn er aanwijzingen dat het met de belasting van de wervelkolom tijdens de groei te maken heeft. De mens heeft een unieke sagittale uitlijning van de wervelkolom, inclusief een naar achteren hellend segment. De oriëntatie van dit segment introduceert, in tegenstelling tot de 'fysiologische' naar voren gerichte belastingen, naar achteren gerichte schuifbelastingen op de wervelkolom, welke zijn aangetoond de rotatiestabiliteit aanzienlijk te verminderen. In totaal werken er dus drie krachten op de wervelkolom: axiaal (naar beneden), anterieur (naar voren) en posterieur (naar achteren). Het is algemeen aanvaard dat overmatige axiale en anterieure krachten tijdens de groei kunnen leiden tot bekende vervormingen, respectievelijk: de ziekte van Scheuermann en spondylolisthesis. De titel van dit proefschrift: Scoliose - een Universele Rotatoire (De)compensatie van de Wervelkolom, suggereert een belangrijke rol voor de derde kracht, de posterieure schuifkracht, en de rol van deze kracht in het mechanisme van het ontstaan van scoliose. Deze hypothese wordt onderzocht in drie delen:

- In het eerste deel wordt de bestaande kennis over de groei van de gezonde wervelkolom verder uitgediept met behulp van moderne medische beeldvorming.
- In het tweede deel worden scoliose van verschillende oorzaak en in verschillende soorten onderzocht, om te bekijken of er een universeel mechanisme aanwezig is.
- In het derde deel wordt een hoog scoliose-risico cohort bestudeerd, en uiteindelijk prospectief geanalyseerd of de mate van posterieure inclinatie van wervelkolom een risico factor is voor het optreden van scoliose.

## Deel I: Groei van de gezonde wervelkolom

Het is vanuit oude anatomische studies al bekend dat de wervelkolom voornamelijk groeit in de lengte door groei van de wervellichamen, en in veel mindere mate door de tussenwervelschijf. Nauwkeurige metingen zijn echter nooit gepubliceerd. In **hoofdstuk 2** werden deze metingen uitgevoerd op CT-scans van de rug van kinderen en werd de sterke toename van de wervellichaamhoogte tijdens de groei bevestigd. Verder werd gezien dat tussenwervelschijven alleen de eerste jaren in hoogte toenemen en daarna stabiel blijven. Omdat het transversale oppervlak tijdens de groei blijft toenemen, neemt de slankheid van de tussenwervelschijven over het algemeen af. Het viel op dat tussenwervelschijven bij meisjes over het algemeen slanker zijn dan bij jongens, het meest uitgesproken rond de groeispurt.

Dit werd bevestigd in de MRI-analyse van **hoofdstuk 3**, bovendien werd waargenomen dat de transversale dwarsdoorsnede van de tussenwervelschijf en het volume consistent toenamen. Daarbinnen was er een stabiele volumeverhouding van de twee belangrijkste componenten: de annulus fibrosus ten opzichte van de nucleus pulposus, met over het algemeen grotere tussenwervelschijven bij jongens. Tijdens de groei was de nucleusoriëntatie binnen de schijf stabiel en gecentreerd in de rechts-links en craniaal-caudale richting. Echter in de anterior-posterieure richting verschuift de nucleus in toenemende mate met de leeftijd, volgens het bekende, S-vormige, sagittale profiel van de wervelkolom. De slankheid van de tussenwervelschijven nam licht af in de eerste drie levensjaren en blijft daarna stabiel. Het interessante is dat vrouwelijke tussenwervelschijven, vooral mid-thoracale en gedurende de vroege adolescentie, slanker waren dan die van mannen. Aangezien idiopathische scoliose zich meestal manifesteert bij meisjes, in het midden van de thorax in de vroege adolescentie, zou kunnen worden gespeculeerd dat dit te maken heeft met de grotere en smallere, dus minder robuuste tussenwervelschijven in dit gebied. Vanuit de literatuur is bekend dat de wervelkolom bij patiënten met scoliose slanker is in vergelijking met de gezonde populatie. Samen met de observaties in dit hoofdstuk suggereert dit dat 'slankheid' van de tussenwervelschijven een potentiële risicofactor is voor het ontstaan van scoliose.

Stabiliteit van de wervelkolom en weerstand tegen rotatiekrachten heeft ook te maken met de manier waarop de tussenwervelschijf aan de wervelkolom is verankerd. De vezels van Sharpey hechten in de ringapofyse en verankeren zo de tussenwervelschijf aan de twee aangrenzende wervels. Aangezien het een zwak punt is, is dit een proces dat belangrijke implicaties kan hebben voor de mechanische stabiliteit van het schijf-wervellichaamcomplex van de thoraco-lumbale gedeeltes op een moment dat de belasting van de wervelkolom snel toeneemt als gevolg van de adolescente groeispurt. In **hoofdstuk 4** werd dit bestudeerd op basis van CT, verschillende RAM-stadia (Ring Apophysis Maturation) die het proces van ossificatie en fusie van de ringapofyse met het wervellichaam beschrijven, werden tijdens de groei in kaart gebracht. Er werd geobserveerd dat RAM relatief later plaatsvond in de mid-thoracale en thoraco-lumbale wervelkolom. Verder was ten opzichte van de timing van de groeispurt waren ringapofyse van meisjes minder volwassen dan die van jongens. Deze bevindingen kunnen belangrijk zijn voor het begrijpen van het pathomechanisme van idiopathische scoliose: gezien scoliose meestal begint in de vroege groeispurt, waarbij de voorkeurslocatie van de apex mid-thoracaal ligt en er oververtegenwoordiging is van vrouwen.

In **hoofdstuk 5** werd gezien dat het thoracale massazwaartepunt verschuift van enigszins rechts op infantiele leeftijd, naar neutraal op juveniele leeftijd, naar links op adolescentie leeftijd. Dit komt overeen met de eerder aangetoonde richtingsverandering van preëxistente rotatie in de normale wervelkolom met de leeftijd, evenals met de bekende verandering van

richting, van links naar rechts, van thoracale curve convexiteit bij scoliose op verschillende leeftijden. Deze bevinding verklaart de richting van de bocht bij scoliose en onderstreept de biomechanische component van AIS. **Hoofdstuk 6** toonde aan dat statistische vormmodellering (SSM) in combinatie met niet-ioniserende ultrasone beeldvorming de subtiele variaties in individuele sagittale vorm kon visualiseren en kwantificeren. De vorm vóór de groeispuurt was een minder uitgesproken sagittale kromming met een minder steil, maar langer achterwaarts hellend segment dat reikte tot in de hogere thoracale gebieden. Na de groeispuurt was er een meer uitgesproken sagittale kromming met een steiler maar korter naar achteren hellend segment.

Vóór deze hoofdstukken was er een algemeen idee dat lengte toename van de wervelkolom tijdens de groei voornamelijk in de wervellichamen plaatsvindt, en dat het sagittale profiel verschuift van een C-vorm bij zuigelingen naar de typische S-vorm van rechtopstaande mensen. De studies van **deel I** geven een veel bredere en nauwkeurigere beschrijving van de morfologie van de elementen waaruit de wervelkolom tijdens de groei bestaat. Verder wordt een meer delicate en stralingsvrije methode voor sagittale vormstudies gepresenteerd. Er zijn echter beperkingen, voornamelijk dat 'groei' werd beschreven op basis van cross-sectionele gegevens van verschillende individuen, terwijl een longitudinaal ontwerp waarschijnlijk nauwkeuriger zou zijn. Dit was niet mogelijk vanwege de beschikbaarheid van gegevens en ethische overwegingen, en door grote steekproeven in deze onderzoeken te hebben, werd geprobeerd voor het cross-sectionele ontwerp te compenseren. De resultaten van deze hoofdstukken zijn een grote hoeveelheid gegevens, die toekomstige studies met specifieke onderzoeksvragen over de etiologie van idiopathische scoliose zullen helpen, maar op zichzelf al enige inzichten geven. Zo zijn bijvoorbeeld de slankheid van de tussenwervelschijf en de ernst van het naar achteren hellende segment al aanwezig in de normale wervelkolom, variërend tussen individuen of tussen jongens en meisjes, maar spelen mogelijk ook een belangrijke rol bij het ontstaan van idiopathische scoliose.

## **Deel II: Scoliose als een universele reactie**

In dit deel werd de morfologie van de scoliosewervelkolom en de mogelijke overeenkomsten tussen scoliose van verschillende etiologieën en soorten bestudeerd. In **hoofdstuk 7** werd een poging gedaan om de stralingsproblemen van conventionele beeldvorming van de wervelkolom aan te pakken, en er werd aangetoond dat Cobb-hoekmetingen van de wervelkolom via echografie een uitstekende correlatie lieten zien met de röntgenfoto's als gouden standaard. De echografie metingen zijn gebaseerd op de locatie van de processus spinosus en de laminae (oftewel de posterieure structuren), bij scoliose is bekend dat deze minder lateraal afwijken dan de meer anterieure wervellichamen die op röntgenfoto's



worden gebruikt voor de metingen. Daarom werd de Cobb-hoek systematisch onderschat. In deze studie werd dit opgelost door omrekenformules te genereren: *thoracale Cobb-hoek* =  $1,43 \times$  *ultrasone hoek* en *lumbale Cobb-hoek* =  $1,23 \times$  *ultrasone hoek*, welke een goede nauwkeurigheid en geen proportionele vertekening vertoonden, wat vervolgens de implementatie van ultrasone beeldvorming ondersteunde.

In **hoofdstuk 8** werd waargenomen dat compensatoire bochten bij congenitale scoliose uitsluitend anterieure verlenging van de tussenwervelschijven vertonen, vergelijkbaar met AIS en neuromusculaire scoliose, wat bevestigt dat dit deel uitmaakt van de driedimensionale deformiteit in verschillende soorten scoliose. Bovendien behielden de benige wervellichamen hun kyfotische vorm zoals ook in AIS vergelijkbaar met de andere scoliosetypen, wat aangeeft dat er geen actieve anterieure benige overgroei is, in tegenstelling tot de eerder gepostuleerde theorie van RASO (relatieve anterieure spinale overgroei). Anterieure verlenging lijkt een passief resultaat te zijn van een scoliotische misvorming, in plaats van gerelateerd te zijn aan de specifieke oorzaak van AIS.

Een ander type scoliose, volwassen degeneratieve scoliose (Adult Degenerative Scoliosis: ADS), werd bestudeerd in **hoofdstuk 9**. ADS wordt algemeen beschouwd als een andere entiteit dan AIS met een andere pathomechanische achtergrond. Er werd waargenomen dat ADS zich normaal 'de novo' ontwikkelt in de lumbale wervelkolom van patiënten met een pelvic incidence dan controles, vergelijkbaar met primaire lumbale AIS. Aangezien de pelvic incidence het sagittale wervelprofiel dicteert, suggereert dit het belang van beide in de etiologie van scoliose, en benadrukt het een andere gedeelde mechanische basis van scoliose misvormingen met verschillende etiologieën. Anders geformuleerd, de bekkenmorfologie dicteert de sagittale uitlijning van de wervelkolom, die de segmenten van de wervelkolom bepaalt die vatbaar zijn voor het ontwikkelen van scoliose, zowel in de groeiende adolescente wervelkolom als in de degeneratieve wervelkolom bij ouderen. Degeneratieve volwassen scoliose kan worden beschouwd als het laatste stadium van idiopathische scoliose.

In **hoofdstuk 10** werd een compensatoire scoliose, welke aanwezig was in het anatomisch normale deel van de wervelkolom bij een gestrande walvis, veroorzaakt door een traumatische verwonding beschreven. Er werd een vergelijkbare apexrotatie in de bocht, convexiteit en anterieure opening van de tussenwervelschijfruimte geobserveerd met sterke gelijkenis met de verschillende scoliosetypen bij mensen, inclusief AIS. Dit suggereert dat elke decompensatie van het evenwicht van de wervelkolom, of compensatie van de wervelkolom geïnitieerd door een externe factor (zoals in het geval van deze walvis), kan leiden tot een tamelijk uniforme reactie, onafhankelijk van de oorzaak of soort. Een walvis heeft een ernstig trauma nodig om

scoliose te ontwikkelen. Het trauma was uiteindelijk - na voldoende tijd om geleidelijk de compenserende scoliose te ontwikkelen – de doodsoorzaak van het dier. Bij mensen zijn, vanwege hun veel minder rotatiestabiele wervelkolomconfiguratie, veel subtielere verstoringen van het evenwicht voldoende om dezelfde reeks gebeurtenissen op gang te brengen.

Ten slotte werd in **hoofdstuk 11** de spinale lengte van de scoliotische bocht in AIS gemeten over vier hoeken: anterieur-convex, anterieur-concaaf, posterieur-convex en posterieur-concaaf. Naast de verwachte globale convexiteitsverlenging en thoracale lordose, werd een sterke verkorting aan de posterieure-concaviteit waargenomen, terwijl de posterieure-convexiteit iets langer was bij AIS in vergelijking met controles. Om de spinale harmonie te herstellen tijdens posterieure chirurgie, moet de posterieure-concaviteit worden verlengd, terwijl de posterieure-convexiteit enigszins kan worden ingekort.

Vóór dit proefschrift was het algemeen aanvaard dat idiopathische scoliose gepaard gaat met een hypokyfose/lordose, met de klinisch aanwezige platte rug of 'flat back', en zichtbaar op röntgenfoto's. In eerdere literatuur werd de geobserveerde relatieve anterieure verlenging bij AIS dus RASO genoemd, met de suggestie dat de normale synchroniciteit van anterieure en posterieure wervelgroei zou zijn verstoord. Dit proefschrift verwerpt zowel het concept van actieve anterieure benige overgroei, alsmede het idee dat anterieure verlenging exclusief is voor AIS. Op basis van de observaties van dit deel, betreffende de segmentale lordose als onderdeel van het scoliosemechanisme, kan worden verworpen dat er enige vorm van benige (over)groei is aan het voorste deel van de wervelkolom. Er werd geobserveerd dat de relatieve anterieure verlenging specifiek de anterieure opening van de tussenwervelschijven is. Bovendien werd bevestigd dat dit mechanisme niet alleen wordt waargenomen bij AIS, maar ook bij scoliose van verschillende etiologieën (neuromusculair, congenitaal en traumatisch) en ook bij een andere soort dan de mens, hoe onwaarschijnlijk het optreden van scoliose bij andere soorten ook is. Daarom bevestigen de resultaten de titel van dit proefschrift, dat scoliose een universele rotatie(de)compensatie van de wervelkolom is, die kan worden geïnitieerd door elke oorzaak van een verstoord evenwicht, in de wervelkolom van elke soort.

### **Deel III. 22q11.2 Deletiesyndroom als model voor scoliose**

Scoliose als onderdeel van het 22q11.2 deletiesyndroom en de gelijkenis met AIS in de gehele populatie, en het potentieel om als 'model' te dienen, werden bestudeerd. Zoals vermeld in **hoofdstuk 12 en 13**, heeft 22q11.2DS een geschatte incidentie van 1 op 2148 levendgeborenen en wordt het gekenmerkt door een scolioseprevalentie van ongeveer 50%. De hypothese om 22q11.2DS-scoliose te gebruiken als een 'model' voor AIS werd

gepostuleerd in **hoofdstuk 14**, waarin werd beschreven dat het 20-voudig verhoogde risico op het ontwikkelen van scoliose ten opzichte van de algehele populatie, de benodigde steekproefomvang voor prospectieve studies sterk verkleint. **Hoofdstuk 15** ondersteunde de legitimiteit van het gebruik van 22q11.2DS-scoliose als een model voor AIS door grote morfologische en dynamische gelijkenis aan te tonen: 98,4% van de 22q11.2DS-patiënten met scoliose had een curve-morfologie volgens vooraf gedefinieerde criteria voor idiopathische curves: acht of minder wervels, een S-vorm en geen deelname van de onderste lendenwervels. Bovendien was curveprogressie aanwezig bij 54,2%, met een gemiddelde progressiesnelheid van 2,5°/jaar, vergelijkbaar met publicaties over idiopathische scoliose.

In **hoofdstuk 16** werd het historische verband uit de literatuur tussen scoliose en congenitale hartafwijkingen (congenital heart disease: CHD) in de algehele populatie onderzocht. De resultaten toonden aan dat de 22q11.2-deletie een grote 'confounder' was in deze relatie, aangezien de prevalentie van scoliose bij mensen met CHD - maar zónder een 22q11.2-deletie - die van de algehele populatie benadert, wat in tegenspraak is met eerdere studies over dit onderwerp. Een ander veel voorkomend fenotype in 22q11.2DS is schizofrenie, en aangezien in de algemene populatie schizofrenie in verband werd gebracht met scoliose, werd de genetische overlap tussen beide bestudeerd in **hoofdstuk 17**. Deze studie toonde aan dat er naast 22q11DS ook genetische overlap is voor 'common genetic variants' in de algehele populatie tussen AIS en schizofrenie. Ook is er overlap in genennetwerken in het risico voor beide aandoeningen, de betrokken 'biopathways' houden verband met cellulaire signalering en neuron- en hersenontwikkeling. Deze processen hebben dus mogelijk een rol in zowel AIS als schizofrenie.

In de laatste drie hoofdstukken werd het 22q11.2DS-scoliose model geëxploreerd en uiteindelijk gebruikt voor prospectieve studies. In **hoofdstuk 18** toonde een 'systematic review' over elastografie van de tussenwervelschijf een uitstekende herhaalbaarheid en reproduceerbaarheid van de ultrasone methode, maar een grote variatie in de correlatie tussen de 'shear wave speed' gemeten in de tussenwervelschijf en de schijnbare stijfheid/elasticiteit van het weefsel. Hoewel de gegevens geen deel uitmaken van dit proefschrift, is er, naar aanleiding van de bevindingen van de systematic review, momenteel een prospectieve studie opgezet en zijn elastografieën uitgevoerd bij zowel 22q11.2DS als asymptomatische kinderen in de leeftijd vóór de groeispurt. De elastografische metingen bij inclusie, van de tussenwervelschijven L4/5 van hun nog rechte wervelkolom, toonden geen significante verschillen tussen 22q11.2DS-patiënten en patiënten uit de algehele populatie. Momenteel volgt er 5 jaar follow-up, waarna ongeveer de helft van de 22q11.2DS-patiënten een scoliose zal hebben ontwikkeld. Dan kan worden geanalyseerd of de elastografische metingen bij inclusie

verschillen tussen de kinderen met 22q11.2DS die wel of geen scoliose ontwikkelden later.

**Hoofdstuk 19** is een eerste 'pilot' studie, waarin een prospectieve verkenning werd gedaan van dit model. Een ongepowerd aantal pre-scoliotische 22q11.2DS-patiënten werden gegroepeerd op basis van geometrische sagittale wervelkolomparameters, er konden vijf axiale deformatiepatronen worden gevormd waarin de patiënten werden gegroepeerd. Na follow-up verschilde de proportie scoliosepatiënten per deformatiegroep, en suggereerde het dus voorspellende waarde.

Ten slotte was de climax van dit proefschrift **hoofdstuk 20**, waar het 22q11.2DS-model ten volle werd gebruikt voor een gepowerde prospectieve studie. In deze studie werd een grotere 'PIT' (Posteriorly Inclined Triangle) in het sagittale wervelkolomprofiel van asymptomatische kinderen met 22q11.2DS geïdentificeerd als een mogelijke risicofactor voor de latere ontwikkeling van scoliose. Bovendien werd bij degenen die scoliose ontwikkelden waargenomen, dat het profiel van de sagittale wervelkolom vóór er enige scoliose was, niet alleen het optreden van scoliose dicteerde, maar ook het type kromming, dat wil zeggen de apex thoracaal versus (thoraco) lumbaal.

De verkenning en validatie van 22q11.2DS-scoliose als een 'biomechanisch model' voor AIS in, en het uiteindelijke gebruik ervan, toonden de belangrijke implicaties aan voor de rol van de tussenwervelschijf en het sagittale wervelkolomprofiel in de etiologie van scoliose. Het gebruik van dit model heeft echter bepaalde limitaties. Eerdere studies beschreven scoliose in 22q11.2DS als 'syndroomaal' of 'neuromusculair', wat het diskwalificeerde om een model voor AIS te zijn. Hoewel de resultaten van dit proefschrift morfologische en dynamische gelijkenis vertonen tussen scoliose 22q11.2DS en AIS, blijft de vertaalbaarheid onzeker en moeten de resultaten met voorzichtigheid worden geïnterpreteerd. Dit geldt voor elk model, het is in het beste geval altijd een benadering van het onderwerp dat wordt bestudeerd. Als belangrijke bevindingen in het 22q11.2DS-model echter kunnen worden gerepliceerd voor AIS in een algemeen bevolkingscohort, kan dit helpen bij het identificeren van degenen die risico lopen op AIS in de gehele populatie.

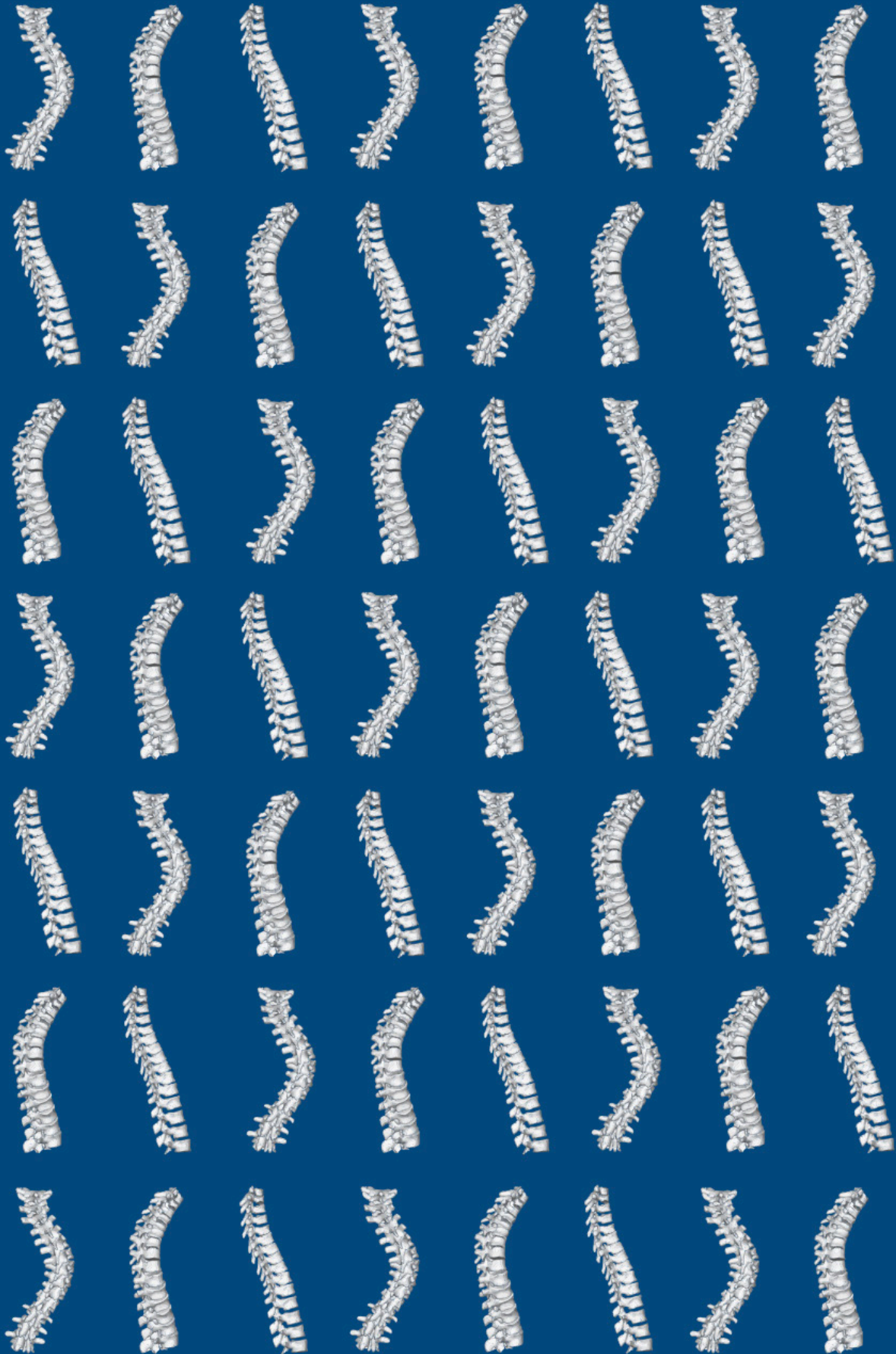
## **Eindconclusies en toekomstperspectieven**

Het unieke karakter van de uitlijning van de sagittale wervelkolom bij de mens en het verband met het specifieke fenomeen adolescentie idiopathische scoliose vormen de basis voor dit werk. Dit proefschrift had tot doel licht te werpen op de rol van zowel het naar achteren hellende segment, als de dorsale schuifbelastingen in de etiologie van AIS. Ten eerste werd

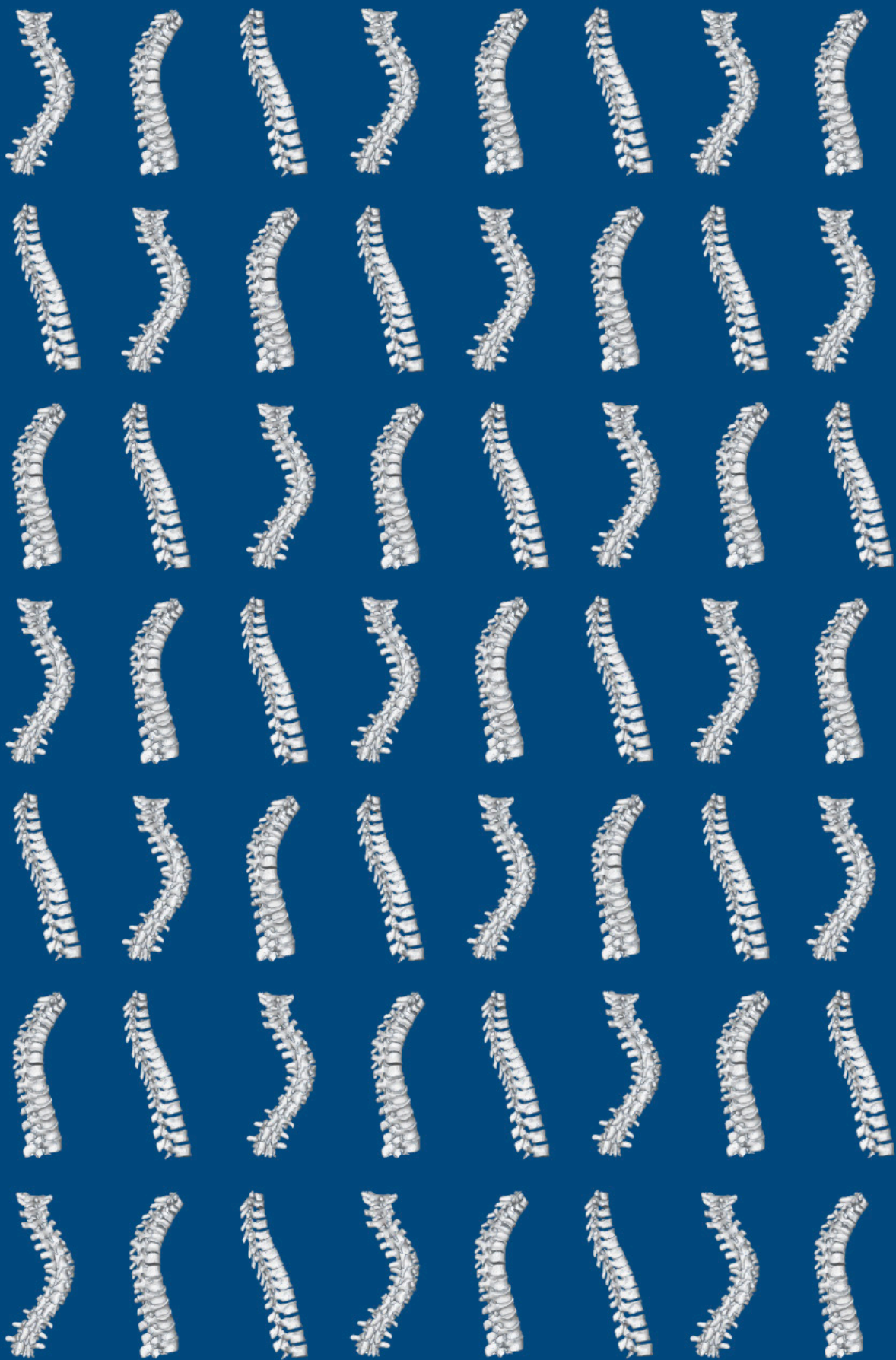
voor de normale wervelkolom waargenomen dat er al discrete verschillen aanwezig zijn, zoals de slankheid van de tussenwervelschijven, vooral bij meisjes mid-thoracaal tijdens de vroege adolescentie, en de ernst van het naar achteren hellende segment, tussen individuen en tussen jongens en meisjes. Welke de potentiële rol van beide in de ontwikkeling van idiopathische scoliose onderstreept. Ten tweede werd bij scoliosis van verschillende etiologieën aangetoond dat rotatie in de bocht, convexiteit en apicale lordose, in het bijzonder anterieure opening van de tussenwervelschijven, een universeel fenomeen zijn, welke een reactie lijkt te zijn op elke oorzaak van verstoring van het evenwicht, in de wervelkolom van welke soort dier dan ook. Ten derde werd aangetoond dat de scoliose in 22q11.2DS morfologisch en dynamisch lijkt op AIS, wat het gebruik als een 'model' ondersteunt en prospectief het belang van de tussenwervelschijf en het sagittale wervelprofiel in de etiologie van AIS bepaalt.

De logische volgende stap is het verder ontrafelen van idiopathische scoliose-etiologie met gepowerde prospectieve studies, wellicht het meest opportuun gebruikmakend van het 22q11.2DS-model, om oorzaak van gevolg te onderscheiden in fenomenen die verband houden met de ontwikkeling van AIS. De identificatie van risicofactoren voor idiopathische scoliose, die al aanwezig zijn in de wervelkolom voordat de curve begint, inclusief maar niet beperkt tot de mechanische eigenschappen van de tussenwervelschijf of sagittaal profiel zoals gepresenteerd in dit proefschrift, zou het belangrijkste doel moeten zijn van toekomstige studies. Ten eerste, hoewel belangrijke aanwijzingen in de etiologie van AIS in het verleden zijn ontleend aan retrospectieve studies, is prospectief onderzoek de enige manier om deze aanwijzingen echt te bevestigen of te verwerpen. Verder kan prospectief onderzoek onderscheid maken tussen oorzaak en gevolg van de stoornis en mogelijk zelfs bijdragen aan de voortdurende inspanning om de letter 'I' van idiopathisch, weg te nemen uit AIS. Ten tweede kan het identificeren van oorzakelijke factoren die al aanwezig waren vóór de ontwikkeling van AIS, worden gebruikt als biomarkers bij het identificeren van degenen die risico lopen op AIS in de algehele populatie. Screening en preventie hebben momenteel bijna geen plaats in de AIS-klinische zorg, terwijl is bewezen dat dit de meest effectieve manier is om een ziekte te bestrijden, zeker op populatieniveau.

Het is tijd om de grote sprong te wagen en de focus te verleggen van waakzaam afwachten en behandeling van secundaire symptomen naar het ontwikkelen van preventie gericht op de primaire oorzaak van de aandoening.



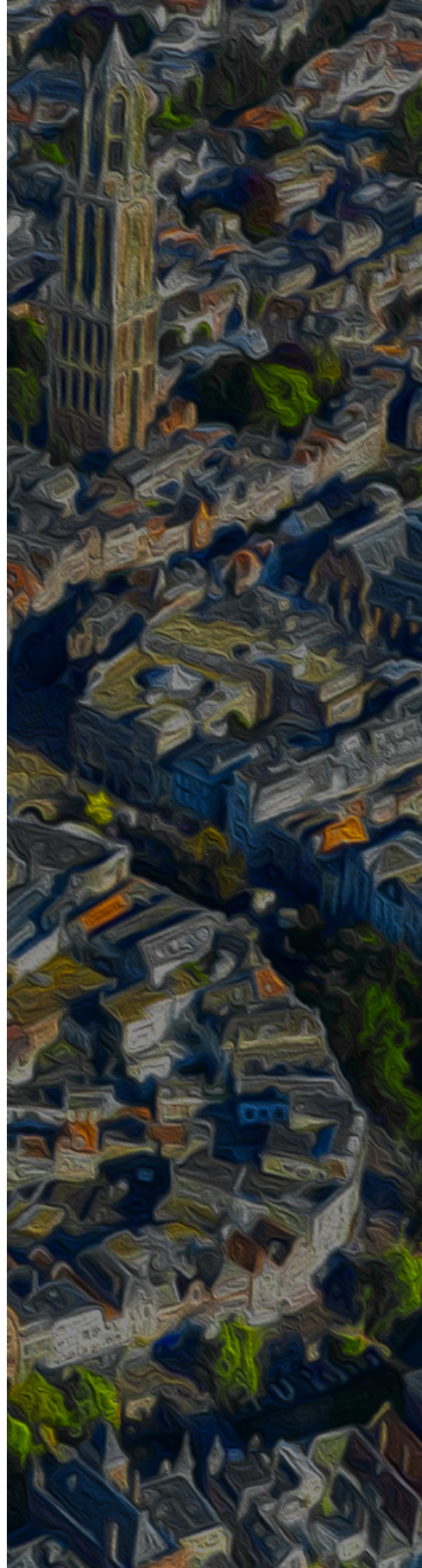








List of Publications,  
Curriculum Vitae  
& Acknowledgements



## List of publications

Part of this thesis

### **1. Disc and Vertebral Body Morphology From Birth to Adulthood**

de Reuver S, Costa L, van Rheenen H, Tabeing CS, Lemans JVC, Schlösser TPC, Kruyt MC, van Stralen M, Castelein RM.

*Spine (Phila Pa 1976)*. 2022 Apr 1;47(7):312-318. doi: 10.1097/BRS.0000000000004278

### **2. Morphology and Orientation of the Annulus Fibrosus and Nucleus Pulposus within the Intervertebral Disc during Growth**

Moens AJBWD, Magré J, Kruyt MC, Castelein RM, de Reuver S.

*Spine (Phila Pa 1976)*. 2023 Jul. ePub ahead of print.

### **3. Ossification and Fusion of the Vertebral Ring Apophysis as an Important Part of Spinal Maturation**

Costa L, de Reuver S, Kan L, Seevinck P, Kruyt MC, Schlosser TPC, Castelein RM.

*J Clin Med*. 2021 Jul 21;10(15):3217. doi: 10.3390/jcm10153217.

### **4. The Changing Position of the Center of Mass of the Thorax During Growth in Relation to Pre-existent Vertebral Rotation**

de Reuver S, Brink RC, Homans JF, Kruyt MC, van Stralen M, Schlösser TPC, Castelein RM.

*Spine (Phila Pa 1976)*. 2019 May 15;44(10):679-684. doi: 10.1097/BRS.0000000000002927

### **5. Sagittal Spinal Profile development during Growth: a Cross-Sectional Pilot Study using Spinal Ultrasound and Statistical Shape Modeling**

de Reuver S, Brink RC, Gielis WP, Lee TTY, Schlösser TPC, Kruyt MC, Castelein RM.

*Under Peer-review*. 2023 Aug. doi: n/a

### **6. Cross-validation of ultrasound imaging in adolescent idiopathic scoliosis.**

de Reuver S, Brink RC, Lee TTY, Zheng YP, Beek FJA, Castelein RM.

*Eur Spine J*. 2021 Mar;30(3):628-633. doi: 10.1007/s00586-020-06652-9

### **7. Anterior lengthening in scoliosis occurs only in the disc and is similar in different types of scoliosis.**

de Reuver S, Brink RC, Homans JF, Vavruch L, Tropp H, Kruyt MC, van Stralen M, Castelein RM.

*Spine J*. 2020 Oct;20(10):1653-1658. doi: 10.1016/j.spinee.2020.03.005.

## **8. The role of sagittal pelvic morphology in the development of adult degenerative scoliosis**

de Reuver S, van der Linden PP, Kruyt MC, Schlösser TPC, Castelein RM.  
*Eur Spine J.* 2021 Sep;30(9):2467-2472. doi: 10.1007/s00586-021-06924-y.

## **9. What a stranded whale with scoliosis can teach us about human idiopathic scoliosis**

de Reuver S, IJsseldijk LL, Homans JF, Willems DS, Veraa S, van Stralen M, Kik MJL, Kruyt MC, Gröne A, Castelein RM.  
*Sci Rep.* 2021 Mar 30;11(1):7218. doi: 10.1038/s41598-021-86709-x.

## **10. Convex-concave and anterior-posterior spinal length discrepancies in adolescent idiopathic scoliosis with major right thoracic curves versus matched controls.**

de Reuver S, de Block N, Brink RC, Chu WCW, Cheng JCY, Kruyt MC, Castelein RM, Schlösser TPC.  
*Spine Deform.* 2023 Jan;11(1):87-93. doi: 10.1007/s43390-022-00566-w.

## **11. Updated clinical practice recommendations for managing children with 22q11.2 deletion syndrome.**

Óskarsdóttir S, Boot E, Crowley TB, Loo JCY, Arganbright JM, Armando M, Baylis AL, Breetvelt EJ, Castelein RM, Chadehumbe M, Cielo CM, de Reuver S, Eliez S, Fiksinski AM, Forbes BJ, Gallagher E, Hopkins SE, Jackson OA, Levitz-Katz L, Klingberg G, Lambert MP, Marino B, Mascarenhas MR, Moldenhauer J, Moss EM, Nowakowska BA, Orchanian-Cheff A, Putotto C, Repetto GM, Schindewolf E, Schneider M, Solot CB, Sullivan KE, Swillen A, Unolt M, Van Batavia JP, Vingerhoets C, Vorstman J, Bassett AS, McDonald-McGinn DM.  
*Genet Med.* 2023 Jan 31:100338. doi: 10.1016/j.gim.2022.11.006.

## **12. Updated clinical practice recommendations for managing adults with 22q11.2 deletion syndrome.**

Boot E, Óskarsdóttir S, Loo JCY, Crowley TB, Orchanian-Cheff A, Andrade DM, Arganbright JM, Castelein RM, Cserti-Gazdewich C, de Reuver S, Fiksinski AM, Klingberg G, Lang AE, Mascarenhas MR, Moss EM, Nowakowska BA, Oechslin E, Palmer L, Repetto GM, Reyes NGD, Schneider M, Silversides C, Sullivan KE, Swillen A, van Amelsvoort TAMJ, Van Batavia JP, Vingerhoets C, McDonald-McGinn DM, Bassett AS.  
*Genet Med.* 2023 Jan 31:100344. doi: 10.1016/j.gim.2022.11.012.

**13. The 22q11.2 deletion syndrome as a model for idiopathic scoliosis - A hypothesis**

Homans JF, [de Reuver S](#), Breetvelt EJ, Vorstman JAS, Deeney VFX, Flynn JM, McDonald-McGinn DM, Kruyt MC, Castelein RM.

*Med Hypotheses*. 2019 Jun;127:57-62. doi: 10.1016/j.mehy.2019.03.024.

**14. 22q11.2 Deletion Syndrome as a Human Model for Idiopathic Scoliosis.**

[de Reuver S](#), Homans JF, Schlösser TPC, Houben ML, Deeney VFX, Crowley TB, Stücker R, Pasha S, Kruyt MC, McDonald-McGinn DM, Castelein RM.

*J Clin Med*. 2021 Oct 20;10(21):4823. doi: 10.3390/jcm10214823.

**15. The role of 22q11.2 deletion syndrome in the relationship between congenital heart disease and scoliosis.**

Homans JF, [de Reuver S](#), Heung T, Silversides CK, Oechslein EN, Houben ML, McDonald-McGinn DM, Kruyt MC, Castelein RM, Bassett AS.

*Spine J*. 2020 Jun;20(6):956-963. doi: 10.1016/j.spinee.2020.01.006.

**16. Genetic Overlap between Idiopathic Scoliosis and Schizophrenia in the General Population**

[de Reuver S](#), Engchuan W, Zarrei M, Vorstman JAS, Castelein RM, Breetvelt EJ.

*Major revisions*. 2023 Aug. doi: n/a

**17. Ultrasound Shear Wave Elastography of the Intervertebral Disc and Idiopathic Scoliosis: A Systematic Review.**

[de Reuver S](#), Moens AJBWD, Kruyt MC, Nievelstein RAJ, Ito K, Castelein RM.

*Ultrasound Med Biol*. 2022 May;48(5):721-729. doi: 10.1016/j.ultrasmedbio.2022.01.014.

**18. Sagittal curvature of the spine as a predictor of the pediatric spinal deformity development.**

Pasha S, [de Reuver S](#), Homans JF, Castelein RM.

*Spine Deform*. 2021 Jul;9(4):923-932. doi: 10.1007/s43390-020-00279-y.

**19. Early sagittal shape of the spine predicts scoliosis development in a syndromic population: a prospective longitudinal study**

[de Reuver S](#), Homans JF, Houben ML, Schlösser TPC, Ito K, Kruyt MC, Castelein RM.

*Under Peer-review*. 2023 Feb. doi: n/a

Publications not part of this thesis

**20. Letter to the editor concerning “Can a bioactive interbody device reduce the cost burden of achieving lateral lumbar fusion?” by Malone et al. JNS spine, 2022**

Duits AAA, de Reuver S, Kruyt MC

*J Neurosurg Spine.* 2023 Feb. doi: 10.3171/2023.2.SPINE23140

**21. Comment on Grivas et al. Morphology, Development and Deformation of the Spine in Mild and Moderate Scoliosis: Are Changes in the Spine Primary or Secondary? J. Clin. Med. 2021, 10, 5901.**

de Reuver S, Schlösser TPC, Kruyt MC, Ito K, Castelein RM.

*J Clin Med.* 2022 Feb 22;11(5):1160. doi: 10.3390/jcm11051160.

**22. Letter to the editor concerning “Vertebral growth modulation by posterior dynamic deformity correction device in skeletally immature patients with moderate adolescent idiopathic scoliosis” by Floman et al., Spine Deformity, 2021**

de Reuver S, Schlösser TPC, Kruyt MC, Castelein RM.

*Spine Deform.* 2021 May;9(3):863-864. doi: 10.1007/s43390-021-00308-4.

**23. A computed tomography-based spatial reference for pedicle screw placement in adolescent idiopathic scoliosis.**

Brink RC, Homans JF, de Reuver S, van Stralen M, Schlösser TPC, Viergever MA, Chu WCW, Ng BKW, Castelein RM, Cheng JCY.

*Spine Deform.* 2020 Feb;8(1):67-76. doi: 10.1007/s43390-020-00032-5.

**24. Reliability and Validity of the Adapted Dutch Version of the Early-Onset Scoliosis-24-Item Questionnaire (EOSQ-24).**

Wijdicks SPJ, Dompeling SD, de Reuver S, Kempen DHR, Castelein RM, Kruyt MC.

*Spine (Phila Pa 1976).* 2019 Aug 15;44(16):965-973. doi: 10.1097/BRS.0000000000003017

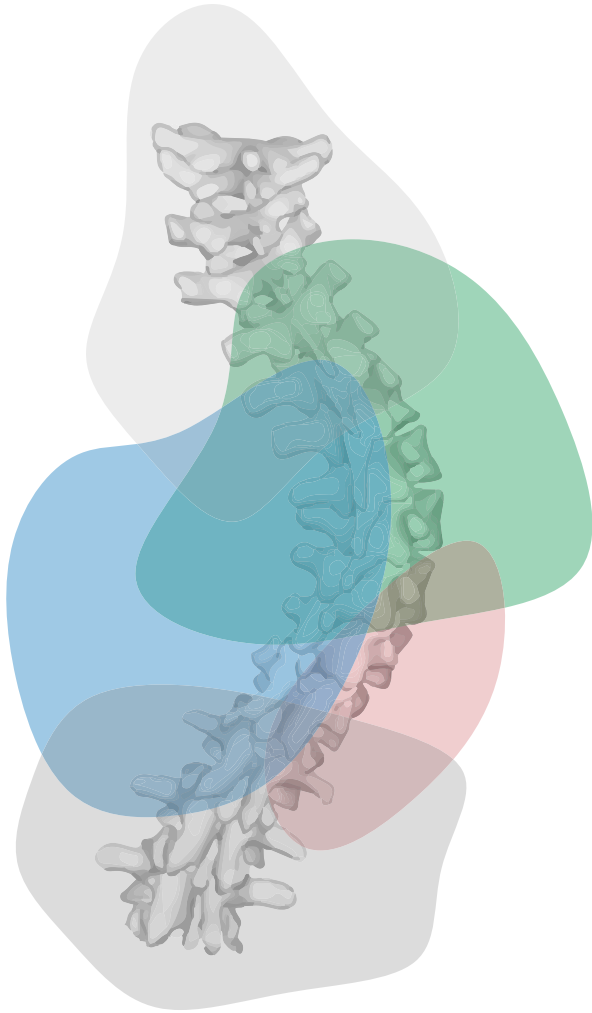
## Curriculum vitae and acknowledgements

Steven de Reuver was born on July 3rd of 1993 in Vlissingen, the Netherlands. He grew up in Middelburg with his father Theo, mother Karin and brother Jimmy, and graduated from Nehalania SSG. After graduating, he moved to Utrecht and studied one year at Law School, before starting Medicine in 2012 at Utrecht University. In 2015, at the start of his Medicine masters, he visited Tygerberg hospital in Cape Town, South Africa, for a clinical rotation in Obstetrics and Gynecology. From 2016 onwards, he joined the scoliosis research group led by prof. dr. René M. Castelein at the Department of Orthopedic Surgery at the University Medical Center Utrecht. A well organized, effective



and pleasant research group, where he was also supervised by prof. dr. Moyo C. Kruyt, dr. Tom P.C. Schlösser, dr. Rob C. Brink and dr. Jelle F. Homans, he did 3 years of part-time extracurricular research in the field of scoliosis etiology, radiation-free imaging and scoliosis in 22q11.2 deletion syndrome. During this time he visited Toronto, Canada twice, to work at the Toronto General Hospital and the Hospital for Sick Children. After receiving his MD degree in 2019, he continued these projects by starting a position of PhD-candidate in the same group at the Department of Orthopedic Surgery at the UMC Utrecht. During these years, he enjoyed a fruitful research period with great supervision by the aforementioned supervisors, and also had the pleasure to work with (and not limited to): pediatrician dr. Michiel L. Houben, psychiatrists dr. Elemi J. Breetvelt, dr. Jacob S. Vorstman and dr. Ania M. Fiksinski, linguists dr. Emma Everaert, dr. Iris S. Selten, dr. Tessel D. Boerma & prof. dr. Frank Wijnen, plastic surgeon prof. dr. Aebele B. Mink van der Molen, imaging engineers dr. Marijn van Stralen & dr. Peter Seevinck, ultrasound engineers dr. Timothy T.Y. Lee and prof. Yong-Ping Zheng, pediatric radiologist prof. dr. Rutger Jan Nievelstein, biomechanical engineer prof. dr. Keita Ito, from the veterinary department dr. Lonneke L. IJsseldijk, dr. Stefanie Veraa, dr. Marja J.L. Kik & prof. dr. Andrea Gröne, and of course the many heroes of the international 22q community led by prof. Anne S. Bassett and prof. Donna M. McDonald-McGinn. Also, with special thanks to the Fondation Yves Cotrel, Scoliosis Research Society and the Annafonds for sponsoring most of the work. Furthermore he enjoyed a great time working at the research headquarters, the 'Q-building' with

amongst others: Rob, Jelle, Willem Paul, Bruce, Sebas, Jasmijn, Floris, Jasper, Justin, Lorenzo, Margot, Mattie, Koen, Joell, Chien, Chien, Ruben, Eva, Dineke, Casper, Bas and Peter. And last but not least, many of these projects would not have succeeded without help from the many students, including Aaron, Hanna, Philip, Max, Micha, Anne-Ruth, Luc, Nick & Abdi. In between all the research, in 2022, he did 10 months of clinical work as resident not-in-training at the Department of Orthopedic Surgery at the UMC Utrecht, together with the great staff (Cumhur, Lodewijk, Charles, Ralph, Jorrit-Jan, Moyo, Bart, Sander, Wouter, Roel, Nienke, Tom, Jasper, Paul, Puck, Michelle, Mechteld, Simone, Mariska, Sandra, Ilse, Barbara, Hilde & Pauline), also good friends and peers (Kiran, Christel, Said, Marianne, Nick, Joost, Paul, Thom, Eric, Mathilde, WP, Mara, Daniel, Fien, Sarina & Dunja), and of course the hero nurses and physiotherapists of D4W. Besides work, his hobbies are working and caring for his 1924 house in the 'Bloesemstraat' where he happily lives with his girlfriend Sari for many years already, furthermore working on cars and other stuff with his dad, and also playing golf, visiting football matches (i.e. Feyenoord), going ice-skating, skiing, some casual maths/physics/geography/history, astronomy with a hobby telescope, chess and traveling. During these years he was able to visit many places to work, including Toronto, Las Vegas, Paris, Split, Prague, Singapore and Cape Town. Finally, from March 2023, he started his training to become an Orthopedic Surgeon.



Thank you